Plenary Lecture I

Chair: Young Hyun Yoo (Korea)

CRISPR genome editing in animals and human embryos

Kim, Jin-Soo[1,2]

[1]Center for Genome Engineering, Institute for Basic Science, Daejeon, South Korea
[2]Department of Chemistry, Seoul National University, Daejeon, South Korea

Genome editing with CRISPR systems that allows targeted mutagenesis in cells and organisms is broadly useful in biology, biotechnology, and medicine. Despite broad interest in CRISPR RNA-guided genome editing, Cas9, Cpf1, and Cas9-fused deaminases (a.k.a., Base Editors) are limited by off-target mutations. We developed nuclease-digested whole genome sequencing (Digenome-seq) to profile genome-wide specificities of Cas9 and Cpf1 nucleases and Cas9-fused deaminases in an unbiased manner. Digenome-seq captured in vitro cleavage sites at single nucleotide resolution and identified off-target sites at which indels or base conversions were induced with frequencies below 0.1%. We also showed that these off-target effects could be avoided by using preassembled ribonucleoproteins (RNPs) and modified guide RNAs. Digenome-seq is a robust, sensitive, unbiased, and cost-effective (< USD 1,500) method for profiling genome-wide off-target effects of programmable nucleases and deaminases.

Key Words: CRISPR, Genome editing, Cas9

Plenary Lecture II

Seeing allergy and anaphylaxis through an evolutionary lens: Roles of mast cells and IgE in innate and adaptive defenses against venoms

Stephen J. Galli

Departments of Pathology and of Microbiology and Immunology, Stanford University School of Medicine, Stanford, CA, 94305-5176, USA

Mast cells and IgE antibodies are thought to promote health by contributing to host responses to certain parasites, but other beneficial functions have remained obscure. Venoms provoke innate inflammatory responses and pathology reflecting the activities of the contained toxins. Venoms also can induce allergic sensitization and development of venom-specific IgE antibodies, which can predispose some subjects to exhibit anaphylaxis upon subsequent exposure to the relevant venom. We found that *innate* functions of mast cells, including degradation of venom toxins by mast-cell-derived proteases, can enhance survival in mice injected with venoms from the honeybee, two species of scorpion, four species of poisonous snakes, or the Gila monster. We also found that mice injected with sub-lethal amounts of honeybee or Russell's viper venom exhibited enhanced survival after subsequent challenge with potentially lethal amounts of that venom, and that IgE antibodies, FcRI, and probably mast cells contributed to such acquired resistance. While there are many other mechanisms that can contribute to host defense against a variety of venoms, our findings in mice suggest that mast cells, and IgE-dependent mast cell activation, can participate substantially in defense against the morbidity and mortality induced by certain insect and snake venoms. This ability to reduce the toxicity of certain venoms may represent an ancient, and beneficial, role of mast cells and IgE-dependent mast cell activation.

Special Lecture I

Chair: Kyung Ah Park (Korea)

The Anatomy Educator: Broadening Horizons

Richard L. Drake

Director of Anatomy and Professor of Surgery, Cleveland Clinic Lerner College of Medicine of Case Western Reserve University, Cleveland, OH, USA

Medical education is changing! Therefore, we/anatomists must also change to remain relevant. If we do not, we will be left behind. And while change is difficult, it invites opportunity. So take advantage of this educational earthquake and explore new directions in your educational program. Your students will welcome the new you!

Key Words: Anatomy education, Innovation

Special Lecture II

Chair: Chang Seok Oh (Korea)

Is the esteem of anatomy in the medical curriculum in decline and, if so, why?

Bernard Moxham

Cardiff School of Biosciences, Cardiff University, Cardiff, Wales, United Kingdom

This talk will investigate the decline in the esteem of anatomy within medical schools in many parts of the world, contrasting this with the views of professional anatomists, medical students and laypersons. It will be argued that reasons for any loss of esteem relate only partly to educational fashion amongst medical authorities (including Deans) and medical educationalists but mainly to misguided notions concerning whether practical anatomical teaching is 'traditional', to an overemphasis on the disease-based model for medicine in contradiction to the health/functionality-based model, and to the shifting of emphasis in medical training from specialisms, and from science to social science, as General Medical Practice becomes the 'endpoint' in the medical curriculum. Remedies for this situation are explored but it may be difficult to recoup the situation since professional anatomists themselves too often choose compromise rather than promulgate the evidence that anatomy is crucial and that dissection by students provides most educational advantages. The consequence is that we could be engaged in a 'spiral down to the bottom!' The talk will feature evidence-based views from both anatomists and medical students as to the most effective ways of teaching and learning gross anatomy.

Keynote Session 1

Chair: Swany KB (Malaysia)

KS-1

Caries and periodontal disease: Which occurred first in human evolution?

Hisashi Fujita

Department of Bioanthropology, Niigata College of Nursing, Japan

Needless to say, the two major oral diseases are dental caries and periodontal disease. Which of the following might have been present during the course of human evolution? The author has investigated dental diseases in many human skeletal remains up to the present. Results from these studies have led many people to believe that periodontal disease preceded the appearance of caries, as many populations have a high rate of periodontal disease but have very low rates of dental caries or no caries at all. While dental caries are not always evident in populations, alveolar bone regression due to periodontal disease has been observed in all populations investigated. This suggests that humans have a preexisting relationship to periodontal disease. This presentation describes caries and periodontal disease, with examples of human skeletal remains from other countries that have been investigated.

KS-2

Biological Effects of Gold Nanoparticles in Lung Cells

Boon Huat Bay[1], Cheng Teng Ng[1,2] Lin-Yue Lanry Yung[2]

[1]Department of Anatomy, Yong Loo Lin School of Medicine, National University of Singapore, Singapore, Singapore
[2]Department of Chemical and Biomolecular Engineering, National University of Singapore, Singapore, Singapore

Gold nanoparticles (AuNPs) have emerging applications in biomedicine, especially as prospective theranostic agents, However, AuNPs are known to have potential adverse effects that may give rise to health risks from direct exposure. We show that 20 nM size AuNPs can easily be taken up by lung fibroblasts and small airway epithelial cells as evidenced by conventional transmission electron microscopy coupled with energy dispersion X-ray microscopy for elemental profiling and advanced microscopy techniques, such as Focus Ion Beam Scanning Electron Microscopy. Internalization of the AuNPs were observed to be via clathrin-mediated endocytosis. Intracellular uptake of AuNPs was concomitant with generation of reactive oxygen species culminating in oxidative stress. The sequelae

of oxidative stress included DNA damage, cytotoxicity, autophagy, alteration of gene and protein profiles affecting cellular and functional processes. A variety of assays were used to demonstrate the toxicological effects of AuNPs. Methodologies used included cell viability assays, Comet Assay, Fluorescence-in situ hybridization (FISH), Gene chip analysis for identifying molecular targets and deciphering of pathways and two dimensional gel electrophoresis for comparative proteomic analysis. *In vivo* experimentation following intravenous administration of AuNPs in Wistar rats revealed inflammatory changes that were associated with altered inflammation-related microRNA expression. Moreover, histopathological examination showed the presence of infiltrating lymphocytes in lung interstitial tissues and enhanced IL-1α immunostaining. The findings show that nano-bio interactions could result in unwanted biological effects affecting cells exposed to AuNPs. The studies have also provided biological insights into the molecular mechanisms underlying the toxicity of AuNPs. Further investigations are warranted to better evaluate the potential health impacts of AuNPs.

Key Words: Gold nanoparticles, Lung cells in vitro, Toxicological profile, Mechanistic insights, *in vivo* experimentation

KS1-3

Good Relationships (Non-Physical Anatomy) Boosting Immune Responses, Getting Healthier, and Comfortable Living

Abdurachman Latief[1], Krisnawan andy Pradana[2], Netty Herawati[3]

[1]Department of Anatomy and Histology, Medical Faculty, Universitas Airlangga, Surabaya, Indonesia
[2]Faculty of Biotechnology, University of Surabaya, Surabaya, Indonesia
[3]Department of Psychology, Trunojoyo University, Bangkalan-Madura, Indonesia

According to famous Einstein's formula, $E \approx m\, C^2$, physical morphology (anatomy) equivalent with non-physical morphology. Physical anatomy equivalent non-physical anatomy. The non-physical anatomy denotes the personality. Human relationships are portion of personality. We checked the potential of good relationships in boosting immune responses. Some articles international standardized related with good relationships in boosting immune response were recorded. Some articles were tabulated to compares the effect of good relationships and bad relationships to immune responses. As a result, good relationships always boosting immune responses while bad relationships decreasing immune responses. Furthermore, good relationships also make healthier and comfortable living. In human living, people must have good relationships to get high quality of immune responses, healthier, and comfortable living.

Key Words: Good relationships, Non-physical anatomy, Immune responses, Healthier, Comfortable living

Keynote Session 2

Chair: Hye-Yeon Lee (Korea)

KS2-1

Body donation and humanistic interaction-based anatomy teaching program (Silent Mentor Program) of the Tzu Chi University

Guo-Fang Tseng

Department of Anatomy, College of Medicine, Tzu Chi University, Hualien, Taiwan

Medical students learn structures by dissecting human bodies. Dissection on unclaimed bodies or donors with undisclosed personal information is the norm in medical schools throughout the world. This practice distances medical schools from the general public. Body donation for medical education remains controversial in many parts of the world. The lack of transparency in treating the bodies and the reluctance of the surviving families to see the bodies subjected to cuts and dismantling are also factors alienating public from donation. Dissecting the unclaimed (without the person's consent) is inconsistent with modern medical educational emphasis on humanity and empathy. We run a humanistic-based gross anatomy curriculum with willed bodies since the first dissection class in 1996 when body donation was practically unheard in Taiwan. Donors are silent mentors or altruistic role models of students. Students connect to the donation by visiting surviving families and learning about the lives of the donors before classes. Families and students joined the ceremonies at the beginning and end of the dissection. Interaction enhances the appreciation of the donation and incites in-depth introspection in students to be caring professionals in the future. It in addition, comforts surviving families and helps to quail public resistance to body donation. In our experience, we are confident that gross anatomy program can be designed to include interaction to connect the learners to the altruistic philosophy of body donors and surviving families. This enriches gross anatomy with empathy cultivation and brings the teaching closer to the aim of modern medical education.

Key Words: Body donation, Gross Anatomy, Silent mentor

KS2-2

Umbilical Cord Care Practices among the Newborns of Gadaba and Konda Dora Tribes

Swany KB[1], G Lakshmi[2], R S Rao[2], L Giridhar[2]

[1]Lincoln University, Kuala Lumpur, Malaysia,
[2]Andhra University, Visakhapatnam, India.

Research question: How the cord care was provided to the Gadaba and Konda Dora

Newborns? Objectives: 1. Know how the cord care is provided to the Gadaba and Konda Dora newborns. 2. Assess the incidence of home-deliveries. 3. Identify the different categories of care providers. 4. Find out the prevailing components of the traditional cord care practices. **Introduction:** Health of a mother and newborn depends not only on the health care received during pregnancy and Intra partum but also during postpartum period. **Settings & Design:** A cross-sectional study was conducted on Gadaba and Konda Dora Tribal populations at random from 95 tribal villages in Vizianagaram district, Andhra Pradesh. Materials & methods: Data were collected from 300 lactating women from each Tribe who were Aged between 15-45 years through in-depth and face to face interview method. **Results:** Nearly one fifth (18.0%-20.0%) of the present Tribal women reported that the Umbilical cord was cut after the delivery of the placenta, and majority of the respondents were not sure/unaware of the time of removing the umbilical cord. Most of the Gadaba (80.3%) and Konda Dora (82.3%) Tribes used the new shaving blade to cut the umbilical cord. After cutting the Umbilical cord, new thread was tied to the stump to arrest the blood flow in 80.3% of Gadaba and 83.0% of Konda Dora newborns. About 96.0% of Gadaba and 95.3% of Konda Dora newborns were applied with variety of oils or ash of vegetative origins and also used different powders to the wound for healing. **Conclusion:** Some of the present study Tribal women have adopted certain unhygienic Practices in cutting the umbilical cord with unsterilized unsafe instruments, tying the wound with available material and also applying the cord stump with different substances which are considered as unhealthy practices.

Key Words: Gadaba, Konda Dora, Newborn, Umbilical cord, Cord stump

1 & 2= Umbilical cord and Placenta of new born, 3&4= Cutter and clams- Safe instruments.

1
2
3
4
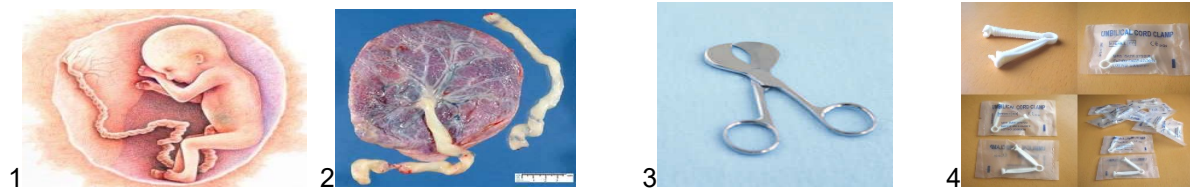
5 to 8= Unsafe and unethical instruments used by Tribal people to cut the Umbilical cord.

5
6
7
8
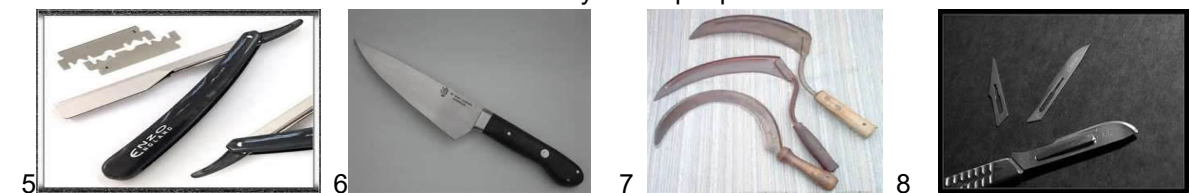
KS2-3

Forensic Osteology Parameters in a Thai Population

Pasuk Mahakkanukrauh, MD*

Professor and Director, Excellence center of osteology research and training and staff in Department of Anatomy, Faculty of Medicine, Chiang Mai University.

Identification of the body remains must be done in all cases as it is the natural right and dignity of human being. Therefore, many techniques have been developed and established for these purposes. Methods for human identification are divided into non-scientific (visual) method and

scientific method by using fingerprint, DNA ect. Data obtained from both methods are used for matching with information from the missing persons. In many cases, such as in crimes, accidents and other violent situations, using of visual identification is impossible. Even using DNA is known to be the most accurate for identification, but in many cases the DNA in remains has degenerated due to many physical and chemical conditions. In case which the body has deceased before the discovery until the remaining is only a skeleton or fragmented bone, forensic osteology would play an important role to help for identification. Scientists can estimate race, age-at-death, sex and stature from many parts of bone remaining. All estimated data establish a biological profile. These estimations lie on the experience and research's result. However, using of estimate techniques according to the research's result in many cases are limited due to different population used. Sex is often the question to be asked. Sexual dimorphism is studied in Thai as follow axial skeleton (base of skull, skull, vertebrae), appendicular skeleton (humerus, radius, ulna, femur, tibia, talus, narvicular bone). One of the challenges of developing a biological profile of unknown skeletal remains is age estimation. There are not many studies in Thai: age estimation from cranial-maxillary suture, vertebral osteophyte and acetabulum. The estimation of stature is a very important step in developing a biological profile for forensic identification. However, little previous work has been done on stature estimation among modern Thai people, despite a growing number of forensic cases in Thailand in recent years. Stature estimation was studied by complete and incomplete of long bone. There are not research in ancestry because of samples limitation.

Key Words: Forensic osteology, Human identification

Keynote Session 3

<div align="right">

30th October, Tuesday
09:00-10:30
Rm 325-326

</div>

Chair: Abdurachman Latief (Indonesia)

KS3-1

Imaging synapse remodeling *in vitro* and *in vivo*

Shigeo Okabe

Department of Cellular Neurobiology / Graduate School of Medicine / the University of Tokyo, Tokyo, Japan

Development of neuronal circuits in vivo depends on precise regulation of synapse formation, elimination and remodeling. In vivo two-photon excitation microscopy is a powerful technique for the detection and analyses of synaptic structures in living animals. Two-photon imaging analyses of synapse development confirmed presence of two phases of synapse dynamics in the mouse cortical pyramidal neurons during postnatal development. In the first 20 days after birth, dynamics of synapses is high with their turnover rate higher than 10% per day. In the second phase, which starts at 3 weeks

postnatal, synapse dynamics is highly suppressed, with the rate lower than 5% per day and with spine elimination rate slightly exceeding spine formation rate. Consistently, the cortical synaptic density increases rapidly in the first phase, while it shows gradual decrease in the second phase. It is likely that both presynaptic and postsynaptic mechanisms are involved in the developmental regulation of synapse stabilization/ destabilization. In this talk I will also discuss multiple mechanisms involved in synapse stabilization and destabilization. These include stabilization of pre- and postsynaptic membranes by cell adhesion system and dense core vesicle-mediated release of a synapse destabilizing factor from the presynaptic compartment. These mechanisms may be important both in normal development of neural network and in pathological changes associated with psychiatric disorders.

Key Words: In vivo synapse imaging, Postnatal synapse development, Dendritic spine, Bone morphogenetic protein (BMP) 4, Superresolution imaging, Autism spectrum disorder (ASD)

KS3-2

Reform of the anatomical sciences education in Peking University

Chang-man ZHOU*, Wei-guang ZHANG

Peking University Health Science Center, 38 Xueyuan Rd, Haidian Qu Beijing China, 100191,

The Peking University Health Science Center (PKUHSC) was founded on October 26, 1912 with the former of Beijing National Medical School. It was China's first government-funded school designated to teach Western medicine. Anatomic science education is always a key course in medical education. However, a Reducing Gross Anatomy class hour has become a general trend. The curricular reduce has been a continuing theme in China medical university for the past 20 years. Current curricular for clinical student in PKUHSC, 88 hours (28 hrs in class room Lecture, 60hrs in libratory) for Gross Anatomy at first year, and 78 hours for topographical anatomy at third year. Thus, the curriculum changes, courses will need to modify their approach accordingly with the new educational paradigm of the institution. A multimodal approach to education involving active learning, contextual learning of applied anatomical sciences, and longitudinal and vertical integration of anatomical curricula with assessments of competencies is the current pedagogical goal. Virtual Anatomy plays an important role in the current anatomic education: Imaging, 3D Virtual dissection, Virtual Reality (VR), Hololens, but Cadavers is always a best ways to learn anatomy, from virtual to reality. The university provides students with a subscription to micro-lectures of E-Anatomy a web based earning program. At the end of third year, when the student finished basic medical courses, Problem-Based Learning (PBL) is a good review for the knowledge of human anatomy.

*Correspondence to Chang-man ZHOU (E-mail: cmzhou@bjmu.edu.cn)

KS3-3

The Myodural Bridge Complex Defined as a new functional structure

Nan Zheng[1], Beom Sun Chung[2], Yi-Lin Li[1], Tai-Yuan Liu[1], Lan-Xin Zhang[1],Yang-Yang Ge[1],Nan-Xing Wang[1], Zhi-Hong Zhang[1], Lin Cai[1], Yan-Yan Chi[1], Jian-Fei Zhang[1], Okoye Chukwuemeka Samuel[1], Min Suk Chung[2] , Sheng-Bo Yu[1]*, Hong-Jin Sui[1]*

[1]Department of Anatomy, College of Basic Medicine, Dalian Medical University, Dalian, P. R. China
[2]Department of Anatomy, Ajou University School of Medicine, Worldcup-ro 164, Suwon 443-749, Republic of Korea.

Introduction: In recent years, multiple studies have revealed that connective tissues exist between the rectus capitis posterior minor (RCPmi), rectus capitis posterior major (RCPma), oblique capitis inferior (OCI), nuchal ligament and the spinal dura mater (SDM). This connective tissue is known as the Myodural Bridges (MDB). However, the spatial relationship of the different connective tissue fibers that form the MDB has remained unclear. It would be demonstrated in this research. This information will be highly useful in exploring the function of the MDB. **Materials and methods:** Three-dimensional visualization model, P45 plastinated slices and histological sections of human MDBs were used in this research to show the MDBs' spatial relationship. **Results:** We found that the MDB originating from the RCPmi, RCPma and OCI coexist. Part of the MDB fibers, which originate from the ventral aspects of the RCPmi together with the cranial segment of the RCPma, pass through the posterior atlanto-occipital interspace and inserted into the posterior aspect of the upper cervical SDM. Meanwhile part of MDBs' fibers, which originate from the dorsal aspect of the RCPmi, the ventral aspect of the caudal segment of the RCPma, and the ventral aspect of the medial segment of the OCI, entered the central part of the posterior atlanto-axial interspace, fused together with the Vertebral Dura Ligament (VDL), and finally connect with the cervical SDM anteriorly. Our finding proved that the MDBs exist as a complex which we termed the 'Myodural Bridge Complex' (MDBC). In the process of head movement along any one of its motor axes, tensile forces could be transported possibly and effectively from some of the subocciptial muscles to the upper part of the cervical SDM by means of the MDBC. **Conclusions:** The concept of MDBC will be beneficial in the overall exploration of the function of the MDB.

Key Words: Myodural Bridge; Three-Dimensional Visualization model; P45 plastinated slices

4th AsACA Symposium

Part I: Head	09:30-10:45
Part II: Upper Limb	11:00-12:15
Part III: Pelvis & Neck	13:30-14:45
Part IV : New challenges in clinical anatomy	15:00-16:15
Special Lecture	16:30-17:30

Part I: Head
Chair: Keiichi Akita (Japan)

AS-1

An Anatomical Study of Maxillary-Zygomatic Complex Using Three-Dimensional Computerized Tomography-Based Zygomatic Implantation

Xiangliang Xu[1], Shijie Zhao[1] , Hui Liu[2], Zhipeng Sun[1], Jianwei Wang[1], Weiguang Zhang[1]

[1]Peking University Health Science Center, Beijing, China
[2]Department of Medical Imageology, Peking University Shougang Hospital, Beijing, China

To obtain anatomical data of maxillary-zygomatic complex based on simulating the zygomatic implantation using cadaver heads and three-dimensional computerized tomography (3D-CT). Simulating zygomatic implantation was performed using seven cadaver heads and 3D-CT images from forty-eight adults. After measuring the maxillary-zygomatic complex, we analyzed the position between the implantation path and the maxillary sinus cavity as well as the distance between the implantation path and the zygomatic nerve. The results showed that the distance from the starting point to the endpoint of the implant was 56.85 ± 5.35mm in cadaver heads and 58.15 ± 7.37mm in 3D-CT images. For the most common implantation path (80.20%), the implant went through the maxillary sinus cavity completely. The projecting points of the implant axis (IA) on the surface of zygoma were mainly located in the region of frontal process of zygomatic bone close to the lateral orbital wall. The distances between IA and zygomatic nerve in 53 sides were shorter than 2 mm. The simulating zygomatic implantation on cadaver skulls and 3D-CT imaging provided useful anatomical data of the maxillary-zygomatic complex. It is necessary to take care to avoid the zygomatic nerve injury during implantation, because it frequently appears on the route of implantation.

Key Words：Zygomatic implantation, Zygoma, Maxilla, Three-dimensional computerized tomography

AS-2

Anatomical Review of Malaris Muscle

Natnicha KAMPAN[1], Keiichi Akita[2], Pasuk Mahakkanukrauh[1,3]

[1]Department of Anatomy, Faculty of Medicine, Chiang Mai University, Chiang Mai, Thailand
[2]Department of Clinical Anatomy, Graduate School of Medical and Dental Sciences, Tokyo Medical and Dental University, Tokyo, Japan
[3]Excellence Center in Osteology Research and Training Center, Chiang Mai University, Chiang Mai, Thailand

The present anatomical textbooks state that the malaris muscle is merely the variation usually found during the study of facial muscles, the malaris muscle, however, has long been described as one of the facial muscles. Numerous studies have attempted to define and examine the existence of the malaris muscle as well as its clinical implication in the facial aesthetic contexts or facial rejuvenation. Various researches have revealed that the malaris muscle relate to the appearance of facial aging especially in the periorbital area. Although many studies have been reported the reasonable explanations about the malaris muscle; in the anatomical context, however, the insight into the malaris muscle remains ambiguous. Many studies have explained the malaris muscle that is the muscle bundle located lateral to the orbicularis oculi muscle, while some have established the malaris muscle consisting of the medial and lateral bundles adjacent to the orbicularis oculi muscle. This present study consequently intends to propose the review of the malaris muscle for the comprehensive understanding. To improve understanding of the malaris muscle, here we focus on the anatomical concept of the malaris muscle as well as the role of the muscle in the facial aesthetic aspect from the previous studies to the current studies. From this review, we will comprehend the change in anatomical viewpoints of the malaris muscle from the morphological examinations of the malaris muscle in various studies. The recent study has exposed that the malaris muscle is not composed of only medial or lateral muscle band but includes the U-shaped muscle band inferior to the orbicularis oculi muscle. Moreover, we will realize the change in concepts of the malaris muscle regarding its role that is considered having the relation to the appearance of the facial aging. The recent study has found the relation between the malaris muscle and the intraorbital fat prominence. This anatomical review will suggest the revised understanding of the malaris muscle.

Key Words: Malaris muscle, Aging, Anatomical

AS1-3

Myodural bridge and cerebrospinal fluid circulation

Hong-Jin SUI

Department of Anatomy, Dalian Medical University, Dalian 116044，China

The concept of MDB was first proposed by Hack in 1995. The dense fibrous connective tissues between the Rectus Capitis Posterior minor (RCPmi) and the Posterior Atlanto-Occipital Membrane (PAO membrane), the PAO membrane and the cervical spinal dura mater (SDM) in the suboccipital region are named as Myodural Bridge (MDB). Subsequent studies have revealed that fibers originating from Rectus Capitis Posterior major (RCPma), Oblique Capitis Inferior (OCI) and nuchal ligament in

the suboccipital region all participate in the formation of the MDB. Multiple researchers infer that MDB might have important functions that the MDB might has implications in avoiding in-folding of spinal dura mater and keeping the subarachnoid space and the cerebellomedullary cistern unobstructed, sensorimotor function and postural control of head, in cervicocephalic pain syndromes. Sui et al. proposed that the motion of the suboccipital muscles may be a dynamic source for the CerebroSpinal Fluid (CSF) circulation via the MDB. Then they found multiple evidences to support the hypothesis though morphology and radiology methods. MDB is a structure having important physiological function. Further researches should be taken to find out the mechanism of MDB involving in the CSF circulation. It may provide new ideas and methods for the diagnosis and curing for the chronic headache of unknown cause.

Key Words: Myodural bridge, Cerebrospinal fluid circulation, Anatomy

Part II: Upper Limb
Chair: Shuwei Liu (China)

AS2-1

Clinical anatomy of the sternoclavicular and acromioclavicular joints, with special reference to articular disc

Kenji Emura

Faculty of Health Care Sciences, Himeji Dokkyo University, Himeji, Japan

The motion of the scapula on the thorax is the result of combined motions of the sternoclavicular joint (SCJ) and the acromioclavicular joint (ACJ). Detailed anatomical information of the SCJ and ACJ is essential to understand the kinesiology of shoulder complex. However, there are scant morphological data on the SCJ and ACJ, especially on their articular disc. Fifty-one SCJs and 52 ACJs were investigated morphologically. We classified the articular discs of the SCJ into three types, namely, discoid type (36 cases), ring type (3 cases), and meniscal type (12 cases). The difference in the shape of the articular disc of the SCJ was due to the difference in the shape of the sternal end of the clavicle, and the shape of the articular surface of the sternum was not different among three types of the articular disc. The motion of the SCJ as a saddle joint could occur mainly between the sternal surface of the articular disc and the manubrium of sternum. We classified ACJs into three major types depending on the articular disc. Type 1 ACJ (2 cases) had an articular disc which completely divided the articular cavity. Type 2 (13 cases) had an articular disc which partially divided the articular cavity. Type 3 (37 cases) had no articular disc. Type 2 and type 3 were further divided into subtypes according to the configurations of the articular surfaces. In total 22 ACJs had articular surfaces like an ellipsoid joint in which the rotation along the long axis was limited.

Key Words: Sternoclavicular joint, Acromioclavicular joint, Articular disc, Articular surface.

AS2-2

Topographical change of neurovascular structures according to variant muscles in upper limb

Jae-Ho Lee

Department of Anatomy, Keimyung University School of Medicine, Daegu, Korea

Variant muscles in upper limb are particularly frequent, and their patterns and types have been studied by many authors. Most frequent variant muscle in arm and forearm is third head of biceps brachii (TBB) and gantzer's muscle (GM), respectively. The presence of these variant muscles might affect the topography of neurovascular structures. The aim of this study was to determine topography of the GM and TBB, and to define the topographical relationship between these muscles and its surrounding neurovascular structure. After identifying the prevalence of the GM and TBB, the topography of these muscles and the neurovascular structures were analyzed and the correlation between the neurovascular structure and variant muscles was investigated. The incidence of the GM was 47.95% (35/73) and the average insertion point of the GM was identified at 49.33 ± 7.47 percentile (119.82 ± 20.80 mm) of the reference line between the medial epicondyle and the pisiform bone. And branch points of the median nerve and the ulnar artery were located 19.91 ± 11.23 percentile (52.21 ± 24.67 mm), 17.45 ± 8.39 percentile (42.53 mm ± 20.54) of the reference line. The presence of the GM had no significant correlation with the position of the nerve branches. On the other hand, the branching point of ulnar artery was distally located in the cases with the presence of the GM (17.35 ± 8.65 vs 19.42 ± 10.87, p = 0.031). There was significant positive correlation between the point of the arterial bifurcation point and the length of the GM (r = 0.407, p = 0.015). The presence of TBB also showed an association with its surrounding neurovascular structure. The present study suggested that variant muscles in upper limb had topographical relation with the neurovascular structures embryologically.

AS2-3

Anatomy based on the common pathologies around the elbow joint

Akimoto Nimura[1] and Keiichi Akita[2]

[1]Department of Functional Joint Anatomy, Tokyo Medical and Dental University, Tokyo, Japan
[2]Department of Clinical Anatomy, Tokyo Medical and Dental University, Tokyo, Japan

As an anatomist half and orthopaedic surgeon the other half, we talk about the elbow anatomy based on the common pathologies around the elbow: the tennis elbow and the ulnar collateral ligament (UCL) injury. The enthesopathy of the origin of extensor carpi radialis brevis (ECRB) is mainly suspected to be the etiology of the tennis elbow. To understand why such changes specifically occurred in the ECRB origin, we analyzed anatomic features of the ECRB origin compared to other extensors, and to identify relationships between the ECRB origin and other deeper structures like as the joint capsule and the supinator. ECRB originated from the most distal part of the lateral epicondyle, and the ECRB origin was simply composed of tendinous portion without muscular parts. The tendinous slip of the supinator originated from the postero-distal part of the ECRB origin, and the supinator did not run over the anterior part of the ECRB origin. The only thin capsule was underlying the anterior side of the ECRB origin without the support of the supinator. This portion seems to be originally fragile to repetitive stress or micro trauma, and could be the lesion for the initiation of the tennis elbow. The anterior oblique ligament (AOL) of the UCL has been thought as the primary static stabilizer against the valgus stress during throwing motion. In addition, the proximal origin of flexor-pronator muscles (FPMs) has been also assumed as the secondary dynamic stabilization. However, the anatomic relationship between them remains unclear. Therefore, we analyzed the relationship between FPMs

and deeper structures, in terms of the surrounding structures such as the tendinous fascia and joint capsule rather than the specific ligaments. By removing muscular parts from the FPMs, the pronator teres muscle (PT) and the flexor digitorum superficialis (FDS) had the common tendinous fascia between two muscles. The PT/FDS common tendinous fascia originated from the anterior slope of the medial epicondyle, distally extended to the sublime tubercle, and posteriorly reflected and continued to the deep fascia of FDS. Based on these findings in perspective with surrounding structures, AOL could be interpreted as the complex, which consists of the PT/FDS common tendinous fascia, the deep fascia of FDS continuing to it, and the joint capsule underlying the fascia. In other words, the contribution of dynamic factors of PT, FDS, and the brachialis to the stabilizing mechanism of the elbow joint against valgus stress could be assumed to be more critical than previously thought.

Key Words: Tennis elbow, ECRB, joint capsule, UCL, AOL, FPMs

Part III: Pelvis & Neck
Chair: Im Joo Rhyu (Korea)

AS3-1

Our gynecologic surgery based on fascia

Kenro Chikazawa[1], Keiichi Akita[2], Ken Imai[1] Tomoyuki Kuwata[1]

[1]Department of Obstetrics and Gynecology, Jichi Medical University, Saitama Medical Center, Japan
[2]Department of Clinical Anatomy, Graduate School of Medical and Dental Sciences, Tokyo Medical and Dental University, Tokyo, Japan.

The relationship between the pelvic fascia and the autonomic nerves is important for pelvic surgery. With knowledge of this relationship, pelvic surgeon could perform the autonomic nerves preservation. Within the field of pelvic surgery, there are many reports and presentations of fascia, space, and cavities. In gynecologic surgery, we take care of three fascia: vesicohypogastric fascia, pre-hypogastric nerve fascia, and fascia outside of ureter which might continue from renal fascia. Three fasciae are useful for avoiding other organ injury and autonomic nerves preservation. We summarize three fasciae with gynecologic operation. We present our operative video clips and pictures. The tips of surgery are following. Vesicohypogastric fascia: the vesicohypogastric fascia ventrally arises at the medial position and leach to ascending branch of the uterine vessel. The lateral side of this fascia is safe in surgery, and the ureter and vessels inhabit a relatively tissue-poor space (avascular space, maintaining distance, called Lazko's pararectal space). Pre-hypogastric nerve fascia: this fascia includes both the sympathetic and parasympathetic neural fibers. They are the important autonomic nerves controlling the urogenital function. Severe damage to the hypogastric nerves may cause postoperative urogenital disorders. Pelvic surgeon take care this fascia mostly. Fascia outside of ureter: this fascia was reported with few studies. We think posterior renal fascia extending to pelvis and covering ureter. This fascia is very thin but important when gynecologist dissecting ureter in laparoscopic surgery.

Key Words: Fascia, Gynecologic surgery, Laparoscopy, Autonomic nerves, Pararectal space

AS3-2

A theoretical management strategy for meralgia paresthetica on the basis of fine

architecture of the pelvic exit of the lateral femoral cutaneous nerve

Xu Z[1,4], Tu L[1] , Zheng Y[2], Ma X[1], Zhang H[3], Zhang M[4]

[1]Department of Anatomy, Anhui Medical University, Hefei, China
[2]Department of Ultrasound, Anhui Medical University, Hefei, China
[3]School of Medicine, University of Otago, Dunedin, New Zealand
[4]Department of Anatomy, University of Otago, Dunedin, New Zealand

Meralgia paresthetica is commonly caused by mechanical entrapment of the lateral femoral cutaneous nerve. The entrapment often occurs at the site where the nerve exits the pelvis. Its optimal surgical management remains to be pinpointed, partially because the fine architecture of the fascial planes around the LFCN has not be elucidated. The aim of this study was to define the fascial configuration around the LFCN at its pelvic exit. Thirty-six cadavers (18 females, 18 males; age range, 38-97 years) were used for dissection (57 sides of 30 cadavers), and sheet plastination and confocal microscopy (2 transverse and 4 sagittal sets of slices from 6 cadavers). Thirty-four healthy volunteers (19 females, 15 males; age range, 20-62 years) were examined for ultrasonography evaluation. This study was performed in accord with our institutional ethical guidelines and approved by the institutional ethics committees. The LFCN exited the pelvis via a tendinous canal within the internal oblique-iliac fascia septum and then ran in an adipose compartment between the sartorius and iliolata ligaments inferior to the anterior superior iliac spine (ASIS). The iliolata ligaments newly defined and termed in this study were 2-3 curtain strip-like structures which superiorly inserted to the ASIS, inferiomedially interwovened with the fascia lata, and laterally continued as skin ligaments anchoring to the skin. Between the sartorius and tensor fasciae latae, the LFCN ran in a longitudinal ligamental canal bordered by the iliolata ligaments. This study defined that (1) the pelvic exit of the LFCN was within the internal oblique aponeurosis and (2) the nature of the fascia lata over the LFCN and upper sartorius was the iliolata ligaments. These results indicated that the internal oblique-iliac fascia septum and iliolata ligaments may make the LFCN susceptible to mechanical entrapment near the ASIS. To surgically decompress the LFCN, it may be necessary to incise the oblique aponeurosis and iliac fascia medial to the LFCN tendinous canal and to free the iliolata ligaments from the ASIS.

Key Words: Fascial Configuration, Lateral Femoral Cutaneous Nerve, Meralgia Paresthetica, Pelvic exit, Epoxy Sheet Plastination

AS3-3

Morphological Study of Cranial and Spinal Roots, and Internal and External Branches of the Accessory Nerve

Hong-Fu Liu[1], In-Hyuk Chung[2], In-Beom Kim[3], Hyung-Sun Won[4]

[1]Department of Anatomy, Binzhou Medical University, Yantai, China
[2]Department of Anatomy, Yonsei University College of Medicine
[3]Catholic Institute of Applied Anatomy, Department of Anatomy, College of Medicine, The Catholic University of Korea, Seoul, Korea
[4]Department of Anatomy, Wonkwang University College of Medicine, Iksan, Korea

Introduction: There has been the controversy surrounding the roots and branches of the accessory nerve. The purpose of this study was to clarify the morphological characteristics of the cranial root (CR) in the cranial cavity, and to illustrate the composition of the internal and external

branches (IB and EB), and to demonstrate the anatomical distribution of each component of the IB of the human accessory nerve. **Materials and Methods:** One hundred-seventeen half heads and necks of 68 adult specimens were used for this study. **Results:** The accessory nerve was easily distinguished from the vagus nerve by the dura mater in the jugular foramen in 80% of 50 cases. In 20% of the cases, there was no dural boundary. In these cases, the uppermost cranial rootlet of the accessory nerve could be identified by removing the dura mater around the jugular foramen where it joined to the trunk of the accessory nerve at the superior vagal ganglion. The IB and EB were mixed with the CR, vagus nerve, and spinal root (SR). The IB was classified into five types and the EB into four types according to their composition. There were 14 combinations of IB and EB types. The most common combination was the IB with the CR and the vagus nerve, and the EB with the SR and CR (31.6%). The combination of IB and EB comprising CR and SR, respectively, was not observed. The IB had three courses: the pharyngeal branch, the descending branch to the thorax, and the recurrent laryngeal nerve. The pharyngeal branch of the IB originated mainly from the vagus nerve, rather than from the CR of the accessory nerve. All of the components of the IB descended to the thorax along the vagus nerve. The recurrent laryngeal nerve comprised the IB and the vagus nerve in all specimens, and was separated into bundles originating from the IB and vagus nerve. Both bundles gave off branches to the trachea and esophagus. The posterior cricoarytenoid, lateral cricoarytenoid, and thyroarytenoid muscles were innervated by the CR and/or vagus nerve, but the distribution pattern was different in each specimen. **Conclusion:** The CR is morphologically distinct from the vagus nerve,confirming its existence. However the vagus nerve and CR can be regarded functionally as the same nerve based on their distribution in the laryngeal muscles. This study shows that there are no IB and EB comprising only the CR and SR, respectively, and the IB and EB have various combinations of the CR, SR, and vagus nerve.

Key Words: Accessory nerve; Cranial root; Spinal root; Internal branch; External branch; Vagus nerve

Part IV: New challenges in clinical anatomy
Chair: Ming Zhang (New Zealand)

AS4-1

Reappraisal of Electromyographic Studies using Cadavers

Im Joo Rhyu[1,2], Dasom Kim[1,2], Se Young Shin[3], Dong Hwee Kim[2,3]

[1]Department of Anatomy, Korea University College of Medicine, Seoul, Republic of Korea
[2]Practical Anatomy Center, Korea University College of Medicine, Seoul, Republic of Korea
[3]Department of Physical Medicine & Rehabilitation, Korea University College of Medicine, Seoul, Republic of Korea

Electrophysiologic tests including nerve conduction studies and needle electromyographic examination (EMG) are usually used for evaluating neuromuscular diseases. Especially, needle EMG localizes neuromuscular lesion by detecting abnormalities in specific muscles. Many textbooks for needle EMG recommended optimal needle insertion sites for each muscle. However, different insertion sites for same muscle can cause confusion to electromyographers and can potentially result in damage of nerve or vessel, especially, in muscles adjacent to neurovascular bundle such as pronator teres, supinator, biceps femoris short head, etc. Also, deep-seated muscles such as rhomboid, pronator quadratus, extensor indicis, extensor halluces longus, etc. can increase the chance of inaccurate or incorrect needle placement, which compromises the diagnostic utility of the procedure for localization of neuromuscular lesion. Quantitative measurements of critical muscles for the

diagnosis of neuromuscular diseases and their relative relationship with nerve or vessel using cadavers provide important information for optimal and safe needle insertion sites and can recommend new and safe needle insertion technique. Anatomical knowledge should be the basis of electrophysiologic tests. Cadaveric studies can give electromyographers a new perspective on needle EMG and newly provide accurate and safe needle insertion of critical muscles for neuromuscular diseases.

Key Words: Electromyography, Cadavers, Neuropathies, Muscles

AS4-2

The new progresses of the digital human anatomy in China

Shuwei Liu[1,2], Yifa Xu[2], Yuchun Tang[1,2], Qunsheng Yin[1,2], Zhenping Li[1,2]

[1]Department of Anatomy, Histology, and Embryology, Shandong University Cheeloo Medical College, Jinan, China;
[2]Institute for Digital Human, Shandong University, Jinan, China

Clinical practice needs high resolution digital human body in order to reveal more detail anatomic structures. Our purpose is to obtain the high resolution sectional anatomic dataset of the human body by using digital freezing milling technique for establishing more precise clinical digital human. 4 Chinese adult cadavers were selected as the specimens for this study. After CT and MRI examinations verification of absent pathological lesions, the specimens was embedded with gelatin in anatomical position and frozen under profound hypothermia, and the specimens were then serially sectioned from feet to head layer by layer with digital milling machine in the freezing chamber. The sequential images were captured by means of a digital linear scanning camera and the dataset was imported to imaging workstation. High resolution digital human bodies were created by using those dataset. The thin serial sections of the human body added up to more than 68 thousands layers with each layer being 0.1 mm in thickness. The picture resolution was 16000×26000. The data size of each section was 2.3GM. The shape, location, structure, internal organ vessels and adjacent structures of man organs were displayed clearly on each layer of the horizontal, sagittal, and coronal sectional slices. CT and MR images through the body were obtained at 1.0 mm intervals. The three dimensional models of some regional structures, for example, hand, were created according to clinical needs. The digital atlas of sectional anatomy was prepared at high resolution level for clinical imaging diagnosis. The methodology reported here has greatly improved the milling methods previously described. It is a new data acquisition method for sectional anatomy and digital human study. The thin sectional anatomic dataset of human body obtained by this technique is of high precision and good quality for establishing clinical digital human with high resolution.

Key Words: Sectional anatomy, Digital freezing milling technique, Dataset, digital human

AS4-3

Contemporary anatomy researches: from cadaveric dissection to practice

Yang Hun-Mu

Department of Anatomy, Yonsei University College of Medicine

Our team (2017-2018) performed a series of clinical anatomical studies to reveal insufficient topographic information for 1) comprehensive understanding of facial connective tissue structure, 2) safe thyroid cancer surgery using an endoscope and 3) efficient regional anesthetic injection in the back and occipital area. To overcome methodological inexactitude of conventional manual dissection, we recruited the enhanced techniques such as micro-CT with PTA preparation (1), stereotactic localization using a 3D digitizer (2) and US- / endoscope- guided simulation using non-embalmed objects (3). Herein, our recent anatomy studies and novel methodological approaches will be introduced. The communication between clinician and clinical anatomist will be also discussed, in respect of its significance for the prehension of clinically meaningful theme and the expeditious application of anatomical research to actual practice.

Special Lecture
Chair: Ki-Seok Koh (Korea)

AS-Special Lecture

Ultrasonography and 3D scanning system; New horizons in anatomical researches and their clinical applications on non-invasive procedures on the face and neck

Hee-Jin Kim, DDS, PhD, Professor*

Division in Anatomy & Developmental Biology, Department of Oral Biology, Human Identification Research Center, BK21 PLUS Project,Yonsei University College of Dentistry, 250 Seongsanno, Seodaemun-gu, Seoul, 120-752, Korea

Anatomically, the face is the most complicated structure of the human body. More specifically, the structure of the facial muscles that include the nerves and vessels is very variable and presents racial differences. Recently, the importance of facial anatomy has been reconsidered since interest on facial aesthetics has been increasing. Aesthetic physicians should therefore understand more about the anatomy of the facial musculature. The BoNT-A and filler injection are widely-applied techniques for managing masseteric hypertrophy, gummy smiling, several facial wrinkles, volume augmentation, and facial asymmetry that includes the asymmetrical smile. However, inaccurate injections sometimes may result in mild side effects such as bleeding, bruising, or muscle bulging, along with more serious side effects including skin necrosis and blindness. Recently, wide ranges of cadaveric studies have been published to prevent these side effects from occurring while optimizing results. In addition to various anatomical studies, the ultrasonography (US)-guided injection technique has been suggested as a method that is safer than other techniques and leads to more accurate injections into the targeted area with less complications. While this US-guided injection technique is safer and more efficient than conventional injection methods (blind injection), clinicians today rarely perform this US-guided injection on the face. It is difficult to identify the facial muscles through ultrasound images that are relative to the upper and lower extremity or trunk muscles because facial expression muscles are interwoven with their surrounding muscles or connective tissues. However, an US-guided injection allows for exact identification of the anatomical information which clinicians were not able to obtain through conventional examinations. This includes anatomical variation, exact location, layers of target muscles, and location of the needle or cannula tip. Other important issues include depth of muscle and thickness of the subcutaneous fat tissue. It is not easy to identify the exact depth of the deep facial expression muscles via blind injection. Furthermore, a needle or cannula with enough length to reach these deep muscles should be used. Furthermore, 3D scanned images of the face are now widely used for the various diagnosis and surgical- or non-surgical evaluations before and after procedures

as well as the aesthetic facial analysis due to easy measurement and high accuracy. In-depth morphological studies of the human body have employed various diagnostic imaging devices. It is now possible for the obtained data to be displayed as three-dimensional (3D) images to facilitate the presentation of locational information in both research and clinical applications. Through my talk, I would like to introduce the US anatomical findings of the face to provide the reference images on each landmark of the face. And overall 3D facial structures (including facial skin, superficial / deep fat, muscle) using a structured-light scanner on the cadaveric faces before and after dissection will be demonstrated. In-depth morphological studies using two diagnostic systems can yield depth and orientation on the skin, fat compartments, facial muscles, blood vessels, and fascial structures of the facial area that were previously impossible to obtain. This provides crucial anatomical knowledge that can be utilized in various clinical applications such as the US-guided pathologic diagnosis and US-guided injections with safety and effectiveness.

* Correspondence to Hee-Jin Kim (E-mail: hjk776@yuhs.ac)

Young Anatomists Session

28th October, Sunday
14:30-17:30
Rm 325-326

Chairs: Ki Hwan Han (Korea)
          Kwon-Moo Park (Korea)
          Boon Huat Bay (Singapore)

YA-1

Anti-Depressant Like Effect Of Curcumin In Olfactory Bulbectomized Model Of Depression In Male Wistar Albino Rats: Antidepressant Behaviour Screening Tests

Shah S[1,*], Koirala B[2], Koirala S[1], Rouniyar GP[2]

[1]Department of Human Anatomy
[2]Department of Clinical Pharmacology & Therapeutics, BPKIHS, Dharan

Depression has become the most prevalent psychiatric disorder and imposes a substantial social burden. Curcumin possesses some interesting properties that justify its use in major depression. The olfactory bulbectomy (OB) in rodents results in a disruption of the limbic-hypothalamic axis with the consequence of behavioral, neurochemical, neuroendocrine and neuroimmune changes, of which many resemble changes seen in depressed patients. The main objective of the study is to investigate the antidepressant like effect of curcumin in olfactory bulbectomized model of depression of male wistar albino rats through behavior screening tests.Bilateral olfactory bulbectomy was performed with rats anesthetized under ketamine (50 mg/kg/i.p.).Twenty male albino wistar rats, weighing 150–220 gm were randomly allocated into four groups (n=5)- Group A (control), Group B(olfactory bulbectomy;OB), Group C (vehicle (0.9% NS, 10 ml/kg) +olfactory bulbectomy,OB) & Group D (curcumin (40 mg/kg)+ olfactory bulbectomy;OB). Immobility time (IT-s) in Forced swim test (FST),Tail suspension time (TST);Swimming time (SWT-s) and struggling time(ST-s) in FST; Sucrose Consumption and water Consumption and sucrose preference percentage in Sucrose preference test

(SFT) were screened. The data were expressed as mean±S.E.M generated. A oneway analysis of variance (ANOVA) was performed for multiple comparisons and post-hoc tests to identify subsequent pair-wise differences. A p<0.05 was considered statistically significant.All the variables were found to have statistically significant differences (p<0.05) between Group (A vs B) and Group (B vs D) but for Group (C vs D),TST(IT-s) was not significant (P=0.247) . Whereas, all variables were not statistically significant differences (p>0.05) between Group (B vs C) and Group (A vs D) except FST(IT-s) and FST(ST-s)(P=0.061).The results of the present study suggest that the curcumin has antidepressant like effect in olfactory bulbectomized-induced depression model in behavior screening tests.

Key Words: Curcumin, Olfactory, Bulbectomized, Model

*Correspondence to Sandip Shah (E-mail: Sandip.shah@bpkihs.edu, Tell: 9842025497)

YA-2

Calculation of Staheli's planter arch index, Chippaux-Smirak index, Clarke's angle and prevalence of flat feet among preclinical undergraduate students: a cross sectional study

Koirala S[1,*], Khanal GP[2], Shah S[1], Khanal L[1], Yadav P[1], Baral P[1]

Department of Human Anatomy, Department of Orthopedics, B.P. Koirala Institute of Health Sciences, Nepal

Introduction: Human foot is the region most affected by anatomical variations which presents a highest level of variability and the medial longitudinal arch and index provides a quantitative measurement of the plantar arch. Objectives: Objectives of the study was to calculate Staheli's planter index, Chippaux-Smirak index, Clarke's angle of feet and to classify the various arches of foot and identify the predictors for flat foot among preclinical undergraduate students. Materials & Methods: A non-interventional study was conducted among 300 preclinical undergraduate students. Ethical clearance was obtained from BPKIHS (IRC-0992-017). Students without any orthopedic surgeries, fractures over foot region were included. Staheli's planter arch index, Chippaux-Smirak index, Clarke's angle and truncated foot length was calculated using Foot Impression gaining kit with Ink Pad. Variables as age, sex, height, weight, navicular height, BMI were noted. Results: Staheli's, Chippaux-Smirak planter index, Clarke's angle on right side foot was found to be 60.98±23.24, 36.09 ±13.94, 32.74±7.8 and 63.85± 24.63, 36.64±14.62, 36.45±8.51 on left foot respectively. Significant difference was present in between BMI, navicular height and truncated foot length (p< 0.05). With respect to Staheli's planter index 3 % (n=9) had flat foot in right and 6.3 % (n=19) on left foot. Pearson's correlation in Staheli's index, Chippaux-Smirak index, normalized truncated foot length was found to be significant with BMI (p< 0.01).   A bivariate logistic regression model was created, which revealed BMI, mid foot length, truncated foot length a strong predictors (regression coefficient, R= 0.94, 0.78, 0.81, p<0.01), which were independently associated with flat foot to be detected by CSI and SPI. Linear Regression line derived from equation, *SPI (R) = y= mx+c; 1.592x CSI (R) + 4.553, (R=0.921, p= 0.003)*. Receiver Operating Curve (ROC) revealed *CSI index (AUC= 0.636, SEE- 0.034, p<0.01)* and *SPI   (AUC= 0.942, SEE-0.018, p<0.01)* was seen to be highly sensitive and specific. Conclusion: Most of student have medium to high medial longitudinal arch. Chippaux-Smirak index and staheli's planter index were sensitive for identification of flat foot.

Key Words: Staheli's index, Chippaux-Smirak index, Clarke's angle, Navicular height, Truncated foot length

YA-3

Learning style preferences among preclinical medical student enrolled in anatomy: an Institutional based study from BP Koirala Institute of Health sciences, Nepal

Khanal L[1], Giri J[2], Shah S[1], Koirala S[3], Rimal J[4]

[1]Associate professor, Department of Human Anatomy, BPKIHS, Dharan, Nepal
[2]Associate professor, Department of Orthodontics, BPKIHS, Dharan, Nepal
[3]Additional professor, Department of Human Anatomy, BPKIHS, Dharan, Nepal
[4]Professor, Department of Oral Medicine and Radiology, BPKIHS, Dharan, Nepal

Transition from under-graduate to first-year medical education can be difficult for students because of the dramatic increase in the volume of content. Student' motivation and performance improves when instruction is adapted to student learning preferences and styles. Present study was conducted to find the preferred mode of learning among first year preclinical students and to compare with age, gender, faculty of students and academic performance of the students using VARK inventory. Materials and methods: A cross sectional study was done among 142 first year students of MBBS and BDS from February to May 2018. Demographic data and various academic performance marks were recorded for each individual. VARK questionnaire (version 7.8) was administered to calculate the score of each component. Mean VARK score was calculated and each student was classified by preferred mode of learning. Preferred mode of learning was compared with gender, nationality, age group and academic performance using Chi Square test, unpaired t-test and Mann Whitney U test. P value less than 0.05 was taken as statistical significant for comparison. Results: Majority of the students (53.52%) were multimodal while unimodal preference was found in 46.48% of students. Most common multimodal mode of preference was bimodal (26.06%), while most common unimodal preference was kinesthetic (29.06%). Total V score, K score and VARK score was higher among males, while A score and R score was higher among females. The difference of total K score (7.96 ± 2.35 in male & 6.96 ± 2.43 in female) was statistically significant (p=0.019). More number of subject with the higher score in theory exam of anatomy were unimodal learner (53.8 %) as compared to multimodal learners (46.2 %). Conclusion: From this study, it could be concluded that our undergraduate students are diverse in their learning styles, but they were mostly multimodal. Though learning styles were found to be varied by gender, age, nationality, blood group and academic performance, the differences were statistically not significant.

Key Words: Medical education; Academic performance; VARK; Learning preference

YA-4

Visualizing and Manipulating Mouse/Human Brain for Metabolism Research

Hyung Jin Choi

Functional Neuroanatomy of Metabolism Regulation laboratory, Department of Anatomy, Neuroscience Research Institute, Department of Biomedical Sciences, Seoul National University College of Medicine, South Korea

Dream Experiment

2013 Nature Neuroscience, Targeting neurons and photons for optogenetics
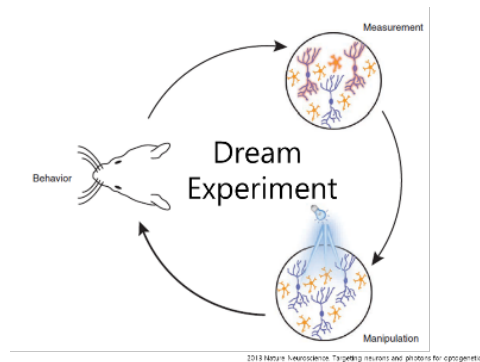
There are growing scientific interests regarding the role of brain on metabolism regulation. Modern rapid rise of obesity is mainly due to modern lifestyle and modern environment with overwhelming exposure to highly hedonic food cues. The cognitive response to these hedonic food cues and behavior consequences are the key pathogenic drivers of obesity. Recent researches have enlightened important insights into the neural circuits controlling energy balance and glucose homeostasis. By translating these neural circuits to clinical therapies, numerous approved drugs and devices are already in clinical use and many promising novel approaches are under development. The talk will cover diverse approaches for evaluating and manipulating the brain for metabolism research.

Neuroscience for Metabolic Disease
Basic–Clinical Translational Research
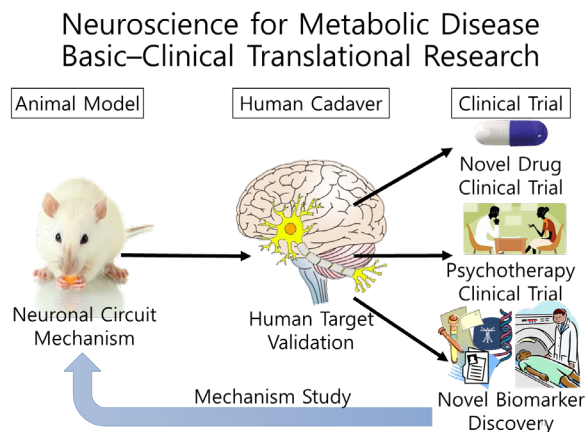
1. Visualizing Brain

1-1. Tissue Clearing 3D Imaging (Mouse/Human)

Tissue clearing and 3D imaging methods are novel techniques which enables three-dimensional visualization of immunostained tissue for the study of circuitry and spatial interactions between cells and molecules in the brain. Tissue clearing methods are widely used to investigate neuron distributions and neural circuits governing metabolism regulation and feeding behavior within hypothalamus and related areas.
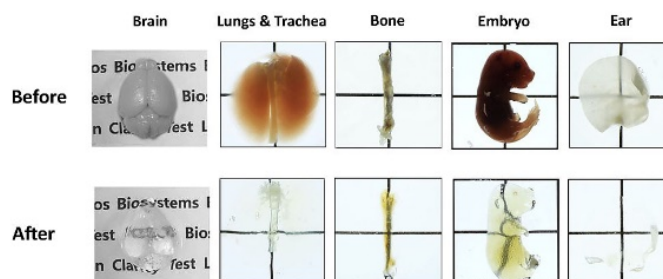

1-2. Miniature Microscope Neuron Calcium Imaging (Mouse)

A microscope lens implanted deep inside a mouse's brain can be used to investigate different patterns of neural activity. Miniature microscopes are used to investigate response pattern and neuron population diversity in live and moving animals. Recent studies identified interesting hypothalamus

neurons which rapidly respond to food related cues. These findings revolutionized the previous understandings on neural regulation of feeding behavior.

Live Neuron Activity - Ca²⁺ imaging

Genetically encoded calcium indicator
(ex. GCAMP, Pericams, Cameleons)
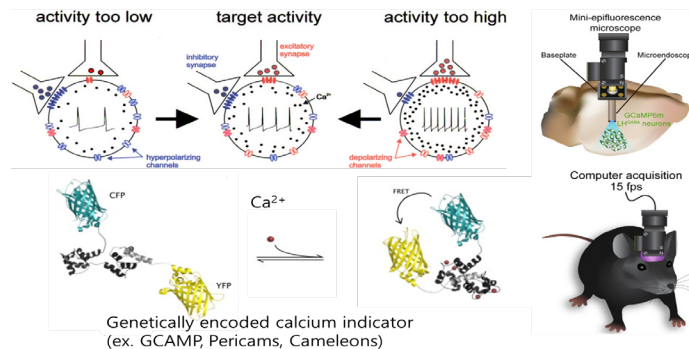
1.3 Functional MRI (Human)

Functional MRI identifies brain areas which show increased neural activity, as measured indirectly by detecting the change in cerebral blood flow associated with the increased energy demand of the activated neurons. By using visual cues related to food and other metabolic interventions, functional MRI can identify brain areas responsible for feeding behavior, food related addictive behavior, obesity and glucose metabolism.

2. Manipulating Brain

2-1. Optogenetics/Chemogenetics (Mouse)

Optogenetics uses light to control the activity of neurons which have been modified to express light-sensitive proteins. Chemogenetics uses chemically engineered receptors (DREADD, Designer Receptors Exclusively Activated by Designer Drugs) and exogenous molecules specific for those receptors, to affect the activity of those cells. Cell-type-specific, location-specific, projection-specific and context-specific neuronal manipulation has become possible by using optogenetics, chemogenetics, transgenic mice, stereotaxic viral injection, location specific light activation and context specific activation methods. These powerful tools unraveled numerous mysteries regarding neural circuits controlling metabolism and feeding behavior.

2016 Cell. Sensory Neurons that Detect Stretch and Nutrients in the Digestive System
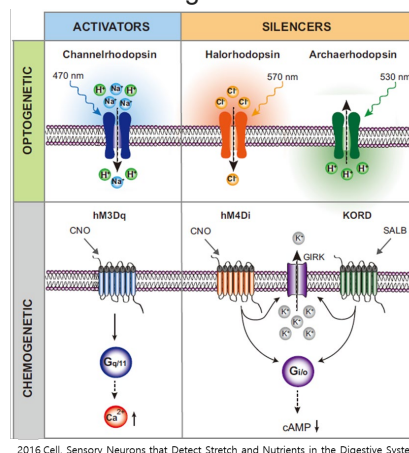
2-2. Neuromodulation (tDCS, vagal nerve modulation) (Human)

Transcranial direct current simulation (tDCS) is a non-invasive neuromodulation technique that allows external manipulation of the human brain in a safe manner, without the requirement of a neurosurgical procedure. Recent studies showed that tDCS can be used to treat obesity. Novel techniques (invasive and non-invasive) have been developed to stimulate or block vagus nerve. Vagal nerve manipulation has been approved by FDA to treat obesity.

2-3. Cognitive Behavior Therapy (Human)

Cognitive behavioral therapy (CBT) is a type of psychological therapy that focuses on the development

of personal coping strategies that target solving current problems and changing unhelpful patterns in cognitions (e.g. thoughts, beliefs, and attitudes), behaviors, and emotional regulation. The goal of obesity CBT is to lose weight in healthy and continuous way as well as to prevent from relapsing weight gains by changing patterns of thinking or behavior that are behind people's difficulties, and so change the way they feel.
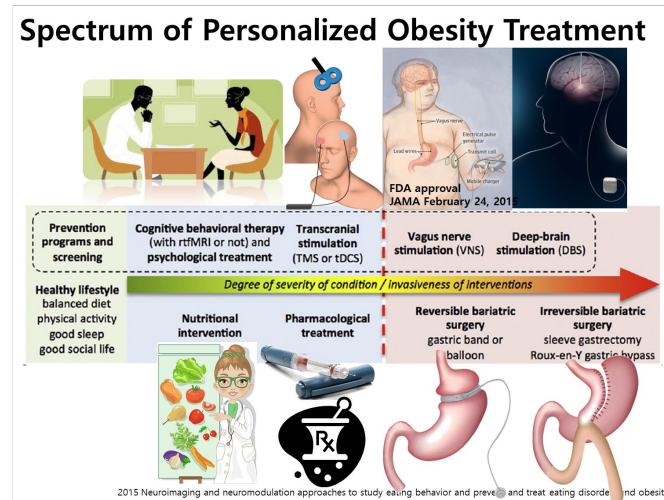
Key Words: Tissue Clearing, Calcium Imaging, Functional MRI, Optogenetics/Chemogenetics, Neuromodulation, Cognitive Behavior Therapy

YA-5

Differential role of parvalbumin-expressing interneurons in reward and action decision

Hyunjung Lee[1], Mootaek Roh[1], Hyunhyo Seo[2], Jihye Kwak[1,] Juhyun Lee[1], Dasom Kwon[1], <u>Kyungmin Lee</u>[1]

[1]Department of Anatomy, School of Medicine, Kyungpook National University, Daegu, South Korea

The orbitofrontal cortex (OFC) and striatum are important parts of a neural network related to reinforcement learning based on goal-directed action and reward-dependent decision making and corticostriatal circuit dynamics are considered to be crucial for value-based action selection. During reinforcement learning, shifting between exploring the alternative options for more information and exploiting the experience-based best opportunities with current information is a critical strategy for survival of animals in dynamic environmental variations. However, the specific neural types, neural activities, and neural circuits involved in exploration-exploitation trade-off have not yet been elucidated. In the present study, we examined which types of neurons in the corticostriatal circuits are involved in decision making for exploration-exploitation action and how reward-based choice is associated with exploitation behavioral decision in the freely behaving mice using dynamic foraging task. As a result, we found that Epac2, an exchange factor activated by cAMP and upstream of Ras activation, is highly involved in the enhancement of exploitation behaviors in a reward-based dynamic foraging task. In addition, we observed that in the corticostriatal circuits, striatal parvalbumin (PV)-positive fast spiking GABAergic interneurons were implicated in the neural responses to unexpected reward during explorative behaviors and choice execution, but PV-expressing interneurons of orbitofrontal cortex were involved in decision of exploratory and exploitive action. Taken together with all of data, PV-positive GABAergic interneurons have a differential role in reward and action decision neural signals

according to the cortical or subcortical neural circuitry.

Key Words: Orbitofrontal cortex, Striatum, GABAergic Interneurons, Exploration, Exploitation, Decision

YA-6

Visualization of intracellular dynamics of transcriptional coactivator reveals novel metabolic system for lactic acid

Takashi Tanida, Ken Ichi Matsuda, Masaki Tanaka

Department of Anatomy and Neurobiology, Graduate School of Medical Science, Kyoto Prefectural University of Medicine, Kyoto, Japan

Lactic acid is a product of glycolysis under hypoxic condition relating to intense exercise, ischemia, and other pathological status. Past studies have demonstrated cellular metabolic process of lactic acid and how this byproduct is effectively utilized to meet energy demand as an aerobic fuel. However, the process that how lactate regulates transcription to metabolize itself have not been fully explained. PGC-1α is a transcriptional coactivator serving as the master regulator for mitochondrial energy production. It drives aerobic gene expressions through the interaction with nuclear receptors including estrogen-related receptor (ERR). Recently, we identified a splicing variant of PGC-1α from rat hypothalamus and confirmed that this variant is a homolog of human and mouse PGC-1 variant form (PGCvf). Interestingly, PGCvf predominantly localizes within cytoplasm, and translocates into nucleus in response to lactic acid via heat shock cognate protein 70-relating mechanism. FRET microscopy revealed the direct interaction between PGCvf and ERRγ in the nucleus following lactic acid stimulation. Lactic acid upregulates ERRγ-mediated transcriptional activity when co-expressed with PGCvf. CRISPR/CAS9-induced knockout (KO) of PGC-1 gene in HepG2 hepatocarcinoma cells decreased the lactate consumption and it was rescued by the expression of PGCvf. Consistent with this finding, reduced mitochondrial membrane potential in PGC KO cells was increased by the expression of PGCvf. These results demonstrate the particular role of PGCvf as a major intermediator of lactic stress to metabolize lactic acid through the activation of mitochondrial respiratory capacity. Our findings further highlight the control of PGCvf-mediated transregulation may be one of the future therapeutic targets for lactic acidosis.

Key Words: PGCvf, ERRγ, lactic acid, nuclear translocation, FRET

YA-7

Optical control of neural activity in *C. elegans* by novel caged compounds

Hironori Takahashi

Dept Anat and Struct Biol, Grad Sch Med, Univ Yamanashi, Chuo, Japan

Optogenetics or caged compounds are useful tools to control neural activity by light stimulation in vitro and in vivo. Ultraviolet to blue light is needed to activate channelrhodopsins or caged compounds, while the short wavelength light evokes the innate photophobic response in *C. elegans* that disturbs accurate analysis of behavioural response. Recently, red-shifted variants of

channelrhodopsin have been developed that can be excited with orange to red light. However, it is difficult to use these opsin-based probes and other fluorescent probes such as green fluorescent Ca^{2+} sensor protein GCaMPs simultaneously because all opsins can be also activated with blue light. To overcome these problems, we developed a novel caged compound based on a fluorescent dye KFL-1 that can be activated with yellow light ($\square$ 580 nm) but not with blue light. Light activation of KFL-1-caged capsaicin induced Ca^{2+} response in ASH sensory neurons expressing capsaicin receptor TRPV1, which could be observed using green fluorescent Ca^{2+} probe GCaMP6s. In freely moving worms, uncaging of KFL-1-caged capsaicin could mimic aversive stimuli mediated by ASH sensory neurons resulting in reversal response. Our novel method to control neural activity by yellow light will allow all optical analysis of neural function and behaviour in vivo without inducing innate photophobic response.

Key Words: Caged compounds, *C. elegans*, Neural activity, ASH neuron, Photophobic response

YA-8

Three-dimensional digital measurement of anatomical parameters for thoracolumbar pedicle screw fixation in patients aged 13 to 14 years with adolescent idiopathic scoliosis

Xiaohe li[1] Baoke Su[1]Zhijun Li[2]Yangyang Xu[2]Huimei Feng[2]

[1,2]Department of Anatomy,Inner Mongolia medical University, Hohhot, China

Background: This study aims to measure anatomical parameters for thoracolumbar pedicle screw fixation by three-dimensional digital reconstruction in patients aged 13 to 14 years with adolescent idiopathic scoliosis (AIS) and compare them with those of normal control subjects, in order to provide support for surgical correction of AIS. **Material and Methods:** Based on CT data randomly collected from 85 patients diagnosed as AIS, 12 patients with Lenke 1 curves were included. All included patients were aged from 13 to 14 years and female. Moreover, CT data of thoracolumbar spine were randomly collected from 25 normal female volunteers in the same age group and used as control. CT data were imported into Mimics 16.01 for three-dimensional reconstruction. Pedicle width, lateral angle, anteroposterior and transverse diameters of the spinal canal, and screw path length were measured and compared between AIS and normal subjects. **Results:** In patients with AIS, the left pedicle width was greater than the right one from the 3rd to 5th thoracic vertebrae (T3 - T5), and the opposite was true for segments below T6. The pedicle width was less than 5 mm from T3 to T9. The right pedicle lateral angle was greater than the left one for T2 - T5, and the opposite was true for T6 - T9. The right pedicle lateral angle was greater than the left one for the 1st to 5th lumbar vertebrae (L1 - L5). The transverse foramen diameter first decreased, then increased, and peaked at L5; and only small changes were observed from T2 to T11, with the average diameter being between 16.89 and 18.41 mm. The anteroposterior foramen diameter generally increased from T1 to L5, and peaked at T12 and L1, with the average diameter being between 14 and 17 mm. Moreover, it was greater in the right pedicle than in the left for T5, T6, and T8, and the opposite was true for T9 - L1 and L3 - L5. There were significant differences in pedicle width and lateral angle of each segment between AIS and normal subjects. The transverse foramen diameter was greater in AIS than in normal subjects for T5, T6, and T8 - L5; and the anteroposterior diameter was significantly greater in AIS than in normal subjects for all segments, except T4, T5, and T8. The screw path was longer in normal subjects than in AIS in all segments, except T1 - T3 and T6. **Conclusion:** In patients with AIS, the concave pedicle width was smaller than the convex one, and smaller than the pedicle width of normal spine. The convex lateral angle was smaller than the concave one. The spinal canal volume and the distance between

the left and right pedicle screws were larger in AIS than in normal subjects.

Key Words: Idiopathic Scoliosis, Thoracolumbar, Digital, Anatomical, Adolescent

YA-9

Effect of tamoxifen a Selective Estrogen Receptor Modulator (SERM) on Cardiac Myocyte of Rat Model of Surgically Induced Estrogen Depleted State

Suresh[1], Ritu Sehgal[2], Raj D Mehra[3], Pushpa Dhar[2]

[1]Health and social sciences cluster, Singapore Institute of Technology, Singapore
[2]Department of Anatomy, All India Institute of Medical Sciences, New Delhi, India
[3]Department of Anatomy, Hamdard Institute of Medical Sciences and Research, New Delhi, India

Introduction: Cardiovascular diseases (CVD) including cardiac hypertrophy, cardiac failure and coronary artery disease are the leading causes of morbidity and mortality in both men and women, although female sex has long considered to be a "protective factor" against CVD. This study evaluated the effect of Selective estrogen receptor modulator (SERM) Tamoxifen (TAM) therapy on myocardium for therapeutic effectiveness in estrogen-depleted states induced by ovariectomy (OVX). **Methods:** We divided the rats into four groups: (I) Sham operated (II) ovariectomized controls without any treatment, (III) ovariectomized rats treated with vehicle sesame oil (IV) ovariectomized rats treated with tamoxifen 1mg/kg, s.c. daily for 60 days. Rats were sacrificed by transcardial perfusion. Different chambers of the heart sections were analyzed by image analysis software after hematoxylin and eosin staining. **Results:** This study reported that an increase in heart weight, cardiac wall thickness and myocytes diameter in response to estrogen depletion that can be effectively reversed by tamoxifen treatment. **Conclusion:** This research revealed that the tamoxifen treatment is the novel strategy to alleviate the post-menopausal problems and prevent the heart failure due to cardiac hypertrophy without the adverse effect of estrogen. This research open a window to develop a cardio selective SERM`s which can be a used in both genders. The further studies are needed to find the molecular mechanisms of tamoxifen over the hypo estrogenic cardiac myocytes.

Key Words: Selective estrogen receptor modulator, tamoxifen, Ovariectomy, Myocyte diameter, Cardiac hypertrophy

Symposium Session

Session 1: Gross Anatomy	Rm 321-322	09:00-10:40 29th October, Monday
Session 2: Brain & Neuroscience (I)	Rm 323-324	
Session 3: Stem Cell & Development	Rm 325-326	
Session 4: Physical Anthropology	Rm 321-322	13:30-15:10 29th October, Monday
Session 5: Immunology	Rm 323-324	
Session 6: Cell Biology (I)	Rm 325-326	
Session 7: Oncology	Rm 321-322	15:30-17:10 29th October, Monday
Session 8: Brain & Neuroscience (II)	Rm 323-324	
Session 9: Cryo-EM Technology	Rm 321-322	09:00-10:40 30th October, Tuesday
Session 10: Anatomy Education (I)	Rm 323-324	
Session 11: Modern Tech in Microscopy	Rm 321-322	13:30-10:40 30th October, Tuesday
Session 12: Anatomy Education (II)	Rm 323-324	

Session 1: Gross Anatomy
-Organized with CAA-

Chairs: Min Suk Chung (Korea)
          Shinich Abe (Japan)

09:00-09:25   Morphological changes about the TMJ and joints of the larynx in the elderly
Shinichi Abe (Tokyo Dental College, Japan)

09:25-09:50   Anatomical features of the incisivus labii superioris and incisivus labii inferioris
Mi-Sun Hur (Catholic Kwandong University, Korea)

09:50-10:15   Development of the fetal brain: assemeement with postmortem 7.0T MRI
Shuwei Liu (Shandong University, China)

10:15-10:40   Application of the sectioned images of cadavers, Visible Korean
Min Suk Chung (Ajou University, Korea)

S1-1

Morphological changes about the TMJ and joints of the larynx in the elderly

Shinichi Abe

Department of Anatomy, Tokyo Dental College, Tokyo, Japan

The morphology of the temporomandibular joint includes a surface formed from evolution and development and a secondary element formed adaptively to the subsequent change in function. As factors influencing the temporomandibular joints, various things can be considered, such as differences in functional strength depending on age and sex, presence or absence of teeth and change in food quality. Therefore, in this presentation, I will explain not only the basic form of temporomandibular joint but also the morphological change accompanying growth, and especially the change occurring after tooth loss. In addition, I will add commentary on aging changes in elderly larynx.

Key Words: Articular disk, TMJ, Lateral pterygoid muscle

S1-2

Anatomical features of the incisivus labii superioris and incisivus labii inferioris

Mi-Sun Hur

Department of Anatomy, Catholic Kwandong University College of Medicine/ Gangneung, Korea

The aim of this study was to clarify the morphological patterns of the incisivus labii superioris muscle (ILS) and incisivus labii inferioris muscle (ILI) and their relationships with the surrounding structures. ILSs and ILSs were investigated in 52 specimens from embalmed Korean adult cadavers. ILSs were observed in all specimens (52/52 specimens, 100%). The ILS has an oblique and linear origin from the incisive fossa of the maxilla to the point just medial to the origin of the levator anguli oris muscle (LAO). The arising fibers of the ILS arched and covered the prominent labial glands at the superior margin of the orbicularis oris muscle (OOr). After the ILS coursed laterally along the anterior part of the upper mucolabial fold, it divided into superficial and deep inserting fibers in 92.3% (48/52 specimens) and it did not divide in 7.7% (4/52 specimens). The superficial inserting ILS fibers and the ILS fibers that did not divide blended with the medial fibers of the LAO to converge toward the modiolus. The deep inserting fibers of the ILS blended with the lateral deep fibers of the OOr in the 92.3% (48/52 specimens), and the deep inserting fibers continued to descend to converge toward the modiolus in 38.5% (20/52 specimens). ILIs were observed in all specimens (100%). The originating muscle fibers of the ILI were intermingled with the upper lateral mentalis (MT) in all specimens (40/40 specimens, 100%). Some of the ILI fibers extended inferomedially to the middle or lower portion of the MT in 55% (22/40 specimens). The ILI muscle fibers that extended to the MT, the amount of which varied between specimens, were intermingled medially with the MT and were connected laterally to the insertions of the ILI. The medial fibers of depressor anguli oris muscle that pass deep to the depressor labii inferioris muscle (DLI) were connected to the ILI in 42.5% (17/40 specimens). The inferior bundle of the ILI was divided from the originating fibers of the ILI, and it was present in all specimens (50/50 specimens, 100%). The inferior bundle of the ILI could be distinguished into the transverse and inferolateral slips according to their courses and locations. The transverse and inferolateral slips were usually attached to the deep fibers of both the platysma lateral to the DLI and

the lateral portion of the DLI via aponeurosis, just below the ILI and above the inferior margin of the mandible, respectively. The new anatomical findings of the present study might contribute to the understanding of the detailed movements of the mouth and lips. This knowledge will be useful for botulinum toxin type A therapies, various facial surgeries, orthodontic treatment, and electromyographic analyses in this area.

Key Words: Incisivus labii superioris muscle, Incisivus labii inferioris muscle, Inferior bundle

S1-3

Development of the fetal brain: assessment with postmortem 7.0T MRI

Shuwei Liu, Zhonghe Zhang, Jinfeng Zhan, Qiaowen Yu, Xinting Ge, Limei Song

Department of Anatomy, Histology, and Embryology, Shandong University Cheeloo Medical College, Jinan, China

During the second trimester, the human fetal brain undergoes numerous changes that may lead to substantial variation in the neonatal and maturing brain in terms of its morphology and tissue types. As fetal MRI is more and more widely used for studying the human brain development during this period, a spatiotemporal atlas becomes necessary for characterizing the dynamic structural changes. Our purpose was to document the sulcal development and obtain quantitative measurements of the fetal brain in the second trimester. In this study, 69 postmortem human fetal brains with gestational ages ranging from 15 to 22 weeks were scanned using 7.0 T MR. We used automated morphometrics, tensor-based morphometry and surface modeling techniques to analyze the data. Then the sequential development of the different fissures and sulci was analyzed, and quantitative measurements of the cerebral cortex were obtained. A spatiotemporal atlase covering the whole period was set up. A new chronology of sulcal development during 12–22 weeks GA was summarized. Most sulci, except for the postcentral sulcus and intraparietal sulcus, were present by 22 weeks GA. Measurements of the fetal brains, each with different growth rates, linearly increased with GA, but no sexual dimorphisms or cerebral asymmetries were detected. A spatiotemporal atlases of each week and the overall atlas covering the whole period with high resolution and contrast were created. These atlases were used for the analysis of age-specific shape changes during this period, including development of the cerebral wall, lateral ventricles, Sylvian fissure, growth direction based on local surface measurements. Our findings indicate that growth of subplate zone is especially striking and is the main cause for the lamination pattern changes. Changes in the cortex around Sylvian fissure demonstrate that cortical growth may be one of mechanisms for gyration. Surface deformation mapping, revealed by local shape analysis, indicates that there is global anterior-posterior growth pattern, with frontal and temporal lobes developing relatively quickly during this period. Our results are valuable for understanding the normal brain development trajectories and anatomical characteristics. These week-by-week fetal brain atlases can be used as reference in in vivo studies, and may facilitate the quantification of fetal brain development across space and time.

Key Words: Fetal MRI, Second-trimester, Atlas, human Brain development

S1-4

Applications of the sectioned images of cadavers, Visible Korean

Min Suk Chung[1], Beom Sun Chung[1], Jin Seo Park[2]

[1]Department of Anatomy, Ajou University School of Medicine, Suwon, Republic of Korea
[2]Department of Anatomy, Dongguk University College of Medicine, Gyeongju, Republic of Korea

The objective of this report is to announce the serially sectioned images, segmented images, three-dimensional images from the Visible Korean (VK), which can be applied to medical education and clinical training. For the VK, a male cadaver was serially sectioned to acquire the sectioned images of whole body. Thereafter, more than 700 structures in the sectioned images were outlined to produce detailed segmented images; the sectioned images and segmented images were volume- and surface-reconstructed to make three-dimensional images. For outlining and reconstruction, we usually did not compose program but just used popular software; the technique is reproducible by other investigators to make their own images. The continuously upgraded technique was applied to another male cadaver's head, a female cadaver's whole body, and another female cadaver's pelvis to produce other series of images. The products of the Visible Korean for learning sectional anatomy and stereoscopic anatomy can be downloaded from the homepage (anatomy.co.kr) free of charge. The VK data, worldwide distributed, have encouraged researchers to develop the virtual dissection, virtual endoscopy, and virtual lumbar puncture.

Key Words: Visible Human Projects, Cross-sectional anatomy, Three-dimensional imaging, User-computer interface

Session 2: Brain & Neuroscience (I)

Chairs: Jong Eun Lee (Korea)
         Woong Sun (Korea)

09:00-09:25   Visualization of neuronal circuit-based biomarkers in the neuronal degeneration diseases
Youngshik Choi (Korea Brain Resesrch Institute, Korea)

09:25-09:50   The cellular anatomy and connectivity of the cerebellar molecular layer: reconstruction and analysis of serial electron microscope images
Jinseop S. Kim (Korea Brain Resesrch Institute, Korea)

09:50-10:15   Anteroposterior gradient of the adhesion and migration properties of neural stem cells in developing spinal cord
Woong Sun (Korea University, Korea)

10:15-10:40   Neural crest cell in secondary neurulation
Yoshiko Akahashi (Kyoto University, Japan)

S2-1

Visualization of neuronal circuit-based biomarkers in the neuronal degeneration diseases

Youngshik Choe

Department of Neural Development and Disease, Korea Brain Research Institute, Daegu, South Korea

Amyloid-containing protein plaques have been the hallmark of the demented aging brains and the spreading of the amyloid proteins has long been studied in the degenerating brain. We utilized brain clearing and three dimensional visualization of the degenerating mouse brains to narrow down the origin of amyloid plaques from the neuronal compartments. Unexpectedly we found that the axonal compartments were mostly degenerating in the mouse model of Alzheimer's disease. In the early stage of Alzheimer's disease, the cortical tissues had increased expression of vesicular markers and extracellular amyloid proteins were observed in the brain vesicles thus we hypothesized this resulted from the defects in axonal transports of vesicles. While the disease worsens, the amyloid plaque forms along the axonal projection and the axonal terminus are engaged in the amyloid plaques in the mouse model of Alzheimer's disease. To examine the contribution of axonal secretory vesicles for the extracellular and axonal accumulation of amyloid proteins, vesicular fractions were analyzed using the cortices of the Alzheimer's mouse model. The proteomic analysis revealed that beta-amyloid vesicles also contained proteins involved in protein trafficking such as intraflagellar transport 88 (Ift88). Closer examination of the axonal bundles in the mouse model of the Alzheimer's disease showed that the hippocampal axonal endings were mostly compromised. In addition, the fluorescent labeling of cortico-cortical connections also showed that the cortical axonal endings were the vulnerable compartment forming amyloid plaques. Mis-regulation of the neuronal Ift88, a novel amyloid protein interacting molecule in the extracellular vesicles, accelerated amyloid accumulation along the neuronal axons. These results suggest that the aberrant axonal transport of vesicular proteins is the physiological biomark for the amyloid plaque formation along the neurites and accumulation of amyloid proteins may imply neural circuit functions in the aged brain.

Key Words: CLARITY, Biomarkers, Alzheimer's disease. Exosome, Proteomics

S2-2

The Cellular Anatomy and Connectivity of Cerebellar Molecular Layer: Reconstruction and Analysis of Serial Electron Microscope Images

Jinseop S. Kim

Department of Structure & Function of Neural Networks, Korea Brain Research Institute, Daegu, Korea

The connectomic analysis of 3D electron microscope images provides the subcellular-resolution morphology of individual cells and the entire connectivity of neural circuits at the same time. While the reconstruction of neurons from the image data is the essential first step, further analyses are also crucial to understand such anatomical features. Here we present the quantitative anatomical properties of cerebellar Purkinje cells in a mouse using computational methods. First, we find the skeleton of the volumetric reconstruction of the cells which contains various information for arborization pattern of the neural processes. Second, we identify individual dendritic spines and separate them from the dendritic branchlets. Combining these, we calculate the dendritic path length and spine distribution of Purkinje cells. We also develop an automated synapse detection method to

find the subcellular wiring specificity between the cells in the cerebellar molecular layer.

Key Words: 3D SEM, Computational analysis, Cerebellum, Purkinje cell, Cellular anatomy

S2-3

Anteroposterior gradient of the adhesion and migration properties of neural stem cells in developing spinal cord

Mohammed R.Shaker, <u>Woong Sun</u>

Department of Anatomy, Brain Korea 21 Plus Program, Korea University College of Medicine, Seoul, 02841, Korea

During the development, mammalian embryos exhibit a transition from head morphogenesis to trunk elongation to meet the demand of axial elongation. Caudal neural tube (NT) is formed with neural stem cells (NSCs) derived from neuromesodermal progenitors (NMPs) localized at the tail tip. However, the molecular and cellular basis of elongating NT morphogenesis is poorly understood. Here, we discovered that cell-cell adhesion properties of NSCs are strongest among the caudal NSCs and decrease gradually along the anteroposterior (AP) axis in the mouse embryo. Strong cell-cell adhesion of caudal NCSs causes collective migration, while rostral NSCs exhibit amoeboid-type migration. These transition of cell migration mode along with the AP axis is also controlled by the local morphogens, Wnt and retinoic acid (RA). Furthermore, RNA-seq analysis uncovered the enrichment of extracellular matrix (ECM) gene expressions in caudal NSCs, and we found that the perturbation of the expression level of them determines the properties of NSC adhesion and migration. Together, these results suggest that progressive reduction of NSCs' adhesion affinity along the AP axis is under the control of Wnt/RA-ECM molecular networks.

Key Words: Neuromesoderm, Neural Stem Cells, Wnt, Extracellular Matrix

S2-4

## Secondary neurulation during tail development

Yoshiko Takahashi

Department of Zoology, Kyoto University, Kyoto, Japan

All the vertebrates possess a tail at their bodies' posterior extremity. The tail allows a variety of diversities, and in many cases tails are specified to particular purposes of habitation (e. g. long vs short tails, decorative appealing for reproductive tactics, etc.). During embryogenesis, the tail forms posteriorly to the hind limb and anus level, and consists of two major components: the ectoderm (nervous system) and mesoderm (muscles and bones). For the tail to form, the tail bud, a mass of mesenchymal cells, plays critical roles. In particular, the tail bud cells that participate in the neural tube formation undergo EMT and MET, and this process is called secondary neurulation (SN), which is completely different from the well-known neural plate folding type of neurulation (primary neurulation) seen in the anterior body. Using chickens as a model animal, we have recently identified the presumptive SN region located posteriorly to Hensen's node in stage 8 chicken embryo (equivalent to

~E8 mouse embryo). Importantly, this region does not contribute to the mesodermal components. Thus, neural tube-forming cells and mesodermal cells are segregated early in the tail-forming region. We have also found that SN-precursors in the tail bud behave as stem cell-like cells, where Sox 2 expression should be maintained at a low level. We will discuss the roles of SN in the tail formation, physiology, and evo-devo.

Key Words: Secondary neurulation, Tail, EMT, MET, Sox 2

Primary- and Secondary Neurulation

Hind limb bud-level

Primary Neurulation (PN)

Secondary Neurulation (SN)
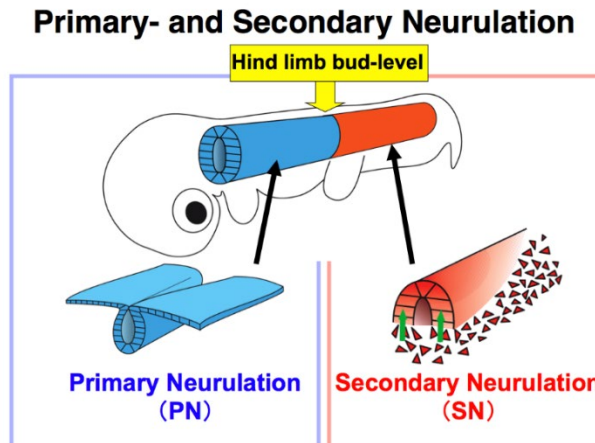
Session 3: Stem Cell & Development

Chairs: Jin Woong Bok (Korea)
          Haeyoung Suh-Kim (Korea)

09:00-09:25   Modeling of spatiotemporal anatomy in neural crest development to study peripheral neuropathies with stem cell technologies.
Yong Joon Kim (Kyunghee University, Korea)

09:25-09:50   A potential therapy of chronic stroke using genetically modified mesenchymal stem cells
Haeyoung Suh-Kim (Ajou University, Korea)

09:50-10:15   A farewell to flat biology: a three-dimensional organoid culture to address the missing link in cellular research
Sik Yoon (Pusan National Univeristy, Korea)

10:15-10:40   Comparative proteomic analysis of fetal and adult tissues
Min-Sik Kim (Kyunghee University, Korea)

S3-1

Modeling of spatiotemporal anatomy in neural crest development to study peripheral neuropathies

Yong Jun Kim

Department of Pathology, College of Medicine, Seoul, Korea

Neural crest stem cell (NCSC) is a 'spatiotemporal' population appeared during gastrulation period. It is well known for migration ability to target various tissues where it generates differentiated cell types such as neurons, glia and pigmented cells. Since NCSC is present in early stage of embryogenesis, it is limited to study pathophysiology of related human disorders. Recent studies have reported that human NSCS can be achieved by using advanced stem cell technologies followed by disease modeling studies with NCSC derivatives. However, cellular and molecular mechanism of NCSC biology are still largely unknown due to difficulties of understanding its biological stage since NCSC is developed through comparably long migration track with various environmental stimulations which known as 'spatiotemporal' to manipulate the cellular fate. Here, our results show that newly developed strategy of NCSC differentiation model a spatiotemporal differentiation of NCSC. Our stage specific NCSC modeled early developmental process of peripheral nervous system, and it shows cellular and molecular phenotypes of NCSC before/after physiologic epithelial-to-mesenchymal transition (EMT), for example, boarder stage early NC has internal property of fate decision for cranial and/or somatic transition during anterior-posterior embryonic elongation in a dish. Our strategy suggest that space and time sensitive NCSC specification can be applied to local peripheral disorders in near future as an innovative tool for modeling and investigating pathological mechanism.

Key Words: Stem cell, Neural crest, Peripheral nervous system

S3-2

A potential therapy of chronic stroke using genetically modified mesenchymal stem cells

Haeyoung Suh-Kim

Department of Anatomy, Ajou University School of Medicine, Suwon, South Korea

Stroke is a dominant cause of sensorimotor disability. Due to a limited or partial spontaneous functional recovery, stroke survivors often suffer from sensory-motor dysfunctions and various degrees of paralysis for several subsequent years.

Mesenchymal stem cells (MSCs) have been shown to ameliorate a variety of neurological dysfunctions. This effect is believed to be mediated by their paracrine functions, since these cells rarely differentiate into neuronal cells. In this talk, I will show that neural induction of MSCs is beneficial for the replacement therapy of neurological diseases. Here we report that expression of Neurogenin1 (Ngn1), a proneural gene that directs neuronal differentiation of progenitor cells during development, is sufficient to convert the mesodermal cell fate of MSCs into a neuronal one. Ngn1-expressing MSCs expressed neuron-specific proteins, including voltage-gated Ca^{2+} and Na^+ channels that were absent in parental MSCs. Most importantly, transplantation of Ngn1-expressing MSCs in the animal stroke

model dramatically improved motor functions compared with the parental MSCs via several ways involving immunomodulation and neuroprotection. However, neural induction of MSCs is not sufficient to reconstruct the neural circuit in the ischemic brain of the chronic phase. We genetically modified MSCs to express several additional genes and transplanted in the chronic stroke brain. Transplantation at one month after the ischemic injury of genetically modified MSCs significantly improved the behavioral and histological deficits when assessed with sensory-motor function tests and MRI. Our genetically modified MSCs satisfied the Stem cell Therapies as an Emerging Paradigm in Stroke (STEP3) guidelines which were suggested for preclinical studies by FDA and NIH (2014) and might provide a potential therapeutic strategy for the treatment of chronic stroke.

Key Words: Ischemic stroke, Mesenchymal stem cells, Neural induction, Transplantation

S3-3

A farewell to flat biology: a three-dimensional organoid culture to address the missing link in cellular research

Sik Yoon

Department of Anatomy, Pusan National University School of Medicine, Yangsan, Gyeongsangnam-do 626-870, Republic of Korea

Cell culture is an indispensable tool and one of the most widely used techniques in a diverse range of basic and clinical *in vitro* biomedical research. Two-dimensional (2D) monolayer cell culture has been the classically preferred method, due to the ease with which cell monolayers can be induced to proliferate on planar surfaces. However, limitations of 2D cell culture such as lack of natural tissue-like structural organization, inability to depict traits exhibited by *in vivo* systems (e.g., altered gene and protein expression), decreased compatibility with *in vivo* systems, increased drug sensitivity and exposed surface hamper its use in both clinical and fundamental investigations. Today, three-dimensional (3D) cell culture is emerging not only as a new tool in biomedical research and early drug discovery, but also as potential therapeutics to treat disease. Since current *in vitro* drug testing models based on 2D cell culture result in disappointing clinical outcomes, the development of efficient research models using 3D cell culture is becoming increasingly important and necessitated. We have fabricated a calcium-free, physically crosslinked, efficient, and bioactive hydrogel for use in 3D cell cultures. Using this technique, we have established an *in vitro* 3D tumor model capable of providing close predictions of *in vivo* drug efficacy. Our tumor model will contribute to enhance our understanding, design, and development of better antitumor therapeutic strategies. Taken together, our hydrogel system could provide an efficient platform for the development of customizable, transparent, biocompatible, functional, easy-to-produce, and cost-effective scaffolds for use in 3D cultures of various cell types, and our 3D tumor model is a promising *in vitro* research platform for studying tumor biology and therapeutic approaches.

Key Words: 3D Cell Culture, Hydrogel, Scaffold, Spheroid, Tumor Model

S3-4

Min-Sik Kim

Session 4: Physical Anthropology

Chairs: Dong Hoon Shin (Korea)
             Myeung Ju Kim (Korea)

13:30-13:55   mtDNA haplo group prediction tool for fragmented DNA samples
                    Kyung Yong Kim (Chung-Ang Uversity, Korea)

13:55-14:15   Caries, antemortem tooth loss and tooth wear observed in indigenous peoples and Russian settlers of 16th to 19th century West Siberia
                    Hye Jin Lee (Seoul National University, Korea)

14:15-14:30   Parasite aDNA of Korean mummies
                    Jong Ha Hong (Seoul National University, Korea)

14:30-14:45   Famine and Stress Markers, with a Focus on Enamel Hypoplasia
                    Shiori Fujisawa (Aomori Chuo Gakuin University, Japan)

14:45-15:10   Arctic mummiesin Salekhard
                    Dong Hoon Shin (Seoul National University, Korea)

S4-1

mtDNA haplogroup in ancient human DNA samples

<u>Kim Kyung Yong</u>[1], Kim Kijeong[2], Hahn Seungho[1], Chung Yoonhi[1]

[1]Department of Anatomy, Chung-Ang University, Seoul, South Korea
[2]Department of Microbiology, Chung-Ang University, Seoul, South Korea

       The study of ancient human DNAs with mummies or skeletons from archeological remains has become a great opportunity for molecular biologists, anthropologist, historians, and forensic scientists. Besides DNA, the proteins, chemiclas, and other substances such minerals and isotopes present great information about the past history of ancient human beings. The ancient DNAs present information about the individual, and the parental, maternal, and biparental genetic relationships of the individual. However, DNA analysis of degraded or ancient samples suffers from reduced reproducibility due to DNA degradation, contamination with other DNA, and the presence of PCR inhibitors. A stringent guidelines with self-critical approach are essential for the DNA of authentication. We have investigated on ancient human DNAs and analyzed relationship and formation of peoples between Asia and Korea through regional and historical aspects. We have built a database of haplogroups and haplotypes of mitochondria and Y chromosome including paternal database of Y-SNP and individual database of autosomal STR. We present several solution for the problems which must be solved for the ancient human DNA Study.

Key Words: Ancient, Human DNA, Skeleton, Haplogroup. mtDNA, Y-SNP

S4-2

Caries, antemortem tooth loss and tooth wear observed in indigenous peoples and Russian settlers of 16th to 19th century West Siberia

Hyejin Lee[1,2], Jong Ha Hong[1], Yeonwoo Hong[3], Dong Hoon Shin[1,*] , Sergey Slepchenko[4,*]

[1]Bioanthropology and Paleopathology Lab, Department of Anatomy and Cell Biology, Institute of Forensic Science, Seoul National University College of Medicine, Seoul 03080, South Korea
[2]Ministry of National Defense Agency of KIA Recovery & Identification, Seoul 06984, South Korea
[3]Department of Cultural Heritage Conservation Science, Kongju National University, Kongju 32588, South Korea
[4]Tyumen Scientific Center of the Siberian Branch of the Russian Academy of Sciences, Tyumen, Russia

There are many previous studies where higher prevalence of dental caries is associated with the shift from hunter-gatherer subsistence to agriculture. We corroborated this conjecture by means of a study on caries prevalence among 16th to 19th century hunter-gatherers and agriculturalists who co-existed in West Siberia. Indigenous people's skeletons (n = 75) exhumed from Tatar, Selkup, Khant, and Nenet graves were examined. Russian settler skeletons (n = 79) from Izyuk were also examined. The prevalences of caries and antemortem tooth loss (AMTL), tooth wear were compared between indigenous peoples and Russian settlers. The resulting statistical inferences were tested using package R. The agriculturalist Russian settlers showed a significantly higher prevalence of dental caries (11.88%) than did the non-agriculturalist indigenous Siberian people (3.85%). Among the latter, the prevalence was the lowest in the Khanty and the highest in the Tatars, suggesting that caries differently affected each sub-group of indigenous Siberian people. Correspondingly to the case of dental caries, the Russian settlers' AMTL prevalence was also higher than that of the indigenous Siberians, regardless of age. In a study on 16th to 19th century West Siberian populations, we were able to corroborate our presumption that agriculturalists ingesting a carbohydrate-rich diet would have higher rates of dental caries and AMTL than would hunter-gatherers.

Key Words: West Siberia, Russian settler, native Siberian, Dental caries; Dental wear; Antemortem tooth loss

S4-3

Parasite aDNA of Korean mummies

Jong Ha Hong[1], Min Seo[3], Chang Seok Oh[1,2], Dong Hoon Shin[1,2,*]

[1]Laboratory of Bioanthropology, Paleopathology and History of Diseases, Department of Anatomy, Seoul National University College of Medicine, Seoul, South Korea
[2]Institute of Forensic Science, Seoul National University College of Medicine, Seoul, South Korea
[3]Department of Parasitology, Dankook University College of Medicine, Cheonan, South Korea

The parasitological information obtained from archaeological specimens can propose speculation about the parasite-infection patterns that prevailed in ancient societies. In archaeooparasitology, which is the study of ancient parasite species, parasite egg remnants in archaeological samples are examined by microscopic or molecular analysis. Although attempts have been made by archaeoparasitologists to detect ancient parasites in samples collected at the excavation site, as for genetic information on ancient parasite species, not many studies are currently available. Multiple parasite genes from multiple ancient feces or precipitates samples obtained from as many archaeological sites as possible were still needed for more advanced analyses. Fortunately, over the past several years in South Korea, our paleoparasitological studies reported on ancient parasites in Korean mummies discovered in 15th- to 18th-century Joseon graves. Briefly, by microscopic examination, we found the ancient parasite eggs of *Ascaris*, *Trichuris*, *Clonorchis*, *Paragonimus*, and *Metagonimus* in the Joseon mummy feces. Utilizing these samples in the present study, we tried to analyze DNA sequences of multiple ancient parasites to understanding their genetic characteristics. After multiple each parasite genes (*Ascaris*: Cytochrome b, Cytochrome c oxidase subunit 1 (COX1), NADH dehydrogenase subunit 1 (NAD1), Internal transcribed spacer 1 (ITS1); *Trichuris*: 18S rRNA, ITS2; *Clonorchis*: COX1, ITS1; *Paragonimus*: COX1, ITS2; *Metagonimus*: 28S rRNA, COX1) in ancient samples were successfully amplified by PCR, consensus sequences determined by the alignment of the sequences of cloned PCR products. The obtained sequences of each parasite gene were highly similar to those of each *Ascaris*, *Trichuris*, *Clonorchis*, *Paragonimus*, and *Metagonimus* spp. reported thus far, but were genetically distinct from other parasite species. This study shows the genetic characteristics of ancient parasites in Joseon period of Korea by comparison with those of modern parasites sequences worldwide. To improve the knowledge about parasites evolution in much detail, multiple parasites gene sequences must be obtained from the regions of much wider geo-historical scope in forthcoming studies.

Key Words: Ancient DNA, Parasite, Mummy, Phylogenetic analysis, Multi-ple parasite gene.

S4-4

Famine and Stress Markers, with a Focus on Enamel Hypoplasia

Shiori Fujisawa

Faculty of Nursing, Aomori Chuo Gakuin University, Aomori, Japan

"Enamel hypoplasia" refers to hypoplasia occurring in the enamel of tooth crowns during their processes of growth. The period of growth for the crowns of permanent teeth is from age 0 to age 6 (for third molars it is from age 9 to 12), and if enamel hypoplasia occurs during this period, the tooth crowns will not be healed or recover even during subsequent growth. Although there are several different possible causes of enamel hypoplasia, regardless of its origin this condition has been shown by epidemiological research to be able to serve as a scale for effectively measuring the health of people in a specific group. By making detailed observations of this abnormality as a stress marker, research is being performed on its rate of occurrence depending on differences in livelihood, such as between hunting/gathering and farming, and depending on differences in social classes, as well as on the trends of weaning periods according to the group-wide ages of people in which it has appeared and the eras of its appearance. In this research project, out of 67 human skeletal remains from the

early modern age, excavated from 4 archaeological sites in Aomori prefecture located at the northern tip of Japan's Honshu island, observation studies were performed on 40 bodies with the crowns of their permanent teeth still intact. The results showed that if only the appearance of enamel hypoplasia was considered while disregarding its severity, it was found in nearly 70% of the examined remains. This is a level far higher than in any other group of human remains from any time period or region in Japan, and is a rate of appearance comparable to those seen in severely malnourished population groups located in present-day developing countries. The location of the study is known to have had a particularly harsh environment among Japan's regional farming areas, with records of a great many villagers starving to death during famines caused by poor harvests which occurred frequently during the early modern era. The people who managed to survive in these types of conditions suffered lasting physical damage from the recurring environmental hardships, and it is believed from the viewpoint of a paleopathological paradox that such traces were left in the bones and teeth of those people.

Key Words: Enamel hypoplasia, Early modern, Famine, Stress Marker, Paleopathological paradox

S4-5

Arctic mummies in Salekhard

Sergey Mikhailovich Slepchenko[1], Alexander Vasilyevich Gusev[2], Evgenia Olegovna Svyatova[3], Jong Ha Hong[4], Chang Seok Oh[4], Do Sun Lim[5], <u>Dong Hoon Shin</u>[4,*]

[1]Institute of the problems of Northern development, Tyumen Scientific Center of the Siberian Branch of the Russian Academy of Sciences, Tyumen, Russia
[2]YaNAO Arctic Research Center, Archeology Department, Archeology and Ethnology Sector, Salekhard, YaNAO, Russia
[3]Institution of Culture of Sverdlovsk Region, Center for Protection and Use of Monuments of History and Culture of Sverdlovsk Region, Scientific and Production Center, Ekaterinburg, Urais, Russia
[4]Department of Anatomy/Institute of Forensic Science, Seoul National University College of Medicine, Seoul, South Korea
[5]Department of Dental Hygiene, College of Health Science, Eulji University, Seongnam 13135, South Korea

Permafrost mummies have been found in 12th to 13th century graves located at the Zeleny Yar (Z-Y) burial ground (66°19'4.54"C; 67°21'13.54"B) of the arctic Western Siberia. In 2013-2016, we excavated the cemetery, locating a total of 47 burials, including several cases of mummies. Some of those mummies had been wrapped in a multi-layered birch bark cocoon. We conducted interdisciplinary examinations using various scientific techniques after the removal of cocoon. Gross anatomical and radiological examinations showed that the internal organs were well preserved inside the body cavities. Light and electron microscopy exhibited that the mummies' histology was very similar to those of naturally mummified specimens discovered in other countries. Ancient DNA analysis showed that the Z-Y mummies' mtDNA haplotypes belong to five different haplogroups: U5a (#34), H3ao (#53), D (#67-1), U4b1b1 (#67-2), and D4j8 (#68). By the results, we presume that the Salekhard mummies were unique combination of Western- and Eastern Siberia-specific mtDNA haplogroups. In the Western Siberia, the anthropological data are still too insufficient to comprehend the bio-cultural details of medieval people of the region. Our current study on Salekhard mummies will provide the information useful for future investigations on medieval mummies reported from the Western Siberian arctic.

Key Words: Salekhard, Russia, Ancient DNA, Anatomy, Radiology

Session 5: Immunology

Chairs: Jeehee Youn (Korea)
           Minsoo Kim (USA)

13:30-13:55   Semaphorin controls immune metabolism and immune diseases
           Sujin Kang (Osaka University, Japan)

13:55-14:20   Recent advances in pharmacologic treatment of severe asthma
           Yong Chul Lee (Chonbuk National University, Korea)

14:20-14:45   Dendritic cells and macrophages in arteriosclerosis
           Jae-Hoon Choi (Hanyang University, Korea)

14:45-15:10   Visualizing and manipulating immunity with light
           Minsoo Kim (University of Rochester, USA)

S5-1

Semaphorin controls immune metabolism and immune diseases

Sujin Kang[1], Atsushi Kumanogoh[2, 3]

[1]Department of Immune Regulation, Immunology Frontier Research Center, Osaka University, Osaka, Japan
[2]Department of Immunopathology, Immunology Frontier Research Center, Osaka University, Osaka, Japan
[3]Department of Respiratory medicine and clinical immunology, Graduate school of medicine, Osaka University, Osaka, Japan

Semaphorins were originally identified as axon guidance cues in the development of the nervous system. In recent years, numerous studies have determined that they are also involved in organogenesis, vascularization/angiogenesis, oncogenesis and bone homeostasis. In addition, the mechanisms underlying the diverse functions of semaphorins and their receptors have been identified. Numerous studies have been made in our understanding of the roles of semaphorins in immune responses, particularly the regulation of macrophage activation. Moreover, dysregulated semaphorin expression causes severe immune disorders, including intestinal bowel disease (IBD). Recently, it has been known that distinct metabolic configurations in different immune cells allows to balance its requirements for energy, molecular biosynthesis, and longevity. However, in addition to facilitating immune cell responses, it is now becoming clear that cellular metabolism has direct roles in regulating immune cell function. However, how these metabolic reprogramming facilitate immune function. This

talk focuses on advanced findings on the role of semaphorins/receptors and their intracellular signaling in the regulation of immune metabolism.

S5-2

Recent advances in pharmacologic treatment of severe asthma

Yong Chul Lee

Division of Respiratory Medicine and Allergy, Department of Internal Medicine, Chonbuk National University Medical School, Jeonju, South Korea

Bronchial asthma is recognized as a heterogeneous clinical syndrome consisting of various disease phenotypes. Each asthma phenotype may have distinct observable molecular, cellular, morphological, functional, and clinical features, all of which can be possibly integrated into specific biological mechanisms, called as endotypes. Considering these backgrounds, the improvement of the characterization of the patients is required to achieve appropriate therapeutic responses for asthma. It is expected that the determination of phenotype and endotype leads to more effective precision medicine. However, to date, pharmacologic treatments for asthma are predominantly nonspecific anti-inflammatory agents such as corticosteroid and bronchodilators including β2 agonists, which are effective in the majority of patients with asthma. However, therapeutic responses to these agents vary. Severe asthma is characterized by uncontrolled symptoms and recurrent exacerbation with excessive chronic airway inflammation despite adequate and even maximum treatment with these current medications. Although multiple factors can cause poor responses and underlying pathogenic differences are being revealed explaining the various therapeutic responses including steroid insensitivity, effective therapeutic modalities for severe asthma are still remained as a major unmet need. Moreover, new members of pharmacological therapeutics and more effective drug-delivery devices (i.e., inhaled device) have been designed but the proportion of severe asthmatic patients remains stable. Recently, many clustering analyses have demonstrated that more specific subpopulations of severe asthmatic patients exist and they are associated with different molecular mechanisms contributing to their own pathogenesis sometimes respectively or cooperatively. As for these findings, in 2006 our research team has reported for the first time that PI3K-δ isoform plays an important pathogenic role in OVA-induced allergic asthma and nowadays, it is believed that phosphoinositide 3-kinases (PI3Ks)-δ contributes to the steroid resistance of severe respiratory diseases and more specifically that oxidative stress directly induces PI3K-δ-dependent Akt activation. In fact PI3Ks play critical roles in inflammation, promoting cell polarization, migration, adhesion, and invasion. Class I PI3Ks are activated by tyrosine kinases and is implicated in a wide range of cellular functions, including induction of Th2-related immune responses. They are cytosolic heterodimers consisting of a catalytic p110 subunit (designated as α, β, γ, or δ) and a particular regulatory subunit (designated as p85, p55, p50, or p101). These proteins are a family of lipid signaling kinases that generate lipid-based second messenger, phosphatidylinositol-3,4,5-trisphosphate (PIP_3) and subsequently phosphorylate effector proteins such as Akt. In mammals, the class I PI3K isoforms are present in all cell types in which expression of the p110α and p110β isoforms are ubiquitous while expression of p110γ and p110δ is restricted in some cells such as leukocytes. The restricted expression profile of PI3K-δ makes it an attractive drug target for various inflammatory conditions such as asthma. In addition, our recent studies have revealed that severe asthma is associated with functions of subcellular organelles such as mitochondria and endoplasmic reticulum (ER). In the pathogeneses, the subcellular organelles seem to have new and different roles from their classic ones

and the new roles are implicated in various inflammatory/immune responses actively. Moreover, PI3K-δ signaling is appeared to relate with the out of control of functions in these subcellular organelles and immunes responses in the pathogenesis of severe asthma. In fact, very recently we have revealed that the role of ER stress in various types of severe asthma and pulmonary inflammation, in which ER stress induces the inflammatory responses through the interplay with PI3K-δ, NF-κB or HIF-1α signaling. Based on these observations, we suggest a hypothesis that the link can exist between subcellular organelles and PI3K-δ signaling in various types of severe asthma in which PI3K-δ isoform plays differential roles in each type of severe asthma. In addition, the therapeutic approach via controlling PI3K-δ isoform is very promising as a precision medicine for severe asthma. In this lecture, recent advances in pharmacologic treatment of severe asthma will be introduced including improved current medications, potent non-specific anti-inflammatory agents, endotype-targeted treatments, specific treatment for comorbidities and potential therapeutic candidates focusing on the modulation of PI3K signaling as well as subcellular organelles associated with immune responses.

S5-3

Dendritic cells and macrophages in atherosclerosis

Jae-Hoon Choi

Department of Life Science, College of Natural Sciences, Hanyang University

Atherosclerosis is a representative chronic vascular inflammatory disease. It has been demonstrated that various immune cells are involved during the atherogenesis. Thus, exact identification of vascular immune population is very important to understand the pathogenesis of atherosclerosis. I published several papers showing the pathophysiological roles of myeloid cells including dendritic cells (DCs) and macrophages in atherosclerosis. I and my collaborators have identified functional DCs in normal and atherosclerotic aortas, and found that pDCs, a subset of DCs, have a protective role in atherosclerosis by controlling regulator T cells. Recently, we have also reported intriguing phenotypes of intimal foam and non-foamy macrophages by analyzing their transcriptome. Today, I will summarize what we found regarding the roles of DCs and macrophages in atherosclerosis. I will also try to suggest a new therapeutic approach.

S5-4

Visualizing and manipulating immunity with light

Minsoo Kim

Department of Microbiology & Immunology, David H. Smith Center for Vaccine Biology and Immunology, University of Rochester Medical Center, Rochester, USA

Recently we identified important cross-talks between innate and adaptive immune systems during influenza virus infection at the respiratory track. In this study, published in *Science* in 2015, using a high-resolution live animal imaging technique, we showed that distinct immune cell subtypes engage in coordinated behavior to control viral infection. The findings reveal, for the first time, how immune cells work together to get to their final destination - the site of an injury or infection. Our current research objective is to determine how the early innate immune responses prime and remodel the tissue microenvironment prior to effector T cell homing and how the tissue-specific inflammatory cues

further modify the chemokine signals, integrin activation and T cell effector functions in the influenza infected airway. Understanding how to control effector T cell homing through the manipulation of local tissue environments has potential applications in many virus infections and chronic inflammatory settings. Immunotherapy for cancer is an exciting topic, as it involves stimulating a patient's own immune system to fight the malignancy. However, tumor microenvironments employ several strategies to attenuate effective immune-mediated tumor killing by interfering with nearly every step required for the host immunity, including prevention of immune cell homing to the tumor sites and suppression of the anti-tumor functions by generating strong immunosuppressive environments. Recently, adoptive cell transfer utilizing genetically engineered cytotoxic T lymphocytes (CTLs) (e.g., chimeric antigen receptor (CAR)-T cells) has emerged as one of the effective immunotherapeutic options against hematological malignancies, but significant clinical success has not yet been achieved for solid tumors. We developed new "optogenetic" approaches to define the checkpoints and identify molecular interactions that can guide successful cancer immunity at the tumor sites. Optogenetics combine "optics" and "genetics" to control defined cellular processes by controlling genetically modified light-sensitive proteins using optical stimulation. Our recent studies highlights the development and application of optogenetic techniques to control (a) recruitment, (b) activation, and (c) off-target cytotoxicity of T cells at the tumor microenvironments using light stimulation..

Key Words: T cell, Neutrophil, Macrophage, Influenza infection, Airway, Intravital microscopy, Cancer immunotherapy

Session 6: Cell Biology (I)

Chairs: Hoon-Ki Sung (Canada)
          Dong Woon Kim (Korea)

13:30-13:55   Regulation of mitosis and organ growth by PP2A and Rad21 in Drosophila
Kwang Wook Choi (KAIST, Korea)

13:55-14:20   Growth control of mammalian optic compartments by Nf2-Hippo-Yap feedback cascade
Jinwoo Kim (KAIST, Korea)

14:20-14:45   Fluid shear stress-based circulating tumor cell models for the study of drug resistance in breast cancer cell lines
Yonghyun Kim (University of Alabama, USA)

14:45-15:10   Intermittent Fasting Improves Metabolic Abnormalities Through Increased White Fat Browning and Reduced Adipose Fibrosis
Hoon-Ki Sung (Toronto University, Canada)

S6-1

Regulation of mitosis and organ growth by PP2A and Rad21 in Drosophila

Lee-Hyang Kim, Sung-Tae Hong, Kwang-Wook Choi

Department of Biological Sciences, Korea Advanced Institute of Science and Technology (KAIST), Daejeon, 34141, Republic of Korea

Cohesin is a conserved protein complex involved in sister chromatid cohesion during mitosis. Rad21/Scc1 is a cohesion subunit essential for proper mitosis. Rad21 is also implicated in gene regulation during development. Here we show that Verthandi (Vtd), the *Drosophila* Rad21/Scc1 homolog, is regulated by Microtubule star (Mts), the catalytic subunit of PP2A. Mutations in *mts* and *vtd* cause synergistic mitotic defects. In addition to the defects in sister chromatid cohesion, *mts/vtd* mutations reveal abnormal spindles and centrosomes. Depletion of Mts and Vtd in developing wing synergistically reduces the Cut protein level, resulting in loss of wing tissues and defective epithelial integrity in developing wing disc. Mts and the PP2A subunit Twins (Tws) physically interact with Vtd protein. Loss of Mts or Tws reduces the level of Vtd protein. Reduced proteasome function suppresses mitotic defects caused by mutations in *mts* and *vtd*. Taken together, PP2A is required for mitosis and organ growth by directly regulating the Vtd level through proteasomal degradation pathway.

Key Words: Cohesin, PP2A, Mitosis, Organ development, Drosophila

S6-2

Growth control of mammalian optic compartments by Nf2-Hippo-Yap feedback cascade

Kyeong Hwan Moon, Jin Woo Kim

Department of Biological Sciences, Korea Advanced Institute of Science and Technology (KAIST)

Growth of vertebrate eyes is a process that adds cells in a spatially ordered fashion. Growth of the double-layered eyecup mainly occurs at the edge, where the retina and retinal pigment epithelium (RPE) make a border structure called cilliary margin (CM). Defects in the CM development therefore result in microphthalmia in mammals including human by a molecular mechanism unidentified yet. We found specific enrichment of neurofibromin 2 (Nf2)/Merlin in mouse CM, suggesting potential roles of Nf2 in the development and maintenance of the structure. In a support of the hypothesis and a clinical report on human *NF2* patient, the mice lacking *Nf2* in these areas show defective CM morphogenesis to develop microphthalmic eyes with pigmeted harmatoma. The hyperplasic phenotypes in the *Nf2*-deficient ocular tissues were largely suppressed by concomitant heterozygous deletions of *Yap and Taz*, key targets of Hippo signaling pathway. In addition to a feedback regulation by Yap/Taz in proliferating CM cells, we also identified activation of *Nf2* expression by Mitf in the RPE and suppression by Sox2 in retinal progenitor cells are necessary for the differential growth of the corresponding cell populations. Together, our findings reveal that Nf2 is a key player that orchestrates the differential growth of optic neuroepithelial compartments during vertebrate eye development.

Key Words: Retina, Ciliary margin, Nf2, Hippo pathway

S6-3

Fluid shear stress-based circulating tumor cell models for the study of drug resistance in breast cancer cell lines

Ursula L. Triantafillu, <u>Yonghyun (John) Kim</u>

Department of Chemical and Biological Engineering, The University of Alabama, Tuscaloosa, AL, USA

Over 90% of cancer-related deaths occur due to cancer metastasis. Metastasis is challenging to treat due to the general lack of specified treatment and detection, in particular for metastatic cells known as circulating tumor cells (CTCs). Here, we developed an in vitro model to test for CTC drug sensitivity and have focused on elucidating how FSS affects CTCs during drug treatment. Breast cancer cell lines MCF7 (estrogen receptor-positive) and MDA-MB-231 (triple-negative) were used to test their drug resistance to paclitaxel (PTX) and doxorubicin (DOX). CTCs were modeled as cells subject to fluid shear stress (FSS) in polyether ether ketone tubings. We found that cells cultured in stemness-enriching conditions were more resistant to both PTX and DOX than those in conventional 2D monolayer cultures. CD44+/CD24- cancer stem cell population was also found to be increased in FSS, FSS+PTX, and FSS+DOX treated cells. There was also correlated increased expressions of MDR1, MRP1, and BCRP drug resistance genes, while drug alone (static conditions) or FSS alone (no drug) did not. These results suggest that CTCs under fluid shear acquire stemness characteristics, which intensifies their resistance to conventional chemotherapeutics. Therefore, our FSS-based CTC model provides motivation for targeting cancer stem cell population in the future as a potential therapy against metastatic breast cancers.

S6-4

Intermittent Fasting Improves Metabolic Abnormalities Through Increased White Fat Browning and Reduced Adipose Fibrosis

Ju Hee Lee[1,2], Eashita Das[1], Yun Hye Kim[1], Joanna Yeung[1], Yanqing Jiang[1], Min-Ah Choi[3], Jae-Ryong Kim[3], <u>Hoon-Ki Sung</u>[1,2]

[1]Translational Medicine, The Hospital for Sick Children, Toronto, Canada,
[2]Laboratory Medicine and Pathobiology, University of Toronto, Toronto, Canada
[3]Department of Biochemistry and Molecular Biology & Smart-aging Convergence Research Center, Yeungnam University, Korea

White adipose tissue (WAT) undergoes dynamic remodeling in response to nutritional, environmental, and physical conditions. This process is essential for whole body energy homeostasis and metabolic adaptation of animals and human. Intermittent fasting (IF), a periodic energy restriction, has been shown to provide health benefits equivalent to prolonged fasting or caloric restriction. However, our understanding of the underlying mechanisms of IF-mediated metabolic benefits is limited. Here we show that isocaloric IF improves metabolic homeostasis against diet-induced obesity and metabolic dysfunction primarily with adipose thermogenesis in mice. IF-induced metabolic benefits require fasting-mediated increases of vascular endothelial growth factor (VEGF) expression in white adipose tissue (WAT). Notably, periodic adipose-VEGF overexpression could recapitulate the metabolic improvements of IF in non-fasted animals. Mechanistically, IF and adipose-VEGF induce alternative activation of adipose macrophage, which is critical for thermogenic activity (brown fat-like change) of WAT. Human adipose gene analysis further revealed a positive correlation of adipose VEGF-M2 macrophage-WAT browning axis. Furthermore, we recently discover that IF and adipose-VEGF are effective for preventing and reverting age-associated adipose fibrosis through activation of adipose progenitor cells (APCs). Uncovering the molecular mechanisms of IF-mediated metabolic benefit, the present study suggests that isocaloric IF can be a preventive and therapeutic approach

against obesity and metabolic disorders.

Key Words: Intermittent fasting, Adipose tissue remodeling, Vascular Endothelial Growth Factor (VEGF), Adipose progenitor cells (APCs), Adipose fibrosis

Session 7: Oncology

Chairs: Dae Young Hur (Korea)
              Chaeyong Chung (Korea)

15:30-15:55   Necroptotic Cell Death Signaling and Tumorigenesis
                        You-Sun Kim (Ajou University, Korea)

15:55-16:20   Regulation of tumor progression and metastasis via the p53/p21 complex,
                        Bcl-2 family proteins, and respiratory complex I
                        Hong-Duck Um (KIRAMS, Korea)

16:20-16:45   Deletion effects of steroidogenic acute regulatory protein (StAR)-related
                        lipid ransfer (START) domain-containing protein 13 (STARD13), a tumor
                        suppressor gene
                        Sookja Kim Chung (The University of Hong Kong, Hong Kong)

16:45-17:10   Role of KEAP1/NRF2 mutations in ariway stem cells and non-small cell
                        lung cancers
                        Youngtae Jeong (Stanford University, USA)

S7-1

Necroptotic Cell Death Signaling and Tumorigenesis

You-Sun Kim

Department of Biochemistry, Ajou University School of Medicine and Department of Biomedical Sciences, Graduate School,   Ajou University, Suwon, KOREA

Receptor-interacting protein kinase-3 (RIP3, or RIPK3) is a crucial player in TNF-induced regulated necrosis (Necroptosis) and genetic and biochemical studies show that the role of RIPK3 in mediating inflammatory diseases is well established. Recently, we have found that the decreased expression of the RIPK3 in most cancer cells leads to decreased sensitivity to necroptosis. Extensive loss/reduction of RIPK3 expression suggests this provides some kind of selective advantage to tumor cells. However, it is unclear whether the cell death function of RIPK3 is central to its role in promoting cancer. Loss of RIPK3 could lead to resistance to necroptosis that may directly act as a checkpoint of tumor growth. In this study we sought to investigate whether *Ripk3* loss potentiates cancer development or progression in tumor-prone mouse models to determine possible mechanisms by which *Ripk3* loss would contribute to tumorigenesis and cancer growth. Here, we present our ongoing

studies of RIPK3's molecular mechanism in Tumorigenesis.

Key Words: Necroptosis, RIP3, Cell death

S7-2

Regulation of tumor progression and metastasis via the p53/p21 complex, Bcl-2 family proteins, and respiratory complex I

HONG-DUCK UM

Division of Radiation Bioscience, Korea Institute of Radiological & Medical Sciences (KIRAMS), Seoul, Korea

The p53 tumor suppressor/transcription factor regulates various cell functions, including the promotion of apoptosis, and suppression of cell migration and invasion. Therefore, mutations in or loss of *p53* are believed to contribute to the resistance of cancer cells to therapies and their metastasis to distant organs. Here, we demonstrated that p53 directly binds to p21[WAF1], a transcriptional target of p53. Subsequent functional studies revealed that the p53/p21 complex suppresses cancer cell invasion and metastasis via at least two mechanisms. First, the p53/p21 complex binds to an E3 ligase Mdm2 and a tumor promoter Slug, facilitating Mdm2-dependent Slug ubiquitination and degradation. Second, the p53/p21 complex binds to pro-survival members of the Bcl-2 family proteins, such as Bcl-2, Bcl-w, Bcl-X_L, and thereby liberating the pro-apoptotic Bcl-2 family members, Bax and Bak, from the pro-survival Bcl-2 proteins. Bax and Bak, in turn, bind to complex I in the mitochondrial respiratory chain, thus inhibiting the enzymatic activity of complex I as well as its ability to generate reactive oxygen species, key mediators of cancer cell invasion and metastasis. Since the Bcl-2 family proteins were originally found as key regulators of apoptosis, we further investigated the possible role of the p53/p21 complex in apoptosis. When cells were exposed to apoptotic stimuli, the liberation of Bax and its apoptotic actions also required the binding of the p53/p21 complex to the pro-survival Bcl-2 proteins. Accordingly, a p53 derivative incapable of binding p21 failed to mediate radiotherapy-induced tumor cell death in mice. Overall, our findings indicate that the p53/p21 complex is a functional unit that acts on multiple cell components, providing a new foundation for understanding the tumor-suppressing functions of p53 and p21. Our data also demonstrate the essential role of complex I in tumor progression and metastasis as well as the regulation of such actions of complex I by Bcl-2 proteins and the p53/p21 complex.

Key Words: Tumor progression & metastasis, p53, p21, Bcl-2 family, respiratory complex I

S7-3

Deletion effects of Steroidogenic Acute Regulatory protein (StAR)-related lipid transfer (START) Domain-containing protein 13 (STARD13), a tumor suppressor gene

SOOKJA K. CHUNG[1]

[1]School of Biomedical Sciences, Faculty of Medicine, The University of Hong Kong, Hong Kong; Beijing Normal University-HK Baptist University United International College, Zhuhai, China

Steroidogenic Acute Regulatory protein (StAR)-related lipid transfer (START) Domain-

containing protein 13 (STARD13), also known as Deleted in Liver Cancer 2 (DLC2), is a member of the family of DLC/STARD genes. This gene encodes a protein containing 1,113 amino acids that shares 51% identity and 65% similarity with the amino acid sequence of DLC1. The DLC2 has a sterile alpha (SAM) domain, a START domain and a Rho GTPase activating protein (RhoGAP) domain. An additional functional domain was identified in residues 322-329 as an ATP/GTP-binding site. The DLC2 was first thought to be a tumor suppressor gene, since it is located on chromosome 13q12.3, a region often deleted in hepatocellular carcinoma (HCC). In addition, DLC2 is reduced in 18% of human HCC samples. The DLC2 exhibited RhoGAP activity specific for RhoA, cdc42 and Rac1, which may modulate stress fiber formation. The increased of its RhoGAP domain inhibited the proliferation of breast cancer cells and HepG2 cells by inactivating RhoA. In addition, increased of its GAP domain inhibited the migration of HepG2 cells. Therefore, we expected the deletion of DLC2 would lead to higher rate of liver tumor. However, our previous study showed that a DLC2-deficient mice appeared to be smaller with less visceral fat and did not lead to the increase in rate of spontaneous liver tumor formation or diethylnitrosamine (DEN)-induced hepatocarcinogenesis. However, the DLC2-deficient mice showed more inflammatory pain. The detailed phenotype of DLC2 mutant mice will be discussed

Key Words: START, STARD13, Liver cancer, Tumor suppressor gene

S7-4

Keap1-Nrf2 antioxidant pathway in lung stem cells and lung cancers

Youngtae Jeong[1,2]

[1]Department of New Biology, Daegu-Gyeongbuk Institute of Science and Technology
[2]Department of Radiation Oncology, Stanford University School of Medicine

Recent large-scale genomic studies revealed that mutations in the Keap1-Nrf2 antioxidant pathway occur in about 1/3 of non-small cell lung cancer patients and about 5% of whole cancer patients. However, their role in lung stem cells and lung cancers has not been well understood, partly due to the lack of optimal assay systems. We therefore developed novel experimental systems, and utilizing these systems, identified the role of *KEAP1/NRF2* and *TP53* mutations in lung stem cells and lung cancers. Utilizing *in vitro* tracheosphere assay system and developing an *in vivo* airway stem cell lineage tracing system, we showed that *KEAP1/NRF2* mutations and *TP53* mutations promote airway stem cells self-renewal. We also developed genetically engineered mouse models for non-small cell lung cancers and discovered that inactivation of *Trp53* and/or *Keap1* in the central airway leads to lung squamous cell carcinoma (LSCC) formation, while inactivation of these same genes in the peripheral airway leads to lung adenocarcinoma (LUAD) formation. Using these mouse models, we further identified that airway basal stem cells are the cell of origin for LSCC and type II pneumocytes and bronchioalveolar stem cells as the cells of origin for LUAD. We further demonstrated that the Keap1-Nrf2 pathway activation contributes to LSCC metastasis, radioresistance and chemoresistance. Finally, by non-small cell lung cancer (NSCLC) patient cohort analysis, we found that *KEAP1/NRF2* mutations are associated with local failure and recurrence after radiotherapy and also with worse prognosis after chemotherapy. Currently we are developing novel targeted therapeutic strategies to overcome therapeutic resistance by *KEAP1/NRF2* mutations. These results expand our understanding of LSCC pathogenesis and identify *KEAP1/NRF2* mutations as predictive biomarkers that could be used for personalizing therapeutic strategies for NSCLCs, and likely other cancers in which they are recurrently mutated. Further, this study highlights how stem cell research could be translated for potential cancer diagnostics and therapeutics.

Key Words: Keap1, Nrf2, antioxidant pathway, lung stem cell, lung cancer, resistance

Session 8: Brain & Neuroscience (II)
-Organized with JAA-

Chairs:　Hwan Tae Park (Korea)
　　　　Hiroshi Kiyama (Japan)

15:30-15:55　Regulation of neuronal apoptosis and axonal degeneration by ZNRF1 ubiquitin ligase.
Toshiyuki Araki (NCNP, Japan)

15:55-16:20　Roles of gaseous molecules in Schwann cells during Wallerian degeneration
Junyang Jung (Kyung Hee University, Korea)

16:20-16:45　A form of Schwann cell plasticity; demyelinating Schwann cell
Hwan Tae Park (Dong-A University, Korea)

16:45-17:10　Mitochondria in the regenerating and degenerating neurons after nerve injury
Sumiko Kiryu-Seo (Nagoya University, Japan)

S8-1

Regulation of neuronal apoptosis and axonal degeneration by ZNRF1 ubiquitin ligase

Toshiyuki Araki, Shuji Wakatsuki

Department of Peripheral Nervous System Research, National Institute of Neuroscience, National Center of Neurology and Psychiatry, Tokyo, Japan.

ZNRF1 is a ubiquitin ligase constitutively expressed in neuronal cells both in CNS and PNS. We previously showed that ZNRF1 promotes Wallerian degeneration by degrading AKT to induce GSK3B activation. Regarding activation mechanism of ZNRF1 in response to stress, we recently reported that oxidative stress serves as an activator of the ubiquitin ligase activity of ZNRF1 by inducing EGFR-mediated phosphorylation at the 103rd tyrosine residue, and that the up-regulation of ZNRF1 activity by oxidative stress leads to neuronal apoptosis and Wallerian degeneration. Our findings suggested that NADPH oxidase activity is required for the EGFR-dependent phosphorylation-induced activation of ZNRF1 and resultant AKT degradation via the ubiquitin proteasome system to induce Wallerian degeneration. These results indicate the pathophysiological significance of the EGFR–ZNRF1 pathway induced by oxidative stress in the regulation of neuronal apoptosis and Wallerian degeneration. We would also like to present and discuss our recent findings on the mechanism of ZNRF1-dependent regulation of axonal degeneration.

Key Words: Axon, Wallerian Degeneration, Apoptosis, E3 ubiquitin ligase, Proteasome, Autophagy, kinase

S8-2

Roles of gaseous molecules in Schwann cells during Wallerian degeneration

Junyang Jung

Department of Anatomy and Neurobiology, College of Medicine, Kyung Hee University, Seoul, Republic of Korea

During Wallerian degeneration, Schwann cells lose their characters (myelinating axons) and change to the state of developmental pro-myelinating cells. The recharacterized Schwann cells help to guide newly regrowing axons to their destination and remyelinate the axons. Thus, the dysfunction of Schwann cells during nerve degeneration is main cause of peripheral neurodegenerative diseases such as diabetic neuropathy and Charcot-Marie-Tooth disease. In mammalian cells, gaseous molecules, hydrogen sulfide (H_2S), carbon monoxide (CO), nitric oxide (NO) play important roles in several cellular events. However, because their physical state is gaseous, it is difficult to demonstrate the exact functions of those molecules in biological system, especially, the nervous system. Thus, in the nervous system, identification of the roles of gaseous molecules is important to discover the therapeutic way for peripheral neurodegenerative diseases. Here, we introduce the roles of gaseous molecules, H_2S, CO, NO in Schwann cells during Wallerian degeneration.

Key Words: Schwann cells, Hydrogen sulfide (H_2S), Carbon monoxide (CO), Nitric oxide (NO), Wallerian degeneration

S8-3

A form of Schwann cell plasticity; Demyelinating Schwann cell

Hwan Tae Park

Department of Molecular Neuroscience, Peripheral Neuropathy Research Center, College of Medicine, Dong-A University, Busan, Korea

The plastic changes of Schwann cells (SCs), that create the peripheral myelin sheath, into repair cells play an essential role in the peripheral axon regeneration after injury. SCs also have the unique ability to destroy the myelin sheath under various demyelination conditions including Wallerian degeneration. Transdifferentiated Demyelinating Schwann cell (DSC) performs irreversible demyelination process in many demyelinating neuropathies that show complete demyelination in an internode, and the cell seems to share a common mechanism of demyelination in Wallerian degeneration. We characterized morphological and biochemical features of DSC in various demyelinating neuropathies. We also proved the presence of DSC in human peripheral neuropathic nerves using serum ELISA and human sural nerve biopsy. Our findings provide insight into the pathophysiological mechanism of demyelination in a variety of demyelinating neuropathies and Wallerian demyelination.

Key Words: Schwann cells, Wallerian degeneration, Demyelinating neuropathy, Regeneration

S8-4

Mitochondria in the regenerating and degenerating neurons after nerve injury

Kiryu-Seo S, Kiyama H

Department of Functional Anatomy and Neuroscience, Nagoya University, Graduate School of Medicine, Nagoya, Japan

Damaged neurons require huge amount of energy to accomplish regeneration, which is supplied by mitochondria. In general, mammalian peripheral nervous system (PNS) neurons have higher potential to regenerate following neuronal injury while central nervous system (CNS) neurons degenerate their axons due to a limited ability to regenerate. In a classical view, mitochondria hold attention as an energy source and harmful reactive oxygen generator in injured neurons. Recent focus has been on how mitochondrial dynamics contributes to axonal integrity in damaged neurons. The accumulation and irregular shape of mitochondria often appear in degenerating axons. It is assumed that axonal transport, mitochondrial fission/fusion and clearance of damaged mitochondria are well-coordinated to supply healthy mitochondria to axonal terminals. Over the last decade, multiple studies have revealed the molecular mechanism concerning mitochondrial dynamics *in vitro* cultured cells with significant progress reported. However, *in vivo* mitochondrial behavior is still poorly understood. *In vivo* studies often face the problem to identify mitochondria in specific neurons because mitochondria reside in most of the cells including neurons, glial cells and fibroblasts endothelial cells and immune cells which are orchestrated with the complexity in brain. To clear the issue, we have generated a new mouse line to visualize mitochondria and induce cre recombinase in a nerve injury-dependent manner. In the mouse, mitochondria are labeled by GFP specifically in injured neurons including dendrites and axons. Here, we discuss recent insights into *in vivo* mitochondrial dynamics during axonal regeneration/degeneration and introduce new finding using the genetically manipulated mouse, which is a powerful tool for nerve regeneration studies. *In vivo* study will contribute to the development of effective strategies for promoting axon regeneration and help find answers to the fundamental questions of how mitochondrial dynamics is associated with successful nerve regeneration.

Key Words: Nerve regeneration, Axonal transport, Mitochondrial dynamics, Nerve injury

Session 9: Cryo-EM Technology
-Organized with JAA-

Chairs: Im Joo Rhyu (Korea),
Masahide Kikkawa (Japan)

09:00-09:25 Electron microscopy and 3D reconstruction of thin filament with myosin-binding protein C
Ji Young Mun (Korea Brain Research Institute, Korea)

09:25-09:50 Cryo-EM analysis revealed how microtubule-associated protein 4 (MAP4) controls microtubule stability and kinesin motility
Tsuyoshi Imasaki (Kobe University, Japan)

09:50-10:15   Structural analysis of poxvirus scaffold using cryo-electron microscopy
Jaekyung Hyun (Korea Basic Science Institute, Korea)

10:15-10:40   Combination of cryo-EM and genetics for studying eukaryotic cilia
Masahide Kikkawa (University of Tokyo, Japan)

S9-1

Electron microscopy and 3D reconstruction of thin filament with myosin-binding protein C

<u>Ji Young Mun</u>[1], Craig Roger[2]

[1]Department of Structure and Function of Neural Network, Korea Brain Research Institute, Daegu, Republic of Korea
[2]Department of Cell and Developmental Biology, University of Massachusetts Medical School, Worcester, MA, USA

Myosin-binding protein C (MyBP-C) is an accessory protein of thick filaments and a modulator of muscle contraction. Defects in the MyBP-C cause muscle dysfuction. MyBP-C comprises immunoglobulin and fibronectin-like domains, and a MyBP-C-specific motif. Several studies show that, in addition to binding to the thick filament via its C-terminal region, MyBP-C can also interact with actin via its N-terminal domains, modulating thin filament motility. Structural observations of F-actin decorated with N-terminal fragments of cMyBP-C suggest that MyBP-C binds to actin close to the low Ca^{2+} binding site of tropomyosin. This suggests that MyBP-C might modulate thin filament activity by interfering with tropomyosin regulatory movements on actin. To determine directly whether MyBP-C binding affects tropomyosin position, we have used electron microscopy (EM) and in vitro motility assays to study the structural and functional effects of N-terminal fragments binding to thin filaments. 3D reconstructions suggest that under low Ca^{2+} conditions, MyBP-C displaces tropomyosin towards its high Ca^{2+} position, and this movement corresponds to thin filament activation in the motility assay. For 3D reconstruction, negative stained TEM and improved resolution images by cryo-TEM were used, but filaments' labile structures showed some limitation to obtaining near-atomic detail. In addition, we also studied the effect of isoform, phosphorylation, and point mutation on MyBP-C structure and on its modulation of tropomyosin position on thin filaments in order to investigate important factors regulating filament's contraction. The data showed phosphorylation reduces MyBP-C's displacement of tropomyosin and its activation of thin filaments, in contrast, specific point mutation like L348P showed reverse effect. These results suggest that MyBP-C may modulate thin filament activity by physically displacing tropomyosin from its low Ca^{2+} position on actin filament, and phosphorylation and point mutation affects its regulation. In addition, each isoforms showed different change of tropomyosin and activation of filament.

Key Words: Actin, Tropomyosin, MyBP-C, IHRSR

S9-2

Cryo-EM analysis revealed how microtubule-associated protein 4 (MAP4) controls

microtubule stability and kinesin motility

Imasaki T[1], Shigematsu H[2], Chihiro Doki[3], Takuya Sumi[1], Mari Aoki[4], Tomomi Uchikubo-Kamo[4], Ayako Sakamoto[4], Kiyotaka Tokuraku[3], Mikako Shirouzu[4], Nitta R[1]

[1]Division of Structural Medicine and Anatomy, Kobe University Graduate School of Medicine, Kobe, 650-0017, Japan
[2]RIKEN SPring-8 Center, Hyogo, 679-5148, Japan
[3]Course of Biosystem, Graduate School of Muroran Institute of Technology, Muroran, Hokkaido 050-8585, Japan
[4] RIKEN Center for Biosystems Dynamics Research, Yokohama, 230-0045, Japan

Tau-family microtubule-associated proteins (MAPs) control microtubule stability and microtubule-based motility through its C-terminal microtubule binding domain (MBD). MBD consists of three to five disordered repeat sequences produced by alternative splicing, altering the function of MAPs. Despite its importance, however, the regulatory mechanism of MAPs through MBD repeats are still poorly understood. To investigate the regulatory mechanism by MAPs, we focused on the microtubule-associated protein 4 (MAP4), which is a member of the Tau-family MAPs. MAP4 has several isoforms with different number of the MBD repeat sequences, which alters microtubule stability and kinesin motility. Using cryo-electron microscopy (cryo-EM), we visualized complex structures of the microtubule, Kinesin-1, and MAP4 MBD 4 repeat (4R-MAP4) or MAP4 MBD 5 repeat (5R-MAP4). Both MAP4 MBD repeats formed complex along the microtubule protofilament, from Kinesin-1 at the minus-end side to the next kinesin-1 at the plus-end side. The strongest density of the MAP4 was observed around the inter-dimer interface of the tubulin. The difference between 4R-MAP4 and 5R-MAP4, and tau protein will be discussed.

Key Words: MAP4, Tau, MAP, Microtubule, Cryo-EM, TEM

S9-3

Structural analysis of poxvirus scaffold using cryo-electron microscopy

Hyeongseop Jeong[1], Jung Jae Park[2], Jongmin Yuk[2], Jaekyung Hyun[1,3]

[1]Electron Microscopy Research Center, Korea Basic Science Institute, Cheongju, Chungcheongbukdo, Republic of Korea
[2]Department of Material Science and Engineering, Korea Advanced Institute of Science and Technology, Daejeon, Republic of Korea
[3]Department of Bio-analytical Science, Korea University of Science and Technology, Daejeon, Republic of Korea

Despite the eradication of smallpox by vaccination in the 1970s, poxviruses remain a concern for human health due to the threat of deliberate release of smallpox virus and occasional zoonosis. In accordance with their structural and genomic complexities, poxviruses undergo dramatic multi-step assembly process in which capsid-like scaffolding protein plays a major role. In particular the scaffolding protein D13 from Vaccinia virus, the prototype of poxvirus family, has been extensively characterized and inhibition of D13 scaffold formation is known to abolish the viral assembly. In the past, taking advantage of simultaneous *in vitro* assembly of purified D13 trimers into honeycomb-shaped crystalline patches and spherical particles that resemble immature Vaccinia virus, we have elucidated a model for molecular organization of D13 in context of assembling immature virion, which

conducts remodeling of host lipid into viral envelope. In addition, x-ray crystallography structure of D13 revealed striking similarities with capsid proteins from seemingly unrelated virus families. In this presentation, we describe an on-going attempts to further understand molecular organization of D13 within immature virus scaffold using cryo-electron microscopy single particle analysis and tomography.

Key Words: Poxvirus, Cryo-electron microscopy, Single particle analysis, Electron tomography

S9-4

Combination of cryo-EM and genetics for studying eukaryotic cilia

Masahide Kikkawa

Department of Cell Biology and Anatomy, Graduate School of Medicine, The University of Tokyo, Tokyo, 113-0033, Japan

Eukaryotic cilia are complex cell organelles and play important roles in various cell, such as propeller and antenna. They consist of hundreds of different proteins that are precisely organized by self-assembly mechanisms. To study such a complex system, we have been using Chlamydomonas genetics and cryo-electron tomography to identify 3D locations of specific proteins. For example, we identified proteins that bind inside of ciliary microtubule that stabilizes doublet microtubules. In addition to Chlamydomonas, we started using zebrafish and mice as model organism, to which we can apply genome editing techniques. Cryo-ET method was established for zebrafish sperm and we systematically studied PIH proteins (Pih1d1, Pih1d2, Ktu, and Twister) in zebrafish and revealed their distinct roles by correlation the swimming phenotype and structures.

Key Words: Cilia, Cryo-EM, Zebrafish

Session 10: Anatomy Education (I)

Chairs: Cagatay Barut (Turkey)
                Hong Tae Kim (Korea)

09:00-09:25   How anatomy teaching can be made more interesting
                Srijit Das (Universiti Kebangsaan Malaysia, Malaysia)

09:25-09:50   Technology for overcoming barriers to active learning in the gross
                anatomy laboratory for 2018 APICA
                Lap Ki Chan (Hong Kong University, Hong Kong)

09:50-10:15   Video-guided anatomy and neuroanatomy lab
                Kyeung Min Joo (Sungkyunkwan University, Korea)

10:15-10:40   Study preferences in anatomy education: perspective of Turkish medical
                students

Cagatay Barut (Bahçeşehir University, Turkey)

S10-1

How anatomy teaching can be made more interesting

Srijit Das

Department of Anatomy, Faculty of Medicine, Universiti Kebangsaan Malaysia, Kuala Lumpur, Malaysia

Anatomy is one of the essential subjects taught at the very beginning of any medical career and it forms the foundation for various other subjects taught later in clinical years. A clear understanding of anatomy is essential for better understanding of surgery and allied subjects. Often, it is difficult to understand the vast subject of anatomy and moreover, the subject is volatile and difficult to remember. To know anatomy, one has to have repeated readings and memorizing is impossible. Teaching requires much skill and didactic lectures are considered to be boring by the undergraduate medical students. While many institutions have developed integrated method of teaching, others still resort to traditional methods. Once anatomy is taught with clinical aspect, it becomes more interesting to the student. Regular training of teachers is essential for imparting better knowledge. Anatomy lectures need more usage of information technology and e-learning methods. 3D visualization, virtual anatomy, electronic version of atlas, online interactive sessions and quizzes make the subject more interesting and contribute to lifelong learning. Shortage of cadavers and teaching staff opens the door to problem based and team based learning methods. Self-learning packages may also help in situations where there is deficiency in teaching staff. Due to shortage of cadavers, prosected embalmed and plastinated specimens are the only means of teaching during any practical class. The assessment methods are also important in any undergraduate curriculum. Mixture of multiple choice questions, modified essays and extended match items make a good question paper. Feedback from students, post-mortem analysis of examination results, regular mentoring of students and audit also helps in managing a good program. Last but not the least, it is also important to infuse the idea of research in the young minds even though time and financial situation may be a constraint.

Key Words: Anatomy, Teaching, Learning, Curriculum, Methods.

S10-2

Technology for overcoming barriers to active learning in the gross anatomy laboratory, for 2018 APICA

Lap Ki Chan

The University of Hong Kong

The gross anatomy laboratory is a small group, highly interactive learning environment that offers rich opportunities for active learning, wherein students engage in activities that promote higher-order thinking. There is accumulating evidence to show that active learning can increase student scores and reduce failure rate. However, there are barriers to implementing active learning, including large class, anxiety on loss of control, and students' failure to engage in high-order learning. Potentially, technology can help teachers and students overcome at least some of these difficulties. In this talk,

the evolution of the use of technology in the gross anatomy laboratory at The University of Hong Kong will be traced. Initially, TV broadcasting system enables efficient delivery of learning materials from the sources (oftentimes the teachers) to the students. The use of video streaming technology, using inexpensive equipment, allows much more flexibility on where and what the teachers can demonstrate and share with the students in the large gross anatomy laboratory. Teachers can broadcast well dissected structures and anatomical variations from any cadavers to the whole class. But true bidirectional interactivities become possible after the installation of tablets, one per dissection team of students, and the use of educational software for collaborative exercises. For example, in problem-oriented dissection, students need to work together to solve clinical problem on their cadavers. The use of a collaborative app allows the student teams to supply individual teams' solutions, via their tablets, to a cloud document and to comment on one another's answers. In the newly developed peer-support system for dissection, the app iClass (developed by the e-Learning Technology Development Laboratory of The University of Hong Kong) is used to foster collaboration. Students can use the tablets to produce short videos, showcasing structures that they have successfully found. The videos produced by different teams are made available to all teams through the iClass platform, from which they can view what other teams have found and how they did it. They can rate these videos and give one another feedback. Our experience shows that the use of technology can overcome some of the barriers to active learning in the gross anatomy laboratory, and can even create new learning opportunities not possible before, by enabling bidirectional interactivities, not just between teachers and students, but even among the students.

S10-4

Study Preferences in Anatomy Education: Perspective of Turkish Medical Students

Barut C[1], Karaer E[2], Yavuz M[3]

[1]Department of Anatomy, School of Medicine, Bahçeşehir University, Istanbul, Turkey
[2]School of Medicine, Bahçeşehir University, Istanbul, Turkey
[3]Department of Public Health, School of Medicine, Bahçeşehir University, Istanbul, Turkey

Anatomy has been taught for centuries. From Edwin Smith Papyrus to 21st century thick anatomy textbooks, it has evolved greatly along with its sources and methods of its education. Due to the course of this evolution, many variations occurred in anatomy education all around the world. Researches that were trying to find the "idealist" method for anatomy education were mostly focused on what is the best teaching method for students, instead of what is the best studying method for them. Due to this, this perspective of anatomy education remains nearly untouched, having only a small amount of articles about itself. Thus, this study aims to identify the study preferences of medical students in Turkey in terms of study methods and sources. 1998 medical students aged between 18-33 years participated in the study. Participants were asked 16 questions related with the education system and study preferences of anatomy: 9 of the questions were related with the education system of their school in general and in terms of anatomy and 7 of the questions were related with their way of studying anatomy; including time spent for studying, preference for a group or individual study, study materials, study methods. Descriptive statistics for categorical variables are given with frequency and percent and categorical independent data were analyzed with Chi-square tests. Students from 35 medical schools of Turkey answered the survey. 50.1% of the respondents were first year students and 36.1% were second year and 13.3% were third year students. 94.68% of the respondents indicated that integrated medical education was the education system used in their school. 80.87% of the respondents indicated that anatomy classes are spread through the 2 years of the curriculum while 10.88% stated that the anatomy classes were spread through the 3 years of the education. Majority

of the respondents preferred studying anatomy alone (72.9%). When the preference for a group or individual study was evaluated according to gender the preferences of males and females were similar (p=0,569), both genders preferred studying anatomy alone. Slide layouts of the theoretical class presentations were the leading preference for anatomy study sources (45.7%). In addition to that, atlases (26.8%) and textbooks (19.6%) were also other preferred sources. When preference of study materials was evaluated according to gender the preferences of males and females were similar (p=0,235), first choice for study materials was slide layouts for both genders. Furthermore, students stated their preference of study methods one or more at the same time and the distribution of these methods were as follows: correlation of structures with relations (18.0%), correlation of structures with functions (14.6%), correlation of structures with clinical situations (13.8%), memorizing with mnemonics (17.5%) or tables and lists (3.3%), flash cards (2.0%), regular repetitions (20.8%). Although most frequent choice for study methods was regular repetitions for both genders there was a statistically significant differences between both genders in terms of study methods (p=0,002). Detailed interpretation of study preferences may lead changes in anatomy curricula in the future.

Key Words: Anatomy, Study preference, Medical education, Medical student

Session 11: Modern Tech in Microscopy

Chairs: Yong Chul Bae (Korea)
              Lai Guan NG (Singapore)

13:30-13:55   3D structural analysis of cilia using cryo-electron tomography
                        Toshiyuki Oda (University of Yamanash, Japan)

13:55-14:20   Watching the great leukocyte migration
                        Lai Guan NG (Singapore Immunology Network, A*STAR, Singapore)

14:20-14:45   Monitoring neural circuit activity during social interaction using in vivo
                        head-mounted fluorescence microscopy
                        Il Hwan Kim (Duke University, USA)

14:45-15:40   Correlative cell biology in 2D and 3D
                        Ruth Chalmers-Redman (Carl Zeiss, Singapore)

S11-1

3D structural analysis of cilia using cryo-electron tomography

Toshiyuki Oda

Department of Anatomy and Structural Biology, University of Yamanashi, Chuo, Japan

        The cilium is a conserved motile organelle that plays essential roles in cellular motility of eukaryotes and development of vertebrates by generating fluid flow. The core structure of the cilium, called the axoneme, is an elaborate and highly-ordered protein complex, composed of hundreds of

subunits. To elucidate the molecular mechanisms of ciliary assembly and motility, it is necessary to "dissect" the three-dimensional ultrastructure of the axoneme. Cryo-electron tomography is a powerful method to reconstruct the three-dimensional structures of organelles and macromolecular complexes to a nanometer-scale resolution. Using this method, we can visualize not only the "9+2" configuration of the microtubules, but also nucleotide-dependent conformational changes in the axonemal dynein motors.   the molecular machinery of cilia requires identification of three-dimensional positions of the axonemal proteins. We have developed a robust structural labeling method based on biotin-streptavidin interaction. Cryo-electron tomography in combination with this labeling technique revealed a molecular ruler and a mechano-signaling system within the cilia.

Key Words: Cryo-electron tomography, 3D structure, Cilia, Dynein

S11-2

Watching The Great Leukocyte Migration

Lai Guan NG

Singapore Immunology Network, A*STAR, Singapore

The migration of leukocytes between tissue compartments is an important aspect of innate immune surveillance. This process is regulated by a cascade of cellular and molecular signals to avoid unnecessary crowding of leukocytes at the periphery, to allow rapid mobilization of leukocytes inresponse to inflammatory stimuli, and to return to a state of homeostasis after the response. Intravital microscopy approaches have been fundamental in unraveling many aspects of leukocyte behavior, providing important mechanistic information on the processes involved in basal and disease states. This talk will provide a broad overview of the current understanding of leukocyte biology, and focus on novel aspects of myeloid cell migration/trafficking, as well as how myeloid cell exploit their regional niches to specialize and maximize their functional properties. Understanding their cellular behavior in each of their specialized microenvironment will eventually allow us to target specific cells and their behavioral patterns for improved vaccine and therapeutic purposes.

Key Words: Innate Immunity, Myeloid Cell, Intravital Imaging

S11-3

Monitoring neural circuit activity during social interaction using in vivo head-mounted fluorescence microscopy

Il Hwan Kim

Department of Psychiatry and Behavioral Sciences, Duke University Medical Center Durham, NC 27710 USA

Psychiatric disorders are highly heritable pathologies of altered neural circuit functioning. How genetic mutations lead to specific neural circuit abnormalities underlying behavioral disruptions, however, remains unclear. Using new circuit-selective transgenic tools, a head-mounted fluorescence microscopy (mini scope), and a mouse model of maladaptive social behavior (ArpC3 mutant), we identify a neural circuit mechanism driving dysfunctional social behavior. We demonstrate that circuit-

selective knockout (ctKO) of ArpC3 gene within prefrontal cortex to basolateral amygdala elevates the excitability of the circuit, leading to disruption of fine tuning of the circuit neurons, resulting in abnormal social behavior. These results highlight a mechanism of how a gene-to-neural circuit interaction drives altered social behavior, a common endophenotype of several psychiatric disorders.

Key Words: Mini scope, Neural circuit

S11-4

Correlative Cell Biology in 2D and 3D

Ruth M.E. Chalmers-Redman

Carl Zeiss Microscopy, Asia Pacific Region, Singapore

Light microscopy is a technique that has evolved into a tool of exquisite labeling and detection that spans resolution scales from macro to micro to super resolution. It offers the unparalleled possibility for multiple labeling that can be detected simultaneously however resolution is limited compared to that which is possible by classical electron microscopy of resin embedded samples. As well, labeling of features for light microscopy, highlights the object(s) of interest while rendering all else invisible to detection. With electron microscopy and other techniques such as x-ray microscopy, this is not the case. All features are visible such that virtually no structure can hide. Recent advances in scanning electron microscopy have led to the re-examination of the classical ultrastructure in 2D and 3D and has led to new discoveries in cellular and organellar connectivity and organization as well as to the identification of cellular populations that were previously not known. The correlation of imaging data from different imaging modalities to such SEM data offers a powerful tool to definitively identify new connectivity and structures. Correlating such data in cell biology brings to and merges the multilabeling advantage to techniques where multilabeling is difficult or not possible. This is leading to the advancement of knowledge of such ultrastructure and in some cases is redefining what we knew and understood from classical 2D TEM data.

Key Words: Correlative Microscopy, Light, Electron, X-Ray, 3D ultrastructure, Multilabeling

Session 12: Anatomy Education (I)

Chairs: Youngbuhm Huh (Korea)
Helen Nicholson (New Zealand)

13:30-13:55 "It's a good learning resource, but it takes a bit of getting used to":
perspectives on utilising cadaveric material for learning anatomy
Helen Nicholson (University of Otago, New Zealand)

13:55-14:20 Medical imaging based anatomy application
Namguk Kim (Asan Medical Center, Korea)

14:20-14:45   3D Simulation/VR/AR based anatomical application
Youngjun Kim (KIST, Korea)

14:45-15:40   Educational research in anatomical sciences: insides from a journal editor
Wojciech Pawlina (Mayo Clinic, USA)

S12-1

"It's a good learning resource, but it takes a bit of getting used to": perspectives on utilising cadaveric material for learning anatomy.

Nicholson HD, Macmillan A, Flack NAMS

Department of Anatomy, University of Otago, Dunedin, New Zealand

Cadaveric dissection is regarded by educators and students as an important teaching tool that provides medical students with a unique opportunity to learn anatomy. However, a growing number of individuals studying anatomy are not medical students. Understanding why and how non-medical students learn anatomy, what they learn, and identifying any barriers is important to ensure the best possible teaching and support is provided. This study aimed to explore the perceptions of non-medical students studying anatomy. All students enrolled in the second (n=328) and third year (n=155) gross anatomy science papers at the University of Otago were invited to take part in two online surveys. Responses from open-ended questions regarding students' perceptions on coping with handling cadaveric material, what they learnt and how they were supported, were analysed by a general inductive approach, identifying common emergent themes. Thereafter, responses were compared to existing data from medical students, to determine any differences or similarities. A total of 223 (n=145 2nd year) students completed the first survey, before interacting with cadaveric material, and 153 (n=101 2nd year) after completing the course. Preliminary analysis shows students' responses were similar across year groups; were generally positive, and commonly conveyed the use of cadaveric material as helpful, exciting and useful for learning anatomy. Largely, students cope well with handling cadaveric material, and if not initially, this mostly improves over time. "Real-life anatomy", "variations" and "anatomical relationships" were identified as the most frequently listed responses of what they learnt. These data are similar to those we identified in medical students. Emergent themes regarding support for non-medical anatomy students suggest that they may benefit from additional support prior to exposure to cadaveric material.

Key words: Cadaveric material, Anatomy students, Learning

S12-2

Medical imaging based anatomy application

Namkug Kim[1,2]

[1]Department of Convergence Medicine, University of Ulsan College of Medicine, Asan Medical Center, Seoul, South Korea
[2]Department of Radiology, University of Ulsan College of Medicine, Asan Medical Center, Seoul, South Korea

While 3D printing technology has been developed in 1984, due to a matter of medical expenses, 3D printing medical application has been recently spotlighted. Besides all developed countries are becoming to the elderly society, the biggest problem of South Korea also reduces health care costs in the near-future elderly society. Similar to precision medicine based on -omics and targeted drugs, the patient-specific medical devices and materials from medical images using a 3D printer to meet the anatomic variations could reduce health care costs, which could be used for medical device of a precision medicine. In this talk, I'll introduces various 3D printers, its theories and available materials especially for minimally invasive surgery. In particular, to produce patient-specific surgery simulators, surgical guides, implants, a 3D printer could be manufactured to medical device of a precision medicine. These patient-specific simulators, surgical guides, implant needs optimal medical imaging technique for obtaining the shape of the patient (including enhancement), the objective modeling of professionals who understand the anatomy, the design for the purposes of CAD specialist, radiologist and confirmation of clinical and physician, 3D printing manufacturing experts, the human body, which is applied cloud systems to share data and processing and management of these workflows. 3D printing technique for this purpose, materials and data creation will be released specifically based on this workflow for such production methods. Particularly in the case of spinal polymer, silicone, ceramic, it can be applied to develop a variety of patient-specific implants in metallic form.

Key Words: 3D Printing, Implant, Medical Imaging, Patient-specific, Precision Medicine, Surgical Guide

S12-3

3D Simulation/VR/AR based anatomical application

Youngjun Kim[1,2]

[1]Center for Bionics, Korea Institute of Science and Technology, Seoul, Korea
[2]Division of Bio-Medical Science & Technology, UST KIST School, Seoul, Korea

Recently, 3-dimensional (3D) software technologies have been applied to anatomical education. Anatomical education based on 3D virtual model of human body has many advantages than cadaver based method. 3D virtual human anatomic model can be virtually cut or visualized layer by layer to give better understanding of the complex structure of organs, muscles, nerves, and skeletons. The state-of-the-art VR/AR medical applications will be introduced and discussed in this talk. For 3D virtual anatomical models, 3D medical image software techniques are essential. In this talk, I will introduce the state-of-art 3D medical image software techniques. Main topics of the talk include 3D human modeling, visualization, virtual reality (VR), and augmented reality (AR). At the end of the talk, my research team's 3D medical image software applications will be presented including VR/AR based anatomical education, virtual surgical simulation for training, and virtual surgical planning.

Key Words: 3D Simulation, Virtual Reality, Augmented Reality, Anatomical Application

S12-4

Educational Research in Anatomical Sciences: Insides from a Journal Editor

Wojciech Pawlina

Department of Anatomy, Mayo Clinic College of Medicine and Science, Mayo Clinic, Rochester, MN.

Publishing results of a research study in peer-reviewed journals is an important part of a successful academic career. However, accomplishing this task can be challenging; especially as it relates to topics in education. To have a successful outcome, anatomy educators should have some understanding of the publication process and what journal editors and reviewers are expecting. The key is the planning process that starts with developing a working hypothesis or a carefully selected objectives and aims for the study. The methodology should be explored very early, taking into consideration both quantitative and qualitative research designs. Attention should be directed towards developing and testing research instruments (surveys and questionnaires) that have required levels of accuracy and consistency (validity and reliability). These should be able to capture the highest possible quality of data for further statistical analysis. Certain requirements should be met (i.e., approval of the research design by the ethical committee at authors' institution) in advance of the experimental phase of the project. Basic elements of scholarly publication design with examples from various types of manuscripts will be discussed in this session.

Oral Presentation I
-Gross Anatomy-

31st October, Wednesday
08:45-11:20
Rm321-322

Chairs: Jun Ouyang (China)
Srijit Das (Malysia)
Changman Zhou (China)

O1-1

New interatrial channels in the heart detected by anatomical dissection and 3-dimensional micro-computed tomography

Mi-Sun Hur[1], Chang-Seok Oh[2], Seunggyu Lee[3], Yeon Hyeon Choe[4]

[1]Department of Anatomy, Catholic Kwandong University College of Medicine, Gangneung, Korea
[2]Department of Anatomy, Sungkyunkwan University School of Medicine, Suwon, Korea
[3]National Institute for Mathematical Sciences, Daejeon, Korea
[4]Department of Radiology, Samsung Medical Center, Sungkyunkwan University School of Medicine, Seoul, Korea

The present study was performed to investigate the interatrial channels in the heart, which had not been reported. Thirty-one hearts from embalmed Korean adult cadavers with no history of heart trauma, interventional or surgical procedures were used in this study. Several tiny holes with various sizes and shapes were found on both the right and left surfaces of the interatrial septum in 22 out of 31 specimens (71.0%), and in two specimens (6.5%) among them the holes on both sides were

found to be connected with each other through a tortuous channel (open channel) by dissection under a surgical microscope. On the right surface of the interatrial septum, the hole was usually found adjacent to the left border of the interatrial septum between the opening of the superior vena cava into the right atrium and the superior margin of the fossa ovalis. On the left surface of the interatrial septum, the holes were usually found adjacent to the superior border of the interatrial septum. The specimens having an open channel were scanned using micro-Computed Tomography (micro-CT), and their serial micro-CT images were reconstructed into 3D models to show the entire channel through the interatrial septum. In 7 (22.6%) and 2 (6.5%) specimens, holes were observed only on one side of the right and left surfaces of the septum, and any hole was not found on any surface, respectively. In the cases that holes on both sides were not connected, or holes were observed only on one side, the holes had obstructed channels, and their depth varied. Some of obstructed channels were also reconstructed into 3D models by serial micro-CT images. An embryologic model for the formation of interatrial channel in the development of atrial septa was discussed. The present study shows a new finding of the interatrial channel of heart, which is expected to be helpful for understanding of the possible symptoms such as stroke caused by the interatrial channel in the absence of classical atrial septal defects.

Key Words: Interatrial channel, Interatrial septum, Dissection, Micro-computed tomography, 3D model

O1-2

Biomechanical research of pedicle-lengthening osteotomy treatment for lumbar spinal stenosis

Ouyang J, Qian L, Zhong S

Department of Anatomy, Guangdong Provincial Key Laboratory of Medical Biomechanics, Southern Medical University, Guangzhou, China

Pedicle-lengthening osteotomy is a new percutaneous minimally invasive surgical procedure for lumbar spinal stenosis, which enlarges the dimensions of the spinal canal and neural foramen through bilateral lengthening of the lumbar pedicles. This new technique increases the volume of the lumbar vertebral canal, maintaining normal spinal kinematics and reducing the risk of blood loss and muscle damage. Three-dimensional reconstructions of CT images were performed for 69 patients (33 men and 36 women) (mean age 49.96 years; 24 to 81). Simulated pedicle-lengthening osteotomies and disc bulge and spinal canal volume calculations were performed using Mimics software. The mean spinal canal volume of the two groups, L4 and L5, were 14 646.81 mm3 (5918.60 to 22 717.77) and 16 408.47 mm3 (8678.21 to 31 204.79), respectively. The mean lengthening distance was 2.17 mm (0.5 to 4.8) and the mean bulge-canal volume ratio was 0.23 (0.05 to 0.48). The pedicle-lengthening distance of the two groups were very strongly correlated with disc bulge volume and bulge-canal volume ratio ($p < 0.001$); the predictive equation was established as L = 0.06 + 9.06R (where L equals the pedicle-lengthening distance and R represents the bulge-canal volume ratio). Our findings indicated that lumbar pedicle-lengthening distance strongly correlates with bulge-canal volume ratio, which can be estimated before surgery from CT images. Followed biomechanical evaluation on lumbar spine specimens showed that the spinal mechanical stability can be preserved for most cases after pedicle-lengthening. The facet joint load between the surgical segment and upper adjacent segment will be increased and the facet joint load between the surgical segment and lower adjacent segment will be reduced.

Key Words: Pedicle-lengthening osteotomy, 3-D reconstruction, spinal stenosis, digital anatomy,

biomechanics

O1-3

MORPHOLOGICAL FEATURES OF MAJOR AND ACCESSORY FISSURES OBSERVED IN LUNG SPECIMENS

Ria Margiana[1], Mochamad Iskandarsyah[1], DIsabella Kurnia Liem[1,*]

[1]Department of Anatomy, Faculty of Medicine, Universitas Indonesia, Jakarta, Indonesia

A case of lung lobes anomaly was found in a male cadaver during anatomical practical session at Department of Anatomy, Faculty of Medicine, Universitas Indonesia. Both of right and left lungs showed anomalies in the minor fissures that affect the lung lobation. The right lung accessory fissure was an incomplete fissure, and seemed to follow a horizontal path from the hilum towards the medial section of the middle lobe. The left lung had three lobes due to the development of a similar minor fissures as a second fissure. Compare to the eleven previous studies demonstrated wide individual varieties on their morphological anomaly, suggesting ecological and hereditary factors in its development. Clinically, documentation and understanding of this anomaly are vital for radiological diagnostics and proper administration of lung pathologies.

Key Words: Accessory fissure, Lung anomaly, Lung lobes, Lung morphology, Lung lobation

*Correspondence to Ria Margiana (E-mail: bellajo04@gmail.com)

O1-4

Computed Tomographic Measurement of Kidney in North Indian Healthy Adults: Correlation with Age, Sex, and Habitus

Dushyant Agrawal[1], Surajit Ghatak[1], Subhash Chandra Upadhyay[2], Gitika Arya Agrawal[2]

[1]Department of Anatomy, All India Institute of Medical Sciences, Jodhpur, India
[2]Department of Anatomy, Sri Ganganagar College of Ayurvedic Science & Hospital, India

Background: Kidney volume is regarded as the most precise indicator of kidney size. However, it is not widely used clinically, because its measurement is difficult due to the complex kidney shape. There is no information on renal size and its relation to age, sex and height in north India. The purpose of this study was to investigate the normal measurements of the kidney in healthy adult subjects. Methods: 320 healthy north Indian subjects aged 18 to 70 years with normal blood pressure, no history of renal disease in them and with normal computed tomographic appearance were chosen for this study. Body parameters (height, body weight, body-surface area, and total body water) and laboratory data were collected. In spiral computed tomographic scan of 640 kidneys in 320 adults, the kidney length pole to pole (LPP), parenchymal (PW) and cortical width (CW) and position of kidneys, were recorded. For length measurements, axes were adjusted individually in double oblique planes using a 3D-software. Analyses of distribution, correlation and multivariate regression analyses were performed. Renal dimensions were correlated with age, height, weight, body mass index, and total body area. Results: LPP was 107.8 ± 11.4 mm for the right, and 110.3 ± 11.9 mm for the left kidney ($p < 0.0001$ each). PW on the right side was 14.8 ± 2.6 mm, slightly less than 15.2 ± 2.4 mm on the

left side (p < 0.0001), the CW was slightly more for the right kidney.   The most significant independent predictors for LPP, CW, and PW were body size, BMI, age, and gender (p < 0.001 each). Conclusion: The result of this study shows the normal values for renal dimensions in Indian males and females, which may be helpful in assessing the size of patients' kidneys in different clinical settings. Due to the complex influences on kidney size, assessment should be made individually. The most important influencing factors are BMI, height, gender, age.

Key Words: Kidney size, Renal length, normal values, computed tomography

O1-5

Sonographic Analysis of the Facial Artery and its Clinical Implication

Han Yuna, Kangwoo Lee, Hyung jin Lee, Hee-Jin KIM, Kyung-Seok Hu

Division in Anatomy and Developmental Biology, Department of Oral Biology, Human Identification Research institute, BK21 PLUS Project, Yonsei University College of Dentistry, Seoul, 03722, Republic of Korea

Previous studies have revealed a various distribution patterns of the facial artery through gross anatomy. However, the sonographic analysis of the facial artery and the its running layer has not been well described. The purpose of this study was to determine the depth of the facial artery from the skin for preventing complications in relation to dermal filler injection and oromaxillofacial surgery. Forty young volunteers (23 male and 17 female; mean age: 25.2 years) were participated in this study. The sonography images were obtained horizontally. Three surface anatomical landmarks were used as follows: antegonial notch (F1), 1 cm lateral to cheilion (F3), and nasal ala (F5). Two additional reference points added at midpoint between F1 and F3 (F2), and between F3 and F5 (F4). The facial artery was observed in every five landmarks of the 40 cases. The depth of the facial artery was 9.31±2.20 mm at F1, 8.85±2.99 mm at F2, 6.88±3.50 mm at F3, 4.85±1.42 mm at F4, and 5.02±1.60 mm at F5, respectively. The results of this study provide useful information regarding precise depth of the facial artery for clinical application in the dentistry fields and cosmetic surgery.

Key Words: Facial artery, Sonography, Filler injection,

O1-6

Morphological analysis of the Fetal Calcarine Sulcus and Lateral Ventricles

Zhuoran Li[1], Feifei Xu[1], Zhonghe Zhang[2], Xiangtao Lin[3], Shuwei Liu[1]*

[1]Research Center for Sectional and Imaging Anatomy, Shandong University School of Medicine, Jinan, China
[2]Department of Medical Imaging, Provincial Hospital Affiliated to Shandong University, Jinan, China
[3]Department of MR, Shandong Medical Imaging Research Institute, Jinan, China

The diagnostic rate of Ventriculomegaly in the prenatal examination is high, mainly due to abnormal central nervous system diseases such as hydrocephalus. The development of lateral ventricle plays an important role in the development of whole fetal brain. This study explores the role of calcarine sulcus in the formation of the lateral ventricle, which can provide some diagnostic basis

for the diagnosis of the ventriculomegaly in clinical work. Fetal brain MRI (3.0T and 7.0T) was performed in 84 fetuses across a gestational age range from 14 to 35 weeks. The lateral ventricle and calcarine sulcus were visualized, and the changes of the lateral ventricle and calcarine sulcus were analyzed. The results show that left calcarine sulcus develops earlier than the right one. The development of the calcarine sulcus increases with the increase of gestational weeks, and no gender difference is detected. The volumes of the lateral ventricles decrease slowly between 14-23 gestational weeks and then increases significantly. Cerebral symmetry and gender difference did not occur in the lateral ventricle volume measurement. With the increase of the depth of the calcarine sulcus, the occipital part of the lateral ventricle is squeezed and the volume decreases accordingly. There is a linear correlation between the depth of the calcarine sulcus and the transverse diameter of the occipital part of the lateral ventricle. The present result is valuable in elucidating the evolution of lateral ventricle development and provides clues for the diagnosis of lateral ventricle abnormality in the prenatal examination.

Key Words：Lateral ventricle, Calcarine sulcus, Fetal brain development, 7.0TMRI, Three-dimentional

O1-7

Three-Dimensional Territory and Depth of the Asian Corrugator Supercilii Regarding to BoNT Injection.

Hyungjin Lee, Young-Jun We, Kang-Woo Lee, Hee-Jin Kim.

Division in Anatomy and Developmental Biology, Department of Oral Biology, Yonsei University College of Dentistry, Human Identification Research institute, BK21 PLUS Project, Seoul, 03722, Republic of Korea.

Facial anatomy is known to be the most important factor when expecting better outcomes following nonsurgical procedures such as BoNT and filler injections. An understanding of the depths of target muscles and of the thicknesses of soft tissues in the area of interest is also significantly important for a successful outcome as it allows the clinician to treat just the target muscle while preventing a diffusion of the adjacent muscle which would lead to unexpected side effects such as paralysis or facial asymmetry. Therefore, the aim of this present study was to provide information regarding the three-dimensional territory and depth of the corrugator supercilii in the forehead area to obtain a satisfactory outcome when performing non-invasive procedures. 31 hemifaces from Korean (12 hemifaces, 12 left; mean age: 79.9 years) and Thai (19 hemifaces, 19 left; mean age 68.6 years) embalmed cadavers were dissected to expose the corrugator supercilii muscle and were scanned by a 3D scanner (Morpheus3D Co.,Ltd). Then, the precise anatomic territory and depth were observed and analyzed from the superimposed images. The corrugator supercilii located consistently on the transected point between the vertical and horizontal line passing through the medial canthus and glabella, respectively. On this point, the depth from the skin to the muscle was 4.7±1.5mm. In addition, the location of the origin of the corrugator supercilii was 15.0±2.1mm superior to the intercanthal line and 7.0mm±1.9 lateral to the midline. The three-dimensional territory and depth of the corrugator supercilii obtained from this study could contribute to successful BoNT injections.

Key Words: Corrugator supercilii muscle, Botulinum neurotoxin injection, Glabellar frown line, Three-dimensional anatomy, Depth of corrugator supercilii

O1-8

Clinical anatomy for the temple augmentation procedures focusing on the depth and location of the deep temporal artery

Hyung-Kyu Bae[1], You-Jin Choi[2], Weeranut Phothong[3], Young-Chun Gil[4], Kyung-Seok Hu[1], Tanvaa Tansatit[5], Hee-Jin Kim[1,6]

[1]Division in Anatomy and Developmental Biology, Department of Oral Biology, Human Identification Research Institute, BK21 PLUS Project, Yonsei University College of Dentistry, Republic of Korea
[2]Department of Anatomy, Yonsei University, College of Medicine, Seoul, Republic of Korea.
[3]Department of Dermatology, Faculty of Medicine, Siriraj Hospital, Mahidol University, Thailand
[4]Department of Anatomy, College of Medicine, Chungbuk National University, Cheongju, Republic of Korea
[5]The Chula Soft Cadaver Surgical Training Center and Department of Anatomy, Faculty of Medicine, Chulalongkorn University, Bangkok, Thailand
[6]Department of Materials Science & Engineering, College of Engineering, Yonsei University Seoul, Republic of Korea.

The temple area is one of the most common sites where filler injections are performed. Since this area is multi-layered and composed of numerous vascular structures, serious vascular complications including blindness can occur due to vascular anastomosis. The aim of this study was to clarify the anatomical features of the deep temporal arteries (DTAs) to optimize the safety and the efficiency during the deep temple augmentation. Thirty-three hemifaces from 20 cadavers (14 males, 6 females; mean age, 79.4) with no history of trauma or surgical procedure on their temple area were dissected for the study. Twenty-two hemifaces were carefully dissected to identify the arterial locations of DTAs with a perpendicular reference line (PL) passing the zygomatic tubercle. Nine hemifaces were dissected to identify the arterial depths of DTAs. Two hemifaces were used to compare two different filler injection methods; the conventional perpendicular approach and the novel oblique bevel-down approach. Both the DTAs were not found in the range of 7.2–12.6 mm lateral from the zygomatic tubercle. In contrast, the locations of the DTAs varied over in wide range at the level of the eyebrow. For the depths of the DTAs, they traveled close to the bone surface as they travel through the temporalis muscle. The DTA depth distribution in the muscle were varied for each specimen. Comparing the two injection methods, the specimens with the perpendicular approach injection revealed a filler deposition at the periosteum and the intramuscular layer whereas the other specimens with the novel oblique bevel-down approach injection demonstrated a rather flat filler deposition only at the periosteal and deep muscular layer. Based on our findings, at the level of the zygomatic tubercle, the area located 1 cm lateral from the PL can be suggested as the safe area for the deep temple augmentation. On the other hand, since the distribution pattern of the DTAs varies at the eyebrow level, oblique bevel-down approach would help locating the bolus most in contact with the periosteum and reducing the vertical piercing effect.

Key Words: Temple augmentation, Filler injection, Temple area, Temporalis, Deep temporal artery, Arterial complication,

O1-9

Submental Artery Passing the Mandibular Border and Its Clinical Implications

Kangwoo Lee[1], Hyun-Jin Park[1], Tanvaa Tansatit[2], Hee-Jin Kim[1]

[1]Division in Anatomy and Developmental Biology, Department of Oral Biology, Human Identification Research institute, BK21 PLUS Project, Yonsei University College of Dentistry, Seoul, 03722, Republic of Korea
[2]The Chula Soft Cadaver Surgical Training Center and Department of Anatomy, Faculty of Medicine, Chulalongkorn University, Bangkok, Thailand

The submental artery (SA) originates from the facial artery and runs on the surface of the mylohyoid muscle along with the border of the mandible. It usually penetrates the mylohyoid muscle and becomes sublingual branch at the mouth floor. In many cases, it is observed that the SA runs anteriorly and pass the border of the mandible to distributes the chin and lower lip. The aim of this study was to elucidate the variational course of the SA to the chin through the border of the mandible to clarify the reason of the of bruising after the injection procedure. Twenty Thai adult embalmed cadaveric faces (12 males, 8 females; mean age: 84 years) were used for the conventional dissections. The variational course of the SA distributing to the chin passing the border of the mandible was observed in nine cases (45%). The location the point passing the border of the mandible was in the side at 8.3±7.5 mm deviated from the midline. The diameter of this vessel was 0.69±0.36 mm. This arterial branch at the chin from SA was communicated with the inferior labial artery or the horizontal labiomental artery (30%). This variational course of the SA at the chin will be helpful in understanding of the cause of bruising after the injection treatment procedure.

Key Words: Submental artery, Inferior labial artery, Horizontal labiomental artery

O1-10

A Bio-anthropological Study of Skeletal Remains from Pallemalala shell Midden in Sri Lanka

Lanka Ranaweera[1] and Gamini Adikari[2]

[1]Department of Anatomy, Faculty of Medicine, University of Kelaniya, Sri Lanka
[2]Postgraduate Institute of Archaeology, University of Kelaniya, Sri Lanka

Sri Lanka occupies a very important place in world archaeology as she possesses the earliest skeletal evidences of anatomically modern human (37,000 B.P.) and the best skeletal record sequence present in South Asia. Adding another to the list, the human skeletal remains, which belong to Mesolithic Culture were found in 1997 at Pallemalala shell midden in Southern Sri Lanka during scientific archaeological investigation under the supervision of Postgraduate Institute of Archaeology, University of Kelaniya. The objectives of this research were to differentiate human bones from animal bones, determine minimum number of human individuals with their age, sex, and pathological conditions. All the osteological materials were in a poor state of preservation and 462 bony fragments were available for the study. Identification of the bones, sex determination and pathology were done

using gross morphological features whereas determination of age was based on teeth eruption, molar wear pattern and epiphyseal fusion. The collection contains abundant human skeletal fragments (233) and animal fragments (229) with some shell species. The minimum number of human individuals for the sample was 7 which includes 5 females and 2 males. The identified age groups were around 20yr, between 35-45yr and above 45 yr. No single indicator of severe disease observed from this population unless some dental pathological conditions such as periodontal diseases, calculus deposits, abscesses and antmortem tooth lost. Pallemalala population was quite healthy and adult population representing more female individuals. Their diet might rich in proteins with fluoride and calcium.

Key Words: Pallemalala, Sri Lanka, Skeletal Remains

Oral Presentation II
-Neuroscience-

31st October, Wednesday
08:45-11:20
Rm323-324

Chairs: Jun Ouyang (China)
Srijit Das (Malysia)
Changman Zhou (China)

O2-1

Recently described telocytes – new interstitial cells for tissue regeneration and homeostasis. Myth or reality?

Varga I[1], Danisovic L[2], Klein M[1] and Kachlik D[3]

[1]Institute of Histology and Embryology, Faculty of Medicine, Comenius University, Bratislava, Slovak Republic
[2]Institute of Medical Biology, Genetics and Clinical Genetics, Faculty of Medicine, Comenius University, Bratislava, Slovak Republic
[3]Institute of Anatomy, Second Faculty of Medicine, Charles University, Prague, Czech Republic

Over the last few years, researchers have been studying telocytes voraciously. It´s documented by more than 300 articles published in Medline/PubMed indexed journals during the last 10 years. Telocytes are currently thought to form three-dimensional networks in various human organs and tissues. They reportedly perform a wide spectrum of functions, such as motility regulation via electrical activity, mediation of intercellular immune signalling, support of tissue regeneration, and promotion of angiogenesis. Our lecture draws attention to the controversies of telocytes focused on the possible discrepancies, confusions and overvalued role of telocytes in human body, in tissue regeneration and in development of different diseases. Importantly, telocytes were discovered only 13 years ago, a very short time from a scientific point of view. This may be the reason that telocytes are not referenced in textbooks or in the internationally accepted nomenclature. Another important reason is that telocytes are a highly controversial topic, research into which frequently produces more questions than answers. Therefore, telocytes are not yet widely accepted as a distinct cell population. The main objective of this lecture is to address the most common, intriguing and debatable questions

about telocytes, which can be summarized into seven classical issues. Confirming telocytes as an individual cell population is important for morphologists, who hesitate to include telocytes in textbooks and incorporate them in the nomenclature. Tissue engineers are interested in the role of telocytes as stem cell 'nurses' and the importance of telocytes in regenerative medicine, where the discovery of a new player could be a game-changer for future therapeutic applications. For histopathologists, the role of telocytes in the pathogenesis of diseases with different aetiologies ('telocytopathies') remains unresolved. Future functional studies of telocytes in vivo will help researchers understand the mechanism by which telocytes contribute to tissue homeostasis.

Key Words: Telocytes, Interstitial Cajal-like cells, Telocytopathies, Histological nomenclature

O2-2

The Effect of Laser Acupuncture on Spatial Memory of the White Rat (*Rattus norvegicus*) Exposed to Chronic Stress

Panji Arga Bintara[1], Selfi Handayani[2], Yunia Hastami[2]

[1]Medical Student, Faculty of Medicine, Universitas Sebelas Maret, Surakarta, Indonesia
[2]Department of Anatomy, Faculty of Medicine, Universitas Sebelas Maret, Surakarta, Indonesia

Introduction: Medical acupuncture is one of the complementary medicine in the medical world that is currently used for medical and psychiatric therapy. Acupuncture is known to increase intelligence and improve cognitive impairment in various pathological conditions. One method of acupuncture is laser acupuncture. This research aims to determine the effect of laser acupuncture on spatial memory of white rats (Rattus novergicus) exposed to chronic stress. **Methods:** This was an experimental quasi laboratory research conducted at the Anatomy and Embryology Laboratory of Faculty of Medicine, Sebelas Maret University. The samples were 24 male white rats (Rattus norvegicus), Wistar strains, grouped randomly into: Control Group (KK), Treatment Group 1 (exposed to acupuncture laser), Treatment Group 2 (exposed to chronic stress), and Treatment Group 3 exposed to chronic stress acupuncture laser). Chronic stress exposure used unpredictable chronic mild stress (UCMS) model for 21 days. Then, it was given acupuncture laser exposure for 14 days. The independent variable in this research was exposure to acupuncture laser, and the dependent variable was spatial memory measured by: Morris Water Maze consisting of Spatial Learning test, Probe test, and sensorimotor test. Data were analyzed by One-way ANOVA test and Kruskal-Wallis test ($α = 0.05$), followed by Post Hoc test. **Result:** One-way ANOVA test on Spatial learning and probe test showed no significant differences between groups ($p > 0.05$), while sensorimotor test showed significant differences between groups ($p = 0.035$). Acupuncture laser can't enhances significant spatial memory in chronic stressful white mice. The results are not significant indicated by spatial learning test and probe test caused by several factors. **Conclusion:** Laser acupuncture can't improve spatial memory of white mice exposed to chronic stress.

Keywords: Acupuncture laser, Spatial memory, Chronic stress, Unpredictable chronic mild stress, Morris Water Maze.

O2-3

Adolescent cocaine exposure causes psychiatric disorders in adulthood: A study on GABAergic transmissions in adult mPFC

Pengbo Shi[1,#], Hou Liu[2,#], Feifei Ge[1,#], Yuehan Li[1], Xu Shen[1], Tifei Yuan[3 *], Xiaowei Guan[1,*]

[1]School of Medicine and Life Sciences, Nanjing University of Chinese Medicine, Nanjing, China
[2]School of Psychology, Nanjing Normal University, Nanjing, China
[3]Shanghai Key Laboratory of Psychotic disorders, Shanghai Mental Health Center, Shanghai Jiaotong University School of Medicine, Shanghai, China

Adolescents are more vulnerable to drugs of abuse than adults. Substance abuse during adolescent period increases the risk of psychiatric disorders in later life, but the underlying molecular mechanisms remain unclear. The present study aims to identify the long-lasting consequences of adolescent cocaine exposure on GABAergic transmission in medial prefrontal cortex (mPFC). Our results here showed that adolescent (P28-42) cocaine exposure enhanced anxiety-like and depression-like behaviors in adult mice, whereas demonstrated intact conditioned place preference (CPP). In addition, a reduced number of c-Fos positive pyramidal neurons were detected at the layer V of adult mPFC, suggesting neuronal hypoactivity following adolescent cocaine exposure. In fact, the synaptic inhibition onto these pyramidal neurons increased. Parallel to changes in inhibitory system, a series of molecule changes were detected, including GABA. An enhanced GABAergic transmission was found in adult mPFC by adolescent cocaine exposure, as indicated by the morphological, electrophysiological and biochemical evidences in this study. Together, these findings provide evidence that adolescent cocaine exposure results in deficits on GABAergic transmission in the mPFC for a long time, even to adulthood, which may contribute to the neuropsychiatric disorders in later life.

Key Words: Adolescent cocaine exposure, GABAergic transmission, Adult mPFC

#Pengbo Shi, Hou Liu and Feifei Ge contribute equally to this work.
*Correspondence to Xiaowei Guan and Tifei Yuan

O2-4

Antidepression Effect of Javanese Music on Stress Rats

Lestari Eliza Handoko[1], Nanang Wiyono[2], Yunia Hastami[2], Muthmainah[2]

[1]Undergraduate Programme, Faculty of Medicine, Sebelas Maret University, Indonesia
[2]Department of Anatomy, Faculty of Medicine, Sebelas Maret University, Indonesia

Stress is one of its cause of depression, and music is now considered as complementary therapy for depression. One of Javanese music, Kebo Giro, is known to be as potential as Mozart's Piano Sonata for music therapy. The aim of this study is to know the effect of Javanese music exposure on depressive behavior in chronic stress-exposed *Rattus norvegicus.* This was a laboratory experiment conducted in Anatomy Laboratory Faculty of Medicine Sebelas Maret University. Samples were 24 male Wistar rats, aged 2 months old and were randomly grouped into: control group (C), treatment group 1 (T1) exposed with chronic stress, treatment group 2 (T2) exposed with chronic stress and classical music, and treatment group 3 (T3) exposed with chronic stress and Javanese music. Chronic stress exposure was using unpredictable chronic mild stress (UCMS) model, were given in the same period as music, both within 21 days. Depressive behavior which were measured as body weight gain, Forced Swim Test (FST), Sucrose Preference Test (SPT). Data was analyzed

with One-Way ANOVA continued with Post Hoc analysis. The results of this study were the mean of body weight gain in C, T1, T2 and T3 were 58.33 ± 6.540 grams, 25.00 ± 5.627 grams, 53.33 ± 5.577 grams, 56.67 ± 3.333 grams respectively   (p = 0.004). The mean of sucrose preference in C, T1, T2 and T3 were 86.95 ± 2.964 %, 57.53 ± 2.460 %, 78.99 ± 3.638 %, 83.72 ± 2.028 % respectively (p = 0.000). The mean of immobility time in C, T1, T2 and T3 were 70.67 ± 14.709 seconds, 187.67 ± 7.641 seconds, 115.83 ± 12.386 seconds, 108.50 ± 18.940 seconds respectively (p = 0.000).   From this research in can be concluded that Javanese music has a potential as antidepression

Key Words: Javenese music, Depression, Sucrose preference test, Forced swim test

O2-5

A Talairach-Tournoux atlas of the hippocampal formation based on the data set of an ultra-high resolution digital human

Liu Weixiang[1], Liu Shuwei[2] and Zhou Shengnian[1]

[1]Department of Neurology, Qilu Hospital Shandong University, Jinan, China
[2]Research Center for Sectional and Imaging Anatomy, Shandong University Cheeloo College of Medicine, Jinan, China.

The purpose of this study is to generate a three-dimensional digital Talairach-Tournoux atlas of the human hippocampal formation (HF) using high-resolution images produced from ultra-thin serial sections and provide morphological basis for the diagnosis and treatment of structural hippocampal lesions. An adult Chinese female cadaver, which was visually examined, computed tomography (CT) and magnetic resonance (MR) scanned to exclude the possibility of craniocerebral lesions, was selected to be sectioned. The entire cadaver was fixed in 10% formalin, frozen at -30°C and serially cross-sectioned at 0.1-mm intervals. High-resolution images (12000 pixels × 8816 pixels) of each cross-section were collected by a line-scan camera. A sequence of 1051 cross-sectional images containing the HF and important adjacent structures (basal nuclei, corpus callosum, lateral ventricle, etc.) was selected and processed for three-dimensional reconstruction. Finally, a volume reconstructed three-dimensional Talairach-Tournoux atlas of adult Chinese female HF was created using OpenGL-based software. The serial sectional images used for three-dimensional reconstruction are of exceptional quality; the display of the atlas is clear and realistic. This atlas provides sagittal, verticofrontal and horizontal view in the Talairach-Tournoux reference system, but also enables the exploration of sectional anatomy of HF and adjacent anatomical structures from any other direction. This atlas will aid medical students and clinicians to acquire a better knowledge of the anatomical structure of HF and its spatial relationship to other anatomical structures, and may be helpful in understanding neurosurgeries of related cerebral regions.

Key Words: Cross-sectional anatomy, Hippocampal formation, Talairach–Tournoux atlas, Digital human

O2-6

The Relationship Between Number of Neuroglia Cells With The Volume of Prefrontal Cortex Ischemia in Rats Brain (*Rattus Norvegicus)* After Transient Bilateral Common Carotid Artery Occlusion (BCCAO)

Ety S. Handayani[1], Nurul Hidayah[2] ,Mislahatil Umami[2]

[1]Departement of Anatomy, Medical Faculty of Universitas Islam Indonesia, Special Region of Yogyakarta, Indonesia
[2]Medical Student of Universitas Islam Indonesia, Special Region of Yogyakarta, Indonesia

One of the examination techniques of ischemia tissue uses 2,3,5-triphenyltetrazolium chloride (TTC) pigmentation. This pigment reacts with the intracellular enzyme LDH. As ischemia tissue experiences neuron damage, LDH level decrease while at the same time result in an increase in the number neuroglia cells. This condition is suspected to influence the pigmentation result of TTC and the volume of rat brain ischemia after transient bilateral common carotid artery occlusion (BCCAO). The aim of the research is to explore the relationship between the number of neuroglia cells with the volume of prefrontal cortex ischemia in rat brains after transient BCCAO. This research used experimental design method known as post-test only control group design. The subjects were 10 male rats (Wistar furrow), that were separated into 2 groups: male rats given a 20 minutes occlusion duration, and a sham-operated group. BCCAO was followed by 2 hours reperfusion. Rat decapitation and collection of the brain was done after 2 hours reperfusion period. Brain tissue sliced into 2 mm samples and pigmented using a 0,05% TTC solution for 30 minutes. Brain ischemia volume was evaluated using *Cavalieri* method. The number of neuroglia was evaluated by histology and prepared with *Toulidin* Blue pigmentation. Statistical analysis was performed using a T-test and linier regression.There was a different mean volume of brain ischemia between the rats in the sham group (1,6 mm^3)   and occlusion group (29,6 mm^3)   (P value 0,005). There was a different mean the number of neuroglia cells in the prefrontal cortex between the sham group (16,8) and 20 minute occlusion group (63,6) (P value 0,000).   The proportion of influence of neuroglia towards the volume of ischemia in rat brains was about 64,3%. BCCAO with 2 hours of reperfusion increased the volume of ischemia and the number of neuroglia cells in the prefrontal cortex of rat brains. The number of neuroglia cells influences the volume of ischemia prefrontal cortex in rats brain after transient BCCAO about 64,3%.

Key Words: Transient BCCAO, Brain Ischemia Volume, The number of neuroglia cells

O2-7

Brain Asymmetry differences between Chinese and Caucasian Populations: A Surface-based Morphometric Comparison Study

Yunxia Lou[1,2], Lu Zhao[3], Shui Yu[4], Bo Sun[1,5], Zhongyu Hou[1,6], Zhonghe Zhang[1,6], Yuchun Tang[1,2*], Shuwei Liu[1,2]

[1]Research Center for Sectional and Imaging Anatomy, Shandong University Cheeloo college of Medicine, Jinan, Shandong, 250012, China
[2]School of Basic Medical Sciences, Shandong University, Jinan, Shandong, 250012, China
[3]Laboratory of Neuro Imaging (LONI), Stevens Neuroimaging and Informatics Institute, Keck School of Medicine of USC, Los Angeles, CA 90032, USA
[4]Department of Radiation Oncology, Shandong Cancer Hospital and Institute, Jinan, Shandong, 250117, China
[5]Shandong Medical Imaging Research Institute, Jinan, Shandong, 250021, China
[6]Department of Medical Imaging, Shandong Provincial Hospital Affiliated to Shandong University, Jinan, Shandong, 250021, China

Asymmetry has been proved to exist in the human brain structure, function and behavior.

This lateralization is thought to originate from hereditary, evolutionary, developmental, cultural and experiential factors. However, most of the current brain asymmetry studies were focused on the brain functions and regional structures, e.g. the language area. Furthermore, most of the extant brain asymmetry findings were originated from the western populations and the studies about the brain structural and functional asymmetries of Chinese people was limited. Extensive evidence suggested that cultural differences e.g. education and language may lead to brain structure and functional differences between various populations. Thus brain structure asymmetry differences may potentially exist between East Asians and Westerners. In this work, using high quality structural magnetic resonance imaging (MRI) data of well-matched right-handed young male adults (age=22-29 years old) from two cohorts, Chinese (n=45) and Caucasian (n=45), we performed a comprehensive surface-based morphometric (SBM) analysis of brain asymmetries in cortical thickness, volume and surface area between the two populations. We revealed the brain structure asymmetry of Chinese people and found that Chinese and Caucasian populations showed different brain asymmetries in the three brain morphological measures in distributed brain regions, including the temporal, frontal, parietal, occipital, insula lobe and cingulate gyrus. More importantly, compared with the Caucasian group, the Chinese group showed greater structure asymmetry in the frontal, temporal, occipital and insular cortices, and smaller asymmetry in the parietal lobe and cingulate gyrus. These findings would provide a new neuroanatomical basis for the distinctions between East Asian and Caucasian in brain functional lateralization.

Key Words: MRI, brain asymmetry, cortical thickness, surface area, cortical volume, surface-based morphometry

O2-8

NSCs transplantation improves learning and memory in the manganese-exposure mice

Hui-Juan Shu, Fang Li, Ping Wang, Jie Tian, Ling Lan, Jian-Gu Gong, Yuan-Yuan Liu, Bo-Ning Yang*, Xiao-Ling Luo*, Guo-He Tan*

[1]Department of Human Anatomy, Guangxi Key Laboratory of Regenerative Medicine & Key Laboratory of Longevity and Aging-related Diseases of Chinese Ministry of Education, Guangxi Collaborative Innovation Center for Biomedicine & School of Preclinical Medicine, Guangxi Medical University, Nanning, Guangxi 530021, China

Chronic Manganese (Mn) exposure usually results in neurological defects, with few effective therapeutic strategies against it. Mn-exposure mice showed space recognition impairment and neurogenesis defect in the dentate gyrus (DG) of mice, however the therapeutical method remains unclear. In this experiment, we have studied the inhibitory effects of neural stem cells (NSCs) transplantation on the pathogenesis of neurological defects after Mn exposure in mice.

The Mn-exposure mouse model were prepared by the two-week $MnCl_2$ administration (20 mg/kg/d, i.p.) and then the histological assays and behavioral tests were performed. After BrdU-labeling, unicell suspension of NSCs was injected into the DG, while the pseudo-transplanted mice were injected with vehicle. We also identified that many of the transplanted NSCs migrated away from the injection sites and survived at least 3 weeks after transplantation.

As a result, the number of nestin-immunopositive cells in SGZ and SVZ was statistically decreased in middle and high-dose manganismus groups, in comparison to the control group, suggesting that manganese exposure inhibits neurogenesis in brain. In the Morris water maze test, the Mn-exposure induced learning and memory impairment was reversed significantly by the NSCs transplantation.

Furthermore, part of the transplanted NSCs in the DG were nestin-positive, while some others were GFAP-, NF-, or NSE-positive in the immunohistochemistry analysis. The results indicate that differentiation of the transplanted NSCs into functional cells might integrate the impaired local circuits, and then provide a possible cellular basis for the improving of Mn exposure-induced memory defect.

Our findings providing a novel strategy against Mn exposure by using intracerebral NSCs transplantation in the DG of mice.

Key Words: Manganese (Mn) exposure, Neural Stem Cells, Learning and memory

*Correspondence to Bo-Ning Yang (E-mail: yangbngx@ sina.com), Xiao-Ling Luo (E-mail: lxllc001@sina.com), Guo-He Tan (tanguohe@gxmu.edu.cn)

O2-9

Differential roles of endodermal signals on Neural crest cells to initiate the middle ear condensations

Harinarayana Ankamreddy[1], Hyehyun Min[1], Jae Yoon Kim[1], Xiao Yang[2], Eui-Sic Cho[3], Un-Kyung Kim[4],, Jinwoong Bok[1,2]

[1]Department of Anatomy, Yonsei University College of Medicine, Seoul, South Korea
[2]State Key Laboratory of Proteomics, Beijing Institute of Lifeomics, Beijing, China
[3]Cluster for Craniofacial Development and Regeneration Research, Chonbuk National University School of Dentistry, Jeonju, South Korea
[4]School of Life Sciences, Kyungpook National University, Daegu, South Korea

Mammalian hearing system consists of outer, middle and inner ears. Middle ear consists of a chain of ossicles: malleus, incus and stapes. These ossicles transmit the sound waves from outer ear to the inner ear in the form of mechanical vibrations. Any developmental defects in the middle ear ossicle can result in conductive hearing loss. These middle ear ossicles are derived from the neural crest cells (NCCs). The NCCs from rhombomere (r) 1 and r2 migrate into pharyngeal arch (PA) 1 to form malleus and incus; and the NCCs from r4 migrate into the PA2 to form stapes. It is still not clear about molecular mechanisms directing the NCCs to their destinations and differentiating into the final target tissue. To examine the roles of Sonic Hedgehog (SHH) or TGF-β signaling on NCC differentiating into middle ear ossicles, a SHH mediator (*Smoothened; Wnt1-Cre;Smo$^{lox/lox}$*) or TGF-β transcriptional mediator (*Smad4; Wnt1-Cre;Smad4$^{lox/lox}$*) was deleted in NCCs. To confirm the sources of these signaling molecules, we also deleted *Shh* (*Foxg1^{Cre};Shh$^{lox/lox}$*) or *Bmp4* (*Foxg1^{Cre};Bmp4$^{lox/Tm1}$*) was deleted in the pharyngeal endoderm. We analyzed gene expression patterns, NCC lineage, cell proliferation and cell death analyses using *in situ* hybridization, *Rosa26* reporter, EdU and TUNEL staining, respectively. When *Smoothened* (*Smo*) gene in the NCCs (*Wnt1-Cre;Smo$^{lox/lox}$*) or *Sonic hedgehog* (*Shh*) in pharyngeal endoderm (*Foxg1^{Cre};Shh$^{lox/lox}$*), malleus-incus condensation was failed to form in the PA1, but not stapes in PA2 at embryonic day (E) 10.5, suggesting endodermal SHH signaling is essential for NCCs to initiate malleus-incus condensation, but not stapes. Interestingly, stapes condensation was lost in both the mutants at E11.5, due to increase in cell death. This demonstrates that SHH signaling is necessary for further development of ossicles through NCC survival. In contrast, when *Smad4* gene in NCCs (*Wnt1-Cre;Smad4$^{lox/lox}$*) or *Bmp4* gene in the pharyngeal endoderm (*Foxg1^{Cre};Bmp4$^{lox/Tm1}$*) was deleted, stapes condensation was failed to form at E10.5, due to lack of NCCs in the prospective stapes region of both the mutants. The malleus-incus condensation was formed in both the mutants. These all results demonstrate that endodermal HH or BMP4 signaling is essential for NCCs to initiate malleus-incus condensation in PA1 or stapes

condensation in PA2, respectively.

Key Words: Endoderm, SHH, BMP4, Neural Crest Cells, Middle ear ossicles

O2-10

Comparing cellular structures and secretory molecules between between adult human multipotent neural cells and brain cancer stem cells

Hyejin Song[1,3,4], Hyun Nam[3,4], Da Eun Jeong[3,4], Sung Soo Kim[2,3,4], Hee Jang Pyeon[1,3], Yoon Kyung Bae[2,3], Jeongseob Won[2,3], Ji Yoon Hwang[1,3,4], So Yeong Cho[1,3], Yu Jeong Noh[1,3], Jee Soo Lee[2,3,4], Kyeung Min Joo[1,3,4]

[1]Department of Anatomy and Cell biology, Sungkyunkwan University School of Medicine, Suwon 16419, South Korea
[2]Department of Health Sciences and Technology, SAIHST, Sungkyunkwan University, Seoul 06351, Korea
[3]Single Cell Network Research Center, Sungkyunkwan University School of Medicine, Suwon 16419, Korea
[4]Stem Cell and Regenerative Medicine Center, Research Institute for Future Medicine, Samsung Medical Center, Seoul 06351, Korea

Neural Stem Cells (NSCs) are located in subventricular zone and subgranular zone, which have capacity of self-renewal and neural differentiation. It has been hypothesized that the origin of brain cancer stem cells (BCSCs) may be derived from NSCs. Despite of the similar characteristics between NSCs and BCSCs, the differences of cellular structures have not yet been compared. Recently, we introduced adult human multipotent neural cells (ahMNCs) derived from temporal lobe of epileptic patients which are comparable to NSC. In this study, we investigated the ultra-structural differences between ahMNCs and BCSCs using electron microscope. Five lines of ahMNCs and four lines of BCSCs were cultured for 3 days. After *in vitro* differentiation with 3-isobutyl-1-methylxanthine (IBMX), cellular structures were observed by scanning electron microscope (SEM) and transmission electron microscope (TEM). As results, the shape, differentiation ratio, and the size of cellular body were similar, which suggested the structural similarities between NSCs and BCSCs. We compared microRNA (miRNA) which were collected by exosomes from NSCs and BCSCs. NSCs and BCSCs showed differential expression of miRNAs. miR-181 was highly expressed in BCSCs compared to NSCs. On the contrary, miR-149 was highly expressed in NSCs compared to BCSCs. We will investigate the reciprocal roles of miR-181 and miR-149 between NSCs and BCSCs in the views of proliferation, apoptosis, and migration. In conclusion, we showed the similar characteristics of cellular ultra-structure between NSCs and BNSCs. However, there were different expression of miRNAs between NSCs and BNSCs which required further investigation about the functional roles of miRNAs and the reciprocal communications between them.

Key Words: ahMNCs, CSCs, Electron microscope, microRNA

O2-11

Inhibitory effects of the enriched environment and radix polygalae treatment on the Aluminum exposure-induced learnning and memory defect in mice

Xue Cheng[1#], Zhong-Xin Guo[1#], Jian-Gu Gong[1], Ling Lan[1], Mei Tang[1], Qiang Huang[1], Xiao-Na Wei[1] ,Guang-Lin He[1], He-Wei Wu[1], Ji-Cong Liu[1], Guo-He Tan[1*], Shao-Ming Huang[1*]

[1]Department of Human Anatomy, Guangxi Key Laboratory of Regenerative Medicine & Key Laboratory of Longevity and Aging-related Diseases of Chinese Ministry of Education, Guangxi Collaborative Innovation Center for Biomedicine & School of Preclinical Medicine, Guangxi Medical University, Nanning, Guangxi 530021, China

Aluminum (Al) exposure is one of the most common occupational diseases, which significantly impairs brain function such as learning and memory. There is few effective therapeutic methods identified currently. In this study, we investigated the effects of the enriched environment and the traditional Chinese medicine radix polygalae on the Al exposure in mice. The Al-exposure mouse model were prepared by $AlCl_3$ solution administration for 40 days. Enriched environment intervention or polygala extract administration were performed during the Al explore. Learning and memory ability was analyzed by Morris water maze test. The expression of the proliferating neural stem cell marker Brdu and the neuron precursor cell marker DCX in SVZ and in SGZ were detected by immunofluorescence analysis. In the Morris water maze test, the high does Al-explore mice (,p.o.) showed longer escape latency compared to control mice from the 3rd day. Since the 5th day, the escape latency of the medium does Al-explore mice (,p.o.) was increased significantly. The increased escape latency in the Al-explore mice was reversed after the enriched environment intervention and polygala extract administration. Additionally, the number of crossing platforms decreased after the Al-explore, either high does or medium does). The enriched environment intervention and polygala extract administration rescued the decreased cross number of the platform in the Morris water maze test. Furthermore, in the immunofluorescence experiment, the expressions of BrdU and DCX in SVZ and SGZ in the Al-exposure mice were lower than those in the control mice. However, both enriched environment intervention and polygala extract administration reversed the decrease expression of BrdU and DCX after the Al explore. These results indicates that Al exposure impairs learning and memory in the adult mice and inhibits the proliferation of neural stem cells and neuronal precursor cells in the brain. Furthermore, enriched environment and polygalae extract can improve learning and memory, and promote neurogenesis in the Al-exposure mice. We demonstrate that the combination of the enriched environment intervention and the Chinese medicine radix polygalae holds great therapeutic potential in treating Al exposure in mice.

Key Words: Aluminum Exposure, Enriched Environment, Radix Polygalae, Learning and memory, Neurogenesis

*Correspondenc to Guo-He Tan (E-mail: tanguohe@gxmu.edu.cn) and Shao-Ming Huang (E-mailshmhuang104@sina.com)

O2-12

Activation of Leptin Receptor-expressing Neurons in Lateral Hypothalamus Enhances Food-seeking without Altering Food Intake in Mice

Younghee Lee[1,2], Dongsoo Ha[1,3], Min Sun Kim[1,2], Ha Young Song[1,2], Cherl NamKoong[1,2], Hyung Jin Choi[1,2]

[1]Functional Neuroanatomy of Metabolism Regulation laboratory, Department of Anatomy, Seoul National Uninversity, College of Medicine, Republic of Korea
[2]BK21Plus Biomedical Science Project, Seoul National Uninversity, College of Medicine, Republic of

Korea

[3]Department of Biological Sciences, KAIST, Republic of Korea

Objective: Our research aimed to identify the food-related behavioral phenotypes that are regulated by leptin receptor-expressing neurons in LHA. **Methods:** We performed food-seeking test, operant conditioning chamber test, overall chow/sucrose/saccharin consumption, preference test and marble burying test. **Results:** We found that chemogenetic activation of LHA leptin receptor neurons only increased 'food-seeking' behavior without altering food intake. However, activation of LHA GABAergic neurons increased both food intake and compulsive behaviors without affecting food-seeking. **Conclusion:** These results suggest that food-seeking is independent from food intake, and LHA leptin receptor neurons are specifically involved in food-seeking behavior that can be targeted to treat eating disorders..

Key Words: Lateral hypothalamus, Chemogenetics, Leptin receptor

Oral Presentation III **-Anatomy Education & Cell Biology-**

31st October, Wednesday
08:45-11:20
Rm325-326

Chairs: Lap Ki Chan (Hong Kong)
Sik Yoon (Korea)
Sookja Kim Chung (Hong Kong)

O3-1

Effectiveness of using Images without Labels during Anatomy Lecture in encouraging Active Learning among students.

Satish R L[1], Tao Ming S[1], Ramya V[1], Bharath RSN[3], Vikaesh M[1], Aishwarya K[2], Lyana S[1].

[1] Department of Anatomy, Yong Loo Lin School of Medicine, National University of Singapore, Singapore
[2]Yishun Junior College, Singapore, [3] School of Medicine, University College Cork, Ireland.

Introduction: In medical education, traditional teaching methods are gradually being supplemented or replaced with new and innovative ones. More interactive forms of teaching are being used to engage students with a hope to increase their knowledge and understanding of the topic taught. In this pilot study, we used arrows with numbers to point to structures in anatomical images on PowerPoint slides which were made available to the students a week prior to the lecture. The educational benefits of this technique were assessed. **Methods:** One hundred and five Life Science students from National University of Singapore were encouraged to participate in this pilot study. Participation in this study was purely voluntary. The teaching session began with an ungraded online

quiz. Subsequently, a printed copy of the answer key to the missing labels was provided to the students. At the end of the teaching session, a survey was conducted to gauge their level of interest and understanding of human anatomy. The survey also asked whether the students preferred this method of interactive teaching and if it was beneficial in their active learning of anatomy. More importantly, the survey sought to find out whether the use of anatomical images without labeling helped the students retain the knowledge they have learnt. **Results:** At the end of the lecture, students were given a 5-point Likert scale questionnaire. The results showed that 78% of the students felt that the missing labels made them more attentive during lectures. Furthermore, 60% of the students indicated better retention of anatomical concepts from the use of missing labels. However, about 49% of the class found it a challenge to study using the PowerPoint Lecture slides without labels. **Discussion:** While some students found it difficult to interpret the anatomical images without labels in the lecture slides, a significant proportion of the cohort found that they were more attentive during the lecture and indicated better assimilation of content. It is hypothesized that students require additional time to get used to learning without labels and will find it easier to study should they be taught with this technique for a longer period of time. Overall, the use of anatomical images without labels was beneficial in the learning of anatomy. A longer-term study would be needed to evaluate whether the students will get used to this mode of teaching. However, given how the students generally retained information better through the use of this technique, I would consider using anatomical images without labels for future lectures.

Key Words: Images without Labels. Active Learning, Human Anatomy, Retention of Knowledge.

O3-2

Exploration and Practice of a Research-based Basic Medicine Experimental Course

Daliang Wang*, Yinyin Wang, Fangli Ren, Xue Li, Xiaoling Liu

Department of Basic Medical Sciences, School of Medicine, Tsinghua University, Beijing, China

The logical thinking, innovation ability and cooperative spirit are the necessary research qualities of medical students. The basic medicine comprehensive experimental course, a research-based lab course, is carried out for second-year medical undergraduate students, which aims to improve the students' ability of knowledge integration and comprehensive research quality. In general, basic medical experiments are often incorporated into different subjects. Students master subject-related experiments separately. Through the creation of innovation course, students properly integrate experimental knowledge and skills of immunology, cellular biology, molecular biology, biochemistry, histology and pathology, etc. into one course, which more simulates a real way of scientific research. Unified teaching center laboratory rooms were provided. Under a general topic and appropriate guidance, students determined experimental designs, analyzed data, made presentation and wrote "manuscripts" by themselves. Twenty students were divided into several groups with 2-3 persons per group. During the experiments, students had division and cooperation. The study found that students in the research-based course had more positive attitudes, higher self-confidence in lab-related tasks, and increased interest in pursuing future research. Compared with traditional experimental teaching scattered in various subjects, students agreed that the course was helpful to improve the logical thinking, the ability of multidiscipline integration, experimental skills, good research habits, and team awareness. In summary, carrying out research-based experimental course is the reform and innovation, which is beneficial to cultivate scientific research qualities of students.

O3-3

Segmenting Students according to Motivation and Perceived Task Performance on the Use of Ultrasound in Anatomy Class: A Q Methodologic Analysis

Ma. Margarita Leticia D. Gellaco[1] , Maria Minerva P. Calimag[2,3,4]

[1]Department of Anatomy, UST Faculty of Medicine and Surgery, Manila, Philippines
[2]Department of Pharmacology, UST Faculty of Medicine and Surgery, Manila, Philippines
[3]Department of Clinical Epidemiology, UST Faculty of Medicine and Surgery, Manila, Philippines
[4]Professorial Lecturer, University of Santo Tomas Graduate School, Manila, Philippines

Medical school educators all over the world face numerous challenges to improve the student's learning processes, among them the need to adapt new technologies into teaching strategies. Ultrasound integration in the medical school curriculum has gained widespread implementation in medical schools all over the world. However, no studies to date have surveyed and examined the learning outcomes on the motivation and learning perceptions of students. The University of Santo Tomas Faculty of Medicine and Surgery is the first medical school in the Philippines to fully integrate ultrasound-based teaching initiatives in its Medical curriculum, beginning academic year 2012-2013. Medical students taking Anatomy classes utilized ultrasound to enhance their knowledge and accuracy in sonologically visualizing anatomical structures and interpreting ultrasound images. In this study, students' opinions and views were used to identify major intrinsic motivators and different learning styles of our students. Four domains were explored, namely autonomy, competence, relatedness, and task value. Using the Q methodology, a research methodology to systematically study subjectivity, three groups of learners emerged namely the acquiescent laggards, the confident adopters and the ambivalent controllers. Results demonstrate distinctions and similarities between the different learning styles but the group of respondents that promoted collaboration and adopted teamwork provided the greatest intrinsic motivators for the learners. This study suggests that medical school educators could use the Q-methodology to individualize and customize their teaching strategies using a learner-focused curricular approach that is adaptable to the learning preferences of the tech-savvy students of the 21st century.

Key Words: Ultrasound integration, Medical curriculum, Intrinsic motivation, Q methodology

O3-4

Creation and use of 3D models in an affordable 3D simulation software for anatomy class

Yang, HeeJun[1], Hyun-Ju Kim[2], SooJung Kim[2], YoungHan Lee[3], Richard G Tunstall[4], HyeYeon Lee[2]

[1]Department of Anatomy, Gachon University College of Medicine, Incheon, Korea
[2]Department of Anatomy, Yonsei University Medical College, Seoul, Korea

[3]Department of Radiology, Yonsei University Medical College, Seoul, Korea
[4]Clinical Anatomy and Imaging, Warwick Medical School, The University of Warwick, Coventry, United Kingdom

Since the emerge of personal computers with high-performance video card, there have been uncountable attempts to teach and learn human anatomy using them. The newest virtual anatomy systems are now with large screens and many useful virtual tools which can be shared via local network. However, the anatomy applications for personal devices are incapable of holding multi-user in same virtual space. In other hand, the large hardware systems for virtual anatomy are so expensive that the teachers and students cannot easily access. Our team set a virtual anatomy learning environment which can be accessed via online with minimal budget. Anatomical image stacks of bones which were taken for diagnostic purpose were converted into 3D surface model and then into 3D voxel models. A virtual world was created by MCJE software which is the client software for the virtual anatomy learning environment. The 3D voxel models of bones were imported into the virtual world and set on proper location, direction and scale so that it was like seeing a set of dismantled human skeletal model. The set of skeletal models was multiplicated as many as the number of students in the anatomy class and the copies were allocated throughout same virtual world. One of the skeletal models was tagged with the names of bones or bony parts to make a demonstration for the students. The virtual world was uploaded to an internet server which were open to the students who had submitted their user IDs for the MCJE software. After the lecture on the skeletal system in the classroom, the students were asked to put tags on bony structures in the virtual world with proper names. The students were asked to answer the questionnaire about using the virtual anatomy environment. The students' performance in the virtual world were various. The teacher could help the students in the online environment instantly. In conclusion, the multi-user virtual anatomy learning environment with various tools to handle the virtual models could be prepared and run in minimal cost and was an enjoyable way to learn human anatomy.

Key Words: Virtual Anatomy, Medical imaging, Multi user online environment

O3-5

Novel histopathologic features of the scalp in androgenetic alopecia

Min Geun Chee[1], Chang Doek Kim[3], Jeung-Hoon Lee[3], Young Ho Lee[2]

[1]Biomedical Research Institute, Chungnam National University Hospital, Daejeon, Korea
[2]Departments of Anatomy, College of Medicine, Chungnam National University, Daejeon, Korea
[3]Dermatology, College of Medicine, Chungnam National University, Daejeon, Korea

Androgenetic alopecia (AGA) is highly heritable condition and the most common form of hair loss in humans. Although androgens are known to be the primary cause of AGA, the actual mechanism is not known yet. Common histopathologic features of the scalp in AGA are microinflammation of the hair follicles, perifollicular fibrosis, and hyperplasia of the sebaceous glands in the hair follicles in AGA. The aim of this study was to find novel histopathologic features of scalp in AGA. We performed H-E, Fontana-Masson, and Oil red O stains, and immunohistochemistry for brain derived neurotrophic factor (BDNF) in the scalp of AGA. Balding (frontal) scalp was thinner, have fewer adipocytes including lipid around the hair follicles, and more melanin pigments in the dermal papilla (DP) of the hair follicles, compared with non-balding (occipital) scalp. BDNF immunoreactivity was increased in the inner root sheath, not in the DP, in the AGA hair follicles, compared with the non-balding hair follicles. In conclusion, novel histopathologic features suggest that there may be a new mechanism in

pathogenesis of AGA in addition to well-known mechanism, hair growth inhibition through action of androgen receptor in the DP of balding hair follicles.

Key Words: Androgenetic alopecia, Pathogenesis, Histopathology, Adipocytes, Melanin, BDNF

O3-6

Multivitamin and albumin supplementations increases body mass index and mid-upper arm circumference at mother in chieldbearing age and has heterozygous Variant D-327-N SHBG genotype (W/v)

Hardy Senjaya[1], ML Edy Parwanto[2]

[1]Department of   Anatomy, Faculty of Medicine, University of Trisakti, Jakarta, Indonesia
[2]Department of Biology, Faculty of Medicine, University of Trisakti, Jakarta, Indonesia

Body mass index (BMI) as a manifestation of genetic and environmental factors. One of the genetic factors that determine BMI is sex hormone binding globulin (SHBG) polymorphism, whereas multivitamin and protein intake as an environmental factor has an effect on BMI. Intake of nutrients such as multivitamins and proteins is one of the environmental factors needed to maintain maternal health. Objective in this study to investigate of multivitamin and albumin supplementation at Indonesian mother in chieldbearing age and has heterozygous variant D-327-N SHBG genotype (W/v). Mother in chieldbearing age who supplemented of multivitamin and albumin for 6 weeks. Three days repeated food recall and record, anthropometric measurement and genotyping of D-327-N SHBG genetic polymorphism were performed for all subjects. Group I is mother in chieldbearing age who supplemented of multivitamin 1 tablet/day. The multivitamin content in 1 tablet are: vitamin A 2000 SI (1.1 mg), vitamin B-1 1 mg, vitamin B-2 1.2 mg, vitamin B-6 0.08 mg, vitamin B-12 1 mcg, vitamin C 30 mg and vitamin D 200 SI (0.005 mg). Group II is mother in chieldbearing age who supplemented of multivitamin 1 tablet + albumin extract 3 grams/day. Characteristics of the study subjects were: age 25.9±5.7 years, undernutrition with BMI <18.5 kg/m^2 and has variant heterozygous (W/v) SHBG genotypes, total energy intake 1308.15±455.1 kcal/day, protein intake 43.14±17.1 gr/day, fat intake 41.5±19.3 gr/day and carbohydrate intake 190.5±76.4 gr/day. Body weight (BW) for group I before supplementation 38,80±2,68 kg and after supplementation 39,46±2,70 kg (p=0,000), while BW for group II before supplementation 40,92±3.05 kg and after supplementation 41.99±3.44 kg (p = 0,000). BMI for group I before supplementation 16.07±0.75 kg/m^2 and after supplementation 16.34±0.84 kg/m^2 (p=0,000), while BMI for group II before supplementation 18.05±0.49 kg/m^2 and after supplementation 18.53±0.86 kg/m^2 (p=0.000). Muscle mass (MM) for group I before supplementation was 29.54±2.51 kg and after supplementation 30.03±3.10 kg (p=0.14), whereas MM for group II before supplementation was 31.06±3, 16 kg and after supplementation of 31.07±2.72 kg (p=0.462). Mid-upper arm circumference (MUAC) for group I before supplementation 22.29±1.3 cm and after supplementation 22.67±1.30 cm (p=0.01), while MUAC for group II before supplementation 23.63±1.81 cm and after supplementation 24,00±1.39 cm (p=0.000). Supplementation of multivitamin 1 tablet/day or albumin extract 3gr/day for 6 weeks increases BW, BMI and MUAC at Indonesian mother in chieldbearing age and has heterozygous variant D327N SHBG genotypes (W/v).

Key words: Multivitamine, Albumin, BMI, SHBG genetic polymorphism, MUAC.

O3-7

Mutation of the Fas-promoter-670 gene, AA to GA in the normal cervix-epithelial-cells of high risk Indonesian mother: A case report

ML Edy Parwanto[1], Wratsangka R[2], Guyansyah A[2], Kirana[2]

[1]Department of Biology, Faculty of Medicine, University of Trisakti, Indonesia
[2]Department of Obstetry and Gynecology, Faculty of Medicine, University of Trisakti, Indonesia

Background: Normalities of the cervix-epithelial-cells can be determined base on the cell morphology and their nucleus. If one of the cervix-epithelial-cells has gene mutations, it will form mutant clones, further growing, developing and malignant. The Fas-promoter-670 gene is allegedly associated with cervical cancer. **Case Presentation:** A 30-year-old of high risk Indonesian mother (human papillomavirus=HPV infected), has 2 childrens, on April 21th 2016 has followed Pap smear examination with thin prep method. Subjects in this case had normal cervix-epithelial-cells. Characteristics of the cervix-epithelial-cells include cell biometrics among others cell length (CL) 11.06 ± 1.57 µm,, cell width (CW) 8.13 ± 2.14 µm, cell area (CA) 73.74 ± 23.15 µm^2, cell perimeter (CP) 32.62 ± 4.92 µm, nucleus area (NA) 1.40 ± 0.54 µm^2 and nucleus perimeter (NP) 4.30 ± 0.78 µm. Fas-promoter-670 genotype in the lymphocytes-cells is AA (normal= wild type), whereas in the cervix-epithelial-cells is GA (heterozygous mutant). **Conclusion:** Base on characteristic of cell biometrics, cervix-epithelial-cells in high risk Indonesian mother is normal. Genotype of the Fas-promoter-670 gene in the lymphocyte cells is AA, whereas in the cervix-epithelial-cells has mutation to GA.

Key Words: Cervix-epithelial-cells, Fas-promoter-670 gene, Cell biometrics, Cell length, Cell width

*Correspondence to ML Edy Parwanto (E-mail: edyparwanto@trisakti.ac.id, Tel +6221-5672731 ext.2302)

O3-8

Construction of the willed body donation program to facilitate the anatomical education in China: Experience from Peking Union Medical College

Hanlin Zhang[1,2], Kang Chen[1,2], Naili Wang[1,3], Di Zhang[1,3], Chao Ma[1]

[1]Institute of Basic Medical Sciences, Department of Human Anatomy, Histology and Embryology, Neuroscience Center, Chinese Academy of Medical Sciences, School of Basic Medicine, Peking Union Medical College, Beijing 100005, China
[2]Eight-year MD Program, Peking Union Medical College, Beijing 100730, China
[3]National Experimental Teaching Demonstration Center of Basic Medicine, Peking Union Medical College, Beijing 100005, China

The value of anatomic dissection is that it allows students to explore in intricacies of the human body, to construct a three-dimensional mental image of the body, and practice surgical skills pre-clinically. Body donation programs are essential for the moral imperative to replace unclaimed bodies or executed prisoners with donations voluntarily made by the individual, which are the main sources of cadavers used for anatomical dissection in Beijing, China. The willed whole-body donation station of Peking Union Medical College (PUMC) was established in May 1999. In 2000, only one of the cadavers used by the medical students was from the body donation program. Since 2001, all cadavers in anatomic dissection class of PUMC have been from the program. By the end of May 2018, 12,458 registrants have registered in the willed body donation program and 1,510 donors have actually

donated their bodies. The Department of Human Anatomy at PUMC has always insisted that each cadaver was dissected by only four medical students to ensure the quality of dissection courses. Up to now, cadavers from the PUMC willed body donation program can satisfy the medical students' needs on anatomic dissection. Surgical demonstration by experts from Yale University or professors from Department of Surgery is established as the operational course in PUMC. Cooperation with PUMC Hospital has been developed to carry out clinical research and clinical training for anesthetists and surgeons. PUMC Human Brain Bank based on body donation station was founded in December 2012. Until March 2018, 207 brain samples have been collected in PUMC Human Brain Bank. It has become the largest human brain bank in China and relevant research on aging and dementia has been conducted over the past five years. Although facing the problem of administration, legislation and dissemination, we will keep on moving to construct the willed body donation program in PUMC, aiming to become a role model for medical schools in China.

Key Words: Anatomic dissection, Body donation, China, Human brain bank.

O3-9

3D animation and printing models to explain development of the heart

Hyeon-Joo Kim[1], Soo-Jung Kim[1], Hee-Jun Yang[2], Hye-Yeon Lee[1]

[1]Department of Anatomy, Yonsei University College of Medicine, Seoul, Korea
[2]Department of Anatomy, Gachon University College of Medicine, Incheon, Korea

To understand the anatomy of the heart, it is important to know the formation of the loop of heart tube during the development. However, it is not easy to explain the fusion of the heart tubes, looping of the tubular heart and three-dimensional development of interatrial septum with the textbooks and illustrations. We created a 3D animation to show the formation of the heart with Cinema4D software. First, we picked and set a series of important phases of the development. The animation was completed by connecting each point of several phases. The five parts of heart; truncus arteriosus, bulbus cordis, atrium, ventricles and sinus venosus were colored differently for easy discrimination in animation. The 3D animation was showed at front, left and diagonal viewpoints for the better understanding. The 3D animation was reinforced by the 3D printed models of coronal section of the heart at several important phases in the sequence. In addition to the 3D animation and models, we also created 2D animation sequences in coronal view. The 2D animation was focused on the formation of the interatrial septum step by step. A two-step 3D printed model showing septum primum and secundum was created for understanding development of foramen ovale. It is expected that these new comprehensive animations and models as educational materials can provide the students with better understanding of the anatomy and development of heart with great effectiveness.

Key Words: 3D animation, 3D printing, 3D printed model, Education, Heart, Embryology

O3-10

Free regional anatomy book, full of schematics and mnemonics

Beom Sun Chung, Min Suk Chung

Department of Anatomy, Ajou University School of Medicine, Suwon, Republic of Korea

In order for medical students to learn anatomy with comfort, a less burdening book with concise contents is needed, and thus, the authors have elaborated a regional anatomy book that fits the purpose. Only anatomical terms essential for basic cadaver dissection are included, along with both schematics and comics that depict anatomy mnemonics and jokes, and the sentences that are comfortably readable. The electronic book titled "Memory Booster of Regional Anatomy" is available on the homepage (anatomy.co.kr) without payment or registration. By the help of volunteer medical students in Korea, the book's educational effects were evaluated. The book reading time was positively correlated to written examination scores and even to tag examination scores. It was an encouraging result that almost 20% students spontaneously read the book regardless of the lecture and examination. The additional descriptive feedback from the students was both positive and negative. Hopefully, the presented book will function as an alternative resource to help medical students learn anatomy efficiently. For the students, this extremely simplified book needs to be supplemented with other anatomy books.

Key Words: Gross anatomy education, Anatomy cartoons, Book, Internet

O3-11

Influence of Naringenin on hyperglycemia-mediated premature atherosclerosis in type 2 diabetic rat model

Nurul Hannim Zaidun, Zar Chi Thent, Syed Baharom Syed Ahmad Fuad, Mardiana Abdul Aziz, Azian Abd Latiff

Faculty of Medicine, Universiti Teknologi MARA (UiTM), Sungai Buloh Campus, Malaysia

Type 2 Diabetes Mellitus (DM) is one of the risk factors in the development of premature atherosclerosis. Decrease nitric oxide production and increase lipid peroxidation in the state of chronic hyperglycemia deteriorates the vascular morphology. Malaysia is blessed with several kinds of herbs or natural products that ameliorate the chronic disease like DM and its major complications. Naringenin (NG), an active compound found in citrus fruits, was proven to possess multiple therapeutics efficacies such as antidiabetic, antihypertensive and anti-hyperlipidemic properties. However, the vasculoprotective effect of NG towards diabetic premature atherosclerosis was not investigated till date. Hence, we aimed to investigate the effect of NG against vascular complication in type 2 DM rat model. We used 30 adult male Sprague-Dawley rats which were induced with fructose and streptozotocin to develop type 2 DM rat model. Following 4 weeks of DM induction, the animal were randomly divided into five(5) groups (n=6); control (C), NG-treated control(CN), non-treated DM (DM), NG-treated DM (DM-NG) (50mg/kg), and metformin-treated DM (DM-MT). The treatment was continued for 5 weeks. We found that DM-NG group had significantly reduced the diastolic blood pressure and malondialdehyde level in aortic tissue. Under light microscope, loss of endothelial cells in tunica intima, disrupted internal elastic lamina and increased thickness of both tunica intima and media were reverted back to normal in DM-NG group. Transmission electron microscopic analysis showed parallel results with light microscopy where the DM-NG group maintained the normal ultrastructural architecture of endothelial lining. Our findings proved that NG improved the vascular deterioration in T2DM rat model by decreasing the lipid peroxidation. Thus, NG can be used as potential adjunct in managing the premature atherosclerosis due to chronic hyperglycemic state.

Key Words: Type 2 Diabetes Mellitus, Naringenin, Atherosclerosis

<Poster Presentation: Day 1 (29ᵗʰ. Oct. 2018)>

P001

Coexistence of Complete Metopic Suture and Inca Bone in Thai Skulls: Incidence, Morphology and Clinical Applications

Nutcharin Pakdeewong[1*], Yoshiyuki Tohno[1]

[1]Department of Anatomy, Faculty of Medicine, Chiang Mai University, Chiang Mai 50200, Thailand

The incidence of the cranial variations was investigated in human populations worldwide. Some specific variations, such as metopic suture and Inca bone, are of clinical importance since they might be misdiagnosed as skull fractures in patients with traumatic head injury. The purpose of this study is to investigate the incidence and morphology of the metopic suture and Inca bone in Thai skulls. The crania from the skeleton collection of the Department of Anatomy, Faculty of Medicine, Chiang Mai University, were examined. From our observation, 7.3% presented with metopic suture; the incomplete type was found in 6.0% and the complete type was found in 1.3%. Different types of the Inca bone were also detected in 2.0%. Among these, 2 skulls happened to coexist with the complete metopic suture and multiple ossicles. The combination of multiple variations in a single braincase is rare. Therefore, the morphometric data and radiography of both skulls were later recorded. The external morphology of such variations mimicked the skull fracture. The cranial radiographs revealed that the metopic suture and additional bones appeared to have sclerotic margins which cannot be found in fractured skull. The physician should take these variations into account to avoid unnecessary management in patients with a history of head trauma. Concerning its uniqueness, it might also be a useful tool as personal identification in forensic medicine by comparing skulls with the antemortem radiographs.

Key Words: Metopic suture, Inca bone, Skull, Thai

P002

Deviation from a norm: congenital anomalies found in isolated female skeleton from Vadnagar, Gujarat

Veena Mushrif-Tripathy[1], Madhulika Samanta[2]

[1]Department of Archaeology, Deccan College Post Graduate and Research Institute, Pune 411006 India
[2]Superintendent Archaeologist, Temple Survey, Archaeological Survey of India, Madhya Pradesh

The present paper is based on the observations conducted on the female skeleton excavated from the site of Vadnagar, Gujarat. The early historic site of Vadnagar located in Mehsana district is known for its domestic and international trading networks in ancient and medieval India. The skeleton under consideration was excavated in the field season of 2016-17 from a locality called Gaontaal in Vadnagar at the eastern bank of Sharmistha Lake. The skeleton was in an extended burial containing no grave goods *per se* and on the basis of associated pottery and other remains can be dated to the early medieval period. It is complete skeleton and preservation is extremely good. While studying the

skeletal remains, various types of congenital anomalies encountered. The left side cervical foramina of axis are not completely fused and C6 or C7 transverse foramen from the left side is divided into two and for right side foramen is smaller in size. It appears that there are only 6 cervical vertebrae. The skeleton was excavated meticulously and documented properly. There is size discrepancy in the first right and left ribs.   Scapula Secondary Ossification Hypoplasia/Aplasia and ulnar styloid Os/Aplasia are also observed. Other than these there were small rounded bone nodules were encountered during cleaning the area near feet. Other than these morphological variations many oral pathologies were also found. Over all this middle aged female is very interesting. There is need to conduct aDNA analysis for the this individual from ancestry and from the point of view of congenital deformities.

Key Words: Congenital anamolies, Hypoplasia/Aplasia, female, Vadanagar, Early medieval

P003

The cross sections of anatomy over the centuries in Persia

Homayoun Naderian[1], Mohammad Ali Atlasi[1], Mohammad Taghi Joghatei[2], Roya Seyedi Rezvani[3]

[1]Department of Anatomy, Kashan University of Medical Sciences, Kashan, Iran
[2]Department of Anatomy, Iran University of Medical Sciences, Teheran, Iran
[3]Education Developmental Center, Kashan University of Medical Sciences, Kashan, Iran

The initial anatomy base medical documents or evidence have been founded in 2800 BC in Persia. They were in southeastern part of Persia in burned city, where the surgical evidence of eye and skull had been discovered. Medical courses and probably anatomy had being taught in ancient Goundishapour University in 500 AC. Bakhtyashu and Mesue were the teachers who worked and dissected based on the Galan experiences. Several medical books have been translated to Latin and taught in University from the ancient to the modern era in Persia. Anatomy was concentrated and emphasized in some of these books based on the author's interest. The most famous books are as follow. Firdous al Hikmat (Paradise of wisdom) was written by Rabban Tabari in 850 AC. It included 7 parts. The second part is about anatomy and organs. Tabari also concentrated on bone, muscles and the kinesiology of the joints. Kitab al Hawi (Liber Continens) and Kitab al Mansuri were written by the famous Persian physician Rhazes in 900 AC. They are about clinical and surgical anatomy. They are used as references for medical students. Hidayat al Mutaallimin (Guideline for Scholars in Medicine) was written by Ahmad Joveini Bukhari in 978 Ac. Bukhari concentrated on anatomy details and muscles fibers. Also the Persian anatomy terminology is explained in this text. Abbas Ahvazi wrote the Kitab al-Maliki (Royal Book) in 990 AC. The Royal Book is about surgical anatomy. Ahvazi explained the surgical procedures based on anatomy. The Cannon of Avicenna is the most famous medical book in 1000 AC. All parts of this book like the modern books started with anatomy. It should be mentioned anatomy as part of the Liber Continens. Royal Book and Cannon were gathered in one book. This book is preserved in library of Leiden University. The first volume of Zakhireyei Khwarazmshahi by Hakim Jorjani in 1120 AC is completely about anatomy. In this book, Jorjani tried to integrate the theoretical and functional anatomy. Tashrih badan insan (The Anatomy of the Human Body) was written in 1390 AC. Yusuf Ibn Ilyas wrote a book about the human anatomy and used pictures to explain anatomy details. During the five centuries cross sections, 7 famous books which concentrated on clinical and surgical anatomy enhanced medicine in Persia. They made ancient physicians to understand the position of anatomy in medicine.

Key Words: Anatomy text, Ancient anatomy, Anatomy in Persia

P004

Visible Korean: Informative 3D PDF file of 297 head structures

Jin Seo Park[1], Min Suk Chung[2], Yong Wook Jung[1]

[1]Department of Anatomy, Dongguk University College of Medicine, Gyeongju, Republic of Korea
[2]Department of Anatomy, Ajou University School of Medicine, Suwon, Republic of Korea

In the Visible Korean, the sectioned images of whole head (0.1 mm X 0.1 mm sized pixel, 48 bits color) were produced. We decided to make informative 3D models from the sectioned images of head. In the sectioned images of head, 297 structures were segmented using Adobe Photoshop to make segmented images. From segmented images, surface models were reconstructed using Mimics software. After the normal shape of structures in the surface models were verified, the surface models were exported to STL format using Deep Exploration software. All STL files and text or figures of anatomical knowledge were assembled and saved as 3 dimensional (3D) PDF file using Adobe Acrobat. As a result, 3D PDF file including surface models of 297 structures were produced. In the 3D PDF file, surface models of 297 structures could be handled freely in model tree window and anatomical knowledge could be shown in bookmark window and another pages. The 3D PDF file will be helpful in anatomical and clinical education. The original files (sectioned images, STL files, and PDF file) are distributed free of charge at neuroanatomy.kr. From original files, a researcher will be able to make 3D models which they need.

Key Words: Visible Human Projects, Cross-sectional anatomy, Three-dimensional imaging, Anatomic models, Neuroanatomy, User-computer interface

P005

Trifurcation of Sciatic Nerve and Multiple Tendons of Peroneus longus Muscle - A Case Report

Abhinitha P[1], Deepthinath R[2], Sudarshan S[3]

[1]Senior Grade Lecturer, [2] Professor, [3]Associate Professor
Department of Anatomy Manipal Academy of Higher Education, Melaka Manipal Medical College (Manipal Campus) Manipal, India

During routine cadaveric dissection for medical undergraduates, we observed left limb of male cadaver aged 67 year old approximately in which there was trifurcation of sciatic nerve with the trifurcated tendon of peroneus longus muscle.Normally the sural communicating nerve arises from the common peroneal nerve opposite the head of the fibula and joins with the sural nerve. Sciatic nerve instead of dividing into its two terminal branches trifurcated into tibial, common peroneal and sural communicating nerves distal to superior angle of the popliteal fossa. However, in the present case, the sural communicating branch was remarkably thicker than its normal thickness and it arose directly from the sciatic nerve as one of its terminal branch and joined with sural nerve arising from tibial nerve. In addition to the variation of the sciatic nerve it was observed in the lateral compartment of the left lower limb that the peroneus longus muscle divided into three tendons of which the middle tendon joined with the tendon in front at the level of the lateral malleolus. After joining it formed a single tendon

and rest of its course as well as its insertion was normal in the foot. The knowledge of the above variation would be considered useful for clinicians as well as surgeons.

Key Words: Sciatic Nerve, Peroneus longus muscle, Trifurcation, Multiple Tendons

P006

The Characteristics of Osteophyte around Lumbar Vertebral Foramina Associated with Spinal Stenosis

Chaimongkhol Thawanthorn[1], Thiamkaew Atiphoom[1], Pasuk Mahakkanukrauh[1,2,3].

[1]Department of Anatomy, Faculty of Medicine, Chiang Mai University, Thailand
[2]Excellence in Osteology Research and Training Center (ORTC), Chiang Mai University, Thailand
[3]Forensic osteology research Center, Chiang Mai University, Faculty of Medicine, Chiang Mai, Thailand

Low back pain is a common condition that can be caused by vertebral osteophytes. The lumbar spine has the highest prevalence of vertebral osteophyte. Osteophyte formation in the vertebral foramina can lead to spinal stenosis. Spinal stenosis most commonly occurs on lumbar vertebrae because of degenerative changes. Thus, this research studied the characteristics of osteophyte development in lumbar vertebrae foramina and association of osteophyte development with lumbar spinal stenosis. We selected all levels of lumbar spines from dry skeletal bone from 31 to 90 years of age. The total number of subjects was 179. The vertebral foramen was divided into six zones. The prevalence and measurements of the length of osteophytes in the vertebral foramina were obtained, then, descriptive statistics and SPSS 22.0 analyzed the data. Population over 31 years old are at risk to develop osteophytes, especially in the laminal and posterior body zone. The prevalence and length of osteophytes in the posterior body zone were higher than the laminal zone, and higher than the pedicular zone, respectively. In each zone, the highest prevalence of osteophytes was at L5, except for the inferior posterior body zone that the highest prevalence is at L4. The length of osteophyte was also in same direction as the prevalence. The prevalence of osteophytes among six zones of each level were compared, and found, in L1 to L4, the inferior posterior body zone generally had the highest prevalence, except in L5, the superior posterior body zone had the highest prevalence. Moreover, prevalence, as well as length, of osteophytes in lumbar vertebral foramina, of all levels, was positively associated with age. Vertebral osteophytes can develop beginning at 31 years of age. Both prevalence and length were positively associated with age. The posterior body of L4 and L5 had the highest risk of osteophyte formation which is one of the causes of spinal stenosis.

Key Words: Vertebral foramina, Osteophyte, Spinal stenosis

P007

Regression analysis to estimate stature from calcaneus

Deog-Im Im[1], Seung-Ho Han[2]

[1]Department of Nursing, Keimyung University, Daegu, Republic of Korea
[2]Department of Anatomy, Chung-Ang University, Seoul, Republic of Korea

The calcaneus is the largest bone in the foot and founded almost intact in the field. It has distinct characteristics enabling it to be distinguished between sexes and population groups. To estimate stature is an important step in identifying human skeletal remains of unknown origin. One hundred calcanei were extracted from the cadavers which known individual information including sex, age, and height. Ten measurements were taken by digital calipers and analyzed statistically to generate equations. All measurements showed the variable values to be useful for estimating stature. Predictive equations derived from simple regression analysis gave better accuracy than did multiple regression analysis. Maximum length in males and maximum height in females proved the best variables to estimate stature. To compare with previous studies, it was differed from results of South African Whites and Blacks. Previous studies, along with the present one, have shown the usefulness of the calcaneus in estimating stature, and we suggest using it when the long bones of remains are incomplete. These findings emphasize the need for equations to estimate stature forensically that matches the characteristics of particular population groups.

Key Words: Calcaneus, Stature, Regression analysis, Mathematic method

P008

A Rare Association of Superficial Brachioulnar Artery with Palmaris Profundus Muscle-A Case Report.

Gaikwad M R[1], Kumar Ravi P[2], Patnaik M[3]

[1]Additional Professor and Head, [2] Senior Resident, [3]Assistant Professor
[1,2,3]Department of Anatomy, All India Institute of Medical Sciences, Bhubaneswar City, Odisha State, India

Arterial variations in superior extremity are often reported commonly. Superficial arterial variations accounting for 4.2 % of all arterial variations are hazardous during any invasive procedures of the upper limb, from routine intravenous injections to surgeries. Recent studies show that these arterial variations are usually associated with muscular variations, the most common being the inverted palmaris longus or its absence. Palmaris profundus, a rare anomalous variation of palmaris longus has been reported in carpal tunnel syndrome as its tendon was associated with median nerve in the carpel tunnel.   The present study reports a unique variation in the upper limb arterial pattern – the presence of bilateral superficial brachioulnar artery (SBUA) associated with palmarisprofundus arising from the deeper aspect of a fleshy palmaris longus in right side and an abnormal radicle of musculocutaneous nerve to the median nerve in the left side.

Key Words: Superficial brachioulnar artery, Palmaris profundus , Arterial variations, Carpel tunnel, Fleshy palmaris longus

P009

Morphology and structural composition of the lateral ligament of adult human ankle joint

Nyo Nyo Myint[1], Laban Hkawn[2], Lucy Kyaw Mya[3]

[1]Professor and Head, Department of Anatomy, University of Medicine 2, Yangon, Myanmar
[2] Professor and Head, Department of Anatomy, University of Medicine Mandalay, Myanmar
[3] Professor and Head (Rtd), Department of Anatomy, University of Medicine 2, Yangon, Myanmar

The purpose of this study was to observe morphology and measurements of all the components of the lateral ligament of ankle joint. The right and left ankle of 30 human cadavers (22 adult males and 8 females) were dissected and studied the attachment, morphology and measurement of the lateral ankle ligaments. The lateral ligaments of ankle joint (anterior talofibular (ATFL), posterior talofibular (PTFL) and calcaneofibular (CFL) were very strong capsular thickening. The attachments of these 3 ligaments were similar as described by the previous researchers. However, in one adult cadaver the calcaneofibular ligament was originated from anterior edge of distal fibula 7.5 mm posterior from origin of anterior talofibular ligament. In the neutral position of right ankle joint the mean length of the anterior talofibular ligament was 12.13 ± 0.63 mm, the width was 8.35 ± 0.63 mm and the thickness was 2.06 ± 0.15 mm. Mean length of posterior talofibular ligament in neutral position was 14.58 ± 0.72 mm, the mean width was 8.92 ± 0 .50 mm and mean thickness was 2.6 ± 0.43 mm. Mean length of calcaneofibular ligament in neutral position was 14.08 ± 0.45 mm, the mean width was 8.27 ± 0.92 mm and the mean thickness was 2.5 ± 0.5 mm. The mean values of each ligament were not significantly different in right and left side of the foot. Measurements of ligament strain in various position of ankle joint showed that anterior talofibular ligament was maximally strained in planterflexion and inversion. The maximum strain was found in posterior talofibular ligament, when the ankle was dorsiflexed and everted and strain in calaneofibular ligament was increased when the ankle was in dorsiflexion and inversion. The significant difference was present in ATFL between the neutral position and planterflexion with inversion and internal rotation. In CFL, the significant difference was present in between the neutral position and dorsiflexion with inversion. In PTFL, the significant difference was present in between neutral position and dorsiflexion with eversion. The length, thickness and width of each lateral ankle ligament in various positions of ankle joint show no significant difference between right and left foot. In histological observation, the result showed that composition of each lateral ligament of ankle joint (ATFL, PTFL and CFL) were fibroblasts, collagen fibres and elastic fibres. They were considered for the stability of ankle joint and provided for the strength of ankle joint. Fibroblast cells were basic functional structures that synthesize collagen and elastic fibres therefore in case of 1st degree ankle sprain, rest and immobilization were the best management in accordance as literatures. Knowledge of the morphology and structural composition of lateral ankle ligaments could be beneficial for the management of ankle injury. The direct anatomical repair of lateral ligament of the ankle should be chosen as valuable method for management of the chronic ankle instabilities. Measurements of these ligaments were also applicable for tenodesis, replacement therapy with tendons (e.g. peroneus longus tendon, palmaris longus tendon).

P010

The Variations in Morphology and Innervation of Palmaris Longus Muscle in Human Adults

Suu Sanda Aye[1], Htar Htar Aung[2], Nilar Shwe[3], Nyo Nyo Myint[4,]

[1]Associate Professor, Department of Anatomy, University of Medicine 2, Yangon, Myanmar
[2]Htar Htar Aung, Senior Lecturer, Human Biology Division School of Medicine, International Medical University, Malaysia
[3] Professor and Head (Rtd), Department of Anatomy, University of Medicine 1, Yangon, Myanmar
[4] Professor and Head, Department of Anatomy, University of Medicine 2, Yangon, Myanmar

Palmaris longus muscle is gaining popularity for its role in reconstructive, plastic and cosmetic surgeries even though several anatomical abnormalities have been reported. Moreover, it is the most suitable autograft material without producing any residual defects in the donor. Variations in Palmaris longus muscle are clinically significant for hand surgeons. Keeping this in view, dissection of 120 upper limbs of 60 Myanmar adult postmortem autopsies (41 males and 19 females, the average age was between 20-80 years) was carried out at the Department of Forensic Medicine, North Okkalapa General Hospital, Yangon, Myanmar, during the span of three years. During the course of study, 5 types of variations were encountered in 7 forearms (5.83%). They could be categorized as (1) unilateral absence (1.67%), (2) bitendinous palmaris longus muscle with the medial slip of the tendon inserted to the flexor retinaculum, thenar fascia and opponens digiti minimi muscle while the lateral slip continued with the palmar aponeurosis and thenar fascia (1.67%), (3) the central muscle belly with the proximal tendinous origin and a distal tendinous insertion (0.83%), (4) the palmaris longus muscle between the proximal fascia and distal tendon (0.83%) and (5) a palmaris longus tendon separated into 2 slips, 2.5 cm below the muscle tendon junction with the accessory hypothenar muscle arising from the medial slip of the tendon (0.83%). Regarding the innervation, the median nerve was classically distributed to the posterior aspect of palmaris longus muscle by a single branch directly in 57 forearms (48.3%) and by a common branch passing through the flexor carpi radialis muscle in 57 forearms (48.3%). Atypical innervation of palmaris longus muscle by an ulnar nerve was encountered in 4 forearms (3.39%) with 2nd, 3rd and 4th types of variants mentioned above. During this study, the incidence of variations in the form of palmaris longus muscle and tendon including agenesis were 5.83 %. These specific anatomic variations described should be anticipated and recognized by the surgeons when they were needed to be appropriately identified during operation, thus increasing the efficacy and safety of the procedures.

Key Words: Palmaris longus, Variations, Morphology, Innervations, Autograft

P011

Comparison of the joint space in different types of malocclusion using three-dimensional models

Eun-Young Jeon[1], Ji-Hyo Kim[2], Won-Jung Han[3], Jeong-Hyun Lee[1], Jong-Tae Park[1]

[1]Department of Oral Anatomy, Dankook University College of Dentistry, Cheonan, South Korea
[2]Department of Career Education, Dankook University College of Liberal Art, Cheonan, South Korea
[3]Department of Dentomaxillofacial Radiology, Dankook University College of Dentistry, Cheonan, South Korea

Harmonious functioning of the temporomandibular joint (TMJ) is crucial to the correct operation of the masticatory system, which makes ideal positioning of the condyle in the TMJ clinically important (1). In addition, widening or narrowing of the joint space is closely associated with TMJ disorders (TMD). A normal joint space is necessary for free movement of the condyle along with the articular disc (2). The CBCT data of 60 patients with malocclusion were obtained in the DICOM (Digital Imaging and Communications in Medicine) format from a CBCT scanner (Alphard 3030, Asahi, Kyoto, Japan). The DICOM files were imported into Mimics software (Materialise, Leuven, Belgium) for constructing 3D models of the skull. Since the joint space corresponds to an empty space, the Mimics files of the 3D-reconstructed skulls were imported into Free form software (3D Systems, Rock Hill, SC, USA) to allow accurate measurements to be made. Areas corresponding to the condyle, fossa, and joint space were cropped out, and the area corresponding to the joint space was filled to construct a

3D model. In this study we reconstructed the CBCT data of patients with malocclusion of classes I, II, and III as 3D models and measured the joint space at different locations to facilitate comparisons of the spatial properties of the TMJ. A Kruskal-Wallis test was used to analyze the joint space according to different types of malocclusion. Significant differences in the measured left and right joint-space values were found between the three experimental groups: in the anterior joint space (AJS) ($\chi 2=12.473$ and $p=0.002$ on the left, and $\chi 2=7.868$ and $p=0.020$ on the right), superior joint space (SJS) ($\chi 2=18.565$ and $p<0.001$, and $\chi 2=13.937$ and $p=0.001$, respectively), and lateral joint space (LJS) ($\chi 2=8.237$ and $p=0.016$, and $\chi 2=9.463$ and $p=0.009$, respectively). A significant interclass difference was observed for the left medial joint space (MJS) ($\chi 2=11.878$, $p=0.003$). This study found that the measured joint space varied with the type of malocclusion. The obtained results will provide deeper insights into malocclusion and TMJ shapes, and suggest that malocclusion can contribute to TMJ deformation.

Key Words: Joint space, Malocclusion, TMJ, Mimics, Freeform

P012

Anatomical variation in branching pattern of brachial plexus and its clinical significance

G Anwer Khan*[1], Shekhar K Yadav[1], A Gautam[1], S Shakya[1], R Chetri[2]

*[1]Department of Anatomy, Chitwan Medical College, CMC, Bharatpur, Nepal.
[2]Department of Anatomy , College of Medical sciences, CMS, Bharatpur , Nepal

Background: Anatomical variations in the branching pattern of the brachial plexus have been described in humans by many authors; however these have not been extensively catalogued. The aim of the study was to describe and observed anomalies in distribution of the branch (branching pattern) derived from the cord of brachial plexus, both in its supraclavicular and infraclavicular parts. **Methods:** This study included thorough dissection of 60 brachial plexuses which belonged to 30 cadavers (male:female ratio = 28:02) with age range of 20-60 years, obtained from the Department of Anatomy, College of Medical Sciences (CMS-TH), following standard guidelines. **Results:** Out of 60 limbs dissected in present study, Normal branching pattern of the posterior cord was encountered in 52 (86.67%) limbs, the remaining 8 (13.33%) being variants in one form or the other. The upper subscapular nerve, the thoracodorsal nerve, the lower subscapular nerve and the axillary nerve were found to arise normally in 91.66%, 96.66%, 96.66% and 98.33% of the limbs respectively. **Conclusion:** The present study carried out on adult human cadavers revealed some rare variations in the branching pattern of the brachial plexus. These variations are of clinical significance are very useful for the anatomists,radiologists, anesthesiologists, neurosurgeons and orthopedic surgeons and general surgeons.

Key Words: Brachial plexus, Branching pattern, Anatomical variation.

P013

Chondroepitroclearis directly compressing the median nerve in Korean cadaver

Yu-Ran Heo[1], Jongwan Kim[1], Yongwook Jung [2], Jae-Ho Lee[1]

[1]Department of Anatomy, School of Medicine, Keimyung University, Daegu, Korea
[2]Department of Anatomy, College of Medicine, Dongguk University, Gyeongju, Korea

Anomalous muscle slips of pectoralis major have been reported on several cases in the literature. Among these, chondroepitroclearis is an extremely rare aberrant muscular slip originating from the pectoral region. During an educational dissection, chondroepitroclearis was found on the right side in a Korean cadaver. Tendinous muscular slip originated from pectoralis major, crossing the neurovascular bundle in the arm, and inserted onto medial epicondyle of the humerus. Clinical significance of these anomalous slip can cause median nerve entrapment and functionally limited movement of the humerus. We report a case of tendinous chondroepitroclearis and discuss its clinical and embryological significance.

Key Words: Chondroepitroclearis, Pectoralis major, Median nerve, Variation

P014

The optimal incision to avoid sural nerve injury in the sinus tarsi approach for calcaneal fracture: A cadaveric study

Jaeho Cho[1,2], Kwang Rak Park[1], Digud Kim[1], Chang Un Choi[1], Hyung Wook Kwon[1], Jeong Hyun Park[1]

[1]Department of Anatomy & Cell Biology, Graduate School of Medicine, Kangwon National University, Kangwon, Korea,
[2]Department of Orthopedic Surgery, Chuncheon Sacred Heart Hospital, Hallym University of Medicine, Kangwon, Korea

The sinus tarsi approach is one of the most commonly applied minimally-invasive approaches for calcaneal fractures. However, postoperative sural nerve-related problems are still reported with this approach. The purpose of this cadaveric study was to describe the anatomical course of the sural nerve in relation to easily identifiable landmarks during the sinus tarsi approach, and to provide a more practical reference for surgeons to avoid sural nerve injury. Twenty-four foot and ankle specimens in adult cadavers were dissected. The bony landmarks were used in the following reference points: point A, the tip of the lateral malleolus; point B, the lateral border of the Achilles tendon on the collinear line with point A; point C, the posteroinferior apex of the calcaneus; point D, the inferior margin of the calcaneus on the plumb line through point A; and point E, the tip of the fifth metatarsal base. After careful dissection, the distances of the sural nerve to points A and B in the horizontal direction (lines D1 and D2, respectively), points A and C in the diagonal direction (lines D3 and D4, respectively), points A and D in the vertical direction (lines D5 and D6, respectively), and points A and E in the diagonal direction (lines D7 and D8, respectively) were measured. Of the 24 specimens, 12 (50%) were from females and 12 (50%) from males. The median ratio of D1 to D1+D2 (R1), D3 to D3+D4 (R3), D5 to D5+D6 (R5), and D7 to D7+D8 (R7) were 0.37 (range, 0.26-0.50), 0.23 (range, 0.16-0.33), 0.35 (range, 0.25-0.45), and 0.32 (range, 0.20-0.45), respectively. There were no significant differences in all ratios by sex and age. We suggest that the optimal incision to avoid the sural nerve in the sinus tarsi approach for calcaneal fractures is by making a straight incision distally from just distal to the tip of the fibula to the level of the calcaneocuboid joint and almost horizontal to the sole of the foot.

Key Words: Cadaveric study, Calcaneus, Fracture, Incision, Sural nerve, Nerve injury

P015

Anatomical variants of "short head of biceps femoris muscle" associated with common peroneal neuropathy in Korean populations: an MRI based study

Hyung Wook Kwon[1], Jaeho Cho[1,2], Kwang Rak Park[1], Digud Kim[1], Chang Un Choi[1], Jeong Hyun Park[1]

[1]Department of Anatomy & Cell Biology, Graduate School of Medicine, Kangwon National University, Kangwon, Korea,
[2]Department of Orthopedic Surgery, Chuncheon Sacred Heart Hospital, Hallym University of Medicine, Kangwon, Korea

In Asians, kneeling and squatting are the postures that are most often induce common peroneal neuropathy (CPNe). However, we could not identify a compatible compression site of the common peroneal nerve (CPN) during hyper-flexion of knee. To evaluate the course of the CPN at the popliteal area related with compressive neuropathy using MRI scans of healthy Koreans. 1.5-Tesla knee MRI scans were obtained from enrolled patients and were retrospectively reviewed. The normal populations were divided into two groups according to the anatomical course of the CPN. Type I included subjects with the CPN situated superficial to the lateral gastocnemius muscle (LGCM). Type II included subjects with the CPN between the short head of biceps femoris muscle (SHBFM) and the LGCM. We calculated the thickness of the SHBFM and posterior elongation of this muscle, and the LGCM at the level of femoral condyles. In Type II, the length of popliteal tunnel where the CPN passes was measured. The 93 normal subjects were included in this study. The CPN passed through the "popliteal tunnel" formed between the SHBFM and the LGCM in 36 subjects (38.7% Type II). The thicknesses of SHBFM and posterior portions of this muscle were statistically significantly increased in Type II subjects. The LGCM thickness was comparable in both groups. In 78.8% of the "popliteal tunnel", a length of 21 mm to < 40 mm was measured. In Korean population, the course of the CPN through the "popliteal tunnel" was about 40%, which is higher than the Western results. This anatomical characteristic may be helpful for understanding the mechanism of the CPNe by posture.

Key Words: Anatomy, biceps femoris muscle, common peroneal nerve, neuropathy

P016

Morphological characteristics of the posterior malleolar fragment according to ankle fracture patterns: a computed tomography-based study

Chang Un Choi[1], Jaeho Cho[1,2], Kwang Rak Park[1], Digud Kim[1], Hyung Wook Kwon[1], Jeong Hyun Park[1]

[1]Department of Anatomy & Cell Biology, Graduate School of Medicine, Kangwon National University, Kangwon, Korea,
[2]Department of Orthopedic Surgery, Chuncheon Sacred Heart Hospital, Hallym University of Medicine, Kangwon, Korea

The posterior malleolar fragment (PMF) of an ankle fracture can have various shapes depending on the injury mechanism. The purpose of this study was to evaluate the morphological characteristics of the PMF according to the ankle fracture pattern described in the Lauge-Hansen classification by using computed tomography (CT) images. We retrospectively analyzed CT data of 107 patients (107 ankles) who underwent surgery for trimalleolar fracture from January 2012 to

December 2014. The patients were divided into two groups: 76 ankles in the supination-external rotation(SER) stage IV group and 31 ankles in the pronation-external rotation (PER) stage IV group. The PMF type of the two groups was assessed using the Haraguchi and Jan Bartonicek classification. The cross angle (α), fragment length ratio (FLR), fragment area ratio (FAR), sagittal angle (θ), and fragment height (FH) were measured to assess the morphological characteristics of the PMF. The PMF in the SER group mainly had a posterolateral shape, whereas that in the PER group mainly had a posteromedial two-part shape or a large posterolateral triangular shape (P = 0.02). The average cross angle was not significantly different between the two groups (SER group = 19.4°, PER group = 17.6°). The mean FLR and FH were significantly larger in the PER group than in the SER group (P = 0.024, P = 0.006). The mean fragment sagittal angle in the PER group was significantly smaller than that in the SER group (P = 0.017). With regard to the articular involvement, volume, and vertical nature, the SER-type fracture tends to have a smaller fragment due to the rotational force, whereas the PER-type fracture tends to have a larger fragment due to the combination of rotational and axial forces.

Key Words: Ankle fracture, Computed tomography, Posterior malleolar fragment, Morphology

P017

The safe zone for avoiding sural nerve injury in medial displacement calcaneal osteotomy: A cadaveric study in Korean populations

Kwang Rak Park[1], Jaeho Cho[1,2], Digud Kim[1], Chang Un Choi[1], Hyung Wook Kwon[1], Jeong Hyun Park[1]

[1]Department of Anatomy & Cell Biology, Graduate School of Medicine, Kangwon National University, Kangwon, Korea,
[2]Department of Orthopedic Surgery, Chuncheon Sacred Heart Hospital, Hallym University of Medicine, Kangwon, Korea

Medial displacement calcaneal osteotomy(MDCO) is a method of surgical correction of the hindfoot valgus and its usefulness is reported in many literature and is generally selected by the majority of surgeons. The sural nerve is distributed on the surface of the of the lateral aspect of the hindfoot and travels along the outer margin of the Achilles tendon, moving away from the Achilles tendon while running about 10cm downward from the heel pad on proximal side. Thus, the sural nerves are vulnerable during an incision for the MDCO. In present study, we hypothesized that identification of the anatomy of the sural nerve in accordance with easily identifiable bony land-marks may minimize the risk of nerve injury during surgical approach for MDCO. Twenty-four foot and ankle specimens in adult cadavers were dissected. Of the 24 specimens, 12(50%) were from females and 12(50%) from males. The bony land-marks were used in the following reference points: A, the tip of the lateral malleolus; point B, the lateral border of the Achilles tendon on the collinear line with point A; point C, the posteroinferior margin of the calcaneus; and point D, the inferior margin of the calcaneus on the plumb line through point A. After careful dissection, the distances of the sural nerve to points A and B in the horizontal direction(lines D1 and D2, respectively), to points A and C in the diagonal direction (lines D3 and D4, respectively), and to points A and D in the vertical direction (lines D5 and D6, respectively) were measured. The median ratio of D1 to D1+D2, D3 to D3+D4, and D5 to D5+D6 were 0.37 (range 0.26 to 0.50), 0.23 (range 0.16 to 0.33), and 0.35 (range 0.25 to 0.45), respectively. There were no significant differences in all measurements by gender and age. In previous study with 20 Chinese cadaveric specimen, Chinese authors suggested that it is relatively safe to make an oblique incision that runs through the point that is no less than one third of the distance from the tip of the lateral malleolus to the posteroinferior margin of the calcaneus. Compared to previous data, our results had no significant difference. Thus, we also suggest that the safe zone for avoiding sural nerve injury

during MDCO in korean populations is one third of the distance from the lateral malleolar tip to the posterior inferior margin of the calcaneus.

Key Words: Cadaver, Calcaneus, Sural nerve, Osteotomy

P018

Unusual variant of distal biceps femoris muscle associated with common peroneal entrapment neuropathy: A cadaveric case report

Digud Kim[1], Jaeho Cho[1,2], Kwang Rak Park[1], Chang Un Choi[1], Hyung Wook Kwon[1], Jeong Hyun Park[1]

[1]Department of Anatomy & Cell Biology, Graduate School of Medicine, Kangwon National University, Kangwon, Korea,
[2]Department of Orthopedic Surgery, Chuncheon Sacred Heart Hospital, Hallym University of Medicine, Kangwon, Korea

The common peroneal nerve (CPN) is the lateral division of the sciatic nerve and it courses from the posterolateral side of the popliteal area around the biceps femoris tendon and the fibular head. 1,2 These anatomical features contribute to the vulnerability of the peroneal nerve to damage around the knee. The most frequent mononeuropathy in the lower extremity has been reported as the common peroneal nerve entrapment neuropathy (CPNe) around the fibular head and neck. 3 Vieira et al. investigated the course of the CPN between popliteal muscles, including the short head of biceps femoris muscle (SHBFM) and the lateral gastrocnemius muscle (LGCM) using magnetic resonance images (MRI). 4 They proposed the possibility of anatomical variation of distal femoris muscle related to the CPNe by entrapment or compression. However, this study had limitation of the lack of cadaveric correlation as a result based on MRI. Herein, we reported a case of unusual variant of distal biceps femoris muscle associated with CPNe in Korean cadaver for first time and discussed its clinical significance.[a]

Key Words: Anatomy, Biceps femoris muscle, Common peroneal nerve, Neuropathy

P019

The distributed pattern of the neurovascular structures under clavicle to minimize structural injury in clinical field: anatomical study

Je-Hun Lee[1], Anna Jeon[2], Seung-Ho Han[2]

[1]Anatomy Laboratory, College of Sports Science, Korea National Sport University, Seoul, Korea
[2]Department of Anatomy, Chung-Ang University, Seoul, Korea

The clavicle is one of the most commonly fractured bones in the human body. Fractures of the clavicle account for 5%–12% of all fractures and 35–44% of injuries to the shoulder girdle. Approximately 81% of these fractures occur in the middle third of the clavicle and are usually accompanied with displacement by the deforming forces from the muscular attachments. These fractures can often be managed by an arm sling or splint with pain medicine; however, the nonoperative management of all clavicular fractures has not good outcomes such as high rates of

nonunion and symptomatic malunion with shortening. Open reduction and internal fixation (ORIF) for a clavicle fracture is performed for a displaced fracture; the pieces of broken bone are not lined up correctly. During an open reduction, the bone pieces back into their proper alignment; then, the bones are connected back in place with hardware, it is called internal fixation. ORIF of clavicle still has potential complications, there are few references to the neurovascular structures of the clavicle. However, the delicately dissected study, even small nerve and vessels are investigated, are difficult to find.   This study was investigated the location and distributed pattern of the neurovascular structures existing superior and inferior of clavicle by detailed dissection.

Key Words: Clavicle fracture, Internal fixation, Supraclavicular nerve, Thoracoacromial artery, Subclavian vein, Anatomy

P020

A unique case of an accessory sartorius muscle

Soo-Jung Jung, Jongwan Kim, Jae-Ho Lee

Department of Anatomy, School of Medicine, Keimyung University, Daegu, Korea

The sartorius muscle (SM) is a long strap muscle originating from the anterior superior iliac spine and inserting onto the medial surface of the proximal tibia. It crosses the anterior compartment of the thigh obliquely and descends towards the medial aspect of the knee. We found an accessory sartorius muscle (ASM) from the inguinal ligament and an original SM bifurcated into medial and lateral heads. The ASM merged with the medial head of the SM and inserted on the medial aspect of the tibia as the pes anserinus. The lateral head of the SM continued inferiorly and inserted on the medial aspect of the patella. We report a unique variation in the morphology of the SM and discuss its functional and clinical implications.

Key Words: Accessory muscle, Sartorius muscle, Thigh muscle, Variation

P021

Morphological significance of the thickness distribution in the gluteus medius tendon with regard to the gluteus medius tendon tears

Masahiro Tsutsumi[1], Akimoto Nimura[2], Keiichi Akita[1]

[1]Department of Clinical Anatomy, Tokyo Medical and Dental University, Tokyo, Japan
[2]Department of Functional Joint Anatomy, Tokyo Medical and Dental University, Tokyo, Japan

Tears of the gluteus medius tendon have been recognized as the potential cause of the lateral hip pain. Despite this, the etiology of these tears and the anatomical background of the gluteus medius tendon remain unclear. Our hypothesis is that the tendinous portions of the gluteus medius itself have the non-uniform structure which contributes to the etiology of the tears. The aim of this study was to examine the three dimensional structure of the gluteus medius tendon. In total of 25 hips from 15 Japanese cadavers, we macroscopically and histologically analyzed 22 and 4 sides, respectively. In all specimens, the three-dimensional morphology of the greater trochanter was examined using micro-

computed tomography (micro-CT: inspeXio smx-100ct, SHIMADZU, Kyoto, Japan). In 10 sides, the thickness distribution of the gluteus medius tendon detached from the greater trochanter were analyzed by micro-CT and the Image J software (version 1.51; National Institutes of Health, Bethesda, MD). Two parts of the gluteus medius tendons, posterior and anterolateral ones, were roughly distinguished based on the aspects of the iliac origins. The posterior part of the gluteus medius tendon ran with a fan-like shape and converged into the posterosuperior facet of the greater trochanter. The anterolateral part ran posteroinferiorly toward the lateral facet of the greater trochanter. These facets of the greater trochanter were identified by the micro-CT before detaching the gluteus medius tendon from the greater trochanter. On the basis of the analysis of the thickness distribution in the gluteus medius tendon, the posterior part was significantly thicker than the anterolateral part. In addition, the border between the 2 parts was identified as the thin region. The histological study showed that both of the 2 parts inserted into the greater trochanter via the fibrocartilage. In conclusion, the gluteus medius tendon consisted of thick posterior and thin anterolateral parts, which were identified by the facet or aspect of the bone structures and thinness of their border region. Given the non-uniform structure of the gluteus medius tendon, the anterolateral part may be associated with the tears of the gluteus medius tendon, which may be limited to the anterolateral part.

Key Words: Gluteus medius tendon, Greater trochanter, Morphology, Thickness distribution

P022

The morphometric study of the inferior peroneal retinaculum and contents of inferior peroneal tunnel

Dangintawat P[1], Apinun J[2], Huanmanop T[3], Agthong S[3], Chentanez V[3]

[1]Ph.D student in Medical Science Program, Faculty of Medicine, Chulalongkorn University, Bangkok, Thailand
[2] Department of Orthopedics, Faculty of Medicine, Chulalongkorn University, Bangkok, Thailand
[3] Department of Anatomy, Faculty of Medicine, Chulalongkorn University, Bangkok, Thailand

The inferior peroneal retinaculum (IPR) had a vital role to stabilize the peroneal tendons fitting in their positions. However, the anatomy of the IPR has not been well explored. Furthermore, the standard anatomy textbooks had described very few about the IPR. Although the incidence of the IPR injury was sporadic, the tear of this retinaculum had been reported as well. One hundred and nine embalmed cadaveric legs were dissected in prone position. The ankle was adjusted into neutral position. The length, width at the origin, width at the middle part, width at the insertion, angle of the IPR to the horizontal axis and thickness of the IPR were measured. The contents of the inferior peroneal tunnel were explored and noted. The IPR was the continuity of the inferior extensor retinaculum. It coursed posterior and inferiorly to attach on the peroneal tubercle and the lateral wall of the calcaneus. The extension of the IPR band from the lateral wall of the calcaneus to the lateral process of the calcaneus was found in 29.36% of cases. The length, width at origin, width at middle part, width at insertion, and thickness of IPR were 23.42 ± 3.54 (17.05 - 33.68), 13.63 ± 4.22 (5.83 - 48.17), 14.50 ± 2.37 (6.68 - 21.34), 10.10 ± 2.63 (4.59 - 19.17) and 0.48 ± 0.16 (0.20 - 0.87) mm, respectively. The angle of IPR to the horizontal axis was 38.51 ± 7.07 (11.67 - 54.00) degrees. The inferior peroneal tunnel was composed of the IPR as its roof and was divided into the upper and lower tunnels by its attachment to the peroneal tubercle which served as the septum. The tendons of peroneus brevis and peroneus longus were lodged in the upper and lower tunnel respectively. The additional content in the upper tunnel was the peroneus digiti quinti muscle. In addition, there were two cases of the peroneus quartus inserted at the septum in the lower tunnel. Moreover, an unusual

accessory peroneal muscle tendon coursed into the lower tunnel and inserted on the peroneal tubercle. The morphometric data of the IPR and the extension of the IPR band to the lateral process of the calcaneus, the information and contents of the inferior peroneal tunnel were reported. These findings might be beneficial in the surgical procedure of the IPR injury.

Key Words: Inferior peroneal retinaculum, Inferior peroneal tunnel, Peroneal tubercle

P023

Mechanical properties of the ligament of the head of femur *in situ*

<u>Vivek Perumal</u>[1], Niels Hammer[1,2,3], Mario Scholze[1,4], Stephanie Woodley[1], Helen Nicholson[1]

[1]Department of Anatomy, School of Biomedical Sciences, University of Otago, Dunedin, New Zealand
[2]Department of Trauma, Orthopedic and Plastic Surgery, University Hospital of Leipzig, Leipzig, Germany
[3]Fraunhofer Institute for Machine Tools and Forming Technology, Dresden, Germany
[4]Institute of Materials Science and Engineering, Chemnitz University of Technology, Chemnitz, Germany

Background: The ligament of the head of femur (LHF) is reported to serve a mechanical stabilising function at the hip joint. Clinically, LHF injuries have a higher incidence in females and in the right hip compared to the left. However, there is no evidence of structural differences of the ligament between men and women or left and right hips. **Aim:** Our study aimed to quantify the mechanical properties of the LHF *in situ under tensile stress*, and to examine potential differences between sex, side, and two physiological joint positions. **Methods:** Twenty-five cadaveric hips were dissected *en bloc* (mean age 85.7 ± 7.5 years; 9 females, 4 males; 13 left, 12 right). The acetabula were cast in resin blocks and mounted onto a mechanical testing machine with the femoral shafts either in a neutral position ($0°$) or $20°$ adduction. A distraction test was performed on the femoral shaft following transection of the capsular ligaments of the hip joint, applying stress to the LHF. The force required to rupture, the initial, yield and failure lengths and the strain of each ligament were documented. Following the experiments, the cross-sectional area of the LHF was obtained from histological sections at their mid-length from which the tensile strength and elastic modulus were computed. Statistical analyses were conducted to compare the mechanical properties of the LHF between sex, side and joint position. **Results:** The mean force required to rupture the LHF was 57 ± 37N (range 3 to 186N). Initial, yield and failure lengths of the LHF averaged 25 ± 5, 40 ± 10 and 64 ± 14 mm, respectively; the mean strain was $59 \pm 33\%$. The mean tensile strength was 3 MPa and the elastic modulus averaged 7 MPa. LHF length at failure was significantly greater in males compared to females (p=0.02). There were no statistical differences in the mechanical properties between females and males nor left or right LHF, irrespective of joint position. **Discussion:** Previous biomechanical studies of the LHF have used younger specimens and mostly tested the rupture force in isolated ligament tissue. Compared to those results, our study using specimens obtained from elderly cadavers showed lower tensile strength and force required to rupture. This finding suggests that these mechanical properties could be age dependent, with an inverse relationship between age of the individual and force needed to rupture the LHF. Mechanical testing did not explain the higher incidence of LHF injuries in females or on the right side in the given small sample size. There could be other anatomical and demographic factors that render the ligament tissue vulnerable to injury in these groups.

Key Words: Ligament, Head of femur, Ligamentum teres, Hip joint, Biomechanics, Mechanical

properties, Tensile strength, Elastic modulus.

P024

Observation of fetal heart veins draining directly into the left and right atria

Ji Hyun Kim[1, 2], Gen Murakami[3], Hiroshi Abe[4], Su Hwan Choi[1], Ok Hee Chai[1, 2], Chang Ho Song[1, 2]

[1]Department of Anatomy, Chonbuk National University Medical School, Jeonju, Korea
[2]Institute of Medical Sciences, Chonbuk National University, Jeonju, Korea
[3]Division of Internal Medicine, Sapporo Asuka Hospital, Sapporo, Japan
[4] Department of Anatomy, Akita University School of Medicine, Akita, Japan

Evaluation of semiserial sections of 14 normal hearts from human fetuses of gestational age 25–33 weeks showed that all of these hearts contained thin veins draining directly into the atria (maximum, 10 veins per heart). Of the 75 veins in these 14 hearts, 55 emptied into the right atrium and 20 into the left atrium. These veins were not accompanied by nerves, in contrast to tributaries of the great cardiac vein, and were negative for both smooth muscle actin (SMA) and CD34. However, the epithelium and venous wall of the anterior cardiac vein, the thickest of the direct draining veins, were strongly positive for SMA and CD34, respectively. In general, developing fibers in the vascular wall were positive for CD34, while the endothelium of the arteries and veins was strongly positive for the present DAKO antibody of SMA. The small cardiac vein, a thin but permanent tributary of the terminal portion of the great cardiac vein, was also positive for SMA and CD34. A few S100 protein-positive nerves were observed along both the anterior and small cardiac veins, but no nerves accompanied the direct drainage veins. These findings suggested that the latter did not develop from the early epicardiac vascular plexus but from a gulfing of the intratrabecular space or sinus of the atria. However, the immunoreactivity of the anterior cardiac vein suggests that it originated from the vascular plexus, similar to tributaries of the great cardiac vein.

Key Words: Great cardiac vein, Anterior cardiac vein, Venae cordis minimae, Smooth muscle actin, CD34, Human fetuses

P025

Morphology of human corpus callosum in Iranian population - An imaging anatomical study

Atlasi M.A, Talari H, Toufighi M, Naderian H

Anatomical Sciences Research Center, Kashan University of Medical Sciences, Kashan, Iran.

Topography of the human corpus callosum has occasionally studied in different populations. The purpose of this study was to evaluation the morphology of human corpus callosum in Iranian population via magnetic resonance imaging. Design of the study was retrospective cross-sectional study. Seven hundred and seven normal magnetic resonance imaging (MRI) were enrolled to our study. The shape, anterior-posterior length and area of corpus callosum as well as their relationship with gender, age, and handedness were assessed. The most common and uncommon form of corpus callosum were splenial bulbosity form (35.6%) and arch mid-body form (7.2%) respectively. Maximum

anterior – posterior (AP) distance of corpus callosum was longer in male and older age individuals compared to female and younger ones respectively. No significant differences were seen in AP distance of corpus callosum between right and left handers. Area of corpus callosum was widened in male and younger age individuals compared to female and older ones respectively. The findings of this study show morphology of corpus callosum in Iranian population. Morphometric parameters of AP and area of corpus callosum are related to sex and age but no to handedness.

Key Words: Morphology, Corpus callosum, MRI, Human

P026

Cerebral blood vessels and Dementia

Patcharaporn Srisaikaew[1], Pasuk Mahhakranukrauh[1,2,3]

[1]Department of Anatomy, Faculty of Medicine, Chiang Mai University, Thailand
[2]Excellence in Osteology Research and Training Center (ORTC), Chiang Mai University, Thailand
[3]Cadaveric Surgical Training Center, Chiang Mai University, Faculty of Medicine, Chiang Mai, Thailand.

Transient ischemic attack (TIA) of the fornix causes a spectrum of memory deficits, which increases the contributions of vascular disease to dementia called early-onset dementia. Several studies showed that approximately 30% of the global population is more likely to develop onset-dementia within six months after the TIA and/or stroke episode and had ten times higher risk than who had no history of TIA and/or stroke. As the fornix, the white matter bundle, serves the major efferent pathway connecting the hippocampus with other human limbic structures, a variety of lesions that damage the fornix could lead to significant memory impairment. Twenty-five fresh human cadaveric heads were used. According to the abilities of formaldehyde and latex solutions, the formaldehyde solution fixation and latex solution injection methods were used to study the anatomy of the fornix and to visualize the branches of the cerebral vasculature, respectively. After review of literature and preliminary studies, it was discovered that formaldehyde solution provided excellent results in fixation method since brains were maintained in the initial condition and no changes were noticed. In coloration method, latex solution could render the visualization of the branches of the vasculature by penetrating into small vessels. Therefore, these aforementioned methods are suitable for studying white matter dissection in cadaveric heads. Moreover, the result showed that the posterior choroidal arteries (PChA) branches anastomoses with the choroidal arteries are supplying crus and body of the fornix counting as 80% of cases. And 40% of cases showed the anterior choroidal arteries (AChA) branches are supplying fimbria of the fornix, the beginning part. These findings provide anatomical knowledge to all researchers, patients and neurosurgeons.

Key Words: Cadaveric heads, Formaldehyde solution, Latex solution, Fornix, Cerebral vasculature, White matter, Dementia

P027

Brain structure differences between Chinese and Caucasian cohorts: a comprehensive morphometry study

Yuchun Tang[1,2], Lu Zhao[3], Yunxia Lou[1,2], Yonggang Shi[3], Rui Fang[1], Xiangtao Lin[1,4], Shuwei Liu[1,2],

Arthur Toga[3]

[1]Research Center for Sectional and Imaging Anatomy, Shandong University Cheeloo College of Medicine, Jinan, Shandong 250012, China
[2]School of Basic Medical Sciences, Shandong University, Jinan, Shandong 250012, China
[3]Laboratory of Neuro Imaging (LONI), Keck School of Medicine of USC, Los Angeles, CA 90032, USA.
[4]Shandong Medical Imaging Research Institute, Jinan, Shandong 250021, China

Numerous behavioral observations and brain function studies have demonstrated that neurological differences exist between East Asians and Westerners. However, the extent to which these factors relate to differences in brain structure is still not clear. The anatomical differences in brain structure play a primary and critical role in the origination of functional and behavior differences. To investigate the underlying differences in brain structure between the two cultural/ethnic groups, we conducted a comparative study on education-matched right-handed young male adults (age=22-29years) from two cohorts, Han Chinese (n=45) and Caucasians (n=45), using high-dimensional structural magnetic resonance imaging (MRI) data. Using two well-validated imaging analysis techniques, surface-based morphometry (SBM) and voxel-based morphometry (VBM), we performed a comprehensive vertex-wise morphometric analysis of the brain structures between Chinese and Caucasian cohorts. We identified consistent significant between-group differences in cortical thickness, volume and surface area in the frontal, temporal, parietal, occipital, and insular lobes as well as the cingulate cortices. Our findings systematically revealed comprehensive brain structural differences between young male Chinese and Caucasians, and provided new neuroanatomical insights to the behavioral and functional distinctions in the two cultural/ethnic populations.

Key Words: Brain structure, MRI, Neuroimaging, Cultural difference, Morphometry, Brain mapping

P028

Nerve distribution pattern of the inferior oblique muscle and its clinical implication

Je-Sung Lee, Shin-Hyo Lee, Tae-Jun Ha, Ki-Seok Koh, Wu-Chul Song

Department of Anatomy, Research Institute of Medical Science, Konkuk University School of Medicine, Seoul, Korea

This study aimed to determine the intramuscular distribution and branching patterns of oculomotor nerve within the inferior oblique muscle (IO) using Sihler's staining. Thirty-five IOs from 27 formalin-embalmed cadavers were investigated. The IO including the branch of oculomotor nerve was finely dissected from its origin to its insertion point into the sclera. The total length of the muscle, muscle width, and distance from the muscle insertion to neuromuscular junction measured. The intramuscular nerve course was investigated after performing Sihler's staining. In addition, arterial distribution pattern of muscle was observed in six IO specimens. The total length of the muscle, muscle width, and distance from the muscle insertion to neuromuscular junction were 30.2 mm, 9.2 mm, 16.9 mm, respectively. The oculomotor nerve enters the muscle around the middle of the IO and then divides into multiple smaller branches without distinctive neuromuscular compartment. The intramuscular nerve distribution within the IO has a root-like arborization and supplies the entire IO width. The intramuscular nerve course (mean length 7.4 mm) finished around the one-third of distal part of IO. Additionally, the arterial blood supply of IO emerged from the muscle origin and typically divided into 3 smaller branches. Sihler's staining is a useful technique for visualizing the entire nerve network of the IO. This new information about the nerve distribution and morphological features will

improve the understanding of the biomechanics of IO and provides an anatomical background for utilization in various clinical and research fields.

Key Words: Branching pattern; Inferior oblique muscle; Intramuscular nerve distribution; Sihler's stain

P029

Reevaluation of the earlobe types in Koreans

Dae-Kwang Kim, Kyeong-Eui Kim, Woo-Jin Song,

Department of Medical Genetics, Keimyung University School of Medicine, 1095, Dalgubeoldaero, Dalseo-Gu, Daegu, Republic of Korea, 42601

The shape of the earlobes has a variety of genetic significance. This study analyzed the frequencies of the earlobe shapes in the Korean population.Data were collected on randomly selected 500 males and 500 females in Daegu Metropolitan City, with all participant ages being in their twenties. Obtuse angled earlobes accounted for 41.2% of the earlobes observed, while acute angled earlobes was calculated at 38.8% and right angled earlobe was 20.0% of the total. In men, the acute angled earlobe was the most frequent type (43.0%), while the obtuse angled earlobe was the most frequent type in females (45.2%). These differences were statistically significant (p=0.015). Overall, attached type earlobe (61.2%) was more frequent than free type earlobe in our study. The attached type earlobe was more common in both sex groups (57.0% in male and 65.4% in female), and the proportion was significantly higher for females (p=0.006). In conclusion, the findings in this study suggest that the attached earlobe type is the most common among Koreans, and the proportion of earlobe types between males and females is significantly different. Further studies are needed to reveal the genetic association with earlobe types among Koreans.

Key Words: Earlobe type, Koreans

P030

Histomorphometric analysis of the palatal mucosa for connective tissue grafts

Sun-Kyoung Yu, Jin Woong Lim, Heung-Joong Kim

Department of Oral Anatomy, College of Dentistry, Chosun University, Gwangju, Korea

The palatal mucosa and gingiva are histologically similar, so are used as autologous donor site for connective tissue grafts in periodontal surgery. Therefore, the aims of this study were to investigate the palatal mucosa to provide a histologic quantitative data, and to compare the topographic relationship of the greater palatal artery (GPA) and the greater palatine nerve (GPN). The 32 hemimaxillae in Korean were prepared using conventional methods of tissue processing and stained with hematoxylin-eosin. The obtained specimens were measured the areas of entire palatal mucosa, submucosa, and glandular tissue, the length from the alveolar crest to the GPA and the GPN, and the depth from the mucosal surface to each artery and nerve. The mean area of the entire palatal mucosa was 59.7, 53.2, 50.6, 57.6, and 73.2 mm^2 and that of the submucosa was 36.6, 35.3, 33.3, 41.8, and 58.0 mm^2 according to the tooth position from the canine, respectively. The glandular tissues were found all in the molar and the mean area was 15.1 and 30.3 mm^2, respectively. The GPA with

the average of 10.1 mm was located on the lateral side than the GPN with the average of 10.8 mm, but there was no statistically significant. Whereas, the depth of the GPA was 4.3 mm, which was statistical significantly deeper than that of the GPN (3.7 mm under the mucosal surface). These anatomical results can be provided the quantitative data on the palatal mucosa as an autologous donor site for connective tissue grafts.

Key Words: Palatal mucosa, Lamina propria, Submucosa, Greater palatine artery, Greater palatine nerve

P031

Anatomical analysis of the distribution patterns of occipital cutaneous nerves and the clinical implications for pain management

Hyun-Jin Kwon[1], Hun-Mu Yang[1], Shin Hyung Kim[2], You-Jin Choi[1]

[1]Department of Anatomy, Yonsei University College of Medicine, Seoul, Republic of Korea
[2]Department of Anesthesiology and Pain Medicine, Anesthesia and Pain Research Institute, Yonsei University College of Medicine, Seoul, Republic of Korea

Establishing the distribution patterns of occipital cutaneous nerves may help us understand their contribution to various occipital pain patterns and ensure that the proper local injection method for treatment is employed. The aim of this study was to demonstrate the detailed distribution patterns of the greater occipital nerve (GON), lesser occipital nerve (LON), and third occipital nerve (TON) using the modified Sihler's staining technique. Ten human cadavers were manually dissected to determine the nerve distributions. Specimens from eight human cadavers were treated using the modified Sihler's staining. In all cases, distinct GON branches proceeded laterally and were intensively distributed in the superolateral area from their emerging point. No twigs were observed at the middle-trisected area, which had a fan-like shape, in the middle-upper occipital region. The LON and TON distribution areas were biased to the lateral side below the superior nuchal line, although these nerves exhibited multiple interconnections or overlapping areas with the GON. Furthermore, a nerve rarified zone in the shape of an inverted triangle was identified in the middle occipital area. Our findings improve our understanding of the occipital nerve anatomy and will aid in the management of occipital pain in clinical practice.

Key Words: Greater occipital nerve, Lesser occipital nerve, Third-occipital nerve, Sihler's stain, Whole mount nerve staining, Occipital neuralgia

P032

Sonographic analysis of the location and depth of the vessels at the forehead midline

Hyun Jin Park[1], Ji-Hyun Lee[1], Kyu-Lim Lee[1], Kyung-Seok Hu[1], Hee-Jin Kim[1,2]

[1]Division in Anatomy and Developmental Biology, Department of Oral Biology, Human Identification Research Institute, BK21 PLUS Project, Yonsei University College of Dentistry, Seoul, Republic of Korea
[2]Department of Materials Science & Engineering, College of Engineering, Yonsei University Seoul, Republic of Korea.

Non-invasive procedures such as autogenous fat grafts and filler injections are frequently performed to treat sunken forehead. However, filler injection on the glabella is one of the most dangerous procedure due to the high risk of embolism and intravascular injection. Therefore, the use of a cannula is highly recommended. Conventionally, the insertion of the cannula is located and proceeded from the forehead middle despite vessels being frequently observed during the anatomical dissections. The aim of this study was to identify the vessels at the forehead midline to provide crucial anatomic information for various non-invasive procedures on forehead. Twenty volunteers (12 males and 8 females, mean age 22.8) participated in this study. Sonographic image scanning was performed at the 4 points on the forehead midline; trichion (P1), metopion (P2), half point between metopion and glabella (P3), and glabella (P4). The vascular course and location were identified and classified according to its proximity to the forehead midline. The vessels running within 15 mm of the forehead midline were identified and observed in 45-55% of cases. The cases that the vessels ran within 1cm of the forehead midline were 10 (6 arteries and 4 veins) at P1, 6 (6 veins) at P2, 5 (2 artery and 3 veins) at P3, and 5 individuals (5 veins) at P4, respectively. The cases that the vessels ran within 1.5 cm of the forehead midline were 12 (7 arteries and 5 veins) at P1, 9 (2 arteries and 7 veins) at P2, 9 (4 arteries and 5 veins) at P3, and 10 individuals (1 artery and 9 veins) at P4, respectively. Except P4 area, the arteries running near the forehead midline tended to be dominant at the right side of the forehead. In 50% of the individuals, the vessels identified at P4 area (glabella) were veins (90%). The vascular depths at the forehead midline were 2.14±0.72 mm in arterial branches and 2.91±0.75 mm in venous branches, respectively. From these results, we confirmed and verified the superficial vascular location running in proximity to the midline of the forehead. This anatomical information can explain the cause for a higher incidence of vascular complications during the conventional filler injection procedures. For safety, the cannula entry point for glabellar augmentation should be reconsidered.

P033

Three-dimensional structure of the orbicularis retaining ligament: an anatomical study using micro-computed tomography

Jehoon O, Hyun-Jin Kwon, You-Jin Choi, Tae-Hyeon Cho, Hun-Mu Yang

Department of Anatomy, Yonsei University College of Medicine, Seoul, Republic of Korea

The orbicularis retaining ligament (ORL) is an important structure for maintaining the eyelid and cheek skin and contouring the characteristic facial appearance. However, the ORL is a delicate structure that is easily damaged in manual dissection. This study aimed to comprehensively investigate the ORL using a micro-computed tomography (mCT) with phosphotungstic acid (PTA) preparation for the acquisition of its three-dimensional information non-invasively. Twenty-two specimens were obtained from non-embalmed human cadaver (mean age 73.7 years). The specimens were dehydrated, stained in 1% PTA solution with 70% ethanol and scanned by Skyscan 1173 (Bruker, Kontich, Belgium) with a minimum voxel size of 5 μm3. The 3D reconstruction of scanned images, modified Verhoeff Van Gieson (VG) and immunofluorescence (IF) staining and were performed. Multidirectional images of the mCT showed that the ORL consisted of continuous tiny plates with a multilayered plexiform shape. The VG and IF revealed a ligamentous tissue consisting of multiple fibroelastic bundles. The preorbicularis fibers of the ORL had more layers and a more

intricate arrangement than its retro orbicularis fibers. The number, complexity and ambiguity of the ORL fibers increased in the lateral area and their density and extent increased near the dermis. Its dermal anchorage was shown as a confluence of its fibroelastic tissue into the dermis. The ORL comprises a multilayered meshwork of very thin continuous fibroelastic plates and its related cutaneous deformities might be a complicated outcome of subcutaneous tissue shrinkage, lipid accumulation and ORL retention.

Key Words: Orbicularis retaining ligament, Micro computed tomography, Phosphotungstic acid, Aging, Dermal anchorage, Midfacial rejuvenation, Blepharoplasty

P034

Location and depth of the exposed winding portion of the facial artery

Ji-Hyun Lee, Hyun Jin Park, Kyu-Lim Lee, Kangwoo Lee, Kyung-Seok Hu, Hee-Jin Kim

Division in Anatomy and Developmental Biology, Department of Oral Biology, Human Identification Research Institute, BK21 PLUS Project, Yonsei University College of Dentistry, Seoul, Republic of Korea

The nasolabial fold is the facial wrinkle that extend from each side of the nose to the mouth corner. To treat this aging phenomenon, various minimally invasive procedures such as the nasolabial fold augmentation are widely performed. Vascular accident of the facial artery (FA) is the most common complication that may occur during these procedures, hence the physician should be aware of the presence and variations of FA. Furthermore, in many cases, the FA runs as being exposed above the muscle layer along the nasolabial fold. Thus, understanding of the location and depth of the exposed winding portion (EWP) of the FA in the facial subcutaneous layer is important during various clinical procedures. The purpose of this study was to provide three-dimensional topography of EWP of FA, which helps to minimize complications during in the clinical procedures. Thirty hemifaces from embalmed adult cadavers (20 male and 10 female cadavers; mean age of 79.7 years) were used for this study. First, the facial skin surface of intact cadavers is scanned using the 3D scanner, then the skin and subcutaneous tissue were carefully dissected and the muscular layer scanning was performed again. Scanned images of dissected and undissected faces were superimposed using Morpheus Dental Solution (version 3.0) software. Then the location of EWP in relation to surface landmarks, and depth of the PFA were measured using the software. The EWP of FA was observed in 80% of the specimens. The exposed patterns of the FA were classified into three categories: type I, one site exposure (63%); type II, two site exposures (21%); type III, linear exposure along the muscle border (16%). The location of the EWP of the FA was related with a line through the otobasion inferius and the cheilion (Oi-Ch line). The EWP was on the Oi-Ch line in 58.3% of cases. The cases that the EWP was above or under the Oi-Ch line was 41.7%. If the EWP was above or below the Oi-Ch line, the average distance from the Oi-Ch line to the EWP was 4.5 mm and 4.0 mm, respectively. From the frontal view, the EWP was related to the mid-pupillary line (MPL). The EWP was on the lateral side of the MPL in 88% of the cases. The cases that the EWP was medial and lateral to the MPL were 8% and 4%, respectively. Average angle between the interpupillary line and the EWP was 92.3°. The average depth of the EWP of the FA from the skin was 7.9 mm (3.1~12.7mm). Whilst performing dermal filler injections, these results on three-dimensional topographic information of the FA will provide the safe clinical guideline for the nasolabial fold augmentation procedure.

Key Words: Nasolabial fold, Exposed winding portion, Facial artery

P035

Localization of the Maxillary Ostium in Relation to the Reduction of Depressed Nasomaxillary Fractures: A Radiological Study

Kun Hwang[1], XiaJing Wu[1], Hun Kim[1], Dae Joong Kim[2]

[1]Department of Plastic Surgery, Inha University School of Medicine, Incheon, Korea
[2]Department of Anatomy, Inha University School of Medicine, Incheon, Korea

The aim of this study was to elucidate the precise location of the maxillary ostium using computed tomography (CT) for reduction of depressed nasomaxillary fractures.
CT images (61 males, 42 females; age range, 3-97 years) were analyzed. Coronal sections were cut every 3mm. The primary maxillary ostium (PMO) was located 24.7%±3.9% of bizygomatic distance (BZD) lateral to septum. The horizontal distance of the PMO significantly increased with age (P=.032). The PMO was located 53.3%±8.0% of nasal length (NL) above superior surface of the palatal bone (SP). The vertical-to-horizontal ratio of the PMO decreased with age (P=.013). The PMO was located 30.3±4.3mm posterior to the tip of nasal bone. The PMO was located 24.6±4.8mm posterior to the anterior nasal spine (ANS). The ANS-PMO distance significantly increased with age (P=.027). The hiatus semilunaris (HS) was located 11.9%±3.2% of BZD lateral to septum. The HS was located 62.4%±10.3% of NL above SP. The vertical distance of the HS significantly decreased with age (P=.019). The accessory maxillary ostium (AMO) was located 14.9%±2.8% of BZD lateral to septum. The horizontal distance of the AMO significantly increased with age (P=.027). The AMO was located 44.8%±6.9% of NL above SP. The vertical distance of the AMO significantly decreased with age (P<.001). The vertical-to-horizontal ratio of the AMO decreased with age (P<.001).
The distances of the ostium from surgical landmarks measured in this study might be helpful when inserting a small curved elevator into the maxillary ostium in the reduction of medial maxillary fractures.

Key Words: Maxillary Fractures, Maxillary Sinus, Anatomy, Cross-Sectional Tomography, X-Ray Computed.

P036

Superficial Fascia in the Cheek and the Superficial Musculoaponeurotic System

Kun Hwang

Department of Plastic Surgery, Inha University School of Medicine, Incheon, Korea

The origins and validity of the term 'superficial musculoaponeurotic system' (SMAS) is reviewed. Gray stated the superficial fascia connects the skin with the deep or aponeurotic fascia, and consists of fibro-areolar tissue. Hollinshead wrote superficial fascia exists throughout the body and contains a variable amount of fat. In the head and neck, it encloses voluntary muscles in its deep portion. Skoog found superficial fascia was fixed to the dense, deep fascia by fibrous adhesions in the temporal, preauricular, and parotid area. Mitz stated "There is a 'superficial muscular and aponeurotic system' (SMAS) in the parotid and cheek areas." SMAS has an intimate relationship with the entire superficial fascia of the head and neck, and divides the subcutaneous fat into 2 layers. Wassef found a continuous fibromuscular layer at the deep limit of the "subcutis," which corresponded to the 'superficial fascia.' Nakajima reported the subcutaneous adipofascial tissue was made up of 2

adipofascial layers. Macchi found 2 different fibroadipose connective layers bounded to the laminar connective tissue layer (SMAS). In the cheek, Hwang found horizontal fibrous connective tissues (membranous layer of superficial fascia) divided the superficial fascia into the superficial fatty layer and the deep fatty layer. Recently, Mitz explained the reason for the term 'SMAS.' The 'musculo+aponeurotic' component is based on histology of muscle cells, including the risorius, in the same structure to be surgically consistent. The aponeurotic cells belong to the same surgical layer. 'SMAS' is not sufficient to replace the old term 'superficial fascia of the cheek area.'

Key Words: Superficial Fascia, Superficial Musculoaponeurotic System, Cheek, Terminology

P037

Human Nasal Adaptation: Balancing Climatic and Metabolic Demands

Suhhyun Kim, Alexa P. Kelly, Scott D. Maddux

Center for Anatomical Sciences, Department of Physiology and Anatomy, University of North Texas Health Science Center, Fort Worth, TX, USA

Studies have shown that indigenous individuals from cold-dry climates exhibit longer, taller, and especially narrower nasal passages compared to equatorial counterparts, enhancing inspiratory air-conditioning (heating and moisturizing) capacity and reducing susceptibility to respiratory tract infections. Concurrently, due to increased demand for thermogenesis, cold-dry climates are also metabolically more expensive than tropical environments, necessitating greater volumetric intake of oxygen. Accordingly, recent research has suggested that while a narrower nose enhances inspiratory air-conditioning, the accompanying restriction on volumetric intake may necessitate increased nasal height to maintain sufficient intake of oxygen. The purpose of this study was to examine the relationship between nasal dimensions, climate, and the metabolic demands. We employed 12 linear measure- ments collected from the nasal skeleton of 837 modern human crania from major geographic (Arctic Circle, Asia, Australia, Europe, Africa) and climatic (polar, temperate, hot-arid, tropical) zones. Anterior-posterior femoral head diameter (FHD) was further employed as a proxy for overall body size and metabolic requirements. Morphological, climatic, and geographic data were then employed in multivariate analyses. Our results indicate that most breadth measurements of the nasal aperture and internal cavity are significantly correlated with climate (all significant R^2 values between 0.29–0.51 with p-values < 0.004), but not FHD. Conversely, height and length measurements of the aperture and cavity were found to be more strongly correlated with FHD (all significant R^2 values between 0.67–0.78 with p-values < 0.0003) compared to climate (all significant R^2 values between 0.36–0.56 with p-values < 0.02). Further, overall nasal passage area was found to be positively associated with FHD ($R^2 = 0.67$, p = 0.0003), while nasal passage shape retained a significant relationship with climate ($R^2 = 0.66$, p = 0.0004) with relatively tall/narrow airways associated with colder-drier environments. Collectively, these results support the assertion that physiological demands for temperature and moisture exchange are predominantly mediated by nasal passage breadth, with airway height representing a compensatory mechanism for ensuring a metabolically sufficient oxygen intake. Additional studies employing more direct measures of metabolic demands are accordingly warranted.

Key Words: Nose, Climate, Thermoregulation, Respiration, Ecogeographic Variation

P38

Three-dimensional analyses of mouth region during smiling

Ozsoy U

Department of Anatomy, Faculty of Medicine, Akdeniz University, Antalya, Turkey

Mimics are important for interpersonal communication in order to express oneself effectively. Smile is a sign of positive feelings and is often used in daily life. The impairment of smile due to neurological diseases or trauma may disrupt social communication. For this reason, to determine morphological changings in mouth region is important for neurologists, plastic and reconstructive surgeons, orthodontists and craniomaxillofacial surgeons. The anatomical assessment of smile is related to the oral area and asymmetry. Therefore, mouth region of twenty (10 male, 10 female) healthy subjects aged between 23 and 45 years were recorded and digitized in 3D during neural face position and smiling face expression. A mirrored image was generated from original digitized image. Then, the asymmetry value of the mouth was calculated by means of the root mean square formula (RMS) by superimposition of original and mirrored images. Additionally, the area of the region was calculated. A statistically significant difference was found between the mean asymmetry values (RMS) of mouth region in neutral face position (0.8±0.3mm) and during smile facial expression (1.7±0.8mm). The area of mouth region was significantly higher during smile expression (4683±812mm^2) than neutral face position (3544±596mm^2). In the present study, we showed that the area and asymmetry of the mouth region was increased while smiling. We think that such increments need to be considered in clinical observation. Our results can help the clinicians as reference data in clinical assessment of facial functional or morphological deterioration.

Key Words: Smile, 3D, Asymmetry, RMS

P039

The boundary of the parotid gland for the clinical application

Ye-Gyung Kim[1], Anna Jeon[1], Je-Hun Lee[2], Jung-A Shin[3], Seung-Ho Han[1]

[1]Department of Anatomy, College of Medicine, Chung-Ang University, Seoul, Republic of Korea
[2]Anatomy Laboratory, College of Sports Science, Korea National Sport University, Seoul, Republic of Korea
[3]Department of Anatomy, School of Medicine, Ewha Womans University, Seoul, Republic of Korea

The parotid glands are the largest and irregular a gland of the salivary glands. It is located between ramus of mandible, mastoid process and sternocleidomastoid muscle. Understanding the location of the parotid glands is important for performing the face-lifting, parotid Botox injection and parotidectomy. Although the parotid gland have been described in numerous literature and articles, it is rare to give accurate information on boundaries and locations. The aim of this study was to examine the accurate location and boundary of the parotid gland. Twenty-four hemifaces from Korean embalmed cadavers (13 males and 11 females; mean age 75.2 years) were used in this study. For the measurement, frankfort horizontal line(orbitale-porion), porion-gonion line, gnathion-gonion line and porion-cheilion line were used as the reference lines. All measurements were taken on the lateral side of the face. The most superior point was 6.85 ± 4.5 mm below the frankfort line. The most inferior point was 10.21 ± 5.5 mm below the gonion-gnathion line. On the porion-gonion line, the most medial and lateral point were located 26.5 ± 7.3 mm anteriorly, 26.5 ± 4.9 mm posteriorly, respectively. On the porion-cheillion line, the most medial point of the parotid gland was 44.8 ± 14.1 mm and the medial

border of the masseter muscle was 69.7 ± 5.9 mm from the porion. The parotid gland has a variety of features, the irregular shape was the most common (54.16 %), followed by the reverse triangle (33.3 %) shape; an falciform form (12.5 %) was noted in on three specimens. All specimens of this study, the boundary of the parotid gland was distributed below the frankfort line and extended over the anterior border of the sternocleidomastoid muscle; not extended over the anterior border of the masseter muscle; down the lower margin of the mandibular body.

P040

Vascular anatomy of the external nose

Tae-Jun Ha, Shin-Hyo Lee, Je-Sung Lee, Ki-Seok Koh, Wu-Chul Song

Department of Anatomy, Research Institute of Medical Science, Konkuk University School of Medicine, Seoul, Korea

Superficial blood supply of the nose can be described as a multidirectional arterial anastomotic system that is formed by branches of the external and internal carotid arteries. Knowledge regarding the nasal arteries is clinically relevant to the practice for aesthetic improvements of the nose. The aim of this study was to identify the overall mapping of the vascular depth of the external nose. The whole of the nasal soft tissues was harvested from twenty-eight noses from formalin-embalmed cadavers using a periosteal elevator and trimmed from the intercanthal line to the marginal border of nostrils. Each specimen was bisected longitudinally and then divided into four pieced of equal length for histological sections and processed using routine histological methods. The depth of the artery from the skin surface and the diameter of that arteries according to levels were measured. Most nasal arteries on the dorsum were located superficial to the fibromuscular layers. Overall arterial depth was 1.9 mm. The nasal skin on the cartilaginous parts receives blood supply from the dorsal nasal artery superiorly and the lateral nasal artery and the columellar artery inferiorly. Some arteries supplied the deep fatty layers and pre-perichondrial layers. The depth to the arteries according to four levels from the superior part were 1.6, 1.6, 2.4, and 2.1 mm, respectively. The diameter of the arteries were 0.3, 0.3, 0.4, and 0.4 mm respectively. Nasal tip vascularization implies the high chance of vascular complications in injection rhinoplasty using filler. The present study provides the vascular proof in aesthetic nose augmentation.

Key Words: Arterial anastomosis, Dorsal nasal artery, Lateral nasal artery, Perichondrium, Fibromuscular layers

P041

Anatomical assessment of sinus lateral wall and Schneiderian membrane for sinus augmentation

Heung-Joong Kim, Byung Soo Park, Sun-Kyoung Yu

Department of Oral Anatomy, College of Dentistry, Chosun University, Gwangju, Korea

When the alveolar bone loss is severe, the sinus augmentation is frequently used to maintain the implant stability. The aim of this study was to investigate the thicknesses and histologic features

of the sinus lateral wall and Schneiderian membrane to provide clinicians with quantitative and qualitative data on sinus augmentation.Thirty five hemimaxillae from 25 cadavers were used (19 males, 6 females, mean death age 59 years). The specimens obtained from first premolar to second molar were embedded in paraffin, stained with hematoxylin-eosin, and observed on light microscope. The thickness of lateral wall and Schneiderian membrane according to tooth site and measurement level was measured by using image-processing software and their histologic feature evaluated. The mean thickness of lateral wall was 2.22, 2.17, 2.64, 2.64 mm from first premolar to second molar according to tooth site, respectively. That mean thickness from the sinus floor was 2.79, 2.24, 2.12 mm according to 0, 2, 8 mm in measurement level, respectively, decreasing as the height from the sinus floor goes up. The mean thickness of the Schneiderian membrane was thicker at the sinus floor (0.41 mm) than 2 mm above the floor (0.38mm), but was not statistically significant. The lateral wall consisted of the outer cortical plate, the trabecular bone at the center, and the inner cortical plate near the Schneiderian membrane. In particular, the inner cortical plate was more porous. These histomorphometric results on the sinus lateral wall and Schneiderian membraneare expected to provide critical information on sinus augmentation.

Key Words: Sinus augmentation, Histomorphometric analysis, Sinus lateral wall, Schneiderian membrane

P042

Sexually dimorphic development of gyrification in the ferret cerebral cortex

Sawada K[1], Kamiya S[1], Aoki I[2]

[1]Department of Nutrition, Faculty of Medical and Health Sciences, Tsukuba International University, Tsuchiura, Japan
[2]Department of Molecular Imaging and Theranostics, National Institute of Radiological Sciences, QST, Chiba, Japan

The present study was attempted to characterize quantitatively the developmental profile of the gyrification of male and female ferrets by MRI-based morphometry. Short TR/TE MR images (typical T_1-weighted parameter setting for conventional MRI) was acquired with a high spatial resolution at 7 tesla from fixed brains of male and female ferrets at postnatal days (PDs) 4 to 90. The cortical convolution was evaluated quantitatively based on 3D MRI data throughout the cerebral cortex by global-gyrification index (global-GI) and in representative primary sulci by sulcal-gyrification index (sulcal-GI), respectively. The global-GI rose in a linear manner from PD 4, plateaued at PD 42 (male, 1.484 ± 0.020; female, 1.460 ± 0.011), and then slightly reduced by PD 90 (male, 1.455 ± 0.026; female, 1.407 ± 0.016). A slight reduction of the global-GI from PDs 42 to 90 in both sexes was altered by changing the shape of cerebral hemisphere: sustaining volume and surface area of the cortex, albeit continuously increasing the fronto-occipital length of the cerebral hemisphere during those ages. Age-dependent sexual difference was obtained by greater global-GI in males than in females on PD 21 and thereafter. Sex difference in the cortical convolution was regionally non-specific on PD 21, but specific in the temporo-parieto-occipital region on PDs 42 and 90. Sulcus-specific sex difference was detected by significantly greater sulcal-GIs in males than in females in the presylvian sulcus and rhinal fissure on PD 42, and further in the splenial sulcus, coronal sulcus, lateral sulcus, and caudal suprasylvian sulcus on PD 90. The present results suggest an age-related appearance of biphasic feature of sexual dimorphism of the gyrification in the ferret cerebral cortex. A greater sulcal infolding in males than in females was allometric by PD 21, and sulcus-specific in evolutionary expanded cortical regions, thereafter. The findings will provide advantageous information regarding sex-related

morphological and functional specification of the cerebral cortex, and keys to understanding pathogenesis of neurodevelopmental disorders with gyrification abnormality and gender vulnerability, i.e., schizophrenia and autism.

Key Words: Cerebrum, Sulcus, Gyrification, Carnivores, Sex difference

P043

Denonvilliers' fascia: Gender differences of its fascial architecture

Zhang M[1], Chapuis P[2], Bokey L[3] , Xu Z[1,4]

[1]Department of Anatomy, University of Otago, Dunedin, New Zealand
[2]Department of Colorectal Surgery, The University of Sydney, Sydney, Australia
[3]Department of Colorectal Surgery, Liverpool Hospital and School of Medicine Western Sydney University, Sydney, Australia
[4]Departments of Anatomy, Anhui Medical University, Hefei, China,

Whereas the existence of Denonvilliers' fascia (DVF) in either sex remains controversial, its identification at operation is considered important when mobilising the distal rectum for cancer or during radical retropubic prostatectomy or rectocoele. The original description of the fascia was based exclusively on Denonvilliers' findings in 12 adult male cadavers though Denonvilliers gave no account of its existence in women. Much of the controversy in the literature concerns the origin and development of the fascia which is said to arise from a "fusion", a "condensation of embryonic connective tissue" or both to form a mature, "multilayered" structure. The aim of this study was to investigate the detailed architecture of DVF in adult cadavers using a combination of epoxy sheet plastination and confocal microscopy techniques. Nine cadavers (6 males, 3 females; age range, 46-87 years) were prepared as nine sets of transverse (4 sets), coronal (1 set) and sagittal (4 sets) plastinated sections. The sections were examined under a confocal laser scanning microscope. This study was performed in accord with our institutional ethical guidelines and approaved by the institutional ethics committees. In the male, the membrane-like structures in the prerectal space represented predominantly fibres originated from the external urethral sphincter (EUS), together with fibres from the longitudinal rectal muscle (LRM) and the connective tissue sheaths of the neurovascular bundles. In the female, at the level of the external anal sphincter, the muscular and tendinous fibres from the rectal and vaginal walls intermingled with each other and no distinct fascial layer was identified. In both male and female, the peritoneum did not descend deeply within the prerectal space.There is no clearly identified membranous layer consistent with DVF in either sex. However, the fascial configuration in the prerectal space appears different between the male and female. The fibers from the EUS in the male and LRM in both male and female may have been misidentified as a multi-layered DVF in previous studies. Thus, the correct plane for anterolateral mobilization of the rectum should be essentially posterior to the multilayered "DVF".

Key Words: Denonvilliers' fascia, Fibrous Architecture, Gender Differences, Prerectal Space

P044

Bilateral difference and sexual dimorphism of the intraparietal sulcus

Qi Zhang[1], Bo Sun[1,2], Shuwei Liu[1]

[1]Research Center for Sectional and Imaging Anatomy, Shandong University School of Medicine, Jinan, China
[2] Shandong Medical Imaging Research Institute affiliated to Shandong University, Jinan, China

The Intraparietal Sulcus (IPS) is a long and deep antero-posterior sulcus, parallel to the interhemispheric fissure, which separates the superior parietal lobe from the inferior parietal lobe. Neuroimaging studies have suggested that IPS is sophisticated, and shows a great relationship to the human cognition, such as attention, notation and simple arithmetic ability. Meanwhile, the IPS can be used as an operative approach for some major operations in the lateral ventricle trigone. In this study, we clarified the differences of the IPS in the gender and bilateral asymmetry using a parametric ribbon method, and explored the types and branches of the sulcus. The IPS was reconstructed and parameterized automatically using a cohort of 107 healthy right-handed subjects. After the reconstruction, the morphologies of the IPS were evaluated by examing its trends, shapes and branches. Next, we calculated the 3D anatomic morphology parameters of the IPS, including the maximum depth (MD), average depth (AD), average width (AW), top length (TL) and bottom length (BL). We found that the IPS can be divided into three types: one segment, two segments, three segments. Left-ward asymmetries of TL and BL were observed both in males and females, and TL and BL of the left hemisphere in the male subjects were larger than that in females. Left-ward asymmetries of AD in males was also observed, while no significant gender differences and lateral differences of AD in female subjects were discovered. There were no significant gender differences in the MD and AW. Our findings indicated that the lateralization of the IPS manifest mainly as sexually different. This study is helpful for clinical imaging researches on development, intelligence and neuropsychiatric disorders in the parietal regions.

Key Words: Intraparietal sulcus, 3D reconstruction, Sulcal pattern, Gender and lateral asymmetry

P045

The correlation of the porosity associated with the age from lumbar vertebrae by image analysis in a Thai population

Nadthaganya Suwanlikhid[1], Sukon Prasitwattanaseree[2], Patison Palee[3], Pasuk Mahakkanukrauh[1,4,5]

[1]Forensic Osteology Research Center, Faculty of Medicine and Graduate School, Chiang Mai University, Chiang Mai, Thailand
[2]Department of Statistics, Faculty of Science, Chiang Mai University, Chiang Mai, Thailand
[3]College of Arts, Media and Technology, Chiang Mai University, Chiang Mai, Thailand
[4]Department of Anatomy, Faculty of Medicine, Chiang Mai University, Chiang Mai, Thailand
[5]Excellence Center in Osteology Research and Training Center (ORTC), Chiang Mai University, Chiang Mai, Thailand

The lumbar vertebrae carried the most weight and hence are more biomechanical stress than any other vertebra. Therefore, the degenerative changes commonly occur in them among the elderly and affect on the vertebral bodies. Thus, we used image analysis which could give rise to the numerical system and clearly more detailed than visual assessment. The aim of this study was to determine the correlation between the quantity of macroporosity and microporosity with age on the endplates from adult lumbar vertebrae in a Thai population. A total of 100 lumbar columns (50 males and 50 females) in the age range of 22 to 89 years were collected from the Forensic Osteology Research Center (FORC), Faculty of Medicine, Chiang Mai University. The macroporosity and microporosity on the endplates were evaluated by using the developed image analysis software. Pearson correlation

coefficient between the porosity index and age was analyzed. The result shows that the highest correlation was the percentage of the macroporosity index on the total surface of the superior surface of L5 vertebra (r = 0.482).   Although it is a moderate correlation, it can evaluate actual age-related changes in the lumbar vertebrae. So, this could be immensely used for distance consultation in the future.

Key Words: Bone, Lumbar vertebrae, Degenerative changes, Macroporosity, Microporosity, Image analysis

P046

Age-dependent changes in geometry of the human aorta in Thai population

Pornhatai Komutrattananont[1], Patison Palee[2], Pasuk Mahakkanukrauh[1,3,4]

[1]Department of Anatomy, Chiang Mai University , Faculty of Medicine, Chiang Mai, Thailand.
[2]College of Arts Media and Technology, Chiang Mai University, Chiang Mai, Thailand.
[3]Excellence in Osteology Research and Training Center (ORTC), Chiang Mai University, Faculty of Medicine, Chiang Mai, Thailand.
[4]Cadaveric Surgical Training Center, Chiang Mai University, Faculty of Medicine, Chiang Mai, Thailand.

Aorta is the largest artery. It is responsible for transporting oxygen through the blood to other parts of the body of humans. There is a change of structure and function which is associated with age. The purpose of the study is to investigate age associated changes of gross morphology, morphometric parameters, and the correlation between parameters and age of the aorta in cadaveric human. A total of 53 specimens were dissected from 4 locations (16 ascending, 10 arch, 17 descending, 10 abdominal) of 27 human aortas from donor and autopsy cadavers. Age ranges from 45 to 90 years. The morphometric parameters including inner circumference, aortic diameter and average thickness of all locations of the aorta were defined and measured by using image analysis program. We establish the program for measuring these parameters and determine the correlation between various morphometric parameters of the aorta and age. The results of this study showed that inner circumference (r=0.60-0.87), thickness (r=0.38-0.76), vertical and horizontal diameter of the aorta (0.59-0.81) were correlated with age. As the age advanced, the inner circumference and vertical and horizontal diameter dilated and arterial wall was thickened. The ascending aorta was the largest segment and diameter of the aorta decrease from the ascending aorta to the abdominal aorta. The thickness was ranged 1.67-2.60 mm of the ascending aorta,1.68-2.95 mm of arch of aorta,1.22-2.61 mm of the thoracic aorta, and the thickness of the abdominal aorta was 1.68- 3.61mm. In conclusion, detailed morphology and morphometry changes in the aorta is important for future clinical therapies and aortic diseases. Possibly, the knowledge of the structural changes with age can be used as an age indicator in the forensic anthropology.

Key Words: Geometry, Ascending aorta, Arch of aorta, Thoracic aorta, Abdominal, aorta, Age changes

P047

Age-associated changes of the morphology of the heart valves in human

Treerat Gumpangseth[1], Patison Palee[2], Pasuk Mahakkanukrauh[1,3,4]

[1]Department of Anatomy, Chiang Mai University , Faculty of Medicine, Chiang Mai, Thailand.
[2]College of Arts Media and Technology, Chiang Mai University, Chiang Mai, Thailand.
[3]Excellence in Osteology Research and Training Center (ORTC), Chiang Mai University, Faculty of Medicine, Chiang Mai, Thailand.
[4]Cadaveric Surgical Training Center, Chiang Mai University, Faculty of Medicine, Chiang Mai, Thailand.

The human heart valves are complex anatomical structures consisting of leaflets and many supporting structures. Through aging, changes can occur in both macroscopic and microscopic structures of the heart valves. The objective is to examine the morphology and dimensions of the tricuspid, pulmonary, mitral, and aortic valves and their relationship with age. Twenty-two fresh human hearts (13 males and 9 females) were obtained from Department of Anatomy and Department of Medical Science, Faculty of medicine, Chiang Mai University, Thailand. The aged of individuals was between 41-90 years. In gross morphometry, the measurement parameters of the tricuspid and mitral valves were taken including: valve circumference, the attachment length of each leaflet, height and area of each leaflet. The parameters of the pulmonary and aortic valves consist of valve circumference, attachment length of each leaflet, height of each leaflet, area of each leaflet. These parameters were measured by using image analysis software. The negative correlation between the height of septal leaflet of the tricuspid valve and age (r=-0.60) was found. The mitral valve showed moderate correlation with age and the attachment length of the anterior leaflet and total circumference of the valve (r=0.48-0.49). For the pulmonary and aortic valve, the valve circumference significantly increased with increasing age (r=0.40-0.53). In most cases, the circumferences of the tricuspid and mitral valves were larger than the pulmonary and aortic valves. Moreover, the tricuspid valves were found with more variation when compared the other valves. These results suggest that the valve circumferences of the mitral, pulmonary, and aortic valves were significantly correlated with age including the height of the tricuspid septal leaflet. Additional knowledge of morphometric features in human heart valve and the relationship between these parameters and age may be applied for age estimation and be useful for optional treatments of the valve diseases.

Key Words: Age changes, Tricuspid valve, Mitral valve, Pulmonary valve, Aortic valve, Morphology

P048

Age Estimation from Vertebral Body Height in a Thai Population

Apichat Sinthubua[1,2,3], Chirapat Inchai[1], Pasuk Mahakkanukrauh[1,2,3]

[1]Department of Anatomy, Faculty of Medicine, Chiang Mai University, 50200, Thailand
[2]Forensic Osteology Research Center, Faculty of Medicine, Chiang Mai University, 50200, Thailand
[3]Excellence in Osteology Research and Training Center (ORTC), Chiang Mai University, Thailand

Age estimation is one of the major components of forensic identification. Morphological changes in the adult human skeleton including cranial suture closure and pubic symphysis have long been regarded as useful indicator for age-at-death estimation. According to human stature related to vertebral column and increasing age, height of vertebral body is useful to study age estimation. The aim was to estimate age from 100 dry vertebral columns in a Thai population with age range from 22 to 94 years housed in Forensic Osteology Research Center, Faculty of Medicine, Chiang Mai University. Height of three parts of vertebral bodies including anterior, middle and posterior parts were measured. Correlation between vertebral body height and age in each parameter was analyzed using Pearson's correlation. The results showed a significant negative correlation between vertebral body height and age. The middle body height was the highest correlation with age followed by anterior and

posterior body heights, respectively. Middle body height of L3 vertebrae revealed the highest correlation with age (r=-0.326, p=0.001). Regression formulae showed the standard error of age estimation (SEE) 13.538 years. Increasing age is related to human stature loss owing to the degenerative process of vertebrae. Hence, this study may help estimate age-at-death from height of vertebral body in forensic anthropological contexts.

Key Words: Age estimation, Vertebral body, Thai population

P049

Age estimation equations using vertebral osteophyte formation in a Thai population: comparison and modified osteophyte scoring method

Sithee Praneatpolgrang[1,2], Sukon Prasitwattanaseree[3,5], Karnda Mekjaidee[4,5], Pasuk Mahakkanukrauh[1,2,5,*]

[1]Forensic Osteology Research Center, Faculty of Medicine and Graduate School, Chiang Mai University, Chiang Mai, Thailand
[2]Department of Anatomy, Faculty of Medicine, Chiang Mai University, Chiang Mai, Thailand
[3]Department of Statistics, Faculty of Science, Chiang Mai University, Chiang Mai, Thailand
[4]Department of Forensic Medicine, Faculty of Medicine, Chiang Mai University, Chiang Mai, Thailand
[5]Excellence Center in Osteology Research and Training Center, Chiang Mai University, Chiang Mai, Thailand, *Corresponding author (presenting author)

Age estimation is an important step in the biological identification of skeletal remains. The main objective of this study is to develop an age estimation equation from vertebral osteophytes for a Thai population. Each vertebra in the cervical, thoracic and lumbar segments were scored for degrees of osteophyte formation according to criteria established by J. Josh Snodgrass et al., Satoshi Watanabe et al., and new modified score by length of vertebral osteophyte for age estimation. 400 individuals (262 males, 138 females) ranged between 22-97 years Thai sample vertebral columns were used: cervical (C2-C7), thoracic (T1-T12), and lumbar (L1-L5) vertebrae. Each vertebra was scored for degree of osteophyte formation and data to statistical analysis. Regression lines of criteria established by J. Josh Snodgrass et al. (five-stage classification) were Y=33.874+13.971X (SE;10.167), Y=33.358+13.581X (SE;10.167), Y=32.308+15.994X (SE;9.506) in mean lumbar for combine sex, males and females, respectively. Regression lines of criteria established by Satoshi Watanabe et al. (four-stage classification) were Y=34.062+15.273X (SE;10.714), Y=32.936+15.087X (SE;10.541), Y=33.202+ 17.226X (SE;10.418) in mean lumbar for combine sex, males and females, respectively. Regression lines of criteria established by new modified score by length of vertebral osteophyte were Y=35.402+10.552X (SE;10.369), Y=34.469+10.342X (SE;10.275), Y=34.260+12.107X (SE;9.813) in mean lumbar for combine sex, males and females, respectively. This study can be applied for age estimation in a Thai population and be useful when dealing with forensic cases.

Key Words: Forensic science, Forensic anthropology, Vertebral osteophytes, Age estimation, Thailand

P50

Fossa vermiana

Kachlik D[1,2], Kunc V[1], Fabik J[1,3,4], Kubickova B[1]

[1]Department of Anatomy, Second Faculty of Medicine, Charles University, Prague, Czech Republic
[2]Department of Health Care Studies, College of Polytechnics, Jihlava, Czech Republic
[3]Department of Developmental Biology, Institute of Experimental Medicine, Academy of Sciences of the Czech Republic, Prague, Czech Republic
[4]Department of Cell Biology, Faculty of Science, Charles University, Prague, Czech Republic

The aim of the study was to state the prevalence and parameters of the fossa vermiana (or fossa occipitalis mediana), a variable bony structure on the internal aspect of the squamous part of the occipital bone. It is a depressed triangular or oval fossa located superior the foramen magnum, at the site of the inferior divergence of the falx cerebelli. 1042 dry skulls of Caucasian race were examined and the variable findings were classified into five types. The fossa vermiana was observed in 29.6%, subdivided into the type I present in 25.3% of cases (not reaching to the foramen magnum), the type II present in 4.3% of cases (reaching to the foramen magnum) and remaining rare variants present in 2.21% of cases. The fossa was absent in 68.1% of skulls. The knowledge of the variant bony fossa vermiana which has a close relationship to the dural venous sinus as well as the vermis of the cerebellum is of utmost importance for neurosurgery procedures in the posterior cranial fossa.

Key Words: Fossa vermiana, Fossa occipitalis mediana

P051

Minimally invasive horizontal intercartilaginous incision during tracheostomy-a cadaveric study

Young Suk Cho[1], Hyung Chae Yang[2], Juhyun Song[1], Chaeyong Jung[1], Kwang Il Nam[1], Kyu Youn Ahn[1], Choon Sang Bae[1]

Departments of [1]Anatomy and [2]Otolaryngology-Head and Neck Surgery, Chonnam National University Medical School, Gwangju, Republic of Korea

We describe a minimally invasive tracheostomy technique that uses an inter-cartilaginous incision without resection of the tracheal cartilage and discuss its feasibility. A total of 20 adult cadavers (13 males and 7 females) were included in this study. The distance from the arch of the cricoid cartilage to the thyroid isthmus, maximal displacement of the thyroid isthmus, number of tracheal rings underneath the thyroid isthmus, and maximally opened distance resulting from an intercartilaginous incision were measured. The mean distance from the arch of the cricoid cartilage to the thyroid isthmus was 21.4±5.0 mm. The thyroid isthmus mainly overlaid the 3rd and 4th tracheal rings. The mean maximal displacement of the thyroid isthmus was 9.0±2.8 mm. Minimally invasive tracheostomy via an intercartilaginous incision is a feasible technique. A skin incision 2 cm below the cricoid cartilage enables exposure of the thyroid isthmus and anular ligament between the 2nd and 3rd tracheal rings. The intercartilaginous incision allows sufficient space for the tracheostomy tube. An intercartilaginous incision without resection of a tracheal ring can be a good alternative tracheostomy technique, especially for patients who require transient tracheostomy.

Key Words: Tracheostomy, Tracheal cartilage, Thyroid isthmus, Cricoid cartilage, Cadaver

P052

An anatomical study of needle electromyography injection points of the teres minor muscle

Eun Ah Hong[1], Mee-Gang Kim[2], Jong-In Lee[2], Yong Seok Nam[1]

[1]Department of Anatomy, Institute for Applied Anatomy, College of Medicine, The Catholic University in Korea, Seoul, Republic of Korea
[2]Department of Rehabilitation Medicine, Seoul St. Mary's Hospital, College of Medicine, The Catholic University of Korea, Seoul, Republic of Korea

Axillary neuropathy is caused by trauma to the axillary nerve from either a compressive force or traction injury following anterior dislocation of the shoulder. During needle electromyography for diagnosis of axillary neuropathy, the teres minor and the deltoid are major target muscles. However, unlike the deltoid, the teres minor is difficult to detect through the skin due to its relatively miniscule size and location depth. The aims of the study are to suggest an effective needle electromyography injection point for the teres minor, and to investigate various patterns of the axillary nerve to the teres minor. Cadaveric dissection of the bilateral shoulders of 15 fresh cadavers were performed. We determined the locations of various landmarks, such as the acromial angle of the scapula (AA), and the inferior angle of the scapula (IA). Measurements were investigated by means of imaginary lines, which were connected between two landmarks: AA-IA. The AA-IA imaginary line passes obliquely above the teres minor, and therefore the upper muscular point and the lower muscular point were formed. The axillary nerve patterns were identified from the quadrangular space, following which its branches to nearby muscular structures were dissected. We classified axillary nerves to the teres minor into 3 types. As a result, the measurement of the AA-IA line was 149.21±11.12 mm. The upper muscular point of the teres minor on the AA-IA line was at 55.72±15.00mm, and the lower muscular point was at 89.30±12.16mm. The nerve entry point to the teres minor was at 37.16±5.71mm. The deltoid and latissimus dorsi, which cover the upper and lower portions of the teres minor, are located adjacent to the upper and lower muscular points of the AA-IA line. Therefore, in order to avoid the deltoid and latissimus dorsi when performing needle electromyography, a practicable injection point of the teres minor should be located at 72.51±13.58mm site of the AA-IA line. The branching pattern of the axillary nerve to the teres minor: 30 shoulders were examined. Results exhibited 3 types of variations in the course and branching pattern of the axillary nerve to the teres minor. In 15 of the 30 specimens (57.6%) examined, the nerve to the teres minor was bifurcated from the posterior branch of the axillary nerve (Type 1). In a single specimen (3.8%), the nerve to the teres minor was bifurcated directly from the axillary trunk (Type 2). In 10 of the 30 specimens (38.5%), the nerve to the teres minor was bifurcated from the posterior branch, which contains not only the nerve to the teres minor, but also the sensory branch. (Type 3). Dissection revealed a proper injection point for needle electromyography of the teres minor, determined as at the ½ site of the AA-IA imaginary line.

Key Words: Axillary nerve, Teres minor muscle, Needle electromyography, Injection point.

P053

Anatomy of the superior hypogastric plexus and its clinical implication in laparoscopic lower para-aortic lymphadenectomy

Hankyu Kim, Yong Seok Nam, In-Beom Kim, Yi-Suk Kim[*]

Department of Anatomy, The Catholic Institute for Applied Anatomy, The Catholic University of Korea, Seoul, Korea

The superior hypogastric plexus (SHP) which conveys autonomic fibers to the pelvic viscera is formed by the bilateral lowest lumbar splachnic nerves (LSNs) and the aortic plexus around the level of the aortic bifurcation. In previous literature, the SHP is described to be overlying anterior from the aortic bifurcation to the sacral promontory, and divided into paired hypogastric nerves. Postoperative complications such as bladder dysfunctions after para-aortic lymphadenectomy were reported. These complications might be related to the SHP injury. Predicting the exact location of the SHP during the operation is required to minimize the complications. The purpose of this study is to reveal the anatomy of the SHP and the lowest LSNs with relevance to generally employed anatomical landmarks and to suggest clinicians a schematic topography of the SHP applicable to laparoscopic para-aortic lymphadenectomy. Several fresh cadavers were dissected. The trapezoid area formed by the following two lines was marked; the superior border of the trapezoid area was an imaginary line connecting the bilateral points at which the abdominal aorta transits into the common iliac arteries, and the inferior border was a connecting line between the point at which the right ureter cross the pelvic brim and the root of the sigmoid mesentery at the pelvic brim level. In this trapezoid area, coordinates presenting the relative locations of the SHP and the lowest LSNs were measured and standardized. In our results, the lowest LSNs converged into the SHP. The origin of the SHP was located 18.12±7.24 mm inferiorly from and deviated 1.65±1.40 mm left to the aortic bifurcation. From the origin, the SHP was fanned out again and then divided into the hypogastric nerves. The termination of the SHP, or the origin of the hypogastric nerves, was located above the sacral promontory in about 60% of the cases. In these cases, the termination was located 44.83±3.31 mm inferiorly from and deviated 7.07±0.58 mm left to the aortic bifurcation point. In general, the SHP was deviated left to the sagittal line crossing the aortic bifurcation point. The hypogastric nerves were closer to the root of sigmoid mesentery than the right ureter at the sacral promontory level. Via standardization of the trapezoid area and the coordinates, the morphometric distribution of the SHP in the area was presented. In our results, right-sided approach considering safety margin of the plexus in the laparoscopic para-aortic lymphadenectomy is required to minimize the autonomic nervous injuries.

Key Words: Superior Hypogastric Plexus, Lumbar Splachnic Nerves, Laparoscopic Para-aortic Lymphadenectomy

P054

How much force is required to perforate a colon during colonoscopy?

Steve Johnson[1,2], Michael Schultz[1,2], Mario Scholze[3], Troy Smith[3], John Woodfield[4], Niels Hammer[3,5,6]

[1]Department of Medicine, Dunedin School of Medicine, University of Otago, Dunedin, New Zealand
[2]Gastroenterology Unit, Southern District Health Board, Dunedin Hospital, Dunedin, New Zealand
[3]Department of Anatomy, University of Otago, Dunedin, New Zealand Department of Anatomy, Dunedin, New Zealand
[4]Department of Surgical Sciences, Dunedin School of Medicine, University of Otago, Dunedin, New Zealand
[5]Department of Orthopedic and Trauma Surgery, University of Leipzig, Germany

[6]Fraunhofer IWU, Dresden, Germany

Colonoscopy is a commonly-performed procedure to diagnose pathology of the larger intestine. Perforation of the colon is a rare but feared complication. It is currently unclear how much force is actually required to cause such injury nor how this is altered in certain diseases. Our aim was to analyze the forces required to perforate the colon in experiments using porcine tissues. Using 3D printing technology, models of two commercially available colonoscope heads were printed under three configurations: straight (I), 90°- bent (L) and fully bent (U). Samples of porcine colon were assessed with the models and configurations under perpendicular and angular load application and these data compared to the maximum force typically exerted by experienced colonoscopists. The force required for perforation was significantly smaller for the I compared to the U configuration (23.0 vs. 27.9 N) under perpendicular loading, and for the I compared to the L configuration under angular loading (14.1 vs. 46.5 N). Similar differences were found for stiffness (I vs. U when loaded perpendicular: 0.65 vs. 1.17 N/m; I vs. L when loaded angular: 0.70 vs. 1.32 N/m). The mode and site of failure varied significantly between the scopes, with delamination of the mucosa/submucosa below the sample (96%) for the I, blunt mucosa/submucosa/muscularis failure adjacent to the loading site (77%) for the L, and failure of all colon layers lateral to the loading site (59%) for the U configuration, respectively. Perpendicular and angulated loading resulted in similar load-deformation values. Maximum forces typically exerted by colonoscopists averaged 13.9 to 27.9 N, depending on the colonoscope model and head configuration. The force required for colon perforation varies depending on the type mode of loading and is likely lower than the force an experienced colonoscopist would exert in daily practice. There is a real risk of perforation, especially when the end of the scope is advancing directly into the colonic wall. The given experimental setup allowed to obtain reliable data of the colon in a standardized scenario, forming the basis for further experiments.

P055

A biomechanical study on the kinematics of the posterior pelvis under physiologic in-vitro sacroiliac joint motion

Niels Hammer[1,2], Mario Scholze[1], Thomas Kibsgård[3], Stefan Klima[1,2], Stefan Schleifenbaum[2], Thomas Seidel[4], Michael Werner[5], Ronny Grunert[2,5]

[1]Department of Anatomy, University of Otago, Dunedin, New Zealand Department of Anatomy
[2]Department of Orthopedic and Trauma Surgery, University Clinics of Leipzig, Germany
[3]Fraunhofer Institute for Machine Tools and Forming Technology IWU, Dresden, Germany
[4]Department of Orthopedics, Oslo University Hospital, Oslo, Norway
[5]Institute of Cellular and Molecular Physiology, Friedrich-Alexander University Erlangen-Nürnberg (FAU), Erlangen, Germany

The sacroiliac joint (SIJ) is a well-known source of low back pain, with increasing interest for both conservative and surgical treatment. Alterations in the kinematics of the pelvis have been hypothesized a major cause of SIJ pain. However, both the range and the extent of physiological movement are defined controversially, and there are no clear baseline data for pathological alterations. The given study combined a novel biomechanical setup allowing for physiologic motion of the lumbosacral transition and pelvis without restricting the SIJ movement *in vitro*, combined with optical image correlation. Six fresh human pelvises (81±10 years, 3 females, 3 males) were tested, with body

weight-adapted loading applied to the fifth lumbar vertebra and both acetabula. Deformation at the lumbopelvises was determined computationally from three-dimensional image correlation data. SIJ motion under the loading of 100% body weight primarily consisted of a sagittal rotation (0.16°) and an inferior translation of the sacrum relative to the ilium (0.32 mm). SIJ flexion-extension rotations were minute (< 0.02°). Corresponding movements to the SIJ were found at the lumbosacral transition, with an anterior translation of L5 relative to the sacrum of -0.97 and an inferior translation of 0.11 mm, respectively. Moreover, a flexion of 1.82° was observed at the lumbosacral transition. Within the innominate bone and at the pubic symphysis, small complementary rotations were seen around a vertical axis, accounting for -0.10° and 0.11°, respectively. Other motions were minute and accompanied by large interindividual variation. The given study provides evidence of different SIJ motion than reported previously when exerted to physiological loading. SIJ kinematics were in the sub-degree and sub-millimeter range, in line with previous *in-vivo* and *in-vitro* findings, and largely limited to the sagittal rotation and an inferior translation of the sacrum relative to the ilium. This given physiologic loading scenario underlines the relevance of the lumbosacral transition when considering the overall motion of the lumbopelvis, and how relatively little the other segments contribute to overall motion.

Key Words: Digital image correlation, Innominate bone motion, nutation, Pelvic girdle pain, Pubic symphysis, Sacroiliac joint kinematics

P056

A Stereological Study of the Growth Plate Volume in Adolescent Rats Stimulated by Laser Acupuncture

Selfi Handayani[1], Bambang Purwanto[2], Koosnadi Saputra[3,4], Didik G Tamtomo[1], Ginus Partadiredja[5], Jens Randel Nyengaard[6]

[1]Department of Anatomy Faculty of Medicine, Universitas Sebelas Maret, Surakarta Indonesia
[2]Department of Internal Medicine, Dr. Muwardi Hospital Surakarta, Indonesia
[3]Acupuncture Reseach Laboratory for Health Services, National Institute of Health of the Republic of Indonesia
[4]Acupuncture Academy, Indonesia
[5]Department of Physiology, Faculty of Medicine, Universitas Gadjah Mada Jogjakarta, Indonesia
[6]Stereology and Electron Microscopy Laboratory, Centre for Stochastic Geometry and Advanced Bioimaging, Aarhus University Hospital, Aarhus, Denmark

Previous studies have demonstrated that laser acupuncture (LA) has positive effect on longitudinal bone growth by changing the histological growth plates. The aim of the study was stereologically to asses the growth plate volume in adolescent rats stimulated by LA. Forty male wistar rats, aged 3 weeks weighing more than 40 g were divided randomly into two groups, A and B, each receiving LA for 10 days and 15 days, respectively. There were four subgroups in each group: control (C), GV20, ST36 and GV20+ST36. The rats were stimulated by LA using the KX Laser GX-2000B (Kangxing), a semiconductor-based low-level laser therapy (LLLT) device emitting a cold red laser (635–680 nm/5 mW) for 60 seconds (0.3 J/cm2). Subgroup GV20 was treated with LA on the GV20 acupuncture point. Subgroup ST36 was stimulated on the ST36 point, and subgroup GV20+ST36 was stimulated on both the GV20 and ST36 points. Before administering the laser stimulation, the area around the point was shaved gently with a razor, then the laser was placed perpendicularly to the skin. Laser stimulation was administered for 60 seconds (0.3 J/cm2). For the control subgroup (C), the laser apparatus was only placed on the acupuncture points without being turned on. After treatment, the

rats were sacrificed and tibia were removed from other tisssue. The proximal tibia was taken, soaked in the formalin and decalcified. Then, it was dehydrated in graded alcohols and embedded in paraffin blocks. The paraffin blocks were sectioned longitudinally using a Leica microtome (RM2125, Germany) at a thickness (t) of 3 μm. The sampled sections were mounted on slides, deparaffinized, rehydrated, and stained with Hematoxylin Eosin. For stereological analysis, we used light microscop with scanner (Olympus BX61VS) and software from Visiopharm Denmark. The growth plate volume was assesed by measuring surface area with nucleator method then it was calculating with Cavalieri principles. The data were statistically analyzed by ANOVA. As a result, all of the growth plate volume in the treatment groups were more than C and the highest volume was ST36 subgroup, in both 10 days and 15 days. ANOVA showed that there were not differences between subgroups significantly. Laser acupuncture on GV20, ST36 and both GV20+S36 increased growth plate volume in adolescen rats, however the increasing did not differ significantly.

Key Words: Laserpuncture, Growth plate volume, Adolescent rat, Stereology, Nucleator.

P057

Topography of the central retinal artery relevant to retrobulbar reperfusion in filler complications

Shin-Hyo Lee, Tae-Jun Ha, Je-Sung Lee, Ki-Seok Koh, Wu-Chul Song

Department of Anatomy, Research Institute of Medical Science, Konkuk University School of Medicine, Seoul, Korea

Vision loss from retrograde occlusion of the central retinal artery (CRA) is a serious complication of cosmetic filler injections because of the anastomotic nature of the facial vasculature and the end artery morphology of the retinal circulation. Salvation methods using hyaluronidase have been proposed recently to restore blood supply to the retina within ischemic tolerance time, 90 to 105 minute. For a practical route of administration in a time-sensitive manner, percutaneous injection of high-dose hyaluronidase directly into the orbit, retrobulbar space has been proposed. Sixty-seven eyeballs of formalin-embalmed cadavers dissected to examine the relevant anatomy of the CRA and the optic nerve. The distance from the posterior margin of the orbit and entry point of the CRA into the dural sheath of the optic nerve was measured. 3D-reconstruction of the optic nerve was performed to observe the intraneural course of a CRA. The CRA ramified from the ophthalmic artery entered the optic nerve inferiorly at a distance of 8.3 ± 1.4 mm from posterior margin of eyeballs. The course of a CRA in the optic nerve showed acute angulation between the fibrous optic nerve sheath and distal center of the optic nerve. Retrobulbar approach for reperfusion with hyaluronidases has been challenged for effective degradation of filler materials at an ophthalmic emergency. Reliable access route implication for hyaluronidase injection aimed at the CRA was suggested 2.5 cm (1 inch) depth from the border of the inferolateral orbital rim to fill inferotemporal quadrant of the orbit. This study aimed to provide a rationale with the detailed anatomy of the CRA to facilitate the technique of retrobulbar administration of hyaluronidase to salvage CRA occlusion.

Key Words: Central retinal artery, Hyaluronidase, Ophthalmic artery, Optic nerve

P058

A Preliminary Test of 4 Recently Proposed Methods for Pronasale Position in Thai Samples

Thitiorul S[1], Prapayasatok S[2], Iamaroon A[3], Sitthiseripratip K[4], Na Lampang S[2], Prasitwattanasare S[5], Mahakkanaukrauh P[1,6,7]

[1]Department of Anatomy, Faculty of Medicine, Chiang Mai University, Chiang Mai, Thailand
[2]Division of Oral and Maxillofacial Radiology, Faculty of Dentistry, Chiang Mai University, Chiang Mai, Thailand
[3]Department of Oral Biology and Diagnostic Sciences, Faculty of Dentistry, Chiang Mai University, Chiang Mai, Thailand
[4]Biomedical Engineering Research Unit, the National Metal and Materials Technology Center, National Science and Technology Development Agency, Pathumthani, Thailand
[5]Department of Statistics, Faculty of Sciences, Chiang Mai University, Chiang Mai, Thailand
[6]Excellence in Osteology Research and Training Center (ORTC), Chiang Mai University, Thailand
[7]Forensic Osteology Research Center, Chiang Mai University, Faculty of Medicine, Chiang Mai, Thailand

This study investigated the accuracy of 4 methods recently proposed for pronasale (prn) prediction in Thai samples. Two prediction guidelines developed from White subjects and the other two guidelines developed from Asian subjects were examined including Stephan et al. (2003), Rynn et al. (2010), Lee et al. (2014) and Utsuno et al. (2016), respectively. Twenty adults (ten females, ten males) age ranged from 21-30 years with normal body mass index were scanned in sitting position using cone-beam computed tomography. Two- and three-dimensional images were established and measured. Then the predicted and actual dimensions of prn were compared. The result suggested that the method of Lee et al. (2014) performed most accurate at predicting nasal tip position in males with mean error 2.55+1.08 mm. The method of Utsuno et al. (2016) was found to perform most accurate in female samples with mean error 1.64+0.86 mm. Regardless of sex, the Utsuno et al. method performed most accurate (mean error = 2.45+1.71 mm), whereas the Rynn *et al.* method performed least accurate (mean error = 4.57+1.98 mm) for prn prediction in Thai samples. These results suggested the ancestry-specific in pronasale prediction models.

Key Words: Accuracy test, Forensic anthropology, Forensic facial reconstruction, Nasal tip prediction, Pronasale

P059

Comparison of injectate spread and nerve involvement between retrolaminar and erector spinae plane blocks in the thoracic region: A cadaveric study

You-Jin Choi[1], Hun-Mu Yang[1], Shin Hyung Kim[2]

[1]Department of Anatomy, Yonsei University College of Medicine, Seoul, Republic of Korea
[2]Department of Anaesthesiology and Pain Medicine, Anaesthesia and Pain Research Institute, Yonsei University College of Medicine, Seoul, Republic of Korea

Although different injection locations for retrolaminar and erector spinae plane blocks have been described, the two procedures have a similar anatomical basis. This cadaveric study was undertaken to compare the dye spread between these two techniques in the thoracic region. After randomization, ten retrolaminar blocks and ten erector spinae plane blocks were performed on the left

or right sides of ten unembalmed cadavers. For each block, 20 ml of dye solution was injected at the T5 level. The back regions were dissected, and involvement of the thoracic spinal nerve was also investigated. Twenty blocks were successfully completed. A consistent vertical spread with deep staining between the posterior surface of the vertebral laminae and the overlaying transversospinalis muscle was observed in all retrolaminar blocks. Moreover, most retrolaminar blocks were predominantly associated with fascial spreading in the intrinsic back muscles. The erector spinae plane block was associated with dye that spread in a more lateral pattern, and fascial spreading in the back muscles was also observed. The number of stained thoracic spinal nerves (median) was greater with erector spinae plane blocks than with retrolaminar blocks (2.0 and 3.5). Regardless of the technique, the main route of dye spread was through the superior costotransverse ligament to the affected paravertebral space. Although erector spinae plane blocks were associated with a slightly larger number of stained thoracic spinal nerves than retrolaminar blocks, both techniques were consistently associated with posterior spread of dye and with limited spread to paravertebral space.

Key Words: Anaesthesia, Cadaver, Paravertebral, Regional, Ultrasonography

P060

The anatomical relationship of neurovascular structures related to tarsal tunnel in a cadaveric study.

Chanatporn Inthasan[1], Tanawat Vaseenon[2], Pasuk Mahakkanukrauh[1,3,4]

[1]Department of Anatomy, Faculty of Medicine, Chiang Mai University, Chiang Mai, Thailand
[2]Department of Orthopaedics, Faculty of Medicine, Chiang Mai University, Chiang Mai, Thailand
[3]Excellence Center in Osteology Research and Training Center (ORTC), Chiang Mai University, Chiang Mai, Thailand
[4]Cadaveric Surgical Training Center, Chiang Mai University, Faculty of Medicine, Chiang Mai, Thailand

The tarsal tunnel syndrome (TTS) arises from compression of nerves, arteries, and their branches within tarsal tunnel which was a rigid space at the medial side of ankle. Currently, surgeons used the surgical procedure for releasing the tarsal tunnel to treat tarsal tunnel syndrome, but this technique may injure nerves. Surgeons tried to maintain completeness of neurovascular structures in the tarsal tunnel because the integrity of neurovascular structures relates to successful surgery. Therefore, the knowledge and understanding of the anatomical relationship of neurovascular structures that relate to tarsal tunnel are important for successful treatment of tarsal tunnel syndrome. The samples in this study were used 20 fresh cadaver legs injected with silicone color to the posterior tibial artery. The reference lines were: a malleolar-calcaneal (MC) axis which started from medial malleolus to medial process of the calcaneal tubercle and a navicular-calcaneal (NC) axis which started from tubercle of navicular bone to medial process of the calcaneal tubercle. We described the length of the MC axis and NC axis including the distance of branching point of posterior tibial nerve and artery on MC axis and the perpendicular distance from the branching point of posterior tibial nerve and artery to MC axis. Moreover, the medial plantar nerve, medial plantar artery, lateral plantar nerve, and lateral plantar artery were measured the location of these structures on MC axis and NC axis. All parameter measurements were reported in mean±SD values. As a result, the length of MC axis was 76.49±4.17 mm and the length of NC axis was 62.60±5.89 mm. The distance of branching point of posterior tibial nerve and artery on MMC axis was 32.70±8.21 mm and 46.70±3.69 mm, respectively. The perpendicular distance from the branching point of posterior tibial nerve and artery to MC axis was 24.26±9.79 mm and 8.41±3.90 mm, respectively. The location of medial plantar nerve, medial plantar artery, lateral plantar nerve, and lateral plantar artery on MMC axis were 39.86±2.97 to

43.57±3.19 mm, 44.62±3.30 to 46.77±3.50 mm, 50.77±3.12 to 54.26±3.26 mm, and 55.80±2.81 to 58.72±2.88 mm, respectively. On NC axis, these structures were 26.75±3.29 to 31.19±3.71 mm, 30.49±4.60 to 32.61±4.78 mm, 41.20±3.87 to 44.71±4.22, and 47.34±3.79 to 49.52±3.99 mm, respectively.

Key Words: Tarsal tunnel, Ankle, Posterior tibial nerve, Posterior tibial artery

P061

Morphological Study of Localization and Branching Pattern of Deep Peroneal Nerve and its Muscular Branches: Cadaveric Study in the Northern Thai Population

Chirapat Inchai[1], Tanawat Vaseenon[4], Pasuk Mahakkanukrauh[1,2,3]

[1]Department of Anatomy, Chiang Mai University, Chiang Mai, Thailand
[2]Excellence in Osteology Research and Training Center (ORTC), Chiang Mai University, Chiang Mai, Thailand
[3]Cadaveric Surgical Training Center, Chiang Mai University, Faculty of Medicine, Chiang Mai, Thailand
[4]Department of Orthopaedics, Faculty of Medicine, Chiang Mai University, Chiang Mai, Thailand

Injury to the common peroneal nerve (CPN) especially the damage deep peroneal nerve (DPN) can lead to weakness and paralysis of dorsiflexor muscles of ankle and toe. The understanding in anatomical basis of the nerve is necessary for the diagnosis and choosing the appropriate treatment. The purpose of the present anatomical study was to examine the origin, course, location of DPN and number of its muscular branches. A total of twenty fresh cadaveric lower extremities were dissected to study the gross morphological characteristic of the deep peroneal nerve and its muscular branches including 1) The bifurcation points of deep peroneal and superficial peroneal nerves from the common peroneal nerve, 2) Branch points of each muscular branch to the tibialis anterior (TA), extensor digitorum longus (EDL) and extensor hallucis longus (EHL muscles, 3) Number of terminal branches to respective muscle. Vernier caliper was used to measure the distance from branch point relative to knee joint line and the fibular head which is the clearly palpable point in surface anatomy. Descriptive statistical analysis was analyzed by using SPSS version 17. The bifurcation points of DPN from the CPN were superior to the fibular head in 9 cases, the average distance was 9.31 mm and inferior to fibular head in 11 cases, the average distance was 12.46 mm while the bifurcation points of DPN from CPN using the knee joint line as a landmark showed 2 case of bifurcation point superior to the knee joint line, average distance was 12.63 mm and there were 18 cases located in the inferior to knee joint line, average distance was 27.43 mm. The motor branches to TA comprise about 2-5 branches, in 45% of all cases was found to have 3 motor branches. The motor branches to EDL comprise about 1-3 branches, in 60% of all cases was found to have 2 motor branches. The motor branches to EHL comprise about 1-3 branches, in 75% of all cases was found to have 2 motor branches. Basic knowledge of exact anatomy of the deep peroneal nerve and its muscular branch patterns and relationships of the nerve to palpable landmarks may help surgeons to prevent injuries and avoid complication during surgical procedures.

Key Words: Common peroneal nerve, Superficial peroneal nerve, Deep peroneal nerve, Fibular nerve, Cadaveric study

P062

A cadaveric study of the left coronary artery variation: intermediate branch

Lelimiska I. Syarif[1], Jefman EM[1], Sitti Rafiah[1], Muhammad Iqbal Basri[1,2]

[1]Department of Anatomy, Medical Faculty of Hasanuddin University, Makassar, Indonesia
[2]Department of Neurology, Medical Faculty of Hasanuddin University, Makassar, Indonesia

Right main coronary artery (RCA) and left main coronary artery (LCA) are two major branches of artery that supply the heart. Mostly, left main coronary artery has two branches, circumflex branch (LCX) and left anterior descending branch (LAD). Some study reports of *trifurcatio*, the variation of left main coronary artery, intermediate branch is the additional branch of left main coronary artery, located between circumflex branch and left anterior descending branch. Other studies report of *Myocardial bridging* as an anatomical variation of coronary artery, known as a congenital anomaly in which a segment of coronary artery lies below the band of heart muscle.

This report is a descriptive quantitative study with random sampling method to describe the distribution of variation of left main coronary artery, intermediate branch. Nine hearts of Indonesian cadavers dissected in Anatomy Laboratory of Hasanuddin University, we performed blunt dissection to remove fat tissue for better identification of the left main coronary artery branches. Furthermore, length of the branches was measured by two persons using centimeter tape. The measurement commenced from the origin of the branch and ended in the terminal of the branch. From nine specimens have been identified, we found intermediate branch in three specimens (7th cadaver, 8th cadaver, and 9th cadaver), length of each sample is 3.0 cm, 1.7 cm, and 3.5 cm respectively. A cadaver showed myocardial bridging (5th cadaver) of left anterior descending branch, and the bride length was 1.1 cm. The other cadavers have no anatomical variation (intermediate branch and myocardial bridging).

Those results suggest that some individual has anatomical variation of coronary artery, especially left main coronary artery which has three branches called *trifurcatio* (left circumflex branch, left anterior descending branch and intermediate branch). And another version of left main coronary artery anatomical variation is myocardial bridging of left anterior descending artery.

Key Words: Cadaveric study, Anatomical variation, Left coronary artery, *trifurcatio*, Intermediate branch, Myocardial bridging.

P063

persons using centimeter tape. The measurement commenced from the origin of the branch and ended in the terminal of the branch. From nine specimens have been identified, we found intermediate branch in three specimens (7th cadaver, 8th cadaver, and 9th cadaver), length of each sample is 3.0 cm, 1.7 cm, and 3.5 cm respectively. A cadaver showed myocardial bridging (5th cadaver) of left anterior descending branch, and the bride length was 1.1 cm. The other cadavers have no anatomical variation (intermediate branch and myocardial bridging). Those results suggest that some individual has anatomical variation of coronary artery, especially left main coronary artery which has three branches called *trifurcatio* (left circumflex branch, left anterior descending branch and intermediate branch). And another version of left main coronary artery anatomical variation is myocardial bridging of left anterior descending artery.

Key Words: Cadaveric study, Anatomical variation, Left coronary artery, *trifurcatio*, Intermediate branch, Myocardial bridging.

P064

Morphological change of aorta in hypertensive rat treated with ethyl rosmarinate

Pantan R[1], Tocharus J[2], Suksamrarn A[3], Tocharus C[1]

[1]Department of Anatomy, Faculty of Medicine, Chiang Mai University, Chiang Mai, Thailand
[2]Department of Physiology, Faculty of Medicine, Chiang Mai University, Chiang Mai, Thailand
[3]Department of Chemistry and Center of Excellence for Innovation in Chemistry, Faculty of Science, Ramkhamhaeng University, Bangkok, Thailand.

Hypertension is a common factor which increases the risk for a variety of other cardiovascular diseases, including stroke, heart failure, and coronary heart disease, that are important causes of mortality and morbidity worldwide. The pathological process leads to change of normal blood vessel characteristics, including the thickness of arterial wall, integrity loss of endothelial cell and elasticity distension. Medicinal plants have widely been interested for using as an alternative treatment in hypertension patient according to its lower adverse effects. The aim of this study is to investigate the effect of ethyl rosmarinate, the effective analog of rosmarinic acid, in order to alter the morphology of the thoracic aorta in hypertensive rats. N_ω-Nitro-L-arginine methyl ester (L-NAME) was used to induce hypertension in male Wistar rat for 4 weeks. Then, ethyl rosmarinate which is an analog of rosmarinic acid was given orally for 6 weeks. After euthanasia, the morphological change of the thoracic aorta was evaluated by hematoxylin and eosin (H&E) staining. Moreover, the presence of endothelial nitric oxide synthase (eNOS), an essential enzyme of endothelial cell function, was determined by immunohistochemistry. As a result, the aortic section prepared from hypertensive rats clearly showed the thickness of the media and the absence of eNOS expression when compared with normotensive rats. However, the results were reversed after treated with ethyl rosmarinate. In addition, hypertensive rats treated with enalapril demonstrated the similar results as shown in ethyl rosmarinate treated group. These obtained results suggest that ethyl rosmarinate would benefit for hypertension patient which may be used as the new alternative treatment received from natural.

Key Words: Aorta, Endothelial cell, Hypertension, Ethyl rosmarinate

P065

Anatomical study of artery and nerve distribution of the subscapularis muscle using

Sihler's staining technique

Tae-Hyeon Cho[1], Sung-Yoon Won[2], Hun-Mu Yang[1]

[1]Department of Anatomy, Yonsei University College of Medicine, Seoul, Republic of Korea
[2]Department of Occupational Therapy, Semyung University, Jecheon, Republic of Korea

The subscapularis frequently applied to surgical approach and the botulinum neurotoxin injection to treat the shoulder pain. Undesirable displacement and resection of tiny nerves and arteries twigs can easily occur during therapeutic approach. In this present study was to establish nerve and artery distribution in the subscapularis using a Sihler's staining technique and suggest reliably and safe surgical approach and injectable treatment. We were performing from respectively ten specimens to establish nerves and arterial distribution in the subscapularis. The ten specimens, latex with a red coloring agent was injected prior to dissection to enable clear distinction of the arterial distribution. The points where nerves and arteries entered the muscle were examined during the dissection procedure, and the extramuscular distribution of the nerves and arteries were meticulously determined. The Sihler's staining protocol was then performed. After staining protocol, the exta- and intramuscular nerves and arterial distribution patterns were comprehensively analyzed by taking photos, notes, and sketches. First, the subscapularis is typically innervated by the upper and lower subscapularis nerve and additionally distributed into the axillary nerve (4/10) and thoracodorsal nerve (2/10). Then, we categorized three types according to the nerve distribution. Second, the subscapularis is generally received an arterial supply of the subscapular artery and additionally observed lateral axillary artery branches (7/10), posterior circumflex artery (5/10), lateral thoracic artery (4/10), circumflex scapular artery (4/10), suprascapular artery (3/10) and dorsal scapular artery (2/10). Then, we classified into three types in anterior facet and three types in posterior face, respectively. The subscapularis is divided into the upper and lower portion by the fascial septa. The nerves and arteries are predominantly distributed according to each portion. This anatomical information of the subscapularis is very important. It will be help clinicians to avoid complications during and after surgical procedure and botulinum neurotoxin injection.

Key Words: Subscapularis, Artery distribution, Nerve innervation, Sihler's staining

P066

MORPHOLOGICAL VARIATIONS OF ORIGIN& TERMINATION THE FACIAL ARTERY IN MYANMAR ADULTS

Tha Zin[1], Saung Akari [2], Myint San Nwe [3]

Department Of Anatomy, University Of Medicine 1, Yangon, Myanmar

The facial artery was the principal artery of the face which arose anteriorly from the external carotid artery in the carotid triangle of the neck. The morphological variations of the facial artery were studied in 19 formalin fixed adult cadavers, 13 in males and 6 in females.
In the present study, the prevalence of usual origin of facial artery was found in 31 facial arteries (81.58%) and high origin was seen in 7 facial arteries (18.42%). The high origins of 5 facial arteries (13.16%) were within the digastric triangle and another 2 facial arteries (5.3%) were arising just above the level of hyoid bone.
In addition, there were 32 facial arteries (84.2%) originated as single branch from the external carotid artery and another variant origin, linguofacial trunk was found in 6 facial arteries (15.8%).The

knowledge of this type of variant origin of facial artery was important in procedures such as extra oral ligature of lingual artery. The hemorrhage caused by a lesion of the lingual artery could occur during a dental procedure by trauma, biopsy and dental implant. If ligation of the lingual-facial trunk, it could diminish the blood flow to the face

The most termination branch was superior labial artery in 16 facial arteries (42.1%). The other termination branches were inferior alar in 9 facial arteries (23.6%), lateral nasal artery in 7 facial arteries (18.4%), inferior labial in 4 facial arteries (10.5%) and angular branches in 2 facial arteries (5.3%). The facial artery was selected as a target for super selective intra-arterial chemotherapy during the treatment of inoperable malignant glioma. The facial artery terminated before reaching the medial angle of the eye as above variations and could not reach the focus.

Key Words: Facial artery, Morphological, Variations, High origin

P067

Testing tools of student's anatomy knowledge

Anita Dabuzinskiene[1], Ausra Burkauskiene[1], Lena Green[2]

[1]Institute of Anatomy, Medical Academy, Lithuanian University of Health Sciences, Kaunas, Lithuania
[2]Faculty of Medicine, Medical Academy, Lithuanian University of Health Sciences, Kaunas, Lithuania

Problem Based Learning (PBL) has been in use in our University since 2005. However, nowadays more accurate knowledge testing tools are required. For instance, the Locomotion module Exam for the Second Year Medical students consists of 13 subject's multiple choice and other type questions. The subject matter of the study of exam results of 400 students is the way the students answer various types of questions on the Anatomy part of the Exam. The first type of question is a multiple choice question with one or more correct answers. The second type of question is related to clinical situations where the students are expected to apply their theoretical knowledge of Anatomy in medical practice. The third type requires students to identify anatomical structures in an image. The students scored the highest in the first type of question, but the accuracy of knowledge assessment is not apparent as the students may guess correct answers rather than display their actual knowledge. The second type of question yielded lower scores notwithstanding the importance of Medical students' proficiency in clinical and applied Anatomy. The identification of structures in given images (the third type of question) scored high enough to show a satisfactory level of the students' understanding of a regional organotopic organization beneficial for the future clinical practice. In conclusion, students subjected to PBL were failing where basic Anatomy knowledge is concerned, making analysis, generalization and synthesis of acquired knowledge primary developmental areas of Anatomy education.

Key Words: Problem Based Learning, Education, Locomotion, Anatomy

P068

The Comparison of Students' Anatomy Practical Exam: Musculoskeletal vs Cardiovascular System

Hidayati, Nurul

Department of Anatomy, Universitas Brawijaya, Malang, Indonesia

The anatomy practical exam from students' end-results presents some interesting values to be evaluated; unfortunately, was rarely explored in content perspective. Most educational program evaluations of students' exam performance likely focuses on students and the surrounding technical program. We compare our students' anatomy practical exam results for the last ten years concentrating at systems of musculoskeletal and cardiovascular. We evaluate our students' practical exam results from the last ten years programs. Accordingly, we have students grades from batch 2007 until 20015 for musculoskeletal and cardiovascular system. Both students' anatomy practical exams were statistically operated using simple calculation for the average results on annual basis. The program applied was minitab 16.0, which is the regular statistical software. Furthermore, the graph lines trend were compared and interpreted using the expert judgments by two subject-based teachers and one medical education expert. As the result, both the graphic lines of musculoskeletal and cardiovascular practical exams show downtrend lines. In fact, the musculoskeletal grades is lower than cardiovascular exam results. Fact that musculoskeletal is addressed on third semester while cardiovascular is placed on fourth semester is not considered as a significant value to compare. Our attention is, then, focused on the grades and the fluctuations between the data sets. The lowest grades of musculoskeletal is at 40.47 while the highest is 60.0. Thus, interestingly, the line of this subject has high fluctuation. The other way, with more stabile line, cardiovascular lowest grade is placed at 59.54 and its average grades from all the year examined is 64.04 showing that the various distances are not far. Consequently, we explore problems of musculoskeletal and use the cardiovascular as the reference to compare. Considering the specific organ structure character between the two, musculoskeletal has a large number of organs to cover but specific feature characters to be identified is not the challenge. In contrary, cardiovascular system has more heterogenic structures that understanding the organ system we need to conceive the functional concept; however, the number of organs to be assessed in practical exam is restricted due to its specificity. Therefore, various sample of questions in cardiovascular may be covered in simple lists of names whilst for musculoskeletal system there is high loading of memory for all muscle names. Hence, the fluctuation of musculoskeletal graph-line can be explained with this perspective since the questions can come from any muscles. Students' anatomy practical exam challenges students in identification various organ structures with all their specific features. The typical organ system may influence students' exam result as the level of difficulty consideration. Finally, it opens future potential investigation to explore students' loading to study in perspective of both structural concept and the number of organ structures to identify.

Key Words: Practical exam, Musculoskeletal, Cardiovascular, Graph-lines, Fluctuation

P069

Self and peer assessment in anatomical sciences courses can foster metacognition awareness in medical students in student-center context

Amrollah Roozbehi[1], Sahar Almasi-Turk[2]

[1]Department of Anatomy, Yasuj University of Medical Sciences, Yasuj, IRAN.
[2]Department of Anatomy, Boushehr University of Medical Sciences, Boushehr, IRAN.

Introduction: Metacognition is a regulatory system that helps a learner understands and controls his own cognitive performance. It involves awareness of how they learn, evaluation of their learning needs, generating strategies to meet these needs and then implementing the strategies.

Learners often show an increase in self-confidence when they build metacognitive skills. Self-efficacy improves motivation as well as learning success. The aim of this study was evaluation of the effects of self and peer assessment method on metacognition awareness in medical students. **Materials and Methods:** This is a participatory action research of 98 medical students (entering in academic year 2017) registered in course of histology and limb anatomy in semester two of year 2017. Contents were divided into five roughly equal parts, each part was assigned to a group of 5-6 students and the students' tasks were determined. Two formal sessions over two weeks were allocated in order to prepare at the level of mastery learning in presentation. Both theoretical and practical units were presented by peer teachers to their classmates while a dedicated tutor was present in each group. All students taught 4-5 of their classmates in peer assisted learning (PAL) groups for two sessions. At the last section of each session a formative exam was taken, the correction key and scores were provided with active participation of students. A few of students were engaged in order to better control of exam correction. Feedback was provided for students. Self and peer assessment characteristics were announced to students in advance. In these studies metacognitive awareness were measured in terms of metacognitive knowledge and cognitive regulation, self-report Schraw and Dennison inventory wa used before mastery learning and at the end of semester. Paired t-tests were used for analyzing the data. **Results:** Paired t-tests analysis showed the three metacognitive knowledge scales in two phases were as follow; declarative knowledge 3.46 ± 0.82 and 3.7 ± 0.63, procedural knowledge 3.77 ± 0.85 and 3.95 ± 0.53, conditional knowledge 3.66 ± 0.84 and 3.89 ± 0.64. And also showed the five cognitive regulation scales in two phases were as follow; planning 3.44 ± 0.76 and 3.75 ± 0.64, information management 3.64 ± 0.81 and 3.84 ± 0.61, comprehension 3.58 ± 0.79 and 3.82 ± 0.64, debugging 3.64 ± 0.81 and 3.84 ± 0.61, evaluation 3.53 ± 0.81 and 3.69 ± 0.72. Comparing mean numbers of two phases showed statistical increases (P ≤ 0.05). **Discussion:** This study showed that cognitive construction was occurred between students. Through implementing this action research implicit knowledge change to explicit knowledge effectively and immediate feedback was received. We can pretend positive performances reinforced and learning errors were managed impressively. Students' self-regulation and self-monitoring will be achieved by such methods, and also self-steam and self-attribution will be developed. In this study we tried not only to engage students in learning processes but also by self/ peer- assessment and immediate feedback promote their metacognition knowledge.

Key Words: Self-assessment, Peer assessment, Metacognition, Peer assisted learning, Medical students and student center

P070

PABZA: Tool for Increasing Cognition in Anatomy via Metacognitive Enhancement

Tg Fatimah Murniwati TM[1], Yasrul Izad AB[1], Ahmed J[2], Asma' H[1], Lakshmi A[1], Nur Farhana CL[1], Sehrish R[2], Sadia S[2], Maryam I[2], Atif AB[1]

[1]Faculty of Medicine, Universiti Sultan Zainal Abidin, Terengganu, Malaysia
[2]School of Health Sciences, University of Management and Technology, Pakistan

Physiology Anatomy Biochemistry through Z to A (PABZA) is an app which is designed for cognitive domain towards learning, understanding and recalling the basic knowledge of anatomy, physiology and biochemistry for the medical and allied health students. The main objective of this app is to develop a new comprehensive method of e-learning for the undergraduate and postgraduate students to enhance their knowledge, skills and productivity. The PABZA app works as a website and also as a phone application. The app is based on curated graphs and animations for teaching purpose

considering the reported recognized RILEAZ (Z to A) method of teaching. We made use of the novel principles of RILEAZ to be implemented for teaching the three most important foundation subjects in medicine and allied health. The conceptual graphics are used as complementary ways to enhance motivation, attention, understanding and recall of the important topics in anatomy, physiology and biochemistry. The method has been complemented with storytelling, is to be incorporated into the existing traditional teaching. This app is targeting the affective learning domains under life-long learning though it can be used for non-integrated or integrated based curriculum. It is still in the early development phase of the contents. In the future, we could improve the PABZA by providing integrated content of the subjects – anatomy, physiology and biochemistry (perhaps pathology), instead of separate topics for each discipline. Comparative analysis of PABZA with the traditional methods and metacognitive levels in academics will be conducted to prove its significance.

Key Words: PABZA, RILEAZ, App, Anatomy, Physiology, Biochemistry

P071

Implementing flipped classroom of anatomical sciences on a blended teaching platform: A step toward community responsiveness

Sahar Almasi-Turk[1], Amrollah Roozbehi[2]

[1]Department of Anatomy, Boushehr University of Medical Sciences, Boushehr, IRAN.
[2]Department of Anatomy, Yasuj University of Medical Sciences, Yasuj, IRAN.

Introduction: Educational excellence depends on an institute's ability to provide all students with the disciplinary knowledge, skills, and dispositions that enable competent participation in our modern, pluralistic society. Our goals are conveyed in our framework, reflective educators for community-responsive education. We need curriculums that provide a wide range of strategies, techniques and differentiated instruction that positively affect student learning. Flipped classroom is a blended learning strategy with the aim to improve student engagement and outcomes. The key purpose of the flipped classroom is to provide a greater focus on students' application of conceptual knowledge rather than factual recall or straight transfer of information. **Materials and Methods:** This is a participatory action research of 108 medical students registered in a blended course of limb anatomy in semester two of year 2016. Contents were given through 5 essential and 20 details videos to students. Books, course and lesson plans were introduced to students. During the first 5 sessions the essential contents and the rest sessions the detail contents were presented. Contents were divided into five roughly equal parts, each part was assigned to a group of 5-6 students and the students' tasks were determined. Two formal sessions over two weeks were allocated in order to prepare by team based learning (TBL) method at the level of mastery learning in presentation. For individual preparedness assurance all students prepared two videos from allocated upper and lower limb content by desktop capturing software. Both theoretical and practical units were presented by peers to their classmates while a dedicated tutor was present in each group. Students studied at home and take part in small group sessions that were managed by same peer tutors. Each tutor taught 4-5 of their classmates in small groups for two sessions. At the last section of each session a formative exam was taken, the correction key and scores were provided with active participation of students. In order to better control of exam correction a few of students were engaged. Feedback was provided for students. Paired t-tests were used for analyzing the data. **Results:** The finding of 5 consecutive formative exams, students' collaboration in TBL phase, students' cooperation in peer assisted learning (PAL) phase and students' satisfaction are came in graph 1 and table 1 to 3. **Discussion:** Community responsive education requires a rigorous, continuing reflection on our

assumptions, aims, and practices as educators who must develop this same reflective and purposeful disposition in our candidates who will teach the next generation of knowledgeable, democratic-minded, and responsible citizens. Flipped classroom is an active method that engaged students in this way. We seek to develop competent educators who: have an in-depth knowledge of their discipline or field of study and understand, value, and apply it in their teaching and learning, accept that all students can learn, and that learning is an active and reciprocal process, recognize and embrace the educational importance of a commitment to diversity, equity, and social justice within the context of a democratic society, understand that all education is rooted in local communities and are reflective practitioners who are committed to the need for life-long learning. These goals provide a foundation for designing programs to educate competent teachers and other educational professionals.

Key Words: Flipped classroom, Anatomical sciences, Blended teaching and community responsiveness

P072

An Adventure Towards The Human Body (AORTA) : Implementing A New Concept to Assess Medical Student's Insight Through A Holistic Approach of Anatomy

Muthiah Nur Afifah, Mufidah Ruslan, Reza Kurniawan Arta, Jamaluddin Madeali, Rizki Darmawan, Muh. Haedar, Asty Amalia

Department of Anatomy, Medical Faculty, Hasanuddin University, Makassar, Indonesia.

Assessment is one of the most important in anatomy education. Varieties of assessment formats are available for assessing anatomical knowledge, understanding, and skill in different domains. The Anatomy Amazing Race Competition, called AORTA (*An Adventure Towards The Human Body*) has been held in Makassar, to assess the medical student's insight of anatomy by categorizing an assessment based on "*Bloom's taxonomy*". AORTA consisted of five posts where each post has various anatomy challenges that represent a different assessment of learning domains from rememberability, understanding, application, analyzability and evaluation. Undergraduate Students from several faculty of medicine throughout Indonesia was invited as participants. Participants were given questionnaire to describe their opinions about the benefit they got from the competition. Each question contained choices of every learning domain, and participant would subjectively choose the assessed domain. Of the forty participants who competed in the competition, there were only twelve who got through all the posts and asked to fill in the questionnaire. They all agreed rememberability (100%) as the assessed domain in the first post, rememberability (100%) and understanding (83.3%) in the second post. In the third post, the assessed domains were rememberability (91%), understanding (75%), application (75%). In the fourth post, the assessed domains were only rememberability (83%) and understanding (75%). In the fifth post, participants only chose rememberability (91%) as the assessed domain and the other domains for each post did not get the standard values (75%). From these results, there was an increase of the learning domain level in the first three posts. While two last post was inappropriate. Overall, AORTA is available for assessing anatomical knowledge based on level competence of undergraduate students (91.67%). In particular, participants noted that the competition also develop their abilities in collaboration (91.67%), strategy (75%), and time management (75%). This study demonstrated that AORTA as a new concept of assessment anatomical knowledge in three different domains of *Bloom's Taxonomy,* there are rememberability, understanding, and application. As other domain was inappropriate, it is expected to be developed so a comprehensive learning domain will be achieved.

P073

Development of Virtual Realty Contents for Third Molar Extration

Jeong- hyun Lee[1], Sa-Beom Park[1], Eun-Young Jeon [1], Hyun-na Ahn[1,] Dea-Won Park[2], Jong-Hoi Kim[3], Jong-Tae Park[1*]

[1]Department of Oral Anatomy, Dan-kook University College of Dentistry, Cheonan, South Korea
[2]Darwin Tech Company, Gwangju, South Korea
[3]Triangle-lab Company, Gwangju, South Korea

Medical technology has seen great improvement in recent years with the use of 3D technology. The purpose of this study is to develop dental treatment models and educational simulations for dental procedures such as third molar extraction, which is almost impossible to practice, through optimized dental modeling standardization. In this study, the entire surgical environment, including the operator and the dental hygienist along with the patient at the center, was filmed in a 360° VR format using three GoPro Hero5 Black (4k, 30fps) cameras equipped with Entaniya 220° angle-of-view lenses. In addition, a 3D parallel camera was used to acquire intraoral super close-up images. To compensate for the drawbacks of VR imaging, a stereoscopic image was acquired in the same direction as the viewer's line of vision by directly mounting the 3D head-mounted camera on a 3D printed head strap. 3D video tracks were edited and displayed in a side-by-side format using the Vegas program. Kolor Autopano Video Pro and Autopano Giga were used to sync and stitch the 360° VR clips and to render the clips in 4K (4096*2160, 30fps) resolution through color correction. The final 3D images and 360° VR clips were replayed on Samsung Gear VR. This study consists of the entire process of third molar surgical extraction including the pre-operative procedure, the surgical procedure, and the post-operative procedure. The practical training process is composed of three stages; the first stage when the demonstrator demonstrates the procedure at an appropriate speed without the explanation of an instructor; the second stage when the instructor explains each part of the surgical extraction; and the third stage when the learner acquires the procedure and principle of the procedure while listening to the explanation of the instructor. Through this three-stage process, the learner can check the entire medical procedure. Such a composition enables the learner to confirm conceptual information, detailed surgical procedure and step-by-step procedures as needed. With the development of simulation-based educational model, this study is expected to suggest a new paradigm of future dental industry. This research was financially supported by the Ministry of Trade, Industry and Energy(MOTIE) and Korea Institute for Advancement of Technology(KIAT) through the Research and Development for Regional Industry(R-0006275)

P074

Developing a mobile learning tools using 3d modeling technology on head and neck anatomy

Sa-Beom Park, Eun-Young Jeon, Jeong-Hyun Lee, Hyun-Na Ahn, Jong-Tae Park

Department of Oral Anatomy, Dankook University College of Dentistry, Cheonan, South Korea

Anatomy practice is necessary for a learner who has entered the field of medicine and dentistry to understand the anatomy and to acquire the basic knowledge of the clinical. Three-dimensional anatomy applications are more effective because they can easily observe the shape of the head bone regardless of time and place. The purpose of this study is to propose an accurate anatomical structure of the head and neck necessary for anatomy practice and to develop a viewer - based mobile learning support tool that provides 3D modeling information about head and neck anatomy. With 2d graphics tools such as Illustrator and Photoshop, we have studied and designed interfaces for user convenience in terms of functionality. The modeling tool such as 3ds Max, Zbrush was used to make the skull bones and muscles. finally, using the mobile programming tool Unity, the 3d head and neck anatomy application was developed. The results of the study showed that the anatomy practice application is a mobile seamless learning that links the lecture room activities including the head and neck anatomy lectures and hands - on activities and the learner's practice and daily learning to the mobile learning support tool. The mobile training support tool was implemented with the structure of the anatomical muscle including the facial information and clinical information on the 3D skull bones, the precise structure through which the nerve, the artery, the vein passes, the clinical variation and clinical practice notes, and the facial muscle. The experts' evaluation on the developed contents shows that the content and function are valid (content validity: 5.0, interface validity: 4.53). The mobile learning support tool developed through this study is considered to be a suitable learning tool to support the mobile seamless learning of students' practice in medicine and dentistry. The 3d anatomy application developed based on this study will be developed into an upgraded version that includes the nerves, arteries, and veins. It is expected to be used not only in the field of plastic surgery requiring clinical knowledge such as botox and filler but also in various fields of medicine and dentistry.

Key Words: Mobile, Application, 3D, Modeling, Head and Neck

P075

Does digital microscopy enhance the learning of Histology?

Pamela David[1], Chia-Wei Phan[2], Murali Naidu[1]

[1]Department of Anatomy, Faculty of Medicine, University of Malaya, 50603 Kuala Lumpur, Malaysia
[2]Department of Pharmacy, Faculty of Medicine, University of Malaya, 50603 Kuala Lumpur, Malaysia

Histology is integral for understanding the underlying mechanisms of disease processes, and a rich knowledge acquisition at tissue level organization is much appreciated in the preclinical years of medical training. In the University of Malaya, the students are exposed to laboratory instructions of histology by way of the conventional microscopy, having an access to a microscope and a set of glass slides. However, digital microscopy featuring labelled illustations with user-friendly navigation steps, has widely emerged as a popular tool to study histology. This study aims to assess the efficacies and compare the effectiveness of conventional microscopy with digital microscopy. The histology sessions of connective tissues, muscle tissue, lymphatic system and nervous system were sampled in this study.
The first year Bachelor of Medicine & Bachelor of Surgery (MBBS) students participated in the study and were randomly divided into two groups. The first group underwent the usual conventional modality of studying the microscopic features of tissues provided, while the second group studied the same

tissues in the computer labs by way of digital microscopy. This was followed by exposing both groups of students to various post-recall tests based on different levels of difficulty, and the knowledge acquired by the students were recored and analysed. A questionnaire survey was also included to explore the students' preference on both the modalities employed. Overall results showed better scores obtained by the digital microscopy group as compared to the conventional microscopy group. The digital microscopy group was also able to identify all (100%) the histological features compared to the conventional microscopy group which identified only 88.9% of the features tested. The post recall tests also revealed better answering skills in the digital microscopy group and this could be due to the fact that the digital images had informative explanatory text and annotations pegged to every photomicrograph viewed during the course of the study. Hence, the current study suggests that digital microscopy enhanced learning. It provides speed, convenience and high quality images that is much useful in an integrated medical curriculum. However, conventional microscopy must not be done away as it gives a 'hand-on' approach in studying histology. Here, we recommend that the conventional microscopy is augmented with a series of self-instructional digital microscopy during the MBBS course to enhance learning histology.

Key Words: Digital microscopy, Conventional microscopy, Histology, Glass slide

P076

Effects of caloric restriction on brown adipose tissue dysfunction in high-fat diet-fed mice

Kyung-Ah Park, Zhen Jin, Jong Youl Lee, Eun Ae Jeong, Hyeong Seok An, Eun Bee Choi, Kyung Eun Kim, Hyun Joo Shin, Gu Seob Roh

Department of Anatomy and Convergence Medical Science, Bio Anti-Aging Medical Research Center, Institute of Health Sciences, College of Medicine, Gyeongsang National University, Jinju, Gyeongnam 52727, Republic of Korea

Lipocalin-2 (LCN2) plays a role in oxidative metabolism and brown adipose tissue (BAT) activation. Caloric restriction (CR) has been shown to help maintain energy homeostasis in adipose tissue. Therefore, in this study we evaluated whether CR can reverse BAT dysfunction via LCN2-mediated oxidative stress and mitochondrial dysfunction in high-fat diet (HFD)-fed mice. C57BL/6 mice were fed an HFD for 20 weeks and then continued on the HFD or subjected to CR (2 g food/day) for next 12 weeks. We evaluated the effects of CR on BAT dysfunction by histological analysis, western blot, and immunostaining, and by measuring triglyceride and iron levels. The BAT of HFD-fed mice showed aberrant iron and triglyceride accumulation and significantly increased levels of LCN2 and proteins associated with oxidative stress, mitochondrial fission, and mitochondrial autophagy. CR significantly attenuated many of the HFD-induced changes. Our findings indicate that CR may be useful to treat obesity-related metabolic disturbances caused by LCN2-mediated oxidative stress and mitochondrial dysfunction in BAT.

Key Words: Caloric restriction; Brown adipose tissue; Lipocalin-2; Oxidative stress; Mitochondrial dysfunction

P077

Lobeglitazone improves insulin resistance and hepatic steatosis in high-fat diet-fed

mice

Jong Youl Lee[1], Zhen Jin[1], Eun Ae Jeong[1], Kyung-Ah Park[1], Kyung Eun Kim[1], Bong-Hoi Choi[2], Jong Ryeal Hahm[3], Gu Seob Roh[1]*

[1]Department of Anatomy and Convergence Medical Science, Bio Anti-aging Medical Research Center, Institute of Health Sciences, College of Medicine, Gyeongsang National University, Jinju, Gyeongnam, Republic of Korea
[2]Department of Nuclear Medicine, College of Medicine, Gyeongsang National University Hospital, Gyeongsang National University, Jinju, Gyeongnam, Republic of Korea
[3]Division of Endocrinology and Metabolism, Department of Internal Medicine, College of Medicine, Gyeongsang National University, Jinju, Gyeongnam, Republic of Korea

Lobeglitazone (Lobe) is a novel thiazolidinedione antidiabetic drug that reduces insulin resistance by activating peroxisome proliferator-activated receptor-gamma (PPARγ). However, the exact mechanisms of antidiabetic effects of Lobe have not been established in an animal model.
The aim of this study was to evaluate the hypoglycemic effects of Lobe and investigate possible factors involved in Lobe-enhanced hepatic steatosis in high-fat diet (HFD)-fed mice. Mice were fed an HFD for 15 weeks. Lobe was administrated orally during the last 9 weeks. Lobe treatment significantly reduced insulin resistance and increased expression of hepatic glucose transporter 4 (GLUT4) and PPARs in HFD-fed mice. However, increased body weight and hepatic steatosis were not reduced by Lobe in these mice. Metabolomics fingerprinting showed that several lipogenesis-related hepatic and serum metabolites in HFD-fed mice had positive or negative correlations with Lobe administration. In particular, increased leptin levels during HFD were further increased by Lobe. HFD-induced signaling transducer and activator of transcription 3 (STAT3) phosphorylation in the hypothalamus was increased by Lobe. In addition, immunohistochemical analysis showed more proopiomelanocortin (POMC)-positive neurons in the hypothalamus of HFD-fed mice (with or without Lobe) compared with normal diet-fed mice. Despite improving leptin signaling in the hypothalamus and enhancing insulin sensitivity in HFD-fed mice, Lobe increased body weight and steatosis. Further research is necessary regarding other factors affecting Lobe-enhanced hepatic steatosis and hyperphagia.

Key Words: Lobeglitazone; Insulin resistance; Hepatic steatosis; Hypothalamus; Obesity

P078

Caloric restriction ameliorates left ventricular hypertrophy through regulation of lipocalin-2-mediated inflammation and oxidative stress in ob/ob mice

Hyeong Seok An[1,2], Eun Ae Jeong[1,2], Jong Youl Lee[1,2], Kyung Eun Kim[1,2], Eun Bee Choi[1,2], Kyung-Ah Park[1,2], Zhen Jin[1,2], Hyun Joo Shin[1,2], Dong Hoon Lee[1], Hyun Joon Kim[1,2], Sang Soo Kang[1], Gyeong Jae Cho[1], Wan Sung Choi[1,2], Gu Seob Roh[1,2]*

[1]Department of Anatomy and Convergence Medical Science, College of Medicine, Gyeongsang National University, Jinju, Gyeongnam 52777, Republic of Korea
[2]Bio anti-aging Medical Research Center, Institute of Health Sciences, College of Medicine, Gyeongsang National University, Jinju, Gyeongnam 52777, Republic of Korea

Obesity has been found to be associated with left ventricular hypertrophy (LVH). Lipocalin-2 (LCN2) is an inflammatory cytokine and obesity-related marker of inflammation. However, little is known about the molecular mechanism between LCN2 and LVH. Obesity-induced metabolic

disturbances were improved by caloric restriction (CR). To investigate effect of CR on LCN2-mediated inflammation and oxidative stress in heart, ob/ob mice were fed normal diet for 20 weeks and continued on normal diet or subjected to CR (2g/day) for 12 weeks. We found that the left ventricular wall thickness were decreased in ob/ob+CR mice compared to ob/ob mice. In particular, CR decreased the expression level of LCN2 in the heart of ob/ob mice. Moreover, inflammatory-related proteins (IL-6 and NF-kB) and fibrogenic proteins (TGF-beta and VEGF) in the heart of ob/ob mice were decreased by CR. In addition, obesity-induced HO-1 and NQO1 expressions in ob/ob mice were decreased by CR.

These findings indicate that CR reverses obesity-induced LCN2 level, inflammation and oxidative stress and ameliorates left ventricular hypertrophy in obese mice.

Key Words: Caloric restriction; heart; lipocalin-2; ob/ob mice

P079

Lipocalin-2 signaling in skeletal muscles regulates inflammation and oxidative stress in ob/ob mice

Eun Bee Choi[1,2], Kyung Eun Kim[1,2], Hyeong Seok An[1,2], Eun Ae Jeong[1,2], Jong Youl Lee[1,2], Kyung-Ah Park[1,2], Zhen Jin[1,2], Hyun Joo Shin[1,2], Dong Hoon Lee[1], Hyun Joon Kim[1,2], Sang Soo Kang[1], Gyeong Jae Cho[1], Wan Sung Choi[1,2], Gu Seob Roh[1,2]*

[1]Department of Anatomy and Convergence Medical Science, College of Medicine, Gyeongsang National University, Jinju, Gyeongnam 52777, Republic of Korea
[2]Bio anti-aging Medical Research Center, Institute of Health Sciences, College of Medicine, Gyeongsang National University, Jinju, Gyeongnam 52777, Republic of Korea

Obesity-associated insulin resistance is attributed to inflammation and oxidative stress, and impaired muscle regeneration. Lipocalin-2 (LCN2) is an iron carrier protein whose circulating level is increased by inflammation in obesity, but its exact role in skeletal muscle in obesity remains controversial. In present study, we investigate how the expression of LCN2 is regulated in skeletal muscles of ob/ob mice. Leptin-deficient *ob/ob* mice *had significant reduction of* muscle diameter compared with wild type (WT) mice. Histological analysis showed that collagen accumulation was increased in ob/ob mice compared to WT mice. In accordance with fibrosis, western blot showed that interleukin-6 (IL-6), nuclear factor-κB (NF-κB), transforming growth factor-β (TGF-β), and α-smooth muscle actin (SMA) expressions were increased in the skeletal muscle of ob/ob mice. In particular, we found that there were increased expressions of LCN2 and its receptor in ob/ob mice. In addition, obesity-induced heme oxygenase (HO-1) was also increased in ob/ob mice compared to WT mice.

Our findings suggest that LCN2 may play an important role in muscle contraction and atrophy of skeletal muscle with insulin resistance or obesity.

Key Words: Lipocalin-2; Skeletal muscle; ob/ob mice

P080

The anti-obesity properties of Phlorotannin rich-Ecklonia Cava extract by regulating central leptin signaling

Myeongjoo Son[1,2], Hyosang Ahn[1,2], Junwon Choi[1,2], Seyeon Oh[2], Hye Sun Lee[2], Ji-Tae Jang[3], You-

Jin Jeon[4], Kyunghee Byun[1,2,*]

[1]Department of Anatomy and Cell Biology, Gachon University College of Medicine, Incheon 21565, Republic of Korea
[2]Functional Cellular Networks Laboratory, Lee Gil Ya Cancer and Diabetes Institute, Gachon University, Incheon 21999, Republic of Korea
[3]AQUA GREEN TECHNOLOGY co., #316. Smart Bidg., Jeju Science Park, 213-3 Cheomdan-ro, Jeju City, Jeju Special Self-Governing Province, 63309, Republic of Korea,
[4] Department of Marine Life Sciences, Jeju National University, Jeju 63243, Republic of Korea.

Generally, it is known that obesity induces hepatic steatosis, lipid accumulation of muscle, increased fat size and various blood circulation diseases. Leptin is one of important obesity factor that controls appetite through receptor of hypothalamus. Recently, researchers were focusing on controlling leptin level for one of method to down regulation of appetite and fat size. However, there are few compound that be able to control this pathway. Here, we used the phlorotannin rich-extract from Ecklonia Cava (ECE) and effective marker B that is one of ECE compounds with leptin-deficiency mice and high fat diet-induced obese mice (DIO) model. In previous studies, there were some specific results that ECE regulated fat metabolism inflammation and the anti-oxidant defense system with DIO mice. We validated more detailed pathways from brain to peripheral organs like liver, muscle and fat tissues. From these results, leptin pathway of hypothalamus in brain was controlled and down-regulation of fat size and inflammation was detected in each fat tissues such as peri-aortic, subcutaneous and visceral fat. These results show that ECE could be leptin substitute for anti-obesity properties.

P081

Fibroblast growth factor 21 alleviates hepatic steatosis and iron overload in HFD-induced NAFLD through upregulating STAMP2 expression

Hye Young Kim, Woo Young Kwon, Joon Beom Park, Hwa Jin Kim, Young Hyun Yoo

Department of Anatomy and Cell Biology, Dong-A University College of Medicine, Busan, Republic of Korea

Fibroblast growth factor 21 (FGF21) has recently emerged as a promising therapeutic candidate for metabolic disorders. Despite the importance of FGF21 in the regulation of glucose, lipid, and energy homeostasis, the mechanisms by which FGF21 functions as a metabolic regulator remain largely unknown. The aim of this study is to evaluate the role of FGF21 in high fat diet (HFD)-induced nonalcoholic fatty liver disease (NAFLD). In this study, we used HFD-induced mouse *in vivo* and oleic acid-induced HepG2 cells *in vitro* NAFLD model. After 10 days of recombinant murine FGF21 treatment (0.5mg/kg/day), metabolic parameters including body weight, blood glucose and lipid levels, hepatic and fat gene expression levels were monitored and analyzed in HFD-induced NAFLD model. Also, fat-loaded HepG2 cells were treated with vehicle or recombinant human FGF21. Recombinant murine FGF21 treatment produced significant improvements in HFD-induced NAFLD, including decreases hepatic steatosis and increases insulin sensitivity. Our previous study suggested that six transmembrane protein of prostate 2 (STAMP2) may be a suitable target for treating NAFLD. Here, we show that rmFGF21 improves HFD-induced NAFLD by upregulating the expression level of hepatic STAMP2. Next we investigated hepatic iron homeostasis because STAMP2 protein has been identified as ferrireductases responsible for the reduction of Fe^{3+}. We observed that rmFGF21 significantly improves HFD-induced hepatic iron overload *in vivo* and *in vitro* NAFLD model. Noticeably, *In vivo* and

in vitro knockdown of hepatic STAMP2 by siRNA undermined effects of rmFGF21 in HFD-induced NAFLD model. In conclusion, FGF21 regulate hepatic iron homeostasis by enhancing hepatic STAMP2 expression, resulting in ameliorates HFD-induced NAFLD models. Our findings indicate that enhancing STAMP2 expression with FGF21 represents a potential therapeutic avenue for treatment of NAFLD.

Key Words: NAFLD, FGF21, STAMP2, Iron overload, Iron homeostasis

P082

The ablation of NADP+-dependent isocitrate dehydrogenase 2 aggravates high-fat diet-induced hypertension.

Mi Ra Noh[1], Jee In Kim[2], Kwon Moo Park[1]

[1]Department of Anatomy and BK21 Plus, School of Medicine, Kyungpook National University, Daegu, Republic of Korea
[2]Department of Molecular Medicine and MRC, Keimyung University School of Medicine, Daegu, Republic of Korea

Obesity is a major risk factor for essential hypertension. Oxidative stress is an important pathogenic mechanism of obesity-induced hypertension. NADP$^+$-dependent isocitrate dehydrogenase 2 (IDH2) plays as a major antioxidant system by production of NADPH, which is an essential player in the glutathione (GSH) and thioredoxin systems for peroxide detoxification antioxidant system. Here, we investigated the role of IDH2 in high fat diet (HFD)-induced hypertension and its underlying mechanism. Eight-week-old Idh2 gene-deleted (Idh2–/–) mice and wild-type (Idh2+/+) littermates were fed control diet (CD) or HFD for 12 weeks. HFD increased blood pressure (BP) both mice from 6 weeks later. BP increases in the Idh2–/– mice was higher compared with that in the Idh2+/+ mice. mRNA levels of renin and angiotensinogen and angiotensin II receptor type I in the kidney, and angiotensin converting enzyme in the lung increased after HFD feeding and these increases were higher in Idh2–/– mice than in Idh2+/+ mice. However, there were no differences in those between CD feeding Idh2–/– mice and Idh2+/+ mice. HFD induced decreased IDH2 activity and expression, accompanying with increases of mitochondrial ROS level and oxidative damages. These HFD-induced mitochondrial ROS formation and oxidative stress were greater in Idh2–/– mouse kidneys than in Idh2+/+ mouse kidneys. Mitochondrial impairments were observed after HFD feeding in both mice and those damages were more severe in the Idh2–/– mice than Idh2+/+ mice. These results indicate that HFD-induced hypertension is worsened by IDH2 gene deletion with greater oxidative stress in the kidneys, suggesting that mitochondrial redox balance impairment is associated with obesity-induced hypertension.

Keywords: Isocitrate dehydrogenase 2, Hypertension, Mitochondria, Reactive oxygen species

P083

Synergistic alveolar bone resorption by diabetic AGE and mechanical forces

Jung-Sun Moon[1], Su-Young Lee[1], Jung-Ha Kim[1], Yoon-Ho Choi[1], Hyun-Mi Ko[1], Jee-Hae Kang[1], Hyun-Jin Kim[2], Min-Seok Kim[1], Sun-Hun Kim[1]

[1]Dental Science Research Institute, School of Dentistry, Chonnam National University, Korea
[2]Department of Oral Anatomy, School of Dentistry, Wonkwang University, Korea

The close association between diabetes mellitus (DM), a major risk for periodontal health, and bone diseases is widely acknowledged; however, the mechanistic pathways leading to the alveolar bone (AB) destruction remain unclear. Accordingly, therapeutic modalities for the DM-associated AB resorption have not been determined yet. This study aimed to elucidate the mechanical forces (MF)-induced AB destruction in DM and its underlying mechanism. *In vivo* periodontal tissue responses to MF were evaluated in streptozotocin-induced diabetic rats. *In vitro* human periodontal ligament (PDL) cells were treated with advanced glycation end-products (AGE) and/or subjected to tension or compressive forces. AB resorption *in vivo* was examined by measuring the increment of tooth movement. Gene and protein levels were measured by real-time RT-PCR, Western blots, and immunohistochemistry. *In vivo*, the transcription of *VEGF-A, CSF-1*, and *Ager* was upregulated in diabetes, whereas changes in *DDOST* and *Glo1* mRNAs were negligible. DM induced VEGF-A protein expression in the vascular cells of the PDL and subsequent angiogenesis, but apparently it did not induce osteoclastogenesis by itself. MF-induced AB resorption was augmented in DM, and this augmentation was morphologically substantiated by the occasional undermining resorption as well as the frontal resorption of the AB by osteoclasts. The mRNA levels of CSF-1 and VEGF in periodontal tissues during MF application were further elevated in diabetic rats, compared to those in normal counterparts. *In vitro*, AGE treatment of human PDL fibroblastic cells elevated *Glut-1* and *CSF-1* mRNA levels via the p38 and JNK pathways, whereas OGT and VEGF levels remained unchanged. MF, especially compressive, upregulated VEGF, CSF-1, and Glut-1 levels in PDL cells and the upregulation was further escalated by AGE treatment. These suggest that excessive MF and AGE metabolites may synergistically aggravate AB destruction by upregulating CSF-1 and VEGF. Thus, the control of both compressive overloading to teeth and diabetic AGE can be a therapeutic modality for managing DM-induced alveolar bone destruction.

Key Words: Mechanical force, VEGF, CSF-1, Diabetes, Alveolar bone

P084

Effect of topical application of virgin coconut oil on fibroblast and myofibroblast of diabetic wounds

Seong Lin Teoh, Soon Kuen Wong, Thanusha A/P Rangiah, Nor Syaqira Aina Binti Bakri, Wan Nazmi Aiman Bin Ismail, Erin Elliey Fazira Binti Bojeng, Mohamad Ali Abd Rahiman, Amro Mohamed Soliman, Norzana Abd Ghafar, Srijit Das

Department of Anatomy, Faculty of Medicine, Universiti Kebangsaan Malaysia, Kuala Lumpur, Malaysia

Wound healing is often impaired in diabetic patients. In the present study, we checked the effect of virgin coconut oil (VCO) on the fibroblast and myofibroblast populations in diabetic wound healing, using immunohistochemistry. A total of 36 male Sprague-Dawley rats were diabetically induced with streptozotocin. Full thickness cutaneous wounds were created with 6 mm punch biopsy needles. The wound tissues were collected from non-treated, VCO-treated, and silver sulfadiazine-treated diabetic rats at day 7 and 14 after wounding. The tissues were then subjected to Verhoeff eosin staining and immunohistology of fibroblast and myofibroblast. Histological analysis showed increased collagen deposition with intact epidermis in the VCO treated wounds compared to reduce collagen deposition with incomplete epithelialization in the non-treated and silver sulfadiazine-treated wounds.

VCO-treated wounds showed significantly reduced fibroblast at day 7 and 14, compared to the silver sulfadiazine-treated and non-treated wounds. Similarly, non-treated wounds contain most abundant myofibroblasts compared to VCO and silver sulfadiazine-treated wounds at day 7 and 14. VCO significantly promoted wound healing process in diabetic rats as evidenced by increased re-epithelialization, collagen fibres deposition and wound contraction. Abnormal fibroblast function and disorganized myofibroblasts may lead to wound healing impairment in non-treated diabetic wounds. These results suggested VCO has a potential to treat diabetic wounds.

Key Words: α-smooth muscle actin, Cutaneous, Ciabetes mellitus, Vimentin, Immunohistochemistry

P085

JAK2/STAT3 Pathway Regulates VEGF Expression in ARPE-19 Cells under Hypoxia

Soohyun Hwang[1], Hyemin Seong[1], Jinhyun Ryu[1], Yong-Seop Han[2], Seokmin Kang[1], Ahmad Fudhaili[1], Juyeong Park[1], Jimin Sim[1], Jiyeon Lee[1], Nayoung Kim[1], Joo Yeon Jeong[1], Dong Hoon Lee[1], Gu Seob Roh[1], Hyun Joon Kim[1], Gyeong Jae Cho[1], Wan Sung Choi[1], Seong Wook Seo[2], Jong Moon Park[2], Sang Soo Kang[1]

[1]Department of Convergence Medical Science and Anatomy, [2]Department of Ophthalmology, Institute of Health Sciences, College of Medicine, Gyeongsang National University, Jinju, 52757, Korea.

Angiogenesis is a blood vessel disorder that causes vascular eye disease like AMD. AMD leads to blindness in elder patients and there is no surgery or drug treatment that returns vision already lost. It is well known that VEGF plays an important role in the pathogenesis of AMD and RPE cells are main sources of VEGF in retina. Hypoxia is a major stimulus that induces VEGF upregulation in various retinopathies. STAT3 which is activated by JAK2 phosphorylation plays roles in regulating the immune response and inflammation in RPE cells. In this study, we confirmed that p-STAT3 and VEGF secretion were upregulated in ARPE-19 cells under hypoxia. Thus when we treated AG490, the inhibitor of JAK2 phosphorylation, both STAT3 phosphorylation and VEGF secretion were reduced under hypoxia. Thus we confirmed that JAK2/STAT3 pathway regulates VEGF expression in ARPE-19 cells under hypoxia. These findings suggest that blocking JAK2/STAT3 pathways under hypoxic condition are considered as a new strategy for AMD.

P086

Structural and Functional analysis of the tuberous sclerosis complex 1 conditional knockout (*Tsc1-cko*) mouse retina

Sharon Jiyoon Jung[1,2], Hyoun Geun Kim[1,2], Ye-Ji Hong[1,2], Seung Hee Lee[1,2], Sun Sook Paik[1, 2], In-Beom Kim[1, 2]

[1]Department of Anatomy, [2]Catholic Neuroscience Institute, College of Medicine, The Catholic University of Korea, Seoul 06591, Korea

Tuberous Sclerosis Complex (Tsc) is a dominant genetic disorder caused by inactivating point mutations in either *Tsc1* or *Tsc2* genes; it is characterized by neurodevelopmental deficits and the formation of benign tumors (hamartomas) in affected organs due to uncontrolled cell growth. Both of these distinct genes usually function as tumor suppressors participated in many pathways including

those that involve cell growth, cell proliferation, and cell migration. Among these two, *Tsc1* is known for an eye-specific genes and to play a significant role in visual pathway development. To explore changes in the retina caused by conditional deletion of *Tsc1*, we examined retinal structure and function in *Tsc1* conditional knockout (cko) mice. In general histology, cell bodies in the inner nuclear layer (INL) of the *Tsc1*-cko mouse appear to be larger than those of control mouse. Thus, the INL was thicker in *Tsc1*-cko mouse retina, while the outer nuclear layer (ONL) where photoreceptors are located was thinner. In *Tsc1*-cko mouse retina, arrangement of protein kinase C-immunoreactive (IR) rod bipolar cell was disrupted, while those of choline acetyltransferase-IR and calbindin-IR amacrine cells appeared to be preserved. In addition, many ectopic ribbon synapses labeled with anti-ribeye (CtBP2) were found frequently in the ONL and often in the ganglion cell layer. Numerous PKC-IR rod bipolar and calbindin-IR horizontal dendrites toward the ectopic ribbon synapses of the photoreceptors were observed. These morphological changes progressed with age. In electroretinographic (ERG) recordings, scotopic and photopic b-waves were significantly increased in *Tsc1*-cko mouse, compared to those in control mice. In conclusion, the retina of *Tsc1*-cko mouse represented structural changes at cellular and synaptic levels, retinal degeneration, and remodeling, suggesting important roles of Tsc1 in regulating cell growth, proliferation, and plasticity. Large b-waves of Tsc1-cko mouse in flash ERG recordings might be caused by large-sized bipolar cells based on morphological finding and known Tsc1 function. This study has been supported by National Research Foundation of Korea(NRF) funded by the Ministry of Science and ICT (NRF-2017R1A2B2005309) and Seoul St. Mary's Hospital (R&D 2016 program).

Keyword: *Tsc1*, Bipolar cell, Horizontal cell, Ribbon synapse, Electroretinography

P087

Morphology and Immunocytochemistry Evaluation of *In Vitro* Corneal Cells in Gelam Honey-Enriched Medium

Norzana Abd Ghafar[1], Muhammad Fairuz Azmi[1,3], Alia Md Yusof[1,4], Taty Anna Kamaruddin[1], Ng Sook Luan[2], Chua Kien Hui[2]

[1]Department of Anatomy, [2]Department of Physiology, Universiti Kebangsaan Malaysia Medical Centre, Kuala Lumpur, Malaysia [3]Department of Anatomy, [4]Department of Basic Sciences, Universiti Teknologi Mara, Malaysia

In vitro cultivation of cells with agent which could promote or retain the expression of favourable phenotypes has long been practiced in cell biology, tissue engineering or in stem cell research. Natural products such as honey has been proven to promote positive effects on skin cells, but its effects on corneal cells have not been elucidated. The aim of the study is to evaluate the morphology and immunocytochemistry of corneal epithelial cells (CEC) and corneal stromal cells (CSC) in Gelam honey (GH)-enriched medium. Corneas were harvested from New Zealand White rabbits. Corneal cells (CEC and CSC) were then isolated using dispase and collagenase type I enzymes respectively. CEC were cultured in epithelial medium only or GH-enriched epithelial medium. The CSC were cultured in stroma medium or GH-enriched stroma medium. The morphology of the CEC and CSC in culture was assessed via a phase contrast microscope. The expression of Cytokeratin 3, specific corneal epithelial differentiation marker and markers for corneal stromal cell phenotypes; vimentin and alpha-smooth muscle actin were assessed by immunocytochemistry. The results showed that in vitro CEC exhibited compact polygonal-shaped cells with distinct cell borders and stained positive for Cytokeratin 3 in both cells cultured in cornea medium only and GH-enriched cornea medium. Cornea stromal cells exhibited elongated, spindle-shaped cells which stained positive

for both vimentin and alpha-smooth muscle actin in both media. GH-enriched cornea and stroma media appeared to have increased the proliferative capacity of both cells based on the density of cells in the culture. In conclusion, CEC and CSC cultured in GH-enriched media have shown to promote proliferation and normal cell morphology while retaining their phenotypical characteristics. These findings suggest the future role of GH in the nutripharmaceutical agent either as an adjunct for a wound healing agent or in the development of honey-based culture medium.

Key Words: Corneal epithelial cells, Corneal stromal cells, Gelam honey

P088

Investigation of the pathogenic role of IL-22 in the development and pathogenesis of experimental autoimmune uveitis and establishment of effective therapeutic ways

Yejin Kim*, Dahae Lee, Yesol Kim, Seul-bee Lee, Hyejung Cho, Younsu Kim, Wang Jae Lee, Jae Seung Kang

Laboratory of Vitamin C and Anti-Oxidant Immunology, Department of Anatomy and Cell Biology, Seoul National University, College of Medicine, Seoul, Korea

IL-22 is a pro- and anti-inflammatory cytokine that is mainly produced by T cells and NK cells. Recent studies have reported the increased number of IL-22 producing T cells in patients with autoimmune noninfectious uveitis; however, the correlation between IL-22 and uveitis remains unclear. In this study, we aimed to determine the specific role of IL-22 and its receptor in the pathogenesis of uveitis. Serum concentration of IL-22 was significantly increased in uveitis patients. IL-22Rα was expressed in the retinal pigment epithelial cell line, ARPE-19. To examine the effect of IL-22, ARPE-19 was treated with recombinant IL-22. The proliferation of ARPE-19 and the production of monocyte chemoattractant protein (MCP)-1 from ARPE-19 were clearly elevated. IL-22 induced MCP-1 which facilitated the migration of inflammatory cells. Moreover, IL-22 increased the IL-22Rα expression in ARPE-19 through the activation of PI3K/Akt. Experimental animal models of uveitis induced by interphotoreceptor retinoid binding protein 1-20 (IRBP1-20) exhibited elevation of hyperplasia RPE and IL-22 production. When CD4+ T cells from the uveitis patients were stimulated with IRBP1-20, the production of IL-22 definitely increased. In addition, we examine the regulatory role of cysteamine, which has an anti-inflammatory role in the cornea, in uveitis through the down-regulation of IL-22Rα expression. Cysteamine effectively suppressed the IRBP1-20-induced IL-22Rα expression and prevented the development of IRBP1-20-induced uveitis in the experimental animal model. These finding suggest that IL-22 and its receptor have a crucial role in the development and pathogenesis of uveitis by facilitating inflammatory cell infiltration, and that cysteamine may be a useful therapeutic drug in treating uveitis by down-regulating IL-22Rα expression in RPE.

Key Words: Interlukin-22, Experimental Autoimmune Uveitis, IRBP, MCP-1

*Correspondence to Yejin Kim (E-mail: bbambaya921@snu.ac.kr)

P089

Vitamin C insufficiency aggravates dextran sulfate sodium (DSS)-induced colitis in *Gulo(-/-)* mice

Yejin Kim, Dahae Lee, Yesol Kim, Seul-bee Lee, Hyejung Cho, Wang Jae Lee, Jae Seung Kang*

Laboratory of Vitamin C and Anti-Oxidant Immunology, Department of Anatomy and Cell Biology, Seoul National University, College of Medicine, Seoul, Korea

Mucosal damage in inflammatory bowel diseases (IBDs) involves the dysfunctional immunoregulation of the gut. Among immunoregulatory factors, oxidative stress is abnormally high level in IBDs, and their destructive effects may contribute to the initiation or propagation of the disease. Vitamin C has both anti-oxidant and immunomodulatory effects. So, we investigated the effect of vitamin C on dextran sulfate sodium (DSS)-induced colitis in Gulo(-/-) mice which cannot synthesize vitamin C. Vitamin C-insufficient Gulo(-/-) mice showed decreased survival with increased oxidative stress and more severe colitis. The production of interleukin (IL)-6 was higher, and STAT3 and Akt were more activated in DSS-treated vitamin C-insufficient Gulo(-/-) mice than in vitamin C-sufficient Gulo(-/-) mice and wild-type mice. In contrast, the production of IL-22, the recruitment of NKp46(+) cells, and the activation of p38 MAPK were decreased in the vitamin C-insufficient Gulo(-/-) mice accompanied by decreased mucin-1 expression. Taken together, vitamin C insufficiency was associated with not only increased oxidative stress and IL-6 production but also decreased production of IL-22, which eventually induces severe colitis and death by DSS treatment. Therefore, our results suggest that vitamin C has a protective effect on DSS-induced colitis by regulating the production of cytokine and the induction of inflammation.

Key Words: Vitamin C, *Gulo(-/-) mice*, Inflammation, IBD

*Correspondence to Jae Seung Kang (E-mail: genius29@snu.ac.kr)

P090

Alloferon and vitamin C increase immune cell activity and decrease lung inflammation induced by influenza A virus/H1N1 infection

Yejin Kim[1], Sun-Hye Lee[2], Haeon Song[2], Daeho Kim[2], Dahae Lee[1], Yesol Kim[1], Seul-bee Lee[1], Hyejung Cho[1], Wang Jae Lee[1], Jae Seung Kang[1,*]

[1]Laboratory of Vitamin C and Anti-Oxidant Immunology, Department of Anatomy and Cell Biology, Seoul National University, College of Medicine, Seoul, Korea
[2]AT-alpha Co. Ltd.

Because Allofreon and vitamin C have immunomodulatory function and anti-viral effect, we investigated whether Alloferon and vitamin C synergistically regulate immune cell function and suppress viral infection. Alloferon and vitamin C were administrated to *Gulo(-/-)* mice, which are incapable of synthesizing vitamin C, with or without influenza A virus/H1N1 infection. Alloferon and vitamin C increased the expression of CD25 and CD69 of PBMCs and natural killer (NK) cells. In

Gulo(-/-) mice, Alloferonand vitamin C increased the expression of NKp46, a natural cytotoxic receptor of NK cells and interferon (IFN)-γ production. Influenza infection decreased the survival rate, and increased inflammation and viral plaque accumulation in the lungs of vitamin C-depleted *Gulo(-/-)* mice, which were remarkably reduced by Alloferon and vitamin C supplementation. Administration of Alloferon and vitamin C enhanced the activation of immune cells like T and NK cells, and repressed the progress of viral lytic cycle. It also reduced lung inflammation caused by viral infection, which consequently increased the survival rate.

Key Words: Vitamin C, Alloferon, *Gulo(-/-) mice*, Inflammation, IBD

*Correspondence to Jae Seung Kang (E-mail: genius29@snu.ac.kr)

P091

Aging-related molecular changes in SMP30/GNL knockout mice exposed to radiofrequency radiation at 835 MHz for 9 weeks

Jin-Koo Lee[1], Hye-Ryoung Lee[1], Ji Ho Ryu[2], Cheol Kyu Oh[3], Min Sun Lee[4], Chang Seok Oh[6] and Myeung Ju Kim[5,*]

[1]Department of Pharmacology, [5]Department of Anatomy, Dankook University College of Medicine, Cheonan, [2]Department of Emergency Medicine, Pusan National University Yangsan Hospital, [3]Department of Urology, Haeundae Paik Hospital, Inje University College of Medicine, Busan, [4]Department of Nursing, Shinhan University, Uijeongbu, [6]Department of Anatomy, Seoul National University College of Medicine, Seoul, South Korea,

As an important animal model of aging research, a number of studies have been conducted on senescence marker-30 (SMP30)/gluconolactonase (GNO) knockout (KO) mice, which cannot synthesize L-ascorbic acid (AA) in vivo. However, biomedical studies still have not yet been conducted on the effects of electromagnetic radiofrequency radiation on the SMP30/GNO KO mice.
In this study, the changes of aging metabolism molecules for 9 weeks exposure to radiofrequency radiation (RFR) using Wave Exposure V20 (835 Mhz, 4.0 W/Kg SAR) for 5hr/day as whole-body exposure method. The mice exposed to 835MHz RFR (SAR 4.0 W/kg) showed a decrease in body weight, blood glucose and survival rate. And also, plasma IL-6 and IL-8 and hypothalamic CRH mRNA levels were increased by RFR in aging mice. These results show that RFR can act as external stressors and further promote aging. Plasma insulin and leptin levels and daily food intake were significantly decreased in aging mice exposed to long-term RFR. The expression of orexigenic neuropeptides and ObRs were further increased by RFR exposure. In contrast, expression of anorexic neuropeptides were further show that RFR affects the metabolism regulation. Lastly, we investigated insulin signaling in RFR-exposure aging mice. The mRNA expression levels of AMPKa1, AMPKa2, FoxO1, FoxO3a, SIRT-1 and PGC-1a and the phosphorylation of PI3K and STAT-3 were significantly increased in the RFR-exposed hypothalamus of aging mice. Taken together, chronic exposure to RFR in aging animal models can lead to hypoglycemia by causing abnormalities in glucose metabolism. The resulting hypoglycemia can aggravate the survival rate in aging mice model.

Key Words: Senescence marker-30, Radiofrequency radiation, L-ascorbic acid, 835 Mhz, Aging

P092

Erdr1 affects shedding of Trem1 through the MMP3 for the anti-inflammatory effect of BV2 cells.

Ju Hye Bae, <u>Min Hye Noh</u>, Seong Han Kim,Dea Young Hur, Yeong Seok Kim

Department of Anatomy, Inje University College of Medicine, 75 Bokji-ro, Busanjin-gu, Busan 47392, Republic of Korea

Erdr1, erythroid differentiation regulator 1, has been identified as a hemoglobin synthesis inducer but also has been demonstrated regulatory functions in anti-cancer effect and anti-inflammation. However, the functional mechanism of Erdr1 remains unknown. Here, we show that Erdr1exerts anti-inflammatory effect by regulation of surface Triggering receptor expressed on myeloid cells-1 (TREM-1) in BV2, murine microglial cells. Upon activation, TREM-1 can directly amplify an inflammatory response. TREM-1 receptor contributes to the pathology of several non-infectious acute and chronic inflammatory diseases. In this study, lipopolysaccharide (LPS) stimulation after Erdr1 transfection in BV2 cells down-regulated pro-inflammatory cytokines, IL-1β, IL-6, and TNF-α with up-regulation of anti-inflammatory cytokines, IL10 and TGF-β. Erdr1 conducts anti-inflammatory functions by shedding off the TREM-1 molecules on the microglial cell membrane by MMP3. With the action of induced MMP3, soluble TREM-1 molecules were liberated into the culture media of Erdr1 transfected BV2 cells, and cleaved TREM-1 on BV-2 cells were defective for inflammatory response. Application of specific inhibitor for MMP3 suppressed soluble TREM-1 liberation and recovered the inflammatory effects of LPS. We discuss pre-clinical studies which show that TREM-1 inhibition, via Erdr1-induced shedding of TREM-1, can be an effective strategy to prevent inflammatory disorders. Further research aimed at identification of detailed functional mechanism involving signal pathways, is required to unravel the therapeutic potentials of Erdr1 for related diseases

Key Words: Erdr1, Trem1, MMP3, BV2, Anti-inflammatory

P093

Carpinus turczaninowii extract alleviates high glucose induced oxidative damage and inflammation in human aortic vascular smooth muscle cells

Oh Yoen Kim[1], So Ra Yoon[1], Kwang Il Nam[2], Chaeyong Jung[2], Juhyun Song[2*]

[1]Department of Food Science and Nutrition, Brain Busan 21, Dong-A University, 37 550beon-gil Nakdongdae-ro, Saha-gu, Busan, 49315, Republic of Korea
[2]Department of Anatomy, Chonnam National University Medical School, Hwasun 58128, Jeollanam-do, Republic of Korea,

Hyperglycemia is one of main cause in atherosclerosis progression. Oxidative stress caused by hyperglycemia triggers severe vascular damage and promotes various inflammatory responses. To treat these processes, many researches tried to prove the beneficial effect of natural compounds on blood vessels under oxidative stress condition. _Carpinus turczaninowii_ (_C.turczaninowii_) as one of natural compounds has been known that it has an antioxidant and anti-inflammatory effects. In present study, we investigated whether or not _C.turczaninowii_ extract attenuates inflammatory response in

human aortic vascular smooth muscle cells (HAoSMCs). We measured cell viability, the expression of gamma H2AX, cytokine's mRNA expressions, the phosphorylation of NF-κB and the expression of AMPK alph2 in HAoSMCs treated with the *C. turczaninowii* extract after high glucose treatment (25 mM) or not. *C.turczaninowii* extract protects HAoSMCs against high glucose induced oxidative stress. In addition, *C.turczaninowii* extract attenuates the expression of pro-inflammatory cytokines such as IL-1beta, TNF-alpha, and the expression of ER stress marker such as CHOP in HAoSMCs against high glucose (25 mM)- induced oxidative stress. Furthermore, the expression of gamma H2AX as a marker of DNA damage, the phosphorylation of NF-kB, and the expression of AMPK alpha2 were reduced by *C.turczaninowii* extract treatment in HAoSMCs against high glucose (25 mM)- induced oxidative stress. In conclusion, this study demonstrated that *C.turczaninowii* might improve inflammatory response in human arterial cells under hyperglycemia. Hence, we suggests that *C.turczaninowii* has a therapeutic potential for hyperglycemia induced atherosclerosis.

Key Words: *Carpinus turczaninowii*; Human aortic vascular smooth muscle cells; High glucose, inflammation, Cytokines, NF-κB

P094

Cyclosporin A aggravates kidney proximal tubular cell death induced by hydrogen peroxide

Daeun Moon[1], Sang Pil Yoon[1,2], Jinu Kim[1,2]

[1]Department of Biomedicine and Drug Development, Jeju National University, Jeju, Republic of Korea
[2]Department of Anatomy, Jeju National University School of Medicine, Jeju, Republic of Korea

Cyclosporin A (CyA) exerts a toxic effect on kidney parenchymal cells, but on the other hand it protects against necrotic cell death through inhibition of mitochondrial permeability transition pore opening.   However, a role of CyA in hydrogen peroxide-induced kidney proximal tubular cell death remains elusive.   In the present study, treatment with CyA further decreased cell viability during exposure to hydrogen peroxide in HK-2 human kidney proximal tubule epithelial cells.   In addition, hydrogen peroxide-induced p53 activation and BH3 interacting-domain death agonist (BID) expression were higher in CyA-treated cells than those in non-treated cells, whereas hydrogen peroxide-induced activation of mitogen-activated protein kinase (MAPK) including p38, c-Jun N-terminal kinase (JNK), and extracellular signal-regulated kinase (ERK) and activation of protein kinase B (AKT) were not significantly altered by CyA.   In oxidant-antioxidant system, reactive oxygen species (ROS) production induced by hydrogen peroxide was further enhanced by treatment with CyA, but expression of antioxidant enzymes including manganese superoxide dismutase (MnSOD), copper/zinc superoxide dismutase (CuZnSOD), and catalase was not altered by both hydrogen peroxide and CyA.   Finally, treatment with CyA further enhanced mitochondrial membrane potential induced by exposure to hydrogen peroxide, but did not alter endoplasmic reticulum (ER) stress as represented by expression of glucose-regulated protein (GRP) 78 and 94. In conclusion, these data suggest that CyA aggravates hydrogen peroxide-induced cell death through p53 activation, BID expression, and ROS production. (NRF-2016R1C1B2012080)

Key Words: Cyclosporin A, Hydrogen peroxide, Kidney proximal tubule, p53, BID, ROS

P095

Cisplatin induces the deciliation of primary cilium in kidney epithelial cell into the urine

Min Jung Kong[1], Jee In Kim[2], Kwon Moo Park[1]

[1]Department of Anatomy, Cardiovascular Research Institute and BK21 Plus, School of Medicine, Kyungpook National University, 680 Gukchaebosang-ro, Junggu, Daegu 41944, Korea
[2]Department of Molecular Medicine and MRC, College of Medicine, Keimyung University, 1095 Dalgubeol-daero 250-gil, Dalseogu, Daegu 42601, Korea

Primary cilium protrudes to the lumen of kidney tubules and plays an important role in kidney functions. The primary cilium length alteration by resorption and deciliation is associated with pathogenesis of several kidney diseases including acute kidney injury (AKI). Cisplatin is widely used as an anticancer drug. However, its nephrotoxicity limits its use. Here, we investigated that cisplatin-induced nephrotoxicity affects primary cilium length and its molecular mechanism. In addition, we investigated whether the length of primary cilium in the kidney tubular epithelial cells and deciliation into the urine can be an indicative kidney injury. Cisplatin shortened primary cilium length in the mouse kidney epithelial cells. Cisplatin injection did not change BrdU-incorporated cell number, and levels of p21 and proliferation cell nuclear antigen (PCNA) expression in the kidney. Cisplatin increased urine primary ciliary protein amounts. Cisplatin-induced shortening and disruption of primary cilium was attenuated by Mito-TEMPO, a mitochondria-targeted antioxidant, treatment along with reduction of cisplatin-induced increases of ROS formation and oxidative stress. These findings indicate that cisplatin induces shortening of renal primary cilium, and this shortening was due to disruption of primary cilium rather than reabsorption into the cell body, via ROS elevation and oxidative stress. Furthermore, data suggest that urine primary ciliary protein and tissue primary cilium length can be useful indicatives of kidney injury.

Key Words: Primary cilia; Cisplatin; Nephrotoxicity; Biomarker; Reactive oxidative species.

P096

Change of Caveolin-2 in the Aging Mouse Model Kidney

Soo-Jin Song, Jung-A Shin*

Department of Anatomy, School of Medicine, Ewha Womans University, Seoul, Korea

Caveolin encoded by the Cav gene family is caveolin-1 (Cav-1), caveolin-2 (Cav-2), and caveolin-3 (Cav-3), and which is the major protein component of the caveolae. Caveolin is known to participate in endocytosis, transcytosis and signal transduction. Especially, Cav-2 is known to play often more direct role in regulating signaling and function in cells and tissues than Cav-1. The aim of this study was to localize Cav-2 in the kidney, and to determine whether it could change in the aging model. Immunohistochemistry for Cav-2 and Cav-1 was conducted in the mouse kidney obtained at 3 month (young), and 19 month (old). In the kidney of normal (young) mouse model, Cav-2 expression is shown in the principle cells of collecting duct, endothelial cells, and glomerulus. In the kidney of old mouse model, Cav-2 staining is increased than young mouse model. Cav-2 staining is seen in the endothelial cells of small and large vessels in old mouse model, while it is observed only in relatively large vessels in kidney of normal mouse model. In addition, in the kidney of the old mouse model, Cav-2 stained cell cluster that cannot be seen in the kidney of the normal mouse model is observed. This cell cluster is also labeled with marker of macrophages and common leukocyte, so Cav-2 stained

cell cluster is seen as immune cell cluster. This suggests that Cav-2 plays important role in the inflammatory response in the aging kidney

Key Words: Caveolin-2, Aging, Kidney, Immunohistochemistry

*Correspondence to Jung-A Shin (E-mail: sja@ewha.ac.kr, Tel: +82-2-2650-2645)

P097

Stronger antioxidant enzyme immunoreactivity of *Populus tomentiglandulosa* extract than ascorbic acid in the rat liver and kidney

Tae-Kyeong Lee[1], Minah Song[1], Hyunjung Kim[1], Cheol Woo Park[1], Young Eun Park[1], Ji Hyeon Ahn[2], Joon Ha Park[2], Jae-Chul Lee[1], Jung Hoon Choi[3], Ki-Yeon Yoo[4], Choong Hyun Lee[5], Moo-Ho Won[1]

[1]Department of Neurobiology, School of Medicine, Kangwon National University, Chuncheon, Gangwon, 24341 Republic of Korea
[2]Department of Biomedical Science and Research Institute for Bioscience and Biotechnology, Hallym University, Chuncheon, Gangwon 24252, Republic of Korea
[3]Department of Anatomy, College of Veterinary Medicine, Kangwon National University, Chuncheon, Gangwon 24341, Republic of Korea
[4]Department of Oral Anatomy, College of Dentistry and Research institute of Oral Biology, Gangneung-Wonju National University, Gangneung Gangwon 25457, Republic of Korea
[5]Department of Pharmacy, College of Pharmacy, Dankook University, Cheonan, Chungcheongnam 31116, Republic of Korea

Populus species have various pharmacological properties including anti-oxidant activity. In this study, we examined effects of *Populus tomentiglandulosa* extract (PTE) on histopathology and antioxidant enzymes in the rat liver and kidney. Sprague-Dawley rats were randomly divided into three groups; (1) normal diet fed group, (2) ascorbic acid-containing diet-fed group as a positive control, (3) PTE-containing diet-fed group. The histopathology in the rat liver and kidney examined by hematoxylin and eosin staining. The effect of PTE was examined in the rat liver and kidney by immunohistochemistry for antioxidant enzymes, copper, zinc-superoxide dismutase (SOD1), manganese superoxide dismutase (SOD2), catalase (CAT) and glutathione peroxidase (GPx). No marked histopathological alterations were observed in the liver and kidney of the PTE-containing diet-fed group. In the liver, the mean number of SOD1, SOD2, CAT and GPx immunoreactive cells were significantly increased in the PTE-containing diet-fed group, compared with those in the normal- and ascorbic acid-containing diet-fed groups. In the kidney, all SOD1, SOD2, CAT and GPx immunoreactive structures were significantly increased in the PTE-containing diet-fed group, compared with those in the normal- and ascorbic acid-containing diet-fed groups.Our results showed that PTE treatment significantly increased antioxidant enzymes in the rat liver and kidney, and we suggest that PTE might have hepato- and nephro-protective potentials against oxidative stress.

Key Words: Histopathology, Oxidative stress, Hepatic cells, Renal tubules, Immunohistochemistry

P098

Some effects of copper oxide nanoparticles (Cuo-NPs) on rat liver: a histopathological study

Paria SHOJAOLSADATI[1], Ferruh YÜCEL[2], Hadi KARIMKHANI[1], Dilek BURUKOĞLU DÖNMEZ[3], Bayram Ufuk ŞAKUL[1]

[1]Department of Anatomy, Faculty of Medicine, Medipol University, İstanbul, Turkey
[2]Department of Anatomy, Faculty of Medicine, Eskişehir Osmangazi University, Eskişehir, Turkey
[3]Department of Histology and Embryology, Faculty of Medicine, Eskişehir Osmangazi University, Eskişehir, Turkey

Copper oxide nanoparticles (CuO-NPs) are increasingly used in several industrial products for different purposes. After intestinal absorption of CuO-NPs, they diffuse into tissues and causes ultrastructural changes. The liver is a target organ for CuO-NP and extreme intake of these nanoparticles may cause some damages in the liver. In the present study, it was aimed to investigate the effects of CuO-NPs in the rat liver by using some quantitative methods and evaluate the mechanism of damage. For this purpose, a total of 40 Sprague-Dawley male rats 6-8 week old (250-300 gr) were used. These rats were randomly divided into two groups: control and CuO-NP (200 mg/kg) received groups. Treatment group animals were administered with 200 mg/kg CuO-NP in serum physiological saline by gavage, once a day for 5 days. The livers of both groups were examined histopathologically using light and electron microscopy (TEM). In the experimental group, the volume fraction (V_v) of sinusoids to whole liver tissue significantly increased. Also, the number of mitochondria per unit area (Na) of cytoplasm of hepatocyte and the volume fraction (Vv) of the mitochondria to the cytoplasm of hepatocyte decreased significantly compared to control group. Presence of Caspase-3 and TUNEL-positive cells in hepatocytes of treated animals is clear evidence for occurrence of apoptosis. On the other hand, after CuO-NP exposure, serum levels of AST markedly increased while ALT decreased. The results obtained in present study show that the mitochondrial pathway of apoptosis seen in CuO-NP administered group of animal is responsible for liver damage. In conclusion, this concentration of CuO-NPs is very toxic for liver and cannot be used in food industry.

Key Words: Copper oxide nanoparticles (CuO-NPs), Hepatotoxicity, AST, ALT.

P099

Ameliorating effects of lagundi and turmeric powder in an alcoholic fatty liver disease Zebrafish (*Danio rerio*) model

Rodel Jonathan S. Vitor II[1,2], Michael Joseph T. Reyes[1,3], Kathleen Juline C. Serato[1,4], Ferdine O. Tolosa[1,5], Maria Michaela S. Valenzuela[1,6], Leandro D. Vila[1,7,8,9]

[1]Department of Physiology, College of Medicine, University of the Philippines Manila, Pedro Gil St., Manila, 1004, Philippines
[2]Biology Department, College of Science, De La Salle University, Taft Ave., Manila 0922, Philippines
[3]Asian Hospital and Medical Center, Civic Dr. Alabang, Muntinlupa City 1780, Philippines
[4]College of Dentistry, University of Perpetual Help System DALTA, Alabang-Zapote Road, Las Piñas City 1750, Philippines
[5]Jonelta Foundation School of Medicine, University of Perpetual Help System DALTA, Alabang-Zapote Road, Las Piñas City 1750, Philippines
[6]Physical Therapy Department, College of Allied Rehabilitation Sciences, University of the East

Ramon Magsaysay Memorial Medical Center, Aurora Boulevard, Quezon City 1113, Philippines
[7]Department of Physiology, College of Medicine, Our Lady of Fatima University, McArthur Highway, Marulas, Valenzuela City 1440, Philippines
[8]Department of Physiology, College of Medicine, Far Eastern University - Nicanor Reyes Medical Foundation, Regalado Ave. West Fairview, Quezon City 1118, Philippines
[9]Department of Physiology, College of Medicine, New Era University, Central Ave., New Era, Quezon City 1107, Philippines

Background: Alcoholic fatty liver disease is considered one of the major complications attributed to excessive alcohol use and abuse. With this, medical practiotiners have warranted the use and discovery of drugs and medicines that can use to ameliorate its unwanted effects. Studies showed that herbal supplements may have the potential to ameliorate the effects of alcohol, specifically in the liver. **Aims and Objectives:** To determine whether there will be an ameliorating effect in the liver of ethanol treated zebrafish. Materials and Methods: Twenty four (24) mature zebrafish were treated with ethanol and were given supplements of lagundi and turmeric at a concentration of 10% wt of powder/wt of Tetramin flakes. After administration with food for 7 days, the zebrafish were sacrificed and the liver harvested for histological analysis. **Results:** Based on histological analysis, lagundi showed better ameliorating effects when compared with turmeric. Also, both treatment performed better than the negative results. **Conclusion:** Lagundi and turmeric has ameliorating effects against alcohol induced fatty liver disease with lagundi performing better than turmeric.

Key Words: Alcohol fatty liver disease, *Danio* rerio, Ethanol, Lagundi, Turmeric, Zebrafish

P100

Fumonisin B1 induces cell proliferation through alterations of CDKs and CDK inhibitors in the mouse liver

Sae-Jin Lee, Yun Soo Chung, Seo Jin Lee, Ki-Hwan Han

Department of Anatomy, Ewha Womans University Medical College, Seoul, Korea

Fumonisin B1 (FB1) is a carcinogenic toxin that induces mitosis in animals and humans. Mitosis is a part of the cell cycle and controlled by complex proteins. The purpose of this was to examine the effects of FB1 on cyclin-dependent kinases (CDKs) and CDK inhibitors, in the mouse liver. C57BL/6 mice groups (n= 10 in each group) were randomly divided and received intraperitoneal injections of FB1 at 0, 2.5, 5, 10, or 20mg/kg doses for 5 days. Liver tissues were processed for immunohistochemistry and immunoblot analysis. H&E stained histology and immunohistochemical labeling of PCNA revealed that FB1 treatment increased cell proliferation by 2.7- (2.5 mg), 4.4- (5 mg), 7.4- (10 mg), and 8.8-fold (20 mg) when compared with normal saline group (0 mg), respectively. FB1 treatment significantly increased protein expression of CDK2, CDK4, and CDK6, while decreased expression of CDK inhibitors, p18 and p27, in the liver. Confocal microscopy double immunofluorescence showed that CDK2 expressed mainly in the nucleus of proliferating PCNA-positive cells. In contrast, expression of p27 was localized in the cytoplasm of hepatocytes after FB1 treatment. These results suggest that expression and intracellular localization of CDKs and CDK inhibitors may play an important role in FB1-induced cell proliferation in the liver.

Key Words: Fumonisin B1, Liver, CDKs, CDK inhibitors

P101

Effect of antimicrobial peptide Nisin on keratinocytes

Norio Kitagawa, Takahito Otani, Kayoko Ogata, Tetsuichiro Inai

Department of Morphological Biology, Fukuoka Dental College, 2-15-1 Tamura, Sawara-ku, Fukuoka 814-0193, Japan

Nisin is a food preservative, which is produced by *Lactococcus lactis subsp. lactis.* and it has a long history of use worldwide. Recently, nisin was found to affect cancer-derived keratinocytes; however, its effects on keratinocytes derived from normal epithelia are not known thus far. In this study, we investigated whether nisin affects keratinocytes by examining the change in the distribution of intermediate filaments in HaCaT human keratinocytes. Owing to their ubiquitous distribution in the cytoplasm, we predicted that intermediate filament protein can be used for the detection of previously undetected alterations caused by nisin. Treatment with 93 µg/ml nisin for 24 h decreased the distribution of the   intermediate filament proteins cytokeratin (CK)5 and CK17 at the cell periphery, which were distributed in a limited area in a ring-like shape. However, this was not observed upon treatment for 6 h. The results of a serial dilution assay revealed that the effect on CK5 and CK17 localization depends on nisin concentration and was observed at concentration ≥ 47 µg/ml. Treatment with nisin also disturbed regular distribution of desmosomal protein desmoglein 3 and adherens junction protein E-cadherin at intercellular contacts. Moreover, Treatment with 93 µg/ml nisin for 24 h disturbed spheroid formation. The results of TUNEL assay showed no apparent increase in apoptotic rate after 24 h of treatment with 93 µg/ml nisin relative to untreated control cells. However, cell viability was marginally decreased. Our findings reveal that Nisin has measurable effects on the HaCaT cells, and CK5 and CK17 can serve as markers for evaluating the effects of nisin on keratinocytes.

Key Words: Cytokeratin 5, Cytokeratin 17, Nisin, HaCaT, Keratinocyte

P102

Melatonin protects hindlimb ischemic injury by increasing autophagy

In-Hye Jeong[1], Jae-Sun Choi[2], Woom-Yee Bae[1], Joo-Won Jeong[1, 2*]

[1]Department of Biomedical Science, Graduate School, Kyung Hee University, Seoul 02447, Republic of Korea
[2]Department of Anatomy and Neurobiology, College of Medicine, Kyung Hee University, Seoul 02447, Republic of Korea

Peripheral artery disease (PAD) is a vascular disease that causes restricted blood supply to the limbs. Melatonin, an indolamines, regulates a variety of physiological functions, including circadian rhythms, neuroendocrine, cardiovascular, neuroimmunological actions and balances the apoptosis and autophagy in physiological conditions. In this study, we investigated the therapeutic effect of melatonin on PAD using the hindlimb ischemia (HLI) model. In order to establish a mouse model of HLI, the left femoral arteries and femoral veins were ligated. The mice were injected intraperitoneally with melatonin (20 mg/kg) everyday for 3 days before surgery, and additionally administered for 7 days after surgery. We showed that administration of melatonin improved foot injury and blood flow in the HLI mouse model. Moreover, microvessel distribution were upregulated in gastrocnemius muscle of HLI mice. Interestingly, we found that the phenomena of autophagy were stimulated by melatonin in

vivo and in vitro ischemia models. These results indicate that melatonin treatment in PAD can improve ischemic injury and blood flow through increasing autophagy and that melatonin may be a potential therapeutic agent for vascular diseases.

Key Words: Hindlimb ischemia, Melatonin, Autophagy

P103

p66Shc deficiency modulates mitochondrial dysfunction by ROS production in osteoarthritis

Hyo Jung Shin[1,2], Hyewon Park[1,2], Sooil Kim[2], Jaewon Beom[3,*], Dong Woon Kim[1,2,*]

[1]Department of Medical Science, Chungnam National University School of Medicine, Daejeon, 35015, Republic of Korea.
[2]Department of Anatomy and Cell biology, Brain Research Institute, Chungnam National University School of Medicine, Daejeon, 35015, Republic of Korea.
[3]Department of Physical Medicine and Rehabilitation, Chung-Ang University College of Medicine, Seoul, 06974, Republic of Korea.

Osteoarthritis (OA) is the most prevalent joint disease, and cartilage loss is a central event in its pathogenesis, but the exact mechanisms of pain in OA remain inadequately understood. In this study, we investigated the impact of p66Shc-derived Reactive oxygen species (ROS) trigger the mitochondrial dysfunction, which is involved in OA pain. since p66Shc, an isoform of the ShcA adaptor protein family, has been characterized as a crucial mediator of mitochondrial ROS generation. We used OA pain model with mono-iodoacetate (MIA), which inhibits the activity of articular chondrocytes, leading to disruption of glycolytic energy metabolism and synthetic processes and eventually to cell death. MIA model showed the reduction of cartilage damage significantly caused by the down-regulation of p66Shc expression. And reduction of p66Shc expression decreases inflammatory cytokines by MIA. Moreover, MIA modulates mitophagy and mitochondrial dysfunction by ROS production in primary human chondrocyte. The silencing of p66Shc by using p66[shc]RNAi mouse results in decreased chondrocyte death in cartilage. Taken together, it suggests that the regulation of p66Shc on ROS levels play a crucial role in mitochondrial dysfunction in chondrocyte degeneration and may be a promising candidate for therapeutic target in OA pain.

Key Words: Osteoarthritis, Mono-iodoacetate, p66shc, ROS, Mitochondrial dysfunction

P104

p66Shc deficiency modulates mitophagy in osteoarthritis

Hyo Jung Shin[1,2], Hyewon Park[1,2], Jaewon Beom[3,*], Dong Woon Kim[1,2,*]

[1]Department of Medical Science, Chungnam National University School of Medicine, Daejeon, 35015, Republic of Korea.
[2]Department of Anatomy and Cell biology, Brain Research Institute, Chungnam National University School of Medicine, Daejeon, 35015, Republic of Korea.
[3]Department of Physical Medicine and Rehabilitation, Chung-Ang University College of Medicine, Seoul, 06974, Republic of Korea.

Osteoarthritis (OA) is the most prevalent joint disease, and cartilage loss is a central event in its pathogenesis, but the exact mechanisms of pain in OA remain inadequately understood. In this study, we investigated the impact of p66Shc-derived Reactive oxygen species (ROS) trigger the mitochondria route of mitophagy, which is involved in OA pain, since p66Shc, an isoform of the ShcA adaptor protein family, has been characterized as a crucial mediator of mitochondrial ROS generation. We used OA pain model with mono-iodoacetate (MIA), which inhibits the activity of articular chondrocytes, leading to disruption of glycolytic energy metabolism and synthetic processes and eventually to cell death. MIA model showed the reduction of cartilage damage significantly caused by the down-regulation of p66Shc expression. And reduction of p66Shc expression decreases inflammatory cytokines by MIA. Moreover, MIA modulates mitophagy and mitochondrial dysfunction by ROS production in primary human chondrocyte. The silencing of p66Shc by using p66shcRNAi mouse results in decreased chondrocyte death in cartilage. Taken together, it suggests that the regulation of p66Shc on ROS levels play a crucial role in mitophagy and mitochondrial dysfunction in chondrocyte degeneration and may be a promising candidate for therapeutic target in OA pain.

Key Words: Osteoarthritis, Mono-iodoacetate, p66shc, ROS, Mitophagy

P105

The role of CREBH in RANKL-induced osteoclastogenesis

Hye Jung Cho[1], Naksung Kim[2], Juhyun Song[1], Chaeyong Jung[1], Kwang Il Nam[1*], Kyu Youn Ahn[1], Choon Sang Bae[1]

Departments of [1]Anatomy and [2]Pharmacology, Chonnam National University Medical School, Gwangju, Republic of Korea

Endoplasmic reticulum (ER) stress is triggered by various metabolic factors, such as cholesterol and proinflammatory cytokines. Recent studies have revealed that ER stress is closely related to skeletal disorders, such as osteoporosis. However, the precise mechanism by which ER stress regulates osteoclast differentiation has not been elucidated. In this study, we identified an ER-bound transcription factor, cAMP response element-binding protein H (CREBH), as a downstream effector of ER stress during RANKL-induced osteoclast differentiation. RANKL induced mild ER stress and the simultaneous accumulation of active nuclear CREBH (CREBH-N) in the nucleus during osteoclastogenesis. Overexpression of CREBH-N in osteoclast precursors enhanced RANKL-induced osteoclast formation through NFATc1 upregulation. Inhibiting ER stress using a specific inhibitor attenuated the expression of osteoclast-related genes and CREBH activation. In addition, inhibition of reactive oxygen species using N-acetylcysteine attenuated ER stress, expression of osteoclast-specific marker genes, and RANKL-induced CREBH activation. Furthermore, inhibition of ER stress and CREBH signaling pathways using an ER stress–specific inhibitor or CREBH small interfering RNAs prevented RANKL-induced bone destruction *in vivo*. Taken together, our results suggest that reactive oxygen species/ER stress signaling-dependent CREBH activation plays an important role in RANKL-induced osteoclastogenesis. Therefore, inactivation of ER stress and CREBH signaling pathways may represent a new treatment strategy for osteoporosis.

Key Words: ER stress, CREBH, RANKL, Osteoclast, Ospeoporosis

P106

Identification of mechanoreceptors in joint capsule

Dasom Kim, Juhyun Han, Im Joo Rhyu

Department of Anatomy, Korea University College of Medicine, Seoul, Korea

The mechanoreceptors present in the joint capsule play an important role in recognizing the movement and posture of the joint and in detecting pain. With the recent increase in the elderly population, the number of joint pain patients is increasing. Therefore, detailed information on nerve fiber receptor distribution is important to understand pathology and treatment of arthralgia. Despite these importance, there is little of understanding and research on mechanoreceptors in the joint capsule. We conducted a study to clearly determine the presence of mechanoreceptors in human knee joints and classification by type. Among the various connective tissues surrounding the knee joint, the quadriceps tendon and the patella ligament in the anterior, medial and lateral collateral ligaments in the bilateral, and joint capsule in the posterior were analyzed. As an initial approach, we tried to identify mechanoreceptors using some labelling methods. The first is the gold chloride method, which has been the most classic method, in which the neural tissue in the tissue is dyed with a deep purple color. The second was immunohistochemistry using two different antibodies, one of which is PGP 9.5, which is known to target neuronal cell bodies and processes. The other was a GT1b-2b targeting the myelinated motor and sensory axon in spinal roots and the PNS. After the labelling, the samples were photographed using a light microscope and a confocal microscope, respectively. In the gold chloride staining, according to the criteria of Freeman & Wyke, we confirmed nerve endings in four types of mechanoreceptors in joint, such as Golgi-tendon organ, Ruffini corpuscle, Pacinian corpuscle and free nerve ending were distinguished in shape and size. Similarly, when immunostaining was performed, we also found lumps that were presumed to be mechanoreceptors in the tissues. However, due to the nature of the fluorescence signal, it was not easy to classify each mechanoreceptor into subtype. To solve this problem, correlated analyses using double labelling, background staining are required for exact understanding. If these problems can be solved and the mechanoreceptors in the tissues can be classified by type, it is expected that it will be a great help to carry out studies related to various joint pain in the future clinical studies.

Key Words: Mechanoreceptor, Knee joint pain, Gold chloride staining, Imunohistochemistry

P107

KHU005 extract inhibits RANKL-induced osteoclastogenesis through NFATc1/c-Fos down-regulation and promote osteoblast differentiation through RUNX2/BMP-2 up-regulation.

Minsun Kim, Jaehyun Kim, Youngjoo Sohn

Department of Anatomy, College of Korean Medicine, Kyung Hee University, Seoul, Republic of Korea

Background: Ostoeporosis is caused by a functional imbalance between osteoblast and Osteoclast. The increased activation of osteoclast that is an osteoporosis results in the progressive loss of bone mass and therefore in an increased susceptibility to bone fractures. KHU005 which originates from Asia and Central Europe is a famous traditional Korean medicine, KHU005 is widely used to treat gynaecopathia, angiocardiopathy, and immunity-related disorders. However, there are no studies on bone of KHU005. The aim of this study was to demonstrate the effects of KHU005 on

osteoclast and osteoblast differentiation. **Methods:** RAW 264.7cells were used as a model for RANKL-induced osteoclastogenesis. Differentiated osteoclasts were stained using TRAP kit and its medium was measured for TRAP activity and function of osteoclast was determined to Pit formation assay. The differentiated cells were lysed to extract the whole protein, and the expression of nuclear factor of activated T-cells (NFATc1) and c-Fos was confirmed by western blot. In addition, MC3T3-E1 cells were used as a model for osteoblast differentiation. Mineralization of osteoblasts was investigated by Alizarin S staining, and we determined osteoblast markers such as BMP-2/RUNX2 using western blotting. **Results:** In the present study, KHU005 decreased the number of TRAP (+) multinucleated cells and inhibited TRAP activity in RANKL-stimulated RAW 264.7 cell. The area of resorption pit lacunae was significantly also reduced by treatment with KHU005. In addition, KHU005 reduced the expression of master regulators of osteoclast differentiation NFATc1 and c-Fos. In the osteoblast, KHU005 enhanced the mineralization through up-regulation of BMP-2/RUNX which are regulator of osteoblast differentiation. **Conclusions:** These suggest that KHU005 possesses potent anti-osteoporotic activity and could provide an alternative therapy for the prevention of bone diseases.

Key Words: KHU005; Osteoclast; Osteoblast; NFATc1/c-Fos; RUNX2/BMP-2; TRAP; Alizarin red S

P108

Claudin-11 regulates bone homeostasis via bidirectional EphB4-EphrinB2 signaling

Sung Chul Kwak[1*], Ju-Young Kim[2*], Jong Min Baek[1,3], Miyoung Yang[1], Min Kyu Choi[1]

[1]Department of Anatomy, School of Medicine, Wonkwang University, Iksan, Republic of Korea
[2]Medical Convergence Research Center, Wonkwang University, Iksan, Republic of Korea
[3]Huons Research Center, Hanyang University in ERICA campus, Ansan, Republic of Korea

Claudins (Cldns) are well-established components of tight junctions (TJs) that play a pivotal role in the modulation of paracellular permeability. Several studies have explored the physiologic aspects of Cldn family members in bone metabolism. However, the effect of Cldn11, a major component of central nervous system myelin, on bone homeostasis has not been reported. In this study, we demonstrate that Cldn11 is a potential target for bone diseases therapeutics, as a dual modulator of osteogenesis enhancement and osteoclastogenesis inhibition. To determine the effect of Cldn11 on osteoclastogenesis or osteoblast differentiation, we examined TRAP staining and Pit assay, or ALP and Alizarin Red-mineralization staining, respectively. The mechanism of Cldn11 by transfection of retrovirus or siRNA analyzed using real-time PCR,western blot, co-immunoprecipitation, and immunofluorescence staining. Moreover, in vivo test performed in lipopolysaccharide-induced bone loss model and calvarial bone formation model. We found that Cldn11 played a negative role in receptor activator of nuclear factor kappa B ligand-induced osteoclast (OC) differentiation and function by downregulating the phosphorylated form of extracellular signal-regulated kinase (ERK), Bruton's tyrosine kinase, and phospholipase C gamma 2, in turn impeding c-Fos and nuclear factor of activated T cells c1 expression. The enhancement of osteoblast (OB) differentiation by positive feedback of Cldn11 was achieved through the phosphorylation of Smad1/5/8, ERK, and c-Jun amino-terminal kinase. Importantly, this Cldn11-dependent dual event in bone metabolism arose from targeting EphrinB2 ligand reverse signaling into OC and EphB4 receptor forward signaling into OB. In agreement with these in vitro effects, subcutaneous injection of Cldn11 recombinant protein exerted anti-resorbing effects in a lipopolysaccharide-induced calvarial bone loss mouse model and increased

osteogenic activity in a calvarial bone formation model.

Key Words: Cldn11, Bone metabolism, EphrinB2-EphB4 signaling, Osteoclast, Osteoblast

P109

Trim38 inhibits RANKL-induced NF-κB activation by mediating lysosome-dependent degradation of TAB2

Kabsun Kim, Jung Ha Kim, Inyoung Kim, Semun Seong, Nacksung Kim

Department of Pharmacology, Chonnam National University Medical School, Gwangju, Republic of Korea

The tripartite motif protein 38 (TRIM38), a member of the TRIM family, is involved in various cellular processes such as cell proliferation, differentiation, apoptosis, and antiviral defense. However, the role of TRIM38 in osteoclast and osteoblast differentiation is not yet known. In this study, we report the involvement of TRIM38 in osteoclast and osteoblast differentiation. Overexpression of TRIM38, in osteoclast precursor cells, attenuated receptor activator of nuclear factor kappa B ligand (RANKL)-induced osteoclast formation, RANKL-triggered NF-kB activation, and expression of osteoclast marker genes, such as NFATc1, osteoclast-associated receptor (OSCAR), and tartrate-resistant acid phosphatase (TRAP); and down-regulation of TRIM38 expression showed the opposite effects. Ectopic expression of TRIM38 in osteoblast precursors induced increased osteoblast differentiation and function. Elevated expression of alkaline phosphatase (ALP), bone sialoprotein (BSP), and osteocalcin was also observed due to blockade of NF-kB activation. Conversely, knockdown of TRIM38 showed the opposite effects. TRIM38 also induced degradation of lysosome-dependent transforming growth factor beta-activated kinase 1 and MAP3K7-binding protein 2 (TAB2), further blocking NF-kB activation. Taken together, our data suggest that TRIM38 plays a critical role in bone remodeling as a negative regulator of NF-kB in both osteoclast and osteoblast differentiation.

Key Words: TRIM38; NF-kB; Osteoclast; Osteoblast; Bone homeostasis

P110

GlcNAc kinase interacts with dynein motor complex and regulates cell migration

Md. Ariful Islam, Syeda Ridita Sharif, Il Soo Moon

Department of Anatomy, Dongguk University Graduate School of Medicine, Gyeongju 38066, Republic of Korea

Recently, we showed that N-acetylglucosamine kinase (GlcNAc kinase or NAGK), an enzyme of amino sugar metabolism, interacts with dynein light chain roadblock type 1 and promotes the functions of the dynein motor. Here we report that NAGK interacts with nuclear distribution protein C (NudC) and lissencephaly 1 (Lis1) in dynein complex. Combination of immunocytochemistry and proximity ligation assay (PLA) revealed NAGK-NudC-Lis1-dynein complex around nuclei and at the leading pole of migrating HEK293T cells and at the tip of migratory processes of cultured rat neuroprogenitor cells. Exogenous expression of RFP-tagged NAGK accelerated migration of HEK293T cells in in vitro wound healing assay, neurons in in vitro neurosphere migration assay and

in in utero electroporation assay, whereas NAGK knockdown by shRNA retarded migration. These data indicate a functional interaction of NAGK with dynein-NudC-Lis1 complex at nuclear envelope and leading process in regulating cell migration.

Key Words: Dynein, Lis1, NAGK, Neuronal migration, NudC

P111

GlcNAc kinase suppresses formation of mHtt and a-Syn protein aggregates in cellular disease models

Md. K. H. Ripon[1], HyunSook Lee [1,2] ‖ Soo Moon[1,2]

[1]Department of Anatomy, [2]Dongguk Medical Institute, Dongguk University Graduate School of Medicine, Gyeongju 38066, Republic of Korea

N-acetylglucosamine (GlcNAc) kinase (NAGK) interacts dynein light-chain roadblock type 1 (DYNLRB1) and promotes the function of dynein in intracellular transport, mitosis and cell migration. In this study we investigated the effects of NAGK in suppressing the formation of mutant huntingtin (mHtt) and the α-synuclein (α-syn) A53T aggregates in cellular Huntington's and Parkinson's disease models. When HEK293T and cortical neurons were co-transfected with pEGFP-mHtt (pQ74) and pDsRed2- or pMyc-DDK-tagged NAGK (pDDK-NAGK), the number and size of the aggregates and the portion of aggregate-positive cells were significantly reduced. The co-transfected cells, however, were green fluorescent throughout the cell, suggesting that the Q74 is still present in the cell but does not form large aggregates. Similar results were also observed in HEK293T and cortical neurons for α-synuclein (α-syn) A53T aggregation, indicating a general role of NAGK in this regard. Conversely, a short hairpin (sh) RNA vector (pSh-NAGK) and the small domain of NAGK (NAGK-DS), which has a dominant-negative effect, increased the aggregate formation and the exogenous expression of NAGK erased the effects of shRNA. A kinase-inactive mutant NAGK (NAGKD107A) also suppressed the formation of Q74 aggregates, indicating that the observed results are a non-canonical function of NAGK. Finally, exogenous expression of NAGK reduced the level of reactive oxygen species (ROS) and maintained the 'thread-like' morphology of mitochondria in a Q74 expressing cellular HD model. Clearance of mHtt aggregates in vivo was also confirmed in mouse brain neurons by electrophoration of the relevant plasmids. Taken together, these results indicate the non-canonical effects of NAGK in clearing or suppressing the formation of protein aggregates.

Key Words: Dynein, GlcNAc kinase, mHtt, Neuron, Proteinopathy

P112

SPG8 spastic paraplegia mutations impair CAV1-integrin-mediated cell adhesion

Seongju Lee[1,2], Ricardo H. Roda[1,3], Craig Blackstone[1*], Jaerak Chang[1,4,5*]

[1]Cell Biology Section, Neurogenetics Branch, National Institute of Neurological Disorders and Stroke, National Institutes of Health, Bethesda, MD 20892, USA
[2]Department of Anatomy and Hypoxia-related Disease Research Center, College of Medicine, Inha University, Incheon 22212, Republic of Korea
[3]Neuromuscular Medicine, Department of Neurology, Johns Hopkins University School of Medicine,

Baltimore, MD 21205, USA
[4]Department of Biomedical Sciences, Ajou University School of Medicine, Suwon 16499, Republic of Korea
[5]Department of Brain Science, Ajou University School of Medicine, Suwon 16499, Republic of Korea.

Mutations in *WASHC5/KIAA0196* cause autosomal dominant hereditary spastic paraplegia (HSP), type SPG8. *WASHC5* encodes the strumpellin/WASHC5 protein, a core component of the Wiskott-Aldrich syndrome protein and SCAR homologue (WASH) complex that activates actin nucleation at endosomes. Though various cellular roles for strumpellin have been described, how SPG8 mutations lead to HSP remains unclear. Protein interactors of the WASH complex were identified by immunoprecipitation and mass spectrometry. Protein function was assessed in cultured cells using both overexpression and RNAi studies, and cell spreading assays were used to investigate cell adhesion. We uncover cellular changes resulting from pathogenic SPG8 mutations. We identify caveolin-1 (CAV1), a key component of caveolae, as a new interacting protein of strumpellin. RNAi depletion of strumpellin reduces CAV1 protein levels, impairing integrin-mediated cell adhesion. Strumpellin proteins harboring SPG8-associated missense mutations are unable to rescue this defect. SPG8 patient fibroblasts exhibit similar defects in CAV1-integrin-mediated cell adhesion that can be rescued by restoring actin nucleation activity of WASH1 at endosomes. These findings provide a clear molecular link between *WASHC5* mutation and CAV1-integrin-mediated cell adhesion, providing important insight into the cellular pathogenesis of SPG8.

Key Words: Spasticity, Neurogenetics, WASH complex, Strumpellin, Motor system, Caveolin, Endocytosis

P113

CD46 stimulated TGFBI enhances cell migration and invasion ability

Manh-Hung Do, Sueun Lee, Kim-Phuong To, Se-Young Kwon, Chaeyong Jung

Department of Anatomy, Chonnam National University Medical School, Hwasun, Jeonnam, Korea

Membrane cofactor protein (CD46) is a transmembrane glycoprotein expressed on all nucleated cells. CD46 was initially discovered as a complement regulatory protein, functioning in protection of cells from complement-mediated cytotoxicity. In addition, CD46 was generally overexpressed in solid tumors including tissues from colorectum, prostate, and bladder. To explore the new role of CD46 in these tumors, CD46 overexpression was made in HT-1376 human bladder cancer cell. Following cDNA microarray analysis showed differential gene expression including *GABRP* (Gamma-Aminobutyric Acid Type A Receptor Pi Subunit)*, RGS4* (Regulator of G Protein Signaling 4)*, MAP4K4* (Mitogen-Activated Protein Kinase Kinase Kinase Kinase 4)*, KRT13* (Keratin 13), and *TGFBI* (Transforming Grow Factor, beta-induced). TGFBI protein is induced by TGF beta, an intriguing cytokine exhibiting dual activities in malignant disease. In this study, over-expression of CD46 leads to an increased cell migration and invasion properties. Following, immunoblotting demonstrated that the enhancement of migration and invasion was mediated through the stimulation of extracellular signal-regulated kinase (ERK), protein kinase B (Akt), c-Jun, and c-Jun N-terminal kinase (JNK). In summary, our data indicated that CD46 in human bladder cancer cells enhanced cell survival, proliferation, and migration via stimulated TGFβ pathway.

Key Words: CD46, TGFBI, HT-1376

P114

PP2A negatively regulates the cardiac hypertrophy by dephosphorylating HDAC2 S394

Hye Jung Cho[1], Eun Jeong Won[2], Gwang Hyeon Eom[3], Hyun Kook[3], Juhyun Song[1], Chaeyong Jung[1], Kwang Il Nam[1*], Kyu Youn Ahn[1], Choon Sang Bae[1]

Departments of [1]Anatomy, [2]Parasitology and [3]Pharmacology, Chonnam National University Medical School, Gwangju, Republic of Korea

Cardiac hypertrophy occurs in response to increased hemodynamic demand and can progress to heart failure. Identifying the key regulators of this process is clinically important. Though it is thought that the phosphorylation of histone deacetylase (HDAC) 2 plays a crucial role in the development of pathological cardiac hypertrophy, the detailed mechanism by which this occurs remains unclear. Here, we performed immunoprecipitation and peptide pull-down assays to characterize the functional complex of HDAC2. Protein phosphatase (PP) 2 A was confirmed as a binding partner of HDAC2. PPP2CA, the catalytic subunit of PP2A, bound to HDAC2 and prevented its phosphorylation. Transient overexpression of PPP2CA specifically regulated both the phosphorylation of HDAC2 S394 and hypertrophy-associated HDAC2 activation. HDAC2 S394 phosphorylation was increased in a dose-dependent manner by PP2A inhibitors. Hypertrophic stresses, such as phenylephrine in vitro or pressure overload in vivo, caused PPP2CA to dissociate from HDAC2. Forced expression of PPP2CA negatively regulated the hypertrophic response, but PP2A inhibitors provoked hypertrophy. Adenoviral delivery of a phosphomimic HDAC2 mutant, adenovirus HDAC2 S394E, successfully blocked the anti-hypertrophic effect of adenovirus-PPP2CA, implicating HDAC2 S394 phosphorylation as a critical event for the anti-hypertrophic response. PPP2CA transgenic mice were protected against isoproterenol-induced cardiac hypertrophy and subsequent cardiac fibrosis, whereas simultaneous expression of HDAC2 S394E in the heart did induce hypertrophy. Taken together, our results suggest that PP2A is a critical regulator of HDAC2 activity and pathological cardiac hypertrophy and is a promising target for future therapeutic interventions.

Key Words: PP2A, HDAC2, Hypertrophy, Cardiac muscle, Heart failure

P115

Direct reprogramming of fibroblasts into diverse lineage cells by DNA demethylation followed by differentiating cultures

Hyun-Mi Ko, Dong-Wook Yang, Yeo-Kyeong Shin, Jung-Sun Moon, Sun-Hun Kim, Min-Seok Kim

Department of Oral Anatomy, School of Dentistry, Chonnam National University, Gwangju, Republic of Korea

Direct reprogramming, also known as a trans-differentiation, is a technique to allow mature cells to be converted into other types of cells without inducing a pluripotent stage. It has been suggested as a major strategy to acquire the desired type of cells in cell-based therapies to repair damaged tissues. Studies related to switching the fate of cells through epigenetic modification have been progressing and they can bypass safety issues raised by the virus-based transfection methods. In this study, a protocol was established to directly convert fully differentiated fibroblasts into diverse

mesenchymal-lineage cells, such as osteoblasts, adipocytes, chondrocytes, and ectodermal cells, including neurons, by means of DNA demethylation, immediately followed by culturing in various differentiating media. First, 24 hr exposure of 5-azacytidine (5-aza-CN), a well-characterized DNA methyl transferase inhibitor, to NIH-3T3 murine fibroblast cells induced the expression of stem-cell markers, that is, increasing cell plasticity. Next, 5-aza-CN treated fibroblasts were cultured in osteogenic, adipogenic, chondrogenic, and neurogenic media with or without BMP2 for a designated period. Differentiation of each desired type of cell was verified by quantitative RT-PCR/western blot assays for appropriate marker expression and by various staining methods, such as ALP/Alizarin red S/Oil red O/Alcian blue. These proposed procedures allowed easier acquisition of the desired cells without any transgenic modification, using direct reprogramming technology, and thus may help make it more available in the clinical fields of regenerative medicine.

Key Words: Direct reprogramming, DNA demethylation, 5-azacytidine, Mesenchymal-lineage cells, Regenerative medicine

P116

An R&E project to understand CRISPR: a test experiment with GlcNAc kinase gene

Ju Yeob Lee[1], Jae Hyeon Lee[1], Seo Jun Hwang[1], Tae Won Choi[1], Jaeha Lee[2], HyunSook Lee[2], Il Soo Moon[2]

[1]Gyeong High School, Gyeongju 38151, Korea
[2]Department of Anatomy, Graduate School of Medicine, Dongguk University, Gyeongju 38066, Republic of Korea

We are high school students and interested in understanding the mechanism of Clustered Regularly Interspaced Short Palindromic Repeats (CRISPR), a recently developed genetic scissor to edit genomes. After studying the background knowledge on the action mechanism of CRISPR, we carried out a serious of test experiments to witness its action with help from a university laboratory. As a test gene, we selected N-acetyl glucosamine (GlcNAc) kinase (NAGK) gene. This gene has been shown to activate cytoplasmic dynein and clear protein aggregates in cells. As a target protein for protein aggregation, we chose mutant huntingtin (mHtt). To produce protein aggregates we introduced by transfection pEGFP-Q74 into a human embryonic kidney 293 (HEK293) cell line. The pEGFP-Q74 contains exon 1 of mHtt and produces peptides with 74 repeats of glutamine (Q74). The exogenously expressed Q74 formed robust green fluorescent protein aggregates which can easily be observed in a fluorescence microscope. Using this Huntington disease cellular model, we tested the effects of NAGK upregulation on the formation of mHtt aggregates. We used CRISPR/gRNA-directed synergistic activation mediator (SAM) to upregulate the gene transcription in a cellular and in vivo model of Huntington's disease. By immununocytochemistry, we found that NAGK protein was increased in CRISPR/gRNA-directed SAM cells and they exhibited reduced the amount of mHtt clusters. In conclusion, our experiments witness that CRISPR/gRNA-directed SAM system recruits transcription factors at the promoter region of NAGK gene in the genome. * Contributed equally to this work.

Key Words: Aggregate, CRISPR, dynein, GlcNAc kinase, mHtt

P117

LMP1 induces Nrf2-mediated Akt expression in Epstein-Barr virus transformed B cells

Sun-mi Yun, Min Hye Noh, Temitope Michael Akinleye, Lata Rajbongshi, Mi Kyung Lee, Yeong Seok Kim, Dae Young Hur

Department of Anatomy and Tumor immunology, Inje University College of Medicine, Busan, Republic of Korea

The transcription factor Nrf2, which regulates the expression of antioxidant and cytoprotective enzymes, contributes to cell proliferation and resistance to chemotherapy. Nrf2 is also dysregulated in many cancer such as lung, head and neck, and breast cancers, but its role in Epstein-Barr virus (EBV)-transformed B cells is still not understood. Here, we investigated EBV infection-induced Nrf2 activation in B cells by analyzing translocation of Nrf2 from the cytosol to the nucleus. In addition, we confirmed expression of the target genes in response to increased Nrf2 activation in EBV transformed B cells. We demonstrated that knockdown of LMP1 blocks the translocation of Nrf2 to the nucleus and reduces ROS production in EBV transformed B cells. Further, we showed that inhibition of Akt prevents Nrf2 activation. Moreover, knockdown of Nrf2 induces apoptotic cell death in EBV transformed B cells. In conclusion, our study demonstrates that Nrf2 promotes proliferation of EBV-transformed B cells through the EBV-related protein LMP1 and Akt signaling, implicating Nrf2 as a potential molecular target for EBV-associated disease.

Key Words: Atmospheric EBV, LMP1, Nrf2, Akt, Apoptosis

P118

MYH11 functions in in male infertility via interacting with CCP1 and USP9Y

Yan-chao Bian, Rui-xiu Li, Jing Liu, Wen-xiu Li, Rui Xiao

Key Laboratory of Molecular Pathology, Inner Mongolia Medical University, Hohhot, P. R. China

Smooth muscle myosin heavy chain (Myosin-11/SMMHC/SM-MHC/MYH11) is a well-known biomarker of vascular physiology, which is involved in vascular or blood disease and different kinds of cancer. However, there are no reports about the function of MYH11 in male reproductive system. Here, we aimed at revealing the expression of MYH11 in mouse testis and its functions in male sterility. As a result, we found that MYH11 was expressed widely in the mouse testis by immunohistochemistry, which was consistent with the results from RT-PCR and western-blot analyses. In addition Myh11 was down-regulated both in mRNA and protein levels in the testes of male sterile pcd (Purkinje cell degeneration) mouse caused by the mutation of cytosolic carboxypeptidase 1 (CCP1). Dramatically, immunoprecipitation combined mass spectrometry revealed that MYH11 might be interacted with CCP1 and USP9Y. The structural model of MYH11 was predicted by Phyre2 software and the functional protein sites were analyzed with Antheprot Editor software, respectively. Moreover, Bioinformatic analysis results suggested that MYH11 might play crucial role in tight junction pathway besides its well-known muscle construction pathway. Our results may shed light on the novel function of MYH11 related to male reproductive system.

Key Words: MYH11, CCP1, USP9Y, Pcd mouse, Male sterility

P119

Usp9y regulates cell proliferation and apoptosis in mouse leydig cells

Wen-xiu Li, Rui-xiu Li, Jia-dong Wu, Yan-chao Bian, Rui Xiao

Key Laboratory of Molecular Pathology, Inner Mongolia Medical University, Hohhot, P. R. China

The Azoospermia factor (AZF) region on the Y chromosome has been considered closely related to spermatogenesis. Ubiquitin specific peptidase 9, Y-linked (Usp9y) gene, located in the AZF region, plays a important role in spermatogenesis. Our previous study found that the Usp9y gene is mainly expressed in mouse Leydig cells. Here we established the Usp9y knockout TM3 mouse Leydig cell line using the Crispr-Cas9 technique. Furthermore, we studied the function of Usp9y to clarify its role in spermatogenesis based on the Usp9y knockout cell model. The cell proliferation and cell cycle were examined by Cell Counter Kit-8 (CCK-8) and flow cytometry, respectively. The expression of Cyclin B1 and Caspase-3 were detected by real-time PCR and western blot, respectively. As a result, the proliferation of Usp9y knockout TM3 cells was inhibited and cell cycle was arrested in G1 phase. The expression of Ccnb1 was increased in the Usp9y knockout cells, and the expression of apoptosis protein Caspase-3 was significantly increased. In a summary, Usp9y knockout resulted in the TM3 cell cycle arrest and cell proliferation inhibition, and induced apoptosis.

Key Words: Usp9y, Leydig cells, Cell proliferation, Apoptosis, Spermatogenesis

P120

Identification of CCP1 interactome in mouse testis

Rui-xiu Li, Jing Liu, Wen-xiu Li, Hao Zhang, Yan-chao Bian, Rui Xiao

Key Laboratory of Molecular Pathology, Inner Mongolia Medical University, Hohhot, P. R. China

CCP1 (Cytosolic carboxypeptidase 1) is identified as a member of M14 subfamily of cytosolic carboxypeptidase. CCP1 autosomal recessive mutation results in Purkinje cell degeneration, male sterility and female sub-fertility. The mechanism of male sterility has not been revealed yet. Therefore, it is important to identify CCP1 interacting proteins in mouse testis for clarifying the function of CCP1 in male reproductive system. Here, we used coimmunoprecipation and LC/MS-MS to identify CCP1 interacting proteins from Balb/C mouse testis in a proteome-wide scale. Subsequently, the bioinformatics analyses using GO, PANTHER and KEGG databases were used to explore the CCP1 interacting proteins function and involved pathways. Finally, we analyzed interactions between CCP1 and its interacting proteins by STRING database. As a result, we identified 325 proteins interacting with CCP1 in mouse testis. Most of them had hydrolase and binding activities with nucleic acids and proteins, which were mainly involved in inflammation process mediated by chemokine and cytokine signaling pathway, nicotinic acetylcholine receptor signaling pathway and Parkinson disease related pathways. The Actb(Actin, cytoplasmic 1), Tubb4b (Tubulin beta-4B chain), Prkaca (cAMP-dependent protein kinase catalytic subunit alpha) and Gnai2 (Guanine nucleotide-binding protein G(i) subunit alpha-2) were the main related proteins. Notably, Tubb4b was in the core of the interacting network. Our study identified CCP1 interacted proteins in proteome-wide scale, and it surely will provide deep insight of CCP1 function and probable related pathways in mouse testis.

Key Words: CCP1,Interactome, Pcd mouse, Male sterility

P121

Inhibitory Effect of Theaflavin Extract from Tea on Melanogenesis

Bo-zhi Tan[1], Seol-A Park[1], Won-Hong Woo[2], Yeun-Ja Mun[1,2]

[1]Department of Herbal Resources, Professional Graduate School of Oriental Medicine, Wonkwang University, Iksan, Korea
[2]Department of Anatomy, School of Oriental Medicine, Wonkwang University, Iksan, Korea

Theaflavin is a natural active substance extracted from tea and it has a good biological activity. Natural products with non-toxic and sustainable properties are nice resources for skin-whitening cosmetic agents when compared to artificial synthetic chemicals. In this study, we investigated the effect of theaflavin on melanogenesis and their mechanisms in melanin biosynthesis. Theaflavin significantly inhibited melanin synthesis and tyrosinase activity of B16F10 cells in a concentration-dependent manner. We also found that theaflavin decreased the expression of tyrosinase, tyrosinase-related protein-1(TRP-1), TRP-2, microphthalmia-associated transcription factor (MITF) and phosphor-cAMP-response element binding protein (p-CREB). The expression of forskolin-stimulated tyrosinase was significantly attenuated by PKA inhibitors (H-89) and completely decreased by concomitant theaflavin. These results indicate that theaflavin down-regulated the intracellular level of tyrosinase through PKA/CREB pathway.

Key Words: Melanogenesis, Theaflavin, Tyrosinase, MITF, PKA inhibitor

P122

Effect of Scopoletin on the Improvement of Photoaging *in vitro* and *in vivo*

Dae-Sung Kim[1], Seol-A Park[1], Yeun-Ja Mun[1,2], Won-Hong Woo[2]

[1]Department of Herbal Resources, Wonkwang University, Iksan, Korea
[2]Department of Anatomy, Wonkwang University, Iksan, Korea

Chronic exposure to UV irradiation over the course of one's lifetime produces changes in skin connective tissues by degradation of collagen, which is a major structural component in the extracellular matrix most likely mediated by matrix metalloproteinases (MMP). In this study, we examined the protective effects of scopoletin on UVB-induced wrinkle formation in hairless mice by topical application or oral administration. First, scopoletin suppressed TNF-α-induced matrix metalloproteinase 1 (MMP-1) secretion and activity in human dermal fibroblast neonatal (HDFn) cells. Therefore, we investigated whether scopoletin inhibits the expression of MMP-13, -3, -9, and collagen in UVB-irradiated hairless mouse skin. Immunohistochemical analysis and Western blotting analysis showed that topical application and oral administration of scopoletin reduced the epidermal thickening and procollagen degradation by UVB radiation. In addition, scopoletin significantly prevented the expression of MMP-13, -3 and -9, which were increased by UVB, whereas markedly restored the expression of IκBα reduced by UVB. UVB-induced oxidative stress lead to damage that may result in premature skin aging. It was also found that water loss by UVB was significantly retrieved with topical application and oral administration of scopoletin. These results demonstrate that topical application and oral administration of scopoletin can protect the UVB-induced procollagen degradation through inhibiting the MMPs. Therefore, scopoletin is a potential agent for the prevention of UV-induced skin photoaging.

Key Words: Scopoletin, Matrix Metalloproteinases, Procollagen, Skin aging, UVB

P123

Organoid in periodontal tissue

Dong-Joon Lee, Qing Ge, Kasun Weerasekara Mudiyanselage, Sushan Zhang, Jong-Min Lee, Han-Sung Jung

Division in Anatomy and Developmental Biology, Department of Oral Biology, Oral Science Research Center, BK21 PLUS project, Yonsei University College of Dentistry, Seoul, Korea.

Organoids are cell-derived in vitro 3D organ models and allow the study of biological processes, such as cell behavior, tissue repair and response to drugs or mutations, in an environment that mimics endogenous cell organization and organ structures. Organoids are now firmly established as an essential tool in biological research and also have important implications for clinical use. They can be used for drug screening to develop individual therapies. And methods of making organoids in many organs have been established.   Periodontal diseases including gingivitis and periodontitis are prevalent both in developed and developing countries and affect about 20-50% of global population. However, the protocol of making organoids of the tissues constituting the periodontal region has not yet been developed. The development of organoids in periodontal tissues implies not only the potential for treatment through transplantation in the lesion area but modeling of the disease. And this can help to answer many important biological questions. This study examines the method of making organoids of periodontal tissue and identifies the character as an organoid. The gingival organoid mimicked the composition of the epithelium of the gingival tissue. This periodontal organoids suggests new alternatives to treatment of periodontal disease can be presented and the origin of personalized treatment can be initialized.

Key Words: Organoid, Periodontal disease, Media components

P124

Comparative histologic analysis of demineralized or undemineralized human dentin block graft with and without micro-holes: An experimental study in rabbits

Yong Suk Moon[1], Soon Wook Kwon[1], Hong Tae Kim[1], Dong Seok Sohn[2]

[1]Department of Anatomy, Catholic University of Daegu, Daegu, Korea
[2]Department of Dentistry and Oral and Maxillofacial Surgery, Catholic University Hospital of Daegu, Daegu, Korea

The aim of this animal study is to evaluate new bone formation in human dentin block grafted on rabbit calvaria according to a comparison of histologic analysis. Human teeth were prepared according to 4 different types of dentin blocks. Group 1 is demineralized and microperforated dentin block (DPDB), Group 2 is demineralized dentin block (DDB), Group 3 is undemineralized and microperforated dentin block (UDPDB), and Group 4 is undemineralized dentin block (UDDB). These 4 different dentin blocks were grafted on 9 rabbit calvaria and animals were sacrificed at 2, 4 and 8 weeks after the surgical procedure for histologic evaluation. In Group 1, histologically, new bone

formation was initiated in the DPDB bottom and micro-holes at 2 weeks, and mature bone was observed at 8 weeks. In Group 3, new bone formation was observed at 8 weeks in the UDPDB bottom and micro-holes. The bone formation ratio of Group 1 was significantly higher at 2, 4, and 8 weeks compared to Groups 2, 3, and 4 ($p < 0.05$). The bone formation ratio in micro-holes at 2, 4 and 8 weeks in Group 1 was significantly greater than in Group 3 ($P < 0.05$). New bone formation of the demineralized dentin block began more rapidly than the undemineralized dentin block, and perforated dentin block was more effective in bone formation than dentin block without micro-holes.

Key Words: Tooth block bone, Demineralization, New bone formation, Ridge augmentation, Dentin block

P125

Lycopus lucidus Turcz improved glucocorticoid induced bone loss in atopic dermitits mice

Bina Lee, Sooyeon Hong, Minsun Kim, Eun-Young Kim, Hyuk-Sang Jung

[1]Department of Anatomy, College of Korean Medicine, Kyung Hee University, Seoul, Republic of Korea

Glucocorticoids (GCs) are commonly used in many chronic diseases widely. However, the usage of GCs in the treatment of immunosuppression following inflammatory diseases is driving to severe side effect including diabetes, a decline of growth as well as bone loss, which can lead to GC-induced osteoporosis (GIOP). The GIOP that results in easy fracturing, fractures are a leading cause of disability in older adults, and a major contributor to medical care costs around the world. Although this is a serious problem, researches for evaluation of medicine in a bone loss by steroid side effect in the actual inflammation situation are not studied yet. *Lycopus lucidus Turcz* (LLT) is has been used to treat amenorrhea, edema, carbuncles and sores. LLT has been studied to anti-inflammation, blood circulation, and cardiac healing effect. However, the effect of LLT in glucocorticoid induced side effect including osteoporosis hed been not reported. In this study, ICR mouse was induced bone loss by steroid side effect in atopic dermatitis condition. LLT has effect especially bone mineral density, trabecular separation and trabecular number. Moreover it improve organ weight loss induced long term glucocorticoid treatment.

Key Words: Glucocorticoid, side effect, GC-induced osteoporosis (GIOP), Bone mineral density (BMD)

P126

Primary cilia dysfunction induces delayed GABAergic interneuron differentiation in infantile spasms

Hyeok Hee Kwon[1,3,4], Hyo Jung Shin[1,2,3], Nara Shin[1,3], Yuhua Yin[1,3], Do Hyeong Gwon[1,3], Juhee Shin[1,3], Hyewon Park[1,3], Jeong-ah Hwang[1], Jinpyo Hong[1,2], Yoon Young Yi[4], Joon Won Kang[2,3,4], Dong Woon Kim[1,2,3]

[1]Department of Anatomy, Chungnam National University, Daejeon, South Korea
[2]Brain Research Institute, Chungnam National University, Daejeon, South Korea
[3]Department of Medical Science, Chungnam National University, Daejeon, South Korea
[4]Department of Pediatrics, Chungnam National University Hospital, Daejeon, South Korea

Primary cilia are sensory organelles that are present in most mammalian cells, play important roles in growth, development, cell cycle progression and function of central nervous system. Recent studies suggest that primary cilia are significantly implicated in neurological diseases. Here, we checked relationship between primary cilia and differentiation of GABAergic neuron in infantile spasms. We used prenatally stressed Sprague Dawley rats and further treatment dams with betamethasone on gestational day 15 (G15) and checked postnatal N – methyl – D - aspartate (NMDA) triggered spasms. We measured length of primary cilia in posterior cortex of postnatal day 15 (P15) rats by immunohistochemistry for the marker of primary cilia, adenylyl cyclase III (ACIII).   As a result, we observed offspring of betamethasone induced prenatal stress exposed rats was decreased the length of primary cilia. And prenatally stressed group showed the decrease of glutamate decarboxylase 67-immunopositive cells in posterior cortex. Our results suggest evidence for prenatal stress induces delayed differentiation of GABAergic neuron in posterior cortex. These finding contributes understanding the mechanism of infantile spasms.

Key Words: Infantile spasms, Primary cilia, GABA, Prenatal Stress, Seizure

P127

Single Cell Analysis of Pathophysiological Mechanisms in Patients with Cortical Dysplaisa

Hee-Jang Pyeon[1,2,3], Hyun Nam[2,3], Ji-Yeoun Lee[6], Kyeung-Min Joo[1,2,3,4,5]

[1]Department of Anatomy and Cell Biology, Sungkyunkwan University School of Medicine, Suwon, South Korea
[2]Single Cell Network Research Center, Sungkyunkwan University School of Medicine, Suwon, South Korea
[3]Stem Cell and Regenerative Medicine Center, Research Institute for Future Medicine, Samsung Medical Center, Seoul, South Korea
[4]Department of Health Sciences and Technology, Samsung Advanced Institute for Health Science & Technology, Sungkyunkwan University, Seoul, South Korea
[5]Samsung Biomedical Research Institute, Samsung Medical Center, Seoul, South Korea
[6]Department of Anatomy and Cell Biology, Seoul National University College of Medicine, Seoul, South Korea

Pediatric focal cortical dysplasia (FCD) is common developmental malformations of cerebral cortex characterized by dysmorphic neurons and disorganization of cortical structure, which are highly associated with medically intractable drug-resistant epilepsy. The etiology of FCD should be multifactorial. Proliferation and differentiation, migration of neural stem cells (NSCs) is one of the multifactorial etiologies. However, the exact pathophysiological mechanisms of FCD are still under elucidation. In the present study, we used single-cell mRNA sequencing (scRNA-seq) to explore gene expression of neural cell components of FCD surgical samples including microenvironmental cells. scRNA-Seq data of 9,341 cells were produced. Gene expression analysis reveals that PTPRZ1, SPARCL1, SERPINE2, FABP7, BCAN, CLU, SCG3, MT3, IGFBP7, and ATP1A2 were identified for top 10 genes with highest expression in neurons compared with the other subtypes. To demonstrate

the validity of discovery of functional disease genes using scRNA-seq, we have isolated and primary cultured NSCs from FCD tissues. Using the NSCs, functional consequences of the high expressions will be explored. Our findings might demonstrate the investigational applicability of scRNA-seq to various congenital neurodevelopmental disorders. The approach may extend the understanding of the pathophysiology of FCD and possibly suggest treatment strategies for FCD.

Key Words: Focal cortical dysplasia (FCD), Single-cell mRNA sequencing (scRNA-seq), *in vitro* stem cell disease modeling

P128

Indocyanine Green Encapsulated Porous Silicon Nanoparticles for Photoacoustic Imaging

Rae Hyung Kang[1], Dokyoung Kim[1,2,3,*]

[1]Department of Biomedical Science, Graduate School, Kyung Hee University, 26 KyungheedaeRo, Dongdaemun-Gu, Seoul 02447, Republic of Korea;
[2]Department of Anatomy and Neurobiology, College of Medicine, Kyung Hee University, 26 Kyungheedae-Ro, Dongdaemun-Gu, Seoul 02447, Republic of Korea;
[3]Center for Converging Humanities, Kyung Hee University, 26 Kyungheedae-Ro, Dongdaemun-Gu, Seoul 02447, Republic of Korea.

Photoacoustic imaging integrates the advantages of optical imaging and ultrasound imaging such as advantage of distinguishing different colors with high resolution and deep tissue penetration. The principle of photoacoustic imaging is that when a short pulse laser enters a living tissue, a part of the energy is absorbed into tissue, converted into heat, and thermally expanded, resulting in the generation of sound waves. In this study, we have developed a new porous silicon nanoparticles (pSiNPs) formulation that photoacoustic imaging agent, indocyanine green (ICG), encapsulated. ICG is a representative FDA-approved photoacoustic imaging contrast agent, which is used to measure heart and liver function and blood flow. We found that ICG can be encapsulated in pSiNPs and shows 17-fold enhanced photoacoustic imaging response when it encapsulated rigid nanostructures. Since pSiNPs have shown low cytotoxicity and excellent biocompatibility relative to metallic nanoparticles, the new pSiNPs-ICG formulation in this study is considered as an improved agent for photoacoustic imaging in the translational research. The photoacoustic imaging efficiency of pSiNPs-ICG formulation is tested in the in vitro assay and ex vivo mouse tissue samples, the results prove that higher signals are generated in the pSiNPs-ICG formulation than bared ICG or PBS control. In conclusion, we demonstrated that pSiNPs can overcome the drawbacks of known photoacoustic imaging agents such as photothermical unstability and maintain the large light-induced heat, which greatly improves the performance.

Key Words: Photoacoustic Imaging, Porous Silicon, Indocyanine Green, Biomedical Imaging

P129

Two-Photon *In Vivo* Imaging with Porous Silicon Nanoparticles

Seohyeon Lee[1], and Dokyoung Kim[1,2,3,*]

[1]Department of Biomedical Science, Graduate School, Kyung Hee University, Seoul 02447, Republic of Korea.
[2]Department of Anatomy and Neurobiology, College of Medicine, Kyung Hee University, Seoul 02447, Republic of Korea.
[3]Center for Converging Humanities, Kyung Hee University, Seoul 02447, Republic of Korea.

Bio-imaging based on fluorescence gives many advantages such as simple operation, cost-effective, non-invasive, high sensitivity, and rapid visualization. Among the imaging tools, the confocal laser scanning fluorescence microscopy (CLSM) is commonly used to bio-imaging. However, CLSM enable to image only a few tens of micrometers in case of tissues imaging, due to the scattering of light and interference of tissue autofluorescence from intrinsic fluorophores. To overcome these issues, two-photon microscopy (TPM) was developed which have enhanced penetration depth and improved spatial resolution owing to the reductions in tissue autofluorescence and scattering associated with the longer wavelengths (650-1000 nm) of both the exciting and emitting lights. In this study, we introduced a porous silicon (pSi) nano-formulation that have high photo-stability, NIR photoluminescence emissive, high two-photon absorption cross-section value, and high quantum yield. The surface of pSi was functionalized with a cancer targeting peptide and its two-photon bio-imaging application was performed in a live cancer xenograft animal model. As a result of the study, the pSi nano-formulation was selectivity accumulated in the disease site and gives bright photoluminescence in the TPM imaging.

P130

A gold ion detection probe based on the disaggregation of aggregation-induced emission molecules and bio-imaging

Na Hee Kim [1], Dokyoung Kim [1,2,3,*]

[1]Department of Biomedical Science, Graduate School, Kyung Hee University, Seoul 02447, Republic of Korea.
[2]Department of Anatomy and Neurobiology, College of Medicine, Kyung Hee University, Seoul 02447, Republic of Korea.
[3]Center for Converging Humanities, Kyung Hee University, Seoul 02447, Republic of Korea

Gold (Au) is widely used as a valuable material from the early stages of technological innovation. Recently, the unique chemical and photophysical properties of gold and gold ions have been used for various applications in the basic medicine and advanced systems. Because of the high biocompatibility of gold, it has been widely applied in biology and medicine, including drug and gene delivery systems, biosensors, bio-imaging materials, anticancer agents, antibiotics and water purification systems. In general, metallic gold [Au(0)] is stable, but under specific conditions (active oxygen species, etc.) it is oxidized in the form of gold ions [Au(III)]. Gold ions have high reactivity and have been are used for catalytic reactions. However, such high reactivity has a problem that it can show potential biological toxicity. To date, various types of analytical methods (i.e. spectroscopy and electrochemical analysis) have been developed for the analysis of gold ions, but these analytical methods were limited in the biological and medical sample analysis. Fluorescence-based probe has recently attracted a great attention, to overcome these problems. Fluorescence-based probes are simple, convenient and cost-effective, high sensitivity and high selectivity, and high biocompatibility. In this study, a new fluorescence probe for the detection of gold ions was developed based on the disaggregation of AIE (aggregation - induced emission) molecules. The developed probe gives strong fluorescence due to their aggregation, but they show the fluorescence disappearance via selective

disaggregation through gold binding. The probe showed high sensitivity to detect a small amount of gold ion, and showed excellent response such as fast reaction time, and high selectivity to other metals. The gold ion probe is expected to be applicable to various fields such as medical and biology for the purpose of analyzing the effect of gold ion on a living body, and verifying bioaccumulation of gold ion particles.

Key Words: Fluorescent probes, Gold ions, Aggregation-induced emission, Fluorescent imaging, Paper-based strip

P131

Development of a New Fluorescent Probe for Bio-imaging of Cells and Tissues.

Yuna Jung[1], Dokyoung Kim[1,2,3,*]

[1]Department of Biomedical Science, Graduate School, Kyung Hee University, 26 KyungheedaeRo, Dongdaemun-Gu, Seoul 02447, Republic of Korea;
[2]Department of Anatomy and Neurobiology, College of Medicine, Kyung Hee University, 26 Kyungheedae-Ro, Dongdaemun-Gu, Seoul 02447, Republic of Korea;
[3]Center for Converging Humanities, Kyung Hee University, 26 Kyungheedae-Ro, Dongdaemun-Gu, Seoul 02447, Republic of Korea.

Various cells and organelles in the body are surrounded by membranes and have an independent environment distinguished from the environment outside the membrane. Many biomolecules that can involve cell phenomena are observed in the cell membrane, and life events such as cell growth, death. In addition, differentiation are affected by structural and chemical changes of cell membrane. Bio-membranes play a significant role in regulating various physiological phenomena and also are known as important research topics in the diagnosis and treatment of diseases. Small molecular probes have been widely used in biological and medical researches as a powerful tool to detect diverse biochemical events occurring in the. Among them, fluorescence based probes enable to identify the physical properties of membranes and visualize the cell membrane. In this study, we developed a small molecular probe based on fluorescence and applied to study cell membrane imaging. The developed fluorescence probe has a merit that it is easy to pretreatment differently from the previously developed cell membrane dyes. Because of its stability and sensitivity, the probe can be applied to biocompatible membrane imaging by interacting the membrane without destroying. Biological imaging studies were conducted using a confocal laser scanning microscope and two-photon microscope, and it was confirmed that the probe selectively labeled only the cell membrane in a biological environment. In addition, it is possible to introduce intrinsic biomolecules, and a targeting functional group with the probe can target cell organelles, so that it is possible to expand research into various research fields including anatomy. The development of multifunctional fluorescent probe is expected to be the core for both basic and applied biological research in that the bio-imaging of cell membranes allows the observation of the dynamic activities of cells involved in disease in the original environment.

Key Words: Molecular probes, Fluorescence imaging, Cellular imaging, Two-photon imaging

P132

High-performance acellular tissue scaffold blended with hydrogel polymers for tissue repair

Eunsoo Lee[1], Hyun Jung Kim[1], Jae Ryun Ryu[1], June Hoan Kim[1], Dai Hyun[1,2], Min Seok Ham[2], Soo Hong Seo[2], Kiwon Lee[3], Neoncheol Jung[3], Youngshik Choe[4], Gi Hoon Son[5], Im Joo Ryu[1], Hyun Kim[1] Woong Sun[1,*]

[1]Department of Anatomy and Division of Brain Korea 21 Plus Program for Biomedical Science, Korea University College of Medicine, 73, Inchon-ro, Seongbuk-gu, 02841 Seoul, Republic of Korea
[2]Department of Dermatology, Korea University College of Medicine, Seoul, Republic of Korea
[3]Logos Biosystems, Inc. Anyang-Si, Gyunggi-Do, 431-755, Republic of Korea
[4]Department of Neural Development and Disease, Korea Brain Research Institute, 701-300 Daegu, Republic of Korea
[5]Department of Biomedical Sciences & Department of Legal Medicine,Korea University College of Medicine, Seoul, Republic of Korea

Decellularization of tissues provides extracellular matrix (ECM) scaffolds for regeneration therapy, and serves as experimental model to understand ECM and cellular interactions. However, technical difficulties for decellularization have limited the use of this technique. Here we present a new tissue decellularization procedure, namely CASPER (*c*linically *a*pplicable *s*caffold *p*olymer-*e*mbedded decellularized tissue for organ *r*epair), which includes steps for infusion and polymerization of hydrogel prior to robust chemical decellularization treatments. Polymerized hydrogels serve to prevent excessive damage to the ECM while maintaining very fast processing times, structures and biological activities of the ECM components. In addition, it can be applied to various organs, including soft tissues (such as brains and embryos) and whole organs of large animals. CASPERized tissues were successfully recellularized *in vitro* and after implantation *in vivo*, suggesting that this method can be used for monitoring cell-ECM interactions *in vitro*, and for surrogate organ transplantation *in vivo*.

Key Words: Decellularization, Tissue scaffold, Extracellular matrix (ECM), Tissue regeneration

P133

Cell type dependent cortical innervation onto globus pallidus in rodent

Karube F[1], Kobayashi K[2], and Fujiyama F[1]

[1]Graduate School of Brain Science, Doshisha University, Kyotanabe, Japan
[2]Section of Viral Vector Development, National Institute of Physiological Sciences, Okazaki, Japan

Previously, we confirmed that motor cortex innervated globus pallidus (GP) in rats, as reported in Naito and Kita (1994). Because GP is a counterpart of the external segment of the GP in the primates, and considered as a relay nucleus of the basal ganglia, direct effect of cerebral cortex has not been taken into account. It would be important to uncover whether the innervation is actually functional. Here we examined details of the innervation using morphological observation and electrophysiology with the aid of optogenetics. Firstly, both of the primary motor cortex (M1) and the secondary motor cortex (M2) innervated GP, and axonal bouton density in GP from those areas were comparable to that in the subthalamic nucleus (STN). The amplitude of optogenetically-induced excitatory postsynaptic currents (oEPSCs) elicited by M1 or M2 terminal stimulation was similar to each other. In addition, oEPSC amplitude recorded in STN and GP neurons was almost equal. Secondary, optical stimulation of cortical terminals did not affect all GP neurons examined, and oEPSC

was detected around one-half to two-thirds of GP neurons. In rodents, recently it is clarified that GP is composed of distinct cell types based on development, molecular profiles, electrophysiological properties, and projection targets. One type is named prototypic neurons. Typically, they project to STN, and express parvalbumin and/or Lim/homeobox 6. Another type is called arkypallidal neurons which exclusively project to the striatum and express forkhead box protein P2. Using combination of retrograde neural labeling of GP neurons and optogenetic stimulation of cortical terminals in slice preparation, we examined whether cortical innervation depended on post synaptic GP cell types. The results implicated that cortical innervation could be dependent on GP cell types, as well as on cortical areas. These results suggested motor cortical inputs could contribute to modulate neuronal activities dependent on GP cell types, and in turn they could differentially affect upstream and downstream basal ganglia circuitry.

Key Words: Cerebral cortex basal ganglia, Globus pallidus, Optogenetics, Synapse

P134

Changed expression of EAAC1 and abnormal behavior in rat model of Neonatal Maternal Separation

Ran-Sook Woo[1]*, Han-Byeol Kim[1], Ji-Young Yoo[1], Seung-Yeon Yoo[1], Jun-Ho Lee[2]

[1]Department of Anatomy and Neuroscience, Eulji University School of Medicine, Daejeon, Korea
[2]Department of Emergency Medical Technology, Daejeon University, Daejeon, 34520, South Korea

Early adverse life events (EALs) are relevant to neuropsychiatric disorder in adulthood. Neonatal Maternal separation (NMS), as one of the EALs, serves as a risk factor for developing emotional disorders. The aim of this study was to determine if stress during developmental stage can bring about depression/anxiety-like behavior observed in the widely accepted maternally separation. A further aim was to determine whether the behavioral changes were accompanied by changes in neuronal excitatory amino acid carrier 1 (EAAC1). Glutamate transporters play a crucial role in physiological glutamate homeostasis, neuronal development and plasticity. We compared with normal control group, NMS rats changed the NMS rats changed the neuronal excitatory amino acid carrier 1(EAAC1) expression. We meassured depression-like behavior using the open field test and forced swim test.

Key Words: Maternal separation, Early life stress, EAAC1, Behavior, Depression

P135

An improved dehydroepiandrosterone-induced rat model exhibiting ovarian and uterine features of polycystic ovary syndrome

Eun-Jeong Kim[1,2], Minhee Jang[2], Jong Hee Choi[1,2], Kyung Sun Park[3], Ik-Hyun Cho[1,2,4,*]

[1]Department of Science in Korean Medicine and Brain Korea 21 Plus Program, Graduate School, Kyung Hee University, Seoul 02447, Republic of Korea
[2]Department of Convergence Medical Science, College of Korean Medicine, Kyung Hee University, Seoul 02447, Republic of Korea
[3]Department of Korean Medicine Obstetrics & Gynecology, College of Korean Medicine, Kyung Hee

University , Seoul 05278, Republic of Korea
[4]Institute of Korean Medicine, College of Korean Medicine, Kyung Hee University, Seoul 02447, Republic of Korea

Complete animal models investigating the pathogenesis and treatment of polycystic ovarian syndrome (PCOS) are not completely established. Although dehydroepiandrosterone (DHEA)-induced pre-pubertal rat model for PCOS has been widely used, the model exhibits weaknesses such as decreased ovary weight. Here, we report an innovative DHEA-induced PCOS model that addresses limitations of the pre-pubertal model. The 21-day-old (pre-pubertal) and 42-day-old (post-pubertal) female rats were subcutaneously injected with DHEA (60 mg/kg body weight) daily for up to 20–30 days. The post-pubertal model showed a steady increase in ovary weight and the number of ovarian cysts as well as uterine weight and thickness, which may be key features of PCOS, compared with the pre-pubertal model. Therefore, a post-pubertal PCOS model induced by DHEA may be an improved model to investigate the etiology of PCOS and development of therapeutic interventions.

Key Words: Polycystic ovary syndrome model, Dehydroepiandrosterone, Post-puberty, rats, Improved model

P136

Animal experimental study of two sutures in reconstruction of biliary-enteric anastomosis after pancreatoduodenectomy

Jing-rui Yang[1], Rui Xiao[2], Jiang Zhou[1], Lu Wang[1], Qian Zhang[1], Jia-xin Wang[1], Jian-xiang Niu[3], Ze-feng Wang[3], Bo Wen[3], Jian-jun Ren[3]

[1]Department of Graduate Studies, Inner Mongolia Medical University, Hohhot, China
[2]Laboratory department of molecular pathology, Inner Mongolia Medical University, Hohhot, China
[3]Department of hepatobiliary surgery, Affiliated hospital of Inner Mongolia Medical University, Hohhot, China

Prolene (Polypropylene) and PDS-II (Polydioxanone) are widely used in reconstruction of biliary-enteric anastomosis. We observed the effect of two different sutures on the diameter and liver function of the experimental dog by making an experimental dog pancreatoduodenectomy model. Six healthy dogs were selected and randomly divided into two groups. Prolene group of three dogs, PDS group of three dogs. After preoperative preparation, reconstruction with simulated pancreaticoduodenectomy was performed. The inner wall diameter and liver function of the common bile duct were observed. As a result, the survival rate at 30 days after surgery was 100% in both groups. In the Prolene group and the PDS group, the intraoperative diameter of the common bile duct was not statistically significant ($P > 0.05$). In the Prolene group, there was no statistically significant difference between the intraoperative diameter of the common bile duct and the diameter of the common bile duct 30 days after the operation ($P > 0.05$). In experimental animals of the PDS group, intraoperative diameter of the common bile duct was compared with that of the common bile duct at 30 days after operation, and the difference was statistically significant ($P < 0.05$). The diameter of the inner wall of the common bile duct was not statistically significant between the Prolene group and the PDS group 30 days after operation($P > 0.05$). Comparing ALT, AST, TBIL and ALKP in the Prolene group and the PDS group, it was found that the differences were not statistically significant before surgery, 7 days after surgery, 14 days after surgery and 30 days after surgery ($P > 0.05$). However, as can be seen

from the line chart, compared with the Prolene group and the PDS group, the postoperative ALT, AST, TBIL and ALKP values were relatively low in the PDS group. In terms of early prognosis, biliary-enteric anastomosis was sutured with Prolene line, which may have less effect on the anastomosis than PDS line. However, the effect on liver function may be less than that of Prolene when biliary-enteric anastomosis is sutured with PDS. Their long-term prognosis still needs further study.

Key Words: Pancreatoduodenectomy, Biliary-enteric anastomosis, Suture selection, Animal experiment

P137

Reproductive Parameters of Male Albina Rats After Induction in Sleep Deprivation Models

Fitranto Arjadi[1], Ika Murti Harini[2], Nur Signa Aini Gumilas[2]

[1]Departement of Anatomy, Medical Faculty, Jenderal Soedirman University, Purwokerto, Indonesia
[2]Departement of Histology, Medical Faculty, Jenderal Soedirman University Purwokerto, Indonesia

Paradoxical sleep deprivation (PSD) and total sleep deprivation (TSD) caused disrupt male infertility but sleep recovery (SR) can improve male reproduction function that connected with occupational works health. The aim of this study was to determine the difference in reproductive parameters in male albino rats after exposed by various sleep deprivation model. This research was experimental post-test only with control group design. Rats were divided into 5 groups (6 animals each group) : negative control, PSD (II), TSD (III), PSD with SR, TSD with SR. Results showed in mean spermatogenic group IV (8.35 ± 0.06) and V (8.27 ± 0.27) had higher scores, group IV has the highest number of Leydig cell (5,91 ± 1,43), group I had the highest rates (40,02 ± 2,04) of number of Sertoli and there are no significant differences in mean diameter (p=0,598) and epithelial height (p=0,895).
There were differences score spermatogenic post-SR, number of Sertoli and Leydig cells, but no differences in diameter and epithelial height of seminiferous tubule after exposed by various sleep deprivation stress model. Sleep recovery in occupational work can repaired the parameter of histological parameter in reproduction quality.

Key Words: Male albino rats, Reproductive parameters, Sleep deprivation models.

P138

Effect of Bisphenol-A to the Fertility of Male Rats

Eryati Darwin[1], Arni Amir[2], Tetra Anestesia Putri[3]

[1]Department of Histology Faculty of Medicine Andalas University, [2]Department of Biology Faculty of Medicine Andalas University and [3] Biomedical Post Graduate Program Faculty of Medicine Andalas University, Padang. Indonesia

Bisphenol A is a chemical found in many hard and clear plastic which is used every day include water bottles, baby bottles, dental and medical devices and coating of metal-based food and beverage cans. High doses of BPA have been linked to the health problems such as cancer,

cardiovascular and reproductive disorders. To determine the effect of BPA to fertility, we studied the effect of bisphenol A to the level of testosterone and number of spermatozoa on rat. The post-only control groups study were carried out on 20 male wistar Rattus norvegicus in the age of eight weeks and 200-250 gr body weight. There were divided in four groups for five each, one group as a control group (C) and the other three groups treated with different doses of BPA. Group 1 (T1) treated with 25 mg/Kg body weight/day, group 2 (T2) 50 mg/Kg body weight/day and group 3 (T3) 100 mg/Kg body weight/day of BPA for 51 days. Blood were collect to measure the level of testosterone and spermatozoa were collected from the duct of epididymis. This study found that testosterone level of control group (C) (7,78±1,4 ng/l) were significantly higher than T3 (4,02±1,0) and it seem tend to be higher than T1 (6,19±3,2 ng/l) and T2 (5,23±0,9 ng/l). Spermatozoa number of control group (39,1±1,0 million/ml) were significantly higher than T1 (30,2±2,3 million/ml), T2 (21,1±2,8 million/ml) and T3 (19,7±3,0 million/ml), and there were also significantly different between groups. Our study shows that high doses of BPA can affect fertility through decline of testosterone levels and spermatozoa number

Key Words: Bisphenol A, infertility, Spermatozoa, Testosterone

P139

The effect of bisphenol-A giving on estrogen hoirmone level and maturation index of vagina epithelial cell *Rattus novergicus* wistar albino strain

Arni Amir[1], Eryati Darwin[2], Rilly Yane Putri[3]

[1]Department of Biology, Faculty of Medicine, Universitas Andalas, Padang, Indonesia
[2]Department of Histology, Faculty of Medicine, Universitas Andalas, Padang, Indonesia
[3]Department of Biomedical Post Graduate, Faculty of Medicine, Universitas Andalas, Padang, Indonesia

Bisphenol-a (BPA) or propan 2,2-bis (4-hydroxyphenyl) compound is the main ingredient of making polycarbonate plastic and epoxy resin making material. Bisphenol-a in its active form, has estrogen hormone activity. Bisphenol-a is also one of the endocrine disruptors compounds that can interfere the biosynthesis, secretion, work, or natural metabolism of a hormone. This study aims to determine the effect of bisphenol-a on estrogen hormone levels and maturation index of vaginal epithelial cells Rattus novergicus strain wistar albino. This study is an experiment post-test only control group design with 20 rats wistar albino strain with age 2-3 month with weight 200-300 gr as samples. Samples were randomly assigned and divided into four groups consisting of the untreated control group, the experimental group with each being given a dose of 25.50 and 100 mg / kg bw / day. Examination of estrogen levels in blood serum using ELISA. Data were analyzed by one way annova test. Analysis of maturation index data using Kruskal Wallis. It was found that there was an effect of bisphenol-a on estrogen hormone level on Rattus novergicus strain Wistar albino (p value = 0,041), and there was an effect of bisphenol-a on the maturation index of vaginal epithelial cell Rattus novergicus Wistar albino strain.

Key Words: Bisphenol-A, Estrogen Hormone, Maturation Index of Vaginal Epithelial Cells

P140

COMPARISON OF BACTERIA ISOLATE IN ANATOMICAL LABORATORY AND OTHER BIOMEDICAL LABORATORIES OF MEDICAL FACULTY MUHAMMADIYAH UNIVERSITY

OF PURWOKERTO

Maulana, A.M.[1], Putra, R.A.N.[1], Putri, P.M.[1], Febriyanti, R.W.[2], Pangestika, T.R.

[1]Anatomy Department, Universitas Muhammadiyah Purwokerto, Indonesia
[2]Microbiology Department, Universitas Muhammadiyah Purwokerto, Indonesia
[3]Undergraduate Student of Medical Faculty, Universitas Muhammadiyah Purwokerto, Indonesia

Background: Infectious diseases are still the top 10 causes of death in the world. Laboratory is a specific environment for the development of infectious bacteria. Anatomical laboratory as a cadaver preparation plays an important role in the development of bacteria that causing laboratory acquired infection. Comparison of bacterial isolate detected in anatomical laboratory and other biomedical laboratories has not been widely known. **Objective**: To know the comparison of bacterial isolate between anatomical laboratory and other biomedical laboratories at Medical Faculty of Muhammadiyah University of Purwokerto **Method**: The sampling technique uses settle down plate method for environmental samples. Samples are taken with 5-point surface swabs from anatomical laboratory and other biomedical laboratories (histology, microbiology and clinical pathology laboratories) at Medical Faculty, Muhammadiyah University of Purwokerto. Samples are grown on Blood Agar, Nutrient Agar and Mac Conkey Agar, and then subjected to gram staining and biochemical tests. Bacterial isolate data are analyzed descriptively. **Result**: Total number of samples for this study are 20 samples. The identified bacteria are *Staphylococcus aureus*, *CoNS*, *Pseudomonas sp.*, *Enterobacter sp.*, *Vibrio vulnificus*, *Aeromonas hydrophila*, *E. coli*, *Enterobacter intermedius*, *Klebsiella pneumonia*, *Serratia fonticola* and *Streptococcus sp*. The Microbiology Laboratory has the highest contamination (63 colonies), while the Anatomical Laboratory is in third rank (17 colonies). The bacterial isolate is founded varied per laboratory. *Vibrio vulnificus* is the dominant bacterium in the Anatomical Laboratory (41.6% of 17 colonies), unlike the Histology Laboratory (*Enterobacter intermedius*), the Microbiology Laboratory (*Pseudomonas sp.*) and the Clinical Pathology Laboratory (*Enterobacter intermedius*). **Conclusion**: There are different bacterial isolate found in each laboratory. The Anatomical Laboratory is dominated by *Vibrio vulnificus*, in contrast to the other three biomedical laboratories.

Keyword: Anatomical Laboratory, bacterial isolate, infection

P141

COMPARISON OF BACTERIA NUMBER BETWEEN ANATOMIC LABORATORY AND OTHER BIOMEDIC LABORATORIES IN MEDICAL FACULTY OF MUHAMMADIYAH UNIVERSITY OF PURWOKERTO BEFORE AND AFTER DISINFECTION WITH ALCOHOL 70%

Putra, R.A.N.[1], Putri, P.M.[1], Febriyanti, R.W.[2], Maulana, A.M.[1] and Pangestika, T.R.[3]

[1]Anatomy Department, Universitas Muhammadiyah Purwokerto, Indonesia
[2]Microbiology Department, Universitas Muhammadiyah Purwokerto, Indonesia
[3]Undergraduate Student of Medical Faculty, Universitas Muhammadiyah Purwokerto, Indonesia

Background: Laboratory is a specific environment for the growth of pathogenic and non-pathogenic bacteria. Anatomical laboratory as a cadaver preparation for practicum of medical student can be a route for bacterial transmission. Disinfection process is useful to reduce bacterial contamination using chemicals such as alcohol70%, as to prevent bacterial transmission. **Objective**:

To know the bacteria number between anatomical laboratory and other biomedical laboratory of Medical Faculty of Muhammadiyah University of Purwokerto, before and after disinfection with alcohol70%. **Method**: Samples are taken from anatomical laboratory and other biomedical laboratory (Histology, Microbiology, and Clinical Pathology Laboratories) Medical Faculty of Muhammadiyah University of Purwokerto. The first and second samples are taken from the surface swab of each sampling point before and after disinfection. Samples are grown on Blood Agar, Nutrient Agar and Mac Conkey Agar, and then subjected to gram staining and biochemical test. Data of bacterial number difference before and after disinfection are analyzed using Paired T test, while data of bacterial number comparison of each laboratory is analyzed by using Independent T test and Mann Whitney. **Result**: The average number of bacteria before disinfection is higher than after disinfection. The difference between the two groups is very significant because the value of significance is p = 0,010 (p <0,05). The Clinical Pathology Laboratory has the highest bacterial contamination, and the Histology Laboratory has the lowest bacterial contamination. There is no bacterial number difference in the Anatomical Laboratory and other biomedical laboratories (p> 0.05). **Conclusion**: Disinfection procedure is useful to reduce bacterial contamination. There is no bacterial number difference in the Anatomical Laboratory and other biomedical laboratories. The number of bacteria in the Anatomy Laboratory is not higher than the Clinical Pathology Laboratory and the Microbiology Laboratory.

Keywords: Anatomical Laboratory, Disinfection, Alcohol 70%

P142

Multimodal Action of Novell Saponin-releasable Carboxymethylcellulose Gel Against Abdominal Post-operative Adhesion

Nahyun Kim[1], Segeun An[1], Jong Hun Ahn[1], Ji Hyun Moon[1], Ji hye Lee[1], Ji Heun Jeong[1], Seong Hee Kang[1], Do Kyung Kim[1], Yeong Gil Jung[1], Nam Seob Lee[1], Seung Yun Han[1,3*]

[1]Department of Anatomy, Konyang University, Daejeon, South Korea
[2]Myunggok research institute, College of Medicine, Konyang University, Daejeon, South Korea

Abdominal postoperative adhesion (APA) commonly occurs after abdominal surgeries and causes serious complications. Although various types of antiadhesives such as carboxymethylcellulose gel (CMC-G) are currently used to prevent APA in clinical field, because of their single-targeted mechanism of action, *i.e.*, physical barriers, do not provide the sufficient salvation against the complex pathogenesis in APA. Given the soybean-derived saponin is well-known for its anti-inflammatory, anti-thrombotic, and anti-fibrotic roles, here, we manufactured a saponin-releasable CMC-G (Saponin@CMC-G) and tested the therapeutic efficacy on mice model of APA. When Saponin@CMC-G was implanted underneath the dorsal skin, the implants itself and the peri-implant inflammatory cell infiltrates were time-dependently reduced and completely disappeared by the 14th day after implantation, revealing the excellences in the biodegradability and the biocompatibility, respectively. Next, Saponin@CMC-G, CMC-G, or, normal saline (NS) used as a vehicle were applied to mice on the interface between the cecal surface and the opposite abdominal wall at the end of procedures of the cecal abrasion operation which was employed as a surgical model of APA. The results from the macroscopic and histologic experiments revealed that the mice with CMC-G showed the significant protection against APA by the demonstration of decreases in wideness, strength, and thickness of adhesion interface as well as in lesional accumulation of fibroblast and collagen-I compared with the mice with NS. However, mice with Saponin@CMC-G showed the further attenuation on all the values when compared with mice with CMC-G. Notably, unlike the mice with CMC-G, mice with Saponin@CMC-G exhibited the marked restoration in the mesothelial morphology,

indicating that the released saponin from the Saponin@CMC-G accelerated the wound healing process apart from the preventive role on the development of APA. Together, this study suggests that the novel synthesized Saponin@CMC-G, which has excellent biodegradability as well as biocompatibility, can inhibit the APA development through the multiple modes of action, *e.g.*, behaving as a physical barrier and accelerating the mesothelial healing.

Key Words: Abdominal post-operative adhesion, Saponin-releasable carboxymethylcellulose (CMC) gel, Biodegradability, Biocompatibility, Fibroblast

P143

Optimization of Immunohistochemical Staining With Anti Protein Gene Product 9,5 (PGP 9,5) Antibodies to Detecting Intraepidermal Nerve Fiber

David Pakaya[1,2], Yustina Andwi Ari Sumiwi[3], Sri Herwiyanti[3], Rina Susilowati[3]

[1]Postgraduate Program of Biomedical Science, Faculty of Medicine, Public Health and Nursing, Universitas Gadjah Mada, Yogyakata, Indonesia
[2]Department of Histology, Faculty of Medicine, Universitas Tadulako, Palu, Indonesia
[3]Department of Histology and Cell Biology, Faculty of Medicine, Public Health and Nursing, Universitas Gadjah Mada, Yogyakata, Indonesia

The intraepidermal nerve fibers are the ending branches of the sensory nerves within the skin. These fibers can be conceived due to the protein gene product 9.5 (PGP 9.5) as a marker which recognized by immunohistochemical. Various studies have visualized these intraepidermal nerve fibers with anti-PGP 9.5 antibodies. However, this study has a differences of immunohistochemical staining methods based on the tissues thickness, the antigen retrieval process and the antibody product used. These differences are related to the laboratory facilities used, so optimization is important to do. Our objective is to find an immunohistochemical staining optimizer with anti PGP 9.5 antibody for the detection of intraepidermal nerve fibers from paraffin blocks. Intraepidermal nerve fiber were determined by mice skin biopsied which stained immunohistochemical method with anti-PGP 9.5 antibodies. This procedure were altered in the dilution, duration and incubation temperature of primary antibodies, the thickness of the tissue and the temperature of the antigen retrieval. The results of the staining were analyzed qualitatively. As a result, Optimization of immunohistochemistry stain entail of 1:2000 dilution of the primary antibody, the thickness of the tissues was 4 µm, overnight incubation and low temperature of antigen retrieval. However, the results were inconsistent. The are some factors that contribute to enhance immunohistochemical staining method with the most optimal anti-PGP 9.5 antibody. There are consist of thin thickness of the tissue, low temperature antigen retrieval, the ratio of antibodies dilution (1: 2000) incubated for overnight at 21°C.

Key Words: Intraepidermal nerve fiber, PGP 9.5, Immunohistochemistry

P144

Neuroprotection against cardiac arrest followed by cardiopulmonary resuscitation with poly(lactic-co-glycolic acid) nanoparticles loaded with erythropoietin

Ji Heun Jeong[1], Seong Hee Kang[1], Jong Hun Ahn[1], Ji Hye Lee[1], Ji Hyun Moon[1], Do Kyung Kim[1], Yeong Gil Jung[1], Nam Seob Lee[1], Seung Yun Han[1,3,*]

[1]Departments of Anatomy, College of Medicine, Konyang University, Daejeon, South Korea
[2]Myunggok research institute, College of Medicine, Konyang University, Daejeon, South Korea

Cardiac arrest followed by cardiopulmonary resuscitation (CA/CPR) often results in dramatic neuronal damage caused by global cerebral ischemia and subsequent reperfusion (GCI/R). Glutamate-induced excitotoxic damage is implicated as the key mechanism of GCI/R. We previously reported that the recombinant human erythropoietin (rhEPO)-loaded poly(lactic-co-glycolic acid) (PLGA) nanoparticles (rhEPO-PLGA-NP), the novel synthesized drug delivery system, exerted the superior protection on *in vitro* neuronal cell against glutamate-induced excitotoxicity than the rhEPO itself. Here, we evaluated the protective effects of the rhEPO-PLGA-NP on a rat model of CA/CPR assessing the number of viable neurons in hippocampal CA1 region and their cognitive performance. First, the rhEPO-PLGA-NPs was fully characterized by both transmission electron microscopy (TEM) and differential scanning calorimetry (DSC). In addition, release profile of rhEPO from the particles and the successful delivery into hippocampal CA1 region were evaluated by *in vitro* release assay and confocal microscopy, respectively. We revealed that the histologic deterioration as well as the cognitive deficit was apparent in all experimental rat groups that previously subjected with 2-vessel occlusion and hypotension (2VOH), an experimental model of CA/CPR, compared to sham-operated. However, when compared to the groups given vehicle or rhEPO only (*i.v.* administered with a dose of 400 IU/head/day for postoperative 3 days), group given rhEPO-PLGA-NPs bearing an equivalent dose of the rhEPO showed the significant increment in number of viable neurons in hippocampal CA1 region. Furthermore, neuroinflammatory events including astrogliosis and microglial activation were significantly diminished in hippocampal CA1 region of rhEPO-PLGA-NPs groups compared with those of vehicle or rhEPO only groups. Most importantly, as demonstrated with Y-maze- and passive avoidance test, 2VOH-induced cognitive deficits were significantly attenuated in rhEPO-PLGA-NPs groups ini comparison with vehicle or rhEPO only groups. Taken together, as corroborate with the *in vitro* results that we previously reported, these data suggest that the rhEPO-PLGA-NPs can confer the protection to the neurons against the CA/CPR-related GCI/R injury histologically and functionally.

Key Words: Cardiopulmonary resuscitation, Neuroprotection, Erythropoietin, Poly(lactic-co-glycolic acid) nanoparticles

P145

Large area imaging using BSE-SEM and large volume reconstruction using serial block-face SEM

Kyung Eun Lee*, Yuna Oh, Jumi Lee, Sang-Jun Kwon

Advanced analysis center, Korea Institute of Sciences and Technology, Seoul, Republic of Korea

The interesting area of many biological tissue for analyzing the ultrastructure is too large to observe their structure using TEM. BSE-SEM (Back-scattered electron scanning electron microscopy) can be used for large area ultrastructure analysis. However to observe the biological tissue using BSE-SEM, the specimen has to be stained with electron dense materials. We examined the various sample preparation methods for BSE-SEM. It was very useful for 3D-SEM as well as for large area imaging using BSE-SEM. 3D-SEM for large volume reconstruction is classified into two techniques. One is serial section SEM that 3D structure is reconstructed using SEM images of serial sections acquired from the outside microtome, and the other is SBF-SEM (serial block-face SEM) using sequential SEM images acquired from a microtome or focused ion beam mounted inside a SEM chamber. We could

reconstructed the 3 dimensional structure with the exact interesting area for using our sample preparation method in the 3D-SEM (both serial section SEM and SBF-SEM).

Key Words: BSE-SEM, 3D SEM, Large area imaging, Large volume reconstruction

P146

TEM Analysis of polystyrene nanoplastics accumulation and abnormal ultrastructural alteration of subcellular organelles in developing zebrafish embryo

Jinyoung Jeong[1], Yang Hoon Huh[2]

[1]Hazards Monitoring Bionano Research Center, Kroea Research Institute of Bioscience and Biotechnology and KRIBB School, University of Science and Technology, Daejeon, 34141 Republic of Korea
[2]Electron Microscopy Research Center, Korea Basic Science Institute, Cheongju, 28119 Republic of Korea

Nanoplastic is a growing issue as an environmental problem due to its potential adverse effects in various organisms including zooplankton and fish. However, the effects of nanoplastics in biosystem are still unknown in spite of the microplastics have been studied in various living organisms. In this study, using the zebrafish embryo (ZFE) as a model animal, we investigated and found the bioaccumulation of polystyrene (PS) nanoplastics (about 50 nm) in brain, eye, yolk and dermis by Bio-HVEM system which is a powerful tool for observation of nanomaterials localized intra- and extra-cellularly in various organisms including vertebrate like ZFE. Also, we confirmed that PS nanoplastics accumulated in ZFE cells were caused the morphological alteration in membrane and cristae structure of mitochondria and the damage in nucleus morphology of eye and brain. This EM ultrastructural analysis of PS in ZFE eimplicates potential risk of nanoplastics in bioorganism.

Key Words: Polystyrene nanoplastics, Zebrafish embryo, Ultrastructure, Bio-HVEM system

P147

The Effect of Aromatherapy Candle as Insecticide from Citrus Extract of Lemongrass (Cymbopogon) to Increase Ae. aegypti Mortality

Aghnia Fikriya N[1], Gea Sonia A[1], Nurul Hidayah[2]

[1]Department of Anatomy, Islamic University of Indonesia, Yogyakarta, Indonesia

Aromatherapy candles are one of the insecticide media that have not been much researched. The active ingredient that is proven to have the effect of insecticide is a citrus extract from lemongrass oil (Cymbopogon). Aromatherapy candles are added by citrus compounds to be insecticidal for Ae. aegypti mosquito that was related to the infectious disease such us dengue fever. This research aims to find out if aromatherapy candles of citrus compounds have an insecticidal effect on Ae. aegypti mosquito. We used true experimental design including posttest only with control group design. The samples are 20 male and female Ae. aegypti mosquitos with aged 1-7 days belong to the inclusion criteria. The subjects were divided into 6 groups, consisting of 1 negative control group and 5 treatment groups with variation concentration are 1%; 2%; 3%; 4%; 5%. Each group will be treated for 2 hours

and observed death after 24 hours. Replication in each group is done 4 times. The results were then tested statistically using Kruskal-Wallis and probit test. Mean of death in negative control group, and treatment group 1%; 2%; 3%; 4%; 5% respectively 0; 1; 0.25; 0; 1 and 1 mosquito. The Kruskal-Wallis test in the study group found no significant difference ($p = 0.178$). The probit analysis showed that LC50 and LC90 were 20.069% and 31.557%. The aromatherapy candle of a citrus compound has an insecticidal effect on the Ae aegypti mosquito.

Key Words: Ae. aegypti insecticide, Aromatheraphy candle, Citrus compound, Lemongrass oil (*Cymbopogon*).

P148

Identification of unexpected object with different color in inattentional blindness

Reza Kurniawan Arta[1], Muthiah Nur Afifah[1], Mufidah Ruslan[1], Jamaluddin Madeali[1], Rizki Darmawan[1], Sitti Rafiah[1], Muhammad Iqbal Basri[1,2].

[1]Department of Anatomy, Medical Faculty, Hasanuddin University, Makassar, Indonesia.
[2]Department of Neurology, Medical Faculty, Hasanuddin University, Makassar, Indonesia.

Inattentional blindness is a phenomenon that has prominent potential to be harmful to everybody in various situations, including traffic accident in which caused by a failure in realizing thing that everyone should see in his or her visual field. A further study concerning this phenomenon is needed to prevent the similar accident occurs in the future. The result of this study also might be used as an input for further research regarding a better traffic sign in Indonesia. This research used 114 senior high school students as the population in which consist of 34 males and 80 females with mean age of 17 years old. The population was tested and 35 people who exceed the 80% confidence level were selected as the sample of the study. Furthermore, we divided the sample into four groups based on the unexpected object color. First group (blue, n=11), second group (yellow, n=6), third group (red, n=8), and controlled group (n=10). All samples were asked to look at the monitor which would show color changing of square object located right in the middle and unexpected object which appeared sometimes located in central vision and peripheral vision. However, they were given only one instruction. The instruction was only to focus their attention to color changing of square object. There were 15 times of color changing and had only 1 second each. Then they would give some response related to its color. Lastly, they were given questions about all objects in the monitor. The author used PsychoPy v1.90.1 as the assessment tool for inattentional blindness. Then, Spearman's correlation was used by the authors to find the correlation between the type of color and level of inattentional blindness. All samples of the first group indicated total inattentional blindness. Second group showed a better result, five samples were categorized as total inattentional blindness and one sample was in partial inattentional blindness. The best result was revealed in the red group with four samples were in total inattentional blindness and the other four samples were in partial inattentional blindness. On the controlled group, six samples were in total inattentional blindness and four samples were in partial inattentional blindness. Spearman correlation resulted in significance of 0.007 ($p<0.05$), and correlation values was -0.528. To conclude, there is a negative intermediate correlation between the type of color and the incidence of inattentional blindness level. It is more likely easier to recognize the unexpected object if its color has a higher spectrum.

Key Words: Inattentional blindness, Vision, Colored unexpected object.

P149

Monoiodoacetate-induced osteoarthritis pain is alleviated by a peptide antagonist of Toll like receptor 4 in rats

Hyewon Park[1,2], Yuhua Yin[1,2], Juhee Shin[1,2], Jinhyun Kim[3], Jaewon Beom[4], Jinpyo Hong[2], Dong Woon Kim[1,2]

[1]Department of Medical Science, Chungnam National University School of Medicine, Daejeon, 35015, Republic of Korea
[2]Department of Anatomy, Brain Research Institute, Chungnam National University School of Medicine, Daejeon, 35015, Republic of Korea
[3]Department of Internal medicine, Chungnam National University College of Medicine, Hospital, Daejeon, 35015, Republic of Korea
[4]Department of Physical Medicine and Rehabilitation, Chung-Ang University College of Medicine, Seoul, 3859, Republic of Korea

Osteoarthritis (OA) frequently develops in the population over 65 years of age with the loss of cartilage and subsequent structural changes of subchondral bones by the progression of aging. Because OA-triggered pain is tightly related with Toll-like receptor 4 (TLR4) signaling cascades, TLR4 is a reasonable target in developing therapeutics for OA pain. Here, we revealed that PAT4, a peptide antagonist of TLR4, debilitated long-termly monoiodoacetate (MIA)-induced OA pain in rats. First of all, we established the MIA-induced OA pain model by an intra-articular injection of MIA into a left knee joint. In the MIA-administrated animals, TLR4 was highly expressed in the synoviocytes. A single intra-articular injection of PAT4 at day 7 after MIA injection attenuated dramatically pain behavior for over 3 weeks in von Frey filaments by reducing the cartilage loss in knee joints and the microglial activation in dorsal horn of spinal cords. Likewise, when PAT4 was delivered to MIA-induced rats, the level of inflammatory cytokines including TNF-α, IL-1β and IL-6 was decreased up to 50% compared with the control. Interestingly, the duration of PAT4 in weakening OA pain remained longer than that of chemical antagonists of TLR4 such as C34 and M62812 lasting for 7 days. Taken together, PAT4 reduced powerfully the strength of OA pain promoted by MIA in rats by blocking TLR4 and its corresponding reactions and could be a prospective medicine for the patients of OA pain.

Key Words: Osteoarthritis pain, TLR4 antagonist, Therapeutics

<Poster Presentation: Day 2 (30th. Oct. 2018)>

P150

Association of intelligence with mitochondrial DNA variations at site of 15925

Dae-Kwang Kim, Ha-Bin Kim, Hyun-Joon Yoon

Department of Medical Genetics, Keimyung University School of Medicine, 1095, Dalgubeoldaero, Dalseo-Gu, Daegu, Republic of Korea, 42601

Intelligence has a huge influences and is very intimately related with human's life. Because intelligence is intangible, people embodied it through examination tools, and named it Intelligence Quotient(IQ). As measuring IQ, researchers noticed there's a wide distribution of IQ, and tried to figure

out the reason by evaluating functional level of brain, and environmental and genetic factors. We found an article about the association between IQ and mitochondrial DNA(mtDNA), and decided to conduct a study. The number of participants was 57 in intellectual disability group and 148 in normal group respectively. We used PCR technique and agarose gel electrophoresis to know participant's mtDNA sequences. All participant's mtDNA sequence 15925 base was C, with no single variants. We proceeded a further study about the variants of mtDNA sequence 15925-15928. 10 variants and 1 variant were detected in normal and intellectual disability group, respectively, but there was no significant value in this study, too. Many trials and documents about new genetic and functional links to intelligence have been published to identify the origin of intelligence. We conducted a study related with this theme, but the result was invaluable. One study announced in Korea concluded that there was no sign of any change at site of 15925 base pair in Koreans. However, there were journals which found variations at site of 15925 base pair in mtDNA with Japanese and Chinese. Considering people of 3 countries diversified from the same race, we need additional study with large samples to figure out association of intelligence with mtDNA variations.

Key Words: Intelligence, Mitochondrial DNA, Variation

P151

The effect of olfactory mental imagery on verbal memory

Muhammad Iqbal Basri[1,2], Budi Sutiono[1], Asty Amalia[1], Sitti Rafiah Husain[1]

[1]Department of Anatomy, University of Hasanuddin, Makassar, Indonesia
[2]Department of Neurology, University of Hasanuddin, Makassar, Indonesia

Remembering pasts experience is related with a smell. The question is, however, which component of smelling facilitates this process. Is it the real odor or imagery odor that helps recognition verbal memory? This research was done to find out the effect of olfactory mental imagery on verbal memory. This research was conducted on 47 medical students (12 male, 35 female) using Italian vocabularies. The participants have never studied the Italian dictionaries before.   The participants were grouped based on their score on Vividness of Olfactory Imagery Questionnaire (VOIQ) into three groups, the real odor (n=14, VOIQ = 33-64), olfactory imagery (n=15, VOIQ = 16-32) and control group (n=18, VOIQ = 64-80). On the first day, participants were assigned to memorize 70 Italian vocabularies in 20 minutes. Group 1 and 2 were asked to smell a specific perfume that was sprayed on a sheet of paper and associated the smell with the wordlists. On the second day, the process was repeated. But after 20 minutes, participants were asked to recognize the vocabularies using PsychoPy software. In this process, participants had to identify 30 words that were included in the wordlists out of 50 words given. Group 1 was asked to smell the paper before underwent the second phase repeatedly. Group 2 was only asked to imagine the smell. This process was repeated on the fourth day. At the eight and fifteenth day, participants were asked to recognize the vocabularies without reading the wordlists. The participants' age average was 18.3 ± 0.68 year. This study found out that at the eighth day, the average increase of recognition level was highest at control group (8.2±1.27) compared to real odor (7.8±1.28) and olfactory imagery (5.3±1.51) group. On the fifteenth day, there was a decrease of recognition level in the control group (1.5±0.59) and real odor (0.64±0.65). However, in olfactory imagery group, there was an increase of recognition level (0.3±0.84). The results of this study showed no significant effect of real odor and olfactory imagery toward the level of recognition in verbal memory. However, there was a tendency of better retention on olfactory imagery and real odor imagery compared to control group. The limitations of this study were the level of smell that gave to the participants might need to be increased. A future research that looks at how the smell effects memory is recommended.

Key Words: Verbal Memory, Olfactory Imagery, Vividness of Olfactory Imagery Questionnaire (VOIQ)

P152

Effects of early life stress on reward seeking behaviors

Mayumi Nishi[1], Nozomi Endo[1], Takayo Mannari[2]

[1]Department of Anatomy and Cell Biology, Nara Medical University, Kashihara, Japan
[2]Department of Food Science and Neutrition, Nara Women's University, Nara, Japan

Early life stress, such as child abuse and neglect, has long-lasting effects on an individual stress response, behavior, and emotion throughout entire life. Early life adverse experiences increase a risk for various kinds of psychiatric diseases including depression, posttraumatic stress disorder, and eating disorder. Maternal separation (MS) is an animal model widely used to study the mechanism underlying the relationship between early-life adverse experiences and the development of the above-mentioned disorders. In the present study, we evaluated whether MS affects the reward and motivation for palatable foods (milk chocolate) by using the conditioned place preference (CPP) test in female mice. Especially, we focused on the mesolimbic pathway in which dopaminergic neurons project from the ventral tegmental area (VTA) to the nucleus accumbens (NAc), associating to the reward circuit and motivated behavior. We examined the expression of the dopamine receptor by real time-PCR and western blot in NAc. Mice were separated from their dam daily for 3h from postnatal day (PND) 1 to14. Following MS procedure, mice were kept with their dam in home cage until weaning at PND21, and then mice were subjected to the CPP test at 9-week-old. The CPP test analysis indicates that control mice showed a significant preference for chocolate–associated compartment, but MS mice did not. And, analysis of the expression of dopamine receptor in NAc indicated that MS significantly decreased the expression of dopamine type 1 receptor (Drd1) compared with control groups. These data suggest that MS experience induced abnormality in the mesolimbic dopamine pathway of female mice, which causes the deterioration in the motivation for palatable food and appetitive behaviors. Furthermore, we examined whether DNA methylation is involved in the regulation of Drd1 gene expression. We will discuss possible alterations in the expression level of genes correlated to the reward system by epigenetic changes caused by MS.

Key Words: Conditioned place preference, Maternal separation, Dopamine receptor, Epigenetics, Reward

P153

Cinnamomum zeylanicum alcoholic extract improves formaldehyde-induced spatial memory deficits via suppression of extrinsic apoptosis pathway and Tau hyperphosphorylation in the hippocampus

Ebrahim Nasiri[1], Sara Sayad Fathi[1], Arash Zaminy[1], and Parvin Babaei[2], Fatemeh Yousefbeyk[3]

[1]Neuroscience Research Center, Department of Anatomical Science, Poursina Hospital, Guilan University of Medical Sciences, Rasht, Iran
[2]Department of Physiology, School of Medicine, Guilan University of Medical Sciences, Rasht, Iran
[3]Department of Pharmacognosy, School of Pharmacy, Guilan University of Medical Sciences, Rasht,

Iran

Formaldehyde can cause memory impairment through different mechanisms such as tau aggregation both *in vitro* and *in vivo* and apoptosis induction. Regarding to its environmental availability and its ability to cross the blood-brain barrier, it may play a key role in Alzheimer's disease pathology. Thus, the aim of this study was to investigate the effect of alcoholic cinnamon extract on apoptosis, Tau protein phosphorylation state, and spatial memory of formaldehyde treated male rats.Thirty-six week old male wistar rats weighing 200-250 gr were assigned to 6 groups: the control group; the group received formaldehyde intraperitoneally at the dose of 60 mg/kg for 30 consecutive days; three treatment groups received alcoholic cinnamon extract orally via a syringe at doses of 100, 200 and 400 mg/kg for 30 consecutive days following formaldehyde treatment and a sham group received the solvent according to treatment groups' regimen. Afterwards, spatial memory was assessed by Morris water maze test and animals were then decapitated under anesthesia and brain tissues were removed. Immunohistochemistry against p-Tau (Thr[231]) was performed to assess phosphorylation state and Hoechst stain was used to assess apoptosis. Quantitative estimation of Caspase-8, Caspase-9 and p-Tau were also performed by western blotting. Injection of formaldehyde significantly increased Tau hyperphosphorylation and the latency to platform, and decreased the time spent in target quadrant. Amounts of cleaved Caspase-8 and p-Tau were also found to be increased in formaldehyde group. Administration of alcoholic cinnamon extract at the dose of 200 mg/kg significantly reduced the amounts of cleaved Caspase-8 and p-Tau, decreased apoptotic cells, and ameliorated spatial memory formation. In conclusion our study indicated that cinnamon has a beneficial effect on MWM test indices through reduction of p-Tau and suppression of extrinsic pathway of apoptosis.

Key Words: Alzheimer's disease, Apoptosis, Cinnamon, Tau, Spatial memory

P154

Adiponectin improves the long term potentiation (LTP) in 5xFAD mouse brain

Ming Wang[1,2], Kyu Youn Ahn[3], Jihoon Jo[1,2,*], Juhyun Song[2,3,*]

[1]Department of Biomedical Sciences, Center for Creative Biomedical Scientists at Chonnam National University, Hwasun 58128, Jeollanam-do, Republic of Korea
[2]Department of Biomedical Sciences, Chonnam National University Medical School, Hwasun 58128, Jeollanam-do, Republic of Korea
[3]Department of Anatomy, Chonnam National University Medical School, Hwasun 58128, Jeollanam-do, Republic of Korea,

Adiponectin as one of the adipokines has been known that it regulates apoptosis pathway, glucose and lipid metabolism, and insulin sensitivity in metabolic diseases. Recent studies have highlighted the positive effects of adiponectin in central nervous system (CNS), including the protection of neuronal cell damage, the inhibition of memory loss, the enhancement of synaptic dysfunction, and the control of neuroinflammation. Recent studies demonstrated that the risk of Alzheimer's disease (AD) as the most common neurodegenerative disease all over the world has involved in the change of metabolites such as adipokines in CNS. In present study, we investigated the effect of adiponectin treatment in Alzheimer's disease (AD) mouse model 5XFAD brain tissue and in SH-SY5Y neuronal cells under amyloid beta (Aβ) toxicity to examine the effect of adiponectin in AD. Our results showed that the reduction of cleaved caspase 3, NF-kB related with apoptosis signaling, the decrease of GSK-3β phosphorylation, APP expression, BACE expression in AD mouse model 5XFAD brain tissue,

based on the measurement of western blotting and real time PCR. Moreover, we examined that adiponectin treatment triggers the long term potentiation (LTP) in AD mouse model 5XFAD brain tissue through electrophysiology experiments. In *in vitro* study, we examined the expression of cleaved caspase 3, the phosphorylation of NF-k B and GSK-3β, and the expression of APP and BACE in SH-SY5Y neuronal cells under Aβ toxicity condition. Our results indicated that the adiponectin reduces the expression of apoptotic signaling, and the phosphorylation of GSK-3β, and the expression of APP, and BACE in both *ex- vivo* and *in vitro* study. Thus, we assume that the adiponectin inhibits neuronal apoptosis mechanisms and promotes LTP in AD brain, involving in cognitive function in brain. In present study, our data showed the therapeutic possibility of adiponectin in AD for the enhancement of LTP, leading to the recovery of memory function.

Key Words: Adiponectin, Long term potentiation (LTP), Alzheimer's disease (AD), 5xFAD

P155

Low-level LED-based light therapy ameliorates cognitive function in the 5XFAD mouse model of Alzheimer's disease

Gwang Moo Cho[1], Seo-Yeon Lee[2,3], Jung Hwa Park[2,3,4], Min Jae Kim[2,3,4], Byung Tae Choi[2,3,4], Yong II Shin[1], Hwa Kyoung Shin[2,3,4]

[1]Department of Rehabilitation Medicine, School of Medicine, Pusan National University, Yangsan, Gyeongnam 50612, Republic of Korea
[2]Korean Medical Science Research Center for Healthy-Aging, Pusan National University, Yangsan, Gyeongnam 50612, Republic of Korea
[3]Graduate Training Program of Korean Medicine for Healthy-Aging, Pusan National University, Yangsan, Gyeongnam 50612, Republic of Korea.
[4]Department of Korean Medical Science, School of Korean Medicine, Pusan National University, Yangsan, Gyeongnam 50612, Republic of Korea

Low-level light-emitting diode therapy (LED-T) can be rapidly applied in neurological and physiological disorders safely and non-invasively. LED-T is effective for chronic disease due to fewer side effects than drugs. Here we investigated the effects of LED-T on amyloid plaques, gliosis, and neuronal loss to prevent and/or recover cognitive impairment, and optimal timing of LED-T initiation for recovering cognitive function in a mouse model of Alzheimer's disease (AD). 5XFAD mice were used as an AD model. Experimental groups receiving LED-T treatment were divided into two groups: an early group starting LED-T at 2 months of age (5XFAD+Early) and a late group starting LED-T at 6 months of age (5XFAD+Delay). Both groups received LED-T treatment 20 minutes per session, three times a week for 14 weeks. The Morris water maze, passive avoidance, and elevated plus maze tests were performed at 10 months of age. Immunohistochemistry and western blotting were performed after behavioral evaluation. The results showed that LED-T treatment at early stages reduced amyloid accumulation, neuronal loss, and microgliosis, and alleviated cognitive function in 5XFAD mice, possibly by increasing insulin degrading enzyme (IDE) related to Aβ degradation. LED therapy may be an excellent candidate for advanced preclinical AD research.

Key Words: Photostimulation, β-amyloid, Gliosis, Neuronal cell death

P156

Blood contacting neurons in the hippocampus in normotensive rats

Hamasaki S, Mukuda T, Koyama Y, Kaidoh T

Department of Anatomy, Tottori University, Yonago, Japan

The blood−brain barrier (BBB) prevents the penetration of blood proteins including hormones into the brain. On the other hand, hypertensive model rats show increased BBB permeability in the hippocampus, which is regulated, at least in part, by angiotensin II (Ang II). However, the control of BBB permeability in the hippocampus under physiological conditions, including the role of Ang II, is largely unknown. Thus, the present study examined the permeability of the hippocampal BBB in normotensive rats using standard histological techniques. Rats were administered a single daily intravenous injection of Ang II (10^{-5} M, 200 µl) for 7 consecutive days to achieve a transient elevation of circulating Ang II within the physiological range. Control animals received intravenous vehicle injection using the same schedule. Evans blue (EB), a fluorescent dye that cannot cross the BBB, was injected intravascularly at 15 min before transcardiac perfusion for fixation on the last day of the experimental period, and EB extravasation was then examined in brain tissue sections. Ang II-injected rats showed marginal EB extravasation in the neuropil along the inner margin of the granule cell layer of the hippocampal dentate gyrus, although this was difficult to analyze quantitatively because of the low signal-to-noise ratio for specific EB fluorescence. On the other hand, intracellular accumulation of EB distinguished in several neurons located in the inner margin of the granule cell layer and hilus of the dentate gyrus in the Ang II-injected rats. Further, unexpectedly, intracellular accumulation of EB was also observed in the vehicle-injected rats. Compared in the number of these EB positive neurons, animals receiving Ang II treatment showed a trend towards an increase. Overall, these data suggest that some neurons in the hippocampal dentate gyrus exhibit constitutive contact with the blood under normal physiology conditions and circulating Ang II levels. Further, Ang II may not always increase hippocampal BBB vascular permeability.

Key Words: Blood-brain barrier, Hippocampus, Angiotensin II

P157

Increase of systemic angiotensin II is key in the exercise-induced enhanced neurogenesis in the adult rat hippocampus

Mukuda T, Koyama Y, Hamasaki S, Kaidoh T

Department of Anatomy, Tottori University, Yonago, Japan

Physical exercise such as running is a robust stimulus for enhancing adult hippocampal neurogenesis. In the regulation mechanisms, direct action of growth factors including vascular endothelial cell growth factor is known to induce cell proliferation, neuronal differentiation and survival. However, the underlying mechanisms of exercise-dependent enhanced neurogenesis, including the pathways by which exercise activates these growth factors, are not yet fully understood. The present study aimed to examine the possible role of angiotensin II (Ang II) in the systemic circulation as a trigger molecule for promoting hippocampal neurogenesis in the rats.
Systemic Ang II rapidly and transiently increased in response to the treadmill running exercise. After undertaking this exercise once daily for 7 days, the number of proliferating cells, incorporating 5-bromo-2'-deoxyuridin, had increased compared with controls. Running wheel exercise for 14 days also enhanced hippocampal cell proliferation, but the beneficial effect was completely abolished by

treatment of an antagonist for Ang II type 1 receptor (AT1R), losartan. Transient increase of systemic Ang II levels, induced by the intravenous injection of Ang II once daily for 7days, increased the number of proliferating cells and immature neurons expressing doublecortin; the effects were cancelled by losartan. Taken together, these findings suggest that the increasing levels of Ang II in the systemic circulation during exercise can give rise to promote hippocampal neurogenesis in the adult rat.

Key Words: Running exercise, Neurogenesis, Angiotensin II, Systemic circulation, Hippocampus

P158

Tetramethylpyrazine attenuates kainic acid-induced neuronal cell death in the mouse hippocampus

Qun Guo[1,2], Mulan Nie[1], Qi Zhang[1], Lu Xu[1], Qianmei Long[1], Wenfang Zhang[2], Dong Wang[2], Yinchuan Jin[1]

[1]Department of Histology and Embryology, Binzhou Medical University, Yantai, PR China.
[2]Department of Cardiology, Affiliated Hospital of Binzhou Medical University, Yantai, PR China

Tetramethylpyrazine (TMP), a biologically active alkaloid extracted from Ligusticum chuanxiong Hort (Umbelliferae). Its effects are mainly related to its antioxidative, anti-apoptosis, and anti-inflammatory actions. Numerous studies indicate that TMP has protective effects in neurological disorders, such as stroke and Parkinson's disease. However, scientific evidence related to its protective effects in epilepsy is largely unclear. In this study, the authors investigated whether TMP has a beneficial effect on KA-induced neuronal cell death. An intracerebro- ventricular (i.c.v.) injection of 0.94 nmol (0.2 μg) of KA produced typical neuronal cell death both in CA1 and CA3 regions of the hippocampus. TMP was found to suppress neuronal cell loss through intranasal delivery. KA-induced gliosis and proinflammatory marker (COX-2, IL-1β, and TNF-α) inductions were suppressed by TMP administration. It is interesting to note here that TMP treatment suppressed NF-κB activity dose-dependently in KA-treated mouse brains, suggesting that this explains in part its anti-inflammatory effect. Together, these results suggest that TMP has therapeutic potential in terms of suppressing KA-induced pathogenesis in the brain, and that these neuroprotective effects are associated with its anti-inflammatory effects.

Key Words: Tetramethylpyrazine (TMP), Epilepsy, Brain, Kainic acid

P159

Effect of short-term heat exposure on hippocampal neurogenesis in adult rats

Koyama Y, Mukuda T, Hamasaki S, Kaidoh T

Department of Anatomy, Tottori University, Yonago, Japan

Adult hippocampal neurogenesis is enhanced by various stimuli including physical exercise. Recently, we found that activation of the angiotensin II (Ang II) type 1 receptor (AT1R) induced by transiently increasing Ang II levels in the systemic circulation plays an important mechanistic role in the regulation of exercise-enhanced neurogenesis in rats. Systemic Ang II is a hormone that is rapidly

synthesized in response to body fluid loss. Because heat exposure, similar to physical exercise, also leads to body fluid loss, it can increase systemic Ang II levels. Thus, the present study examined the effects of short-term heat exposure on hippocampal neurogenesis in adult rats. Rats received 1 h of heat exposure (36.0±0.1°C) daily for 7 consecutive days (hyperthermic group). Normothermic group rats received exposure to normal environmental conditions (25.0±0.8°C). For pharmacological blockade of AT1R, some of rats in each group were chronically given an AT1R antagonist candesartan. There was a significant 1.4-fold increase in the number of doublecortin-immunoreactive newborn neurons in the hippocampus in hyperthermic animals compared with controls. However, there was no change in the number of Ki67-expressing stem cells. Vascular endothelial cell growth factor, which is known to enhance newborn cell survival, was increased in the hippocampus by short-term heat exposure. These effects of hyperthermia were abolished by pretreatment with candesartan. These data suggest that the short-term heat exposure can enhance hippocampus neurogenesis via Ang II-AT1R signaling, likely by increasing newborn cell survival mediated by vascular endothelial cell growth factor release.

Key Words: Hippocampus, Neurogenesis, Ang II, VEGF

P160

Reduced expression of HCN1&2 channels in the aged hippocampus

Young Eun Park[1], Minah Song[1], Cheol Woo Park[1], Hyunjung Kim[1], Tae-Kyeong Lee[1], Joon Ha Park[2], Ji Hyeon Ahn[2], Jae-Chul Lee[1], Ki-Yeon Yoo[3], Choong Hyun Lee[4], Jung Hoon Choi[5], Moo-Ho Won[1]

[1]Department of Neurobiology, School of Medicine, Kangwon National University, Chuncheon, Gangwon, 24341 Republic of Korea
[2]Department of Biomedical Science and Research Institute for Bioscience and Biotechnology, Hallym University, Chuncheon, Gangwon, 24252, Republic of Korea
[3]Department of Oral Anatomy, College of Dentistry and Research institute of Oral Biology, Gangneung-Wonju National University, Gangneung, Gangwon, 25457, Republic of Korea
[4]Department of Pharmacy, College of Pharmacy, Dankook University, Cheonan, Chungcheongbuckdo, 31116, Republic of Korea
[5]Department of Anatomy, College of Veterinary Medicine, Kangwon National University, Chuncheon, Gangwon, 24341, Republic of Korea

Hyperpolarization-activated cyclic nucleotide-gated (HCN) channels plays important roles in various hippocampal functions, such as the regulation of long-term potentiation, synaptic plasticity and hippocampal-dependent cognitive process. In the present study, we investigated the age-related changes in HCN1 and HCN2 immunoreactivity in the gerbil hippocampus at various ages. HCN1 and HCN2 immunoreactivity was markedly increased in pyramidal neurons of the hippocampus proper as well as in granule cells of the dentate gyrus in the postnatal month 3 (PM3) group, compared to that in the PM 1 group. In the hippocampus proper of the PM 12 group, HCN1 immunoreactivity was similarly observed with that in the PM 3 group, whereas HCN2 immunoreactivity was significantly decreased. In addition, marked reductions of HCN1 and HCN2 immunoreactivity in the hippocampus proper of the PM 24 group was found, compared to that in the 12 group. In the granule cells of the dentate gyrus, HCN1 and HCN2 immunoreactivity were decreased age-dependently after PM 3. These results indicate that normal aging process has effect on the expressions of HCN1 and HCN2 in the hippocampus, and that marked reduction of HCN1 and HCN2 expression in the age hippocampus might be associated with a decline of hippocampus-dependent functions.

Key Words : Aging, Gerbil, Hippocampus, HCN channel

P161

The mechanism of selective clearance of tau protein

Ji Young Im[1,*], Suehee Huh[2,*], Sang Il Ahn[1], Sun Ah Park[2,3]

[1]Department of Neurology, Soonchunhyang University Bucheon Hospital, Bucheon 14584, Republic of Korea
[2]Department of Anatomy, Ajou University School of Medicine, Suwon 16499, Republic of Korea
[3]Department of Neurology, Ajou University School of Medicine, Suwon 16499, Republic of Korea
*Co-first author

The abnormal accumulation of tau protein is the core pathological feature of neurodegenerative disorders with tauopathy. In various tauopathies, sequestosome-1/p62 (p62) protein is often associated with neurofibrillary tangles composed of tau protein and ubiquitin. Previously, we identified that the protein expression of p62 was inversely correlated with abnormal tau protein accumulations in diabetic rat brains. To know the molecular mechanism, we established transient overexpression cell models of p62 and tau proteins using plasmid constructs and lentiviral vectors. In accordance with *in vivo* data tau protein expression was reduced according to the increase of p62 expression in cultured cell lines and primary rat neurons. When the selective inhibitors of proteasome and autophagic pathways were applied p62-dependent tau reduction was found diminished. It suggests that both proteasomal and autophagic pathway contribute to p62-mediated clearance of tau protein. Further, using the mutant constructs the protein-protein interactions between tau and p62 were explored, which demonstrated that the critical role of tumor necrosis factor receptor-associated factor 6 (TRAF6)-binding (TB) domain in physical interaction. Co-immunoprecipitation and glutathione S-transferase (GST) pull-down assays confirmed that p62 interacts with tau through its TB domain. And the interaction through this domain was found critical for tau clearance. Because TB domain is also important for TRAF6 binding. We checked if TRAF6 binding to TB domain affects the efficiency of tau-p62 interaction thereby tau clearance. Additionally, because ubiquitinations of the proteins are known to enhance protein degradation both through proteasomal and autophagic pathway, and TRAF6 is a type of E3 ligase mediating ubiquitinations, we checked the relation of ubiquitinations of tau proteins in p62-mediated tau clearance. Interestingly, the ubiquitination of tau was enhanced by co-expression with wild-type p62, but not by the TB domain-deleted p62 mutant. Taken together, p62 plays a pivotal role in tau clearance through its TB domain-mediated direct interaction with tau protein and augmentation of tau ubiquitination.

Key Words **:** Autophagy, Protein clearance, Ubiquitin, Tau

P162

Classifying transcriptomic class of neuron by electrophysiological property using machine learning

Incheol Seo[1], Hyunsu Lee[2]

[1]Hapcheon geriatric hospital, Gyeongsangnam-do, Korea
[2]Department of Anatomy, Keimyung University School of Medicine, Daegu, Republic of Korea

The task of classifying neurons, an essential component of the nervous system, has been tried in a variety of ways. The transcriptomic approach has become more accessible with the development of genetic engineering techniques. Considering the information process function of the brain, however, it is necessary to conceive the electrophysiological characteristics of neurons. Recently, the Allen Brain Institute has published the electrophysiological characteristics of neurons tagging with a transgenic reporter. We have used these electrophysiological features to classify the transcriptomic class of neurons. Using the linear regression, random forest, and artificial neural network, we compared the performance of supervised machine learning model to classify transcriptomic classes of neurons. As a result, in the binary classification problem classifying excitatory and inhibitory neurons, the accuracy was 90% or more regardless of the model. It showed better performance than merely distinguishing by suprathreshold features such as firing rate. However, when the excitatory neuron was classified, the accuracy was less than 40%, and the accuracy of classifying the inhibitory neuron was ~60%. The present study is based on the results of electrophysiological experiments to determine whether transcriptomic classes of neurons can be classified. Future research will be needed to add morphological features and projection targets to the neuron classification.

Key Words: Neuron, Electrophysiology, Transgenic mice, Machine Learning

P163

Whole-brain map of inputs to cholecystokinin neurons in suprachiasmatic nucleus

Ruixi Li[1], Haohua Wei[1], Xiangshan Yuan[1], Zhili Huang[2]

[1]Department of Anatomy, [2]Department of Pharmacology, School of Basic Medical Science, Fudan University, Shanghai, China

It has been known that a small group of neurons expressing Cholecystokinin (CCK) in suprachiasmatic nucleus (SCN) acted as a principal pacemaker driving circadian rhythms, in which the CCK neurons may act in non-photic regulation mediating clock information. However, the inputs to CCK neurons, by which the functions of CCK neurons were mediated, remain poorly characterized. Here, using a recently developed rabies virus-based cell-type-specific retrograde tracing system, we mapped the inputs of the SCN CCK neurons from whole brain. After 50nl of mixed Cre-dependent AAV carrying TVA and RG were stereotaxically injected into the unilateral SCN of CCK-Cre mice for 3 weeks, 200 nl of EnvA-pseudotyped, RG-deleted and mCherry-expressing rabies virus was injected to same area. With this rabies virus-mediated monosynaptic retrograde tracing, the afferents connecting the SCN CCK neurons from numerous brain regions were identified. The results showed high dense inputs to CCK neurons from the diencephalon, including supraoptic nucleus (SON), medial preoptic nucleus (MPO), paraventricular hypothalamic nucleus (PVH). Moreover, several nuclei sent the moderate inputs to CCK neurons, such as zona incerta, periventricular hypothalamic nucleus, lateral septum. In addition, slight afferent neurons were also observed in the cerebral cortex and brain stem. However, no any input from retina ganglion cell. Moreover, SCN CCK neurons were preferentially innervated by the ipsilateral AVP neurons from PVH and SON than contralateral, whereas, the contralateral PVT sent more projections to CCK neurons than ipsilateral. These results expand our knowledge about the connectivity of SCN CCK neurons, provide some candidate neurons through which the reinforcement signals are conveyed to SCN CCK neurons and new the perceptive for future explorations of neural circuit mechanism mediating the SCN functions except circadian rhythm, such as, the ingestive behavior and osmotic stability.

Key Words: Cholecystokinin neuron, Suprachiasmatic nucleus, Circadian rhythm, Neural pathway

P164

Assessment of cognitive functions in touchscreen-based automated battery system with animal model of high-fat diet-induced metabolic stress

Saeram Lee[1,2,], Jae Young Kim[1], Jong Youl Kim[1], Eosu Kim[2,3], KyoungYul Seo[4], Chul Hoon Kim[2,5], Ho-Taek Song[6], Lisa M. Saksida[7,8,9], Jong EunLee[1,2,*]

[1]Department of Anatomy, [2]BK21 PLUS Project for Medical Science, and Brain Research Institute; [3]Department of Psychiatry, [4]The Institute of Vision Research, Department of Ophthalmology, [5]Department of Pharmacology, [6]Department of Radiology, Yonsei University, College of Medicine, Seoul, Korea, [7]Department of Psychology and MRC/Wellcome Trust Behavioural and Clinical Neuroscience Institute; University of Cambridge, Cambridge, UK, [8]Canada Research Chair in Translational Cognitive Neuroscience, [9]Department of Pharmacology & Physiology, University of Western Ontario, London, ON, Canada

Obesity-related metabolic disorders can affect not only systemic health but also brain function. Recent studies have elucidated that amyloid beta deposition cannot satisfactorily explain the development of Alzheimer's disease (AD) and that dysregulation of glucose metabolism is a critical factor for the sporadic onset of non-genetic AD. Identifying the pathophysiology of AD due to changes in brain metabolism is crucial; however, it is limited in measuring changes in brain cognitive function due to metabolic changes in animal models. The touchscreen-based automated battery system, which is more accurate and less invasive than conventional behavioral test tools, is used to assess the cognition of mice with dysregulated metabolism. This system was introduced in humans to evaluate cognitive function and was recently back-translated in monkeys and rodents. We used outbred ICR mice fed on high-fat diet (HFD) and performed the paired associates learning (PAL) test to detect their visual memory and new learning ability loss as well as to assess memory impairment. The behavioral performance of the HFD mice was weaker than that of normal mice in the training but was not significantly associated with motivation. In the PAL test, the average number of trials completed and proportion of correct touches was significantly lower in HFD mice than in normal diet-fed mice. Our results reveal that HFD-induced metabolic dysregulation has detrimental effects on operant learning according to the percentage of correct responses in PAL. These finding establish that HFD-induced metabolic stress may have an effect in accelerating AD-like pathogenesis.

Key Words: Metabolic disorders, High-fat diet, Cognitive impairment, Paired Associates Learning test, Alzheimer's disease

P165

Transcriptomic analysis of high fat diet fed mouse brain cortex

Choon Sang Bae[1], Kyu Youn Ahn[1], Kwang Il Nam[1], Chaeyong Jung[1,3], Young-Kook Kim[2,3], <u>Juhyun Song</u>[1,3,*]

[1]Department of Anatomy, Chonnam National University Medical School, Hwasun 58128, Jeollanam-do, Republic of Korea
[2]Department of Biochemistry, Chonnam National University Medical School, Hwasun 58128, Jeollanam-do, Republic of Korea
[3]Department of Biomedical Sciences, Center for Creative Biomedical Scientists at Chonnam National University, Hwasun 58128, Jeollanam-do, Republic of Korea

High fat diet leads to metabolic diseases such as obesity and diabetes, which are chronic inflammatory diseases with high prevalence worldwide. Recent studies have reported the cognitive dysfunction in obesity patients caused by high fat diet, and accordingly, it is called as "type 3 diabetes" or "diabetic dementia". Although dysregulation in protein coding genes was extensively studied, the profiling of non-coding RNAs including lncRNAs and circRNAs was not conducted. In the present study, we conducted the analysis of diverse RNAs profile and presented the patterns of their alteration in high fat fed brain cortex compared to the normal brain cortex. To investigate the regulatory roles of both coding and noncoding RNAs in high fat diet brain, we used the RNA sequencing of rRNA-depleted RNAs and identified genome-wide lncRNAs and circRNAs expression and co-expression pattern with mRNAs in high fat diet mouse brain cortex. We showed those mRNAs related with neurogenesis, synapse, or calcium signaling were most highly changed in high fat diet fed cortex. In addition, numerous differentially expressed lncRNAs and circRNAs were identified. Our study provides the valuable expression profiles and potential function of both coding and noncoding RNAs in high fat diet fed brain cortex.

Key Words: Noncoding RNA, Long noncoding RNAs, Circular RNAs, High fat Diet, Brain cortex

P166

Effect of myeloid sirtuin1 deletion on hypothalamic neurogranin in mice fed a high-fat diet

<u>Kyung Eun Kim</u>[1,2], Eun Ae Jeong[1,2], Jong Youl Lee[1,2], Eun Bee Choi[1,2], Hyeong Seok An[1,2], Kyung-Ah Park[1,2], Hyun Joo Shin[1,2], Zhen Jin[1,2], Gu Seob Roh[1,2]

[1]Department of Anatomy and Convergence Medical Science, Institute of Health Sciences, Gyeongsang National University School of Medicine, Jinju, Gyeongnam, Republic of Korea
[2]Bio anti-aging Medical Research Center, Gyeongsang National University School of Medicine, Jinju, Gyeongnam, Republic of Korea

Sirtuin 1 (SIRT1) is the most conserved mammalian NAD^+-dependent protein deacetylase that has emerged as a key metabolic sensor in the hypothalamus. Previous study have demonstrated that myeloid SIRT1 deletion increases hypothalamic inflammation in mice fed a high-fat diet (HFD). Neurogranin, a calmodulin-binding protein, is abundantly expressed in the ventromedial hypothalamus (VMH). However, the myeloid SIRT1 deletion in the context of food intake regulation in VMH is largely unknown. To investigate the effect of neurogranin on food intake in HFD-fed mice, myeloid-specific SIRT1 deficiency (KO) mice were fed a HFD or normal diet for 20 weeks. We found that POMC mRNA expression were decreased in the arcuate nucleus of KO mice compared to wild type (WT) mice. In particular, neurogranin expression were decreased in VMH of male KO mice compared to female KO

mice. SIRT1 deletion promoted HFD-induced insulin resistance compared to HFD-fed WT mice. In particular, expression levels of neurogranin in hypothalamus were decreased in HFD-fed KO mice compared to that in HFD-fed WT mice. Moreover, microglial activation were increased in the arcuate nucleus of HFD-fed SIRT1 KO mice compared to HFD-fed WT mice. In addition, hypothalamic expression levels of parvalbumin and phosphorylated AMPK were decreased in HFD-fed KO mice compared to HFD-fed WT mice. These findings suggest that myeloid SIRT1 deletion may play an important role in food intake through VMH-specific neurogranin-mediated AMPK signaling.

Key Words: Obesity, SIRT1, Neurogranin, Hypothalamus

P167

RNA editing in the nucleus accumbens is involved in alcohol drinking behavior

Tanaka M[1], Shirahase T[1], Taguchi K, Tanida T[1], Watanabe Y[2]

[1]Department of Anatomy and Neurobiology, Kyoto Prefectuiral Universityof Medicine, Kyoto, Japan
[2]Department of Basic Geriatrics, Kyoto Prefectuiral Universityof Medicine, Kyoto, Japan

The nucleus accumbens (NAc) in the forebrain is known to have an important role in the addiction and reward system. Messenger RNA editing, particularly RNA editing of neurotransmitter receptors such as serotonin 2C receptor (5-HT$_{2C}$R) is closely related to various neuronal functions. We previously found that chronic ethanol exposure elevated the RNA editing frequency of 5-HT$_{2C}$R in the NAc of alcohol-preferring C57BL/6J mice. In this study we generated NAc-specific ADAR2 knockout mice using AAV-GFP/Cre, and performed various behavioral analyses including assessment of alcohol-drinking behavior. Unlike control mice injected with AAV-GFP, NAc-specific ADAR2 knockout mice did not show enhanced alcohol consumption and alcohol preference after chronic ethanol vapor exposure. This result suggests that alcohol-drinking behavior and alcohol preference are regulated by RNA editing in the NAc.

Key Words: RNA editing, ADAR2, Nucleus accumbens, 5-HT$_{2C}$ receptor, Alcohol drinking

P168

Interneurons secrete prosaposin, a neurotrophic factor, after kainic acid-induced neurotoxicity

Hiroaki Nabeka[1]

[1]Department of Anatomy and Embryology, Ehime Graduate School of Medicine, Toon, Japan

Prosaposin (PS) is a precursor of sphingolipid activator proteins saposins A, B, C and D. PS is not only a precursor protein but also PS is a neuroprotective factor. PS is up-regulated after the excitotoxicity induced by kainic acid (KA), a glutamate analog. Excessive glutamate release plays a pivotal role in numerous neuropathological disorders, such as ischemia or seizure. An 18-mer peptide (LSELIINNATEELLIKGL; PS18) derived from the PS neurotrophic region significantly protected hippocampal synapses against KA-induced destruction. PS immunoreactivity in the hippocampal and cortical neurons showed significant increases on day 3 after KA injection, and high PS levels were maintained after 3 weeks. The increase in PS, but not saposins, detected by immunoblot analysis

suggests that the increase in PS-like immunoreactivity after KA injection was not due to an increase in saposins as lysosomal enzymes after neuronal damage, but rather to an increase in PS as a neurotrophic factor to improve neuronal survival. Furthermore, several neurons with slender nuclei inside/outside of the pyramidal layer showed more intense PS expression than other pyramidal neurons. These are parvalbumin (PV) positive GABAergic inhibitory interneurons. It suggests that axonal transported PS protects surrounding hippocampal pyramidal neurons from neurotoxicity after KA injection.

Key Words: Prosaposin, Kainic acid, Neuroprotection, Axonal transport

P169

Chemokine production by microglia mediates blood derived-monocytes trafficking in neuroinflammation

Meiying Huang[1,2], Jong Youl Kim[1], Joo Hyun Park[1,2], Jong Eun Lee[1,2,3,*]

[1]Department of Anatomy, [2]BK21 Plus Project for Medical Science, [3]Brain Research Institute, Yonsei University College of Medicine, Seoul, 03722, Korea

The inflammatory response following acute ischemic stroke is a well-known and widely studied phenomenon, but the mechanism is still unclear. After ischemic stroke, microglia and recruited macrophages play major roles in neuroinflammation after ischemic stroke. We explored how these cells affect counterpart's polarization and infiltration and revealed some chemokines and chemokine receptors can be important modulators of these interactions. BV2 (microglia cell line) were treated with lipopolysaccharides (LPS) or interleukin-4, and the supernatant was collected as M1 or M2 conditioned media of BV2. The supernatant of PMA differentiated THP-1 (monocyte cell line) followed by LPS treatment or interleukin-13 & IL-4 co-treatment was collected as M1 or M2 conditioned media of THP-1. After BV2 or THP-1 cultured in conditioned media, the activation and polarization were assessed by ICC and confocal microscopy for CD11b, CD86 and CD206. Transwell inserts of 3 and 8 µm pore membrane were used for THP-1 infiltration and BV2 migration assay. M1/M2 conditioned media of BV2 and THP-1 and the brain tissue of ischemic mouse model were assessed by proteome profiler array (PPA) to find target cytokine and chemokine. THP-1 pretreated with antagonists of candidates chemokines were used to infiltration assay, the expression of chemokine receptor in THP-1 were confirmed by western blotting. THP-1 and BV2 expressed CD206 in M2 conditioned media of BV2 or THP-1. M2 conditioned media of BV2 increased the infiltratory ability of THP-1 while M1 conditioned media of THP-1 enhanced BV2 migration. After ischemic stroke, chemokines were significantly expressed at 3 days than at 7 days in the PPA and several chemokines were match to the conditioned media of BV2 while the related receptor shows high expression in THP-1. Antagonists were significantly reduced the infiltration ability of THP-1 to BV2 M2 conditioned media. Our study suggests a new insight into the interaction of microglia and monocyte through their ability to expression of cytokine and chemokine after ischemic stroke. Chemokines and receptors can be strong candidates of target protein in new therapeutic strategies to acute brain inflammation by modulating the functions of microglia and monocytes.

Key Words: Microglia, Macrophage, Chemokine, Neuroinflammation

P170

Palmitate induces lipoapoptosis in Schwann cells through ROS generation-mediated STAMP2 downregulation

Park JB[1], Lee SW[2], Kim HJ[1], Lee SY[2], Chung WT[2], Rho JH[1], Yoo YH[1]

[1]Department of Anatomy, Dong-A University College of Medicine, Busan, Republic of Korea
[2]Department of Rhematology, Dong-A University College of Medicine, Busan, Republic of Korea

Free fatty acids (FFAs) are considered the principal inducers of lipotoxicity, leading to cell dysfunction and/or cell death. Lipotoxicity in Schwann cells (SCs) damages neurons, which may be associated with peripheral neuropathies and axon degeneration. However, the molecular mechanism by which FFAs exert lipotoxicity in SCs remains to be established. In the present study, we demonstrate that palmitate exerts lipotoxicity in SCs through apoptosis and that palmitate-induced lipotoxicity in SCs is mediated through reactive oxygen species (ROS) generation. We observed that the six-transmembrane protein of prostate 2 (STAMP2), which plays a pivotal role in lipid homeostasis, is expressed in SCs. We further demonstrate that palmitate induces lipoapoptosis in SCs through ROS generation-mediated STAMP2 downregulation and that STAMP2 depletion accelerates the palmitate-exerted lipoapoptosis in SCs, indicating that STAMP2 confers on SCs the ability to resist palmitate-induced lipotoxicity. In conclusion, palmitate induces lipoapoptosis in SCs through ROS generation-mediated STAMP2 downregulation. Our findings indicate that ROS and STAMP2 may represent suitable targets for pharmacological interventions targeting lipotoxicity-associated peripheral neuropathies and axon degeneration.

Key Words: Lipotoxicity, Palmitate, ROS, STAMP2, Schwann cells

P171

Isolation and characterization of cell-to-cell transmissible α-synuclein seeds

Katsutoshi Taguchi[1], Yoshihisa Watanabe[2], Atsushi Tsujimura[2], Masaki Tanaka[1]

[1]Department of Anatomy and Neurobiology, Graduate School of Medical Science, Kyoto Prefectural University of Medicine, Kyoto, Japan
[2]Department of Basic Geriatrics, Graduate School of Medical Science, Kyoto Prefectural University of Medicine, Kyoto, Japan

α-Synuclein (αSyn) is one of major components of Lewy bodies (LB) and Lewy Neurites (LN), which are well-known pathological hallmarks of synucleinopathies including Parkinson's disease (PD) and dementia with Lewy bodies (DLB). These intracellular aggregates, LB and LN, are formed by recruitment of intrinsic soluble αSyn into the insoluble aggregate core. Therefore, endogenous expression of αSyn and seeds which accelerate αSyn polymerization are required for the aggregate formation. Furthermore, accumulated evidence suggests that prion-like cell-to-cell transmission of pathogenic αSyn seeds in brain is a critical event for neurodegeneration. However, biochemical properties of these pathogenic molecules remain to be elucidated. According to the previous studies, preformed fibrils prepared from recombinant αSyn can induce the formation of LB-like aggregates in neurons. Here, using this experimental system, we isolated characteristic αSyn oligomer species recovered from conditioned culture medium of pathological neurons harboring LB-like aggregates.

These extracellular αSyn oligomers showed uniform molecular weight in Native-PAGE and successfully induced LB-pathology in cultured hippocampal neurons. Now, we are further characterizing the pathogenic oligomer species of αSyn. These molecules will be a better target to inhibit the disease propagation through the cell-to-cell seed-transmission in PD and DLB brain.

Key Words: Parkinson's disease, Lewy bodies, Lewy neurites, Preformed fibrils, Propagation, α-synuclein oligomers

P172

Spatiotemporal distribution of extracellular osteopontin and its association with neuroglial cells in the striatum of rats treated with the mitochondrial toxin 3-nitropropionic acid

Tae-Ryong Riew[1], Soojin Kim[1], Xuyan Jin[1], Hong Lim Kim[2], Mun-Yong Lee[1]

[1]Department of Anatomy, Catholic Neuroscience Institute, College of Medicine, The Catholic University of Korea, Seoul 06591, Republic of Korea
[2]Integrative Research Support Center, Laboratory of Electron Microscope, College of Medicine, The Catholic University of Korea, Seoul 06591, Republic of Korea.

(Osteopontin (OPN), an adhesive glycoprotein, has recently been reported to with the spatiotemporal progression of calcification in the striatum of rats treated with the mitochondrial toxin 3-nitropropionic acid (3-NP). Induced OPN immunoreactivity in lesioned striatum was recognized two distinct forms, intracellular OPN (the Golgi complex) within brain macrophages and small granular extracellular OPN, which was identified as degenerated neurites coated by OPN. The present study was designed to investigate the spatiotemporal relationship between extracellular OPN deposition with astroglial and microglial reactions elicited by 3-NP injection. Three days post-lesion, extracellular OPN was confined to the periphery of the lesion core, in which activated microglia/macrophages accumulated, but not in microglia-free epicenter. In particular, activated microglia were preferentially localized within the striatal white matters in the lesion periphery, and most of them contained intracellular OPN. At this time point, reactive astrocytes in the peri-lesional area were localized at a distance from area where extracellular OPN was present in the lesion periphery, and OPN-negative microglia were present between GFAP- and extracellular OPN-rich areas. At 7 days post-lesion when activated microglia/macrophages were evenly distributed throughout the lesion core, extracellular OPN was scattered throughout the lesion core except in white matter bundles in which most intracellular OPN-positive cells were clustered. At the lesion edge, reactive astrocytes showed distinctive, elongated morphologies and long cellular processes, which were frequently in close apposition to, but not overlapping with extracellular OPN-rich area. By 14 days post-lesion, extracellular OPN, which appeared to decrease in number, was preferentially localized to the periphery of the lesion core. In this lesion periphery, extracellular OPN-rich area, GFAP and Iba1 had overlapping spatial distribution. In particular, extracellular OPN appeared to be frequently located in close proximity to astroglial processes and activated microglia/macrophages, but not within their cytoplasm. At 28 days, there was a notable decrease in the number of dot-like OPN, but had a close spatial relationship with astroglial processes and activated microglia/macrophages in the lesion core. Our data indicated that the extracellular OPN accumulation during the early phase of injury occurred in association with activation and recruitment of microglia/macrophages, and became correlated spatially with astroglial fibers forming the astroglial scar which appeared to move gradually inward toward the lesion core over time post-lesion.

Key Words：Osteopontin, 3-NP, Acute brain injury, Astrocyte, Microglia, Glial scar

P173

A crosstalk between gut microbiota and methamphetamine addiction: signaling from gut microbiome-derived butyrate to histone acetylation in orbitofrontal cortex

Xue Lu[1,2,#], Yali Chen[1,2,#], Feifei Ge[1,2,#], Yuehan Li[2], Pengbo Shi[2], Jiaxun Nie[2], Wei Zhu[3], Xu Shen[1], Tifei Yuan[4,*], Xiaowei Guan[1,2,*]

[1]State Key Laboratory Cultivation Base for TCM Quality and Efficacy, School of Medicine and Life Sciences, Nanjing University of Chinese Medicine, Nanjing, China
[2]Department of Human Anatomy and Histoembryology, School of Medicine and Life Sciences, Nanjing University of Chinese Medicine, Nanjing, China
[3]Department of Human Anatomy, School of Basic Medicine, Nanjing Medical University, Nanjing, China
[4]Key Laboratory of Psychotic disorders, Shanghai Mental Health Center, Shanghai Jiaotong University School of Medicine, Shanghai, China

Gut microbiota (GM) serves as important regulator for brain functions and contribute to different psychiatric diseases. Recently, emerging evidence demonstrated that substance use result in the alteration of GM profiles, which may conversely trigger addiction. The present study investigated the effects of chronic methamphetamine (MA) exposure on gut microbiota composition. The results showed significant decrease in butyrate-producing bacteria in colonal feces following long-term withdrawal from MA, together with decreased butyrate and increased HDAC activity in orbitofrontal cortex (OFC) in the brain. Taken together, the results argued for the importance of gut microbiota in psychostimulants evoked behavioral changes and its potential molecular gut-brain signaling. Thus, keeping hemostasis of GM might be a new therapeutic strategy for treating drugs-caused psychiatric disorders, and gut-derived Short chain fatty acids (SCFAs) may be a potential intervention target for addiction.

Key Words**:** Methamphetamine, Gut microbiota, Butyrate, Orbitofrontal cortex, Histone acetylation

[#]Xue Lu, Yali Chen, and Feifei Ge are contributed equally to this work
*Correspondence to Xiaowei Guan and TiFei Yuan

P174

Stigmasterol stimulates neuronal migration through reelin signaling

Md. Nazmul Haque, Il Soo Moon

Department of Anatomy, Dongguk University Graduate School of Medicine, Gyeongju 38066, Republic of Korea

Stigmasterol (ST), a phytosterol, is found in diverse food. Previously, in a transcriptomics

study, we found ST upregulated migration-related genes. In the present study, we carried out in vitro neurosphere migration assays to investigate the effects of ST on neuronal migration. For this purpose, neurospheres were produced by culturing rat (Sprague-Dawley) E14 cortical neurons. The addition of ST (75 µM) to culture medium increased not only the numbers of migratory neurons by 15% but the distance of movement up to 120 µm from the centers of neurospheres as compared to vehicle cultures. Immunocytochemistry showed ST upregulated the expressions of Reelin (Reln) and its downstream signaling molecules like phospho-JNK (c-Jun N-terminal kinase), doublecortin (DCX) and dynein heavy chain (DHC) in migratory neurons. Furthermore, in silico molecular docking simulation indicated that ST interacts with Relin receptor ApoER2 by forming a hydrogen bond with Lys2467 and other van der Waals interactions. Taken together, our study shows that ST upregulates Reln signaling and promotes neuronal migration and suggests that ST supplementation be considered a potential means of treating migration-related CNS disorders.

Key Words: Dynein, JNK signaling, neurosphere, Reln, Stigmasterol

P175

Stigmasterol enrich glutamatergic synapses in cultures of brain neurons

Md. Nazmul Haque, Mohammad Maqeshudul Haque Bhuiyan, Il Soo Moon

Department of Anatomy, Dongguk University Graduate School of Medicine, Gyeongju 38066, Republic of Korea

The phytosterol stigmasterol (ST) ameliorates scopolamine-induced memory impairment. Therefore, in this study, we investigated the hypothesis that ST promotes spinogenesis and the formation of glutamatergic synapses and thus improves memory in cultured rat hippocampal neurons. Immunoblots showed that ST activated extracellular signal–regulated kinase 1/2 (Erk1/2) and cAMP response element binding protein (Creb), and upregulated actin-related protein 2 (Arp2) and cell division cycle 42 (Cdc42), central components in actin organization and spine head development. Consistently, DiO staining of live neurons showed that ST increased the densities of dendritic filopodia andmushroom-typemature spines, and immunocytochemistry showed an increase in the expressions of the GluN2A and GluN2B subunits of N-methyl-D-aspartate receptors (NMDARs) at synapses. Finally, staining the recycling membranes with FM1-43 showed that ST increased the sizes of synaptic vesicle pools at presynaptic terminals. Together, our data indicate that ST upregulates Cdc42-Arp2/3 and Erk1/2-Creb signaling and thus induces the formations of mushroom-type spines and glutamatergic excitatory synapses.

Key Words: Erk1/2, FM1-43, NMDAR, Spinogenesis, Stigmasterol, Synaptogenesis

P176

Effects of stigmasterol on neuronal gene expression: Transcriptome Analysis

Md. Nazmul Haque, Il Soo Moon

Department of Anatomy, Dongguk University Graduate School of Medicine, Gyeongju 38066, Republic of Korea

Stigmasterol (ST), a phytosterol, facilitates neuromodulatory effects. To identify underlying affected genes by ST, total RNA was isolated from rat primary hippocampal neurons and mRNA-Seq was performed. Among the differentially expressed 17337 RefSeq genes, 445 genes (up/down 293/157) passed the p-value <0.05 criterion, 52 genes (up/down; 37/13) had a p-value <0.05 and a false discovery rate (FDR) q-value of <0.2, and 24 genes (up/down; 20/4) passed the more stringent criterion of both p <0.05 and q <0.05. After applying a stringent FDR q-value cutoff of <0.2, it was found ST induced many immediate early genes (IEGs), and that a major proportion of upregulated genes were related to CNS development (neurite outgrowth or synaptic transmission). In a Venn diagram for CNS development Gene Ontologies (GOs) (i.e., axon development, dendrite development, modulation of synaptic transmission), Reln emerged as a central player in these processes. The study indicates that ST upregulates genes for neuritogenesis and synaptogenesis, and suggests ST be viewed as a potential resource for improving brain functions.

Key Words: mRNA-seq, Neuron, Reelin, Stigmasterol, Transcriptome

P177

Reduced gyrification with cerebral cortical thickening in ferrets with neonatal exposure to valproic acid

Kamiya S[1] , Aoki I[2], Sawada K[1]

[1]Department of Nutrition, Faculty of Medical and Health Sciences, Tsukuba International University, Tsuchiura, Japan
[2]Department of Molecular Imaging and Theranostics, National Institute of Radiological Sciences, QST, Chiba, Japan

The purpose of this study quantitatively evaluated morphological changes of the cerebral cortex in ferrets with an exposure neonatally to valproric acid (VPA). Male ferrets received VPA (200 mg/kg of body weight) at postnatal days 6 and 7, and were perfused with 4% paraformaldehyde solution at postnatal day 20, when completed primary sulcogyrogenesis. Three-dimensional short TR/TE MR images (typical T1-weighted parameter setting) at 7-tesla were acquired with a high spatial resolution from fixed brains. On a basis of 3D MRI data, the degree of sulcal infolding was evaluated throughout the cerebral cortex by global-gyrification index (global-GI), in four divisions of the cerebral cortex (i.e., prefrontal, frontal, temporoparietal and occipital divisions) by local gyrification index (local-GI), and in representative primary sulci by sulcal-gyrification index (sulcal-GI), respectively. We further measured cerebral cortical thickness in representative primary sulcal and gyral regions. The global-GI of VPA-treated ferrets was significantly lower than that in control ferrets. This involved a reduction in the local-GI of the frontal and temporoparietal divisions in VPA-treated ferrets, significantly. The sulcal-GI in VPA-treated ferrets was specifically reduced in presylvian, splenial and rostral suprasylvian sulci, which extended horizontally from prefrontal to temporoparietal divisions. Notably, the cerebral cortex was thickened specifically in floors of spenial and rostral suprasylvian sulci in VPA-treated ferrets. On the other hand, the anterior sigmoid gyrus, which convoluted in the prefrontal division, was also thickened significantly in VPA-treated ferrets, without altering the local-GI. The present study suggests that neonatal exposure to VAP causes hypogenesis of cerebral sulci intended through the frontal and temporoparietal divisions with thickening their floor cortex.

Key Words**:** Cerebrum, Valproric acid, Gyrification, Ferret, Sulcus, Gyrus

P178

CTCF is required for maintenance of auditory hair cells and hearing function in the mouse cochlea

Ji-Hyun Ma[1], Hyeon-Joo Kim[1], Hyoung-Pyo Kim[2,3], Jinwoong Bok[1,3,4], Jeong-Oh Shin[1,*]

[1]Department of Anatomy, [2]Department of Environmental Medical Biology, [3]BK21 PLUS Project for Medical Science, [4]Department of Otorhinolaryngology, Yonsei University College of Medicine, Seoul 03722, Republic of Korea

Auditory hair cells play an essential role in hearing. These cells convert sound waves, mechanical stimuli, into electrical signals that are conveyed to the brain via spiral ganglion neurons. The hair cells are located in the organ of Corti within the cochlea. They assemble in a special arrangement with three rows of outer hair cells and one row of inner hair cells. The proper differentiation and preservation of auditory hair cells are essential for acquiring and maintaining hearing function, respectively. Many genetic regulatory mechanisms underlying hair-cell differentiation and maintenance have been elucidated to date. However, the role of epigenetic regulation in hair-cell differentiation and maintenance has not been definitively demonstrated. CTCF is an essential epigenetic component that plays a primary role in the organization of global chromatin architecture. To determine the role of CTCF in mammalian hair cells, we specifically deleted *Ctcf* in developing hair cells by crossing *Ctcf*^{fl/fl} mice with *Gfi1*[Cre/+] mice. *Gfi1*[Cre]*; Ctcf*^{fl/fl} mice did not exhibit obvious developmental defects in hair cells until postnatal day 8. However, at 3 weeks, the *Ctcf* deficiency caused intermittent degeneration of the stereociliary bundles of outer hair cells, resulting in profound hearing impairment. At 5 weeks, most hair cells were degenerated in *Gfi1*[Cre]*; Ctcf*^{fl/fl} mice, and defects in other structures of the organ of Corti, such as the tunnel of Corti and Nuel's space, became apparent. These results suggest that CTCF plays an essential role in maintaining hair cells and hearing function in mammalian cochlea.

Key Words: CCCTC-binding factor (CTCF), Hearing loss, Hair cell

P179

Changes in primary afferent fiber projections and motoneuronal perineuronal nets after spinal cord transection of juvenile rats

Masahito Takiguchi[1], Yoshihiko Ikeda[2], Kengo Katsuki[2], Takashi Akaike[2], Kaoru Shindo[2], Kengo Funakoshi[1]

[1]Department of Neuroanatomy, Yokohama City University, Yokohama, Japan
[2]School of Medicine, Yokohama City University, Yokohama, Japan

Complete spinal cord transection in adult rats results in poor recovery of hindlimb function, while rats that received neonatal spinal transection show spontaneous recovery of hindlimb function. We demonstrated that after neonatal spinal transection, primary affrent fibers projecting to the spinal cord are increased to compensate the loss of the descending projections. In this study, we investigated whether primary afferent fibers would increase after spinal transection at postnatal day 20 (P20) because it was reported that rats that received spinal transection after P14 failed to recover from hindlimb dysfunction. Furthermore, we studied chondroitin sulphate (CS)-A and CS-C expression in the perineuronal nets (PNNs) of rats 2 weeks after spinal transection at P5, P10, P15, or P20.

Interestingly, primary afferent fibers were increased after spinal transection at P20 although hindlimb locomotor function was deteriorated. Observation of CS-A- and CS-C- positive PNNs on motoneurons revealed that CS-A expression in PNNs of intact rats retained high until P29, and was decreased at P34, while CS-C expression in PNNs was low at P19 and was increased thereafter until P34. CS-A expression in PNNs of rats that received spinal transection at P15 (P15 ST) or P20 ST was low 2 weeks after injury, but that of P5 ST or P10 ST was high 2 weeks after injury. CS-C expression in PNNs of P5 ST or P10 ST, on the other hand, was low 2 weeks after injury, but that of P15 ST or P20 ST was high 2 weeks after injury. Significant differences were observed in CS-A expression between P15 ST and intact rats, and in CS-C expression between P10 ST and intact rats. These results may suggest that altered expressions of CS-A and CS-C on motoneuronal PNNs could be involved in functional recovery of hindlimb locomotor.

Key Words：Spinal cord injury, Perineuronal nets, Motoneuron, Juvenile rats

P180

Mechanisms of Degeneration And Regeneration In Spinal Cord Injury

Mohammad Taghi Joghataie

Faculty of Advanced Technologies in Medicine, Department of Neuroscience, Iran University of Medical Sciences, Tehran, Iran .Cellular and Molecular Research Center, Iran University of Medical Sciences, Tehran, Iran

The trend in the major causes of death has changed over the past years from infectious diseases to cardiovascular diseases, cancers and road traffic accidents. Road traffic accident is one of the main causes of Spinal Cord Injury (SCI), a debilitating disease, which leads to progressive functional damages. It is estimated that the annual incidence of spinal cord injury is approximately 50 per 1 million people. SCI represents an injury with catastrophic outcomes, both for the individual on a personal level, and for society with respect to the extent of burden on the health care and living expenses. Although, considerable research efforts were undertaken, only limited rehabilitating therapies are available in human patients. Unlike the peripheral nervous system (PNS), the adult mammalian the CNS have limited capacity to spontaneously regeneration following an injury. Because of this is a condition which cannot be treated, Many approaches were used by investigators in order to facilitate axonal regeneration and consequent functional recovery following SCI. Here, we will explain briefly different strategies applied by researchers and our colleagues in animal models of SCI and clinical trials. Injury to the CNS induces tissue damage, which creates barriers to regeneration. One of the main barriers is the glial scar, in which astrocytes and some other cells establish a dense cellular response surrounding the lesion site These cells express several inhibitory molecules including chondroitin sulfate proteoglycans (CSPGs) and keratan sulfate proteoglycans (KSPGs) which fill the extracellular matrix (ECM) surrounding the lesion site. The astrocyte response to injury is referred to as reactive gliosis. As axons cannot regenerate beyond the glial scar, this extracellular glial scar is thought to be a major limiting factor following CNS injury; However, increasing evidences suggests a beneficial role of this scar tissue in reestablishing the physical and chemical integrity of the CNS. Another event which makes more complex the regeneration process is progressive cavitation in which, after days to weeks, a CNS injury can expand in size; leading to a scar-encapsulated cavity more expanded the size of initial lesion. Recently, basic scientists have being applied several strategies aimed to provide new treatments. These include (a) promoting the survival and growth of damaged axons using different neurotrophins; (b) neutralizing inhibitory molecules associated with the failure of axonal regeneration, (c) providing a permissive growth environment by transplanting neural

cells, and (d) gene therapy, (e) and some cutting-edge tools for use in drug or cell delivery, including nanoparticles, matrix-mimetics, scaffolds, tissue engineering etc. We observed a significant improvement in motor function of rats when stromal derived factor-1 was used to attract innate stem cells to the injury site. In conclusion, it seems that co-transplantation of different cells accompanies with other factors like enzymes and growth factors via new delivery systems may yield better results in SCI.

Key words: Cell therapy, Regenerative medicine, Stem cell, Spinal Cord Injury

P181

In vivo distribution of U87MG cells injected into the lateral ventricle of rats with spinal cord injury

Yu Jeong Noh[1,2,5,] Jeong-Seob Won[1,2,3]Ji-Yoon Hwang[1,2,5]Hee Jang Pyeon[1,2,5], Sung Soo Kim[1,2,3], Hye Jin Song[1,2,5], Yoon Kyung Bae[1,2,3], So yeong Cho[1,2,5], Jee soo Lee[1,2,3] Da Eun Jeong[1,2], Hyun Nam[1,2,4], Hye Won Lee[1,5], Sun-Ho Lee[2,3,4*], Kyeung Min Joo[1,2,3,5,*]

[1]Single Cell Network Research Center, Sungkyunkwan University School of Medicine, Suwon, South Korea
[2]Stem Cell and Regenerative Medicine Center, Research Institute for Future Medicine, Samsung Medical Center, Seoul, South Korea
[3]Department of Health Sciences and Technology, SAIHST, Sungkyunkwan University, Seoul, South Korea
[4]Department of Neurosurgery, Samsung Medical Center, Sungkyunkwan University School of Medicine, Seoul, South Korea
[5]Department of Anatomy & Cell Biology, Sungkyunkwan University School of Medicine, Suwon, South Korea

Stem cells could be the next generation therapeutic option for neurodegenerative diseases including spinal cord injury (SCI). However, several critical factors such as delivery method should be determined before their clinical applications. Previously, we have demonstrated that lateral ventricle (LV) injection as preclinical simulation could be used for intrathecal administration in clinical trials using rodent animal models. In this study, we further analyzed in vivo distribution of cells that were injected into LVs of rats with SCI at thoracic level using in vivo imaging techniques. When 5×10^6 U87MG cells labelled with fluorescent magnetic nanoparticle (FMNP-labelled U87MG) were administrated into LVs at 7 days after SCI, FMNP-labelled U87MG cells were observed in all regions of the spinal cord at 24 hours after the injection. Compared to water-soluble Cy5.5 fluorescent dye or rats without SCI, in vivo distribution pattern of FMNP-labelled U87MG cells was not different, although migration to the spinal cord was significantly reduced in both Cy5.5 fluorescent dye and FMNP-labelled U87MG cells caused by the injury. The presence of FMNP-labelled U87MG cells in the spinal cord was confirmed by quantitative PCR for human specific sequence and immunohistochemistry staining using antibody against human specific antigen. These data indicate that LV injection could recapitulate intrathecal administration of stem cells for SCI patients. Results of this study might be applied further to the planning of optimal preclinical and clinical trials of stem cell therapeutics for SCI.

Key Words**:** Spinal cord injury (SCI), Cy5.5, U87MG, lateral ventricle (LV), *in vivo* optical imaging

P182

Foxp3 plasmids-encapsulated PLGA nanoparticles reduce neuropathic pain behavior in spinal nerve ligation-induced rats

Juhee Shin[1], Jinpyo Hong[2,*], Dong Woon Kim[1,2,*]

[1]Department of Medical Science, Chungnam National University School of Medicine, Daejeon, 35015, Republic of Korea.
[2]Department of Anatomy, Brain Research Institute, Chungnam National University School of Medicine, Daejeon, 35015, Republic of Korea.

Neuropathic pain from damage or dysfunction of the nervous system is a highly debilitating chronic pain state and is often resistant to currently available treatments. It has become clear that neuroinflammation mediated by proinflammatory cytokines and chemokines from microglia plays an essential role in the development of central sensitization during the establishment and maintenance of neuropathic pain. Here, we succeeded in alleviating spinal nerve ligation (SNL) induced neuropathic pain by inhibiting the microglial activation through plasmids encoding foxp3-loaded PLGA nanoparticles (Foxp3-PLGA-LP). We revealed that the Foxp3-PLGA-NP decreased the expression of proinflammatory genes such as TNF-alpha, IL-1beta and iNOS in BV2 cells. Moreover, neuropathic pain generated by SNL was effectively diminished in rats administrated intrathecally with the Foxp3-PLGA-NP in behavioral test. Similarly, the loss of microglial activity was also confirmed during histological and cytokine analysis. Taken together, these data suggest that enhanced regulation of Foxp3 in spinal microglia with PLGA nanoparticles efficiently relieves SNL-induced neuropathic pain, and it would be therapeutic value for treating neuropathic pain.

Key Words: Neuropathic pain, Nanoparticle, Foxp3, Microglia

P183

p66shc-PLGA nanoparticles reduce by pain behavior in neuropathic pain model following spinal nerve ligation

Nara shin[1,2], Hyo Jung Shin[1], Sooil Kim [1], Dong Woon Kim[1,2]

[1]Department of Anatomy, Brain Research Institute, Chungnam National University College of Medicine, Daejeon, 35015, Republic of Korea.
[2]Department of Medical Science, Chungnam National University College of Medicine, Daejeon, 35015, Republic of Korea.

AIMS: Reactive oxygen species has been suggested as a key player in neuropathic pain, causing central sensitization by glia activation and loss of GABAergic interneuron in spinal dorsal horn. However, it remains unclear as to what type of reactive oxygen species changes what aspect of glia activation and GABAergic interneuron for central sensitization in neuropathic pain conditions. In this study, we investigated whether mitochondrial superoxide affects both excitatory in spinal dorsal horn neurons after peripheral nerve injury. **RESULTS:** Downregulation of mitochondrial superoxide level by p66shc-PLGA nanoparticles alleviated neuropathic mechanical hypersensitivity caused by L5 spinal nerve ligation. In SNL model (Spinal nerve ligation model), superoxide product DHE signal was highest at 9 days postoperatively. In SNL condition, the DHE signal, pain behavior and inflammatory cytokine and decreased after p66shc-PLGA nanoparticles in spinal dorsal horn. In addition, superoxide and inflammatory cytokine level were attenuated in microglia and neuronal cell line by p66shc-PLGA

nanoparticle co-treatment after LPS and Glutamate treatment. **CONCLUSION:** These results suggest that, high levels of mitochondrial superoxide through p66shc in spinal dorsal horn neurons and microglia increase sensory threshold after peripheral nerve injury and contribute to neuropathic mechanical hypersensitivity.

.

Key Words**:** Neuropathic pain, Spinal cord ligation, p66shc, Nanoparticle, ROS

P184

Single intrathecal administration of a peptide antagonist of Toll-like receptor 4 alleviates neuropathic pain induced by spinal nerve ligation in rats

Yuhua Yin[1,2,3], Hyewon Park[1,2], Won Hyung Lee[3], Jinpyo Hong[2], Dong Woon Kim[1,2]

[1]Department of Medical Science, Chungnam National University College of Medicine, Daejeon, 35015, Republic of Korea
[2]Department of Anatomy, Brain Research Institute, Chungnam National University College of Medicine, Daejeon, 35015, Republic of Korea
[3]Department of Anesthesia and Pain Medicine, Chungnam National University Hospital, Daejeon 35015, Republic of Korea

Neuropathic pain is caused by tissue damage or lesions in peripheral fibers and central neurons. Inflammation is one of the mechanisms of neuropathic pain, which is mainly mediated with the TLR4 signaling pathway. Therefore, because blocking TLR4 with specific molecules could be reasonable in alleviating neuropathic pain, in this study, we examined the therapeutic effect of a peptide antagonist of TLR4 (PAT4) in spinal nerve ligation (SNL)-operated rats. TLR4 was highly expressed in microglia of ipsilateral sides of spinal dorsal horns in SNL-induced rats. When LPS-induced BV2 microglia cells induced by LPS (100 ng/ml) were incubated with PAT4 (10 μM), the level of proinflammatory mediators, such as TNF-α, IL-1β, and IL-6, were dramatically reduced by ~70% in quantitative PCR. We also confirmed that FITC-conjugated PAT4 was primarily targeted in spinal microglia of SNL rats. Thus, when PAT4 was administrated intrathecally to SNL rats at day 7 post-operation, pain behavior was lessened for ~2 weeks in von Frey filaments test. In PAT4-delivered SNL rats, microglial activity in spinal dorsal horns was apparently decreased in Iba1 staining. Likewise, the fluorescent intensity of Dihydroethidium in detecting reactive oxygen species (ROS) and the expression of proinflammatory genes were decreased in PAT4-injected SNL rats. Taken together, these data suggested that PAT4 could relieve neuropathic pain behavior in SNL rats by suppressing microglia activation and subsequently the production of ROS and cytokines. Therefore, it would a believable medicine to treat the patients of neuropathic pain.

Key words: Neuropathic pain, TLR4 antagonist, Spinal nerve ligation, Inflammation

P218

Tissue clearing technique for evaluating peripheral neuropathy: A quantification of intraepidermal nerve fiber density with ACT-PRESTO

Dai Hyun Kim[1], Se Jeong Lee[1], Ji Hyuck Hong[2], Soo Hong Seo[2], Hyo Hyun Ahn[2], Byung-Jo Kim[3],

Woong Sun[1,4], Im Joo Rhyu[1,4]

[1]Department of Anatomy, Korea University College of Medicine, Seoul, Korea
[2]Department of Dermatology, Korea University College of Medicine, Seoul, Korea
[3]Department of Neurology, Korea University College of Medicine, Seoul, Korea
[4]Division of Brain Korea 21 Plus Program for Biomedical Science, Korea University College of Medicine, Seoul, Korea

The skin nerve biopsy has been being considered a few reliable evaluation tool for diagnosing peripheral neuropathies. However, the method has an inevitable limitation due to the sectioning process and subsequent two dimensional imaging using few thin sections. The tissue clearing technique could clear whole biological tissues without deteriorating an original tissue architecture and also accelerate antibody penetration into thick specimens by applying pressure. The purpose of the present study was to identify the possibility of tissue clearing technique in assessment of intraepidermal nerve fiber density(IENFD) for evaluating peripheral neuropathies.
A total of 9 subjects including 5 normal people and 4 patients with peripheral neuropathies were participated for the study and two skin samples were collected from each subject. One of the biopsied tissues was cryosectioned and immunostained with two different method including 3,3'-diaminobenzidine(DAB) stain and fluorescent labeling. The other one was proceeded through the rapid tissue clearing and immunolabeling method called ACT-PRESTO. The IENFDs were quantified from the two and three dimensional images obtained through the former conventional method and latter latest technique respectively. The tissue clearing and immunolabeling with ACT-PRESTO provided not only rapid and highly reproducible three dimensional images of cutaneous nerve fibers within four days but also reliable quantified data of IENFDs compared with the results obtained from conventional methods. The average values of IENFDs of normal group were 6.14 and 6.05 fibers/㎜ obtained by DAB and immunofluorescent stain respectively. The average values of patient group were 2.79 and 2.73 respectively. The three dimensional images resulted from ACT-PRESTO also produced significantly different IENFDs between normal and neuropathy group. The IENFDs of normal and patient group in cleared whole skin were 96.23 and 54.42 fibers/㎟ respectively. The speed and consistency of ACT-PRESTO for quantification of IENFD will provide a promising way to improve the conventional assessment tool for peripheral neuropathies.

Key Words: Skin nerve biopsy, Tissue clearing technique, Intraepidermal nerve fiber density, Peripheral neuropathy

P186

In vivo Monitoring of Monoamine Oxidase Activity in Alzheimer's Disease using Two-photon excitable Fluorescent Probe

Jongmin An[1], Dokyoung Kim[1,2,3,*]

[1]Department of Biomedical Science, Graduate School, Kyung Hee University, 26 KyungheedaeRo, Dongdaemun-Gu, Seoul 02447, Republic of Korea;
[2]Department of Anatomy and Neurobiology, College of Medicine, Kyung Hee University, 26 Kyungheedae-Ro, Dongdaemun-Gu, Seoul 02447, Republic of Korea;
[3]Center for Converging Humanities, Kyung Hee University, 26 Kyungheedae-Ro, Dongdaemun-Gu, Seoul 02447, Republic of Korea.

Monoamine oxidases (MAOs) are commonly found the outer membrane of mitochondria in

most cell. It is important to regulate biogenic amines such as dopamine, serotonin, or norepinephrine in brain. Thus, some physiological disorders and diseases are found to be correlation to the abnormal activity of MAOs.In this study, we developed a fluorescent probe which can detect the increased activity of MAOs dependent on the aging of mice with Alzheimer's disease (AD) by using two-photon *in vivo* imaging. The enzymatic reaction of MAOs and cascade intramolecular cyclization convert the structure of probe to a fluorophore which is two-photon excitable and sensitive to the amyloid-beta plaque (AD biomarker). Also, this fluorophore has a dipolar character, changing it weakly emissive outside Aβ plaques (indicate the MAOs 's activity), meanwhile highly emissive inside Aβ plaques (indicate the AD progress). These signal changes at the amyloid-beta plaque (indicate the AD progress) and background (indicate the MAOs 's activity) were monitored by *in vivo* two-photon microscopy. The upregulated activity of MAOs was observed over the progress of AD from the *in vivo* deep-tissue imaging. The correlation between MAOs activity and AD progress proposed that the increased activity of MAOs can be a potential biomarker for AD diagnosis.

Key Words: MAOs, Alzheimer's disease, Two-photon imaging, Biomarker

P187

Optimizing Tissue Clearing Method for Human Brain Tissue : Preparing Methods, Clearing Efficiency, Staining Methods, and Imaging Strategy

Min Sun Kim[1], Ahn Jang Ho[1], Mo Ji Eun[2]

[1]Funtional Neuroanatomy Metabolisom of Regulation, Seoul National University, Seoul, Koera

Currently, the tissue clearing method is actively used in neuroscience research. However, a protocol applicable for human brain tissue has not yet been optimized because of difficulty to gain fresh human samples. We aimed to optimize human brain clearing and imaging methods using fresh human samples. Fresh human brain samples obtained at autopsy and cadavers donated for medical school practice were used. We applied active electrophoretic clearing for human brain tissue. We quantified the degree of transparency, noise and brightness of DAPI staining using Image J. Antibody and chemical dye were stained for 4 days, 11 days in PBS and we applied commercial staining kit to human brain tissue. The staining efficiency according to the different staining strategy was compared. Confocal microscope was used to investigated staining depth. Fresh human brain samples showed higher clearing efficiency compared with cadaver samples (time required for 80% transparent; 4hr vs. 40hr). In addition, as the clearing progresses, both samples became weaker, especially cadaver samples could be confirmed to be broken. Although a tendency of higher noise was observed with less transparent samples, fresh human brain samples showed fewer noise compared with cadaver samples. DAPI was stained to over 500μm at least 16hr incubation for fresh human brain samples. The surface's fluorescent brightness was increased according to incubating duration. In contrast to fresh brain samples, only a few cadaver samples showed DAPI staining. Respect to antibody staining efficiency, fresh and cadaver samples showed similar penetration depth (about 65um). Longer antibody incubation with PBS buffer samples showed deeper staining depth. A commercial staining kit showed higher efficiency. The present study investigated and compared both classic and innovative technology regarding human brain clearing, staining and imaging. These pioneering results provide valuable information to the human brain researchers.

Key Words: Human Brain, Brain, Clearing, Clarity, Imaging

P188

Dlx1/2 and Otp coordinate the production of hypothalamic GHRH- and AgRP-neurons

Bora Lee[1], Janghyun Kim[2], Taekyeong An[3], Sangsoo Kim[3], Esha M. Patel[6], Jacob Raber[6], Soo-Kyung Lee[4], Seunghee Lee[5], Jae W. Lee[2]

[1]Center for Neuroscience, Korea Institute of Science and Technology (KIST), Seoul, 02792, Korea
[2]Neuroscience Section, Papé Family Pediatrics Research Center, Department of Pediatrics, Oregon Health and Science University, Portland, OR, 97239, USA.
[3]Department of Bioinformatics and Life Science, Soongsil University, Seoul, 06978, Korea.
[4]Vollum Institute, Oregon Health and Science University, Portland, OR, 97239, USA
[5]College of Pharmacy and Research Institute of Pharmaceutical Sciences, Seoul National University, Seoul, 08826, Korea.
[6]Department of Behavioral Neuroscience, Oregon Health and Science University, Portland, OR, 97239, USA.

Despite critical roles of the hypothalamic arcuate neurons in controlling the growth and energy homeostasis, the gene regulatory network directing their development remains unclear. Here we report that the transcription factors Dlx1/2 and Otp coordinate the balanced generation of the two functionally related neurons in the hypothalamic arcuate nucleus, GHRH-neurons promoting the growth and AgRP-neurons controlling the feeding and energy expenditure. *Dlx1/2*-deficient mice show a loss-of-GHRH-neurons and an increase of AgRP-neurons, and consistently develop dwarfism and consume less energy. These results indicate that Dlx1/2 are crucial for specifying the GHRH-neuronal identity and, simultaneously, for suppressing AgRP-neuronal fate. We further show that Otp is required for the generation of AgRP-neurons and that Dlx1/2 repress the expression of Otp by directly binding the *Otp* gene. Together, our study demonstrates that the identity of GHRH- and AgRP-neurons is synchronously specified and segregated by the Dlx1/2-Otp gene regulatory axis.

Key Words: Dlx1/2, Otp, GHRH, AgRP, Arcuate nucleus

P189

The spatiotemporal expression of GRP78 on blood vessels of rats subjected to 3-nitropropionic acid: its correlation with blood-brain barrier disruption

Xuyan Jin[1], Tae-Ryong Riew[1], Hong Lim Kim[2], Soojin Kim[1], Mun-Yong Lee[1]

[1]Department of Anatomy, Catholic Neuroscience Institute, College of Medicine, The Catholic University of Korea, Seoul 06591, Republic of Korea
[2]Integrative Research Support Center, Laboratory of Electron Microscope, College of Medicine, The Catholic University of Korea, Seoul 06591, Republic of Korea

The 78-kDa glucose-regulated protein (GRP78), chaperone protein located in the endoplasmic reticulum (ER), has recently reported to be involved in the neuroglial response to ischemia-induced ER stress. The present study was designed to further substantiate the detailed distribution of and the cell types involved in the induction of GRP78 expression in rats treated with the mitochondrial toxin 3-nitropropionic acid (3-NP). Immunoreactivity for GRP78 was almost exclusively

localized to striatal neurons in saline-treated controls, but it was induced in activated glial cells including reactive astrocytes and activated microglia/macrophages in striata treated with 3-NP. In the lesion core, GRP78 immunoreactivity was also induced in association with vasculature; this was evident in the lesion periphery of the core at 3 days post-lesion, and was evenly distributed throughout the lesion core by 7 days after lesion induction. Vascular GRP78 expression appeared to correlate temporally and spatially with infiltration of activated microglia into the lesion core. In addition, this was coincident with the time and distribution of blood-brain barrier (BBB) leakage, detected by the extravasation of the established BBB permeability marker fluorescein isothiocyanate-albumin. Vascular GRP78-positive cells in the lesion core corresponded to endothelial cells, smooth muscle cells, and adventitial fibroblast-like cells, in which GRP78 protein was specifically localized to the cisternae of the rough ER and perinuclear cisternae, but not to other organelles such as mitochondria, or nuclei. Thus, our data provide a novel insights into the phenotypic and functional heterogeneity of GRP78-positive cells within the lesion core, suggesting its involvement in the activation/recruitment of activated microglia/macrophages and its potential role in the BBB impairment in response to neurotoxic insults by 3-NP. This research was supported by the National Research Foundation of Korea (NRF) [grant number NRF-2017R1A2B4002922].

Key Words：78-kDa glucose-regulated protein, Striatum, Endoplasmic reticulum, 3-nitropropionic acid, Blood-brain barrier, Blood vessels

P190

Extracerebellar expression of glutamate receptor GluD2 in adult mice and marmosets

Konno K, Watanabe M

Department of Anatomy, Hokkaido University Faculty of Medicine, Sapporo, Japan

GluD2 is exclusively expressed in cerebellar Purkinje cells (PCs) and selectively localized at parallel fiber (PF) synapses. GluD2 plays a key role in the formation, maintenance, and regeneration of PF-PC synapses, which are mediated through selective binding of GluD2 with presynaptic neurexins via granule cell-derived Cbln1. Mutation of the GluD2 gene in mice and humans causes cerebellar ataxia. Intriguingly, several human cases of de novo and inherited mutations display not only cerebellar ataxia, but also cognitive impairment. Indeed, GluD2 mRNA is expressed outside of the cerebellum, albeit at much lower levels than in the cerebellum. The present study undertook to clarify extracerebellar expression of GluD2 in adult mice. Highly-sensitive chromogenic *in situ* hybridization revealed widespread expression of GluD2 mRNA, with relatively higher levels in the mitral cell layer of the olfactory bulb, retrosplenial granular cortex (RSG), arcuate nucleus, locus ceruleus, and parabrachial nucleus. In the RSG, a limbic cortical region highly interconnected with the hippocampus and anterior thalamic nucleus, GluD2 mRNA was mainly detected in glutamatergic neurons expressing VGluT1 mRNA. By immunohistochemistry, GluD2 was detected as bright coarse puncta, an enriched in the layer I and layer II/III, where they tightly apposed to VGluT2-positive nerve terminals and overlapped with PSD-93 and GluA3. Post-embedding immunogold microscopy demonstrated selective labeling of the postsynaptic membrane at VGluT2-positive asymmetrical synapses. These expression profiles in mice were conserved in the cerebellum and RSG of marmosets. These findings suggest that GluD2 functions as a fundamental component of the synaptic adhesion system between specific inputs and targets in the extracerebellar regions of mammalian

brains, as is the case in the cerebellum.

Key Words: Glutamate receptor, GluD2, Retrosplenial cortex, Synapse formation

P191

Detailed characterization of neuroglial response after L-NIO-induced focal ischemia in adult mice

Soojin Kim[1], Tae-Ryong Riew[1], Xuyan Jin[1], Mun-Yong Lee[1]

[1]Department of Anatomy, Catholic Neuroscience Institute, College of Medicine, The Catholic University of Korea, Seoul 06591, Republic of Korea

A selective nitric oxide synthase inhibitor, N (5)-(1-iminoethyl)-L-ornithine dihydrochloride (L-NIO), has been reported to result in acutely compromised blood-brain barrier function and focal ischemia, causing tissue inflammation and chronic neurodegeneration. Our aim was to determine the spatiotemporal distribution and detailed characterization of glial responses in the mouse striatum after stereotaxic instratriatal injection of L-NIO. Depending on astrocytic/microglial responses and neuronal viability, three distinct regions in the ipsilateral striatum were clear: ischemic lesion core, peri-lesional edge, and penumbra. Fluoro-jade B, neurosilver staining and loss of DARPP-32, Iba1, and GFAP immunoreactivty showed pan-neural cell death in the lesion core, starting at 6 hours to 1 day post-lesion. At 2 days post-lesion, Iba1+ cells infiltrated in the peri-lesional edge, characterized by the loss of GFAP immunoreactivity, thus clearly distinguished from penumbra. Peri-lesional Iba1+ cells were mostly amoeboid highly proliferative. After 3 days, amoeboid Iba1+ cells start to fill the degenerated white matter tracts in the lesion core adjacent to peri-lesional edge, while gray matter was relatively salvaged. Scar-forming reactive astrocytes begin to become polarized in the penumbra. Infiltration of Iba1+ cells in all degenerated white matter bundles in the lesion core become more prominent at days 7. At days 10, Iba1+ cells were distributed in the gray matter, rather in reactive form with elongated processes than amoeboid. Fulminant formation of astrocytic scar with polarization of astrocytes with distinctive elongated morphologies were evident in the penumbra at days 10. After 14 days, Iba1+ cells were evenly distributed throughout the lesion core. Iba1+ cells were distributed in the gray matter around the striatal white matter bundles, and were evenly distributed throughout the lesion core by day 14. These data demonstrated the characteristic time-dependent distribution patterns for activated microglia/macrophages and reactive astrocytes in the lesion core and penumbra after L-NIO injection, indicating this model has advantages in the study of a detailed characterization of the time course of activated neuroglial cell compared with other ischemic stroke model, because well-demarcated striatal lesion does not spread to the cerebral cortex, thus providing a better-preserved lesion core and penumbra areas.

Key Words: L-Nio, Focal ischemia, Microglia, Macrophage, Astrocyte, Neuroinflammation, Glial scar

P192

Expression of vesicular glutamate transporter 1 (VGLUT1) and VGLUT2 in the axons and somata of the rat trigeminal primary sensory neurons in the normal condition and

following inflammation

Yi Sul Cho, Jin Young Bae, Hye Min Han, Yong Chul Bae

Department of Anatomy and Neurobiology, School of Dentistry, Kyungpook National University, Daegu, Korea, Republic of

Informations on the expression of vesicular glutamate transporter (VGLUT) in the axons and somata of the primary sensory neurons may help understand glutamate signaling mechanism associated with transmission of various sensory informations. This study, in order to elucidate type of VGLUTs and axons associated with craniofacial acute and inflammatory pain, examined expression of VGLUT1 and VGLUT2 in the rat trigeminal ganglion and peripheral sensory root in the normal condition and following CFA-induced inflammation by behavioral assay, light- and electron-microscopic immunohistochemistry and quantitative analysis. In normal rats, VGLUT1 was expressed mostly in the medium- and large-sized neurons whereas VGLUT2 was expressed mostly in the small- and medium-sized neurons. Most of the VGLUT1+ (71.8%) and VGLUT2+ (97.3%) axons were unmyelinated and small myelinated (< 20 μm^2 in cross-sectional area, equivalent to Aδ fiber size). A large number of VGLUT1+ (28.2%), but few VGLUT2+ (2.7%) axons were large myelinated. Fractions of VGLUT1+ and VGLUT2+ unmyelinated axons of all examined axons were increased significantly whereas fractions of VGLUT1+ and VGLUT2+ small and large (>20 μm^2 in cross-sectional area, equivalent to Aβ fiber size) myelinated axons were not changed when thermal hypersensitivity was developed following CFA-induced inflammation compared to control. These findings suggest that VGLUT1- and VGLUT2 are involved in the acute pain associated glutamate signaling and VGLUT1- and VGLUT2 in the unmyelinated fiber are involved in the inflammatory pain associated glutamate signaling.

Key Words: VGLUT, fiber type, Nociception, Inflammation, Trigeminal

P193

Deficiency of SREBP-1c induces schizophrenia-like behavior in mice

Sueun Lee[1], Sohi Kang[1], Mary Jasmin Ang[1], Juhwan Kim[1], Jong Choon Kim[1], Sung-Ho Kim[1], Tae-Il Jeon[2], Chaeyong Jung[3], Seung-Soon Im[4], Changjong Moon[1,*]

[1]Department of Veterinary Anatomy and Animal Behavior, College of Veterinary Medicine and BK21 Plus Project Team, Chonnam National University, Gwangju 61186, South Korea
[2]Department of Animal Science, College of Agriculture & Life Science, Chonnam National University, Gwangju 61186, South Korea
[3]Department of Anatomy, Chonnam National University Medical School, Gwangju 61469, South Korea
[4]Department of Physiology, Keimyung University School of Medicine, Daegu 42601, South Korea

Schizophrenia is a hereditary disease that ~1% of the worldwide population develops. Many studies have investigated possible underlying genes related to schizophrenia. Sterol regulatory element-binding protein (SREBP) has recently been suggested as a susceptibility gene in patients with schizophrenia. SREBP controls cellular lipid homeostasis by three isoforms: SREBP-1a, SREBP-1c, and SREBP-2. This study used SREBP-1c knockout (KO) mice to examine whether a deficiency in SREBP-1c would affect their emotional and psychiatric behaviors. Altered mRNA expression in genes upstream and downstream from SREBP-1c was confirmed in the brains of SREBP-1c KO mice. Schizophrenia-like behavior, including hyperactivity during the dark phase, depressive-like behavior,

aggressive behavior, and deficits in social interaction and prepulse inhibition were observed in SREBP-1c KO mice. Furthermore, increased volume of the lateral ventricle was detected in SREBP-1c KO mice. The mRNA levels of several γ-aminobutyric acid (GABA)-receptor subtypes and glutamic acid decarboxylase 65/67 decreased in the hippocampus of SREBP-1c KO mice. Thus, SREBP-1c deficiency may contribute to enlargement of the lateral ventricle and development of schizophrenia-like behaviors and be associated with altered GABAergic transmission.

Key Words: Behavior, GABAergic transmission, Mice, Schizophrenia, SREBP-1c

P194

Effects of 72-hour sleep deprivation on heterozygous Disc1 mutant mice

Chih-Yu Tsao[1], Li-Jen Lee[1,2,3]

[1]Graduate Institute of Anatomy and Cell Biology, National Taiwan University, Taipei, Taiwan, ROC.
[2]Institute of Brain and Mind Sciences, National Taiwan University, Taipei, Taiwan, ROC.
[3] Neurobiology and Cognitive Science Center, National Taiwan University, Taipei, Taiwan, ROC.

Schizophrenia is a severe mental disorder that occurs in the early stage of life and affects approximately 1% of the population. One susceptibility gene related to neurodevelopmental mental diseases is Disrupted-in-Schizophrenia 1 (DISC1). We have generated a Disc1 mutant mouse line and both homozygous (Homo) and heterozygous (Het) knockout mice exhibit subtle behavioral difference compared with wildtype controls. We therefore considered these mutant mice are in a prodromal stage. The full-blown psychiatric symptoms might be expressed subsequent to certain challenges. Sleep problems are commonly reported by patients with psychiatric disorders while insufficient sleep may deteriorate the symptoms of mental diseases, suggesting a mutual contribution between insufficient sleep and mental illness. Animals with Disc1 mutation exhibit altered sleep-activity pattern, indicating a role of Disc1 in sleep homeostasis. We therefore adopted the multiple platform-over-water paradigm of sleep deprivation (SD) as an environmental challenge and examined the interplay between Disc1 mutation and sleep insufficiency. In particular, the degree of adult neurogenesis in the dentate gyrus (DG) and the responses of microglia proximal to this neurogenic niche after 72 hour SD were examined. In the present work, the density of Ki67-positive cells were significantly decreased in SD groups of WT and Disc1 Het mice compared with home cage (HC) or big-platform (BP) control groups, indicating the impact of 72-hour SD on the neurogenic activity. The density and morphology of microglia, resident phagocytes in the CNS involved in the homeostasis of neurogenesis, were then examined. In Disc1 Het mice, microglial density was increased in the subgranular zone (SGZ) after SD, but not in other subregions. Besides, significant changes of microglial morphology were noticed in Het mice. Reduced numbers of bifurcation nodes, terminal ends, segments, and complexity were found in SD group of Het mice, especially in microglia collected from the hilus and SGZ. These changes would lead to reduced total process length. Together, these results indicated signs of microglial activation in after SD in Het mice particularly in the hippocampal neurogenic niche. The mRNA levels of three pro-inflammatory cytokines, including TNF-α, IL-1β, and IL-6, were measured. The level of IL-1β was increased in SD groups of both genotypes, whereas the level of IL-6 was augmented only in the SD group of Disc1 Het mice, suggesting a greater inflammatory reaction in Het mice after SD relative to that in WT mice. The mRNA and protein levels of BDNF were increased in the SD group of WT mice but not in Het mice, suggesting a fault of neuroprotective BDNF expression in Het mice after 72h SD. Our results suggested an interaction between sleep deprivation and genetic disruption of Disc1 in the reaction of microglia and neuroinflammatory status in the hippocampus which might contribute to the pathogenesis of mental disorders.

P195

Phenotypic characterization of mice lacking exons 4-13 of Disc1 gene

Pei-Fen Siow, Li-Jen Lee

Graduate Institute of Anatomy and Cell Biology, National Taiwan University, Taipei, Taiwan

Schizophrenia is a chronic mental disorder that affects a person's feeling, thoughts, and behaviors. One of the candidate susceptibility gene related to the pathogenesis of this disease is *Disrupted-in-Schizophrenia 1* (*DISC1*). We have established a *Disc1* mutant mouse line in which the exons 4 to13 were deleted by the expression of *Emx1-Cre* in the excitatory neurons of the forebrain. Both homozygous (Homo) and heterozygous (Het) forebrain-specific *Disc1* knockout (Fb*Disc1* KO) mice were apparently normal with no significant physical impairment. Behavioral examinations were then conducted. In the open field test, wildtype (WT) and mutant (Het and Homo) mice behaved similarly in distance travelled and time spent in central and peripheral regions. In the novel object recognition test, Homo mice displayed impaired short-term recognition memory, while WT and Het mice had comparable performances. In the elevated plus maze test, Homo mice spent more time in the open arms than WT and Het mice and no difference was noticed between WT and Het groups. In the forced swim test, no significant difference was found among the three genotypes. Our preliminary results showed behavioral abnormalities in Homo Fb*Disc1* KO mice in cognition and emotional aspects while Het mutants seemed to be normal.

Key Words: Schizophrenia, Animal model, Behavior, cognition, Emotion

P196

Active avoidance results do not directly reflect classic depression behavior in learned helplessness mice model

Jin Yong Kim[1], Soo Hyun Yang[1], Minhyuk Kwon[2], Hyun Woo Lee[1], Hyun Kim[1]

[1]Department of Anatomy, College of Medicine, Korea University, Seoul, Korea
[2]Department of Biomedical Engineering, Viterbi School of Engineering, University of Southern California, Los Angeles, California, USA

Learned helplessness model is a widely used animal model of depression. To induce learned helplessness, an unpredictable and inescapable electrical foot shock is used in mice. After exposure to inescapable foot shocks, the state of learned helplessness of the animal is assessed by active avoidance test. If the animal is in learned helplessness (LH), mice fail to avoid foot shock even it is escapable. Whereas, some mice still try to escape the foot shock and succeed to escape (non-learned helplessness, NLH). However, there was no studies that directly correlated active avoidance results with classic depression behavior tests. Therefore, we performed active avoidance test and classic depression behavior tests in same mice. We found that both LH and NLH mice show anhedonia and anxiety, but not despair. Notably, the mice which received inescapable foot shock showed similar behavior irrespective of their active avoidance results. In conclusion, active avoidance test results do

not directly reflect classic depression behavior test results in electric foot shock induced learned helplessness mice model.

Key Words: Learned helplessness, Animal model, Depression, Active avoidance, Mouse

P197

Function of habenular cholinergic system in depression

Soo Hyun Yang[1], Jin Yong Kim[1], Seojung Mo[1], Esther Yang[1], Ki Myung Song[1], Byung-Joo Ham[2], Gustavo Turecki[3], Minhyuk Kwon[4], Hyun Woo Lee[1], Hyun Kim[1]

[1]Department of Anatomy, College of Medicine, Korea University, Seoul 136-705, Korea
[2]Department of Psychiatry, College of Medicine, Korea University, Seoul 136-705, Korea
[3]Department of Psychiatry, McGill University, Douglas Mental Health University Institute, Montreal, QC H4H 1R3, Canada
[4]Department of Biomedical Engineering, Viterbi School of Engineering, University of Southern California, Los Angeles, California, USA, 90089

Dysfunctions of cholinergic neurons in the brain have been known to be associated with depression. However, the relationship between the functional abnormality of habenular cholinergic neurons and depressive symptoms is further to be. Here we show that cholinergic signaling genes (CHAT, VACHT, CHT, CHRNA3, CHRNB3 and CHRNB4) are reduced in rat habenula using a chronic constriction stress (CRS) animal model. In addition, down-regulation of choline acetyltransferase (CHAT), which is responsible for the production of acetylcholine in rat habenula, is sufficient to induce anhedonia, but not anxiety and despair. Chronic administration of the selective serotonin reuptake inhibitor, fluoxetine, failed to restore anhedonia. To determine whether habenular cholinergic signaling affects dopaminergic neurons and serotonergic neurons in the ventral tegmental area (VTA) and dorsal raphe nucleus (DRN), we used designer receptors exclusively activated by designer drugs (DREADD) system in CHAT: cre transgenic mice. Pharmacological activation of habenular cholinergic neurons induced dopaminergic neuron excitation in VTA and reduced the immune-reactivity of 5-hydroxytryptamine (5-HT) in DRN. Finally, down-regulation of habenular cholinergic genes was recapitulated in postmortem habenula of suicide victims diagnosed with major depressive disorder (MDD).

Key Words: Habenula, Cholinergic signaling, Depression, Anhedonia, Monoaminergic center

P198

3-Dimensional reconstruction and volumetric analysis of mouse habenula

Esther Yang[1], Minhyuk Kwon[2], Soo Hyun Yang[1], Jin Yong Kim[1], Hyun Woo Lee[1], Hyun Kim[1]

[1]Department of Anatomy, College of Medicine, Korea University, South Korea,
[2]Department of Biomedical Engineering, Viterbi School of Engineering, University of Southern California, Los Angeles, California, USA, 90089

Habenula is known to act as a central mechanism of depression related monoamine neuronal circuit in the brain, hence, it has become an important target for the treatment of depression. Although

the expression of few markers has been reported in tissue sections of habenula, the detailed 3-dimentional (3D) structure of habenula and related expression profile are yet to be conducted. Here, we performed volumetric analysis of habenula using mouse depression model and compared to control mouse. For the 3-dimensional volumetric analysis of habenula in mouse depression model, we 1) subdivided the cell groups in habenula with nuclear staining, 2) provided an 3D reconstruction of habenular subdomains using Amira segmentation software, 3) generated the 3D reconstruction of habenular based on the nuclear, 4) volumetric analyzed habenula in both control and depression models, and finally 5) compared the 3D structure of habenula in both control and depression model. As a result, we reconstructed habenula (control and depression model) in a 3D volume and found that there is a difference in habenula, where depression mouse has a significant smaller volume of habenula compared to control mouse.

P199

Bioinformatics and experimental analyses for adhesion G protein-coupled receptor B1 regulation in Parkinson's disease

Jae-Sun Choi[1], Woom-Yee Bae[2], Joo-Won Jeong[1,2]*

[1]Department of Anatomy, Name of University/Institute/Company, City, Country1Department of Anatomy and Neurobiology, College of Medicine, Kyung Hee University, Seoul 02447, Republic of Korea
[2]Department of Biomedical Science, Graduate School, Kyung Hee University, Seoul 02447, Republic of Korea

Progressive dopaminergic neurodegeneration is responsible for the cardinal motor defects in Parkinson's disease (PD). However, understandings of the key molecular events that provoke the selective dopaminergic neurodefects in this disease are yet to be revealed. The present study examined whether adhesion G protein-coupled receptor B1 (ADGRB1) participates in the pathway of dopaminergic neuronal loss by using bioinformatics and PD models. In the ParkDB and a transcriptomics dataset, decrease of ADGRB1 was observed. Then, we constructed a PD model to evaluate the role of ADGRB1 on neuronal cell survival. C57BL/6 mice were administrated MPTP. Moreover, mouse mesencephalic neurons and SH-SY5Y cells were treated with 1-methyl-4-phenylpyridinium (MPP+), a toxic metabolite of MPTP. ADGRB1 immunostaining of brain sections from MPTP-group showed that ADGRB1 was significantly decreased in dopaminergic neurons in the substantia nigra. In primary mouse mesencephalic neurons and human neuroblastoma cell lines, the expression of ADGRB1 was decreased by MPP+. We applied a network generation tool, Ingenuity Pathway Analysis®, with the transcriptomics dataset to extend the upstream regulatory pathway of ADGRB1 expression. AMP-activated protein kinase (AMPK) was predicted as a regulator, and consequently an AMPK-activator reduced the ADGRB1 protein level. Moreover, ADGRB1 overexpression decreased nuclear condensation induced by MPP+. Downregulated ADGRB1 by activation of AMPK induces neuronal cell death in MPTP-treated mice, suggesting that ADGRB1 could play as a cell survival factor in the neurodegenerative pathway of PD.

Key Words: Parkinson's disease, adhesion G protein-coupled receptor B1, AMP-activated protein kinase

P200

Neuroprotective effects of a traditional multi-herbal medicine Kyung-Ok-Ko in an animal model of Parkinson's disease; Inhibition of the MAPKs and NF-κB pathways and activation of the Nrf2-ARE pathway

Jong Hee Choi[1,2], Minhee Jang[2], Ik-Hyun Cho[1,2,3,*]

[1]Department of Science in Korean Medicine and Brain Korea 21 Plus Program, Graduate School, Kyung Hee University, Seoul 02447, Republic of Korea
[2]Department of Convergence Medical Science, College of Korean Medicine, Kyung Hee University, Seoul 02447, Republic of Korea
[3]Institute of Korean Medicine, College of Korean Medicine, Kyung Hee University, Seoul 02447, Republic of Korea

A traditional multi-herbal medicine, Kyung-Ok-Ko (KOK) has been widely used in Oriental medicine as a restorative enforcing the vitality of whole organs and as a medicine to treat age-related symptoms including lack of vigor and immunity. However, the beneficial value of KOK on neurological diseases such as Parkinson's diseases (PD) is largely unknown. We examined the protective effect on neurotoxicity in a 1-methyl-4-phenyl-1,2,3,6-tetrahydropyridine (MPTP)-induced mouse model of PD. Pre-treatment of KOK (2.0 and 1.0 g/kg/day, p.o.) showed significantly mitigating effects in neurological dysfunction (motor and welfare) as measuring using pole, rotarod, and nest building tests, and in the survival rate. The positive effects were related to the inhibition of the loss of tyrosine hydroxylase–positive neurons, the reduction of MitoSOX activity, increase of apoptotic cells, microglia activation, and upregulation of inflammatory factors [interleukin (IL)-1β, IL-6, cyclooxygenase-2, and inducible nitric oxide], and reduced blood-brain barrier (BBB) disruption in the substantia nigra pars compacta (SNpc) and/or striatum after MPTP intoxication. Interestingly, these multi-effect of KOK against MPTP neurotoxicity associated with the inhibition of phosphorylation of the mitogen-activated protein kinases and nuclear factor-kappa B signaling pathways and the up-regulation of the nuclear factor erythroid 2-related factor 2 pathways in the SNpc and/or striatum. Collectively, our findings suggest that KOK may mitigate neurotoxicity in MPTP-induced mouse model of PD via multi-effects including anti-neuronal and anti-BBB disruption activities through anti-inflammatory and anti-oxidative activities, suggesting that KOK may a potential strategy for prevention and/or treatment of PD.

Key Words: 1-methyl-4-phenyl-1,2,3,6-tetrahydropyridine, Parkinson's disease, Kyung-Ok-Ko, nuclear factor erythroid 2-related factor 2

P201

The Dendritic Changes of Striatal Neurons in Parkinsonian rats

Sinem Gergin , Özlem Kirazlı , Hatice Boracı, Sercan Doğukan Yıldız, Ümit S.Şehirli

Marmara University, School of Medicine, Department of Anatomy, Istanbul, Turkey

Introduction: Parkinson's disease(PD) is the second most common neurodegenerative disease which is charecterized by the loss of dopaminergic neurons found within the substantia nigra pars compacta and striatum. Neurodegenerative disorders are mainly caused by oxidative damage.

Melatonin is an indole mainly produced in the pineal gland which has been shown to have potent endogenous antioxidant actions. Beside the medical treatment, the physical therapy programmes are being involved as one of the mainstay in the treatment options. **Objectives:** We aimed to observe the changes in striatal neurons due to effect of exercise and melatonin. **Material Method:** 6-OHDA is injected unilaterally to the medial forebrain bundle of Wistar rats (n=48) by stereotaxic method. Rats are divided into eight groups; PD-four and Sham-four groups (vehicle-SF injection). These four groups are; melatonin, swimming exercise, both melatonin and swimming exercise and sedentary. Melatonin injection is applied by intraperitonally for 30 days. Exercise groups were regularly floated for 6 weeks (30 min/day, 5 days/week). At the 21th and 30th day following to the 6-OHDA injection, stepping and rotation tests (apomorphine 0.25mg/kg sc) are applied. Brain excision was performed after transcardiac perfusion. Tyrosine hydroxylase immunohistochemistry protocol and golgi staining technique were applied to the sections. Neuron analyzes were obtained by Neurolucida system (Microbrightfield Inc). **Findings and Conclusion:**

The number of rotations of both melatonin and exercise groups were found to be less when compared to the sedentary group with a statistically significant difference. The stepping test results reflect positive effects of therapy groups. Dendritic spine types were defined in all groups by Neurolucida analyses system. Stubby types which are related with degeneration decrease in PD group with melatonin and swimming exercise. Whereas thin type spines were increased in PD group with swimming exercise prominently compared other groups.

Key Words: Parkinson's disease, exercise, melatonin, neurolucida, dendritic spine

P202

Cinnamic aldehyde inhibits autophagy-induced cell death in Parkinson's disease modes

Woom-Yee Bae[1], Jae-Sun Choi[2], Joo-Won Jeong[1,2,*]

[1]Department of Biomedical Science, Graduate School, Kyung Hee University, Seoul 02447, Republic of Korea
[2]Department of Anatomy and Neurobiology, College of Medicine, Kyung Hee University, Seoul 02447, Republic of Korea

Parkinson's disease (PD) is a progressive neurodegenerative disorder and is characterized by selective dopaminergic neuronal loss in the substantia nigra and striatum of the brain. Cinnamic aldehyde (CA) is a key flavor compound in cinnamon essential oil. It has been identified that CA is effective for treatment of various neurodegenerative disorders, including PD. In the present study, we found that CA inhibited the selective dopaminergic neuronal death in the 1-methyl-4-phenyl-1,2,3,6-tetrahydropyridine (MPTP)-mediated mouse model. Recent studies have revealed that deregulated excessive autophagy can cause in most cases of neurodegenerative disorders. We, here, showed that stimulated LC3 puncta and down-regulated p62 mediated by MPTP treatment was decreased and increased by the administration of CA, respectively. Moreover, 1-methyl-4-phenylpyridinium (MPP$^+$)-mediated cell death is diminished by blockage of autophagy using autophagy inhibitors. Taken together, our results suggest that CA has a neuroprotective effect in PD and inhibition of autophagy might be a promising therapeutic target for PD.

Key Words: Cinnamic aldehyde, Autophagy, Parkinson's disease, MPTP, MPP+

P203

Cytoarchitecture of the dentate gyrus in the laggard mutant mouse

Junaedy Yunus[1], Tomiyoshi Setsu[2], Satoshi Kikkawa[2], Toshiaki Sakisaka[3], Toshio Terashima[2]

[1]Department of Anatomy, Faculty of Medicine, Public Health, and Nursing, Yogyakarta, Indonesia
[2]Division of Developmental Neurobiology, Department of Physiology and Cell Biology, Kobe University Graduate School of Medicine, Kobe, Japan
[3]Division of Membrane Dynamics, Department of Physiology and Cell Biology, Kobe University Graduate School of Medicine, Kobe, Japan

The laggard mutant mouse, characterized by hypomyelination and cerebellar ataxia, is a spontaneously occurring mutant mouse caused by the mutation in Kif14 (Fujikura et al., 2013). In this mutant, the laminated structures, such as cerebral and cerebellar cortices and dentate gyrus, are cytoarchitecturally abnormal. We studied the cytoarchitecture of the lag mutant dentate gyrus on the basis of Nissl staining and immunohistochemistry in the mouse pups at various pre- and postnatal ages. BrdU labeling analysis was performed to determine cell proliferation, while the TUNEL assay was performed to determine cell apoptosis. As a result, Nissl staining revealed that the dentate gyrus of the mutant mouse was smaller in size than the normal counterpart. The features and lamination of the mutant dentate gyrus appeared to be normal in general, but detailed analysis had demonstrated that the three layers were dramatically reduced in depth. In the mutant, the granule cell layer was cytoarchitecturally disorganized and arranged in a multiple layer instead of being arranged in a single layer, as also revealed by anti-NeuN immunostaining. Efferent projection of the granule cells to the CA3 pyramidal cells of the hippocampus appeared to be normal, as shown by anti-calbindin immunostaining. BrdU-positive cells were decreased in number and TUNEL-positive cells were increased in number, suggesting that the decreased population of the granule cells in the laggard mutant mouse is caused by the decreased cell proliferation and increased apoptotic cell death. In conclusion, the dentate gyrus of the laggard mutant mouse is cytoarchitecturally affected, suggesting that the protein encoded by Kif14 gene has multiple effects on the development of the laminated structures in the central nervous system in addition to the myelin formation.

Key Words: Laggard, Kif14, Dentate gyrus, Development, Apoptosis

P204

Adeno-Associated Viral Vector Serotype DJ-Mediated Overexpression of N171-82Q-Mutant Huntingtin in the Striatum of Juvenile Mice Is a New Model for Huntington's Disease

Minhee Jang[1], Seung Eun Lee[2], Ik-Hyun Cho[1,3]

[1]Department of Convergence Medical Science, College of Korean Medicine, Kyung Hee University, Seoul, South Korea
[2]Virus Facility, Research Animal Resource Center, Korea Institute of Science and Technology (KIST), Seoul, South Korea
[3]Brain Korea 21 Plus Program and Institute of Korean Medicine, College of Korean Medicine, Kyung

Hee University, Seoul, South Korea

Huntington's disease (HD) is an autosomal-dominant inherited neurodegenerative disorder characterized by motor, psychiatric and cognitive symptoms. HD is caused by an expansion of CAG repeats in the huntingtin (HTT) gene in various areas of the brain including striatum. There are few suitable animal models to study the pathogenesis of HD and validate therapeutic strategies. Recombinant adeno-associated viral (AAV) vectors successfully transfer foreign genes to the brain of adult mammalians. In this article, we report a novel mouse model of HD generated by bilateral intrastriatal injection of AAV vector serotype DJ (AAV-DJ) containing N171-82Q mutant HTT (82Q) and N171-18Q wild type HTT (18Q; sham). The AAV-DJ-82Q model displayed motor dysfunctions in pole and rotarod tests beginning 4 weeks after viral infection in juvenile mice (8 weeks after birth). They showed behaviors reflecting neurodegeneration. They also showed increased apoptosis, robust glial activation and upregulated representative inflammatory cytokines (tumor necrosis factor-alpha (TNF-α) and interleukin (IL)-6), mediators (cyclooxygenase-2 and inducible nitric oxide synthase) and signaling pathways (nuclear factor kappa B and signal transducer and activator of transcription 3 (STAT3)) in the striatum at 10 weeks after viral infection (14 weeks after birth) via successful transfection of mutant HTT into neurons, microglia, and astrocytes in the striatum. However, little evidence of any of these events was found in mice infected with the AAV-DJ-18Q expressing construct. Intrastriatal injection of AAV-DJ-82Q might be useful as a novel in vivo model to investigate the biology of truncated N-terminal fragment (N171) in the striatum and to explore the efficacy of therapeutic strategies for HD.

Key Words: Huntington's disease; N171-82Q, Adeno-associated viral vector serotype DJ, Mutant huntingtin, Polyglutamine expansion

P205

Electroacupuncture on the scalp over the motor cortex ameliorate behavioral deficits via activation of neural stem cells in neonatal hypoxia-ischemia of rats

Da Hee Jung[1,2], Malk Eun Pak[1,2], Hong Ju Lee[1,2], So Young Kim[3], Sung Min Ahn[3], Hwa Kyoung Shin[1,2,3], Byung Tae Choi[1,2,3*]

[1]Department of Korean Medical Science, School of Korean Medicine, Pusan National University, Yangsan 50612, Korea
[2]Graduate Training Program of Korean Medicine for Healthy-Aging, School of Korean Medicine, Pusan National University, Yangsan 50612, Korea
[3]Korean Medical Science Research Center for Healthy-Aging, Pusan National University, Yangsan 50612, Korea

Electric acupuncture therapy, alternating current stimulation, on the scalp over the motor cortex (hereafter, EASM) is used for the treatment of brain disorders. Neonatal hypoxia-ischemia (HI) is a devastating injury resulting in severe neurological disabilities, such as sensorimotor deficits and memory impairments. We investigated whether EASM could promote functional improvement in a HI rat model via the enhancement of activating neural stem cells. HI underwent EASM (2 Hz with 1, 3, and 5 mA) for 20 min from 4–6 weeks after birth. HI rats with EASM improved motor and memory function, with the greatest improvement after 3 mA EASM. The corpus callosum was significantly thicker and showed a significant increase in proliferating cells and oligodendrocytes in the 3 mA EASM group. We observed proliferating cells, and an increase in newly developed neurons and astrocytes in the subventricular zone and dentate gyrus in the 3 mA EASM group compared with the HI group.

Moreover, HI rats showed increased expression of oligodendrocytes and neuron markers in the corpus callosum and hippocampus in the 3 mA EASM group. These results suggested that EASM treatment promotes functional improvements following neonatal HI assault, *via* the proliferation and differentiation of neural stem cells. This effect was strongest after 3 mA EASM, suggesting that this is the optimal treatment dose.

Key Words: Electric acupuncture, Alternating current stimulation, Scalp, Neonatal hypoxia-ischemia, Neural stem cells

P206

Alarmin HMGB1 induces brain and systemic inflammatory exacerbation in the post-stroke infection rat models

Hahnbie Lee[1,2], Il-Doo Kim[1,2], Dashdulam Davaanyam[1,2], Ja-Kyeong Lee[1,2]

[1]Department of Anatomy, Inha University School of Medicine, Inchon, Republic of Korea
[2]Medical Research Center, Inha University School of Medicine, Inchon, Republic of Korea

Post-stroke infection (PSI) is known to worsen functional outcomes of stroke patients and accounts to one-third of stroke-related deaths in hospital. In our previous reports, we demonstrated that massive release of high-mobility group box protein 1 (HMGB1), an endogenous danger signal molecule, is promoted by N-methyl-D-aspartic acid-induced acute damage in the postischemic brain, exacerbating neuronal damage by triggering delayed inflammatory processes. Moreover, augmentation of proinflammatory function of lipopolysaccharides (LPS) by HMGB1 via direct interaction has been reported. The aim of this study was to investigate the role of HMGB1 in aggravating inflammation in the PSI by exacerbating the function of LPS. PSI animal model was produced by administrating a low-dose LPS at 24 h after post-middle cerebral artery occlusion (MCAO). Profound aggravations of inflammation, deterioration of behavioral outcomes, and infarct expansion were observed in LPS-injected MCAO animals, in which serum HMGB1 surge, especially disulfide type, occurred immediately after LPS administration and aggravated brain and systemic inflammations probably by acting in synergy with LPS. Importantly, blockage of HMGB1 function by delayed administrations of therapeutic peptides known to inhibit HMGB1 (HMGB1 A box, HPep1) or by treatment with LPS after preincubation with HMGB1 A box significantly ameliorated damages observed in the rat PSI model, demonstrating that HMGB1 plays a crucial role. Furthermore, administration of Rhodobacter sphaeroides LPS, a selective toll-like receptor 4 antagonist not only failed to exert these effects but also blocked the effects of LPS, indicating its TLR4 dependence. Together, these results indicated that alarmin HMGB1 mediates potentiation of LPS function, exacerbating TLR4-dependent systemic and brain inflammation in a rat PSI model and there is a positive-feedback loop between augmentation of LPS function by HMGB1 and subsequent HMGB1 release/serum. Therefore, HMGB1 might be a valuable therapeutic target for preventing post-stroke infection.

Key Words: HMGB1, Post-stroke infection, Inflammation, TLR4

P207

Positive effects of α-asarone on neural progenitor in a murine model of ischemic stroke

Hong Ju Lee[1,2], Sung Min Ahn[3], Malk Eun Pak[1,2], Da Hee Jung[3], So Young Kim[3], Hwa Kyoung Shin[1,2,3],

Byung Tae Choi[1,2,3*]

[1]Department of Korean Medical Science, School of Korean Medicine, Pusan National University, Yangsan 50612, Korea
[2]Graduate Training Program of Korean Medicine for Healthy-Aging, School of Korean Medicine, Pusan National University, Yangsan 50612, Korea
[3]Korean Medical Science Research Center for Healthy-Aging, Pusan National University, Yangsan 50612, Korea

NPCs transplantation, a type of stem cell therapy, has been effective for the recovery of behavioral function in neurodegenerative diseases involving ischemic stroke. This study investigated the effects of α-asarone on the neural progenitor cells (NPCs) in primary culture and in a murine model of ischemic stroke. *In vitro* assay, treatment with α-asarone induced significant NPC proliferation and increased the number of cells expressing neuronal marker NeuN. Treatment with α-asarone also increased the expression of β-catenin, cyclin D1, and phosphorylated ERK compared to vehicle treatment. In a murine model of ischemic stroke, treatment with α-asarone and transplanted NPCs alleviated stroke-related functional impairments. Combined treatment with α-asarone and NPC transplantation had greater-than-additive effects on sensorimotor function. Moreover, α-asarone treatment promoted the differentiation of transplanted NPCs into neuron-lineage cells, expressing NeuN-, GFAP-, PDGFR-α-, and CNPase-immunoreactions.These results suggest that α-asarone promotes NPC proliferation and differentiation into neuron-lineage cells via the activation of β-catenin, cyclin D1, and ERK. Moreover, α-asarone treatment facilitated neurofunctional recovery after NPC transplantation in a murine model of ischemic stroke. Therefore, α-asarone is a potential adjunct treatment of NPCs therapy for functional restoration after brain injuries such as ischemic stroke.

Key Words: Asarone, Ischemic stroke, Neural progenitor cells, Neuronal differentiation

P208

p66shc RNAi-encapsulated PLGA nanoparticles alleviate ischemia injury in Rose Bengal-induced photothrombosis stroke model

Jeong-ah hwang[1,3], Dong Woon Kim[1,3], Hee-Jung Song[2]

[1]Department of Medical Science, Chungnam National University School of Medicine, Daejeon, 35015, Republic of Korea.
[2]Departments of Neurology, Chungnam National University Hospital, Daejeon, Republic of Korea.
[3]Department of Anatomy, Brain Research Institute, Chungnam National University School of Medicine, Daejeon, 35015, Republic of Korea.

Growing evidence showed an association between ischemic stroke and increased systemic and local production of ROS. The p66Shc adaptor protein regulates oxidative stress, inflammation, apoptosis via ROS signaling. Here, we show inhibition of p66Shc on ischemic injuries by siRNA nanoparticles (NPs) in Rose Bengal photothrombosis stroke model. Rose Bengal (RB) is photosensitizer and RB induced ischemia model is developed by 560nm illumination. Two days before exposure photo-light at intact skulls, p66Shc siRNA NPs were administered to mice with through intrathecal administration. We observed that p66Shc siRNA NP treated group preserved blood–brain barrier integrity that resulted in improved stroke outcome, as identified by smaller lesion volumes, decreased neurological deficits, and increased survival. Also, we showed that decreased of microglia / astrocyte activation by p66Shc siRNA NP treated in stroke induced mice through tissue staining.

These results suggest that inhibition of p66Shc attenuate Rose bengal-induced ischemia damage by inhibiting microglia and astrocyte activation followed inflammation. Therefore, targeting the activity of p66Shc might be an interesting strategy to treat ischemia damage induced inflammation.

Key Words: Rose Bengal, Stroke, p66shc, PLGA nanoparticle

P209

Involvement of indoleamine 2,3-dioxygenase-dependent neurotoxic kynurenine metabolism in spatial restraint stress-treated mice after ischemic stroke

Young Soo Koo[1,2,3], Hyunha Kim[1,2,3], Jung Hwa Park[1,2,3], Min Jae Kim[1,2,3], Byung Tae Choi[1,2,3], Seo-Yeon Lee[1,2,3], Hwa Kyoung Shin[1,2,3]

[1]Department of Korean Medical Science, School of Korean Medicine, Pusan National University, Yangsan, Gyeongnam 50612, Republic of Korea.
[2]Korean Medical Science Research Center for Healthy-Aging, Pusan National University, Yangsan, Gyeongnam 50612, Republic of Korea.
[3]Graduate Training Program of Korean Medicine for Healthy-Aging, Pusan National University, Yangsan, Gyeongnam 50612, Republic of Korea.

Post-stroke depression (PSD), which occurs in approximately one-third of stroke survivors, is clinically important because of its association with slow functional recovery and increased mortality. In addition, the underlying pathophysiological mechanisms are still poorly understood. In this study, we used a mouse model of PSD to examine the neurobiological mechanisms of PSD and the beneficial effects of aripiprazole, an atypical antipsychotic drug. PSD was induced in mice by combining middle cerebral artery occlusion (MCAO) with spatial restraint stress. The body weight, sucrose preference, and forced swim tests were performed at 5, 7, and 9 weeks and the Morris water maze test at 10 weeks after completing MCAO and spatial restraint stress. Mice subjected to MCAO and spatial restraint stress showed significant depressive-like behavior in the sucrose preference test and forced swim test as well as cognitive impairment in the Morris water maze test. The PSD-like phenotype was accompanied by an indoleamine 2,3-dioxygenase 1 (IDO1) expression increase in the nucleus accumbens, hippocampus, and hypothalamus, but not in the striatum. Furthermore, the increased IDO1 levels were localized in Iba-1(+) cells but not in NeuN(+) or GFAP(+) cells, indicating that microglia-induced IDO1 expression was prominent in the PSD mouse brain. Moreover, 3-hydroxyanthranilate 3,4-dioxygenase (HAAO), quinolinic acid (QA), and reactive oxygen species (ROS) were significantly increased in nucleus accumbens, hippocampus, and hypothalamus of PSD mice. Importantly, a 2-week aripiprazole (1 mg/kg, per os) regimen, which was initiated 1 day after MCAO, ameliorated depressive-like behavior and impairment of cognitive functions in PSD mice that was accompanied by downregulation of IDO1, HAAO, QA, and ROS. Our results suggest that the IDO1-dependent neurotoxic kynurenine metabolism induced by microglia functions in PSD pathogenesis. The beneficial effect of aripiprazole on depressive-like behavior and cognitive impairment may be mediated by inhibition of IDO1, HAAO, QA, and ROS.

Key Words: Post-stroke depression, Aripiprazole, Indoleamine 2,3-dioxygenase 1 (IDO1)

P210

Temporal alteration of infiltrated macrophage and resident microglia following focal

cerebral ischemia model in mice

Joohyun Park[1,2], Jong Youl Kim[1], Young Min Hyun[1], Hosung Jung[1,2,3], Jong Eun Lee[1,2,3,*]

[1]Department of Anatomy, [2]BK21 Plus Project for Medical Science, [3]Brain Research Institute, Yonsei University College of Medicine, Seoul, 03722, Korea

Stroke, a devastating brain damage, is the second cause of adult disability and death following the heart disease worldwide.[1,2] As the blood supply is insufficient to the brain tissue followed by occlusion of the cerebral artery, molecular cues generated by cerebral ischemia activate the components of innate immunity, promote inflammatory signaling and contribute to tissue damage. Microglia known as an immune cell in the central nervous system (CNS) has functions similar to those of macrophages in the periphery. At the functional point of view, resident microglia (M0) can be polarized by molecular cues: M1 phase microglia and M2 phase microglia – former is related to pro-inflammatory responses and the latter is associated with anti-inflammatory responses. Moreover, blood-brain barrier (BBB) causes the extravasation of blood-derived monocytes. However, the interaction between the microglia and blood-derived macrophage is still unknown. We used CX3CR1::EGFP transgenic mice to visualize the microglia and blood-derived monocytes dynamics on neuroinflammatory responses. CX3CL1, a cell surface–bound chemokine constitutively expressed by neurons, suppresses microglial activation through its microglial receptor CX3CR1. In this study, our aim is to time-dependently observe the dynamics of microglia and macrophages using various techniques on neuroinflammation by focal cerebral ischemia. Our preliminary data showed that it is morphologically possible to distinguish activated microglia and infiltrated macrophages from the resident microglia specifically in FACS and Immunohistochemistry. In addition, blood-derived macrophages and brain microglia showed different polarization patterns by specific markers in time-dependent manners (n=5 /sham, 6 hours, 1, 3, 5, 7 days) after tMCAO. Furthermore, we performed the cytokine/chemokine array to evaluate the level of specific cytokine/chemokine on ischemic stroke using the brain tissue. In results, the levels of brain tissue of specific cytokine/chemokine showed different levels in all experimental time courses. Taken together, the overall data demonstrated that dynamics of microglia and blood-derived macrophage using specific type of transgenic mice could be a novel strategy for regulating the M2 anti-inflammatory microglia phenotype rather than M1 pro-inflammatory microglia and finding the optimal time point of drug treatment attenuating ischemic stroke.

Key Words**:** Macrophage, Neuroinflammation, Microglia, Ischemia

P211

Suppression of microRNA *let-7a* expression promotes neurogenesis in arginine decarboxylase-neural stem cells after ischemia

Yumi Oh[1,2], Sumit Barua[1], Jong Youl Kim[1], Jae Young Kim[1], Jong Eun Lee[1,2,3,*]

[1]Department of Anatomy, [2]Brain Korea 21 PLUS Project for Medical Science, [3]Brain Research Institute, Yonsei University College of Medicine, 03722, Seoul, Korea

Neural stem cells (NSCs) have been studied to treat the central nervous system (CNS)

disorders due to the potential of differentiation into neuron. To increase therapeutic efficiency of NSCs, recent researchers have focused on the study of the role of microRNA in CNS. MicroRNA *let-7a* (*let-7a*), a regulator of cell differentiation, also regulates genes associated with CNS neurogenesis. Agmatine, an endogenous primary amine produced by decarboxylation of L-arginine by arginine decarboxylase (ADC), has neuroprotective effects and contributes to cellular proliferation and differentiation. Moreover, human ADC gene delivery into the NSCs using retroviral vector (*vh*ADC) prevents the cell death and improves cell survivability against oxidative insult *in vitro*. The purpose of this study is to investigate the role of arginine metabolic enzyme which regulated *let-7a* in neural stem cell differentiation. *In vitro* study suggested that high levels of *let-7a* promoted the expression of TLX and c-Myc, as well as repressed DCX and ERK expression. In addition, agmatine attenuated the expression of TLX and increased the expression of ERK by negatively regulating *let-7a*. To confirm the effects of arginine metabolic enzyme and *let-7a in vivo*, mice were subjected to distal middle cerebral artery occlusion (dMCAO). Following dMCAO, mice were treated agmatine by intraperitoneal injection, *let-7a* mimic by osmotic pump and *vh*ADC-NSCs via intracranial injection at the corpus callosum. We found that *vh*ADC-NSC and *let-7a* co-treatment group reduced the infarct volume, increased the expression of DCX, Neurogenin2, Olig2, and attenuated the expression of GFAP. Therefore, our study suggests that the therapeutic efficiency of the *vh*ADC-NSC on neural stem cell differentiation through suppression of *let-7a* in ischemic disorders.

Key Words: Neural stem cell, MicroRNA *let-7a*, Agmatine, Human arginine decarboxylase, Cerebral ischemia

P212

Induced arginine decarboxylase can promote neural stem cell differentiation after ischemic stress

Jae Young Kim[1], Won Taek Lee[1], Jong Eun Lee[1,2,3,*]

[1]Department of Anatomy, [2]BK21 PLUS Project for Medical Science, [3]Brain Research Institute, Yonsei University, College of Medicine, Seoul, 03722, Korea

Cell replacement therapy by neural stem cells (NSCs) after ischemic stroke is a promising potential therapeutic strategy, but still lacking efficacy for the human CNS therapeutics. Recently, we reported that over-expression of human arginine decarboxylase (ADC) promotes neuronal differentiation of mouse NSCs in vitro study. In this study, we focused on the underlying cellular mechanism concerning cell proliferation and differentiation and the therapeutic feasibility of ADC-mNSCs after ischemic stroke. Firstly, we over expressed ADC in mouse NSC (mNSC) by retroviral plasmid vector and evaluate the role ADC-mNSCs in both in vivo and in vitro ischemic models. To mimic the cerebral ischemia in vitro; mNSCs were subjected to oxygen-glucose deprivation (OGD). Over expression of ADC induced the mNSCs differentiation which was related to the excessive intracellular calcium-mediated cell cycle arrest and the phosphorylation of the ERK1/2, CREB and STAT1 signaling cascade after ischemic stress. Besides, the induced ADC resisted the mitochondrial membrane potential collapse in the increasing excessive intracellular calcium environment in mNSCs. Following these results, transplanted ADC-mNSCs have suppressed infarct volume, promoted neural differentiation, synapse formation and motor behavior performance in the in vivo tMCAO rat model. Therefore, transplantation of ADC-mNSCs in the brain suggests a promising avenue of cell

replacement therapy by after ischemic stroke.

P215

A combination therapy of electroacupuncture and TrkB-expressing mesenchymal stem cells for ischemic stroke

Sung Min Ahn[1], So Young Kim[1], Malk Eun Pak[2,3], Hong Ju Lee[2,3], Da Hee Jung[2,3], Hwa Kyoung Shin[1,2,3], Byung Tae Choi[1,2,3]

[1]Korean Medical Science Research Center for Healthy-Aging, Pusan National University, Yangsan, Republic of Korea
[2]Department of Korean Medical Science, School of Korean Medicine, Pusan National University, Yangsan, Republic of Korea
[3]Graduate Training Program of Korean Medicine for Healthy-Aging, Pusan National University, Yangsan, Republic of Korea

We prepared and grafted tropomyosin receptor kinase B (*TrkB*) gene-transfected mesenchymal stem cells (TrkB-MSCs) into the ischemic penumbra, and investigated whether electroacupuncture (EA) treatment could promote functional recovery from ischemic stroke. For the behavioral test, TrkB-MSCs+EA resulted in significantly improved motor function compared to MSCs+EA or TrkB-MSCs alone. At 30 days after middle cerebral artery occlusion (MCAO), the largest number of grafted MSCs was detected in the TrkB-MSCs+EA group. Some differentiation into immature neuroblasts and astrocytes was detected; however, only a few mature neuron-like cells were found. Compared to other treatments, TrkB-MSCs+EA upregulated the expression of mature brain-derived neurotrophic factor (BDNF) and neurotrophin-4 (NT4) and induced the activation of TrkB receptor and its transcription factor cAMP response element-binding protein (CREB). At 60 days after MCAO, EA highly promoted the differentiation of TrkB-MSCs into mature neuron-like cells compared to MSCs. A selective TrkB antagonist, ANA-12, reverted the effect of TrkB-MSCs+EA in motor function recovery and survival of grafted MSCs. Our results suggest that EA combined with grafted TrkB-MSCs promotes the expression of BDNF and NT4, induces the differentiation of TrkB-MSCs, and improves motor function. TrkB-MSCs could serve as an effective treatment for ischemic stroke if used in combination with BDNF/NT4-inducing therapeutics.

P216

Early Histone deacetylase inhibition mitigates ischemia/reperfusion brain injury by reducing the activation and modulating the phenotype of microglia

Yuhua Ji, Shi Haiyan, Fei Ding

Key Laboratory of Neuroregeneration of Jiangsu and Ministry of Education, Co-innovation Center of Neuroregeneration, Nantong University, Nantong, China

Histone deacetylase inhibitors (HDACis) are promising drugs for treating stroke, but the mechanisms underlying their multiple neuroprotective effects remain unclear. Neuroinflammation mediated by resident microglia and infiltrated macrophages plays a critical role in the pathophysiology of ischemic brain injury and recovery. The present study evaluated the effects of the pan-HDACi suberoylanilide hydroxamic acid (SAHA) on inflammatory responses induced by ischemic/reperfusion (I/R) injury, and the involvement of resident microglia and infiltrated leukocytes. Transient middle cerebral artery occlusion (tMCAO) was induced for 60 minutes in C57BL/6 mice. A single dose of SAHA (50 mg/kg, i.p.) was injected immediately or 12 h after ischemia onset. Infarct volume was detected by Tetrazolium chloride (TTC) staining and the neurological deficits were evaluated by rotating beam test. Gene expression of inflammatory cytokines was examined using quantitative real-time PCR (qRT-PCR). The dynamics of microglia and infiltrated leukocytes and the levels of microglia polarization markers were examined by immunohistochemistry (IHC) and/or flow cytometry (FACS). Immediate SAHA treatment significantly decreased the infarct volume and improved long-term neurological recovery, providing more neuroprotection than delayed treatment. The protective effect was accompanied by the suppression of pro-inflammatory cytokine overexpression, and was closely associated with the reduction of activated microglia in the early phase of I/R brain injury when the infiltrated neutrophils and monocytes were few. Notably, SAHA treatment suppressed pro-inflammatory cytokine expression (IL-6, TNF-α and iNOS)while promoted the expression of anti-inflammatory cytokines (Arg-1 and IL-10) in LPS-challenged primary microglia. Further FACS analysis showed SAHA treatment enhanced CD206 levels (M2 marker) and suppressed CD86 levels (M1 markers) in microglia isolated from the ipsilateral hemisphere. Our data demonstrated early SAHA treatment mitigated I/R brain injury by reducing the activation and modulating the phenotype of microglia in a tMCAO mouse model.

Key Words: Stroke, Ischemia/reperfusion injury, Inflammation, SAHA, Microglia/macrophages, Polarization

P217

Rhus Verniciflua Extracts Protects Focal Cerebral Ischemic Mice Model of Diabetes Mellitus through Restoration of the Cerebral Blood Flow

Ji Hye Lee, Ji Heun Jeong, Jong Hun An, Ji Hyun Moon, Seong Hee Kang, Do-Kyung Kim, Nam-Seob Lee, Young-Gil Jeong, Seung Yun Han[*]

Department of Anatomy, College of Medicine, Konyang University, Daejeon, 35365, Republic of Korea.

Diabetes mellitus (DM) is known to aggravate concomitant cerebral ischemia through hampering the compensatory restoration of cerebral blood flow (CBF). The extract of Rhus Verniciflua (RVE), an herbal plant medicine, is revealed to promote the blood circulation. Therefore, the current study examined the therapeutic potential of RVE on focal cerebral ischemic mice model of DM focusing on the possible modulation of CBF. First, DM was induced with intraperitoneal injection of streptozotocin on C57/BL6 mice and the animals were randomly divided with two groups and orally administered with 500 mg/kg RVE or distilled water used as a vehicle daily for further 14 days.

Subsequently, the former (*i.e.*, DM+FCI+RVS) and the latter (*i.e.*, DM+FCI) as well as the healthy mice (*i.e.*, FCI) were subjected with 60 min-of-middle cerebral artery occlusion and reperfusion (MCAO/R) surgery for induction of focal cerebral ischemia. Next, the infarct volume, motor deficit, CBF, and the collaterals development was assessed. The 2,3,5-triphenyltetrazolium chloride stain and a batteries of motor performance tests, *i.e.*, grip strength, inverted screen, and rotarod tests, revealed the marked increases in the infarct volume and the motor deficit in DM+FCI compared with FCI, respectively. Furthermore, Doppler flowmetry indicated the significant reduction of CBF in ischemic penumbra of DM+FCI compared with that of FCI. Both macroscopic and microscopic visualization of the collaterals suggested the marked structural deterioration on vascular niche in ischemic penumbra of DM+FCI compared with that of FCI. However, all the pathologies seen in the DM+FCI were significantly reversed in DM+FCI+RVE. Notably, it was revealed that all the positive findings seen in DM+FCI+RVE was totally abolished by the intracerebral injection of Bevacizumab, a selective antibody against vascular endothelial growth factor (VEGF), suggesting that the VEGF signaling is crucially involved in the therapeutic mechanism of RVE. Together, we concluded that the oral intake of RVE could minimize the cerebral ischemic damage when DM is superimposed, and this effect is, at least partly, due to the restoration of CBF.

Key Words: Diabetes mellitus, Rhus Verniciflua Extracts, Focal cerebral ischemia, Cerebral blood flow, Vascular endothelial growth factor

P218

Role of heterotrimeric Go protein in development of cerebellar cortex

<u>Jung-Mi Choi</u>[1], Hye-Lim Cha[1], Huy-Hyen Oh[1], Dong Cheol Jang[3,4], Sang Jeong Kim[3,4], Young-Don Lee[1,2], Sung-Soo Kim[1], Lutz Birnbaumer[5,6], Haeyoung Suh-Kim[1,2]

Departments of [1]Anatomy and [2]Biomedical Sciences, The Graduate School, Ajou University School of Medicine, Suwon, South Korea; Department of [3]Physiology, and [4]Neuro-Immune Information Storage Network Research Center, Medical Research Center, Seoul National University College of Medicine, Jongno-gu, Seoul, South Korea; [5]Neurobiology laboratory, National Institute of Environmental Health Sciences, Research Triangle Park, NC, USA; and [6]Institute of Biomedical Research (BIOMED), School of Medical Sciences, Catholic University of Argentina, C1107AFF Buenos Aires, Argentina.

Heterotrimeric Go protein is a member of the $G_{i/o}$ family, which is widely expressed in the brain including cerebrum, corpus striatum, hippocampus, thalamus, and cerebellum. Even though G_o is suggested to transduce signals of neurotransmitters in those regions, the precise role of Go protein has not been identified. G_o comprises three subunits: a unique α subunit G_o ($G\alpha_o$) and the common $\beta\gamma$ subunits that are shared by other G proteins. Here, we investigated the expression of $G\alpha_o$ during the development of cerebellar cortex. We found that the $G\alpha_o$ protein is highly targeted to the plasma membrane. Thus, Purkinje cells appeared to be devoid of $G\alpha_o$ protein despite the expression of *Gnao* (the gene encoding $G\alpha_o$ protein) mRNA in the perikaryon. Since the low survival rate of *Gnao* knockout mice hampered the study on $G\alpha_o$ in the brain, we created conditional knockout (cKO) mice using *Gli-creER[T2]* to induced specific deletion of $G\alpha_o$ in the developing cerebellum. We performed histological analyses and investigated the effect of Go deficiency in *Gnao* cKO mice. We will discuss the results on how the Go regulate the maturation of Purkinje cells and synaptic network during early postnatal development of cerebellum.

Key Words: $G\alpha_o$ protein (GTP-binding Protein α subunit, Go), Purkinje cell, Cerebellum, hypoplasia,

Synaptic boutons, Climbing fiber, Gi-Go

P219

Transcriptome analysis of neuromesodermal progenitor cells in tailbud of chick embryo

<u>Veronica Jihyun Kim</u>[1], Seungbok Lee[3], Saet Pyoul Kim[1], Jinju Park[1], Kyu Chang Wang[2], Ji Yeoun Lee[1,2]

[1]Department of Anatomy, Seoul National University College of Medicine, Seoul, Republic of Korea
[2]Department of Pediatric Neurosurgery, Seoul National University Children's Hospital, Seoul, Republic of Korea
[3]Department of Pediatrics, Seoul National University Children's Hospital, Seoul, Republic of Korea

The tailbud of chick embryo is commonly known as the caudal cell mass (CCM) which consists of a population of neuromesodermal progenitor cells. CCM is known to be a key player in secondary neurulation, a critical developmental process that shapes the neuraxis, where it contributes to the developing secondary neural tube. We analyzed the transcriptomic profile of the CCM to better understand its exact role and underlying mechanism in secondary neurulation. CCM tissue was microdissected from chick embryos of developmental stages HH16, HH20, HH28 where secondary neurulation is most active and the CCM is most prominent. Pooled mRNA was sequenced using next generation sequencing technology and analyzed. Principal component analysis (PCA) and sample clustering analysis revealed that gene expression well represented their developmental stages. HH20 in the PC2 axis seemed to be apart from the other two indicating that HH20 is not only intermediate but also has unique properties in secondary neurulation. Differentially expressed gene (DEG) analysis using gene ontology (GO) and KEGG pathways showed enrichment in a variety of processes including mesenchyme development, somite development, anterior posterior pattern specification, and notch signaling. Through this study we expect that identifying pathways and DEGs regulated by CCM may provide novel mechanistic insight in secondary neural tube formation and a potential therapeutic strategy for neural tube defects.

Key Words: Chick embryo, Neurulation, Neuromesodermal progenitor, Transcriptome

P220

Human neural organoid model exhibiting early neural tube morphogenesis

<u>Ju-Hyun Lee</u>[1], Mohammed R. Shaker[1], Hyun Jung Kim[1], June Hoan Kim[1], Hyogeun Shin[2], Minjin Kang[3], Tae Hwan Kwak[4], Im Joo Rhyu[1], Hyun Kim[1], Dong Wook Han[4], Il-Joo Cho[2], Dongho Geum[3], Woong Sun[1]

[1]Department of Anatomy, Brain Korea 21 Plus Program for Biomedical Science, Korea University College of Medicine, Seoul, Republic of Korea; [2]Center for BioMicrosystems, Brain Science Institute, Korea Institute of Science and Technology (KIST), Seoul, Republic of Korea; [3]Department of Biomedical Sciences, Korea University College of Medicine, Seoul, Republic of Korea; [4]Department of Stem Cell Biology, School of Medicine, Konkuk University, 120 Neungdong-ro, Gwangjin-gu, 05029 Seoul, Republic of Korea

The neural tube is an embryonic neural tissue that give rise to the central nervous system formation. It develops through an early developmental morphogenesis called neurulation, which is regulated by highly sophisticated cellular and molecular events. However, these regulatory mechanisms have been studied only in animal models due to ethical regulation towards research involving human subjects. Thus, it has remained challenging to develop in vitro model that recapitulate the human neurulation. Here, we established a novel method for producing neuruloids exhibiting neural tube morphogenesis using human pluripotent stem cells. Our neuruloids show specific features of neurulation, such as the induction and folding of the neural plate and the formation of neural tube. This is a highly reproducible method for producing a large quantity of neuruloids rapidly, allowing for the robust quantification of the generated neuruloids. Furthermore, we have extended the culture to further mature neuruloids toward spinal cord–like organoids that can form neuromuscular junctions and exhibit synchronized neural network activity. Neuruloids will be a useful tool for assessing genetic and environmental factors affecting neural tube development, and screening 'personalized drugs' for spinal cord diseases such as Amyotrophic Lateral Sclerosis (ALS).

Key Words: Organoid, Spinal cord, Development, Neurulation, Neural tube defects, Disease modeling.

P221

Development of CPNE7-derived Functional Peptide for Tubular Dentin Regeneration

Yoon Seon Lee, Joo-Cheol Park

[1]Laboratory for the Study of Regenerative Dental Medicine, Department of Oral Histology-Developmental Biology, School of Dentistry, Seoul National University

Aged odontoblasts at resting phase do not actively react to external stimuli by mineral deposition. Our previous study demonstrated that CPNE7, identified in preameloblast-conditioned medium, induces odontoblast differentiation and mineralization in vitro, and promoted tertiary dentin formation in beagle dog indirect pulp capping model. In this study, we investigated the role of CPNE7 in stimulating physiologic dentin formation using few different tooth defect models, and developed functional peptide derived from CPNE7 sequence. We observed tertiary dentin formation in both the dentin and pulp exposure models. The regenerated dentin showed the characteristics of physiologic dentin, regardless of the cavity depths. Dentinal tubule structure was clearly observed beneath the remaining dentin, instead of bone-like osteodentin commonly formed in MTA capping. In the case of dentin matrix protein complex treatment, tubular dentin was regenerated as previously reported. However, the number of dentinal tubules decreased remarkably when CPNE7 was neutralized. The same effects were observed for the functional peptide, KH001. In conclusion, CPNE7 seems to induce both the odontoblast differentiation and reactivation. The depth of cavities, in other words, the extent of the external stimuli determines whether CPNE7 induces pulp stem cells to differentiate into new odontoblasts, or simply reactivates the underlying odontoblasts at resting phase. In both cases, physiologic dentin retaining dentinal tubules were regenerated in vivo. The development of the functional peptide may pave the way to potential therapeutic application for dental caries.

Key Words: Odontoblast, Dentin, Regeneration, Copine, Medication

P222

Expression of the Hutchinson-Gilford Progeria mutation leads to aberrant dentin

formation

Hwajung Choi[1], Tak-Heun Kim[1], Ju-Kyung Jeong[1], Charlotte Strandgren[2], Maria Eriksson[2], Eui-Sic Cho[1]

[1]Cluster for Craniofacial Development and Regeneration Research, Institute of Oral Biosciences, Chonbuk National University School of Dentistry, Jeonju, South Korea
[2]Department of Biosciences and Nutrition, Center for Innovative Medicine, Karolinska Institutet, Huddinge, Sweden

Hutchinson-Gilford progeria syndrome (HGPS) is a rare accelerated senescence disease that manifests in dental abnormalities and which has several symptoms suggestive of premature aging. Although irregular secondary dentin formation in HGPS patients has been reported, pathological mechanisms underlying aberrant dentin formation remain undefined.

In this study, we analyzed the mandibular molars of a tissue-specific mouse model that overexpresses the most common HGPS mutation (*LMNA*, c.1824C>T, p.G608G) in odontoblasts.

In the molars of HGPS mutant mice at postnatal week 13, targeted expression of HGPS mutation in odontoblasts results in excessive dentin formation and pulp obliteration. Circumpulpal dentin of HGPS mutants was clearly distinguished from secondary dentin of wild type (WT) littermates and its mantle dentin by considering the irregular porous structure and loss of dentinal tubules. However, dentin was significantly thinner in the molars of HGPS mutants at postnatal weeks 3 and 5 than in those of WT mice. *In vitro* analyses using MDPC-23, a mouse odontoblastic cell line, showed cellular senescence, defects of signaling pathways and consequential downregulation of matrix protein expression in progerin expressing odontoblasts. These results indicate that expression of the HGPS mutation in odontoblasts disturbs physiological secondary dentin formation. In addition, progerin expressing odontoblasts secrete paracrine factors that can stimulate odontogenic differentiation of dental pulp cells. Taken together, our results suggest that aberrant circumpulpal dentin of HGPS mutant results from defects in physiological secondary dentin formation and consequential pathologic response stimulated by paracrine factors from neighboring progerin-expressing odontoblasts.

Key Words**:** HGPS, Premature senescence, Circumpulpal dentin, Tertiary dentin

P223

β-catenin is essential for the fate determination of Hertwig's epithelial root sheath

Tak-Heun Kim, Siqin Yang, Ju-Kyung Jeong, Eui-Sic Cho

Cluster for Craniofacial Development and Regeneration Research, Institute of Oral Biosciences, Chonbuk National University School of Dentistry, Jeonju, South Korea

Wnt/β-catenin signaling plays multiple roles in both dental epithelium and mesenchyme during various stages of tooth development. Previously, we reported that Wnt/β -catenin signaling is essential in odontoblasts for tooth root formation. However, it remains unknown whether Wnt/β-catenin signaling is required in Hertwig's epithelial root sheath (HERS), essential for tooth root formation. To address the contribution of Wnt/β-catenin signaling in HERS during root development, we analyzed mice with inducible *β-catenin* disruption or stabilization allele in HERS.

Following the disruption of *β-catenin* induced by tamoxifen administration, HERS was prematurely dissociated in the developing root apex and further root elongation was impaired. In contrast, HERS

dissociation was failed after root dentin formation and it covered the root dentin surface following the induction of *β-catenin* stabilization. Moreover, neither acellular cementum nor cementoblasts were observed and mineralization of the neighboring root dentin was severely impaired. These results indicate that Wnt/β-catenin signaling is necessary to maintain cellular integrity of HERS until completion of root formation, and that excessive Wnt/β-catenin signaling disturbs HERS dissociation after root dentin formation and leads to impaired acellular cementum formation and dentin mineralization. Taken together, it is suggested that Wnt/β-catenin signaling plays an essential role in root and cementum formation through the fate determination of HERS. These findings may provide new insight to understand molecular and cellular events underlying root and cementum formation.

Key Words**:** Wnt signaling, Inactivation, Stabilization, HERS, Dissociation

P224

Light- and drug-gated optogenetic technique for the regulation of Wnt signaling

Seung Hwan Lee[1,2], Woong Sun[1,2], Dongmin Lee[1,2]

[1]Department of Biomedical Science, Brain Korea 21 PLUS, College of Medicine, Korea University, Seoul, Republic of Korea
[2]Department of Anatomy, College of Medicine, Korea University, Seoul, Republic of Korea.

Optogenetic techniques which control intracellular biomolecules with light have been applied to various biological fields due to their precise manipulation power with high spatio-temporal resolution. Especially, optogenetic control is the most suitable approach to turn on or off critical differentiation factors in the developmental study. Recently, new optogenetic method was successfully established to control the Wnt signaling, one of the most critical differentiation pathways, by light-dependent clustering of CRY2 and LRP6c. However, continuous blocking of room-light brings procedural troubles in long-term period experiments and the single trigger system using light alone accumulates undesired backgrounds. Hereby, we design AND-gate based Wnt3a signaling regulatory system by combining chemogenetic and optogenetic modules, FRB-FKBP and CRY2, respectively. We construct two-component synthetic proteins consisting of CRY2-FKBP and FRB-LRP6c. In HEK293T cell-line test, both blue light and Rapamycin induce faithful gene-expression by SEAP reporter system, indicating light- and drug-dependent Wnt activation. This double trigger system will provide user defined time-windows for Wnt signaling regulation and effectively reduce a background activity during in vivo or long-term culture experiments.

Key Words: Optogenetics, Wnt signaling, CRY2, FRB, FKBP

P225

Primary Cilium Plays Differential Roles During Cochlear Development

KyeongHye Moon[1], HongKyung Kim[1], Jeong-Oh Shin[1], Ji-Hyun Ma[1], Sun Myoung Kim[2], Ping Chen[2], Doris K. Wu[3], Hyuk Wan Ko[4], Jinwoong Bok[1]

[1]College of Medicine, Yonsei University, Seoul, South Korea
[2]School of Medicine, Emory University, Atlanta, GA, USA
[3]National Institute on Deafness and other Communication Disorders, Bethesda, MD, USA

[4]College of Life Science and Biotechnology, Yonsei University, Seoul, Korea

The primary cilium serves as a signaling center for several cellular pathways important for development including Sonic hedgehog (SHH). Defects in the primary cilium are associated with a range of genetic disorders known as ciliopathies, which include hearing loss. Previous studies showed that ciliary defects resulted in a shortened cochlear duct and abnormal hair cell polarization. While the hair cell polarization defect is attributed to defective planar cell polarity (PCP) signaling, the cause for shortened cochlear duct and precise etiology of the hearing loss in ciliopathies remain unclear. To understand the role of primary cilia in the inner ear, we analyzed three different ciliary mutants, *Broad-minded* (*Bromi*) mutant, *Intestinal cell kinase* (*Ick*) knockout (KO), and conditional knockout of *Ift88* (*Pax2-Cre; Ift88^{lox/lox}, Ift88* cKO). *Ift88* cKO mutants lack the primary cilium, while *Bromi* and *Ick* mutants show abnormal morphology and length of the cilium. All three mutants exhibited shortened cochlear duct, extra rows of hair cells in the apex, premature hair cell differentiation, and decreased hair cell number. In addition, *Bromi* and *Ift88 cKO* developed ectopic vestibular-like hair cells in the Kölliker's organ and exhibited reversed hair cell differentiation wave. Moreover, the expression of an apical cochlear marker, *Msx1*, which requires high levels of SHH signaling, was reduced or absent. These phenotypes closely resemble those of mutants carrying defective SHH signaling. Indeed, *Ptch1* expression, which is a direct readout of SHH signaling, was compromised in the developing inner ears of the ciliary mutants. These results indicate that the major cause of cochlear phenotypes of ciliary mutants is misregulated SHH signaling. Interestingly, we observed that there is a transition from the primary cilia to the kinocilia at the onset of hair cell differentiation. Although we did not observe an obvious difference in their microstructures, there was a clear change in their ability to respond to SHH signaling. We are currently investigating how such transition contributes to mediate diverse roles of SHH signaling essential for cochlear development. Taken together, our results demonstrate the complexity of ciliary mutants and the importance of the primary cilia in mediating multiple roles of SHH signaling during cochlear development.

Key Words**:** Primary Cilia, Shh Signaling, Cochlea, Auditory Hair Cell, Development, Hearing Loss

P226

The Comparasion of *Eucommia ulmoides* And *Cibotium barometz* Ethanol Extract On Fetal Growth of Wistar Rat Fetus

Heddy Herdiman[1], Jeanny Ervie Ladi[2], Cherry Azaria[2], Christian Edwin[3], Syani Lesmana[3]

[1]Department of Anatomy Faculty of Medicine Maranatha Christian University, Bandung, Indonesia
[2]Department of Histology Faculty of Medicine Maranatha Christian University, Bandung, Indonesia
[3]Faculty of Medicine Maranatha Christian University, Bandung, Indonesia

Eucommia ulmoides and *Cibotium barometz* are traditional Chinese medicine that is widely consumed all over the world, especially by pregnant women to strengthen the womb. Safety in consuming *Eucommia ulmoides* and *Cibotium barometz* needs to be investigated because most of the consumers are pregnant women who feared those herbs would affect fetal development. The purpose of the study is to find the effect of *Eucommia ulmoides* (EU) and *Cibotium barometz* (CB) ethanol extract on fetal growth. By experimental research, using male and female rats mated up until pregnant. Pregnant female rats were divided into 7 groups which were given the treatments of: CMC

1% as negative control, EU 400 mg/kgBW, EU 800 mg/kgBW, EU 1600 mg/kgBW, CB 500 mg/kgBW, CB 1000 mg/kgBW, and CB 1500 mg/kgBW at 11 days of gestation and dissected when the pregnancy was at 20 days to retrieve the rat's fetus sample. Data measured were weight (g), length (cm), and calcification length of femur (mm) of fetal rat using Alizarin Red color staining. The data was analyzed using one way ANOVA followed by LSD test. Generally, *Eucommia ulmoides* and *Cibotium barometz* ethanol extract showed statistically significant ($p<0.05$) increase in body weight, body length, and calcification length of the rat fetus' femur. Among other, the EU 400 mg/kgBW group showed no difference in the means of femur calcification length compared to control. We concluded that *Eucommia ulmoides* and *Cibotium barometz* ethanol extract increases body weight, body length, and the calcification length of the femur of rat's fetus.

Key Words: *Eucommia ulmoides*, *Cibotium barometz*, Body weight, Body length, Calcification of femur bone, Wistar rat fetus

P227

Transcription Factor Tbx5 Promotes Cardiomyogenic Differentiation of Cardiac Fibroblasts Treated with 5-azacytidine

Yangyang Jia[1], Yuqiao Chang[1], He Li [2], Zhikun Guo[1]

[1]Henan Key Laboratory of Medical Tissue Regeneration, Xinxiang Medical University, Xinxiang 453003, PR China
[2]Department of Histology and Embryology, Tongji Medical College, Huazhong University of Science and Technology, Wuhan 430030, PR China

Cardiac fibroblasts (CFs) are assumed to possess multidirectional differentiation potential similar to stem cells. The cardiac-specific transcription factor Tbx5 is considered to be an important factor in myocardial development. The aim of this study is to investigate the cardiomyogenic differentiation potential of rat CFs treated with 5-azacytidine (5-aza) and the effect of Tbx5 on CFs during myocardial differentiation. The CFs were initially isolated and identified, then were cultured in induction medium to induce cardiomyogenic differentiation. Morphological changes and cardiac troponin T (cTnT) expression of CFs were evaluated by phase-contrast microscopy and immunofluorescence, respectively. Cell viability and contractility were monitored using a real-time cell analyzer (RTCA) Cardio Station. Cardiac specific genes and proteins expression were determined by RT-PCR and Western blotting. Vectors harboring Tbx5 or empty vectors were transferred into CFs. The expression of Tbx5 and cTnT were analyzed by immunostaining and western blotting. Morphologically, the induced cells exhibited a lower proliferative capacity, appeared thicker and refractive on phase-contrast microscopy, and with a rod-like shape or a long spindle shape. Immunofluorescence staining showed that the differentiated cells expressed sarcomeric proteins cTnT. On day 28 after induction, the cTnT positive rate in 10μmol/L and 15μmol/L 5aza-induced group were $7.92 \pm 0.6\%$ and $10.64 \pm 0.28\%$. Correspondingly, the rate was $0.74 \pm 0.03\%$ in the cells without 5-aza. However, the contractility was not detected. RT-PCR and western blotting analyses showed that the 5-aza treated cells expressed a broad range of cardiac genes and multiple cardiac-specific proteins at different time. The addition of Tbx5 up-regulated the expression of sarcomere proteins cTnT in CFs more efficiently at weeks 3 compared with 5aza-treated alone ($p<0.05$). The overexpression of Tbx5 plays an important role in the process of cardiogenic differentiation, which can enhance the myocardial differentiation of CFs induced by 5aza.

Key Words: 5-aza, Myocardial differentiation, Tbx5, Cardiomyocytes, Cardiac fibroblasts

P228

A new structure from cardiac cells cultured *in vitro*: cardiomyocyte-annulation

Li Cixia, Chang Yuqiao, Jia Yangyang, Guo Zhikun

Henan Key Laboratory of Medical Tissue Regeneration, Xinxiang Medical University, Xinxiang 453003, PR China

To explore the formation, morphological characteristics, cell composition, and differentiation potential of cardiomyocyte annulation (cardio-annulation) during *in vitro* culture of cardiac cells. Rat cardiac cells were isolated and cultured. A live-cell imaging system was used to observe cardio-annulation. Cardiac troponin-T (cTnT) and vimentin were labeled with double immunofluorescence staining, and coexpressions of cTnT and connexin43 (Cx43), cTnT and nanog, c-kit and nanog, and c-kit and stem cell antigen (sca-1) were detected. The location of various types of cells within the cardio-annulation structure was observed. Adipogenic- and osteogenic-inducing fluids were used separately for *in situ* induction to detect the multidirectional differentiation potential of cells during the annulation process. After 3-6d, cardiac cells migrated and formed an open or closed annulus with a diameter of 800-3500μm. The annulus wall comprised the medial, middle, and lateral regions. The cells in the medial region were small, abundant, and laminated, those in the middle region were larger with fewer layers, and those in the lateral region were less abundant, and loosely arranged in a single layer. Cardiomyocytes were distributed mainly on the surface of the medial region; nanog$^+$, c-kit$^+$, and sca-1$^+$ cells were located mainly at the bottom of the annulus wall and fibroblasts were located mainly between these layers. The annulus cavity contained a large number of small, round cells and telocytes. Cx43 was expressed in all cell types, and nanog$^+$, c-kit$^+$, and sca-1$^+$ were coexpressed in the cardio-annulation cells, which possess adipogenic and osteogenic differentiation potential. Cardio-annulation was discovered during an *in vitro* culture of cardiac cells. The structure contains cardiomyocytes, fibroblasts, telocytes, and abundant stem cells. These results provide insight into the relationship among cardiac cells *in vitro*.

Key Words: Cardiac cells, *In vitro* cell culture, Cardiomyocyte annulation, Cardiosphere, rats

P229

Kruppel like factor 4 (KLF4) induces apoptosis in granulosa cells involving the Bcl-2/Bax pathway during periovulatory period

Doyeon Kim, Hyeonhae Choi, Jaesook Roh*

Laboratory of Reproductive Endocrinology, Dept. of Anatomy & Cell Biology, College of Medicine, Hanyang University, Seoul 133-791, South Korea

The important role of *KLF4* in proliferation and differentiation was evident from its highly restricted expression pattern and from its involvement in transcriptional control of genes relevant for cell cycle and apoptosis in the epithelial cells of several organs. There is considerable evidence that *KLF4* is one of transcription factors highly induced by the luteinizing hormone (LH) surge in ovarian granulosa cells (GCs), suggesting that it could play a role in cell survival during the periovulatory period.

Therefore, we evaluated if *KLF4* involves in cell survival of GCs during the LH surge-induced luteal transition. Primary GCs were obtained from preovulatory follicles of PMSG-primed rat ovary. *KLF4, Bax* and *Bcl-2* mRNA levels in GCs treated with different doses of LH were analyzed by Real-time RT-PCR. Cell viability was measured with CCK-8 assays and apoptosis was analyzed with Annexin-AAD staining by flow cytometry. In this investigation, we demonstrated the expression of *KLF4* in mature GCs isolated from preovulatory follicles and found that *KLF4* level was significantly increased by ovulatory dose of LH treatment, suggesting a potential role for *KLF4* in cell differentiation. Moreover, apoptosis and delayed growth of cells induced by overexpression of *KLF4* further demonstrated the hypothesis. Thus, we conclude that *KLF4* has an important role in the regulation of LH-dependent signaling pathways in the luteinization.

Key Words: KLF4, Granulosa Cells, LH surge, Apoptosis, Proliferation

P230

NOX1 AND NOX4 EXPRESSION DURING MOUSE LIVER AND LUNG DEVELOPMENT

Kasun Weerasekara Mudiyanselage, Sushan, Zhang, Qing Ge, Kim Hyun-Yi, Jung Han-Sung

Division of Anatomy and Developmental Biology, Department Oral Biology, BK21 PLUS Project, Yonsei University College of Dentistry, Seoul, South Korea

Despite differences in the pathology, the role of nicotinamide adenine dinucleotide phosphate (NADPH) oxidases 1 (NOX1) and NOX4 during organ development is still not well elucidated. In this study, we examined their expressions at different stages of developing mouse liver and lung. Immunofluorescence staining indicated that NOX1 and NOX4 are highly localized in early liver and lung development but were decrease late gestation. By contrast, mRNA expressions of *NOX4* in liver and *NOX1* in lung were gradually upregulated over time. Importantly, NOX4 was clearly localized in the proximal airway smooth muscle (ASMC). *NOX1* expression was significantly elevated in NOX4 knockout mice embryonic lung at E17.5. 48 hours *in-vitro* lung culture data indicated that the inhibition of few NOX enzymes at once, airway branching was dysregulated. Following pan-NOX inhibitor (NOX1, NOX2, and NOX4), GKT137831 treatment (100μM), the airway thickness was decreased, in contrast, the number of developing lung buds were increased. Taken together, our results suggest that NOX1 and NOX4 are essential in the liver and lung development. Specially, NOX family enzymes might play a pivotal role in the airway branching morphogenesis and could prevent from late pathological anomalies. Further experiments are necessary to elucidate the correlation among NOX4 mediated redox signaling in ASMC and airway branching morphogenesis.

Key Words: NOX, Airway smooth muscle, *in vitro* lung culture, GKT137831

P231

LEPR Gene Polymorphism in Osteoporosis among Mulao ethnic in Chinese

Xiaoyun Bin, Lianfei Yin, Minzhou, Yandong Huang, Xiufeng Huang, Chuhan Liang, Juan Wu

Preclinical college, Youjiang medical university for nationalities, China,533000

Aims: Osteoporosis is a complex multifactorial disorder of gradual bone loss and increased

fracture risk. While previous studies have shown the importance of many genetic factors in determining peak bone mass and fragility fractures and in suggesting involvement of Leptin receptor (LEPR) in bone metabolism and bone mass, the relationship of LEPR genetic diversity with bone mass/osteoporosis has not yet been revealed. **Materials and methods:** The current study investigated the potential relevance of LEPR gene polymorphism in osteoporosis among a Mulao ethnic Chinese cohort of 623, including 237 normal bone mass controls, and 386 osteoporosis of different ages. Bone density was examined by calcaneus ultrasound attenuation measurement, and single nucleotide polymorphisms (SNPs) and linkage disequilibrium analyses were performed on five SNP loci of LEPR gene. **Results:** Significant difference in BMD was found between 45yrs group and above 75 yrs group in males, and the same was detected between all groups above 55yrs and 45yrs group, between 70yrs group, above 75yrs group and the rest ones in females. The proportion of osteoporosis gradually increased with age from 0 to 19% in males and from 0 to 50% in females. Pearson correlation analysis showed that BMD was negatively correlated with age, while positively and significantly correlated with weight, height and BMI. Out of 6 SNPs, significant difference was found in the genotype frequency of LEPR rs1751492, rs2767485 in OP groups compared to control subjects ($P < 0.001$). Regarding the rs1751492, the prevalence of C allele compared to T allele was significantly different among the groups ($P = 0.008$), while rs2767485 the prevalence of T allele compared to C allele was significantly different among the groups ($P = 0.002$). Results of multinomial regression analysis indicated that T allele carriers in the recessive genetic model (TT vs. CC+ CT) of rs1751492 had a significantly risk protective effect of OP (OR = 1.167; 95% CI = 1.041–1.307; $P = 0.008$), while the T allele carriers in the recessive genetic model (TT vs. CC+ CT) of rs2767485 had a protective effect t(OR = 0.292; 95% CI = 0.131–0.648; $P = 0.001$). **Significance:** The findings of present study revealed that the LEPR rs 1751492 gene polymorphism might serve as predisposing factor, while rs2767485 serve as a protective factor in OP.

*Correspondence to E-mail: bxy889@163.com, Tel:+8615277699551

P232

Mining of the co-expressed genes of Myh-11 related to spermatogenesis

Hao Zhang, Rui-xiu Li, Wen-xiu Li, Rui Xiao

Key Laboratory of Molecular Pathology, Inner Mongolia Medical University, Hohhot, P. R. China

Myosin has been involved in spermatogenesis and plays an important role in acrosome formation, nuclear morphogenesis, mitochondrial translocation and sperm individualization. Myosin heavy chain MYH-11, a marker of the smooth mucle cells, affects the sperm tube wall contraction and sperm movement process, leading to the male infertility and other related diseases. Therefore, it is important to identify the co-expressed genes of MYH-11 to explore the MYH-11 function and the molecular mechanism underlying male infertility. In this study, bioinformatics analysis of Myh-11 (mus musculus) co-expression network was performed. The predicted Myh-11 co-expression genes were identified and classified by GO analysis, KEGG pathway and litterature study. As a result, Actg2 is considered as a major co-expressed genes with Myh-11, and may play an important role in male sterility. Further study needs to be done to confirm it.

Key Words: Myh-11, bioinformatics, male sterility, Actg2

P233

The genetic structure of Sui people in southwest China

Xiufeng Huang[1], Chaowen Lin[1], Rongyao Wei[1], Xiaoyun Bin[1], Chuanchao Wang[2]

[1]Preclinical college, Youjiang medical university for nationalities, China
[2]Department of anthropology and ethnology,Xiamen University, China

The Sui people are one of the 56 officially recognized ethnic groups living mostly in Guizhou and Guangxi, southwest China. However, there is no genomic data reported from this group until now. Here we collected 68 Sui samples from Huanjiang, Yizhou, Dushan, Sandu, Libo, Duyun, and Nandan, and genotyped with more than half million genomewide single nucleotide polymorphisms (SNPs). We used Principal Component Analysis (PCA), ADMIXTURE analysis, f statistics, qpWave and qpAdm to infer the population genetic structure and admixture. Our data revealed that Sui people are genetically similar to the Kam-Sui speaking populations in southwest China, which is consistent with their language affinity. We also observed genetic substructure in Sui people. The Sui people in Huanjiang compared with other Sui groups share more alleles with Miao people and the Sui people in Yizhou share more alleles with Tibetans, suggesting gene flow between Sui and other surrounding populations.

*Correspondence to Xiufeng Huang (E-mail:hxflcw@163.com, Tel:+8613707768113)

P234

Single Nucleotide Polymorphisms at C677T and A1298C of Methylenetetrahydrofolate Reductase (MTHFR) Gene in mothers with Down syndrome children in Myanmar

Ei Ei Lwin[1], Zaw Zaw Latt[1], Nyo Nyo Myint[2], Myint San New[3]

[1]Associate Professor, Department of Anatomy, University of Medicine 2, Yangon, Myanmar
[2]Professor and Head, Department of Anatomy, University of Medicine 2, Yangon, Myanmar
[3]Professor and Head, Department of Anatomy, University of Medicine 1, Yangon, Myanmar

Down syndrome is a genetic disease resulting from the presence of three copies of the genes located on chromosome 21. Advanced maternal age is the only fully accepted risk factor for trisomy 21, however several young women aged less than 35 year give birth to Down syndrome children, suggesting a susceptibility to early chromosome malsegregation. The present study evaluated the two polymorphisms in genes encoding the folate metabolizing enzyme methylenetetrahydrofolate reductase namely, C677T and A1298C in 70 Myanmar mothers of Down Syndrome child and 70 matched control mothers, using Polymerase Chain Reaction - Restriction Fragment Length Polymorphism (PCR-RFLP). Frequencies of MTHFR C677T genotypes (CC, CT, and TT) and also combination of heterozygous and homozygous variant genotypes (CT or TT) demonstrated significant difference between mothers of children with Down syndrome and mothers of children without Down syndrome. Variant genotypes of MTHFR A1298C (AC or CC) were also significant differences when compared between the two groups. The combined presence of both polymorphisms was associated with a greater risk pregnancy with Down syndrome than the presence of either alone. T allele of SNP 677 was 4.63 fold and C allele of SNP 1298 was 2.823 fold increased risk of pregnancy with Down syndrome. When a person have both risk alleles of haplotypes of both SNPs (SNP 677 and SNP 1298), the risk of developing pregnancy with Down syndrome became 3.5 times of those having one risk alleles of either SNP 677 (or) SNP 1298.The data presented in this study found that Single nucleotide

polymorphisms at C677T and A1298C of methylenetetrahydrofolate reductase gene are associated with increased maternal risk of pregnancy with Down syndrome in Myanmar women.

Key Words: Methylenetetrahydrofolate reductase (MTHFR), Down syndrome, Polymorphism, Trisomy 21, MTHFR 677C> T polymorphism;,MTHFR 1298A>C polymorphism

P235

Microvesicles from brain-extract-treated mesenchymal stem cells promote neuro behavior function in a rat model with stroke

Ji Yong Lee[1], Byung Pil Cho[1,2], Won Gil Cho[1], Young Chul Yang[1], Byoung Young Choi, Han-soo Kim[3,4,*]

[1]Department of Anatomy, Yonsei University Wonju College of Medicine, Wonju-si, Korea
[2]Institute of Lifestyle Medicine, Yonsei University Wonju College of Medicine, Wonju, Korea
[3]Department of Biomedical Sciences, Catholic Kwandong University College of Medical convergence, Gangneung-si, 25601, Korea
[4]Institute for Healthcare and Life Science, International St. Mary's Hospital and College of Medicine, Catholic Kwandong University, Incheon, Korea

Transplantation of mesenchymal stem cells (MSCs) was reported to improve functional outcomes in a rat model of ischemic stroke, and subsequent studies suggest that MSC-derived microvesicles (MVs) can replace the beneficial effects of MSCs. Here, we evaluated three different MSC-derived MVs, including MVs from untreated MSCs (MSC-MVs), MVs from MSCs treated with normal rat brain extract (NBE-MSC-MVs), and MVs from MSCs treated with stroke-injured rat brain extract (SBE-MSC-MVs), and tested their effects on ischemic brain injury induced by permanent middle cerebral artery occlusion (pMCAO) in rats. NBE-MSC-MVs and SBE-MSC-MVs had significantly greater efficacy than MSC-MVs for ameliorating ischemic brain injury with improved functional recovery. We found similar profiles of key signaling proteins in NBE-MSC-MVs and SBE-MSC-MVs, which account for their similar therapeutic efficacies. Immunohistochemical analyses suggest that brain-extract—treated MSC-MVs reduce inflammation, enhance angiogenesis, and increase endogenous neurogenesis in the rat brain. We performed mass spectrometry proteomic analyses and found that the total proteomes of brain-extract—treated MSCMVs are highly enriched for known vesicular proteins. Notably, MSC-MV proteins upregulated by brain extracts tend to be modular for tissue repair pathways. We suggest that MSC-MV proteins stimulated by the brain microenvironment are paracrine effectors that enhance MSC therapy for stroke injury. (Grant supported by the National Research Foundation, MSIP, 2012M3A9B4028639, 2017M3A9B4042583,)

Key Words: Microvesicles, mesenchymal stem cells, middle cerebral artery occlusion, cerebral ischemia, paracrine signaling

P236

Isolation and Differentiation of Neural Stem/ Progenitor Cells From Subventricular Zone of One Adult Rat

Mohammad Hossein Asadi[1], Bahman Jalali Kondori[1], Hossein Bahadoran[1]

[1]Department of Anatomical Sciences, School of Medical Sciences, Baqiyatallah University of Medical

Sciences, Tehran, Iran.

Introduction: In adult mammalian brain, neural stem cells are isolated from both the dentate gyrus and subventricular zone. This study aimed to isolate neural stem cells from adult rat subventricular zone and differentiate them into neurons and astrocytes. **Methods:** In this study, the whole brain was removed after full anesthesia and creating cervical dislocation. Under a microscope, subventricular zone was dissected by a coronal incision in optic chiasm zone. Enzymatic digestion was performed using trypsin-EDTA. The isolated cells from one brain were cultured in serum free DMEM/F12 medium, containing bFGF (basic Fibroblast Growth Factor) and EGF (Epidermal Growth Factor) growth factors. **Results:** Neurospheres were observed five days after culturing. Immunocytochemistry was used to investigate nestin gene expression and identify neural stem cells. Neural stem cells were differentiated in poly-L-lysine coated plates in the absence of growth factors. The expression of GFAP, β tubulin III, and nestin genes were analyzed by RT-PCR. The results of immunocytochemistry confirmed nestin gene expression in the neural stem cells. Phenotype of neurons and astrocytes were observed 5 days after cell culture in differentiation medium. RT-PCR analysis revealed the expression of GFAP and β tubulin III genes. **Conclusion:** The results of this research show that only one rat brain is needed for neural stem cells isolation and differentiation to neurons and astrocytes.

Key Words**:** Neural stem cells, Astrocytes, Neurons, Cell differentiation

P237

Neuronal restoration effect of secretome from pluripotent stem cell-derived neural precursor cells in rat model with stroke

Ji Yong Lee[1], Byung Pil Cho[1,2], Won Gil Cho[1], Young Chul Yang[1], Byoung Young Choi, Han-soo Kim*[3,4]

[1]Department of Anatomy, Yonsei University Wonju College of Medicine, Wonju-si, Korea
[2]Institute of Lifestyle Medicine, Yonsei University Wonju College of Medicine, Wonju, Korea
[3]Department of Biomedical Sciences, Catholic Kwandong University College of Medical convergence, Gangneung-si, 25601, Korea
[4]Institute for Healthcare and Life Science, International St. Mary's Hospital and College of Medicine, Catholic Kwandong University, Incheon, Korea

Recently, cell-based therapy has been highlighted as an alternative to treating ischemic brain damage in stroke patients. We previously showed that the transplantation of pluripotent stem cell-derived neural precursor cells (NPCs) improve functional outcomes in a rat model of ischemic stroke. NPCs exerted the beneficial effects, in part, through paracrine mechanism. Subsequent studies using the same model have suggested that NPC secretome replace the beneficial effects of NPCs. In this study, we investigated the ability of NPC secretome to attenuate ischemic brain injury induced by permanent middle cerebral artery occlusion (pMCAO) in rats. To examine the therapeutic benefits of NPCs secretome in an ischemic stroke model, intravenous (I.V) injections (0.2 mg/kg) were administered to Sprague-Dawley rats 1 day after pMCAO. Our results demonstrated that NPCs secretome ameliorated ischemic brain injury with improved functional recovery. To investigate its underlying events, immunohistochemical (IHC) analysis was performed on rat ischemic brains. Immunohistochemical analyses showed that NPCs secretome evidently lowered the positivity of microglial ED-1 and astrocytic GFAP, suggesting a suppression of adverse glial activation in the ischemic area of host brain. In addition, NPCs secretome elevated the expression of CD31(+) and won-willebrand factor (vWF) immunoreactivity indicating angiogenic stimulation in the host brain.

Finally, NPCs secretome elevated the expression of BrdU (+) cells in the ipsilateral subventricular zone (SVZ) indicating neurogenic stimulation in the ischemic injured brain. Taken together Taken together, NPCs secretome reduced inflammation, enhanced angiogenesis with increased endogenous neurogenesis in rat injured brain. In conculsion, NPCs secretome promotes the functional recovery of damaged stroke brain via modulation of anti-inflammation, angiogenesis and neurogenesis. Thus, NPCs secretome closely recapitulated the effects seen upon NPCs transplantation

Key Words**:** Secretome, Neural precursor cells, Middle cerebral artery occlusion, Paracrine

P238

Optimizing clump culture method to isolate adult human multipotent neural cells

Ji-Yoon Hwang[1,3,4], Hye Won Lee[1,3], Hee Jang Pyeon[1,3,4], Jeong-Seob Won[2,3,4], Yoo-Jung Roh[1,3,4], Hyun Nam[1,3,4,*], Kyeung Min Joo[1,2,3,4,*]

[1]Department of Anatomy & Cell Biology, Sungkyunkwan University School of Medicine, Suwon, 16419, South Korea
[2]Department of Health Sciences and Technology, SAIHST, Sungkyunkwan University, Seoul, 06351, South Korea
[3]Single Cell Network Research Center, Sungkyunkwan University School of Medicine, Suwon, 16419, South Korea
[4]Stem Cell and Regenerative Medicine Center, Research Institute for Future Medicine, Samsung Medical Center, Seoul 06351, South Korea;

Neurodegenerative diseases (NDs) are incurable and irreversible, because damaged neurons could not be regenerated spontaneously. Stem cells could be therapeutics for NDs. Previously, we reported adult human multipotent neural cells (ahMNCs) isolated from temporal lobe of epileptic patients, which have similar characteristics of neural stem cells (NSCs). However, the difficulty of primary isolation and culture condition of ahMNCs lead to the limited application of ahMNCs. In this study, we developed primary clump culture method of ahMNCs with high efficiency. Brain tissues were partially digested with enzyme with mechanical mincing. Dissociated clumps were collected with different sizes of strainers, which were divided into four types of clumps including Clump I (clumps > 100-µm), Clump II (70-µm < clumps < 100-µm), Clump III (40-µm < clumps < 70-µm), and Clump IV (clumps < 40-µm). At 3 and 6 days after culture, Clump III showed the highest number of adherent colonies. ahMNCs derived from Clump II (ahMNCs-Clump II) showed similar characteristics to ahMNCs established by Percoll-density gradient. ahMNCs-Clump II differentiated into neuron (Tuj1+ and MAP2+) and astrocyte (GFAP+). In the results of in vivo Matrigel plug assay, ahMNCs-Clump II could make microvessels. In conclusion, we established novel clump culture method to isolate ahMNCs from human brain with high efficiency via optimizing clump size.

Key Words**:** Adult human multipotent neural cells Clump culture, Neural differentiation, Angiogenic potential

P239

Agmatine enhances differentiation of murine neural stem cells into neuronal lineage in mRNA level

Jae Hwan Kim[1], Jaemu Kim[2], Minah Suh[1,2]

[1]Biomedical Institute for Convergence at SKKU (BICS), Sungkyunkwan University, Suwon 16419, Korea (ROK)
[2]Center for Neuroscience Imaging Research, Institute for Basic Science (IBS), Suwon 16419, Korea (ROK)

Stem cell therapy has high therapeutic potential in CNS diseases. Spinal cord injury (SCI) has still needed optimal therapy to cure, so stem cell therapy is hopeful in SCI. In many research, neural stem cell therapy has shown meaningful effect in SCI but the lineage-specific differentiation efficiency of neural stem cell transplanted *in vivo* has room for improvement. Agmatine has displayed a neuroprotective effect in CNS diseases and improved functional recovery was found in spinal cord injured mice received agmatine-producing neural stem cell. These findings make us expect the synergy effect of combining neural stem cell transplantation and agmatine treatment in SCI. In this study, the effect of agmatine on differentiation of murine nerual stem cells was elucidated *in vitro*. Neural stem cells was induced to differentiate under favorable condition for differentiation or unfavorable condition for differentiation. Agmatine enhanced differentiation of neural stem cells without lineage-specificity under unfavorable condition. The mRNA expressions of MAP2, dcx, GFAP were increased. Under favorable condition, agmatine strengthened neuronal differentiation. Neuronal markers, MAP2 and dcx were increased but Glial marker, GFAP was decreased in mRNA expression. Oligodendrocyte marker, Olig2 had no difference in mRNA expression with or without agmatine treatment. Based on these results, it is presumed that agmatine enhance differentiation of neural stem cells transplanted in vivo. In next study, this hypothesis will be confirmed in CNS injury animal models, SCI and cerebral ischemia.

Key Words: Agmatine, Neural stem cell, Stem cell differentiation, Spinal cord injury, Cerebral ischemia

P240

Perinatal Stem Cells Have Better Differentiation Potency Than Bone Marrow-Derived Mesenchymal Stem cells in A Rat Ischemic Heart Injury Model

Yong Soo Park[1,2], Bong-Woo Park[3], Hyeok Kim[3], Ye-Ji Hong[1,2], Sung Won Jung[1,2], Seung Hee Lee[1,2], Sun-Sook Paik[1,2], Hun-Jun Park[4], In-Beom Kim[1,2,5]

[1]Department of Anatomy, The Catholic University of Korea
[2]Catholic Neuroscience Institute, The Catholic University of Korea
[3]Department of Life Science, College of Medicine, The Catholic University of Korea
[4]Cardiovascular Center, Seoul St. Mary's Hospital, The Catholic University of Korea
[5]Catholic Institute for Applied Anatomy, The Catholic University of Korea

Stem cell therapy for ischemic heart disease has emerged as a new treatment method to reduce progression of the heart failure, after myocardial infraction (MI). However, the effect of stem

cell therapy is still controversial, and needs further optimization. For the therapy, bone marrow (BM)-derived mesenchymal stem cells (MSCs) have been commonly considered because of their relatively ease acquisition and usability, but it has been reported that their survival and differentiation were limited. To test the possibility that perinatal stem cells can be used in stem cell therapy for MI, we applied two kinds of MSCs, chorion (C)-derived MSCs and umbilical cord (UC)-derived MSCs in a rat ischemic heart injury model and compared their effects to those of BM-MSC application. 8-week-old Fischer 344 rats were anesthetized with 2% inhaled isoflurane and intubated via the trachea for mechanical ventilation. Left ventricle was visualized through the left thoracotomy, and then left anterior descending artery was permanently ligated to induce myocardial infarction. Cells were labeled by DiI and injected in the border zone of the infarcted myocardium right after ligation with PBS and extracellular matrix. Echocardiogram was performed at 1, 2, 4, and 8 weeks after artery ligation and measured left ventricle ejection fraction (LVEF) and fraction shortening (FS). Hearts were perfused with PBS for 15 min, and fixed in 4% paraformaldehyde overnight. Tissues were embedded in paraffin and sectioned in 4 μm thickness. Three different cardiac markers, anti-human α-Sarcoplasmic action (α–SA), cardiac troponin-T (cTnT) and connexin 43 (CX43) were immunostained to evaluate degrees of differentiation into cardiomyocyte. In functional assessment, echocardiograms showed no differences in LVEF and FS among control injured group and MSC-injected groups (ANOVA, $p>0.05$). In tissue sections containing DiI-labled MSCs were apparently observed. In both C-MSC- and UC-MSC-injected groups, DiI-labeld MSCs expressed α-SA, cTnT and CX43 immunoreactivities, while in BM-MSC-injected group, MSCs did not. These results demonstrate that perinatal MSCs, UC-MSCs and C-MSCs have better differentiation potency than BM-MSCs in a rat ischemic heart injury model, suggesting that there are differences in differentiation potency among various kinds of MSCs. Perinatal MSCs could be better candidates for stem cell therapy for heart disease such as MI than BM-MSCs.

Key Words: Mesenchymal stem cell, Myocardial infarction, Differentiation, Cardiac markers

P241

Mesenchymal stem cells decrease oxidative stress in bowel of IL-10 knockout mice

Kyong-Jin Jung[1], Tae-Jin Lee[1], Joo-Young Kim[1], Eon-Gi Sung[1], Kun Woo Lee[2], Chul Hyun Park[2], Lee Byung Ik Jang[3] and In-Hwan Song[1]

[1]Department of Anatomy, Yeungnam University College of Medicine, Daegu, Republic of Korea
[2]Department of Orthopedic Surgery, Yeungnam University College of Medicine, Daegu, Republic of Korea
[3]Department of Internal Medicine, Yeungnam University College of Medicine, Daegu, Republic of Korea

Inflammatory bowel disease (IBD) is an autoimmune disease characterized chronic inflammation mainly in large intestine. The interleukin-10 knockout (IL-10 KO) mouse is a well-known animal model of IBD which develops spontaneous intestinal inflammation that resembles Crohn's disease. Oxidative stress is considered a leading cause of cell and tissue damage. Reactive oxygen species (ROS) itself can cause direct cell injury and/or cause indirect cell injury by secretion of cytokines from damaged cell. In this study, human bone marrow-derived mesenchymal stem cells (MSCs) was injected to IL-10 KO mice (MSC) and oxidative stress and inflammation levels were

evaluated in the large intestine and compared with those of control IL-10 KO mice (CON) and wild control mice (Wild). The levels of ROS (superoxide and hydrogen peroxidase) and secondary end product of lipid peroxidation (malondialdehyde) were significantly higher in CON but superoxide dismutase (SOD) and catalase levels were lower in MSC. Inflammation related markers (INF-γ, TNF-α, IL-4, and CD8) expression and inflammatory changes in histological analysis were much milder in MSC compare than CON. We conclude that MSCs have effects for redox balance this lead to suppression of IBD.

Key Words: Inflammatory bowel disease, Mesenchymal stem cells, Oxidative stress, Inflammation

P242

The expression of TGF-β, CK-14 in the treatment of scar wound by the bone marrow mesenchymal stem cells

Enhe jirigala, Weiming Xu, Xiaohe Li, ShaHuang, YanWu, Wenzhong, Liu Xiaobin Fu

Department of Anatomy, Inner Monglia Medical University, Hohhot, China

Objective: Study of repair effect on scar wound by transplantation of BMSCs. It provides experimental basis for the clinical application of BMSCs transplantation in the treatment of scar wounds and other related diseases. **Methods:** 1. BMSCs were isolated from the C57BL/6-GFP mouse bone marrow (2-3week) by whole bone marrow culture method and purified, cultured and amplified in vitro. The configuration and morphology of the stem cells were observed under inverted microscope and a stable isolation culture system of C57BL/6-GFP mouse bone marrow mesenchymal stem cells were established. Expression of BMSCs at the fourth passage isolated and cultured by this system were detected by flow cytometer. The proliferative ability of these cells were accessed by MTT test and a growth curve was drawn. 2. Using C57BL/6 mouse, to build the back skin excessive fibrosis model. 3.It is divided into two groups: injection of physiological saline as control group (group A), BMSCs transplantation group (groupB), To observe the GFP-BMSCs transplantation on fibrosis wound repair effect, and the repair mechanism research by GFP-BMSCs cells tracer detection, detection of apoptosis, histopathological staining, immunofluorescence detection of TGF-β, CK-14 factors method. **Results:** 1. Phase contrast microscopy from cells after cultivating 3 days demonstrated a fibroblast-like, spindle-shaped morphology. In later 14 days, the the spindle-shaped cells began to display a broadened, flat morphology, and arrange like a group of fish. Through the adipogenic differentiation of osteogenic induction training, have proved their multilineage differentiation capacity. Flow cytometric analysis showed: MSCs, CD29 (positive) 97.34%; CD90 (positive) 95.22%; CD45 (negative) 1.47%; CD105 (positive) 96.88%. MTT growth curve showed GFP-BMSCs proliferation are normal. 2. After seventh days of treatment control group without any changes in thickness, the average thickness of 52mm BMSCs group and control group had significant difference (P < 0.05). After fourteenth days control group the mean values of 57mm, BMSCs transplantation group the average thickness of 48mm, which were significant difference with control group (P < 0.01). Cell tracing display, BMSCs group at 1 hours, 6 hours, 12 hours can be tracer, cell number was decreasing, 24 hours without signal. Detection of apoptotic cells results showed that the apoptotic cells in group B were 6 hours more obvious, the most obvious 12 hours. Immunofluorescence revealed after 7 days, 14 days of transplantation group TGF-βexpression is relatively lower than the control group.While the changes in the expression of CK-14 for transplantation group than those in the control group expressed strong. **Conclusion:** The GFP-BMSCs transplantation in the wound subcutaneous, that make the skin fibrosis degree is reduced, and the skin epithelial degree is increased. visible GFP-BMSCs on wound healing have stimulative effect.

Key Words: Wound healing, Bone marrow mesenchymal stem cells, Green fluorescent protein-transgenic mice, Fibrosis

P243

Xenogeneic and allogeneic immunogenecity of human umbilical cord- and adipose tissue-derived mesenchymal stem cells

Jun Man Hong[1], Jin Hee Kim[2], Young-il Hwang[1]

[1]Department of Anatomy and Cell Biology, Seoul National University College of Medicine, Seoul, Korea
[2]Department of Biomedical Laboratory Science, College of Health Science, Cheongju University, Cheongju, Korea

Recently, efforts have been made to use mesenchymal stem cells (MSCs) for regenerative medicine and for the treatment of several immune and inflammatory diseases. To support such attempts, many animal experiments have been carried out using human MSCs. For correct interpretation of the results from these experiments, effects of xenogeneic immune responses must be considered, which has not been frequently described yet. Another issue in the use of MSCs is the so-called "off-the-shelf" usage of allogeneic MSCs. So far, MSCs are believed not to elicit allogeneic immune responses owing to their low expression of type II MHC molecules and their immunosuppressive characteristics. However, the possibility of alloimmune response by MSCs has been continuously suggested by some authors. This issue should be clarified for safe use of allogeneic MSCs. Here, we explored xenogeneic and allogeneic immune responses elicited by human MSCs derived from adipose tissue (Ad-MSCs) and umbilical cord connective tissue (UC-MSCs). Immuno-competent mice were injected with naive or activated Ad-MSCs or UC-MSCs twice with a 3-week interval to determine the xenogeneic immune response. Animals were sacrificed seven days after the second injection. The presence of xenogeneic immune responses were evaluated by immunoglubulin titration in the serum, staining of MSCs with immune serum, FACS profiling of splenic T cells, and germinal center staining in the spleen. For the evaluation of allogeneic immunity, multiple donor peripheral mononuclear cells (PBMCs) were co-cultured with MSCs or MSC lysates, and PBMC proliferation was estimated. As results, antibody titers of each isotypes, as well as total, were increased in mice immunized with MSCs, and these immune serum stained MSCs as revealed by FACS. Analysis of splenic T cells showed increased frequencies of memory and effector T cells compared to those from control mice. Also, developed germinal centers were observed in the spleen of MSC-injected mice with immunohistochemical staining for proliferating nuclear antigen. BrdU uptake by PBMCs increased in the co-culture with mitomycin-treated MSCs and cell lysates. Our results clearly shows that MSCs, which are known to have immunosuppressive capacity across species, apparently induced xenogeneic immune responses. Additionally, allogeneic immune responses were observed in *in vitro* experiments, which suggests a possible *in vivo* provocation of immune reaction by allogeneic MSCs. Attention should be paid to in the *in vivo* usage of allogeneic MSCs as a therapeutic purpose.

Key Words: Human mesenchymal stem cell, Adipose-derived mesenchymal stem cells, Umbilical cord-derived mesenchymal cells, Allogeneic immune response, Xenogeneic immune response

P244

Regeneration of taste sense by taste bud organoid

Sushan Zhang, Kasun Weerasekara Mudiyanselage, Qing Ge, Jong-Min Lee, Han-Sung Jung

Division in Anatomy and Developmental Biology, Department of Oral Biology, Oral Science Research Center, BK21 PLUS Project, Yonsei University College of Dentistry, Seoul, South Korea,

Taste sense is one of the primary sense of human, which is essential for human's life quality. Taste disorder rate increase due to population ageing, tumor and its therapy side effect, etc. Previous studies have reported that stable maintenance and regeneration of taste receptor cells requires for nerve innervation. In this study, we focus on the regeneration of taste receptor cells with innervated taste axons during organoid culture and transplant into tongue tissue. Circumvallate papillae is located in posterior tongue both human and mouse. Circumvallate papillae have numerous taste buds in its epithelial trench region. The taste progenitor cells located in circumvallate papillae are marked with leucine-rich repeat containing G protein-coupled receptor 5 and its homolog, Lgr6, which are adult stem cells marker in various organs including the tongue papillae. Taste organoids derived from single Lgr5 and Lgr6 positive taste progenitor cells expressed differentiated taste receptor cell markers. However, nerve innervation technique of taste bud organoid is not elucidated. To overcome the limitation of current taste bud organoid, such as cell arrangement of taste receptor cells and axons innervations, we reconstruct taste papillae with taste bud organoid and transplant into mouse tongue to confirm the function of taste bud organoid. This study shows the future practical using taste bud organoid to regenerate taste sense, which is an essential step for clinical treatment of taste disorder.

Key Words: Taste disorder/Taste bud regeneration/ Lgr5/taste bud organoid/nerve innervation

P245

RAE1 promotes epithelial-mesenchymal transition and breast cancer metastasis by enhancing *ZEB1* expression

Ji Hoon Oh[1], Ji-Yeon Lee[1], Sungsook Yu[2], Yejin Cho[2], Ki Taek Nam[2,*], Myoung Hee Kim[1,*]

[1]Department of Anatomy, and Brain Korea 21 PLUS Project for Medical Science, Yonsei University College of Medicine, Seoul, Korea
[2]Severance Biomedical Science Institute and Brain Korea 21 PLUS Project for Medical Science, Yonsei University College of Medicine, Seoul, Korea

Breast cancer metastasis accounts for most of the deaths from breast cancer. Since epithelial-mesenchymal transition (EMT) plays an important role in promoting metastasis of cancer, many mechanisms regarding EMT have been studied. We previously showed that Ribonucleic acid export 1 (RAE1) is dysregulated in breast cancer and its overexpression leads to aggressive breast cancer phenotypes by inducing EMT. Here, we evaluated the functional capacity of RAE1 in breast cancer metastasis by using a three-dimensional (3D) culture system and xenograft models. Furthermore, to investigate the mechanisms of RAE1-driven EMT, *in vitro* studies were carried out. The induction of EMT with RAE1-overexpression was confirmed under the 3D culture system and *in vivo* system. Importantly, RAE1 mediates upregulation of an EMT marker ZEB1, by binding to the promoter region of *ZEB1*. Knockdown of ZEB1 in RAE1-overexpressing cells suppressed invasive and migratory behaviors, accompanied by an increase in epithelial and a decrease in mesenchymal markers. Moreover, Kaplan-Meier survival analysis indicated that breast cancer patients with high expression of RAE1 and ZEB1 expression level had poor prognosis. Taken together, these data

demonstrate that RAE1 contributes to breast cancer metastasis by regulating a key EMT-inducing factor ZEB1 expression, suggesting its potential as a therapeutic target.

Key Words: RAE1, ZEB1, Breast cancer, Metastasis, Epithelial-mesenchymal transition

*Correspondence to Ki Taek Nam (E-mail: kitak@yuhs.ac, +82-2-2228-0754) and Myoung Hee Kim (E-mail: mhkim1@yuhs.ac, +82-2-2228-1647)

P246

Current Brain Tumor Therapy Induces NUPR1α Expression in Primary GBM Cell Lines

Jiyeon Lee, Joo Yeon Jeong, Seokmin Kang, Hyemin Seong, Ahmad Fudhaili, Juyeong Park, Soohyun Hwang, Jimin Sim, Nayoung Kim, Jinhyun Ryu, Dong Hoon Lee, Gu Seob Roh, Hyun Joon Kim, Gyeong Jae Cho, Wan Sung Choi, Sun Ha Paek, Sang Soo Kang*

Department of Convergence Medical Science and Anatomy, College of Medicine, Gyeongsang National University, Jinju, 52727, Korea.

Glioblastoma multiforme (GBM) is the most malignant and aggressive form of primary brain tumors. GBM is characterized by rapid proliferation, high invasiveness, and the ability to infiltrate and damage the surrounding arears of the brain. The current standard of care for GBM patients is surgical resection followed by radiotherapy with chemotherapy. In treating GBM, there are several obstacles that hinder the effectiveness of treatment, such as poor prognosis, rapid recurrence, and multi-drug resistance. Radiotherapy (RT) plays a crucial role in the treatment of GBM, doubling survival when compared with surgery alone. Temozolomide (TMZ) is an oral alkylating agent that induces DNA methylation of guanine at the O^6 position. It triggers mismatch repair, which leads to cell cycle arrest and apoptosis. Concomitant and adjuvant TMZ is applied with radiotherapy in order to improve the survival of GBM patients currently. Nuclear Protein 1 (NUPR1) is a small protein whose expression is induced by several stresses and which is overexpressed in cancer cells and tissues. NUPR1 expression allows cancer to counter the effects of chemotherapeutic drugs. The potential role of NUPR1 in making cancer resistant to the effects of conventional chemotherapeutic agents is suggested in several types of cancer, for example, pancreatic and breast cancer. It plays a role in mediating resistance to a broad spectrum of anti-cancer drugs. We suggested that NUPR1α, also known as an isoform of NUPR1, is induced by radiotherapy and chemotherapy. To investigate whether NUPR1α is up-regulated in response to chemotherapy agent and radiation, we first examined correlation between NUPR1α expression and TMZ treatment. NUPR1α expression is increased by TMZ treatment in primary GBM cells. Further, after radiation exposure, GBM cells showed increase in NUPR1α expression and combination treatment also up-regulated its expression level. These findings suggest that NUPR1α is involved in radiotherapy and chemotherapy, current treatments for GBM patients.

P247

Bmal1, a key circadian rhythm gene, inhibits tumorigenesis of glioblastoma cells and further promote Temozolomide-mediated cell death

Do hyeong Gwon[1,2], Nara Shin[1,2], Won-hyung Lee[3], Sun Yeul Lee[3], Jinpyo Hong[2], Dong Woon Kim[1,2]

[1]Department of Medical Science, Chungnam National University School of Medicine, Daejeon, 35015, Republic of Korea.
[2]Department of Anatomy, Brain Research Institute, Chungnam National University School of Medicine, Daejeon, 35015, Republic of Korea.
[3]Department of Anesthesia and Pain Medicine, Chungnam National University Hospital, Daejeon 35015, Republic of Korea.

Background: Brain and muscle aryl hydrocarbon receptor nuclear translocator-like 1 (*Bmal1*), an important molecule for maintaining circadian rhythms, inhibits the growth and metastasis of tumor cells in several types of cancer, including lung, colon, and breast cancer. However, its role in glioblastoma has not yet been established. Here, we addressed the function of Bmal1 in glioblastoma cells with two approaches, loss and gain of function. **Methods:** To understand the role of *Bmal1* in tumorigenesis, U87MG cells treated with Bmal1 small interfering RNA (siRNA) or adenovirus were used to analyze the cell proliferation by MTT assay, migration by wound healing assay, and invasion by Matriegel invasion assay. To reveal the mechanism how *Bmal1* regulates the tumorigenesis, Bmal1 siRNA or adenoviruses-treated U87MG cells were also examined by flow cytometry and western blot. Furthermore, we investigated whether Bmal1 could enhance the sensitivity of U87MG cells to Temozolomide (TMZ) by MTT assay. **Results:** In the loss of function experiments, cell proliferation in U87MG cells transfected with Bmal1 siRNA was increased by approximately 20% via upregulation of Cyclin B1. In addition, migration and invasion of Bmal1 siRNA-treated glioblastoma cells were elevated by approximately 20% and 200%, respectively, due to the accumulation of phosphorylated AKT (p-AKT) and matrix metalloproteinase (MMP)-9. Gain of function experiments revealed that adenovirus-mediated ectopic expression of Bmal1 in U87MG cells resulted in a 22% decrease in cell proliferation compared with the control via downregulation of Cyclin B1 and increased apoptosis due to changes in the levels of Bax, Bcl-2, and cleaved Caspase-3. Likewise, migration and invasion were attenuated by approximately 30% and 50%, respectively, in Bmal1-overexpressing U87MG cells following downregulation of p-AKT and MMP-9. Moreover, Bmal1 elevated the sensitivity of U87MG cells infected with Bmal1 adenovirus to TMZ. **Conclusions:** Our results suggest that *Bmal1* acts as an anti-cancer gene by altering the proliferation, migration, and invasion of glioblastoma cells and can synergistically enhance cell sensitivity to TMZ. Therefore, the *Bmal1* gene could be a potential therapeutic target in the treatment of glioblastoma.

Key Words: Bmal1, Glioblastoma, Temozolomide, Anti-cancer

P248

Compound from *Lindera Strychnifolia* Suppress Xenograft Tumor Growth of Human Glioblastoma Multiforme Cells through Bcl-2/Caspase-3/PARP Pathway

Ji Young Hwang[1,2,3], Jung Hwa Park[1,2,3], Min Jae Kim[1,2,3], Jin Ung Baek[4], Byung Tae Choi[1,2,3], Seo-Yeon Lee*[2,3], Hwa Kyoung Shin*[1,2,3]

[1]Department of Korean Medical Science, School of Korean Medicine, Pusan National University, Yangsan, Gyeongnam 50612, Republic of Korea.
[2]Korean Medical Science Research Center for Healthy-Aging, Pusan National University, Yangsan, Gyeongnam 50612, Republic of Korea.
[3]Graduate Training Program of Korean Medicine for Healthy-Aging, Pusan National University, Yangsan, Gyeongnam 50612, Republic of Korea.
[4]Division of Humanities and Social Medicine, School of Korean Medicine, Pusan National University, Yangsan, Gyeongnam 50612, Republic of Korea

Objective: Glioblastoma (GBM) is the most common brain tumor in adults which is highly malignant and incurable. Compounds from plant extracts are a potential source to develop more potent anti-cancer medicine. In this study, we found that compound from *Lindera strychnifolia* (termed as "LS03") suppresses U-87 human glioblastoma cell proliferation through apoptosis. **Method:** U-87 glioblastoma cells were treated with LS03, and cell proliferation, Annexin-V flow cytometry and LDH release were observed. Western blot, real-time PCR and immunohistochemistry for apoptotic cell death-associated molecules were performed. Growth inhibition of subcutaneous GBM by LS03 was examined in mouse xenograft model *in vivo*. Tumor tissue was pulled out and weighed. **Results:** Glioblastoma cells treated with LS03 decreased cell proliferation, increased apoptotic cell death and also increased the LDH release. LS03 suppressed the expression of Bcl-2, an anti-apoptotic protein, but Bax level showed no significant difference compared with control. LS03 significantly increased the level of cleaved caspase-3 and the cleaved poly (ADP-ribose) polymerase (PARP). In addition, intraperitoneal injection of LS03 significantly suppressed tumor growth. Tumor weigh was significantly lower in the group receiving LS03 ($p<0.01$). We observed TUNEL and cleaved caspase-3 in tumor tissue by immunohistochemistry, and found TUNEL and cleaved caspase-3 fluorescence were increased in LS03 injection group. **Conclusion:** Taken together, LS03 from *Lindera strychnifolia* inhibits U-87 GBM cell proliferation and induces apoptosis by stimulating Bcl-2/Caspase-3/PARP pathway, and LS03 may become a potential candidate for anti-glioblastoma drug development.

Key Words: Glioblastoma, Xenograft, Apoptosis, Plant extract

*Correspondence to Seo-Yeon Lee (E-mail : brainsw@gmail.com) and Hwa Kyoung Shin (E-mail : julie@pusan.ac.kr)

P249

Anti-angiogenic effects of compound from *Lindera Strychnifolia* on human glioblastoma cells *in vitro* and *in vivo*

Jung Hwa Park[1,2,3], Ji Young Hwang[1,2,3], Woo Jean Kim[4], Min Jae Kim[1,2,3], Byung Tae Choi[1,2,3], Seo-Yeon Lee[2,3,*], Hwa Kyoung Shin[1,2,3,*]

[1]Department of Korean Medical Science, School of Korean Medicine, Pusan National University, Yangsan, Gyeongnam 50612, Republic of Korea.
[2]Korean Medical Science Research Center for Healthy-Aging, Pusan National University, Yangsan, Gyeongnam 50612, Republic of Korea.
[3]Graduate Training Program of Korean Medicine for Healthy-Aging, Pusan National University, Yangsan, Gyeongnam 50612, Republic of Korea.
[4]Department of Anatomy, College of Medicine, Kosin University, Busan 49267, Republic of Korea

Glioblastoma (GBM) is a lethal type of brain tumor with a median survival of 12 to 15 months after diagnosis. In particular, blocking agent against vascular endothelial growth factor (VEGF) such as bevacizumab has been used for the GBM treatment. Despite being the only FDA-approved anti-angiogenic agent, resistant patients often develop and frequently fail to prove significantly better survival. Compounds from plant extracts are a promising source for developing potent anti-cancer medicine. In this study, we found that compound from *Lindera strychnifolia* (termed as "LS03") has an anti-angiogenic activities against human glioblastoma cells *in vivo* and in *vitro*. We first evaluated whether LS03 inhibited tumor growth *in vivo* animal tumor model. In a human GBM xenograft mouse model, administration of LS03 significantly reduced tumor volume and tumor weight. To identify the

molecular mechanisms involved in the tumor growth inhibition, two human glioma cell lines (U-87, U-373) were treated with LS03 under hypoxic conditions. LS03 treatment significantly decreased VEGF mRNA, protein and VEGF secretion. In addition, human brain microvascular endothelial cells (HBMECs) were treated with LS03 in the presence of recombinant human VEGF and were investigated the effect on angiogenic processes. LS03 treatment inhibited cell proliferation and capillary-like tube formation, yet did not affect cell migration. Furthermore, administration of LS03 decreased angiogenesis *in vivo* mouse Matrigel plug assay. Because the activity of VEGF is mediated through receptor tyrosine kinases, we observed VEGFR2 and its downstream pathway. Phosphorylation of VEGFR2, FAK and ERK was decreased by LS03. Taken together, LS03 from *Lindera strychnifolia* exhibits anti-angiogenic effect through suppression of VEGF in hypoxic GBM cells and proliferation and capillary-like tube formation in HBMECs, suggests LS03 as a promising anti-cancer medicine candidate.

Key Words**:** Angiogenesis, Xenograft, Plant extract, Tumor growth

*Correspondence to Seo-Yeon Lee (E-mail : brainsw@gmail.com) and Hwa Kyoung Shin (E-mail : julie@pusan.ac.kr)

P250

Chemical hypoxia induces caspase-dependent apoptosis via ROS/caspase-1 in T98G glioblastoma cells

<u>Yeo Wool Kang</u>, Jin suk Lee, Min-ho Jung, Byung Young Choi, Young Chul Yang, Byung Pil Cho, Won Gil Cho*

Department of Anatomy, Yonsei University Wonju college of Medicine / Wonju, Gangwon province, South Korea

Hypoxia is a condition in which the body or a region of the body is deprived of oxygen supply. Among them, cerebral hypoxia (brain hypoxia) is a major cause of brain damage. Astrocytes are essential for the survival and functioning of neurons not only under hypoxic condition, but in physiological conditions. Therefore, protection of astrocytes from death during hypoxia is one of the therapeutic strategies. For this purpose, the mechanism of hypoxia-induced astrocytic cell death should be fully elucidated. Reactive oxygen species (ROS) were generated in response to chemical hypoxia. NADPH oxidases are a family of enzyme dedicated to the generation of ROS via reduction of molecular oxygen. Among them, NOX2 is one of the main source of ROS generation in astrocytes. Cobalt chloride-induced chemical hypoxia transcriptionally upregulate NOX2 mRNA level and simultaneously downregulates anti-oxidant enzyme catalase. Increase ROS induced by chemical hypoxia activated caspase-1. Active caspase-1 induced activation of caspase-8/9, caspase-3/7 and cleavage of PARP and mediate apoptotic cell death during hypoxia.

Key Words: Hypoxia, Astrocyte, ROS, Caspase-1, NOX2

P251

Three-dimensional in vitro hydrogel-based cell culture model of human ovarian cancer for the evaluation of tumor progression and malignancy

Yejin Ok, Ye Seon Lim, Chang-Hyun Kim, Hae Yeong Kang, Seonyoung Hwang, Sik Yoon*

Department of Anatomy, Pusan National University School of Medicine, Yangsan, Gyeongsangnam-do 626-870, Republic of Korea

Ovarian cancer is one of the most deadly malignancies in women because of its poor prognosis and that a majority of patients are diagnosed at advanced stage. Therefore, chemotherapy becomes the most important treatment option in most ovarian cancer cases. Current in vitro drug testing models based on 2D cell culture lack natural tissue-like structural organization and result in disappointing clinical outcomes. The development of efficient drug testing models using 3D cell culture that more accurately reflects in vivo behaviors is vital. Our aim was to establish an in vitro 3D ovarian cancer model that can imitate the in vivo human ovarian cancer microenvironment. Using this model, we explored strategies to evaluate tumor progression and malignancy. Ovarian cancer cells grown in this model exhibited excellent biomimetic properties compared to conventional 2D culture including (1) enhanced chemotherapy resistance, (2) suppressed rate of apoptosis, (3) upregulated expression of drug resistance genes (MDR1 and MRP1), (4) elevated levels of tumor aggressiveness factors including Notch (Notch, VEGF and MMPs), and (5) enrichment of a cancer stem cell markers (Sox-2 and Nanog). Therefore, our data suggest that our 3D ovarian cancer model is a promising in vitro research platform for studying ovarian cancer biology and therapeutic approaches.

Key Words: Hydrogel, 3D Culture, Tumor Spheroid, Resistance, Ovarian Cancer

P252

Three-dimensional human ovarian cancer model for evaluation of tumor progression and drug resistance

Seonyoung Hwang, Ye Seon Lim, Yejin Ok, Chang-Hyun Kim, Hae Yeong Kang, Sik Yoon*

Department of Anatomy, Pusan National University School of Medicine, Yangsan, Gyeongsangnam-do 626-870, Republic of Korea

Conventional 2D cell culture models do not reflect the true biological activities of human ovarian cancer cells in vivo, and thus drug screening and testing in 3D ovarian cancer cell culture models are more effective than conventional 2D monolayer culture system. In the present study, we established a hydrogel-based 3D ovarian cancer culture system using various human ovarian cancer cell lines. It was found that cells cultured in the hydrogels grow as tumor-like clusters in 3D formation when compared to cells cultured in 2D monolayer culture. Histological examination demonstrated the formation of spheroids, whereas none of the cell types in 2D formed any spheroids. RT-PCR, Western blot, drug resistance and immunofluorescence staining analyses revealed that the expression of various genes related with ovarian cancer malignancy was significantly up-regulated in 3D cell culture when compared to 2D cell culture. Furthermore, increased migration and invasion of the human ovarian cancer cells were observed in cells cultured in 3D compared to those in 2D. Therefore, this study provides a novel hydrogel-based 3D culture technique for human ovarian cancer cells that closely mimicked in vivo cancer progression. Furthermore, our data may provide a useful platform technology to develop functional and biocompatible scaffolds for 3D culture of various cancer cell types.

Key Words: Hydrogel, 3D Culture, Tumor Spheroid, Resistance, Ovarian Cancer

P253

CD46 expression in prostate cancer

Sueun Lee, Manh-Hung Do, To Kim Phuong, Se-Young Kwon, Kwang Il Nam, Juhyun Song, Kyu Youn Ahn, Choon Sang Bae, Chaeyong Jung[*]
Department of Anatomy, Chonnam National University Medical School, Gwangju 61469, South Korea

CD46 is a human type I transmembrane glycoprotein, and regulates the complement system. CD46 expression is increased in various cancer cells. We studied CD46 expressions in human prostate cancer cell lines and human prostate cancer tissues. Increased CD46 expression was confirmed in human prostate cancer cell lines including LNCaP, C4-2 and CWR22Rv1. Sixty human prostate cancer tissues were investigated for CD46 expression by immunohistochemistry, and the expression was compared with Gleason score, the grading system for evaluating aggressiveness and prognosis of prostate cancer. The tendency of CD46 expression was inversely correlated to Gleason scores. CD46 expression was decreased on progression of Gleason scores, both combined and primary. CD46 was also inversely correlated with T stage. Therefore, we suggest that CD46 expression in prostate cancer may dictate the prostate cancer prognosis.

Keywords: CD46, Prostate cancer, Gleason score

[*]Correspondence to: Chaeyong Jung (E-mail: chjung@jnu.ac.kr)

P254

3D human prostate cancer model for evaluation of tumor characteristics

Ye Seon Lim, Yejin Ok, Chang-Hyun Kim, Hae Yeong Kang, Seonyoung Hwang, Sik Yoon*

Department of Anatomy, Pusan National University School of Medicine, Yangsan, Gyeongsangnam-do 626-870, Republic of Korea

Conventional 2D prostate cancer cell culture models do not reflect the true biological activities of prostate cancer cells in vivo, and thus drug screening and testing in 3D prostate cancer cell culture models are more effective than conventional 2D monolayer culture system. In the present study, we established a hydrogel-based 3D prostate cancer culture system using various human prostate cancer cell lines (LNCaP, DU145 and PC3). It was found that cells cultured in the hydrogels grow as tumor-like clusters in 3D formation when compared to cells cultured in 2D monolayer culture. Histological examination of all the three types of prostate cancer cells demonstrated the formation of spheroids, whereas none of the cell types in 2D formed any spheroids. RT-PCR, Western blot, drug resistance and immunofluorescence staining analyses revealed that the expression of various genes related with prostate cancer malignancy was significantly up-regulated in all the three types of cells in 3D cell culture when compared to 2D cell culture. Furthermore, increased migration and invasion in all three types of the human prostate cancer cells were observed in cells cultured in 3D compared to those in 2D. Therefore, this study provides a novel hydrogel-based 3D culture technique for human prostate cancer cells that closely mimicked in vivo cancer progression. Furthermore, our data may provide a useful platform technology to develop functional and biocompatible scaffolds for 3D culture of various

cancer cell types.

Key Words: Hydrogel, 3D Culture, Tumor Spheroid, Prostate Cancer

P255

Zinc inhibits expression of androgen receptor to suppress growth of prostate cancer cells

Phuong Kim To, Manh-Hung Do, Young-Suk Cho, Se-Young Kwon, Chaeyong Jung*

Department of Anatomy, Chonnam National University Medical School, Gwangju 61469, Korea

The prostate gland contains a high level of intracellular zinc, which is dramatically diminished during prostate cancer (PCa) development. Owing to the unclear role of zinc in this process, therapeutic applications using zinc are limited. This study aims to clarify the role of zinc and its underlying mechanism in the growth of PCa. $ZnCl_2$ suppressed proliferation of androgen receptor (AR)-retaining PCa cells, whereas it did not affect AR-deficient PCa cells. In LNCaP and TRAMP-C2 cells, zinc downregulated expression of AR in a dose- and time- dependent fashion. Zinc-mediated AR suppression accordingly inhibited androgen-mediated transactivation and expression of the androgen target PSA. This phenomenon resulted from facilitated protein degradation, not transcriptional control. In studies using mice bearing TRAMP-C2 subcutaneous tumors, intraperitoneal injection of zinc significantly reduced tumor size. Analyses of both xenograft tumors and normal prostate showed reduced expression of AR and increased cell death. Considering the significant loss of intracellular zinc and dominant growth-modulating role of AR during PCa development, loss of zinc may be a critical step in the transformation of normal cells to cancer cells. This study provides the underlying mechanism by which zinc functions as a PCa suppressor, and the foundation for developing zinc-mediated therapeutics for PCa.

Keywords: Zinc, Prostate cancer, Androgen receptor

P256

Yeast extract inhibits proliferation of renal cell carcinoma cells via regulating iron metabolism

Jinu Kim[1], Sang-Pil Yoon[1,2]

[1]Department of Anatomy, School of Medicine, Jeju National University, Jeju, Republic of Korea
[2]Institute for Medical Science, Jeju National University, Jeju, Republic of Korea

Microbiome has recently gained an interest for scientific research. We incidentally found that reinforced clostridium media (RCM) for microbiome culture had anti-tumor effects on renal cell carcinoma cells when compared to the microbiome 'X'. Anti-tumor effects of RCM were investigated for all of ingredients of RCM, which showed yeast extract could be a candidate for this phenomenon. Further experiment including MTT assay, cell counting, cell death analysis, cell cycle analysis and Western blotting was done with yeast extract on renal cell carcinoma cells (Caki-1 and Caki-2) and normal human proximal tubular cells (HK2). As a result, yeast extract showed dose-dependent anti-tumor effects on Caki-1 and Caki-2, while little effects on HK2. Yeast extract did not effect on necrosis

or apoptosis of Caki-1 and Caki-2 based on cell death analysis, but showed cell cycle arrest with increased G0/G1 fraction and decreased S fraction. Quantitative analysis showed that p21 increased with yeast extract treatment, which was regulated by decreased transferrin receptor and increased ferritin in Caki-1 and Caki-2. These results showed that yeast extract might inhibit proliferation of renal cell carcinoma cells via regulating iron metabolism. Since increased iron requirement is a classic phenomenon of cancer cells, yeast extract might be a candidate for an adjuvant treatment of renal cell carcinoma.

Key Words: Yeast extract, Renal cell carcinoma, Iron metabolism

P257

Neferine-induced apoptosis is dependent on the suppression of Bcl-2 expression via down-regulation of p65 in renal cancer cells

Eun-Ae Kim, Eon-Gi Sung, In-Hwan Song, Joo-Young Kim, Tae-Jin Lee

Department of Anatomy, College of Medicine, Yeungnam University, 170 Hyeonchung-ro, Nam-Gu, Daegu 705-717, Korea

Neferine is an alkaloid extracted from a seed embryo of Nelumbo nucifera and has recently been shown to have anticancer effects in various human cancer cell lines. In present study, we found that neferine induced apoptosis in a dose-dependent manner in Caki cells, which was attenuated by pretreatment with z-VAD, pancaspase inhibitor. Treatments with neferine dose-dependently down-regulated Bcl-2 expression at transcriptional level. The forced expression of Bcl-2 attenuated the neferine-mediated apoptosis in Caki cells. Finally, we found that treatment with neferine induced apoptosis by inhibiting NF-kB pathway through downregulation of p65 expression. Collectively, this study demonstrates that neferine-induced apoptosis is mediated by the down-regulation of Bcl-2 expression via repressing NF-kB pathways in renal cancer cells.

Key Words: Neferine, Caki, Bcl-2, NF-kB, p65

P258

Could spleen tyrosine kinase (SYK) be a useful marker for identifying epigenetic changes in cervical cancer?

Min Jun Kim, Han Ju Lee, Mee Young Choi, Min Young Kim, Akhtar Ali, Yoon Sook Kim, Wan Sung Choi[*]

Department of Anatomy and Convergence Medical Science, College of Medicine, Gyeongsang National University, Institute of Health Sciences, Jinju, Gyeongnam, Republic of Korea

Human papillomavirus (HPV) infection causes virtually all cervical cancer patients but how causes or regulating development from the initial lesion to invasive carcinoma still unknown. HPV upregulates and augments DNA methyltransferase (DNMT) and histone deacetylase (HDAC) activities which induce epigenetic changes. Epigenetic alterations may modify the expression of host genes, leading to silencing of tumor suppressor genes (TSGs) by promoter hyperrmethylation. Here, we identified CpG methylation region and sites in cervical cancer tissues and cervical cancer cell lines by

methylation specific array assay. And we found 16 hyper-methylated genes related to carcinogenesis and selected 5 TSGs from these hypermethylated genes. Among them, we focus on Spleen tyrosine kinase (SYK) which is a non-receptor protein tyrosine kinase that has been proposed to play important roles in tumor suppression. And it also has been reported that promoter region of SYK was hypermethylated in many types of cancer, including gastric cancer, melanoma and breast cancer. In our study, we found that expression of SYK was decreased in cervical cancer patients. Next, we are trying to find the methylation status of SYK promoter in cervical cancers. We hypothesize that SYK could be a useful marker for identifying epigenetic modulation in cervical cancer.

Key Words: Epigenetic markers, Methylation modification, Tumor suppressor genes, SYK, cervical cancer

P259

Metformin induces cell cycle arrest and cell death through the down-regulation of O-GlcNAcylated AMPK in cervical cancer cells

Min Young Kim[1], Min Jun Kim[2], Ali Aktar[2], Mee yeong Choi[2], Han Ju Lee[2], Yoon Sook Kim[2], Wan Sung Choi[1,2]

[1]Department of Anatomy and Convergence Medical Science, School of medicine, [2]Institute of Health Sciences, Gyeongsang National University, Jinju, Gyeongnam, Republic of Korea

Cancer and diabetes have something in common which need high glucose condition. Recently, anti-diabetes drugs that decrease the blood glucose are known as effective in cancer treatment. Metformin has an effect of reducing blood glucose and many researches discussing the effects of metformin in cancer were reported. In this study, we investigated whether metformin induces cell death in cervical cancer cells(HeLa). We first performed 4,5-dimethylthiazol-2-yl-2, diphenyl-tetrazoliumbromide (MTT) assay to compare the apoptotic cell death of HeLa to normal keratinocyte (HaCaT) cells after metformin treatment. We found that cancer cells were more sensitive to metformin than normal cells. Then, we also found that metformin induced cell cycle arrest by using Fluorescence activated cell sorting(FACS) analysis. Westernblot analysis, sWGA assay and immunoprecipitation analysis showed that metformin increased the expression of p-AMPKα, p27 and p21 and decreased the expression of OGT, O-GlcNAc level and AMPKa in HeLa cell. We also found that metformin down-regulated the global O-GlcNAcylation and decreased the O-GlcNAcylated AMPK level. In conclusion, our results suggest that metformin is effective in regulating of O-GlcNAcylation in cancer cells and could be used as anti-cancer drug in cervical cancer.

Key Words: Cervical cancer, O-GlcNAcylation, Metformin, Apoptosis, Cell cycle

P260

LCA induces miR21 expression through ERK1/2 and AP-1 signals in colorectal cancer cells

Thinh Nguyen Thi, Thuan Ung Trong, Li Shinan, Young Do Jung

Research Institute of Medical Sciences, Chonnam National University Medical School, Gwangju 501-190, Republic of Korea

Our study found that secondary bile acid, lithocholic acid (LCA), stimulates the expression of miR21 in colorectal cancer cells, HCT116 by quantitative PCR assay. Promoter activity assay showed that LCA strongly stimulates miR21 promoter activity in HCT116 cells by time and dose dependence. Sequential deleted promoter revealed that transcription factor AP-1 is a crucial in LCA induced miR21. Chemical inhibitor studies also indicated that Erk1/2 and AP-1 signals are involved in this mechanism of LCA-induced miR21 in HCT116 cells. Furthermore, it is found that LCA inhibits tumor suppressor protein expression, phosphatase and tensin homolog (PTEN), and stimulates cell cycle regulating signaling, PI3K/Akt, that were proved to be subsequence of miR21 expression enhancement. Inhibitors of signals involved in LCA-induced miR21 mechanism, Erk1/2 and AP-1, also reversed the effect of LCA on PTEN. In conclusion, LCA induces miR21 expression in colorectal cancer cells, HCT116, and subsequently down-regulates PTEN expression and stimulates PI3K/Akt signaling.

Key Words: PTEN, miR21; Lithocholic acid (LCA)

P261

FAM188B functions as a putative oncogene in colorectal carcinoma

Hamadi MADHI[1], Eun-Seok CHOI[2], Myoung Hee KIM[1], Sung-Ho GOH[2,*]

[1]Department of Anatomy, Embryology Laboratory, and Brain Korea 21 PLUS project for Medical Science, Yonsei University College of Medicine, Seoul 03722, Korea
[2]Research Institute, National Cancer Center, Goyang, 10408, Korea

FAM188B is a novel protein that is evolutionarily conserved among mammals. FAM188B protein has been reported recently as a probable Lys48 deubiquitinase which is important for many cancers as its expression showed a substantial exon usage. However, the exact role and the expression level of FAM188B in colon cancer remains elusive. Here we report that FAM188B knockdown based on an siRNA strategy triggers cell cycle arrest and apoptosis in colon cancer cells. More importantly, knockdown of FAM188B triggers p53, a key pro-apoptotic protein activation and upregulation. Furthermore, FAM188B knockdown dramatically reduces tumor size in xenografted mice. Hence, targeting FAM188B might be a new strategy to inhibit colon cancer growth. In addition, further research on FAM188B regulatory mechanisms, as well as conditions relative to p53 mutations might increase our understanding of FAM188B as a potential therapeutic target.

Key Words: FAM188B, Cell survival, p53, USP7, Colorectal cancer

P262

Silibinin Suppresses Cell Invasion and Migration through the Wnt/β-catenin Signaling Pathway

Dan-Bi Park[1,2], Jin-A Park[1,2], Hae-Mi Kang[1,2], Su-Bin Yu[1], In-Ryoung Kim[1], Bong-Soo Park[1,2]

[1]Department of Oral Anatomy, School of Dentistry, Pusan National University, Yangsan, Korea
[2]BK21 PLUS Project, School of Dentistry, Pusan National University, Yangsan, Korea

In tumor development, Epithelial-Mesenchymal Transition (EMT) is known to play an important role in cancer progression. During the EMT process, epithelial cells acquire fibroblast-like properties and show reduced intercellular adhesion and increased motility. Oral squamous cell carcinoma (OSCC) is the most common malignant tumor in the oral and maxillofacial region. Generally, OSCC is treated with a combination of chemotherapy and radiotherapy after extensive surgical resection. Thus, it is necessary to develop novel chemotherapeutic agents to improve overall survival rates. Silibinin is a major biologically active compound of milk thistle and has strong anti-oxidant and radical scavenger activities. Also it has shown strong anti-cancer efficacy against various cancers. Taken together, this study demonstrates that the silibinin treatment strongly inhibits cell migration and prevents EMT via Wnt/β-catenin signaling pathway in OSCC lines. For these reasons, silibinin may have anti-cancer effect and suppression of metastasis in OSCC cell lines.

Key Words: Silibinin, Oral squamous cell carcinoma, Epithelial-mesenchymal transition, Apoptosis

P263

Development of 3D Microfluidic Chip for Drug Screening and Drug Resistance Analysis in Brain Tumor Microenvironments

Jee Soo Lee[1,2], So Yeong Cho[1,3], Hyun Ho Kim[4], Da Eun Jeong[1, 3], Hyun Nam[1], Hee Jang Pyeon[1,3], Hye Jin Song[1,3], Sung Soo Kim[1,2], Yoon Kyung Bae[1,2], Jeong Seob Won[1,2], Ji Yoon Hwang[1,3], Yu Jeong Noh[1,3], Hye Won Lee[1,2,3*], Seok Chung[4*], Kyeung-Min Joo[1,2,3*]

[1]Stem Cell and Regenerative Medicine Center, Research Institute for Future Medicine, Samsung Medical Center, Seoul 06351, South Korea
[2]Department of Health Sciences and Technology, Samsung Advanced Institute for Health Science and Technology (SAIHST), Sungkyunkwan University, Seoul, 135-710, South Korea
[3]Department of Anatomy and Cell biology, Sungkyunkwan University School of Medicine, Samsung Biomedical Research Institute, #300 Cheoncheon-dong, Jangan-gu, Suwon, Gyeunggi-do, 440-746, South Korea
[4]Department of Mechanical Engineering, Korea University, Seoul, South Korea

Understanding the tumor microenvironment (TME) is important in the study of tumor. Brain tumor consist of complicated microenvironment, such as astrocytes, neurons, oligodendrocytes, immune cells and brain endothelial cells. These cells secrete numerous cytokines and soluble factors which promote tumor cells survival. Current 2D-culture system poses limitation on fully recapitulating TME characteristics of a tumor, due to high complexity and poor understanding of the heterogeneous microenvironment conditions in cancer pathogenesis. The complicated interaction in TME can lead to unexpected results like drug resistance. In an effort to address such issues, strategic culture system is required. To make environment similar to TME and earn credible results from drug screening, we developed a new 3D-patient's tumor model designed to contain extracellular matrix hydrogel, patient's tumor cell, astrocytes and brain endothelial cell.
Through this study, we expect our tri-culture model shows effect of TME to tumor cells growth, molecular properties and their mechanism. Also, tri-culture model is optimized for drug screening. It allows us to better understand the changes in drug response. Furthermore, our study will help to overcome the limitations of present targeted therapy.

Key Words: Tumor Microenvironment, Microfluidic chip, Tri culture, Drug screening, Brain tumor

P264

Differential cell death on 2D and 3D culture systems in EGFR mutant HCC827cell and HCC4006 cell by erlotinib

Min Hye Noh[1], Akinleye Temitope Michael[1], Lata Tajbongshi[1], Hyun-Kyung Lee[2], Seong Han Kim[1] and Yeong Seok Kim[1] and Dea Young Hur[1]

[1]Department of Anatomy, Inje University College of Medicine, 75 Bokji-ro, Busanjin-gu, Busan 47392, Republic of Korea
[2]Division of Pulmonary and Critical Care Medicine, Department of Internal Medicine, Inje University Pusan Paik Hospital, 75 Bokji-ro, Busanjin-gu, Busan 47392, Republic of Korea

Non-small cell lung cancer (NSCLC) patients with epidermal growth factor receptor (EGFR) mutation have been shown to good responsiveness to erlotinib, a receptor tyrosine kinase inhibitor for EGFR. Cell death pathways by erlotinib in 2 dimensional (2D) culture system of EGFR mutant lung cancer cell lines were already well known. However, those of 3D culture system were not determined yet. In this study, we found that the cell death pathways of 2D and 3D were different. Treatment with erlotinib to 2D and 3D cultures induced a typical caspase-dependent apoptosis. Interestingly, caspase 8 which is a main initiator caspase in receptor-mediated apoptosis was activated only 3D cultures but not 2D cultures by erlotinib. These cell death in 3D cultures were mediated through upregulation of TNF-related apoptosis-inducing ligand (TRAIL) expression. Surprisingly, autophagy induction by erlotinib activated the expression of TRAIL only in 3D cultures. Furthermore, TRAIL-induced cell death increased the expression of c-Jun N-terminal kinase (JNK) and treatment of SP600125, a chemical inhibitor for JNK, significantly inhibited erlotinib-induced cell death only in 3D cultures. These results suggested that erlotinib differentially induces apoptotic cell death through Autophagy-TRAIL-JNK pathway in 3D cultures and mitochondria-mediated apoptotic cell death in 2D cultures.

Key Words: NSCLC, EGFR, 3D culture, Erlotinib, TRAIL

P265

CD99-derived Agonist Peptide CD99CRIII3 Inhibits Tumor Growth by Suppressing EGFR Dimerization and Activation through PTPN12

Yuri Kim, Hyung Jin Won, Kyeong Han Park, Jung Hyun Park, Dae Joong Kim and Jang-Hee Hahn[*]

Department of Anatomy and Cell Biology, School of Medicine, Kangwon National University, Chuncheon, Korea

CD99 protein, a 32 kDa type I transmembrane glycoprotein, is known to be expressed in most tissues of the human body. It plays a significant role in the regulation of receptor activation, cell adhesion and migration. Epidermal growth factor receptor (EGFR) is a 170 kDa transmembrane protein, activation of which results in its dimerization and tyrosine autophosphorylation and subsequent recruitment of downstream signaling molecules that mediate cell proliferation, regeneration, and migration. Dimerization and clustering of receptor tyrosine kinases, which are modulated by actin cytoskeleton remodeling, are the important procedures in their activation of signaling pathways. However, molecular mechanisms underlying dimerization and clustering of receptor molecules are still unclear. This study aims at investigating whether CD99 inhibits tumor growth by suppressing EGFR activation in breast cancer cells and its underlying mechanism. This

study shows that EGF-derived tripeptide YAC induced the physical interaction among EGFR/Grb2/SOS/Shc/FAK/c-Src complex, which leads to cell proliferation. Transfection of MCF-7 cells with either dominant negative FAK or FAK siRNA reduced EGFR dimerization and subsequent endocytosis of EGFR, which leads to blocked interactions of RhoA, Rac1 and Cdc42 with FAK. In addition, dominant-negative RhoA, Rac1 or Cdc42 abrogated tripeptide YAC-induced endocytosis of EGFR. These results indicate that EGF and tripeptide YAC induces EGFR dimerization and activation through FAK-mediated activation of Rac1-Wave2-Arp2 and RhoA-Rock2-Ezrin signaling axes. Interestingly, tripeptide YAC-induced EGFR signaling was attenuated by CD99-derived agonist peptide CD99CRIII3. Transfection of PTPN12 siRNA, constitutively active RhoA or Rac1 abrogated the inhibitory effect of CD99CRIII3 on the EGFR clustering, suggesting that CD99 could inhibit EGFR-FAK-RhoA or Rac1-mediated actin cytoskeleton remodeling and tumor growth via PTPN12. CD99CRIII3 suppresses cell proliferation and migration induced by tripeptide YAC *in vitro*. Taken together, these results indicate that CD99 may inhibit EGFR dimerization and activation through PTPN12, suggesting that the CD99-derived agonist tripeptide CD99CRIII3 might be useful for inhibiting EGFR-induced tumor cell growth in patients with breast cancer.

Key Words: CD99, EGFR clustering, Actin cytoskeleton remodeling, FAK, PTPN12

P266

Effect of laminarin on the proliferation and apoptosis of human hepatoma HepG2 cell line

Fa-Rong Mo[1,2], Chun-Mei Li[1], Lin Tian[1], Wei-Xia Nong[1], Guo-Rong Luo[1,2]

[1]Department of Histology and Embryology, Guangxi Medical University, Nanning, China
[2]Guangxi Colleges and Universities Key Laboratory of Human Development and Disease Research, Guangxi Medical University, Nanning, China

The aim of this study was to elucidate the anticancer effect and the corresponding underlying mechanism of laminarin by assessing the effect of different concentrations of laminarin on the proliferation and apoptosis of human hepatoma HepG2 cell lines. HepG2 cells were seeded in 96-well plates at approximately 5000 cells/well. The control cells were treated with normal saline, while the experimental groups were respectively treated with 5-, 10-, 20-, and 30-mg/ml laminarin. Each group was established in triplicate. Morphological changes in HepG2 cells of each group were observed under an inverted microscope at 24 h, 48 h, and 72 h post-treatment. In addition, the potential inhibitory effects of laminarin on HepG2 cell proliferation and apoptosis were assessed using a CCK-8 assay and an Annexin V-fluorescein isothiocyante (FITC)/propidium iodide (PI) double staining method, respectively. Microscopy observations showed that compared to the control HepG2 cells that grew well, the laminarin-treated HepG2 cells displayed volumetric shrinkage and cell condensation. The number of adherent cells gradually decreased with an increasing concentration of laminarin. The HepG2 cells in the 30 mg/ml group exhibited the most remarkable deformation after 72 h of treatment. Results from the CCK-8 assay showed that laminarin exerted an inhibitory effect on the proliferation of HepG2 cells, which was positively correlated with the concentration of laminarin. Treatment with 30 mg/ml laminarin for 72 h resulted in the most significant inhibition of proliferation, with an inhibition rate of 83.2% and statistically significant differences between groups ($P<0.05$). Flow cytometry results showed that the apoptosis rate increased with increasing concentrations of laminarin. The apoptosis rate in the control group was $3.68 \pm 0.77\%$, while that in the laminarin groups (5-, 10-, 20-, and 30-mg/ml) was significantly different ($P<0.05$) from the control, at $5.30 \pm 1.21\%$, $9.47 \pm 2.44\%$, $21.7 \pm 2.13\%$, and $28.3 \pm 1.57\%$, respectively.

In conclusion, laminarin exerts an inhibitory effect on HepG2 cell growth, probably via inhibition of proliferation and induction of apoptosis.

Key Words: Laminarin, HepG2 cells, Proliferation, Apoptosis

P267

SAC3D1: a novel prognostic marker in hepatocellular carcinoma

Ji-Young Kim, Myoung-Eun Han, Ga Hyun Kim, Si Young Park, Yun Hak Kim[*], Sae-Ock Oh[*]

Department of Anatomy, School of Medicine, Pusan National University, Yangsan, Republic of Korea

Centrosome-associated proteins are recognized as prognostic factors in many cancers because centrosomes are critical structures for the cell cycle progression and genomic stability. SAC3D1, however, is associated with centrosome abnormality, although its prognostic potential has not been evaluated in hepatocellular carcinoma (HCC). In this study, 3 independent cohorts (GSE10186, n = 80; TCGA, n=330 and ICGC, n=237) were used to assess SAC3D1 as a biomarker, which demonstrated SAC3D1 overexpression in HCC tissues when compared to the matched normal tissues. Kaplan-Meier survival analysis also showed that its overexpression was associated with poor prognosis of HCC with good discriminative ability in 3 independent cohorts (GSE10186, P=0.00469; TCGA, P=0.0000413 and ICGC, P=0.0000114). Analysis of the C-indices and AUC values further supported its discriminative ability. Finally, multivariate analysis confirmed its prognostic significance (GSE10186, P = 0.00695; TCGA, P = 0.0000289 and ICGC, P = 0.0000651). These results suggest a potential of SAC3D1 as a biomarker for HCC.

Key Words: TCGA, Hepatocellular carcinoma, HCC, SAC3D1

P268

Aripiprazole, an atypical antipsychotic is drug to treat schizophrenia, inhibits the cell proliferation of non-small cell lung cancer H1299 cells

Jimin Sim, Joo Yeon Jeong, Seokmin Kang, Hyemin Seong, Ahmad Fudhaili, Juyeong Park, Jiyeon Lee, Soohyun Hwang, Nayoung Kim, Jinhyun Ryu, Dong Hoon Lee, Gu Seob Roh, Hyun Joon Kim, Gyeong Jae Cho, Wan Sung Choi, Sang Soo Kang*

Department of Convergence Medical Science and Anatomy, College of Medicine, Gyeongsang National University, Jinju, 52727, Korea.

Recently, many studies were reported that the patients with schizophrenia have a lower risk of cancer. From these findings, it can be inferred that medicines used to treat schizophrenia have anti-cancer effect. Cancer is the second leading cause of death globally. Among them, lung cancer is the most common cause of cancer death. Lung cancer has two main types small cell lung cancer (SCLC) which accounts for 15% and non-small cell lung cancer (NSCLC) which accounts for 85%. It is commonly known that cisplatin is a widely used drug for lung cancer patients and has been used to treat lung cancer even recently. It is necessary that the new drug except cisplatin because many patients already have the resistant to cisplatin. In recent years, Drug repositioning has been very popular in study development of new drugs. Drug repositioning is that drugs known as medicine to

treat some diseases are also being made available to treat other diseases. When NSCLC cells (A549, H460, H1299, H1975, H23, H358) were treated with atypical antipsychotics (Quetiapine, Olanzapine, Risperidone, Aripiprazole, Ziprasidone) and assessed cell proliferation by MTT assay, we found out that aripiprazole has the greatest anti-cancer effect. We also discovered that anti-cancer effect is strongest in H1299 cells than other NSCLC cell lines. To identify molecular mechanism of aripiprazole atypical antipsychotics, we proceeded cell cycle analysis with flow cytometry and discovered aripiprazole induces G1 phase arrest. In addition, we also analyzed mRNA expression levels of cell proliferation marker by real –time PCR. The results indicate that aripiprazole inhibits cell proliferation of H1299 cells.

According to this finding, aripiprazole can be used as a new anti-cancer drug for lung cancer patients.

P269

Anti-cancer effects of eucalyptols a novel DNA methylation inhibitor in lung cancer cells.

Ji Wook Moon, Won Seok Byun, Hyeon Soo Kim, Sun-Hwa Park

Department of Anatomy, Korea University, College of Medicine, Seoul, Republic of Korea

Objectives: Eucalyptols as a major composition of eucalyptus, is known to induce anti-inflammatory and anti-oxidant effects. However, the anti-tumor effect and DNA demethylating effect in lung cancer cells is not clear. The aim of this study was to explore whether eucalyptol has an inhibitory ability on the DNA methylation in lung cancer cells. **Methods:** The cell proliferation of normal and various cancer cells to eucalyptol was analyzed by MTT assay. Following eucalyptol treatment, the expression of DNA methyltransferase 1 (DNMT1) mRNA and protein was detected by qRT-PCR and Western blot analysis, respectively. Using qMSP and qRT-PCR, methylation status and mRNA expression levels of hypermethylated genes were determined in two lung cancer cell lines and two normal lung cell lines. **Results:** MTT data showed that eucalyptol had higher sensitivity in lung cancer cells (A549 and PC-9) compared with normal lung cells (MRC-5 and BEAS2B). Eucalyptol inhibits various human cancer cells growth in a dose- and time-dependent mannar. Eucalyptol decreased the expression of DNMTs mRNA (DNMT1, DNMT2, DNMT3a, and DNMT3b) in A549 cells. In PC-9 cells, eucalyptol decreased the expression of DNMT2, DNMT3a, and DNMT3b, but MRC-5 and BEAS2B cells was not changed the DNMTs after treatment eucalyptol. Eucalyptol reduced the methylation status of 5 hypermethylated genes (BTG4, IGF2, IGFBP3, RUNX3, and ZNF272) and restored the mRNA expression levels in lung cancer cell lines. **Conclusions:** These results demonstrated that eucalyptol could be associated with DNA demethylation and thus provides eucalyptol as new therapeutic candidate of lung cancer treatment.

Key Words: Eucalyptol, DNA methylation, Lung cancer

P270

The establishment of spontaneous tumor models using transgenic mouse with K-ras$^{(LSL-G12D/+)}$ and p53$^{(fl/fl)}$ and Adenovirus-Cre-GFP system for studying tumor microenvironment.

Yoon Kyung Bae[1,2], So Yeong Cho[2,3], Hyun Nam[2], Da Eun Jeong[2], Hee Jang Pyeon[2,3], Hye Jin Song[2,3], Sung Soo Kim[1,2], Jeong Seob Won[1,2], Ji Yoon Hwang[2,3], Jee Soo Lee[1,2], Yu Jeong Noh[2,3], Hye Won

Lee[2,3]*, Kyeung-min Joo[1,2,3]*

[1]Department of Health Sciences and Technology, Samsung Advanced Institute for Health Science and Technology (SAIHST), Sungkyunkwan University, Seoul, 06351, South Korea
[2]Single Cell Network Research Center, Sungkyunkwan University of Medicine, Suwon, 16419, South Korea.
[3]Department of Anatomy and Cell biology, Sungkyunkwan University School of Medicine, Suwon, 16419, South Korea. *Corresponding Authors.

Cancers are composed of billions of cells; each cell has different characteristics, because they gain mutations through cell divisions. This intratumoral heterogeneity affects response to anti-cancer therapy, tumor invasion capacity and tumor progression. Additionally, the tumor microenvironment (TME) is also known as a key factor in disease progression. In this study, to identify interaction between tumor cells and TME, genetically engineered mouse model that has oncogenic mutation in Kras (K-ras$^{LSL-G12D/+}$) and floxed p53 allele (p53$^{fl/fl}$) were used. These mutated genes were expressed simultaneously under Cre recombinase existence. Kras mutations are very common mutations in various human cancers. Representatively, lung adenocarcinoma, pancreatic ductal adenocarcinoma, and urothelial bladder cancer are known to have frequent Kras mutation. To establish lung adenocarcinoma, pancreatic ductal adenocarcinoma, and urothelial bladder cancer model, K-ras$^{LSL-G12D/+}$;p53$^{fl/fl}$ mouse had a surgical operation to inject Adenovirus-Cre-GFP for Cre recombinase expression. 40 days after Ad-Cre injection, K-ras$^{LSL-G12D/+}$;p53$^{fl/fl}$ mouse for lung adenocarcinoma show several small and big nodules on their lung. Furthermore, 50 days after Ad-Cre injection, K-ras$^{LSL-G12D/+}$;p53$^{fl/fl}$ mouse for pancreatic ductal adenocarcinoma has a number of tumor lumps in their abdominal cavity, and tumor cells are seemed to spread to several parts of the abdominal cavity. Taken together, we established several spontaneous tumor models through orthotopic injection of Adenovirus-Cre-GFP to K-ras$^{LSL-G12D/+}$;p53$^{fl/fl}$ transgenic mouse, which could be useful preclinical platform for elucidating the roles of tumor microenvironment in tumor evolution.

Key Words: Tumor microenvironment, Tumor heterogeneity, Kras, p53, Cre recombinase

P271

Targeting CD46 enhances anti-tumoral activity of adenovirus type 5 for bladder cancer

Manh-Hung Do, Young-Suk Cho, Kim-Phuong To, Se-Young Kwon, Kwang Il Nam, Kyu Youn Ahn, Choon Sang Bae, Chaeyong Jung

Department of Anatomy, Chonnam National University Medical School, Hwasun, Jeonnam, Korea

CD46 is generally overexpressed in many human cancers, representing a prime target for CD46-binding adenoviruses (Ads). This could help to overcome low anti-tumoral activity by coxsackie-adenoviral receptor (CAR)-targeting cancer gene therapy viruses. However, because of scarce side-by-side information about CAR and CD46 expression levels in cancer cells, mixed observations of cancer therapeutic efficacy have been observed. This study evaluated Ad-mediated therapeutic efficacy using either CAR-targeting Ad5 or CD46-targeting Ad5/35 fiber chimera in bladder cancer cell lines. Compared to normal urothelia, bladder cancer tissue generally overexpressed both CAR and CD46. While CAR expression was not correlated with disease progression, CD46 expression was inversely correlated with tumor grade, stage, and risk grade. In bladder cancer cell lines, expression levels of CD46 and CAR were highly correlated with Ad5/35- and Ad5- mediated gene transduction and cytotoxicity, respectively. In a human EJ bladder cancer xenograft mouse model, with either

overexpressing or suppressed CD46 expression levels, Ad5/35-tk followed by ganciclovir (GCV) treatment significantly affected tumor growth, whereas Ad5-tk/GCV had only minimal effects. Overall, our findings suggest that bladder cancer cells overexpress both CAR and CD46, and that adenoviral cancer gene therapy targeting CD46 represents a more suitable therapy option than a CAR-targeting therapy, especially in patients with low risk bladder cancers.

Key words: CD46, CAR, adenovirus, gene therapy, bladder cancer

P272

The role of HOTAIRM1 on tamoxifen-resistance in ER+ breast cancer cells

Clara Yuri Kim, Ji-Yeon Lee, Myoung Hee Kim*

Department of Anatomy, and Brain Korea 21 PLUS Project for Medical Science, Yonsei University College of Medicine, Seoul, Korea

Breast cancer is one of the most commonly occurring cancers in women worldwide. Approximately 40% of breast cancer patients acquire endocrine-resistance following therapy with tamoxifen. Many explanations for the development of endocrine-resistance have been put forward, one of them being the dysregulation of long non-coding RNAs (lncRNAs), as lncRNAs are the most diverse group of non-coding RNAs that are known to play important functions in various cellular and physiological processes. In fact, a number of lncRNAs have been reported to be involved in endocrine-resistance, as well as breast cancer progression and metastasis.
In this study, we show that HOTAIRM1, an intergenic lncRNA located between HOXA1 and HOXA2 is up-regulated in tamoxifen-resistant MCF7 (MCF7-TAMR) cells. We demonstrate that this up-regulation results from an increase in the enrichment of H3K4me3, and a decrease in the enrichment of H3K37me3 marks in MCF7-TAMR cells compared to MCF7 cells. The knockdown of HOTAIRM1 in MCF7-TAMR cells significantly decreased cell proliferation and viability through the re-sensitization of cells to tamoxifen. Further characterization of the role of HOTAIRM1 in controlling gene expression and its interaction with chromatin modifiers may elucidate novel insight into the molecular mechanisms of HOTAIRM1 involved in the pathogenesis of breast cancer.

Key Words: HOTAIRM1, HOX genes, breast cancer, resistance, long non-coding RNA

*Correspondence to Myoung Hee Kim (E-mail: mhkim1@yuhs.ac, Tel: +82-2-2228-1647)

P273

Regulatory Mechanism for ID1 expression in cholangiocarcinoma

Ga Hyun Kim, Myoung-Eun Han, Ji-Young Kim, Si Young Park, Yun Hak Kim*, Sae-Ock Oh*

Department of Anatomy, School of Medicine, Pusan National University, Yangsan, Republic of Korea

ID1 is known to inhibit differentiation and enhance cell proliferation. It is also highly overexpressed in over 20 cancers including and plays important roles in tumorigenesis in a wide range of tissues. Due to its late diagnosis and chemoresistance, the survival rate of cholangiocarcinoma (CCA) is less than 5 % for 5 years if surgery is impossible. So new development of biomarker for its

diagnosis and treatment are necessary. Unfortunately, the regulatory mechanisms for its expression are poorly characterized in CAA. To reveal regulatory mechanism for ID1 expression in CCA, we examined whether serum can regulate ID1 expression. After the serum starvation, serum-stimulation increased ID1 expression in a time-dependent manner. We also treated various inhibitors for signal pathways known to be related to ID1 expression such as NF-Kb, Raf/MEK, Akt, JAK-3, PI3K and BMP pathways. Interestingly, K02288 (ALK1,2,6 inhibitor) and LDN214117 (ALK2 inhibitor), LDN193189 (ALK2,3 inhibitor) and ML347(ALK1,2 inhibitor) effectively inhibited serum-induced ID1 expression in CAA. Among them, LDN214117 (ALK2 inhibitor) inhibited the expression of ID1 most effectively. These results suggest that the expression of ID1 in cholangiocarcinoma is possibly regulated through ALK2.

Key Words: ID1, Cholangiocarcinoma

P274

Discovery of a novel prognostic marker in gastric Cancer

Si Young Park, Myoung-Eun Han, Ga Hyun Kim, Ji-Young Kim, Yun Hak Kim, Sae-Ock Oh

Department of Anatomy, School of Medicine, Pusan National University, Yangsan, Republic of Korea

Gastric cancer is the third leading cause of cancer deaths worldwide. Various chemotherapies have been developed to slow the progression of cancer, but surgery is still the only treatment. Cancer stem cells can cause recurrence and metastasis because they have ability to regenerate and to differentiate. To find out new diagnostic or therapeutic targets, we compared mRNA expression between gastric cancer stem cells and differentiated daughter cells after sorting by use of CD44+/EPCAM surface marker. After *in silico* study of overexpressed genes in gastric cancer stem cell, we examined the clinical significance of Gene A using TCGA database. In Kaplan Meier analysis, we found gene A was associated with poor prognosis of gastric cancer patients. Moreover, Gene A siRNA decreased the proliferation and migration rate of gastric cancer cells. To find out underlying mechanisms, we examined effect of BMP inhibitors because Gene A is associated with BMP pathway. These results suggest Gene A can be used as an important prognostic marker of gastric cancer. Further studies are required to identify underlying mechanisms in detail.

Key Words: Gastric cancer, BMP pathway, Prognostic marker

P275

GIANT: an online resource for comprehensive survival analysis from The Cancer Genome Atlas

Myoung-Eun Han[1], Tae Sik Goh[2], Dae Cheon Jeong[3], Chi-Seung Lee[4], Ji-Young Kim[1], Hokeun Sun[5], Sae-Ock Oh[1], Kyoungjune Pak[6*], Yun Hak Kim[1*]

[1]Department of Anatomy, School of medicine, Pusan National University, Yangsan, Republic of Korea
[2]Department of Orthopedic Surgery, Pusan National University Hospital, Busan, Republic of Korea
[3]Deloitte Analytics Group, Deloitte Consulting LLC, Busan, Republic of Korea
[4]Biomedical Research Institute, Pusan National University Hospital and School of Medicine, Busan, Republic of Korea
[5]Department of Statistics, Pusan National University, Busan, Republic of Korea

[6]Department of Nuclear Medicine, Pusan National University Hospital, Busan, Republic of Korea

Prognostic genes or gene signatures have been widely used to predict patients' survival and aid the decision of therapeutic options. Although few web-based survival analysis tools to identify them have been developed, they only provide limited information. To overcome limitations of previous web-based tools and provide comprehensive survival analysis, we developed GIANT, an online resource for identifying prognostic biomarkers in pan-cancer from The Cancer Genome Atlas (TCGA). We used R program to code survival analysis based on RNA-seq data from TCGA. To perform survival analyses, we excluded patients and genes that have insufficient information. The GIANT is programmed by applying appropriate cross validation methods and survival analysis methods to provide three analysis services (survival analysis by mRNA, cancer type, or gene/variable signature). It can perform comprehensive survival analysis to identify prognostic genes or gene signatures with subgroup analysis. Using RNA-seq, clinical data and pathway databases in combination, it provides gene/variable signature by grouped variable selection methods (least absolute shrinkage and selection operator, Elastic Net regularization, Network-Regularized high-dimensional Cox-regression) that has better discriminatory power than single gene. Users also can find prognostic values of gene and statistically significant genes in specific cancer. All results are presented as Kaplan-Meier curve with median/optimal cutoff value, C-index, and area under the curve (AUC) value at t-years. Moreover, users can easily obtain results from the website. The GIANT (https://giantonline.org/) will help oncologists of those who are vulnerable to computer technology to do database analysis can easily perform survival analysis.

Key Words**:** Survival analysis; Grouped variable selection; The Cancer Genome Atlas; Web Tool

P276

Crosstalk between Apoptosis and Autophagy by Fisetin in Human Oral Squamous Cell Carcinoma

Jin-A Park[1,2], Dan-Bi Park[1,2], Hae-Mi Kang[1,2], Su-Bin Yu[1], In-Ryoung Kim[1], Bong-Soo Park[1,2]

[1]Department of Oral Anatomy, School of Dentistry, Pusan National University, Yangsan, Korea
[2]BK21 PLUS Project, School of Dentistry, Pusan National University, Yangsan, Korea

Fisetin (3,3-,4-,7-tetrahydroxyflavone), a naturally occurring flavonoid, has antioxidant, anti-inflammatory, and anticancer effects. Oral squamous cell carcinoma (OSCC) has a 5-year survival rate lower than that of most other carcinomas, and can create functional and aesthetic problems for the patient. New therapies for OSCC are necessary, and treatment using plant-derived natural substances has recently become a trend. It has been suggested that autophagy may play an important role in cancer therapy. Several studies demonstrated that autophagy inhibition enhances apoptotic cell death. Therefore, autophagy inhibition might be a promising therapeutic method against OSCC. Our results showed that fisetin exhibited anticancer activity via apoptosis of the human tongue squamous cell lines CAL-27 and CaA9-22. Our results showed that the fisetin exhibited anti-cancer activity via apoptosis in OSCC cell lines CAL-27 and CaA9-22. We confirmed the autophagy process in fisetin-treated Ca9-22 cells and found that fisetin clearly induced autophagy in Ca9-22 cells. Taken together, the combination of fisetin and an effective autophagy inhibitor could be a potentially useful treatment for oral cancer.

Key Words: Fisetin, Oral squamous cell carcinoma, Autophagy, Apoptosis

P277

Cancer Prevention effects of Delphinidin in Human Osteosarcoma Cells

Hae-Mi Kang[1,2], Dan-Bi Park[1,2], Jin-A Park[1,2], Su-Bin Yu[1], In-Ryoung Kim[1], Bong-Soo Park[1,2]

[1]Department of Oral Anatomy, School of Dentistry, Pusan National University, Yangsan, Korea
[2]BK21 PLUS Project, School of Dentistry, Pusan National University, Yangsan, Korea

Delphinidin is major anthocyanidin that is extracted from many pigmented fruits and vegetables. This substance has anti-oxidant, anti-inflammatory, anti-angiogenic, anti-cancer and anti-migration and invasion of various cancer cells during tumorigenesis. Although delphinidin has anti-cancer effects, little is known about its functional roles in osteosarcoma (OS). For these reasons, we have demonstrated the effects of delphinidin on OS cell lines. The effects of delphinidin on cell viability and growth of OS cells were assessed using the MTT assay and colony formation assays. Hoechst staining indicated that the delphinidin-treated OS cells were undergoing apoptosis. Flow cytometry, confocal microscopy, and a western blot analysis also indicated evidence of apoptosis. Inhibition of cell migration and invasion was found to be associated with epithelial-to-mesenchymal transition (EMT), observed by using a wound healing assay, an invasion assay, and a western blot analysis. Furthermore, delphinidin treatment resulted in a profound reduction of phosphorylated forms of ERK and p38. Taken together, our results suggest that delphinidin strongly inhibits cell proliferation and induces apoptosis. Delphinidin treatment also suppresses cell migration and prevents EMT via the MAPK-signaling pathway in OS cell lines. For these reasons, delphinidin has anti-cancer effects and can suppress metastasis in OS cell lines, and it might be worth using as an OS therapeutic agent.

Key Words: Delphinidin, Osteosarcoma, Epithelial-to-mesenchymal transition, Apoptosis

P278

Effect of the recombinant MAGED4 loaded dendritic cells in the specific immunotherapy for glioma

Qing-Mei Zhang[1], Shui-qing Bi[1], Bin Luo[1], Ying-Ying Ge[1], Jun Fu[1], Xi-Sheng Li[2], Ya Peng[1], Fang Chen[1], Wei-Xia Nong[1], Guo-Rong Luo[1], Su-Fang Zhou[1], Xia Zeng[1], Chang Liu[1], Shen-ao Li[1], Gao-shui Guo[2], Shao-Wen Xiao[2,*], Xiao-Xun Xie[1,*]

[1]Department of Histology and Embryology, School of Pre-clinical Medicine, [2]Department of Surgery, First Affiliated Hospital, Guangxi Medical University, Nanning 530021, Guangxi Zhuang Autonomous Region, China;. *Corresponding author

Introduction: MAGED4 is overexpressed in glioma whilst restricted expression in normal tissues. Here, we examine the immunogenicity of MAGED4 in glioma to determine its potential as an immunotherapeutic target. **Methods:** Dendritic cells (DCs) was generated from adherent PBMCs of a HLA-A2^{+} healthy donor and identified by flow cytometry. MAGED4-specific CTLs targeting glioma were induced from CD8^{+} T cells isolated from PBMCs using CD8 magnetic microbeads, by two stimulations with MAGED4-loaded DCs. IFN-γ production was analyzed by ELISPOT assay and cytotoxicity was performed by LDH release. **Results:** Mature DCs expressed higher levels of CD83, CD80, CD86 and HLA-DR, and lower level of CD14, compared to immature DCs. MAGED4 specific CTLs can effectively produce IFN-γ and lyse MAGED4-expressing HLA-A2[+] U251 instead of MAGED4-expressing HLA-A2[-] A172 in dose-dependent and HLA-A2-restricted manners. **Discussion:** These results suggest that

MAGED4 protein may serve as a specific immunotherapeutic target for treating HLA-A2 patients with glioma.

Key Words: MAGED4, DC, CTL, Glioma

P279

CALCITRIOL ATTENUATES KIDNEY FIBROSIS VIA DECREASING TUBULAR INJURY, M1-M2 MACROPHAGE RATIO, AND MYOFIBROBLAST

Rizka Adi Nugraha Putra[1*], Dwi cahyani Ratna Sari[2], Santosa Budiharjo[2], Nur Arfian[2]

[1]Departement of Anatomy Faculty of Medicine, Universitas Muhammadiyah Purwokerto, Indonesia
[2]Departement of Anatomy Faculty of Medicine, Universitas Gadjah mada, Indonesia

Background. Chronic Kidney Disease (CKD) is the global health issues with bad prognosis outcome, characterized by kidney fibrosis. Unilateral Ureteral Obstruction (UUO) is the most representative experimental model to obtain kidney fibrosis. Kidney fibrosis observed with progressive injury of parenchymal kidney and extracellular matrix aggregation of type I and III collagen. This study was aimed to explore the effect of calcitriol administration toward the expression of M1-M2 macrophage, tubular injury and myofibroblast in male mice by using UUO.
Methods. Twenty-five Switzerland furrowed mouse were divided into 5 equals groups; control group (SO), UUO3, UUO7, UUOD3 and UUOD7. UUO groups received 0.2% ethanol and UUOD groups received 0.5 µg/kg BM calcitriol for 3 and 7 days exposure. Twenty-five paraffin-embedded section of kidney tissue were analysed by Periodic Acid Schiff and immunohistochemical staining against antibody anti-CD68, Arginase I and αSMA. Data were shown in the proportion of tubular injury, M1-M2 macrophage, and myofibroblast accumulation with imageJ software for scoring. Data were analysed using one way anova using SPSS22 software with $p < 0.05$ considered to be statistically significant. **Results.** UUO treated increased the tubular injury, M1 macrophage and myofibroblast accumulation but decreased M2 macrophage ($p < 0.05$) compared to SO group. This study revealed the poorer prognosis in different exposure of treatment ($p < 0.05$). But calcitriol (UUOD) administration to the treatment decreased the tubular injury, M1 macrophage and myofibroblast accumulation and increased M2 macrophage ($p < 0.05$) compared to UUO groups.
Conclusion. Calcitriol decreased chronic kidney disease by reducing tubular injury and M1-M2 macrophage ratio and inducing myofibroblast in mice.

Keywords: Calcitriol, UUO, M1-M2 Macrophage ratio, Tubular Injury, Myofibroblast

*Correspondence to Rizka Adi Nugraha Putra (E-mail: rizka.adinp@gmail.com)

P280

Semaphorin 6D reverse signaling controls macrophage lipid metabolism and anti-inflammatory polarization

Sujin Kang[1], Atsushi Kumanogoh[2]

[1]Department of Immune Regulation, Immunology Frontier Research Center, Osaka University, Osaka,

Japan
[2]Department of Immunopathology, Immunology Frontier Research Center, Osaka University, Osaka, Japan

Polarization of macrophages into pro-inflammatory or anti-inflammatory states has distinct metabolic requirements with mTOR kinase signaling playing a critical role. However, it remains unclear how mTOR regulates metabolic status to promote polarization of these cells. Here, we show that an mTOR–Semaphorin 6D (Sema6D)–Peroxisome proliferator receptor γ (PPARγ) axis plays critical roles in macrophage polarization. Inhibition of mTOR or loss of Sema6D blocked anti-inflammatory macrophage polarization, concomitant with severe impairments in PPARγ expression, uptake of fatty acids, and lipid metabolic reprogramming. Macrophage expression of the receptor Plexin-A4 is responsible for Sema6D-mediated anti-inflammatory polarization. We found that a tyrosine kinase, c-Abl, which associates with the cytoplasmic region of Sema6D, is required for PPARγ expression. Furthermore, Sema6D is important for generation of intestinal resident CX3CR1[hi] macrophages and prevent development of colitis. Collectively, these findings highlight crucial roles for Sema6D reverse signaling in macrophage polarization, coupling immunity and metabolism via PPARγ.

Key Words: Macrophage, Lipid metabolism, Semaphorin, Neuron, Inflammation

P281

Lipogenesis regulation properties of Ecklonia cava via RAGE ligands control secreted from macrophage

Junwon choi[1,2], Seyeon Oh[2], Myeongjoo Son[1,2], Hyesun Lee[2], Kyunghee Byun[1,2,*]

[1]Department of Anatomy and Cell Biology, Gachon University Graduate School of Medicine, Incheon, Republic of Korea
[2]Functional Cellular Networks Laboratory, Lee Gil Ya Cancer and Diabetes Institute, Gachon University, Incheon, Republic of Korea

The positive properties of Brown algae in obesity and inflammation are published and studied by the researchers these days. The Ecklonia Cava is sort of brown algae and cultivated in Jaejoo island. Polyphenol substrates of Ecklonia Cava were extracted and separated by using a chemical process to validate the anti-obesity and anti-inflammation effects. Obesity caused by excessive energy consumption induces chronic inflammations in major organs such as liver, kidney and even in adipose tissue. The chronic inflammations are generated by pro-inflammatory cytokines such as IL-6, TNF-α and free fatty acids(FFA) released from lipid droplets through upregulation of lipolysis. On the other hands, Adipose tissue macrophages(ATMs) regulate inflammations and anti-inflammations depends on the environments where it resides in. In the lean state, most of the macrophages are M2 type characteristics and secrete anti-inflammatory cytokines such as TGF-β, IL-10 to prevent the inflammation. However, In the obese state, ATMs are promoted to differentiate inflammatory macrophages characteristics affected by inflammatory cytokines and FFAs. Those inflammatory macrophages not only recruit not only immune cells from the blood vessel by secreting pro-inflammatory cytokines and chemokines such as MCP-1, CCK2 but also express and secrete RAGE and RAGE ligands as well. It has been discovered that receptor of AGEs(RAGE) and RAGE ligands such as Aged glycation end-products(AGEs), High mobility group box-1 proteins(HMGB-1) play an important role in hypertrophy in a recent study. In this study, we studied the mechanisms of Ecklonia Cava on controlling macrophage differentiation via regulating the RAGE pathway and the modulation of RAGE-ligand as well. As a result, the lipogenesis pathway is down-regulated by controlling the

RAGE pathway in adipose tissue.

Key Words: Lipogenesis, Macrophage, RAGE, Obesity, Ecklonia Cava

P282

Effects of Isoflavone-enriched Soybean (Glycine max) Leaves Extract on Anti-inflammatory and Anti-osteoporosis

<u>Dong Hoon Lee</u>, Juyeong Park, Seokmin Kang, Hyemin Seong, Joo Yeon Jeong, Jinhyun Ryu, Sang Soo Kang

Department of Convergence Medical Science and Anatomy, College of Medicine, Gyeongsang National University, Jinju, 52727, Korea

Postmenopausal osteoporosis accounts for 80% of incidence of osteoporosis and affects 200 million women worldwide. Moreover, osteoporotic fractures caused can lead to chronic pain, deformity, depression, disability and even death. Hormone replacement therapy (HRT) is regarded as the effective treatment for postmenopausal osteoporosis, but it can result in some side effects. Soy isoflavones are well known as active phytoestrogens and are widespread accepted as natural alternative or supplement of HRT. In previous study, we found that ethylene-treated soybean (Glycine max) leaves have unprecedented levels of total isoflavones of up to 13,584 µg/g, which is far higher than those of 2,300 µg/g in the common soybean leaves. To identify the beneficial effect of isoflavone-enriched soybean leaves (IESLs) on postmenopause osteoporosis, lipopolysaccharides-stimulated RAW264.7 cells and an ovariectomized (OVX) rat model were used in the present study. Results showed aglycone daidzein and genistein from IESLs significantly inhibited LPS-induced inflammatory response by suppressing the mRNA expression of iNOS, COX-2, IL 6 and IL β. Oral administration of IESLs to OVX rats (18.8 mg isoflavone/kg/day) significantly ameliorated OVX-induced bone loss as reflected by improving microarchitecture indices of trabecular bone such as Bone mineral density, number of trabecular bone, trabecular bone separation and bone volume compared with the OVX group. According to mRNA expression in femurs, IESLs exert its benefit effects on postmenopausal osteoporosis by down-regulation the mRNA expression of osteoclastic protein (RANKL/OPG., OC and cathepsin K) and inflammatory-related genes (IL6, NFκB, and COX-2). Therefore, IESLs can be used as functional food for a prevention and therapy of postmenopausal osteoporosis.

Key Words: Postmenopause, Osteoporosis, Isoflavone, Ovariectomy, Anti-inflammation

P283

Interleukin-10 protects ureteral obstruction-induced renal fibrosis by attenuating endoplasmic reticulum stress, oxidative stress and apoptosis

Kyong-Jin Jung, In-Hwan Song

Department of Anatomy, Yeungnam University College of Medicine, Daegu, Republic of Korea

Chronic kidney disease (CKD) is one of major incurable disease disturbing quality of life. Rregardless of initial trigger, fibrosis is the common final pathway to CKD and inflammation plays a key role. Interleukin (IL)-10 is a potent immunomodulatory cytokine with anti-inflammatory properties.

Endoplasmic reticulum stress (ERS) contribute to the pathophysiologic changes of kidney fibrosis. However, the role of IL-10 against ERS during renal fibrosis has remains poorly elucidated. We investigated the mechanisms of IL-10 on ERS-induced renal fibrosis in IL-10 knockout (KO) mice using unilateral ureteral obstruction (UUO) model. ERS and profibrotic protein levels were measured by western blotting. Periodic acid Schiff and Masson's trichrome stain were used for analyzed histologic changes and collagen deposition. Oxidative stress levels (O_2^-, H_2O_2, malondihydrogenase (MDA) and 4-HNE) were also checked in kidney sample. Kidney tubular epithelial cells (TMCK-1) were used for *in vitro* study. Cells were cultured in ERS inducers (tunicamycin, thapsigargin, and brefeldin A) with or without IL-10. In addition, CHOP or IL-10 siRNA transfection were used to confirm effect of CHOP or IL-10 deletion to fibrosis. In this study, fibrosis, tubular damage (tubular dilation, cast formation, tubular atrophy and infiltration of cells), oxidative stress, and collagen deposition were more prominent in UUO-induced IL-10 KO mice. In addition, IL-10 KO mice expressed higher level of profibrotic genes (α-SMA and COL1), ERS genes (GRP78/Bip and CHOP) and apoptosis related genes (cleaved caspase-3) after UUO. IL-10 treatment reduced apoptosis and fibrosis in the cell cultured with ERS inducer. IL-10 siRNA increased expression of ERS and profibrotic genes but CHOP siRNA showed opposite results. ERS inhibitor, sodium 4-phenylbutyrate (PBA), treatment reversed both of above *in vivo* and *in vitro* results. Our results suggested that IL-10 can protect kidney fibrosis by suppression of the ER stress, oxidative stress and apoptosis.

Key Words: Chronic kidney disease, UUO, IL-10, ER stress, Oxidative stress, Apoptosis

P284

Piper Nigrum extract prevents OVA-induced nasal epithelial barrier disruption

Nguyen Thi Van[1], Thi Tho Bui[1], Chang Ho Song[1,2], Ok Hee Chai[1,2]

[1]Department of Anatomy, Chonbuk National University, Jeonju, South Korea
[2]Institute for Medical Sciences, Chonbuk National University, Jeonju, South Korea

P. nigrum has been reported to have anti-oxidant, anti-bacterial, anti-tumor, anti-mutagenic, anti-diabetic, and anti-inflammatory properties. However, the protective role of *P. nigrum* on *upper respiratory tract injury* in an allergic rhinitis (AR) mouse model has been unclear. This study aims to investigate the effects of *P. nigrum* fruit extract (PNE) on the *upper respiratory tract* in an ovalbumin (OVA)-induced AR model. AR mouse model was established by intraperitoneal injection with 200 μl saline containing 50 μg OVA adsorbed to 1 mg aluminum hydroxide, and intranasal challenge with 20 μl per nostril of 1 mg/ml OVA. Besides, mice were orally administrated once daily with PNE and dexamethasone in 13 days. The nasal symptoms, inflammatory cells, OVA-specific immunoglobulins, cytokines, nasal histopathology, and immunohistochemistry were evaluated. The PNE oral administrations inhibited allergic responses via reduction of OVA-specific antibodies levels and mast cells histamine release, accordingly, the nasal symptoms in the early-phase reaction were also clearly ameliorated. In both nasal lavage fluid and nasal tissue, PNE suppressed the inflammatory cells accumulation, specifically with eosinophils. The intravenous Evans blue injection illustrated the permeability reduction of nasal mucosa layer in PNE-treated mice. Also; PNE treatments protected the epithelium integrity by preventing the epithelial shedding from nasal mucosa; as a result of enhancing the strong expression of the E-cadherin tight junction protein in cell-to-cell junctions, as well as inhibiting the degraded levels of zonula occludens-1 (ZO-1) and occludin into the nasal cavity. Additionally, PNE protected against nasal epithelial barrier dysfunction via enhancing the expression of Nrf2 activated form which led to increasing synthesis of the anti-inflammation enzyme HO-1. These results suggest that PNE has a promising strategy for immunotherapy in allergic rhinitis treatment.

P285

Anti-inflammatory and anti-oxidant effects of mangiferin on OVA-induced allergic rhinitis

Chun Hua Piao[1], Suhwan Choi[1], Hyoung-Tae Kim[1,2], Eui-Hyeog Han[1], Chang Ho Song[1,2], Ok Hee Chai[1,2]

[1]Department of Anatomy, Chonbuk National University Medical School, Jeonju, Korea
[2]Institute for Medical Sciences, Chonbuk National University, Jeonju, Korea

Mangiferin (MF), usually isolated from a variety of natural plants such as mango trees. MF is considered to protect against various organ injuries arising from different causes, and it has anti-inflammatory, anti-apoptotic, and antioxidant benefits. However, anti-allergic inflammatory effect of MF and some of its mechanisms in allergic rhinitis model is unknown well. The aim of the present study was to investigate the mechanisms underlying the protective action of MF in OVA-induced allergic rhinitis (AR) models. Allergic rhinitis was induced in BALB/c mice by sensitization and challenge with OVA. Each various concentration of MF (5 mg/kg, 20 mg/kg) and Dexamethasone (Dex, 2.5 mg/kg) was administrated by oral gavage on 1 hour before ovalbumin (OVA) challenge. Mice of control group were treated with saline only. Then mice were evaluated for the presence of nasal mucosa inflammation, the production of allergen-specific cytokine response and the histology of nasal mucosa and lung tissue. Here, MF significantly ameliorated the nasal symptoms and the inflammation in nasal mucosa of OVA-induced AR. MF markedly reduced the infiltration of eosinophils and mast cells in these tissues and epithelial disruption. Meanwhile, MF evidently inhibited the overproduction of Th2/Th17 cytokines (IL-6, IL-13, IL-17 and TNF-α) and transcription factor (GATA-3 and ROR-γ), and increased reduction of HO-1/Nrf2 pathways in nasal lavage fluid (NALF) and oxidative stress biomarker (MDA) by OVA. Moreover, Furthermore, MF inhibited the levels of NF-κb and IκB signaling pathway activation in NALF. Overall, MF exerts anti-inflammatory and anti-oxidant activities on OVA-induced AR by inhibiting NF-κB and activating HO-1/Nrf2 pathways. Therefore, these results imply that the MF might be new therapeutic approach for the treatment of AR.

P286

Gallic acid alleviates nasal inflammation in the OVA-induced allergic rhinitis mouse model

Yan Jing Fan[1], Eui-Hyeog Han[1,2], Hyoung-Tae Kim[1], Chang Ho Song[1,2], Ok Hee Chai[1,2]

[1]Department of Anatomy, Chonbuk National University Medical School, Jeonju, Jeonbuk, Republic of Korea
[2]Institute for Medical Sciences, Chonbuk National University, Jeonju, Jeonbuk, Republic of Korea

Allergic rhinitis (AR) is an allergic nasal disease characterized by nasal obstruction, rhinorrhea, sneezing, and itching. Type 1 helper T cells (Th1)/ type 2 helper T cells (Th2) imbalance

has been identified as an important immunological mechanism of AR. In addition, upregulation of type 17 helper T cells (Th17) also increase the risk of developing AR. Gallic acid (3, 4, 5-trihydroxybenzoic acid, GA), a polyphenol natural product, is obtained from various herbs, red wine and green tea. It is known to have diverse biological effects such as anti-oxidation, anti-inflammation, anti-microbial and anti-cancer. In the present study, the effect of GA on airway inflammation and expression of Th1, Th2 and Th17 cytokines in an ovalbumin (OVA)-induced AR mouse model were investigated. AR was developed in BALB/c mice by sensitized with OVA emulsified in aluminum on days 1, 8 and 15, then nasal installation challenged with OVA from days 22 to 28. On days 16 to 28, mice of GA (20, 40, 80 mg/kg) and dexamethasone (Dex, 2.5 mg/kg) groups were administrated 200 μL of GA or Dex by oral gavage, and from days 22 to 28, mice were received treatment 1 hour before OVA challenge. Mice of naive group were treated with saline and without sensitization and challenge. GA alleviated the nasal allergic symptoms, reduced the thickness of nasal mucosa, attenuated goblet cell hyperplasia and eosinophil cell infiltration in the nasal mucosa, decreased the levels of interleukin (IL)-4, IL-5, IL-13 and IL-17 in nasal lavage fluid, and diminished the levels of OVA-specific IgE and OVA-specific IgG1 in serum. However, GA increased the expression of interferon-gamma and IL-12 in NALF. Taken together, it suggests that GA may be used as a therapeutic agent for AR.

Key Words: Gallic acid, Allergic rhinitis, Airway inflammation, Th cytokines

P287

The effect of Epigallocatechin gallate on OVA-induced allergic rhinitis by controlling Th1/Th2 cytokines balance and suppressing oxidative stress

Eunjin Hyeon[1], Suhwan Choi[1], Ok Hee Chai[1,2], Chang Ho Song[1,2]

[1]Department of Anatomy, Chonbuk National University Medical School, Jeonju, Jeonbuk, Republic of Korea
[2]Institute for Medical Sciences, Chonbuk National University, Jeonju, Jeonbuk, Republic of Korea

Epigallocatechin gallate (EGCG) is found in high content in the dried leaves of green tea, white tea, and in smaller quantities, black tea. Several researches reported EGCG has antioxidant activity, anti-angiogenesis, anti-tumor, cardiovascular protection and blood lipid regulation functions. However, it has not fully known the effect of EGCG on OVA-induced allergic rhinitis model. Therefore, the purpose of this study is to demonstrate the suppressing effect of EGCG on allergic rhinitis murine model. In this study we analysed the control influence of EGCG by inflammatory cell numbers, various cytokines and HO-1 (Heme oxygenase-1), the major anti-oxidative and cytoprotective enzyme, from nasal lavage fluid and histological changes. As well as level of OVA-specific IgE and IgG1 were checked from serum. Oral treatment of EGCG groups were significantly decreased inflammatory cells (epithelial cells, eosinophils, neutrophils and macrohpages), also Th2 cytokines such as interleukin 4, interleukin 13 and Th17, interleukin 17 were significantly reduced. In contrast, Th1 cytokines like interferon γ and interleukin 12 were markedly increased especially in 20 mg/kg EGCG group and treated groups tended to reinforce HO-1. Moreover, the level of OVA-specific IgE was down regulated. In histological analysis, treated groups with EGCG were significantly alleviated hyperplasia of goblet cell in the epithelial wall. From these results, we suggest that Epigallocatechin gallate could be a therapeutic potential in OVA-induced allergic rhinitis model though keeping the Th1 and Th2 balance via enhancing HO-1 pathway.

Key Words: Epigallocatechin gallate, Allergic rhinitis, Inflammatory cells, Th1/Th2 cytokines, HO-1

P288

Splenic Gr1⁺CD11b⁺ myeloid cells regulate humoral immunity in autoimmune disease models

Eunkyeong Jang, Suksan Choi, Jeehee Youn

Laboratory of Autoimmunology, Department of Anatomy & Cell Biology, College of Medicine, Hanyang University, Seoul, Korea

Chronic systemic autoimmune diseases are driven by the continuous activation of autoreactive B cells that receive help from Th subsets. A hallmark of such diseases is splenomegaly that is in part composed of abnormally accumulated Gr1⁺CD11b⁺ myeloid cells (SPMC), but the exact role of these cells in the disease process remains largely unknown. To address this question, we conducted in situ and in vitro experiments using a sanroque mouse model of systemic lupus erythematosus and a SKG mouse model of rheumatoid arthritis. We found that SPMC were composed of heterogeneous cells having diverse shapes of nucleus and mixed phenotypes of $Ly6G^{hi}Ly6C^{low}CD11b^+$ and $Ly6G^{low}Ly6C^{hi}CD11b^+$. They were accumulated within extrafollicular area adjacent to T cell zone. In in vitro co-culture settings, SPMC directly inhibited the proliferation of CD4⁺ T cells in a cell-contact-dependent manner. However, SPMC promoted the differentiation of naive CD4⁺ T cells into Th1 and Tfh cells in a contact-independent manner. Moreover, SPMC significantly enhanced the development of IgG1-switched B cells and the expression of costimulatory molecules CD80 and CD86 on B cells without affecting their proliferation. These effects occurred in a manner independent of cell contact, arginase 1 and iNOS. Most importantly, SPMC reduced the apoptosis of plasma cells in a cell contact-dependent manner. These results suggest that SPMC can promote humoral autoimmunity through enhancing Th help to B cells, B cell maturation, and plasma cell survival. This study may be exploited to develop new therapies for human autoimmune disease.

Key Words: Splenic myeloid cells, Follicular helper T cells, Plasma cells

P289

HISTOLOGICAL PROFILE OF MAST CELLS IN BUCCAL MUCOSAE OF MYANMAR HUMAN ADULTS

Hay Man Tun [1], Phyu Win Ei [2], Myint San Nwe[3]

Department of Anatomy University of Medicine 1 (Yangon), Myanmar

Mast cells serve a fundamental role within the immune system. They are key effector cells in both innate and acquired immunity. The number of mast cells are variable in oral submucous fibrosis and oral squamous cells carcinoma.The buccal mucosae were prepared by tissue processing and staining methods.The mast cells were identified by routine Haematoxylin and Eosin staining. . Haematoxylin and Eosin stain was not specific due to various morphologies of mast cells. So the metachromatic stains, Toluidine Blue and Giemsa stains were more reliable to detect the mast cells granules. Mast cells were oval or elongated shaped and centrally placed nuclei in both Toluidine Blue

and Giemsa stains. These cells were detected by purplish red granules with blue nuclei by Toluidine Blue staining in which mean number of mast cells was 7.11 $\pm$ 3.16. In Giemsa stain, the mast cells appeared purplish red granules with baby blue nuclei among pink background and mean number of these was 8.56 $\pm$ 3.05. Giemsa stain was good staining intensity stains for detecting of the mast cells followed by Toluidine Blue and Haematoxylin and Eosin. The fining of the mean number of mast cells in buccal mucosa could provide the basic information for comparing the variation of mast cells number in oral diseases.

Key words: Mast cell, Toluidine Blue stain, Giemsa stain

P290

STUDY ON GASTRIN PRODUCING G CELLS AT PYLORIC ANTRUM REGIONS OF MYANMAR ADULTS

Kay Thi Than Naing[1], Thida Than[2], Saw Wut Hmone[3], May Thwe Linn[4] and Myint San Nwe[5]

Department Of Anatomy, University Of Medicine 1, Yangon, Myanmar

Gastrin producing G cells were mainly distributed within lamina propria of the human pyloric antrum regions and it stimulated the parietal cells to secrete gastric acid (Hydrochloric acid) which was required for digestion of nutrients and killing of pathogens and other microbes. The aim of this study was to identify the endocrine cells and gastrin producing G cells at the pyloric antrum of human adult stomach by using Haematoxylin and Eosin staining and polyclonal rabbit anti-gastrin antibodies. A total of 30 human adult stomachs (23 males and 7 females) from human autopsies were studied. By Haematoxylin and Eosin staining, endocrine cells in pyloric antrum were pyramidal in shape with vesicular nucleus at the base of the pyloric gastric glands. The tissue sections were immune-histochemical stained with polyclonal rabbit antigastrin antibodies and found that the brown cytoplasmic staining of gastrin immunoreactive G cells were located in the middle and base of the pyloric gastric gland within lamina propria of human stomach. G cells exhibited rounded or pyramidal or irregular in shape with brownish cytoplasm surrounding the central nucleus. Most of the G cells were closed type and the remaining cells were opened type. It was observed that some of the G cells appeared as the brown cytoplasmic staining which was evenly dispersed around the central nucleus and in the other G cells staining density was more increased in infranuclear part of the cells within individual case. The median number of G cell examined under light microscope (400X) (5 visual fields) was 21.5.

Key Words: Stomach G cells, Endocrine cells, H and E stain, Immunohistochemical stain

P291

ODAM expression in healthy and inflamed human periodontal tissues

Geumbit Hwang, Joo-Cheol Park

Laboratory for the Study of Regenerative Dental Medicine, Department of Oral Histology and Developmental Biology, School of Dentistry and Dental Research institute, Seoul National University,

Seoul, Republic of Korea

ODAM, an odontogenic ameloblast-associated protein, has been implicated in diverse functions such as ameloblast differentiation, enamel maturation, junctional epithelial formation and regeneration, and tumor growth and metastasis. ODAM was expressed in the normal epithelium of healthy teeth but absent in the pathologic pocket epithelium of diseased periodontium. Therefore, the aim of this study was to investigate ODAM expression in inflamed periodontal tissue compared with healthy periodontal tissue. We obtained periodontal tissues of 13 people from Ajou University Hospital, Suwon, Republic of Korea. The tissue samples were divided into two types, healthy and inflamed periodontal tissues. To compare ODAM expression in healthy and inflamed periodontal tissues for histology, we conducted H&E staining and immunohistochemistry after tissue fixation, processing, embedding and section. We observed ODAM expression in different parts of healthy and inflamed periodontal tissues. ODAM is expressed in epithelium layer of healthy periodontal tissue. By comparison, ODAM was detected in connective tissue layer of inflamed periodontal tissue. These results suggest that ODAM in epithelial tissue of healthy periodontal tissue is secreted to connective tissue of inflamed periodontal tissue. In addition, the ODAM protein was expressed in GCF from periodontitis patients. Therefore, we propose that ODAM in GCF and connective tissue could be used as a protein biomarker for periodontitis diagnosis.

Key Words: ODAM, Odontogenic ameloblast-associated protein, periodontitis, connective tissue, epithelial tissue

P292

Effect of periodontal pathogens *P. gingivalis* and *F. nucleatum* on FABP4 Expression

Da Jeong Kim[1,3], Eun Young Lee[1,3,4], Bok Hee Woo[1,3,4], Jeom IL Choi[2], Hae Ryoun Park[1,3,4]

Department of Oral Pathology[1], Department of Periodontology[2], BK21 PLUS Project[3] Periodontal Disease Signaling Network Research Center(MRC)[4], School of Dentistry, Pusan National University, Mulgeum-up, Yangsan 50612, South Korea

Objectives: we observed whether the periodontal pathogens, P. gingivalis and F. nucleatum, affect FABP4 expression in macrophages and further investigated the mechanism that modulates FABP4. Through this study, we intend to gain knowledge on the correlation between periodontitis and systemic diseases in a mechanistic way. **Methods:** Raw264.7 were grown in 75-cm2 flasks in Dulbecco's modified Eagle's medium (DMEM) supplemented with 10% heat - inactivated fetal bovine serum (FBS). Cells were maintained at 37°C in a 5% CO2 humidified incubator. Fusobacterium nucleatum polymorphum and Porphyromonas gingivalis strain 381 were maintained in GAM broth containing 5 mg/mL hemin and 5 μg/mL vitamin K in an anaerobic chamber at 37°C. P. gingivalis and F. nucleatum were suspended in reduced transport fluid (RTF) and 4% sterile carboxymethylcellulose (CMC) for oral administration. Six-weekold-female C57BL/6 mice from KOATECH (Korea) were maintained in groups and housed in cages. **Results:** P. gingivalis and F. nucleatum induce morphological changes and increase FABP4 expression in Raw264.7 macrophages. FABP4 expression by periodontal pathogens is dependent on both Mitogen Activated Protein (MAP) kinase and PI3K/Akt pathways. Mice administered with F. nucleatum showed increased FABP4

expression. Mice administered with P. gingivalis or F. nucleatum exhibited higher levels of glucose and serum insulin levels compared with the control group. **Conclusions:** Our results show that the levels of FABP4 were more elevated in the serum of mice administered F.nucleatum than in non-infected or P. gingivalis-infected mice. Additionally, the insulin levels were higher in mice administered F. nucleatum than in non-infected or P. gingivalis infected mice. These findings suggest that F. nucleatum may play a role in insulin resistance.

Key Words: Periodontal, Fusobacterium nucleatum, Porphyromonas gingivalis, FABP4

P293

The Immunoreactivity of PI3K/AKT Pathway After Prenatal Hypoxic Damage

Yonghyun Jun, Yoonyoung Chung

Department of Anatomy, School of Medicine, Chosun University, Gwang-ju,

Background/Aim: There is no consensus on the effect of hypoxia on neurogenesis. In this study, we investigated the immunoreactivity of BDNF and PI3K/Akt signaling after uterine artery ligation in pregnant rats. **Materials and Methods:** Unilateral uterine artery ligation was performed at 16 days of gestation (dg). Fetuses from one horn with ligated artery were allocated to the hypoxic group. Immunohistochemistry was performed with primary antibodies; NeuN, BDNF, PI3K, Akt and phospho-Akt (pAkt). **Results:** The densities of NeuN- and BDNF-immunoreactive (IR) cells in the cerebral cortex were lower in the hypoxic fetuses than in the controls at 21 dg. The density of PI3K and pAkt-IR cells in the cortex of the hypoxic group significantly decreased. The results in dentate gyrus were similar to the results in the cerebral cortex. **Conclusion:** These results suggested that prenatal hypoxia reduced Akt phosphorylation, which affected neuronal survival in the cortex and dentate gyrus.

Key Words: Prenatal hypoxia, Neurogenesis, Akt, pAkt, PI3K

P294

Role of hepcidin - ferroportin axis during Salmonella pathogenesis

Daejin Lim[1,2], Kwang Soo Kim[1,2], Hyung-Ju Lim[1], Jae-Ho Jeong[1,2]

[1]Department of Microbiology and Immunology, Chonnam National University Medical School, Gwangju, 61468, Republic of Korea
[2]Department of Molecular Medicine (BK21plus), Chonnam National University Graduate School, Gwangju, 61468, Republic of Korea

Macrophages release iron into the bloodstream via a membrane-bound iron export protein, ferroportin (FPN). The hepatic iron-regulatory hormone hepcidin controls FPN internalization and degradation in response to bacterial infection. Salmonella typhimurium can invade macrophages and proliferate in the Salmonella-containing vacuole (SCV). Hepcidin is reported to increase the mortality of Salmonella-infected animals by increasing the bacterial load in macrophages. Here, we assess the iron levels and find that hepcidin increases iron content in the cytosol but decreases it in the SCV through FPN on the SCV membrane. Loss of FPN from the SCV via the action of hepcidin impairs the

generation of bactericidal reactive oxygen species (ROS) as the iron content decreases. We conclude that FPN is required to provide sufficient iron to the SCV, where iron serves as a cofactor for the generation of antimicrobial ROS rather than as a nutrient for Salmonella.

Key Words: Salmonella typhimurium, Hepcidin, Ferroportin, Iron, Reactive oxygen species

P295

Examination of *prenatal immune activation* effects on placental *Psg* genes and pregnancy outcome

Da Som Jeong, Ji-Yeon Lee, Myoung Hee Kim

Department of Anatomy and Brain Korea 21 PLUS Project for Medical Science, Yonsei University College of Medicine

The pregnancy-specific glycoproteins (PSGs), members of the immunoglobulin (*Ig*) superfamily, are the most abundant fetal proteins produced by placenta during pregnancy and have possible roles in immune tolerance to fetus. Decreased PSG levels in human maternal serum are associated with adverse pregnancy outcomes including intrauterine growth retardation, preterm labor and pre-eclampsia (PE). There is accumulating evidence that maternal prenatal stress or infection induces placental inflammation and causes abnormal pregnancy outcomes in a fetal sex-dependent manner. Interestingly, our previous work showed that many immune-related genes including *Psg* genes were dysregulated by administration of synthetic glucocorticoid, dexamethasone, on pregnant mice. To investigate the placental gene expression alterations after maternal immune activation, pregnant mice were intraperitoneally injected lipopolysaccharide (LPS) at gestation day 15 (GD15). After 48 hr, placenta samples were analyzed to examine the expression patterns of immune-related genes. Maternal LPS exposure resulted in reduced embryo size and length, and induced placental expression of pro-inflammatory cytokine genes in a sex-specific manner. In addition, the effects of maternal LPS on *Psg gene expression were dose-dependent* and *sex-specific.* The *possible* mechanisms behind the *association* between *Psg gene expression and* sex-specific immunoregulatory responses during pregnancy will be further examined.